Synthetic Studies toward Bacillaene and Analogues

Dissertation

zur

Erlangung des Doktorgrades (Dr. rer. nat.)

der

Mathematisch-Naturwissenschaftlichen Fakultät

der

Rheinischen Friedrich-Wilhelms-Universität Bonn

vorgelegt von

Maximilian Johannes Guhlke

aus

Köln

Bonn, 2025

Angefertigt mit der Genehmigung der Mathematisch-Naturwissenschaftlichen Fakultät

der Rheinischen Friedrich-Wilhelms-Universität Bonn

Gutachter/Betreuer: Prof. Dr. Dirk Menche

Gutachter: Prof. Dr. Andreas Gansäuer

Tag der Promotion: 09.10.2025

Erscheinungsjahr: 2025

Die vorliegende Dissertation wurde im Zeitraum von September 2019 bis Dezember 2024 unter der Leitung von Prof. Dr. Dirk Menche am Kekulé Institut für Organische Chemie und Biochemie der Mathematisch-Naturwissenschaftlichen Fakultat der Rheinischen Friedrich-Wilhelms-Universitat Bonn angefertigt.

Teile dieser Arbeit wurden bereits veröffentlicht:

M. Guhlke, J. Herbst, T. G. Nguyen, A. Schneider, J. S. Dickschat, D. Menche, *Org. Lett* **2025**, *27*, 2317–2322. DOI: https//doi.org/10.1021/acs.orglett.4c04750

„Wer bei der Verfolgung der Wissenschaft nach unmittelbarem praktischen Nutzen jagt, kann ziemlich sicher sein, dass er vergebens jagen wird.“

-Hermann von Helmholtz

Danksagung

Zunächst möchte ich Herrn Prof. Dr. *Dirk Menche* für die Aufnahme in seinen Arbeitskreis und die Unterstützung bei der Themenwahl und der Forschung danken. Insbesondere schätze ich die Aufnahme in den Sonderforschungsbereich TRR 261 und die damit verbundene Tagung in Bad Boll sehr. Zudem möchte ich mich herzlich für die Möglichkeit bedanken, an der RSC-Konferenz in Oxford teilnehmen zu können. Nicht zuletzt danke ich Prof. *Menche* für seine Ermutigung, trotz der nahezu aussichtslosen Synthese nicht aufzugeben und für die hervorragende Zusammenarbeit beim Verfassen der Veröffentlichung.

Herrn Prof. Dr. *Andreas Gansäuer* danke ich für die Übernahme des Zweitgutachtens, seine inspirierenden Vorlesungen und die angenehmen Gespräche während der Betreuung des organischen Grundpraktikums.

Ebenso möchte ich mich bei allen meinen ehemaligen und aktuellen Kolleginnen und Kollegen bedanken, insbesondere meinem Laborpartner *Tim Treiber* und meinem geschätzten Diskussionspartner *Jonas W. Meringdal*. Meinen Bachelor- und Masteranden *Leon C. Honsdorf*, *Damla Aydemir*, *Mohamad* "DIBAL" *Dib Al Dubel*, *Gero H. Steffens*, *Alexander Terekhov*, *Johannes Herbst* und *Tra Giang Nguyen* danke ich für die angenehme Zusammenarbeit und die hervorragenden Ergebnisse. Zudem möchte ich mich bei *Max Seul* und *Max Schönenbroicher* für unseren gemeinsamen Sieg beim Institutslauf 2022 bedanken.

Ein großer Dank gilt ebenso der analytischen Abteilung der Universität Bonn. Im Bereich der NMR-Analyse danke ich Frau Dr. *Senada Nozinovic*, *Karin Prochnicki*, *Hanelore Spitz* und *Ulrike Weynand*. Ebenso bedanke ich mich ganz besonders bei *Andreas J. Schneider* für die vielen HPLC-Analysen und Trennungen sowie bei Frau PD Dr. *Marianne Engeser* für die LC/MS-Messungen. *Karin Peters-Pflaumbaum* danke ich besonders herzlich für die massenspektrometrischen Analysen. Dem AK *Krbek* danke ich für das Leihen der UV-Lampen und der Nutzung des UV-Spektrometers und dem netten Umgang in der gemeinsamen Etage. Allen Mitarbeitern des Instituts gilt mein Dank für den stets freundlichen und unkomplizierten Kontakt. Zudem möchte ich Dr. *Jochen Möllmann* und Dr. *Gabriele Richardt* für ihre technische und organisatorische Leitung danken.

Zuletzt gilt mein tiefster Dank meiner Familie und meinen Freunden, insbesondere meiner zukünftigen Frau *Anna M. H. M. Garbade*, die mich während der gesamten Zeit mit großer Unterstützung begleitet hat, sowie unserem ungeborenen Kinde, welches im Juni das Licht der Welt erblicken wird. Ebenso danke ich meinen Schwiegereltern *Hermann* und *Hedwig* herzlich dafür, dass ich während des Verfassens dieser Arbeit stets bestens bewirtet und motiviert wurde.

Abbreviations

2,2-DMP	2,2-Dimethoxypropane
Ac	Acetyl
ACP	Acyl Carrier Protein
AT	Acyltransferase
B(MIDA)	*N*-Methyliminodiacetat boronate
b.p.	Boiling point
BHT	Dibutylhydroxytoluene
Boc	*Tert*-Butoxycarbonyl
Bpin	Pinacol boronate
Bu	Butyl
CDI	Carbonyldiimidazole
CH	Cyclohexane
CHMP	4-Cyclohexylmorpholine
COSY	Correlation spectroscopy
d.r.	Diastereomeric ratio
DCC	*N*,*N*'-Dicyclohexylcarbodiimide
DCM	Dichloromethane
DDQ	2,3-Dichloro-5,6-dicyano-1,4-benzoquinone
DH	Dehydratase
DIAD	Diisopropyl azodicarboxylate
DIM	diiodomethane
DIPEA	*N*,*N*-Diisopropylethylamine
DMSO	Dimethylsulfoxide
EDC	1-Ethyl-3-(3-dimethylaminopropyl) carbodiimide
EF-G	Elongation factor G
Epin	1,1,2,2-tetraethylethylene glycol
ER	Enoylreduktase
Et	Ethyl
EtOAc	Ethylacetate
Fmoc	Fluorenylmethyloxycarbonyl
GT	Glycosyltransferase
HATU	Hexafluorophosphate Azabenzotriazole Tetramethyl Uronium
HBTU	Hexafluorophosphate Benzotriazole Tetramethyl Uronium
HMBC	Heteronuclear Multiple Bond Correlation
HOBt	Hydroxybenzotriazole
HPLC	High Performance Liquid Chromotagraphy
HRMS	High resolution mass spectrometry
HSQC	Heteronuclear single quantum coherence
IBX	2-Iodoxybenzoic acid
***i*PP$_2$BH**	Diisopropylprenyl borane

KR	Ketoreductase
KS	Ketosynthase
KS^0	Nonfunctional ketosynthase
LAH	Lithium aluminium hydride
λ_{ex}	Excitation wavelength
LDBBA	Lithium diisobutyl-tert-butoxyaluminum hydride
LHMDS	Lithium bis(trimethylsilyl)amide
LiTMP	Lithium tetramethylpiperidide
LLS	Longest linear sequence
***m*CPBA**	*meta*-Chloroperoxybenzoic acid
Me	Methyl
MIC	Minimum inhibitory concentration
MIDA	*N*-Methyliminodiacetic acid
MS	Mass spectrometry
MT	Methyl transferase
MyTSA	*N*-methyltoluenesulfonamide
NBSH	*ortho*-Nitrobenzenesulfonylhydrazide
neop	Neopentyl glycol
NHC	*N*-Heterocyclic carbene
NHMDS	Sodium hexamethyldisilazide
NIS	*N*-Iodosuccinimide
NMR	Nuclear magnetic resonance
NOE	Nuclear overhauser effect
NOESY	Nuclear overhauser effect spectroscopy
OBz	Benzoyl
OTf	Triflate
OTos	Toslyate
PCP	Peptidyl Carrier Protein
PGPR	Plant growth promoting rhizobacteria
Ph	Phenyl
PKS	Polyketidsynthase
PMBTCA	*para*-Methoxybenzyl trichloroacetimidate
p-TsOH	*para*-Toluenesulfonic acid
PyBOP	Benzotriazol-1-yloxy-tripyrrolidinophosphonium hexafluorophosphate
R_f	Retention factor
RP	Reversed phase
RP-C18	Reversed phase (ocatedylsilane)
S_N2	Bimolecular nucleophilic substitution
TBAF	Tetra-*n*-butylammoniumfluorid
TBS	*tert*-Butyldimethylsilyl
TBDPS	*tert*-Butyldiphenylsilyl
TE	Thioesterase
Teoc	2-(Trimethylsilyl)ethoxycarbonyl
TES	Trietyhlsilyl
TFA	Trifluoroacetic acid
TFAA	Trifluoroacetic acid anhydride

THF	Tetrahydrofurane	**TPPO**	Triphenylphosphane oxide
TLC	Thin layer chromatography	**Tr**	Trityl
TMS	Trimethylsilyl	**UV/vis**	Ultraviolett-/visible light (specroscopy)

Table of Contents

Abstract

Thirty years after its first isolation[1], bacillaene (**1**) (Figure 1), a polyketide and polyene antibiotic initially discovered in *Bacillus subtilis*, remains a subject of ongoing research. While significant contributions to the study of this natural product have come from the fields of biochemistry and molecular biology,[2] no contributions were reported from the field of synthetic organic chemistry.

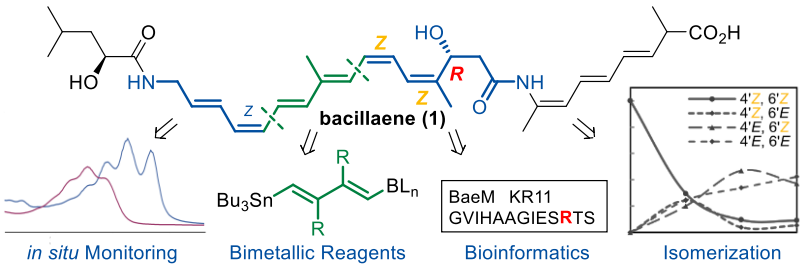

Figure 1. The natural product bacillaene and some key techniques involved during the pursuit of its total synthesis and other investigations. Reprinted with permission from Guhlke, M.; Herbst, J.; Nguyen, T. G.; Schneider, A.; Dickschat, J. S.; Menche, D. *Org. Lett.* **2025**, *27*, 2317–2322. Copyright **2025** American Chemical Society.

Despite its intriguing structure, the synthesis of bacillaene (**1**) is severely hampered due to its highly labile molecular architecture.[3]

In this work, the great challenge of developing a total synthesis of the natural product bacillaene (**1**) and a simplified analogue was pursued. It features improved syntheses of bimetallic linchpin[4,5,6] reagents, iterative cross-coupling strategies and investigations into isomerization processes. Furthermore, the purification and isolation of unstable polyenes is described in detail. Additionally, a valuable method for monitoring polyene iteration via UV-vis shift analyses was developed.

The synthesis of the hexaene core of bacillaene (**1**) was achieved with excellent geometrical purity and subsequently compared to the authentic natural product. A first bacillaene analogue was successfully synthesized, however its final isolation and characterization was not achieved.

Additionally, methods for the synthesis of the enamide sidechain were explored. The *Peterson* olefination method for enamide formation, as described by *Fürstner,*[7] was successfully implemented on a test system. Finally, based on the insights gained from this work, a synthetic strategy is proposed that might enable a future total synthesis of the natural product bacillaene (**1**).

[1] P. S. Patel, S. Huang, S. Fisher, D. Pirnik, C. Aklonis, L. Dean, E. Meyers, P. Fernandes, F. Mayerl, *J. Antibiot.* **1995**, *48*, 997–1003.

[2] S. Miao, J. Liang, Y. Xu, G. Yu, M. Shao, *J. Cell Physiol.* **2024**, 239:e30974.

[3] Guhlke, M.; Herbst, J.; Nguyen, T. G.; Schneider, A.; Dickschat, J. S.; Menche, D. *Org. Lett.* **2025**, *27*, 2317–2322.

[4] M. Altendorfer,D. Menche, *Chem. Commun.* **2012**, *48*, 8267–8269.

[5] R. S. Coleman, M. C. Walczak, *J. Org. Chem.* **2006**, *71*, 9841–9844.

[6] J. Cornil, A. Guérinot, J. Cossy, *Org. Biomol. Chem.* **2015**, *13*, 4129–4142.

[7] A. Fürstner, C. Brehm, Y. Cancho-Grande, *Org. Lett.* **2001**, *3*, 3955–3957.

1. Introduction

Natural products are a class of organic molecules produced by living organisms and can be divided into primary and secondary metabolites.[1] While primary metabolites are directly involved in living cell processes, secondary metabolites, such as polyketides, terpenoids, or alkaloids, often play a role in signaling, resistance, and defense mechanisms of microorganism and plants.[2]

The study of this latter class of natural products has played a major role in the discovery of antibiotics since the "golden age" in the mid-20th century[3] when many classes of antibiotics such as the penicillins, erythromycins and tetracyclines (Figure 2) were first isolated.[4] Up to this day, natural products and their derivatives are the major source for new antibiotic compounds.[5] In light of the serious antibiotic crisis with increasing numbers of (multi)drug resitancies, the discovery of new antibiotics but also the identification of new antiobiotic targets remains an ongoing challenge.[3]

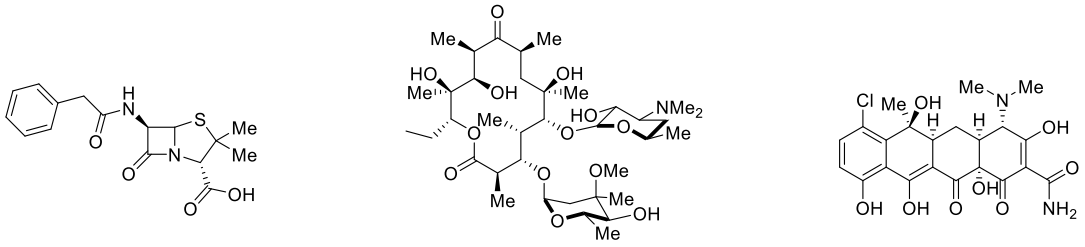

penicillin G (**I**) (1928) erythromycin A (**II**) (1952) chlortetracycline (**III**) (1945)

Figure 2. The structural diversity of the well-known antibiotics penicillin G (**I**), erythromycin A (**II**), and chlortetracycline (**III**), isolated as secondary metabolites from various natural sources during the "golden age" of antibiotics, along with the year of their first isolation.[4]

Within the the exploration of natural products, total synthesis evolved as a discipline for the purpose of structure determination during a time when modern methods for structure elucidations were not available. The structural identity of natural products was therefore facilitated by degradation and partial synthesis of fragments or the total synthesis of the natural product itself. Until today, full sterochemical assignments as well as structural modifications are often only possible through the total synthesis of the compound of interest.[4,6]

Therefore, although total synthesis is sometimes considered a "mature field",[7] it remains an important area within the field of organic chemistry as it allows for structural assignments and the targeted modifications of natural prodcuts.

1.1 Overview of bacillaenes and their significance

Bacillaene (**1**) belongs to the class of polyketide natural products[8] and is a secondary metabolite produced by certain bacteria of the *bacillus* species, particularly the non-pathogenic[9] soil bacteria *B. subtilis, B. amyloliquefaciens* and *B. mehtylotrophicus*.[10]

The discovery of various bacillaenes (**1**-**6**) (Figure 3) stems from research of the last three decades focused on identifying bioactive substances produced by microorganisms and the elucidation of their biosynthetic pathways. However, 12 years passed between the first isolation in 1995[11] and the full structural elucidation of this natural product in 2007 presumably owing to its notorious instability.[12,13,14]

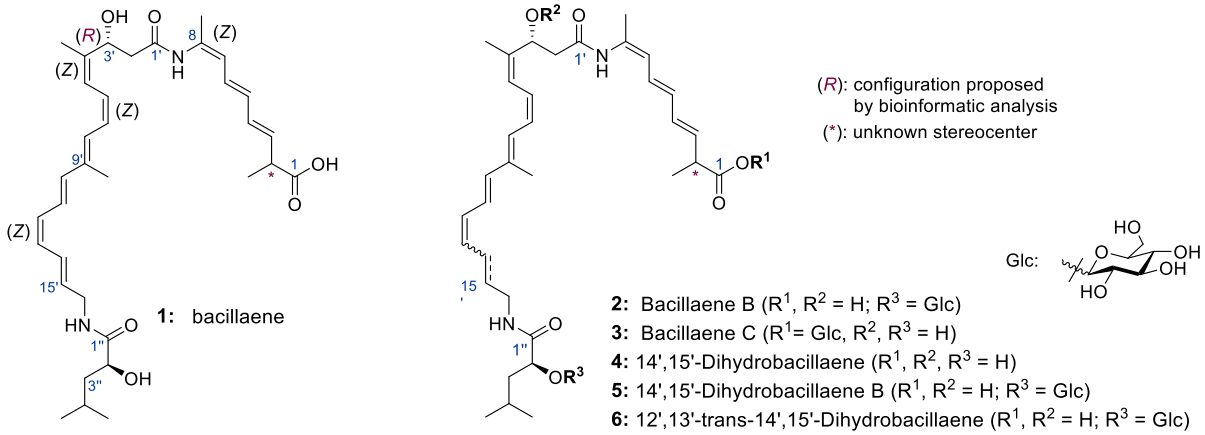

Figure 3. The family of bacillaenes (BAEs) (**1**, **4)** and glycosylated bacillaenes (gBAEs) (**2**, **3**, **5**, **6**).

The overall accepted structure of the bacillaenes (**1**-**6**) features a hexaene backbone with a series of six conjugated double bonds, three of which are in a thermodynamically unfavoured *Z*-configuration. This central hexaene core, or pentaene in case of the dihydrobacillaenes (**4**-**6**), is combined with a likewise singular β,γ-unsaturated trienoic acid, which is linked to the central polyene core by a trisubstituted *Z*-enamide.[16]

While the stereochemistry of the *C2''*-center was experimentally verified by determination of the reduction chirality of the corresponding ketoreductase (KR) domain,[15] the *R*-configuration of the other hydroxyl-bearing stereocenter at *C3'* was later determined by a bioinformatical analysis in our group[16] in cooperation with *Jeroen S. Dickschat* based on methods of *McDaniel* and *Caffrey*.[17,18] Lastly, no sterochemical proposal for the configuration of the *C2*-center exists up to this day.

Structural diversity among bacillaenes (**1**-**6**) arises from variations in double bond geometries and differences in *O*-glycosylsation, enabling the control of biological activities.[19] While higher stabilities

were observed with derviatives glycosylated at 2''-*OH* or 1-*OH*, a reduced antibacterial efficacy was observed.

Bacillaenes (**1**-**6**) are known for their extraordinary sensitivities toward light, heat and oxygen[12] leading to rapid decomposition even at ambient temperature. Recent studies have shown, that the decomposition is triggered by an initial isomerization of the *C4*',*C5*'-double bond from a *cis*- to a *trans*-configuration resulting in a decomposition cascade.[20] However, a systematic understanding of its instabilities remains elusive as photosensitivity cannot be the only reason.[16]

In fact, decomposition of bacillaene (**1**) was observed even in the absence of light while the *O*-glycosylated bacillaene B (**2**) proved significantly more stable.[10] Unlike **1**, glycosylated bacillaene B (**2**) remained largely intact when incubated in an aqueous solution at 37 °C in the dark for a period of 18 hours, while bacillaene (**1**) decomposed quickly under these conditions.[20]

The observed labile nature of this natural product might also explain why a total synthesis of bacillaene (**1**) or its derivatives (**2**-**6**) has not been achieved yet, despite 30 years of active research (Figure 4) on this unique polyene antibiotic.

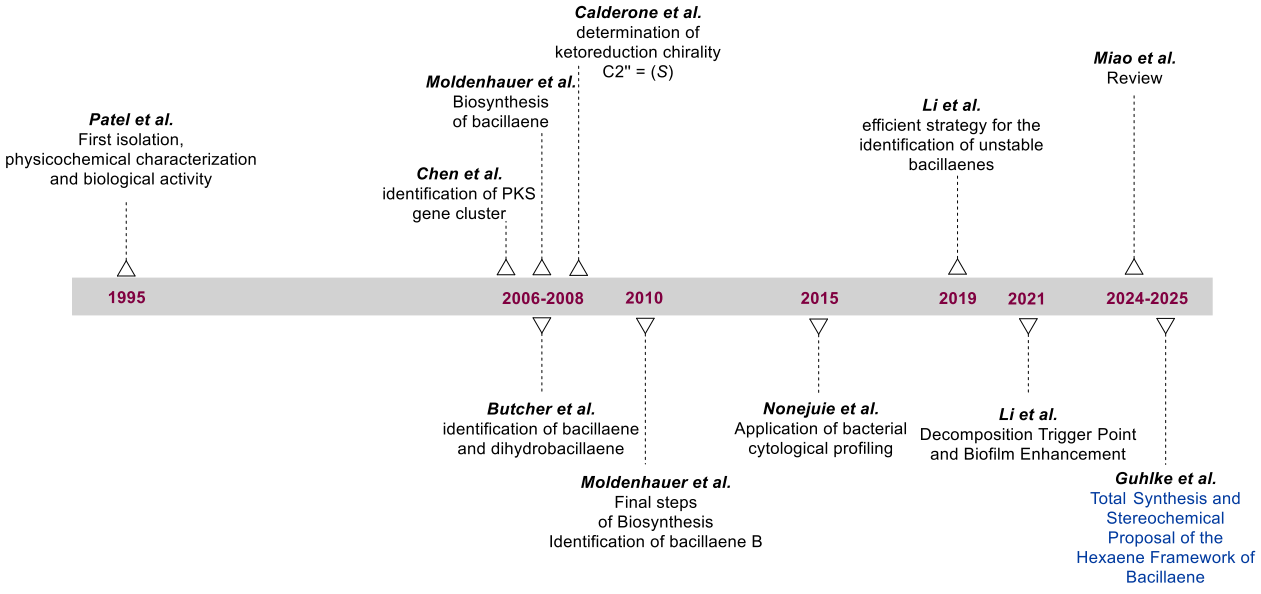

Figure 4. Timeline of the most impactful publications[11,21,12,13,8,22,19,14,20,10] related to bacillaene (**1**), covering its isolation, gene cluster analysis, structural elucidations, biosynthetic pathways, identification of its decomposition trigger point, and the first partial total synthesis developed during this work.[16]

1.2 Biological significance of bacillaene

B. subtilis belongs to the class of plant growth-promoting rhizobacteria (PGPR)[23] and its secondary metabolite bacillaene (**1**) exhibits a broad activity against Gram-positive and Gram-negative bacteria, including *Escherichia coli, Enterococcus faecium, Klebsiella pneumoniae, Proteus vulgaris, Salmonella typhimurium, Serratia marcescens, Staphylococcus aureus,* and *Campylobacter jejuni*.[10,11] Anti-fungal activity was observed toward the fungi *Penicillium digitatum*[24] and *Fusarium oxysporum*.[25]

The antibacterial activity of bacillaene was initially assessed using agar plate diffusion assays, revealing a bacteriostatic effect through selective inhibition of prokaryotic protein synthesis. In these studies, bacillaene was particularly effective against hyper-permeable strains of *E. coli*, with a minimum inhibitory concentration (MIC) of <1.0 µg/mL.[11]

The mechanism of action was studied by *Molina-Santiago* et al. in *Pseudomonas chlororaphis* strains.[26] According to this study, bacillaene (**1**) binds to the elongation factor EF-G (FusA) showing the same mode of action as the antibiotic fusidic acid by blocking ribosomal translocation.[27] This interaction between bacillaene (**1**) and EF-G was further verified by *in-silico* molecular docking studies.[26]

Additionally, effects of a sub-inhibitory concentration (< MIC) were observed for bacillaene (**1**) causing a behavioral change in other bacteria. It was shown, that very low concentrations of bacillaene (**1**) inhibit the biofilm formation of *Campylobacter jejuni*,[28] a bacterium frequently causing foodborne infections.[29] Such antibiofilm properties extend the spectrum of bacillaene's (**1**) biological activity beyond mere growth inhibition.

1.3 Biosynthesis of Bacillaene

The *pksX* gene cluster related to the production of bacillaene (**1**) encodes a large (2.5 MDa) trans-AT hybrid PKS/NRPS-complex.[30] Spanning approximately 80 kb (kilobases), this gene cluster comprises around 2% of the entire *B. subtilis* genome, indicating the significant biological importance of bacillaene (**1**).[12]

Unlike conventional PKS modules, bacillaene's (**1**) enzyme complex includes free-standing acyltransferase (trans-AT) enzymes, placing it within the trans-AT PKS family.[13] These complexes are characterized by the absence of AT domains in their synthetic modules, instead relying on AT enzymes that act "*in trans*" to incorporate monomers.[31]

The biosynthesis of bacillaene (**1**) was reported by two independent research groups, namely, the *Piel* group (*B. amyloliquefaciens* CH12)[13] and the *Clardy* group (*B. subtilis* 3610 *albA− pksX+*)[12], with only six months between the publication of their results.

The main difference in the proposed biosynthetic pathways described by these groups involved the saturation in the *C14*'-*C15*' region. The *Piel*-group proposed a biosynthetic pathway leading to 14',15'-dihydrobacillaene with post-PKS enzymatic dehydrogenation facilitated by P450.[13]

Instead of the typical acetyl-CoA starter module, the biosynthesis was initially reported to begin with an α-hydroxyisocaproic acid (α-HIC) unit, catalyzed by the PksJ/BaeJ-module, followed by incorporation of glycine via the NRPS modules.[12,13]

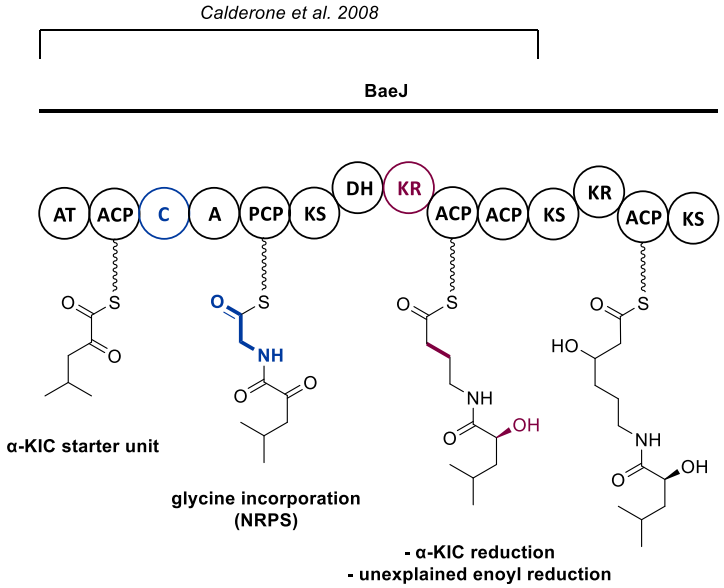

Scheme 1. First steps of the biosynthesis of bacillaene (**1**) with the unusual α-KIC starter unit in the BaeJ-domain.[15] Abbreviations: AT: acyltransferase; ACP: acyl carrier protein; A: adenylation domain; C: condensation domain; KS: ketosynthase; DH: dehydratase; KR: ketoreductase; MT: methyltransferase; PCP: peptidyl carrier protein; KS^0: nonfunctional ketosynthase; TE: thioesterase.

Later research by *Calderone et al.*[15] revealed that the actual starter unit is α-ketoisocaproic acid (α-KIC), which is subsequently reduced by the ketoreductase (KR) in the BaeJ domain. This study also proposed the *S*-configuration of the *C2*''-center.

With the BaeJ domain lacking an enoylreductase (ER), the formation of an α,β-unsaturated intermediate, rather than a fully saturated one, would typically be expected. However, deletion of the TE domain, which off-loads all premature intermediates from the PKS, showed masses two Da higher than expected,

consistent with a fully reduced intermediate in BaeJ.[32] This represents a second surprising feature of this domain.

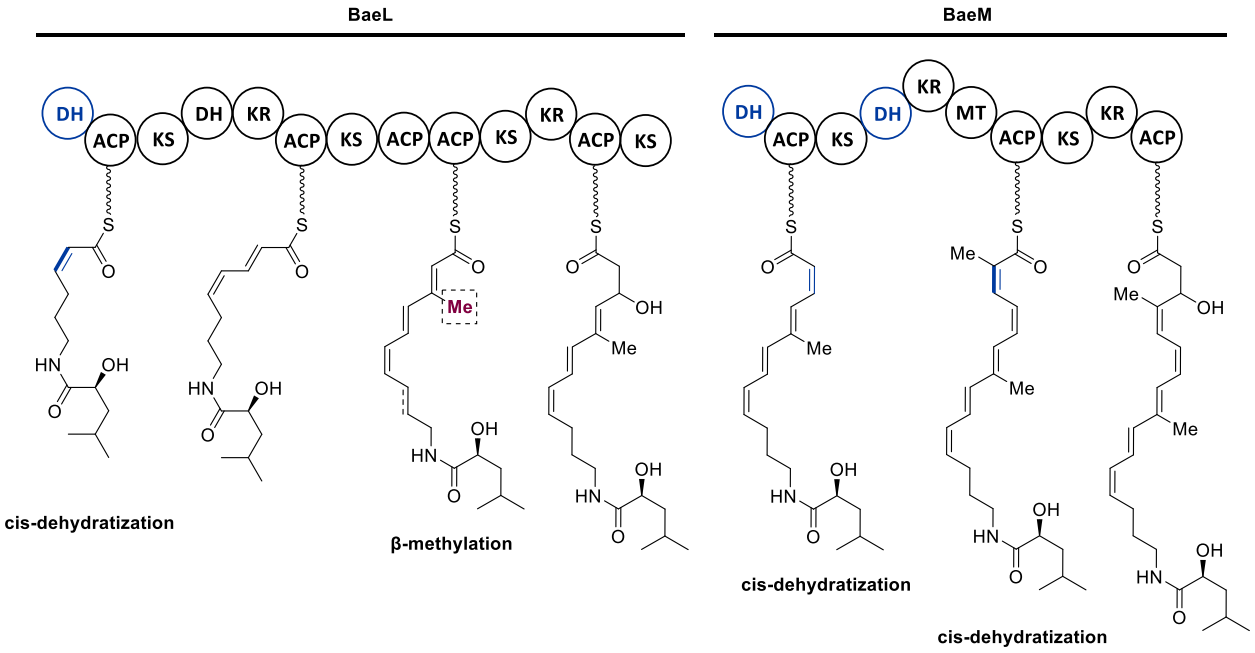

Scheme 2. Further chain elongation within the BaeL and BaeM domains. Abbreviations: ACP: acyl carrier protein; KS: ketosynthase; DH: dehydratase; KR: ketoreductase; MT: methyltransferase; PCP: peptidyl carrier protein.

Subsequent modules BaeL and BaeM iteratively add and modify the extender-units through reduction and dehydration reactions, resulting in the formation of the highly conjugated polyene core. This process introduces the characteristic cis double bonds.[12]

Notably, two of the three *cis* double bonds are generated at the interfaces of the split-modules BaeJ-BaeL and BaeL-BaeM, while the third *cis* double bond is facilitated by an embedded DH domain that, according to bioinformatical analysis, would typically catalyze a *trans*-dehydration.

The introduction of the unusual β-methyl group is reported to be mediated by five enzymes and an external thiolation domain.[12]

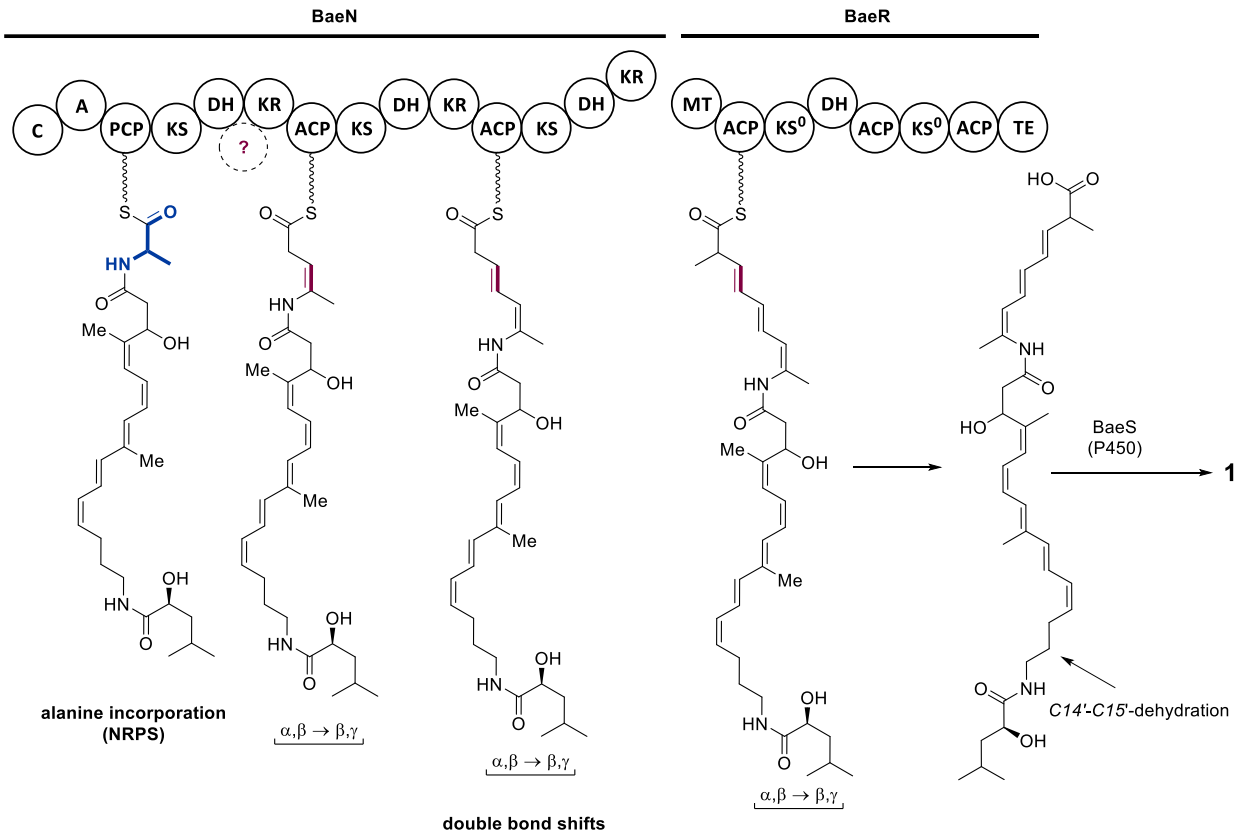

Scheme 3. Proposed final steps of bacillaene (**1**) biosynthesis with the likeliest scenario of a double bond shift during the chain elongation in the BaeN-module. Abbreviations: ACP: acyl carrier protein; A: adenylation domain; C: condensation domain; KS: ketosynthase; DH: dehydratase; KR: ketoreductase; MT: methyltransferase; PCP: peptidyl carrier protein; KS^0: non-functional ketosynthase; TE: thioesterase.

Following the addition of an alanine unit via NRPS, subsequent propagation steps are atypical because the resulting triene is not conjugated with the terminal carboxylic acid. NMR studies on off-loaded intermediates in a TE deletion mutant revealed that these double-bond shifts occur during elongation steps, likely as a series of α,β- to β,γ-shifts following DH activity.[22]

The pks-pathway ends with the P450 enzyme PksS, which catalyzes the final dehydrogenation step, yielding bacillaene (**1**) in its biologically active form.[12] Further modification may occur through glycosylation at *2''-OH*, producing bacillaene B (**2**).[22]

Recent research has shown that the required glycosyltransferase (GT) enzyme, although not part of the *pksX* gene cluster, is encoded within a conserved putative macrolide GT gene (*bmmGT1*) found across genomes of bacillaene-producers.[33,34]

1.4 Aim of this project

The primary objective of this dissertation was the modular total synthesis of the labile polyene antibiotic bacillaene (**1**) along with the development of structurally modified analogues (Figure 5). A key aspect of this synthetic endeavor was the stereoselective construction of the hexaene core by an iterative cross coupling strategy, the investigation of its stability and the elucidation of the stereochemistry at the remaining unassigned or experimentally unconfirmed stereocenters.

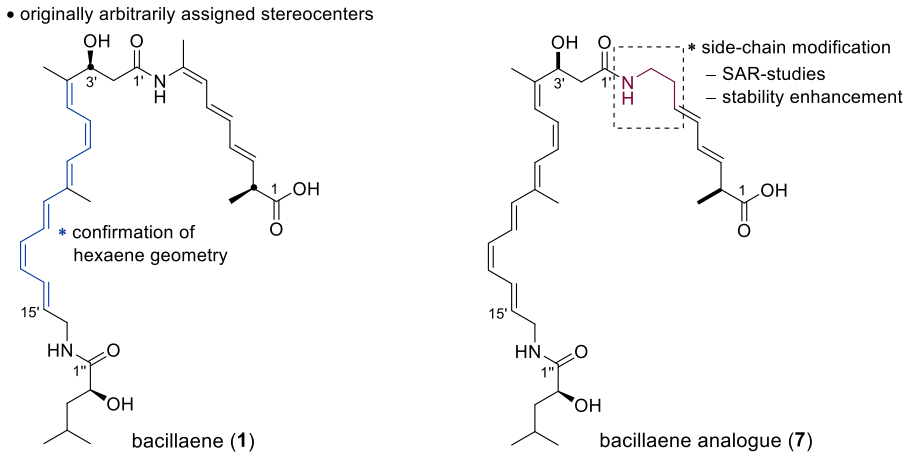

Figure 5. The two target structures bacillaene (**1**) and the bacillaene analogue (**7**).

Since bacillaene (**1**) selectively inhibits prokaryotic protein synthesis but not eukaryotic protein synthesis,[11] it could serve as a lead structure for novel antibiotics that cause minimal harm to human cells. However, due to bacillaenes (**1**) notorious instability, caused by the highly conjugated polyene scaffold and the labile enamide side chain, isolation and potential pharmaceutical applications are inherently challenging.

The synthesis of the bacillaene analogue (**7**) with potentially increased stability by omitting the enamide motif was therefore pursued. In this analog, the methyl group at the *C8*-position was also left out, to prevent the formation of a new unnatural stereocenter. The synthesis of bacillaene analogue (**7**) is also of interest for SAR studies, as alterations in biological activity upon removal of the enamide motif could provide further insights into bacillaene's (**1**) mode of action.

In the case of the cytotoxic natural product salicylihalamide A, the absence of the enamide-structure resulted in a significant loss of biological activity.[35,36] To this end, a large influence depending on the presence or absence of the enamide motif would be expected and as a result also a partial identification of the pharmacophore.

Fundamentals & Theory

2.1 Challenges and Strategies in the Synthesis of Polyenes and Enamides

Conjugated polyenes are olefins with two or more units of alternating double and single bonds.[37] This alternating structure of π- and σ-bonds provides conjugated polyenes with unique electronic properties due to the delocalization of π-electrons across the system resulting in their characteristic absorption spectra.[38]

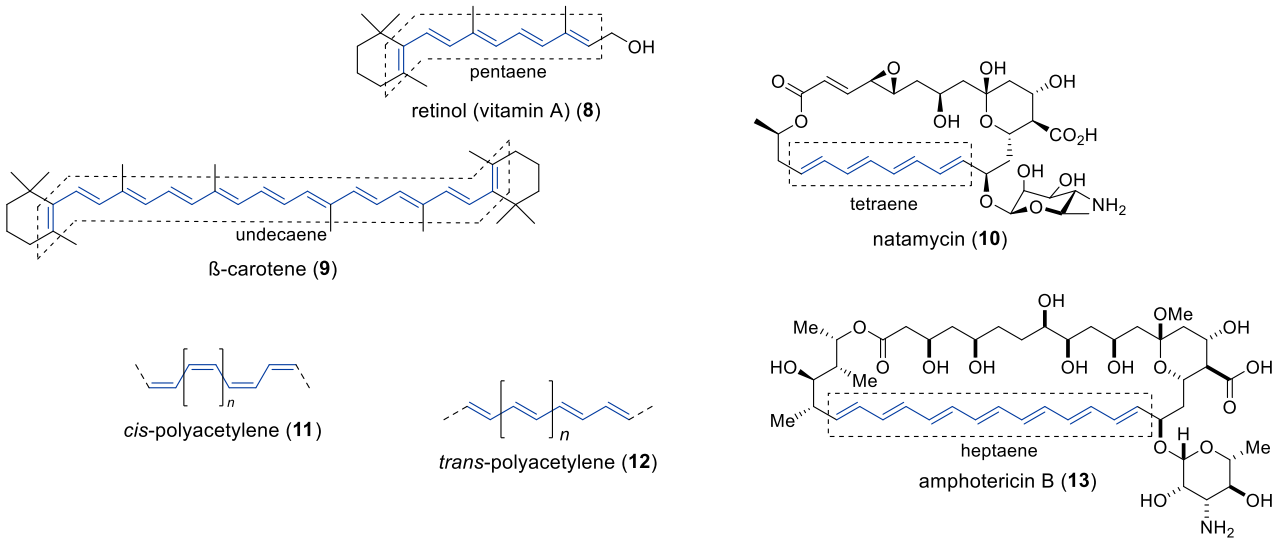

Figure 6. Representative examples of natural and synthetic cyclic and acyclic polyenes.

Polyenes are ubiquitous in nature (Figure 6), serving as key structural components in various biological systems. For instance, carotenoids, which are long-chain polyenes, play crucial roles in light absorption and photoprotection in plants, algae, and photosynthetic bacteria.[39] Their "fission" products, the apocarotenoids, play a major role in vision, through their role as retinoids. Retinal, an aldehyde derivative of vitamin A (**8**) derived from β-carotene (**9**), is a critical component of rhodopsin, the visual pigment in the retina that enables vision in low light. [40,41]

Similarly, polyene macrolides, such as amphotericin B (**13**) and natamycin (**10**), are natural antifungal agents produced by certain microorganisms. These compounds exploit the lipophilic nature of their conjugated polyene chain to interact with cell membranes, forming pores that disrupt fungal cell integrity.[42]

Beyond nature, polyenes are foundational in synthetic chemistry and materials science, where their conjugated structures impart desirable optical, electronic, and mechanical properties.[43]

2.2 The role of homo- and heterobifunctional linchpins in polyene synthesis

2.2.1 Introduction

In organic synthesis, the use of bifunctional linchpins (Figure 7) has become a ubiquitous strategy for the synthesis of polyenic frameworks due to their high modularity and chemoselectivity.[44] While pioneering work dates back until 1991 by the group of *Naso*,[45] the most impactful contributions for for this work were made in the early 2000s by the group of *Coleman*[45] with their use of hetero-bimetallic Sn-B-linchpins **17** and *Burke* with their utilization of MIDA-protected haloboronic acid building blocks **19** in iterative cross-coupling.[46,47,48]

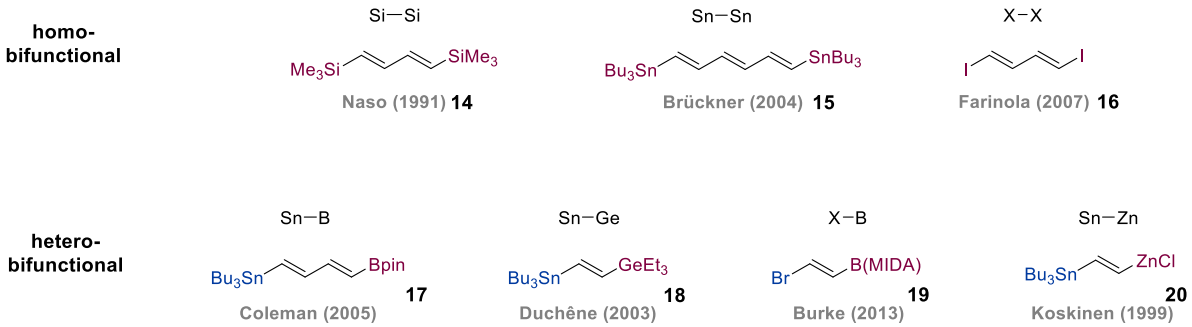

Figure 7. A selection of diverse homo- and heterobifunctional linchpin-olefins.

Linchpin olefins, as named in the literature, are bifunctional building blocks in which two functional groups, usually metals or halides, are separated by a typically sp^2-hybridized carbon chain.[44] This arrangement allows for diversification at both ends of the carbon chain in a consecutive fashion.

The functional groups of the linchpin can be identical (homo-bifunctional) or different (hetero-bifunctional) and typically consist of metals capable of acting as a nucleophile during the transmetalation step of cross-coupling reactions. In some cases, the metal of the linchpin can be converted into a halide through halodemetalation, reversing its reactivity.[49]

Conversely, halide linchpins can be transformed into nucleophiles by insertion of a metal into the carbon-halide bond. Halide linchpins, however, are much less common in the literature due to their lower stability compared to their metal counterparts.[40,50] For instance, vinyl iodides often exhibit poor light stability while lower halides, such as bromides or chlorides, are frequently volatile, making them less practical to handle.[40]

2.2.3 Homobifunctional linchpins

Homo-bifunctional linchpins can be used in desymmetrization approaches[52] but are usually rather utilized for the synthesis of symmetrical molecules e.g. 1,4-diarylbutadienes[50,51] or for ring-closing purposes.[53]

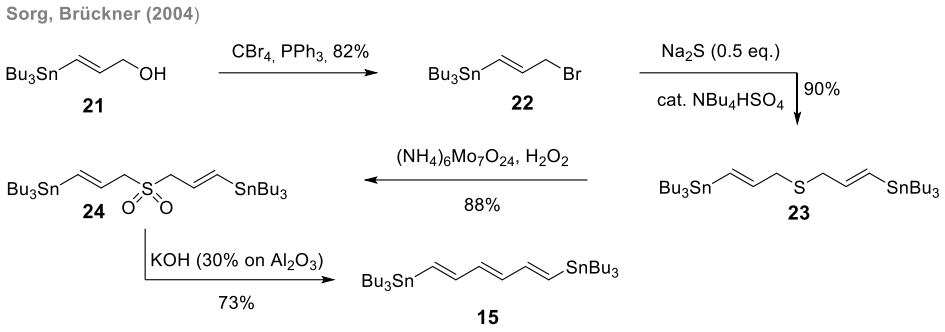

Scheme 4. Synthesis of (1*E*,3*E*,5*E*)-hexatrienyl-1,6-bisstannane **15** a homo-bifunctional linchpin by *Sorg* and *Brückner*.[54]

In 2004, the *Brückner*-group synthesized the symmetrical homo-bimetallic Sn-Sn-linchpin **15** (Scheme 4) via the tin containing disulfide **23**, a subsequent oxidation to the sulfone **24** followed by a *Ramberg-Bäcklund* reaction.[55]

Within their total synthesis of xerulinic acid[54] (**28**) (Scheme 5), they demonstrated that an unsymmetrical coupling of the identical termini of **15** was indeed possible. In this case, a transmetalation cascade (Sn → Li → Zn) on a single terminus of the Sn-Sn-linchpin **15** was accomplished, followed by a *Negishi* coupling. This procedure provided better yields of the mono-coupled product **26** compared to a predominantly statistical driven mono-*Stille* coupling.

An impressive utilization of the same linchpin **15** was its use in a tandem double-*Stille* ring closure as the final step of the total synthesis of pentamycin **31** (Scheme 5) by my former colleague Dr. *Alexander Babczyck*.[53]

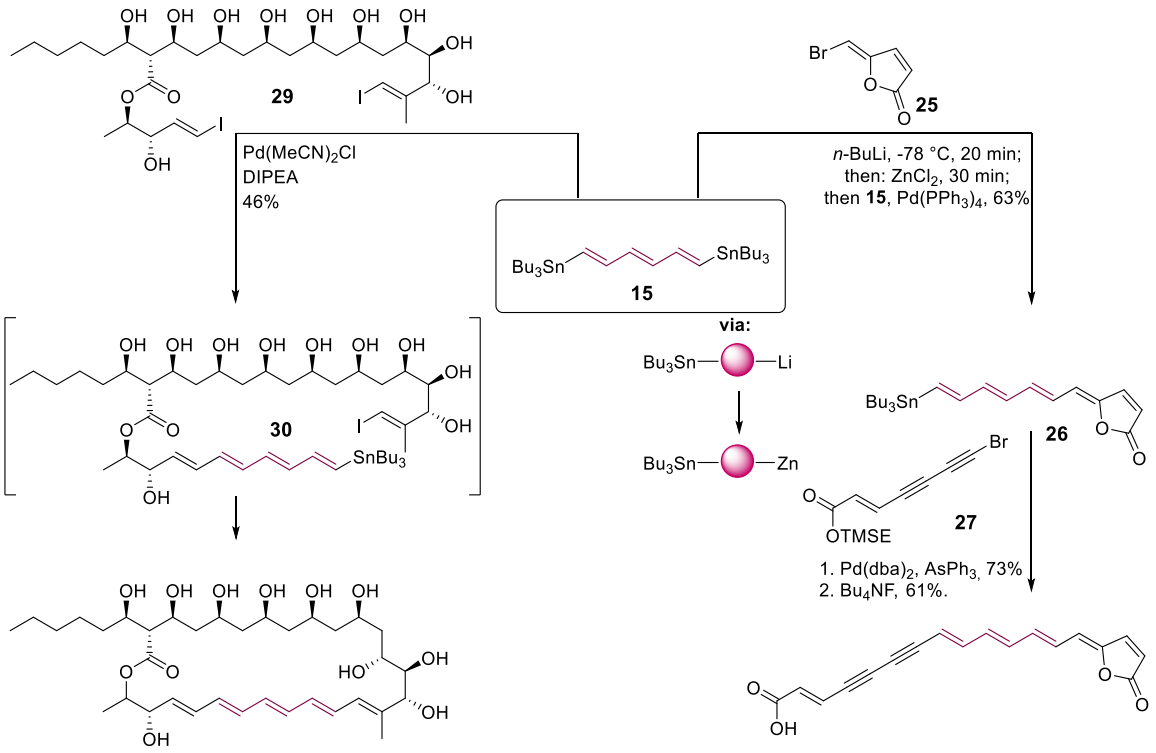

Scheme 5. Utilization of homo-bimetallic Sn-Sn-linchpin **15** in the total syntheses of the polyene natural products pentamycin (**31**) by a double *Stille* reaction (*Babczyk*, *Menche*) and Xerulinic acid (**28**) (*Sorg*, *Brückner*) with a mono-transmetalation *Negishi* coupling followed by a *Stille* coupling.[53,54]

The demand for more site- and chemoselective transformations has driven the evolution of linchpin-olefins toward hetero-bifunctional building blocks, as a combination of different metals allows chemists to exploit their unique transmetalation activities in palladium catalyzed cross-coupling reactions.

2.2.4 Heterobifunctional linchpins

In 2005, the *Coleman*-group synthesized the first Sn-B-linchpin **17** (Scheme 7) and demonstrated a selective coupling of the differentially metalated termini on numerous examples, including the polyene side chain of the natural product lucilactaene (**47**) (Scheme 8).[45]

The synthesis of the Sn-B-linchpin **17** (Scheme 6) started with a *Lipshutz* type stannylcupration[46] of diethoxypropyne (**32**), followed by an acidic deprotection of the acetal. The obtained aldehyde **33** was then converted to the vinyl pinacolboronate by a boryl-*Takai*[57] reaction delivering (Sn-B)-linchpin **17** in a straight-forward fashion.

A slightly different approach to obtain aldehyde **33** was carried out by *Altendorfer*[58] with a palladium catalyzed hydrostannylation[59], followed by an allylic oxidation using activated MnO_2.

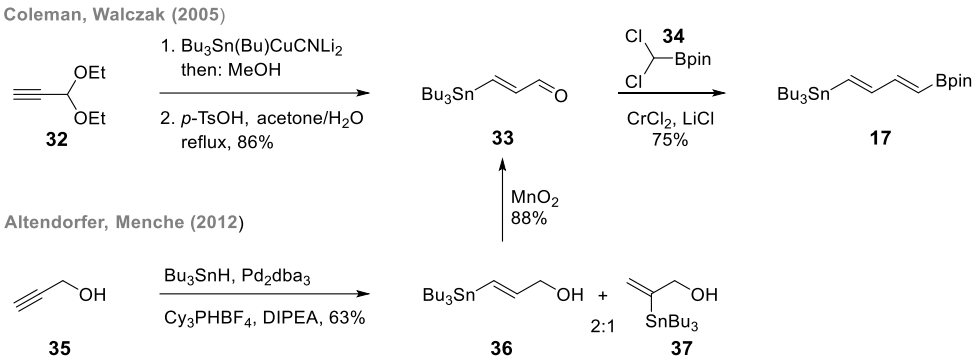

Scheme 6. Comparison of the syntheses of the hetero-bimetallic (Sn-B)-linchpin diene **17** by the *Coleman* group (top) and the *Menche* group (bottom).[45,58]

Besides lower yields, the palladium catalyzed hydrostannylation poses the disadvantage of a rather poor anti-*Marknovnikov* selectivity of 2:1 urging a more tedious chromatographic purification.

While no *Markovnikov* product was observed for the *Lipshutz* type stannylation, the addition of higher order cuprates offers another advantage as the intermediate stannylcuprates can be trapped with various electrophiles[60], thus allowing access to β-branched compounds. This reactivity was indeed utilized for the synthesis of the β-methyl-branched Sn-B-linchpin II (**121**) and will be discussed later.

Both, the our group and the *Coleman*-group successfully carried out sequential *Stille* and *Suzuki-Miyaura* cross coupling reactions (Scheme 7) with the boron-terminus proving unreactive under *Stille* reaction conditions due to the absence of a base. This procedure allowed for an efficient synthesis of the polyene side chains of their target natural products etnangien (**42**) and lucilactaene (**46**) or analogs thereof.[45,58]

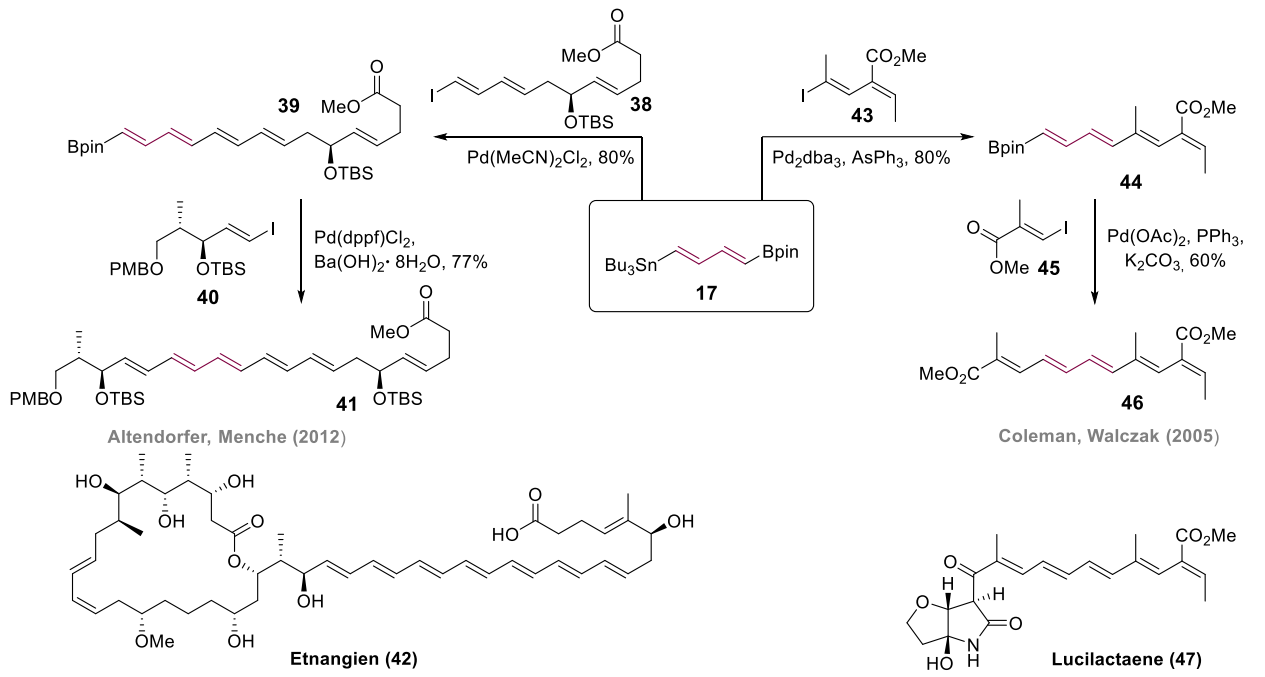

Scheme 7. Utilization of (Sn-B)-linchpin **17** for the synthesis of the polyene side chain (-analogs) of the natural products Etnangien (**42**) (*Altendorfer*, *Menche*) and Lucilactaene (**47**) (*Coleman*, *Walczak*) by sequential *Stille*- and *Suzuki-Miyaura* cross coupling reactions.

2.3 The unique role of MIDA-protected haloboronic esters

While the previously discussed homo- and heterobimetallic linchpins take a fixed place in the synthetic organic chemists tool box, the main disadvantage is their limited ability to serve in iterative cross couplings as their number of iterations is usually limited. In contrast, most biomolecules, e.g. peptides, are in fact synthesized by a more or less unlimited iterative coupling of bifunctional building blocks.[47]

In 2007, *Gillis* and *Burke* published the use of MIDA-protected haloboronic acids as a strategy for small molecule synthesis by iterative *Suzuki-Miyaura* cross couplings (Scheme 8). In analogy to polypeptide synthesis they relied on a protection/deprotection strategy using the MIDA-ligand as a stable but readily cleavable protecting group for the boron center.[46]

MIDA-boronates are the condensation products (anhydrides) of a boronic acid and *N*-methyliminodiacetic acid (MIDA, **48**), a heteroatomic tridentate ligand.[61] They are usually highly crystalline, indefinitely bench stable solids and compatible with chromatography. Due to their sp^3-hybridization, they are unreactive under standard anhydrous *Suzuki-Miyaura* cross coupling conditions, as a vacant p-orbital of the boron center is crucial for the transmetalation step in this

reaction. Therefore, MIDA (**48**) can be seen as a ligand that is capable of reversibly attenuating the reactivity of the boron center by rehybridization.[47]

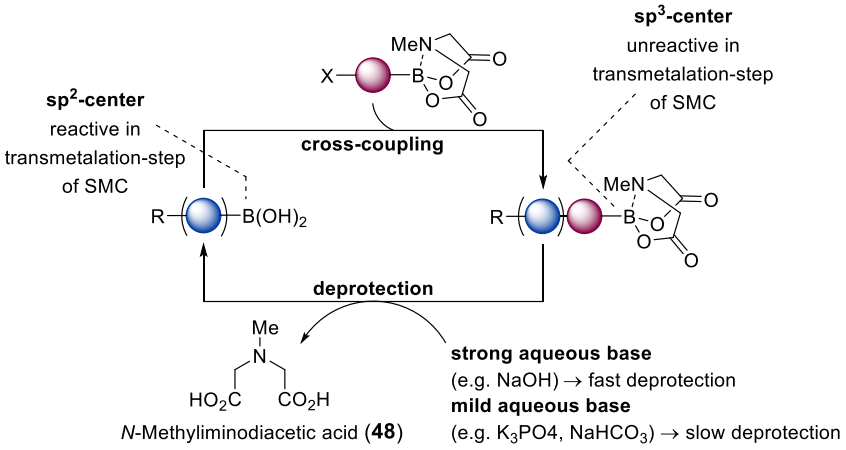

Scheme 8. The conceptual use of MIDA protected haloboronic acids in iterative *Suzuki-Miyaura* cross coupling adapted from E.P. Gillis, M. D. Burke, *J. Am. Chem. Soc.* **2007**, *129*, 6716−6717.

Unlike most organoboronates and other organometallics, MIDA-boronates stand out due to their tolerance towards a wide range of chemical transformations such as oxidations, reductions, protections and deprotections, nucleophilic displacements, additions of carbanions, electrophilic substitutions, additions across triple bonds and transition metal catalytzed reactions including cross metatheses.[62] Such a stability across a manifold of reaction conditions allows their use in multistep syntheses, which is highly desirable from a total synthesis point of view.

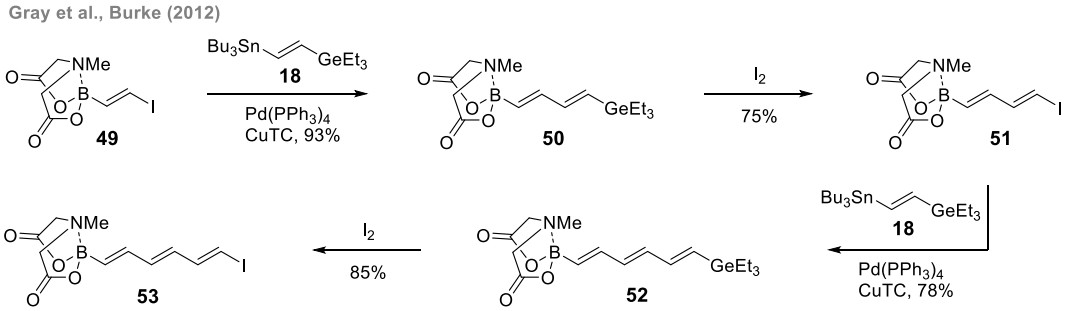

Scheme 9. Synthesis of MIDA protected haloboronic triene linchpin **53** by a linchpin strategy.[49]

An interesting example is the synthesis of MIDA protected haloboronic triene linchpin **53** (Scheme 9) as it was synthesized, again by a linchpin strategy and exemplifies some of the reactivities mentioned at the beginning of this chapter. Here, the final triene **53** is elaborated by an iterative addition of the

(Sn-Ge)-linchpin **18**. After coupling of the Sn-terminus, the polarity of the second terminus is reversed (umpolung) through a iododegermylation allowing a subsequent iterative chain growth.

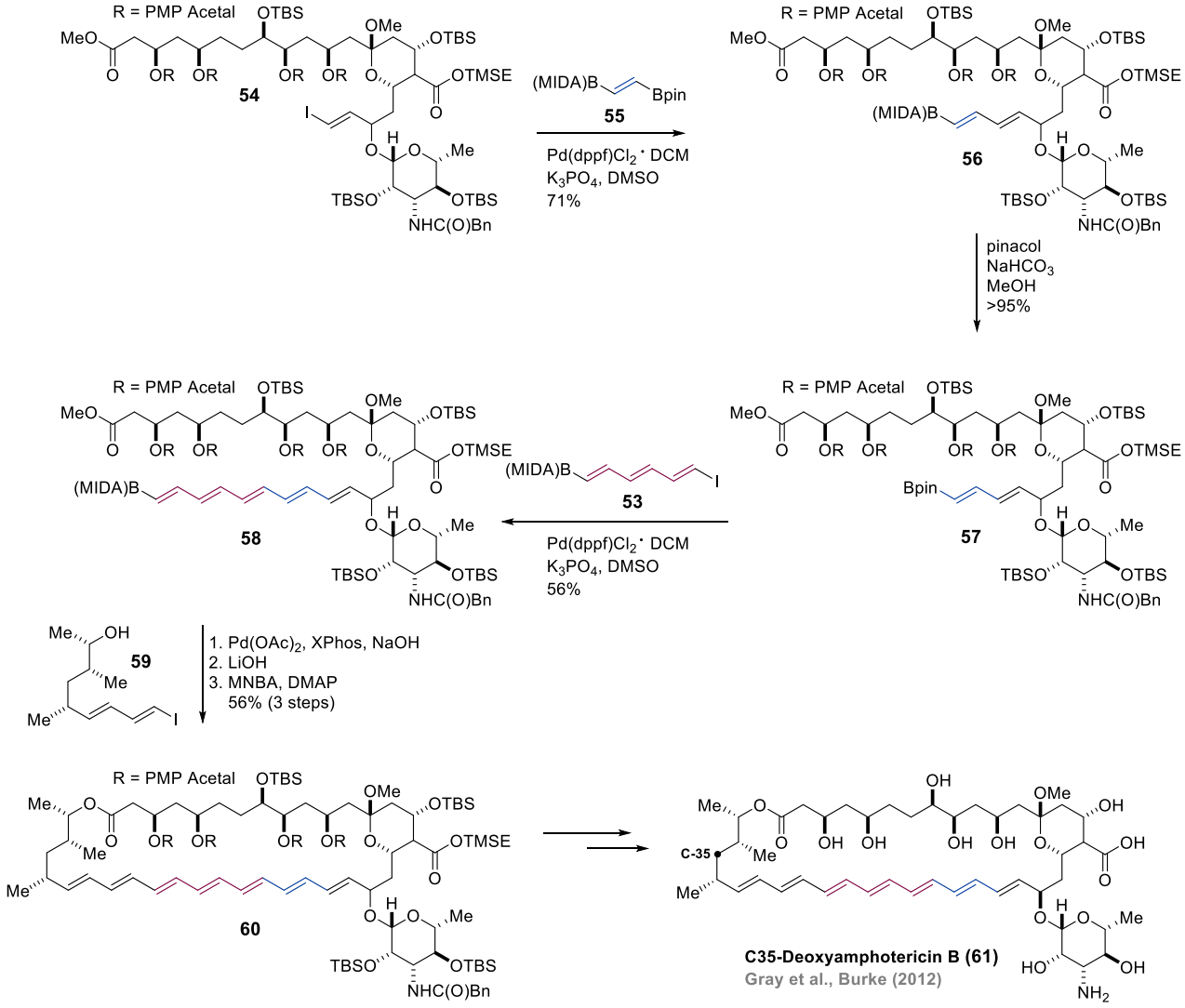

Scheme 10. Utilization of MIDA-boronates **55** and **53** in the semi-synthesis of C35-Deoxyamphotericin B (**61**).[49]

The last example in this chapter is *Burke's* semi-synthesis of C35-Deoxyamphotericin B (**61**) by a linchpin strategy.[49] The sequence starts with an anhydrous *Suzuki-Miyaura* coupling of vinyl iodide **54** with the bis-boronate B(MIDA)-B(pin)-linchpin **55** resulting in a site-selective coupling at the sp^2-boron center. The obtained MIDA-diene **56** is then rehybridized by a ligand exchange with pinacol, regenerating a reactive sp^2-boron center in molecule **57**, which allows subsequent coupling of triene **53**, again under anhydrous conditions. In contrast, the final coupling step of the obtained MIDA-boronate **58** with vinyl

iodide **59** was carried out under aqueous conditions under which the MIDA-ligand is cleaved, releasing the reactive sp^2-boronic acid. After saponification and subsequent macrolactonization, the obtained macrocycle **60** was deprotected to yield the desired C35-Deoxyamphotericin B (**61**).

In conclusion, this chapter explored the utility of bifunctional linchpins as key tools in polyene synthesis and iterative cross croupling. Beginning with homo-bifunctional linchpins, their application in ring-closure reactions was discussed. The chapter then highlights hetero-bifunctional linchpins, such as tin-boron systems, which allow for easier site-selective and sequential couplings. The development of MIDA-boronates represents a breakthrough for iterative cross-coupling, enabling chemists to mimic peptide assembly processes. Selected examples, such as the syntheses of pentamycin (**31**) and C35-deoxyamphotericin B (**61**) illustrate the impact of these linchpins in modern polyene synthesis. Many more interesting examples are among the literature.

Following the exploration of bifunctional linchpins, the next chapter will focus on the total synthesis of enamide containing natural products. These $N_{\alpha,\beta}$-unsaturated amides often play a central role in the biological activity of natural products.[63] The chapter will discuss strategies for constructing enamide-containing frameworks and give examples of successful syntheses from literature.

2.4 Synthesis of enamide containing natural products

2.4.1 Introduction

Enamides are a versatile functional group in organic chemistry, characterized by a carbon-carbon double bond conjugated to an amide group (*N*-vinyl amides). Their unique electronic and structural properties make them valuable intermediates in numerous synthetic applications.[63,64] Enamides are present in many biologically active natural products, such as the crocacines (**62, 68, 79**), lituarines (**63**), and salicylhalamides (**64**).[65,66,67,68]

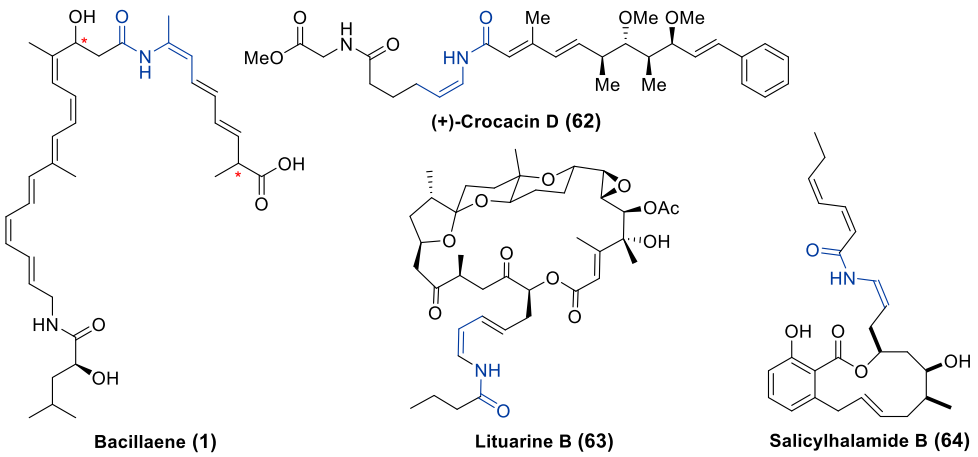

Scheme 11. A selection of *Z*-enamide containing natural products including the synthetic target bacillaene (**1**).

Enamides can be seen as *N*-acylated enamines, with the electron-withdrawing acyl group on the nitrogen reducing the electron density of the nucleophilic sites. Their reactive sites remain similar, with nucleophilic activity at the nitrogen and N_β-carbon and electrophilic reactivity at the N_α-carbon.[69]

Tautomerism between enamides and *N*-acyl imines has been observed, however the imine form is energetically less favored compared to enamine/imine-tautomerism.[70] The presence of a carbon-carbon double bond allows for stable *E*/*Z*-isomerism. Additionally, atropisomerism introduces axial chirality due to restricted rotation around the C-N bond.[71]

Among the many methods described in the literature, this work highlights a small selection, focusing on those assessed capable of synthesizing the α-methyl *Z*-enamide motif found in the natural product bacillaene (**1**). Many of these methods have evolved around the year 2000 and were exemplified in the total syntheses of various crocacines (**62**, **68**, **79**).

2.4.2 Enamide synthesis by C-N coupling

The first example in the list of suitable methodologies is the copper(I)-mediated (catalyzed) vinylic substitution by *Porco* and co-workers (Scheme 12).[72]

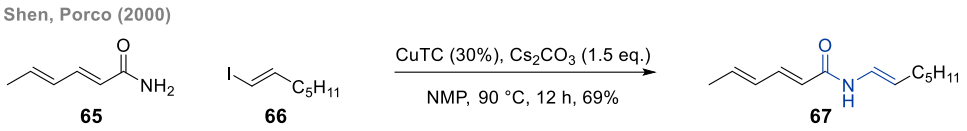

Scheme 12. Copper(I)-catalyzed vinylic substitution by *Porco* and co-workers.[72]

As a copper-mediated *C-N* coupling, this coupling can be regarded as a special case of the *Goldberg*-coupling,[73] which was originally a coupling between amines and aryl halides. Later a wider substrate scope was reported by *Buchwald*, along with the synthesis of *Z*-enamides by a refined method using copper(I) iodide in combination with diamine ligands.[74] A disadvantage of this method is that it typically requires relatively high temperatures.

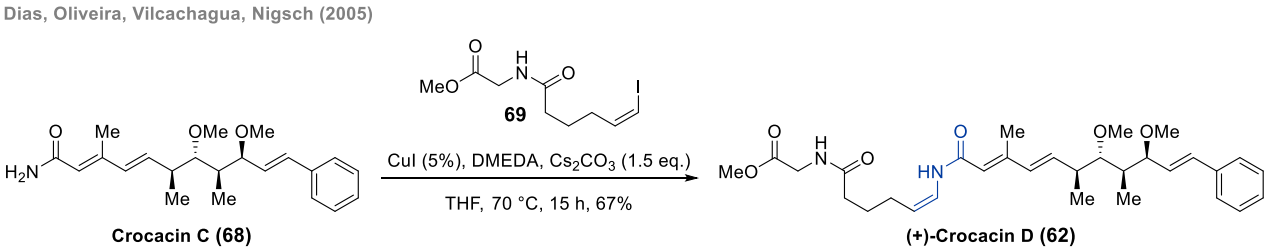

Scheme 13. The copper-catalyzed coupling of crocacin C (**68**) with vinyl iodide **69** as the final step of the total synthesis of (+)-crocacin D (**62**).[75]

An example of this methodology in total synthesis is the synthesis of (+)-crocacin D (**62**) by *Nigsch* and co-workers (Scheme 13). Treatment of crocacin C (**68**) and *Z*-vinyl iodide **69** using *Buchwalds* conditions gave (+)-crocacin D (**62**) as the final step of their total synthesis in 67% yield. Purification of this sensitive enamide required the use of NEt_3-deactivated silica gel.[75]

This successful coupling together with a coupling of methyl *cis*-3-iodocrotonate by *Buchwald*[76] demonstrate the potential to synthesize the α-methyl *Z*-enamide motif present in bacillaene (**1**).

This approach was also employed by my former colleague, *Reuter-Schniete*, during her work on the synthesis of bacillaene's (**1**) eastern fragment. However, her results are not available to me and will not be discussed in this work. Additionally, I actively chose not to use this method during my research to avoid duplicating my former coworker's results.

2.4.3 Enamide synthesis by Peterson-olefination

The synthesis of enamides by a *Peterson* olefination was first reported in the late 80's and early 90's. Back then, geminal *N*-disilylmethylamides were reacted with aldehydes in presence of a fluoride source resulting in the formation of enamides, however with poor stereochemical control.[77,78]

In 2001, *Fürstner* and co-workers published a stereoselective synthesis of enamides[79] (Scheme 14) from vinylsilanes **70** by a sequence comprising of epoxidation, silicon directed[80] ring opening of the resulting epoxysilanes **71** with sodium azide followed by a reduction of the azide **72** to obtain an α-amino-β-hydroxysilane **73**. After amide coupling the enamide **74** is obtained from a base induced *syn*-elimination.[81]

One advantage of this method are the basic conditions under which the enamide is formed, avoiding issues related to the inherent lability of enamides toward acid catalyzed hydrolysis.[82]

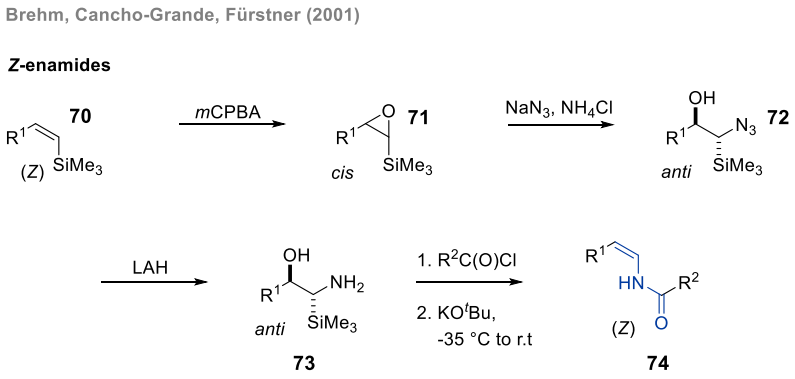

Scheme 14. *Fürstner´*s stereoselective synthesis of *Z*-enamides by a *Peterson* reaction manifold.[79]

As the elimination process of the *Peterson* olefination takes place via a *syn*-periplanar transition state under basic conditions,[81] both *E*- and *Z*-enamides can be obtained by this sequence, depending on the double bond geometry of the starting vinyl silane which ultimately determines the *syn*- or *anti*-configuration of the corresponding β-hydroxysilanes prior to elimination.

The main disadvantage of this method is the requirement for multiple reaction steps, coupled with potential regioselectivity issues during epoxide openings, although 2,3-epoxysilanes are known to preferentially open at the silyl-bearing position.[80]

An example of this methodology in total synthesis is the synthesis of (+)-crocacin A (**79**) (Scheme 15), another member of the crocacine family, by *Chakraborty* and *Laxman*.[65]

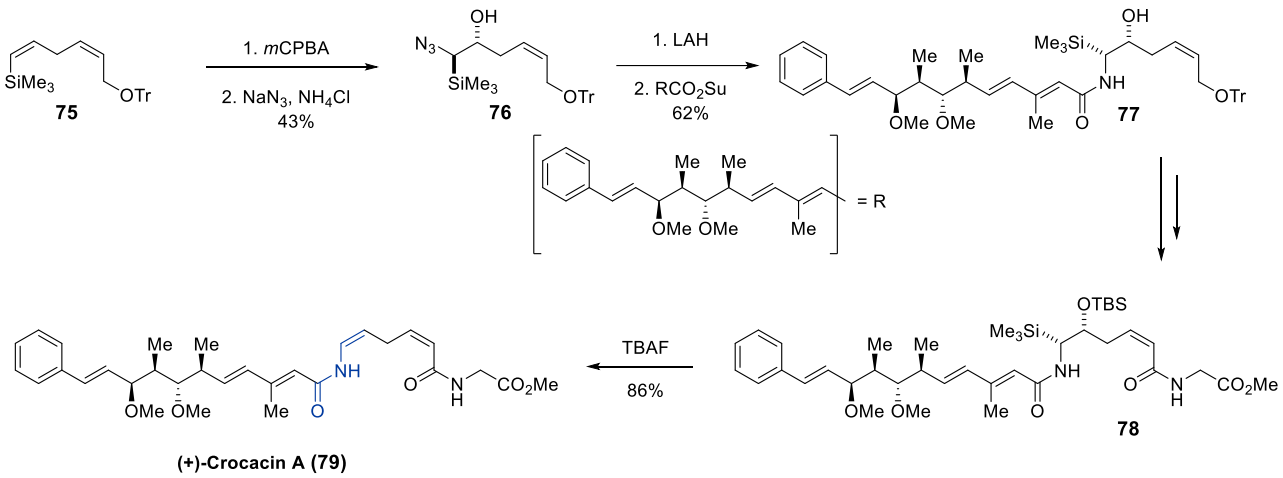

Scheme 15. An example of *Fürstners* peterson olefination approach utilized in the total synthesis of (+)-crocacin A (**79**).[65]

This example illustrates the versatility of the *Fürstner* method, which enables the incorporation of the corresponding enamide-precursor at an arbitrary stage of the synthesis as the use of a simple TBS protecting group enables further modifications of other parts of the molecule. Once the remaining functionalities are installed, the elimination can be initiated through a tandem deprotection/*Peterson* elimination process by adding TBAF. This approach liberates the sensitive enamide functionality in the final step of the synthesis, while the underlying amide bond has been securely installed many steps earlier.

2.4.4 Enamide synthesis from alkenyl isocyanates

Another suitable method was published by *Taylor* in 2000, namely a *Grignard* addition to vinyl isocyanates to prepare several simple naturally occurring enamides.[83]

The sequence starts from the readily available alkenyl acyl azide **80** (Scheme 16), which is converted to the alkenyl isocyanate **81** by a curtius rearrangement.[84] The resulting highly reactive alkenyl isocyanate **81** can then be trapped with with a *Grignard* reagent or other nucleophiles such as organo cuprates or organo lithium compounds.[83]

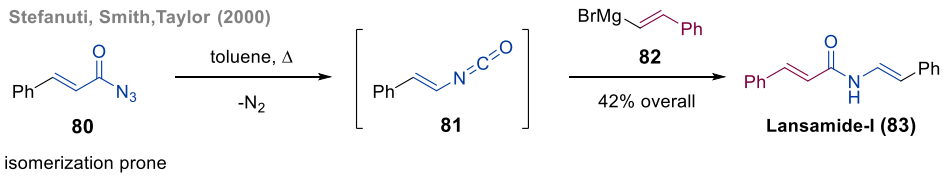

Scheme 16. Synthesis of Lansamide-I (**83**) by a *Grignard* addition to alkenyl isocyanate **81**. [83]

The synthesis of *Z*-enamides through this method was however thwarted due to isomerization during the formation of the alkenyl acyl azides. However, in the same year, *Kitahara* solved this issue by using diphenylphosphoryl azide (DPPA) in combination with sodium hydride at 0 °C. These conditions reduced isomerization and enabled the synthesis of *Z*-vinyl isocyanates with this method.[85]

An example (Scheme 17) of using isocyanate addition for enamide synthesis is demonstrated in the preparation of (+)-crocacin D (**62**).[66] In this specific case, the *Z*-alkenyl isocyanate **85**, obtained with *Kitaharas* conditions[85] was first reacted with TMS-ethanol (**86**) to form the *Teoc*-protected enecarbamate **87**. Subsequently, the carboxylic acid **89** was converted into the acid chloride **90** after deprotonation.

A solution of the anion, generated by deprotonation of the enecarbamate **87** with NaHMDS in THF, was then added to the crude acid chloride **90**. Following chromatographic purification, this sequence yielded the desired enamide **91** which was later deprotected using TBAF.

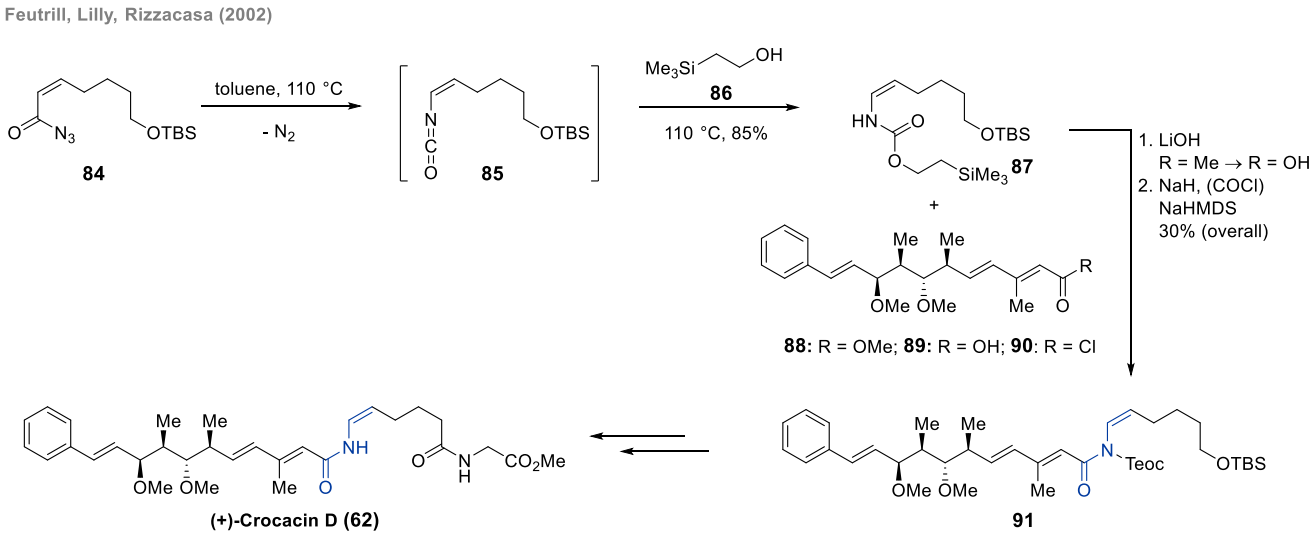

Scheme 17. An example of enamide synthesis by addition to alkenyl isocyanates from the total synthesis of (+)-crocacin D (**62**).[66]

2.4.5 Enamide synthesis by acylation of methyl 3-aminocrotonate

The acylation of methyl 3-aminocrotonate (**92**) (Scheme 18) is another promising and straightforward method for enamide syntheses.

Amide coupling between carboxylic acids and enamines is usually thwarted by the tautomerism involved with the corresponding enamine precursors. Methyl 3-aminocrotonate (**92**) however depicts a special case as the *Z*-configuration of this enamine **92** is locked by hydrogen bonding with the neighboring acyl group. However, due to the *C*-nucleophilicity of the β-carbon, *C*-acylation is a considerable side-reaction.[86]

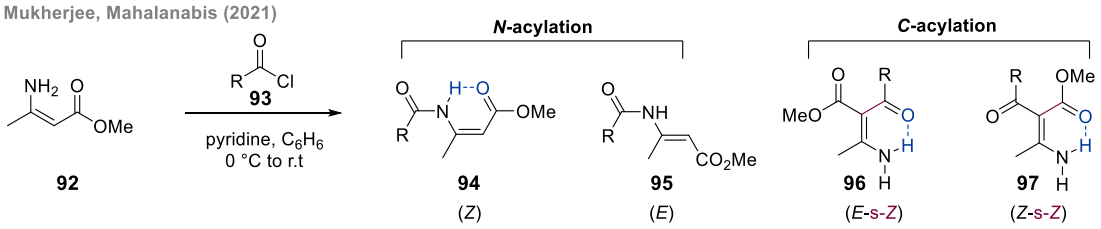

Scheme 18. The acylation products of methyl 3-aminocrotonate (**92**).[86]

In 2021, a systematic study explored the acylation of methyl 3-aminocrotonate (**92**).[86] According to the study, the regioselectivity in the *C*- and *N*-acylation of **92** is influenced by factors such as the nature of the acid chlorides and the added organic base.

While a *Z*-selective *N*-acylation would yield the α-methyl *Z*-enamide motif found in bacillaene (**1**) in a single step, no literature is available regarding further functionalization of the ester function of enamidoesters **94** except from ester hydrolysis[67] and hydrogenations.[87] As we will see in the discussion part (Chapter 6.2), selective acylation and further reduction of the resulting enamidoester **94** poses a significant challenge.

2.4.6 Enamide synthesis by σ-C–C bond eliminative borylation of cyclopropylamides

The newest and highly intriguing method for the synthesis of enamides is the synthesis by σ-C–C bond eliminative borylation of cyclopropylamides (Scheme 19).[88]

In this process, *N*-cyclopropylamides such as **98** are reacted with boron trichloride in presence of 4-cyclohexylmorpholine (CHMP), resulting in an insertion into the less substituted bond of the cyclopropane ring. As intermediates, γ-boryl enamides such as **99** are obtained, which can either be classically complexed with pinacol or oxidized to the corresponding alcohols using sodium perborate.

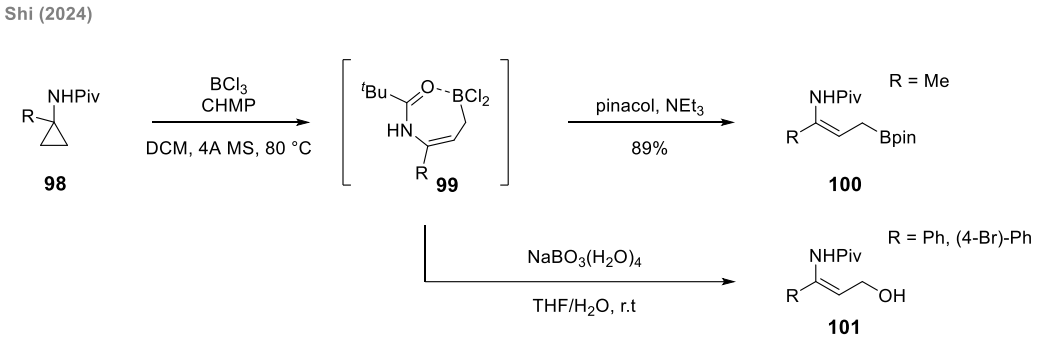

Scheme 19. Enamide synthesis by σ-C–C bond eliminative borylation of *N*-cyclopropylamides.[88]

The advantages of this reaction include its *Z*-selectivity, the (commercial) availability of various *N*-cyclopropanamines, and the relatively mild reaction conditions.

The ability to access allylic alcohols such as **101** through this method enables subsequent oxidation to aldehydes, thereby providing a pathway to further olefination reactions.

Notably, the substrates **102** and **105** (Scheme 20) derived from gemfibrozil (**104**) and abietic acid (**107**) were converted into the corresponding enamide derivatives **103** and **106** with high yields and high stereocontrol demonstrating the versatility of this reaction sequence.

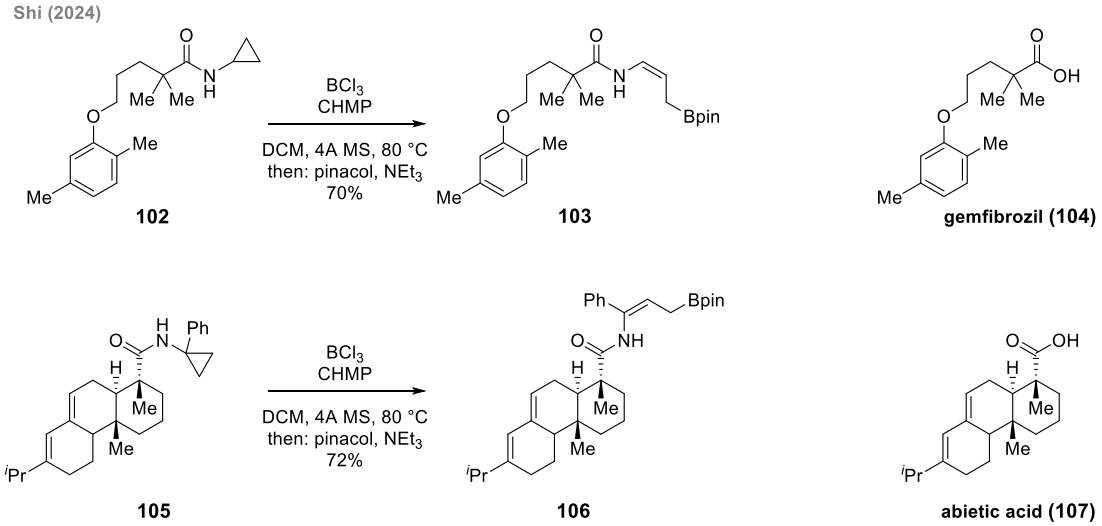

Scheme 20. The σ-C–C bond eliminative borylation carried out on derivatives of gemfibrozil (**104**) and abietic acid (**107**).[88]

Unfortunately, this work was published only after synthetic efforts on bacillaene (**1**) were completed.

Part 2: Retrosynthesis and Syntheses of Fragments

3.1 Retrosynthetic approach for bacillaene (1)

3.1.1 First generation

The first attempt at a total synthesis of bacillaene (**1**) was a collaborative project based on a retrosynthetic analysis in our group by *Reuter-Schniete*, and me (Scheme 21). The underlying strategy was an iterative cross coupling approach, partially inspired by synthetic studies on etnangien (**42**) by *Altendorfer* and *Menche*[58] (Chapter 2.2.4), utilizing a hetero-bimetallic Sn-B-linchpin reagent **113**.

In this retrosynthesis, the sensitive hexaene core of bacillaene (**1**) was divided into three diene units to minimize the propensity for isomerization. These strategic cuts yielded four key fragments, namley the western fragment (**112**), Sn-B-linchpin I (**113**), the central fragment (**109**), and the side-chain fragment (**110**), which together would constitute the framework of bacillaene (**1**).

For the synthesis of the sensitive enamide fragment (**108**), *Reuter-Schniete* proposed a copper-catalyzed C-N coupling between **109** and **110** as a key step (as discussed in 2.4.2).

In this plan, the tetraene **111**, accessible by a *Stille* coupling between the Sn-B-linchpin I (**113**) and the western fragment **112** was envisioned to be combined with the enamide-fragment **108** in a final *Suzuki* coupling.

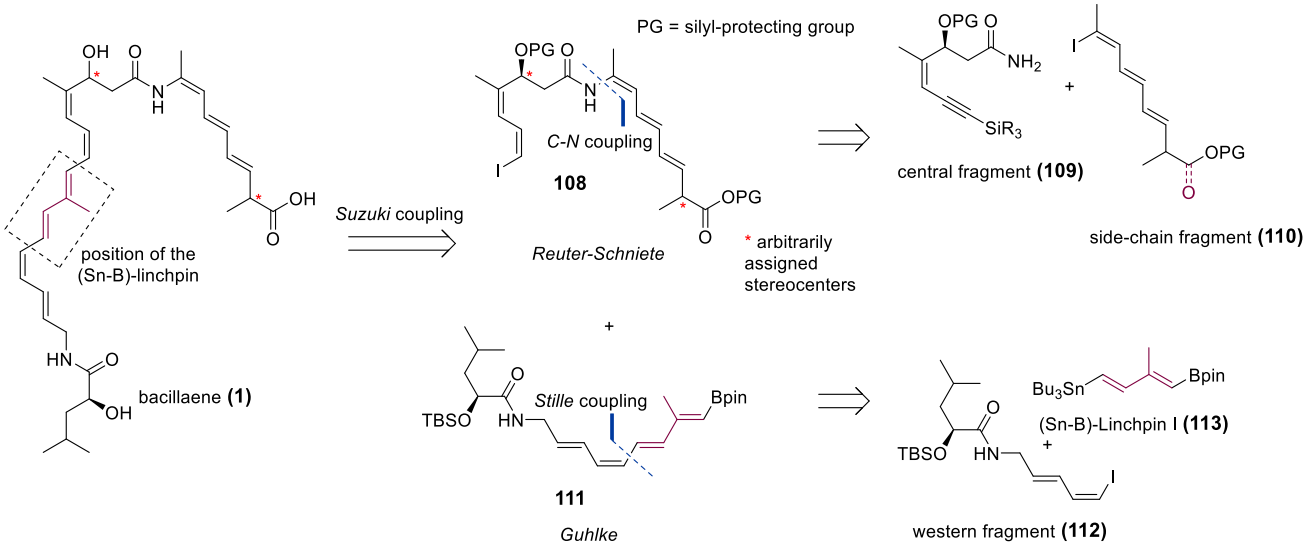

Scheme 21. First retrosynthetic approach for the authentic natural product bacillaene (**1**).

For the initital retrosynthesis (Scheme 21) the following two scenarios (Scheme 22, 23) were possible.

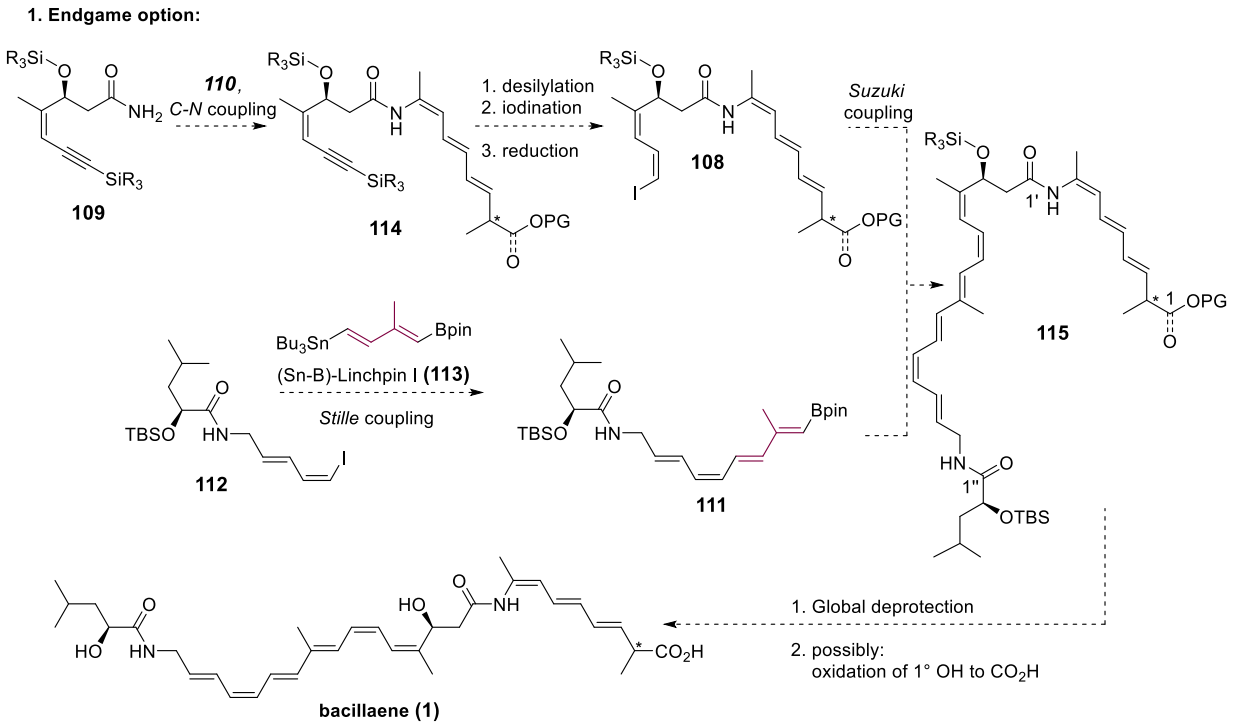

Scheme 22. First endgame scenario resulting from the first generation retrosynthesis of bacillaene (**1**).

In the first scenario (Scheme 22), the central fragment (**109**) would initially be coupled with the sidechain fragment (**110**) (Scheme 21) using the copper catalyzed *C-N* coupling.

The advantage of this sequence is that the *C-N* coupling, a less established transformation compared to *Stille*- or *Suzuki* couplings is carried out relatively early in the synthesis. After coupling of these fragments, the plan called for a conversion of the silylenyne **114** into the corresponding *Z,Z*-iododiene **108** by a sequence of desilylation, iodination, and reduction. This transformation would furnish the first half **108** of the desired natural product.

Final assembly of the hexaene scaffold was planned by a *Suzuki* coupling between the fragments **108** and **111**. This route has the benefit of forming the isomerization-prone hexaene core (**115**) at a late stage of the synthesis. Finally, a global deprotection of intermediate **115** would be performed and, if necessary, the oxidation state at *C1* could be adjusted to deliver the natural product bacillaene (**1**). (Various oxidation states at *C1* of fragments **114** and **108** were considered by *Reuter-Schniete*).

However, the early installation of the enamide poses stability risks. At least five additional steps would be required after the formation of enamide **114**, and due to the known sensitivities of enamides, purification of the following intermediates would be challenging. Moreover, the behaviour of a

trienamide as part of a β,γ-polyunsaturated carboxylic acid is largely unexplored. As discussed for the biosynthesis of bacillaene (**1**) (chapter 1.3), such a trienamide is proposed to be the final intermediate in the biosynthesis of **1**.[22]

Therefore, an isomerization accompanied by a proton shift could occur resulting in an α,β-unsaturated carboxylic acid, effectively obliterating the enamide functionality. If the side-chain fragment (**110**) (Scheme 21) comprises a protected homoallyl alcohol instead of the carboxylic acid as proposed by *Reuter-Schniete*, a subsequent oxidation to the carboxylic acid would still be necessary after the global deprotection of **115**. This would require a selective oxididation of a primary alcohol in the presence of a secondary alcohol on a reportedly oxygen sensitive molecule.[12]

In summary, this scenario is feasible but carries the described risks due to the unpredictable behavior of the early-installed trienamide side chain in **114**. A late-stage oxidation, if necessary, poses another unpredictable challenge due to the sensitive nature of the natural product (**1**).[12,13,14]

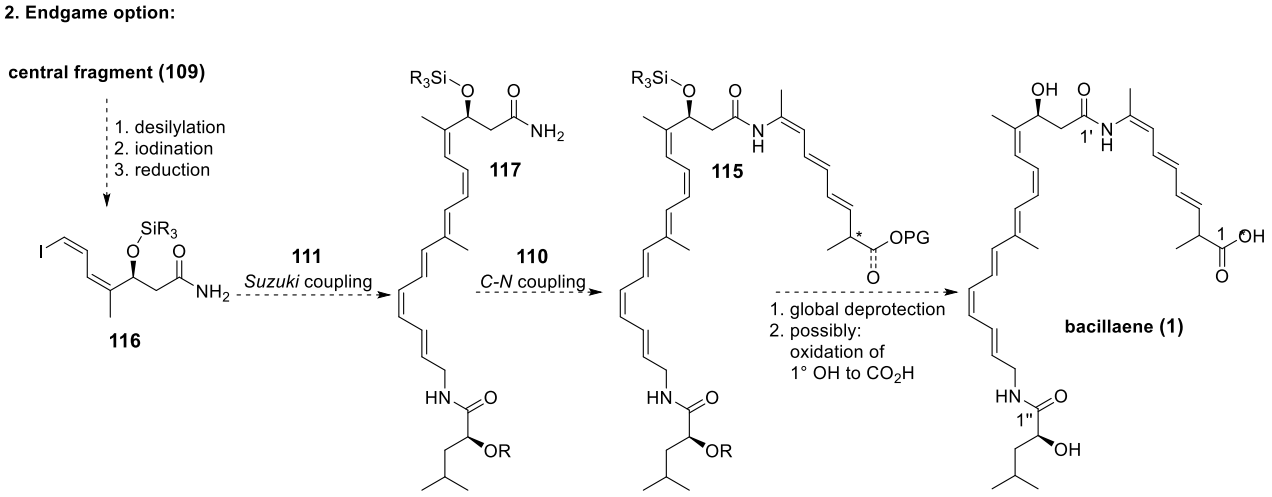

Scheme 23. Second endgame scenario resulting from the first generation retrosynthesis of bacillaene (**1**).

In the second scenario (Scheme 23), the *C*-*N*-coupling is moved to the final step, placing the manipulation of the central fragment **109** earlier in the sequence leading to *Z*,*Z*-iododiene **116**.

After the *Suzuki* coupling of **116** with the tetraene **111** (Scheme 22), the hexaene fragment **117** could be obtained. The enamide side chain would then be installed in a final copper catalyzed *C*-*N* coupling step, followed by global deprotection to form bacillaene (**1**).

Similar to the first scenario, an oxidation may be required as the final step of the total synthesis, depending on the oxidation state of *C1* in **115**.

This plan faces the issue of executing the challenging *C-N* coupling step after completion of the sensitive hexaene scaffold **117**. This type of reaction is typically conducted at temperatures around 70 °C (for examples see 2.4.2), which are relatively "harsh" given the reported instabilities of **1**. The issues of a final oxidation, if required, were described in the previous section.

3.1.2 Second generation

The second-generation retrosynthesis of bacillaene (**1**) (Scheme 24) was developed during the course of this work, with several key modifications aimed at addressing the shortcomings of the first-generation plan.

The most significant change was the introduction of a third cross-coupling disconnection at the enamide side chain, leading to a revised plan in which an intermediate **118** and a new eastern fragment **119** emerged.

The use of Sn-B-linchpins in combination with a MIDA-protected haloboronic acid (Chapter 2.3) would enable three consecutive palladium-catalyzed cross couplings. In this case, site discrimination would be achieved through the selection of different metals (Sn, B) as well as the hybridization state of the boron centers. In practice, selective coupling of the boron-centers would be achieved by selecting appropriate reaction conditions (anhydrous vs. aqueous conditions).[47-49]

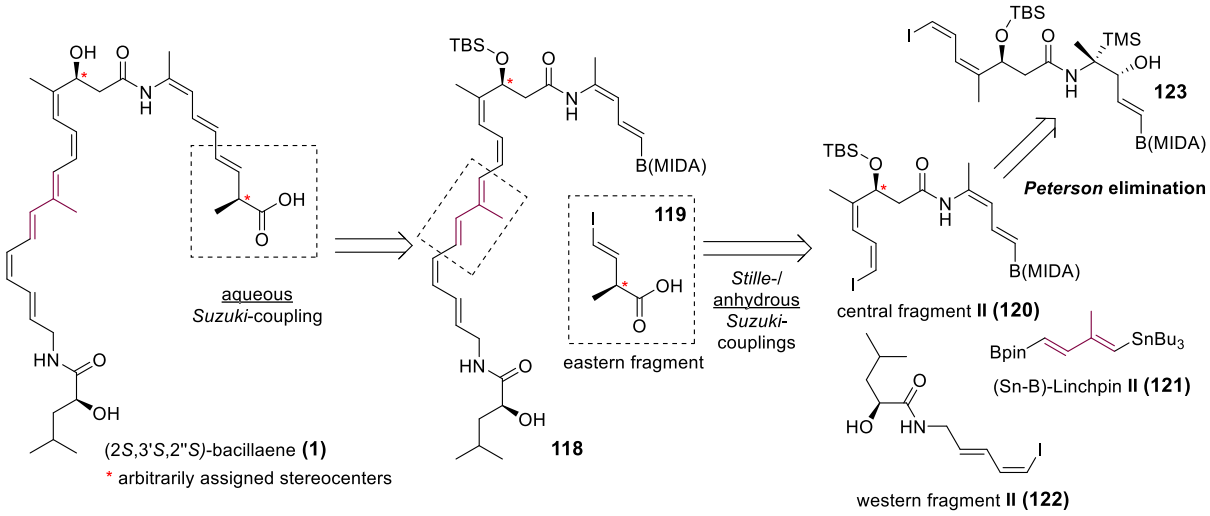

Scheme 24. Second retrosynthetic approach for the authentic natural product bacillaene (**1**).

The new eastern fragment **119**, is known from the total synthesis of the shellfish toxins (-)-isodomoic acids B, E, and F, where it was subsequently used for a cross coupling and diene synthesis.[89] In this case, a *Stille* coupling was employed to couple fragment **119**.

Notably, a *Suzuki* coupling with a vinyl-MIDA boronate in the presence of a free carboxylic acid (similar to a coupling between **119** and **118**) has been demonstrated in *Burke*'s synthesis of β-parinaric acid.[90] This suggests an overall positive outlook regarding the feasibility of this additional third and final coupling step.

The second major change in this approach, was the use of *Fürstner's Peterson* olefination method[79] (Chapter 2.4.3), to generate the enamide-motif of the new central fragment II (**120**) which could be obtained after *Peterson* elimination of **123**. The synthetic approach to **123** is briefly discussed in chapter 6.3.

The third major modification was the utilization of Sn-B-linchpin II (**121**) which allows for a reversed coupling order. This adjustment was made after experimentally observing that the reversed coupling order yielded better results than the originally planned sequence (Chapter 5.2.4). Similarly, the western fragment I (**112**) was changed to the unprotected western fragment II (**122**) as it showed better results during the attempted *Stille* couplings throughout this work.

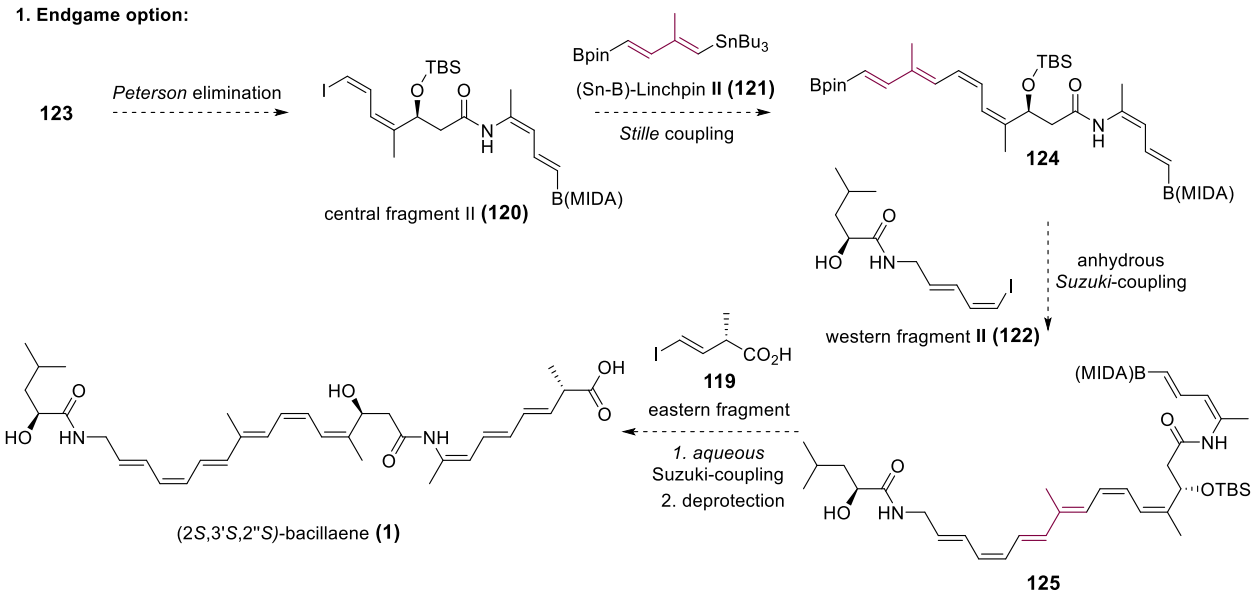

Scheme 25. First endgame option for for the second generation retrosynthesis of bacillaene (**1**).

For the endgame sequence, two major options were considered. Firstly, after *Peterson* elimination of **123** (Scheme 24) the enamide containing central fragment II (**120**) would be obtained, followed by a *Stille* coupling with Sn-B-linchpin II (**121**) to form the tetraene **124** (Scheme 25).

Afterwards, a selective anhydrous *Suzuki* coupling at the sp^2-boron center of **124** with the western fragment II (**122**) followed by an aqueous *Suzuki* coupling of **119** with the MIDA-bearing center was planned. Subsequent deprotection of the single TBS-protecting group would yield bacillaene (**1**) with the

given arbitrarily assigned stereochemistry. The weaknesses of this approach, are the early introduction of the sensitive enamide motif in **120** and the required additional *Suzuki* coupling with **119** after formation of the sensitive hexaene core **125**.

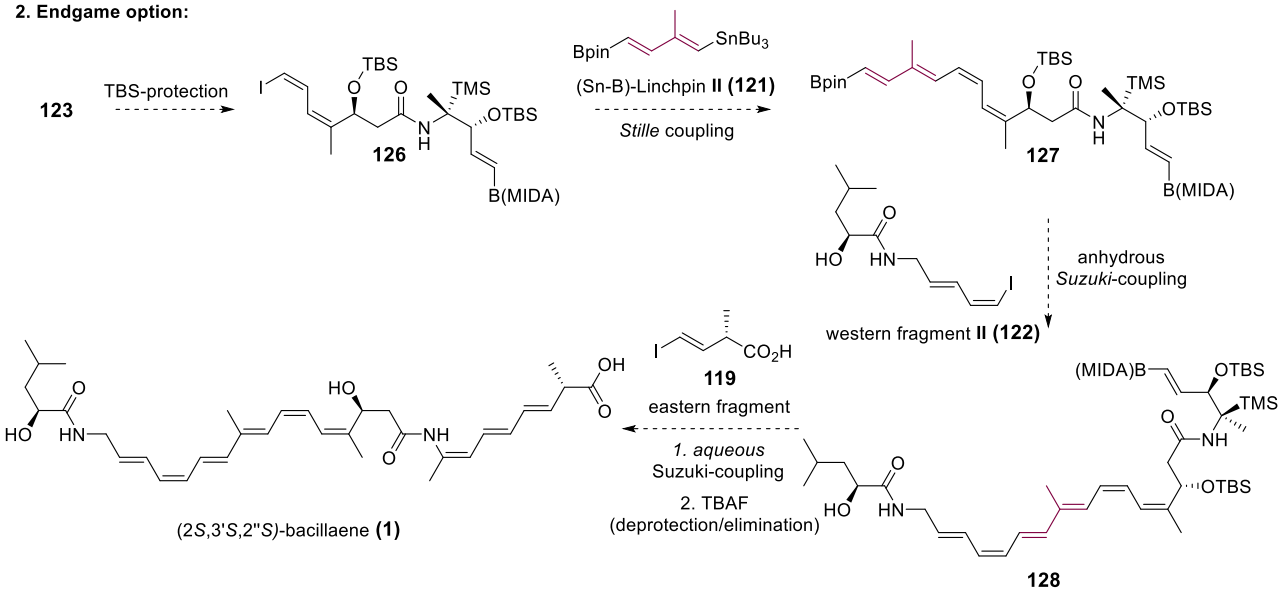

Scheme 26. First endgame option for for the second generation retrosynthesis of bacillaene (**1**).

The second endgame scenario (Scheme 26) derived from the 2nd generation retrosynthetic analysis is based on the total synthesis of (+)-crocacin A (**79**)[65] (see 2.4.3). By employing a TBS protection for the hydroxy group of **123**, the formation of the unstable enamide would be postponed to the final step of the total synthesis. After the formation of **126**, the same coupling sequence as for the first endgame (Scheme 25) would be pursued, resulting in tetraene **127** and hexaene **128** both bearing the corresponding enamide precursor. Then, after the final Suzuki-coupling with **119** a deprotection/elimination cascade would be triggered using TBAF in analogy to the synthesis of (+)-crocacin A (**79**).[65] The remaining weakness of this approach would be the required *Suzuki*-coupling after formation of the sensitive hexaene core **128**.

For both strategies, the key fragment **123** (Scheme 27), would be required, which should be obtained from carboxylic acid **129** and compound **130** after deprotection of the *Boc*-group of **130** and subsequent amide coupling (Scheme 27).

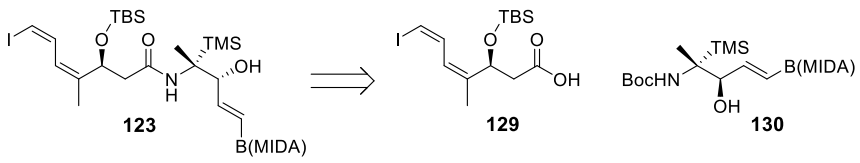

Scheme 27. Retrosynthesis of the key fragment **123** required for enamide synthesis by *Peterson* olefination.

3.2 Retrosynthetic approach for the bacillaene analogue (7)

3.2.1 First generation

The 1st generation retrosynthesis of the bacillaene analogue (**7**) and the 2nd generation retrosynthesis of bacillaene (**1**) both have the same underlying coupling strategy as they were developed simultaneously. In fact, the rationale behind this was to first evaluate the coupling conditions for this simplified analogue (**7**) and later, if successful, transfer the strategy onto the authentic natural product (**1**).

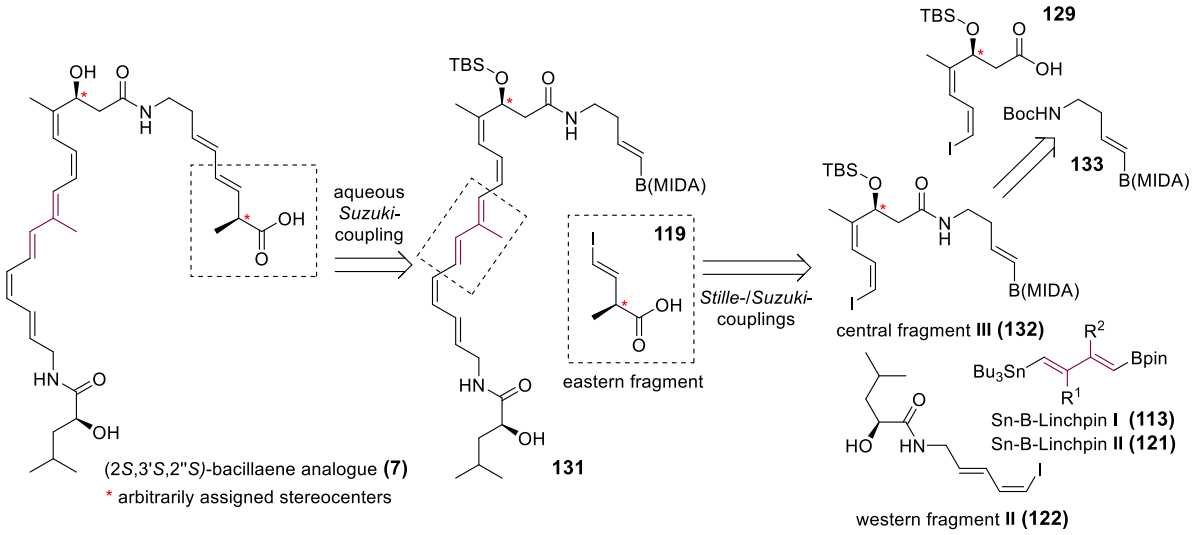

Scheme 28. Retrosynthetic approach for the bacillaene analogue (**7**).

The only difference from the 2nd generation retrosynthesis of bacillaene (**1**) lies in the simplified central fragment III (**132**) containing a saturated amide instead of an enamide and the omitted methyl group. Central fragment III (**132**) should be obtained again from carboxylic acid **129** and the simplified building block **133** after deprotection of the *Boc*-group and subsequent amide coupling.

Depending on which Sn-B-linchpin would be used, two different coupling strategies, namely the "left-to-right" approach (Scheme 29) or the "center-to-edges" (Scheme 30) approach, are obtained.

The "left-to-right" approach (Scheme 29) starts with the western fragment II (**122**) together with Sn-B-linchpin I (**113**) with an initial *Stille* coupling to form the tetraene **134**.

The resulting tetraene **134** is then combined with the central fragment III (**132**) in an anhydrous *Suzuki* coupling leading to hexaene **131**. Finally, the desired analogue (**7**) would be obtained after an aqueous *Suzuki* coupling with eastern fragment **119** at the MIDA-bearing site and subsequent deprotection.

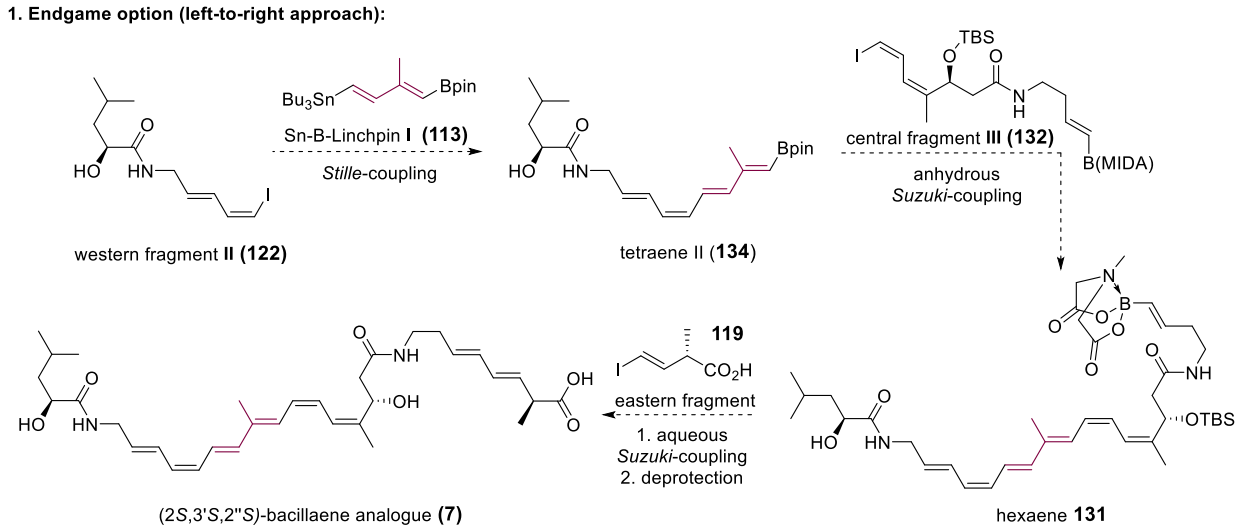

Scheme 29. First endgame option (left-to-right approach) resulting from retrosynthesis of the bacillaene analogue (**7**) using Sn-B-linchpin I (**113**).

In contrast, the second "center-to-edges" approach (Scheme 30) starts with the central fragment III (**122**) together with the other Sn-B-linchpin II (**121**) with an initial *Stille* coupling to form the bis-boronate tetraene **135** bearing two differently hybridized boron centers.

In this case, the two edges of the final molecule are added in the last coupling steps again by an anhydrous *Suzuki* coupling with the western fragment II (**122**) resulting again in the hexaene **131**. Similar to the "left-to-right" approach, the desired analogue (**7**) would be obtained after an aqueous *Suzuki*-coupling with eastern fragment **119** at the MIDA-bearing site and subsequent deprotection.

The choice between the "left-to-right" approach (Scheme 29) or the "center-to-edges" approach (Scheme 30) for the synthesis of analog (**7**) ultimately depends on the efficiency of the respective coupling reactions.

Another key factor is the stability of the intermediate tetraenes **134** and **135** as different isomerization behaviors of these tetraenes are expected.

While both routes converge to the same hexaene **131**, the viability of the initial cross couplings may lead to significantly different yields. Also, potential isomerization during the reactions may play a critical role. In practice, the decision which route to pursue, would depend on experimental results specifically, which sequence provides higher yields and which sequence provides a better integrity of the polyene geometry.

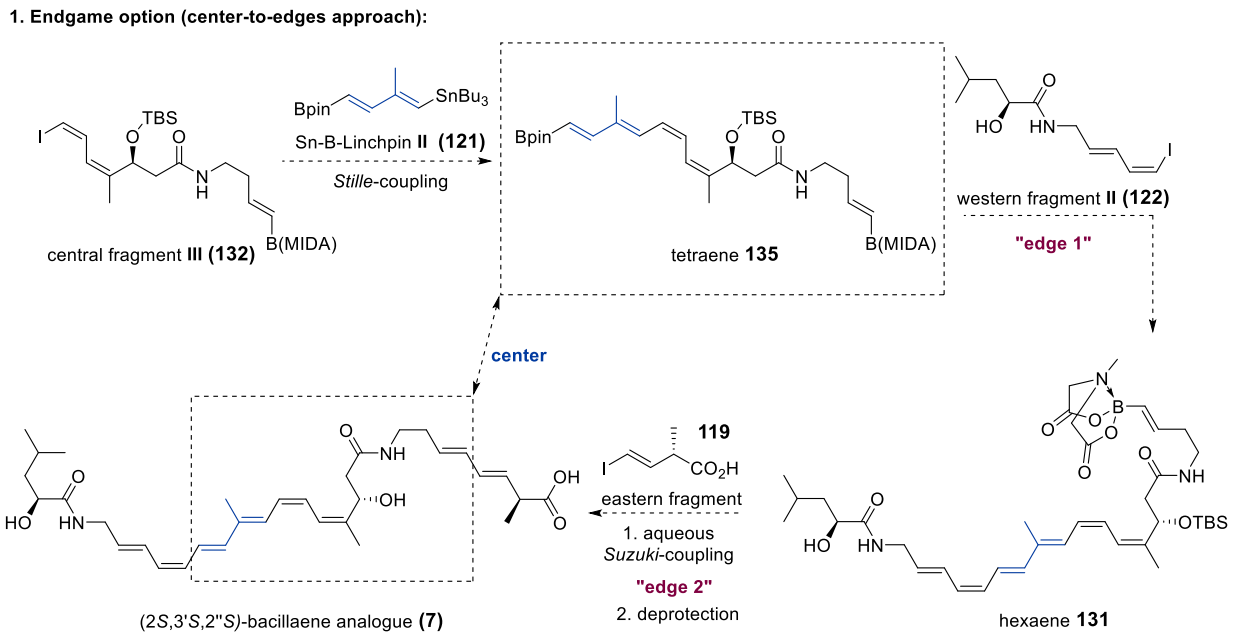

Scheme 30. Second endgame option (center-to-edges approach) resulting from retrosynthesis of bacillaene analogue (**7**) using Sn-B-linchpin II (**121**).

In summary, the retrosynthetic analysis for bacillaene (**1**) and its analogue (**7**) are all based on an iterative cross coupling strategy which evolved during the course of this work. While the first-generation plan for bacillaene (**1**) was developed in a collaborative project, the second-generation retrosynthesis was developed within this work and included an additional cross coupling disconnection, new linchpin reagents, MIDA protected haloboronic acids[46-49] together and the use of *Fürstner's* strategy for a late-stage introduction of the labile enamide-functionality.[65,79]

The bacillaene analogue (**7**) served as a simplified model to test the underlying cross coupling strategies. This work will show that the order of fragment assembly and intermediate stability are critical factors for a successfull assembly of this sensitive polyene framework.

4. Synthesis of Fragments

4.1 Synthesis of the western fragment

For the synthesis of western fragments **122** and **112**, several approaches were explored, namely a linear approach and several modular approaches. The first two procedures (4.1.1 and 4.1.2) were initially developed during my master thesis,[91] but they are included here for the sake of completeness. Also, further optimizations on 4.1.2 were completed during this work.

4.1.1 Linear approach

The linear 7-step approach toward western fragment **112** (Scheme 31) began with the literature-known[92] synthesis of protected α-hydroxy isocaproic acid (**137**) (α-HIC) from L-Leucine (**136**) via deamination[93], followed by TBS protection to form **138**.

Notably, the deamination reaction proceeds with retention of stereochemistry due to a double-inversion mechanism. The initially formed α-diazo acid **136.a** undergoes an intramolecular S_N2-attack by the carboxy group with a first inversion of the configuration, leading to the formation of an α-lactone **136.b**. This intermediate is subsequently attacked by water resulting in the corresponding α-hydroxy acid **137** with a second inversion (net retention) of the configuration.[94]

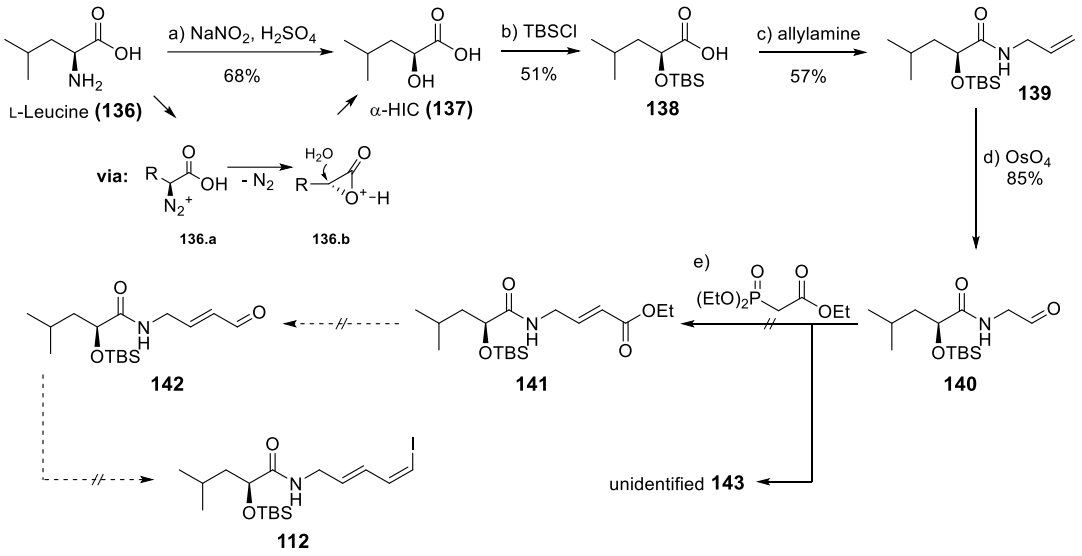

Scheme 31. Linear unsuccessful approach for the synthesis of western fragment I (**112**). Conditions: a) $NaNO_2$ (2.3 eq.), H_2SO_4 (1.2 eq.), H_2O, 0 °C to r.t, overnight, recrystallization, 68%; b) TBSCl (2.5 eq.), imidazole (4.8 eq.), DMF, 16 h, 51%; c) allylamine (1.3 eq.), PyBOP (1.2 eq.), HOBt (1.2 eq.), DIPEA (1.4 eq.), DCM/DMF, 57%; d) OsO_4 (0.03 eq.), $NaIO_4$ (3.5 eq.), 1,4-dioxane/H_2O, 85%; triethyl phosphonoacetate (2.0 eq.), *n*-BuLi (1.9 eq.), THF, 93% (**143**).

After TBS-protection, the formation amide **139** was facilitated by PyBOP[95] mediated peptide coupling with allylamine followed by an oxidative cleavage with osmium(VIII) oxide (*Lemieux-Johnson* oxidation).[96] The resulting aldehyde **140** was intended to be converted to enoate **141** by a standard *Horner-Wadsworth-Emmons* (HWE) procedure.[97] However, only a series of unidentified side-products (**143**) was observed.[91]

Due to the failure of the linear approach at the *HWE*-stage, several modular approaches were explored. The modular approaches were developed to prioritize the efficient construction of the iododienamine core **154** (Scheme 32).

These approaches can be divided into two main strategies:

Either the late introduction of the *Z*-vinyl iodide or the late incorporation of nitrogen into the desired intermediate. The primary challenge with the early introduction of the *Z*-vinyl iodide lies in their low stabilities and their resulting propensity for isomerization. On the other hand, the introduction nitrogen often requires the use of hazardous reagents such as azides or hydrazine.

However, the late introduction of the *Z*-vinyl iodide has the disadvantage of a limited number of viable reactions, such as *Stork-Zhao Wittig*[98,99] reaction or stereoselective reductions of iodoalkynes,[100,101] which are especially in the case of iodoenynes sometimes unstable.

4.1.2 Allylamine approach

The first modular approach (Scheme 32) started with a *Boc*-protection of allylamine (**144**)[102] followed by an oxidative cleavage of **145** using *Lemieux-Johnson*[96] conditions which gave boc-glycinal **147** in good yield.[91] Retrospectively, following a literature known[103] reduction Boc-Gly-N(OMe)Me would have been a safer option considering the high health risk of osmium(VIII) oxide.[104]

After *HWE*-reaction to form enoate **148** and subsequent reduction allylalcohol **149** was obtained in only moderate yields.[105]

Therefore, another literature known[106] metathesis approach was followed starting from *Boc*-protected allylamine **145** and crotonaldehyde which gave γ-amino enal **150** in a very good yield of 81%. Despite the reported instability,[106] aldehyde **150** proved stable when stored under argon at −30 °C. Subsequent *Stork-Zhao*[99] reaction gave the core intermediate **152** in fair to good yield. After deprotection and amide coupling with **138**, western fragment I (**112**) was obtained during my master thesis.[91]

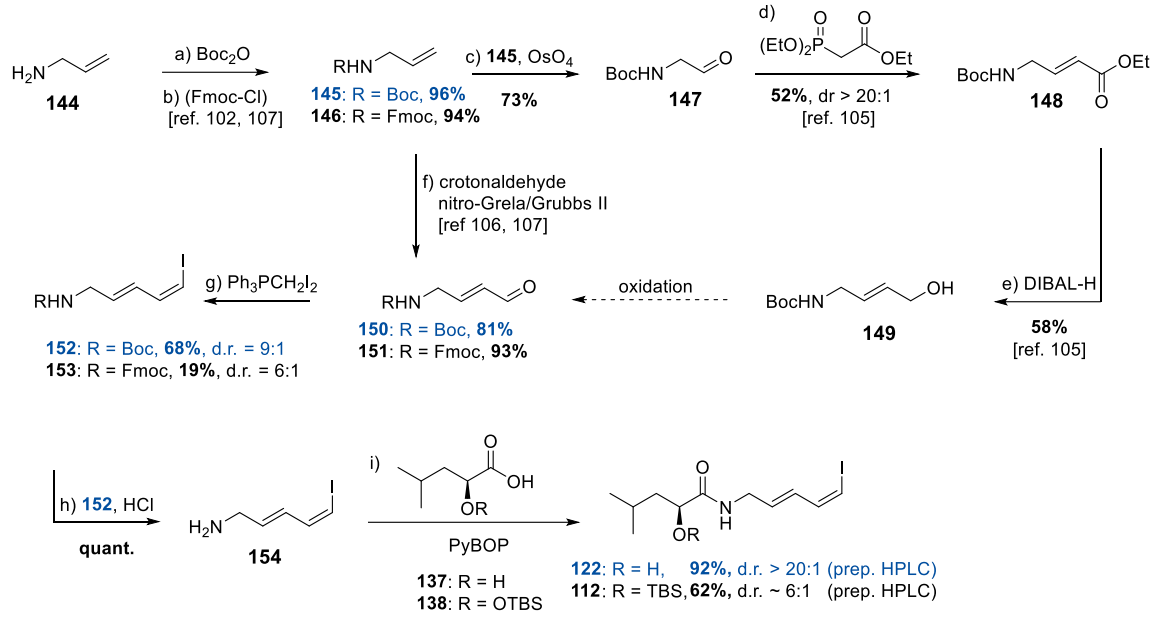

Scheme 32. Modular successful approach for the synthesis of western fragment I/II **112**/**122**. Conditions: a) Boc_2O (1.1 eq.), DMAP (0.6 mol-%), DCM, 0 °C, 1.5 h, 96%; b) allylamine (1.5 eq.), Fmoc-Cl (1.0 eq.), $NaHCO_3$ (2.5 eq.), 1,4-dioxane, 0 °C to r.t., 20 h, 94%; OsO_4 (0.7 mol-%), $NaIO_4$ (3.0 eq.), 1,4-dioxane/H_2O (1:1), r.t., 3 h, 73%; d) triethylphosphonoacetate (1.15 eq.), *n*-BuLi (1.1 eq.), LiCl (0.5 eq.), DME/THF (2:1), −78 °C to r.t., 4 h, 52%; e) DIBAL (3.6 eq.), DCM, −78 °C, DCM, 2 h, 58%; f) R = *Boc*: crotonaldehyde (11 eq.), nitro-Grela (2 mol-%), DCM, 50 °C, 4 h, 81%; R = *Fmoc*: crotonaldehyde (10 eq.), BHT (0.1 eq.), Grubbs II (2 mol-%), toluene, 65 °C, 21 h, 93%; g) R = *Boc*: $Ph_3PCH_2I_2$ (1.15 eq.), NaHMDS (1.1 eq.), THF/DMI (7:1), −78 °C, 3 h, 81%; R = *Fmoc*: $Ph_3PCH_2I_2$ (1.05 eq.), NaHMDS (0.95 eq.), THF, −78 °C, 5 h, 19%; h) HCl (1.25 M in EtOH, 5.0 eq.), 50 °C, 2 h, quant.; i) R = H: **137** (1.2 eq.), PyBOP (1.2 eq.), HOBt (1.2 eq.), DIEPA (5.0 eq.), DMF, r.t., 5 h, 92%, d.r. > 20:1 after semi-prep. HPLC separation; R = OTBS: **138** (1.0 eq.), PyBOP (1.1 eq.), HOBt (1.1 eq.), DIEPA (9.2 eq.), DCM/DMF (1:1), r.t., 1.5 h, 62%, dr = 6:1 after semi-prep. HPLC separation.

One drawback of this fragment **112** was its propensity towards isomerization combined with an only moderate peak resolution obtainable by hplc. This lead to a worse geometrical purity (dr = 6:1) than what was obtained for diene **152** after the *Stork-Zhao* reaction (d.r. = 9:1).

In contrast, when coupled with the unprotected hydroxy-acid **137**, western fragment II (**122**) appeared to be less prone to isomerization and a better hplc peak resolution was achievable leading to a higher geometrical purity (d.r. > 20:1) which is mandatory, given the context of a polyene synthesis.

In the comparison of the ^{1}H-NMRs (Figure 8) of both fragments **112** and **122** (both after semi-preparative HPLC purification) it is clearly visible, that the TBS-protected fragment **112** contains considerable amounts of isomeric impurities, while for fragment **122** the integral ratio is 99:1.

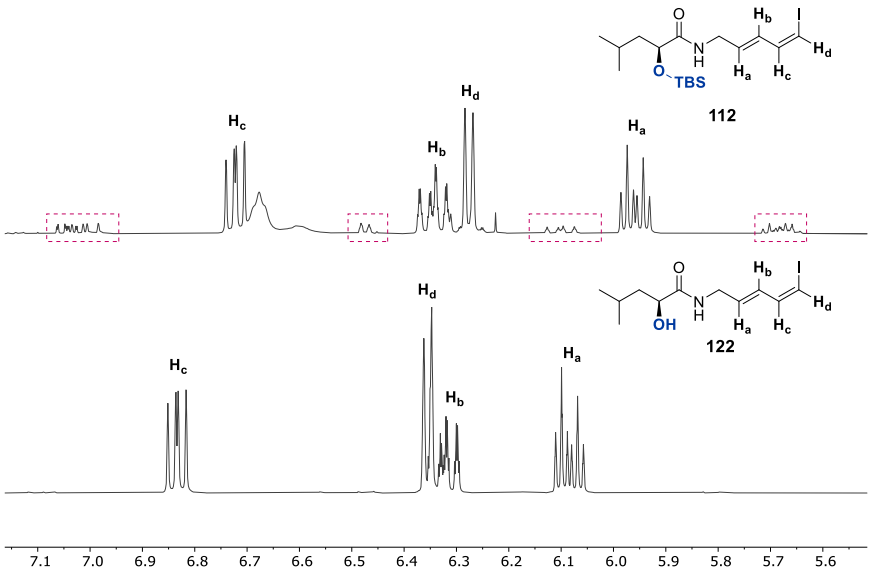

Figure 8. Comparison of the ^{1}H-NMRs (olefinic region) of TBS-protected western fragment I (**112**) (500 MHz, $CDCl_3$; top) and unprotected western fragment II (**122**) (500 MHz, acetone-d6; bottom), both after semi-preparative HPLC purification with isomeric impurities (dr = 6:1) labelled for fragment **112**.

To overcome the dependency on HPLC-purifications, this route was repeated with an *Fmoc*-protecting group instead of the *Boc* group. The idea behind this was to exploit the higher crystallinity of the *Fmoc*-protected intermediates to obtain a better geometrical purity of **153** by recrystallizations.

The initial *Fmoc*-protection of allylamine (**144**)[107] was facilitated with comparable yields and subsequent metathesis gave the α,β-unsaturated aldehyde **151** in excellent yield. In the next step, applying standard *Stork-Zhao* conditions to form **153** resulted in a very poor yield of 10% with no starting material present, presumably due to a deprotection of the base sensitive *Fmoc*[108] group by the phosphonium ylide.

In order to keep the concentration of ylide low, it was slowly added to the aldehyde **151** over the course of 4 hours. This procedure allowed to nearly double the yield to a however still poor 19%. Given the fact that the resulting diene **152** decomposed during a recrystallization attempt, that route was not further pursued.

4.1.3 Propargylamine-approach

As mentioned in the introduction of this chapter, besides *Stork-Zhao* olefination a second viable method to generate *Z*-vinyl iodides is the stereoselective reduction of iodoalkynes.[100,101]

To test this alternative approach, a literature known 5-step procedure[108] to enyne **160** was performed (Scheme 33) starting from *Boc*-propargylamine (**156**).

After *Boc*-protection of **155**,[109] the alkyne **156** was hydrostannylated to form **157** using *in-situ* generated *Lipshutz* higher order stannyl cuprate[111] followed by a iododestannylation to obtain vinyl iodide **158**, which can be easily monitored visually as the elemental iodine immediately reacts with **157** to the colorless **158**. Therefore, the completeness of the reaction is indicated when no more decoloration occurs upon dropwise addition of an iodine solution.

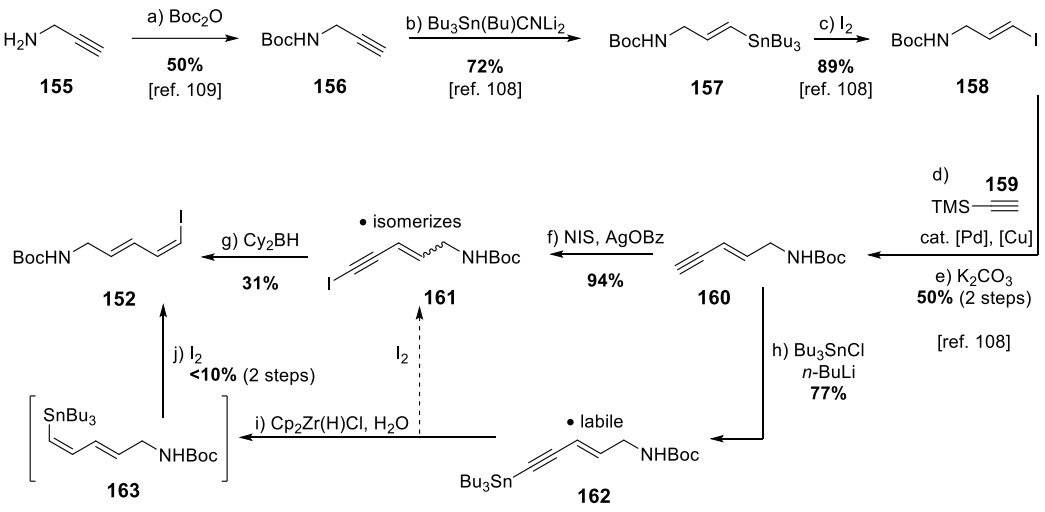

Scheme 33. Modular semi-successful approach to **152**. Conditions: a) Boc_2O (1.2 eq.), DCM, 0 °C to r.t., 8 h, recrystallization, 50%; b) CuCN (1.0 eq.), *n*-BuLi (2.1 eq.), Bu_3SnH (2.1 eq.), THF, −78 °C, 45 min, 72%; c) I_2 (1.1 eq.), DCM/Et_2O, 0 °C, 15 min, recrystallization, 89%; d) TMS-acetylene (1.2 eq.), CuI (0.1 eq.), $Pd(PPh_3)_2Cl_2$ (3 mol−%), DIPEA (12 eq.), THF, −78 °C to r.t., 2 h, 88%; e) K_2CO_3 (1.0 eq.), MeOH, r.t., 1 h, recrystallization, 57%; f) NIS (1.2 eq.), AgOBz (0.1 eq.), acetone, r.t., 30 min, 94%; g) BH_3 • THF (2.5 eq.), cyclohexene (5.8 eq.), Et_2O, 0 °C 1 h, then: acetic acid (23 eq.), 0 °C, 30 min, 31%; h) *n*-BuLi (1.5 eq.), Bu_3SnCl (2.0 eq.), THF, −78 °C to r.t., 1 h, 77%.

Subsequent *Sonogashira* reaction with TMS-acetylene (**159**) and a mild K_2CO_3 mediated desilylation[112] gave enyne **160** in moderate yields.

Notably, a considerable amount of product was lost during the three recrystallization steps conducted during this route (compounds **156**, **158**, **160**), which could have been reduced by further optimization of the crystallization conditions.

Next, the preparation of stannylenyne **162** (Scheme 34) was approached as a better stability towards light and therefore a higher geometrical purity was expected for **162** in contrast to iodoenyne **161**.

When enyne **160** was treated with *n*-BuLi and tributyltin chloride, no reaction was observed in presence of 1.0 or 1.5 equivalents of Bu_3Sn−Cl. Next, an alternative methods using tributyltin oxide (TBTO)[113] in presence of 3 Å molecular sieves also gave no intended product, even at forcing conditions (5 eq. TBTO, toluene, 130 °C).

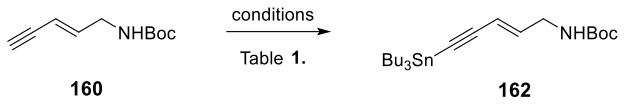

Scheme 34. Synthesis of the stannylenyne **162**.

Table 1. Screened conditions for the synthesis of stannylenyne **162**.

entry	electrophile]	conditions	crude NMR	purification	yield
1	Bu_3SnCl (1.0 eq.)	*n*-BuLi (1.5 eq), THF, −78 °C to r.t	no reaction	-	-
2	Bu_3SnCl (1.5 eq.)	*n*-BuLi (1.5 eq), THF, −78 °C to r.t	no reation	-	-
3	$(Bu_3Sn)_2O$ (0.5 eq.)	THF, 3 Å MS, 60 °C	no reaction	-	
4	$(Bu_3Sn)_2O$ (5.0 eq.)	toluene, 3 Å MS, 130 °C	no reaction	-	
5	D_2O	*n*-BuLi (1.5 eq), THF, −78 °C to r.t	alkyne signal vanished		
6	Bu_3SnCl[a] (2.0 eq.)	*n*-BuLi (1.5 eq), THF, −78 °C to r.t	reaction succeeded	column chromatography	decomposed
7	Bu_3SnCl[a] (2.0 eq.)	*n*-BuLi (1.5 eq), THF, −78 °C to r.t	reaction succeeded	column chromatography, Silica/K_2CO_3 (9:1); CH/EtOAc/NEt_3 (10:1:0.5)	**77%**

[a]: dried over 3 Å molecular sieves for at least 48 hours.

To explore, whether the failure of the first two reactions was due to an initial “deprotonation problem” or a problem with the electrophile, **160** was treated under the same conditions as for entry 1 and 2 but quenched with deuterium oxide.

As a result the ^{1}H-NMR signal of the alkyne vanished, indicating that the deprotonation and deuteration worked as intended.

A recorded ^{1}H-NMR of Bu_3Sn-Cl however revealed a significant contamination with water. Therefore, the reaction was repeated with tributyltin chloride previously stored over molecular sieves for at least 48 hours, with the crude NMR indicating product formation.

Purification by standard column chromatography led to destannylation (entry 6) which could be avoided by addition of triethylamine (5%) to the eluent while using a potassium carbonate doped stationary phase.[114] The carbonate doped silica serves two purposes namely, the deacidification of the silica but generally more importantly the retention of electrophilic tin-(*pseudo*)halide and tin-oxide species which are immobilized by the doped stationary phase.[114]

Subsequent hydrozirconation[115] using *Schwartz* reagent yielded the *Z*-vinylstannane **163** (Scheme 33) after hydrolysis and work-up. The crude product was directly treated with an iodine solution to obtain the intended *Z*-vinyl iodide **152**. However, only a yield below 10% was achieved, again with isomers present.

A direct iodination of alkyne **160** was achieved by reaction with NIS in presence of AgOBz, which resulted in nearly quantitative yields. The resulting *E*-iodoenyne **161** (J = 15.9 Hz) isomerized to the thermodynamically less stable *Z*-enyne (J = 10.8 Hz) when purified by column chromatography (*E*/*Z* = 2.8:1) and was therefore used without further purification.

Subsequent *Z*-selective reduction by *in-situ* generated dicyclohexylborane[100] followed by treatment with acetic acid gave Z-vinyl iodide **152** however accompanied by a cumbersome purification due to residual dicyclohexyl-boron side products. An improvement of the geometrical purity of **152** (d.r. = 6.5:1 to d.r. = 9:1) was achieved by recrystallization from *n*-heptane.

The overall route was evaluated worse than the allylamine approach (4.1.2) in terms of isomer formation, number of steps and chemical hazards and was ultimately discarded.

4.1.4 iodoacrylate-approach

One final route exploration (Scheme 35) was facilitated by a complimentary method which exploits the use of *Z*-iodoacrylate **165**, which can be readily synthesized from ethyl propiolate (**164**) by heating with sodium iodide.[116] The advantage of this reaction is the excellent *Z*-selectivity, which was also exploited by *Negishi et al.* to form dienoate **167** by reduction of **165** to the corresponding *Z*-iodoacroleine (**166**) and subsequent *HWE* reaction.[117]

While **166** is known and *experienced* to be a volatile highly lachrymatory substance,[118] it is usually obtained highly pure after reduction with DIBAL at −78 °C with no observable over-reduction to the corresponding allylalcohol. However, during the reduction and subsequent workup of **166**, only low boiling solvents such as DCM and Et_2O should be used, the solvent should never be entirely removed and subsequent reactions should be setup immediately after workup, ideally in a light-subdued environment.

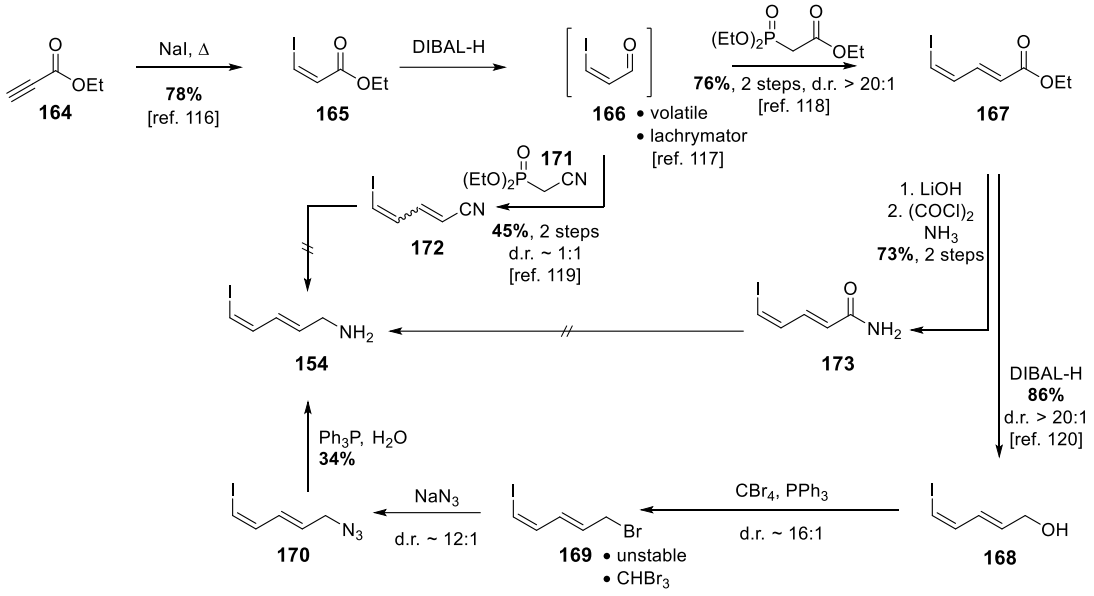

Scheme 35. Modular semi-successful approach to **154**. Conditions: a) NaI (2.0 eq.), AcOH, 70 °C, 22 h, 78%; b) DIBAL-H (1.05 eq.), DCM, −78 °C, 5 min, then: diethyl cyanomethylphosphonate (1.5 eq.), *n*-BuLi (1.5 eq.), −78 °C to r.t., overnight, 45% (2 steps), d.r. ≈ 1:1; c) DIBAL-H (1.05 eq.), DCM, −78 °C, 5 min, then: triethylphosphono acetate (1.5 eq.), *n*-BuLi (1.5 eq.), −78 °C to r.t., overnight, 76% (2 steps), d.r. > 20:1; d) LiOH (7.6 eq.), THF/H_2O (2:1), r.t., 6 h, 80%; e) oxalylchloride (0.94 eq.), cat. DMF, DCM, r.t., 1 h, then: NH_3 (2 M in *i*-PrOH, 6.0 eq.), 0 °C, 30 min, 91%; f) DIBAL-H (2.5 eq.), DCM, 0 °C, 45 min, 86% ,dr > 20:1; g) CBr_4 (2.2 eq.), PPh_3 (2.0 eq.), DCM, 0 °C, 30 min; h) NaN_3 (2.5 eq.), DMF, 60 °C, 3 h; i) PPh_3 (1.0 eq.), 0 °C, 2h, then: H_2O, r.t., 20 h, 31% (3 steps).

One possible route from iodoacroleine **166** was a literature known *HWE* reaction using cyanomethyl phosphonate.[119] While the literature stated only the formation of 2*E*,4*Z*-isomer, the 2*Z*,4*Z*-isomer of **172** was as well isolated with an observed d.r. of 1:1 (24:21) with 45% overall yield. Notably, these isomers showed a remarkable ΔR_f of 0.25 which is the highest value observed within this work for *E*/*Z*-Isomers.

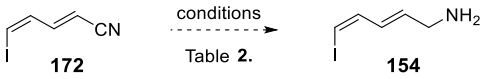

Table 2. Screened conditions for the reduction of dienenitrile **172**.

entry	reductant	conditions	yield
1	$LiAlH_4$	DME, r.t.	-
2	$NaBH_4$, $NiCl_2(H_2O)_6$	EtOH, r.t.	-
3	$NaBH_4$, $CoCl_2$	MeOH, r.t.	-
4	Red-Al®	Et_2O, r.t.	-

The subsequent reduction of dienenitrile **172** to dienamine **154** did not yield any product under several conditions (Table 2). Besides strong complex metal hydrides like LAH or Red-Al® (entries 1 and 4) also *in-situ* prepared Nickel/Cobalt borides[121] (entries 2, 3) were tested with no observed product formation. Eventually, the route was discarded due to the low yielding and unselective *HWE* reaction and the subsequent failed reduction.

From literature known[118] iododienoate **167** two pathways were possible (Scheme 36). A saponification of the ester **167** followed by generation of the corresponding acid chloride which is quenched with ammonia to form the primary amide **173** with a subsequent reduction to the amine **154**. Secondly, an initial reduction of **167** to allylalcohol **168** followed by an *Appel* reaction[122] and nucleophilic displacement of the resulting allylbromide **169** with sodium azide and a subsequent *Staudinger* reduction.[123]

In the first case, the resulting iododienamide **173** was obtained in a very good yield of 73% over two steps, however the final reduction using $LiAlH_4$ yielded an inseparable mixture of desired iododienamine **154** and overreduction (alkene → alkane) products, which were not observed in the absence of iodine.[124]

In the second case, the initial reduction of the enoate **167** to the corresponding alcohol **168**[120] was performed with a very good yield of 86%.

The following *Appel* reaction was suitable to convert the allylalcohol **168** to the allylbromide **169** which however proved unstable on silica.

This was highly problematic due to the side products of the *Appel* reaction (TPPO and bromoform). While TPPO does not interfere with the subsequent S_N2-reaction with sodium azide, the presence of bromoform causes safety issues, as the formation of highly explosive triazidomethane cannot be ruled out. Additionally, the resulting iododieneazide **170** only has a C/N-ratio[125] $(n_{carbon} + n_{oxygen})/n_{nitrogen} = 1.67$ (2.0 if iodine is counted) implying that the desired compound **170** constitutes a safety risk itself, especially when scaled up and should have been evaluated *non-suitable* before starting the reaction sequence.

Another observation during the exploration of this route was the fact that the geometrical purity of the compounds decreased with each synthetic step merely due to the exposition of environmental influences such as light, heat but also purifications using silica gel.

For that reason, the initially excellent Z-selectivity of the starting product **165** does not provide any advantages as the number of steps for this route is larger than for the previous sequences.

4.1.5 Summary for the synthesis of western fragment I/II

The synthesis of the western fragments **112** and **122** was approached through both linear and modular strategies, each with distinct advantages and challenges summarized below (Table 3).

The linear method (4.1.1), while conceptually straightforward, failed at the *Horner-Wadsworth-Emmons* reaction due to formation of an unexpected side product.

Table 3. Summary of the explored routes toward the western fragments **112** and **122**.

entry	approach	strengths	weaknesses	outcome
4.1.1	linear	sequential, (pseudo)biomimetic	failed at *HWE* reaction	abandoned
4.1.2	modular (allylamine)	high yields for metathesis steps	selectivity of *Stork-Zhao* reaction, HPLC purification	**viable** with limits (HPLC)
4.1.3	modular (propargylamine)	crystallinity of intermediates (purification)	organotin compound early in the sequence, cumbersome reduction	less favourable
4.1.4	modular (iodoacrylate)	high *Z*-selectivity	instability of intermediate **169,** safety risk involving iodoacroleine **166** azide **170**, many steps	less favourable

The modular approaches (4.1.2-4.1.4), on the other hand, were successful synthetic methods. Among these, the allylamine approach (4.1.2) stood out for its efficiency in the metathesis steps, which provided γ-amino enals (**150**, **151**) with high yields. However, obtaining a high diastereomeric ratio of the western fragments **112** and **122** (d.r. > 20:1) required a semi-preparative HPLC separation ideally shortly before further use.

The propargylamine approach (4.1.3) was hindered by low overall yields and complex purification steps, making it less practical for large-scale synthesis.

The iodoacrylate approach (4.1.4) demonstrated excellent *Z*-selectivities and high diastereomeric purities, which however decreased with an increasing step count. The route involved safety issues, particularly during the introduction of the nitrogen using sodium azide, which limited its feasibility.

Considering these outcomes, the allylamine (4.1.2) approach, originally developed during my master thesis,[91] was rated the most practical and scalable synthesis route for western fragment I/II (**112**/**122**).

4.2 Synthesis of homo- and hetero bimetallic linchpin dienes

During this work, several linchpin systems were developed with focus on methyl branched or, more precisely homo- and heterobimetallic 1,4-difunctionalized isoprene derivatives as shown below (Scheme 36).

For the synthesis of these branched linchpins several methods needed to be explored mostly relying on hydro-, carbo- and metallometalations of alkynes (enynes) in combination with transmetalations and electrophilic trapping of metal-carbon intermediates. These reactions types are particularly well-suited as key transformations since they often meet the requirements for high regio- and stereoselectivity and typically proceed in a quantitative manner.

This is especially important considering the challenges of purification, as the bis-metalates shown below are generally unstable towards silica and often exhibit very low polarities. As a result these molecules, if stable towards silica, often run with the solvent front on normal phase chromatography, while likewise purification via reversed phase (RP) chromatography leads to problematic recoveries due to overly high retentions.

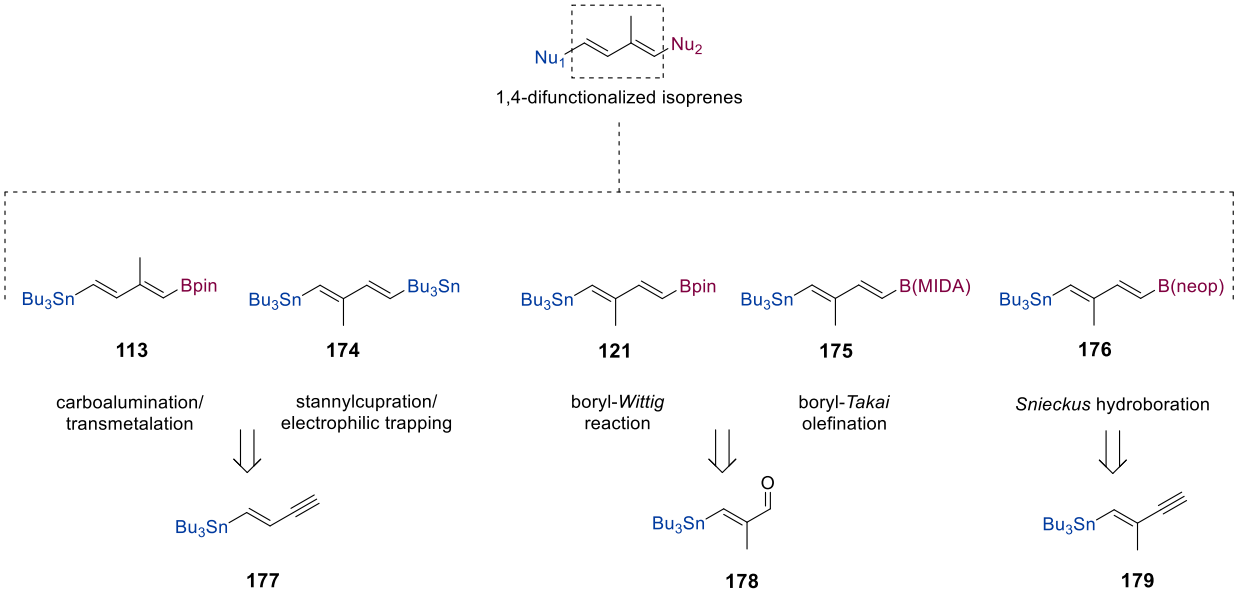

Scheme 36. A selection of methyl branched homo- and heterobimetallic linchpins synthesized during the course of this project with key steps and common precursors included.

4.2.1 Synthesis of Sn-B(pin)-Linchpin I

For the synthesis of the linchpin **113** a method needed to be found to facilitate the additional methyl-branching in β-position to the boron center.

As the existing methods by *Coleman*[45] and our group[58] relied on use of the boryl *Takai* olefination[57] for the introduction of the vinyl pinacolboronate motif, a different pathway needed to be explored as ketones are usually unreactive under takai-conditions.[57]

A suitable solution (Scheme 37) had already been found during my master thesis,[91] using a *Colvin* rearrangement[127] to convert aldehyde **33** into the homologated enyne **180** according to a known procedure from *Roush* and co-workers.[128] However, only poor yields of **113** were obtained in the subsequent zirconocene catalyzed carboalumination[129] of the terminal alkyne **180**.

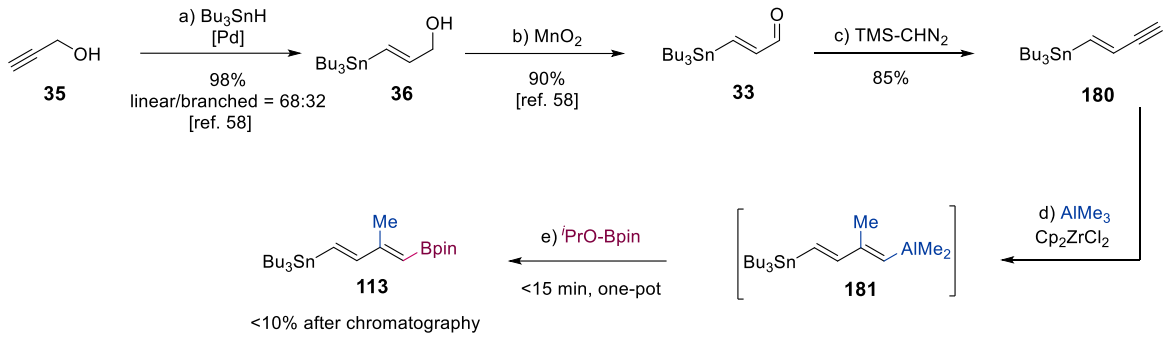

Scheme 37. First synthetic approach of Sn-B-linchpin I (**113**) developed during my master thesis.[91] Conditions: a) Pd_2dba_3 (2 mol-%), Cy_3PHBF_4 (8 mol-%), DIPEA (0.16 eq.), Bu_3SnH (1.2 eq.), DCM, 0 °C, 2 h, 98% linear/branched = 68:32; b) activated MnO_2 (20 eq.), DCM, r.t., overnight, 90%; c) TMS-CHN_2 (1.5 eq.), *n*-BuLi (1.3 eq.), THF, −78 °C to 0 °C, 2 h, 85%; d+e) Cp_2ZrCl_2 (0.3 eq.), $AlMe_3$ (2.0 eq.), −78 °C, 10 h, then: ^{i}PrOBpin (1.5 eq.), −41 °C, 15 min, 0-18%.

A careful TLC monitoring of all reaction steps revealed that **113** remained stable throughout the transmetalation (Al → B) step, quenching, extraction, drying, and evaporation of the solvent.

Next, the stability towards several stationary phases was examined, revealing that silica and basic alumina resulted in full decomposition of **113**, while triethylamine deactivated silica only showed slow decomposition. No decomposition was observed in combination with RP-silica or Florisil®.

However, their retentions were either too low for Florisil or too high for RP-Silica, when tested with the corresponding RP- or Florisil-TLC plates.

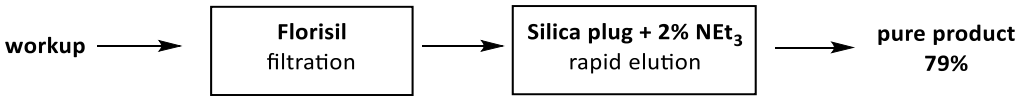

Scheme 38. Purification method for Sn-B(pin)-Linchpin I (**113**).

Based on these observations, a purification protocol (Scheme 38) was developed using an initial filtration over Florisil® followed by a second filtration over a triethylamine deactivated Silica plug. The overall protocol is rather simple and yields highly pure product after only two filtration steps with a very good recovery of 79%.

The synthesis of stannylacrylaldehyde **33** following the *Normant* protocol[130] proved more straightforward due to excellent anti-*Markovnikov* selectivity of the utilized stannylcupration. It was theorefore integrated into the synthesis of linchpin **113**, resulting in the final optimized synthetic route (Scheme 39) with an overall yield of 56% over 4 steps.

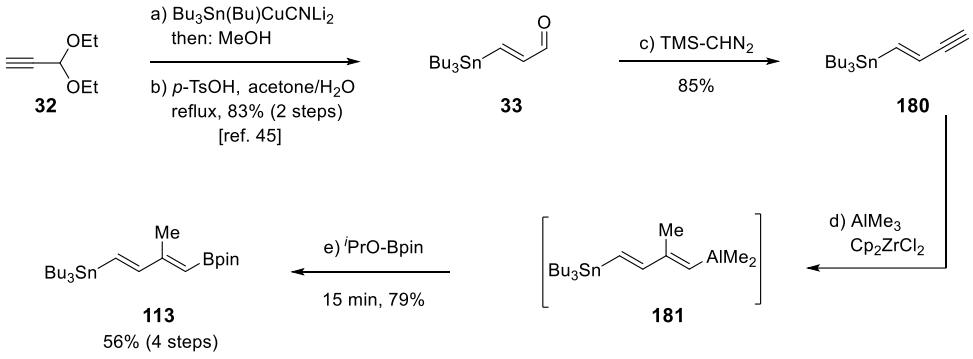

Scheme 39. Optimized synthesis of Sn-B(pin)-linchpin I (**113**). Conditions: a) CuCN (1.2 eq.), *n*-BuLi (2.4 eq.), Bu_3SnH (2.4 eq.), −78 °C, 2 h; b) *p*-TsOH (0.1 eq.), acetone/H_2O (15:1), reflux, 24 h, 83% (2 steps), c) $TMSCHN_2$ (1.5 eq.), *n*-BuLi (1.3 eq.), THF, −78 °C to 0 °C, 2 h, 85%; d+e) Cp_2ZrCl_2 (0.3 eq.), $AlMe_3$ (2.0 eq.), −78 °C, 10 h, then: ^{i}PrOBpin (1.5 eq.), −41 °C, 15 min, 79%.

4.2.2 Synthesis of Sn-Sn-Linchpin 174

Although not used for the total synthesis of **1** and **7**, the Sn-Sn-linchpin **174** was synthesized for conceptual purposes (Scheme 40) providing a method to synthesize homo-bimetallic linchpins with additional methyl-branching in β-position to one of the tin-centers.

Therefore, starting from stannylenyne **180** a suitable carbostannylation method needed to be found. Again, a stannylcupration was the method of choice, as the intermediate alkenyl cuprate **182** readily reacts with various electrophiles[60] including iodomethane as demonstrated in this reaction.

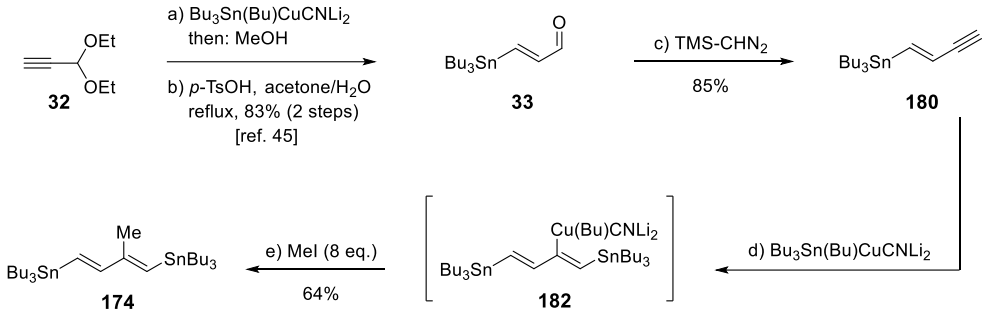

Scheme 40. Synthesis of the Sn-Sn-linchpin **174**. Conditions: a) CuCN (1.2 eq.), *n*-BuLi (2.4 eq.), Bu_3SnH (2.4 eq.), −78 °C, 2 h; b) *p*-TsOH (0.1 eq.), acetone/H_2O (15:1), reflux, 24 h, 83% (2 steps), c) $TMSCHN_2$ (1.5 eq.), $TMS\text{-}CHN_2$ (1.5 eq.), *n*-BuLi (1.3 eq.), THF, −78 °C to 0 °C, 2 h, 85%; d+e) CuCN (1.2 eq.), *n*-BuLi (2.4 eq.), Bu_3SnH (2.4 eq.), −78 °C, 1 h, then: MeI (8.0 eq.), −78 °C to r.t., overnight, 64% (after hplc).

Although synthesized in 4 steps and 45% overall yield, the drawback of this bis-stannne **174** was the requirement of a HPLC purification using an RP-C18 stationary phase in combination with a low-polarity chloroform/acetonitrile eluent mixture.

Moreover, this product was undetectable by MS and proved unstable upon prolonged exposure to $CDCl_3$, leading to decomposition during ^{13}C-NMR measurements. However, switching from $CDCl_3$ to acetone-d6 provided full NMR-data of **174**.

4.2.3 Synthesis of Sn-B(pin)-Linchpin II 121

The synthesis of Sn-B(pin)-linchpin II (**121**) was the only one for which a literature procedure was available as it was used in the syntheses of paracentrone[131] and allene containing apocarotenoids.[132] However, their synthetic procedure consisted of a cumbersome 7-step route with an overall yield of 17% as shown in (Scheme 41).

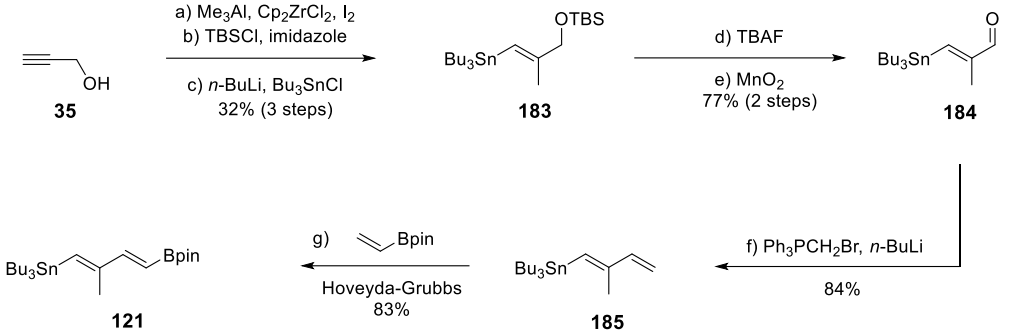

Scheme 41. Literature procedure for the synthesis of Sn-B(pin)-linchpin II (**121**).[131,132] Conditions: a) Cp_2ZrCl_2 (0.25 eq.), Me_3Al (3.0 eq.), 0 °C to r.t., then: I_2 (1.2 eq.), −30 °C, 1 h, **75%**; b) TBSCl (1.1 eq.), imidazole (2.0 eq.), DMF, 0 °C to r.t., overnight, 77% c) *n*-BuLi (1.6 eq.), Bu_3SnCl (1.6 eq.), Et_2O, −78 °C, 3 h, 55%; d) TBAF (1.2 eq.), THF, 0 °C, 1 h, 92% e) MnO_2 (10 eq.), DCM, r.t., 84%; f) Ph_3PCH_2Br (1.6 eq.), *n*-BuLi (1.6 eq.), −78 °C to 0 °C, 40 min, 84%; g) vinylpinacolboronate (2.0 eq.), Hoveyda-Grubbs (0.15 eq.), DCM, reflux, 19 h, 83%.

The literature procedure starts with a zirconocene catalyzed carboalumination[133] of propargylic alcohol **35**, followed by an electrophilic trapping of the alkenylaluminium intermediate with iodine.

After TBS-protection of the allylic alcohol, the tributyltin group is introduced via lithium-halogen exchange of the intermediate vinyl iodide which is reacted with tributyltinchloride in a nucleophilic displacement to obtain molecule **183**.[134]

After deprotection of the TBS-group the resulting allylic alcohol is oxidized to the corresponding aldehyde **184** using manganese dioxide[135] and after a *Wittig*[126] reaction, the obtained diene **185** is converted to the final linchpin using a cross-metathesis reaction.[131]

Inspired by the successful carbostannylation during the synthesis of Sn-Sn-linchpin **174** (4.2.2) it was hypothesized that a more streamlined route towards aldehyde **184** could be obtained using the stannylcupration of diethoxypropyne **32** followed by an electrophilic trapping of the alkenylcuprate **186** with iodomethane (Scheme 42), which indeed proceeded with a yield of 73% including the subsequent cleavage of the diethoxy acetal **187**. However, care must be taken to avoid any traces of water in this reaction, as it results in the formation of **33** (Scheme 40) as a non-separable side-product.

Next, a homologation to form alkyne **188** was pursued using again the *Colvin*[127] rearrangement giving the homologated alkyne **188** in a moderate yield of 66%. Again, a hydrozirconation/transmetalation

procedure was chosen to convert the resulting enyne to the corresponding alkenyl pinacolboronate and final structure **121**.

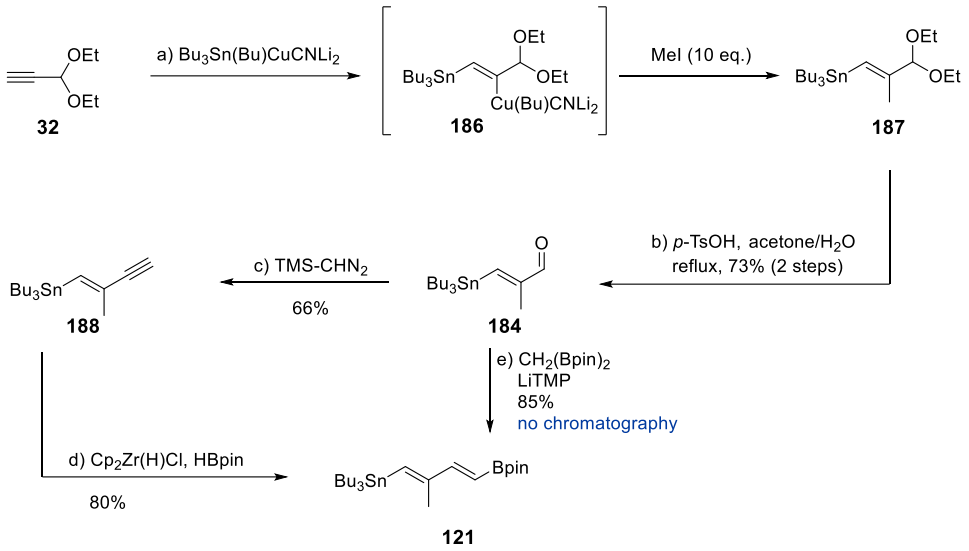

Scheme 42. Improved synthesis of Sn-B(pin)-linchpin II (**121**). Conditions: a) CuCN (1.2 eq.), *n*-BuLi (2.4 eq.), Bu_3SnH (2.4 eq.), −78 °C, 1 h, then: MeI (10 eq.), −78 °C to r.t., 5 h**;** b) *p*-TsOH (0.1 eq.), acetone/H_2O (15:1), reflux, 20 h, 73% (2 steps), c) $TMSCHN_2$ (1.4 eq.), *n*-BuLi (1.45 eq.), THF, −78 °C to 0 °C, 1 h, 66%; d) $Cp_2Zr(H)Cl$ (0.5 eq.), HBpin (1.8 eq.), DCM, r.t., 18 h, 80%; e) $CH_2(Bpin)_2$ (2.0 eq.), LiTMP (1.8 eq.), THF, −78 °C to r.t., 20 h, 85%.

The resulting Sn-B(pin)-linchpin II (**121**) however proved less stable towards (deactivated) silica, than Sn-B(pin)-linchpin I (**113**) resulting in decomposition when the same purification protocol (Scheme 38) was applied. Only an RP-C18 column with a step-gradient MeCN/H_2O → MeCN → MeCN/Et_2O was capable of providing pure product.

Therefore, an alternative protocol was developed using aldehyde **184** in combination with a boryl-*Wittig* olefination.[137] This reaction resulted in 100% conversion with an excellent diastereomeric ratio (d.r. > 20:1).

Moreover, the resulting pinacolborinate (*HO*-Bpin) and other by-products could be separated from the product by a simple sequence of several washing and extraction steps avoiding the necessity for any chromatographic purification leading to pure Sn-B(pin)-linchpin II (**121**) after 3 steps with an overall yield 62%.

4.2.4 Synthesis of Sn-B(MIDA)-Linchpin 175

The synthesis of Sn-B(MIDA)-linchpin (**175**) was initially expected to be a simple task as direct trans-esterification of vinylpinacolboronates[138] as well as the $NH_4OAc/NaIO_4$ protocol[139] for the conversion of the pinacolester to the corresponding boronic acid followed by complexation were available as suitable protocols.

However, both methods failed to proceed with Sn-B(pin)-linchpin II (**121**) resulting in isolation of the starting material (Scheme 43).

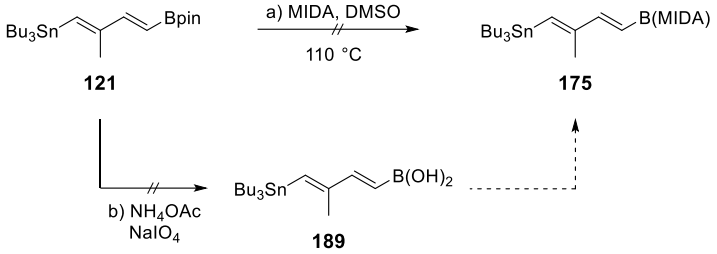

Scheme 43. Unsuccessful attempts of the conversion of Sn-B(pin)-linchpin II (**121**) to Sn-B(MIDA)-linchpin (**175**) via transesterification/transligation. Conditions: a) MIDA (6.0 eq.), DMSO, 110 °C, 24 h. b) NH_4OAc (2.5 eq.), $NaIO_4$ (2.5 eq.), acetone/H_2O 2:1.

Therefore, inspired by the first literature protocols by *Coleman*[45] and our group[58] *(2.2.4),* synthesis by boryl-*Takai* olefination was considered. To test the feasibility of this reaction, the new *Takai*-reagents **192** and **195** were synthesized (Scheme 44) inspired by a literature precedented synthesis of the common *Takai* reagent dichloromethylboronicacid pinacolester.[140,141]

The reactions (Scheme 44) started with the formation of the corresponding lithium carbenoids (**190.a**/**193.a**) by deprotonation of dichloro- (**190**) or diiodomethane (**193**) at −100 °C for which LHMDS was reported to be a more suitable base in case of diiodomethane.[142]

Subsequent addition of trimethylborate results in the formation of the corresponding -ate complexes (**190.b**/**193.b**) and hydrolysis with hydrochloric acid gave the corresponding sensitive dihalomethylboronic acids **191** and **194**, which were not isolated but immediately reacted with MIDA under *Dean-Stark* conditions to facilitate the condensation process. Both *Takai* reagents **192** and **195** were obtained in rather low yields presumably due to the poor stability of the sensitive carbenoid intermediates (**190.a**/**193.a**) involved in this reaction.

In contrast to the complexation with pinacol which typically proceeds at room temperature, the complexation with MIDA is carried out under rather forcing conditions (110 °C) which probably leads to partial decomposition of the corresponding boronic acids **191** and **194** before completion of the complexation process.

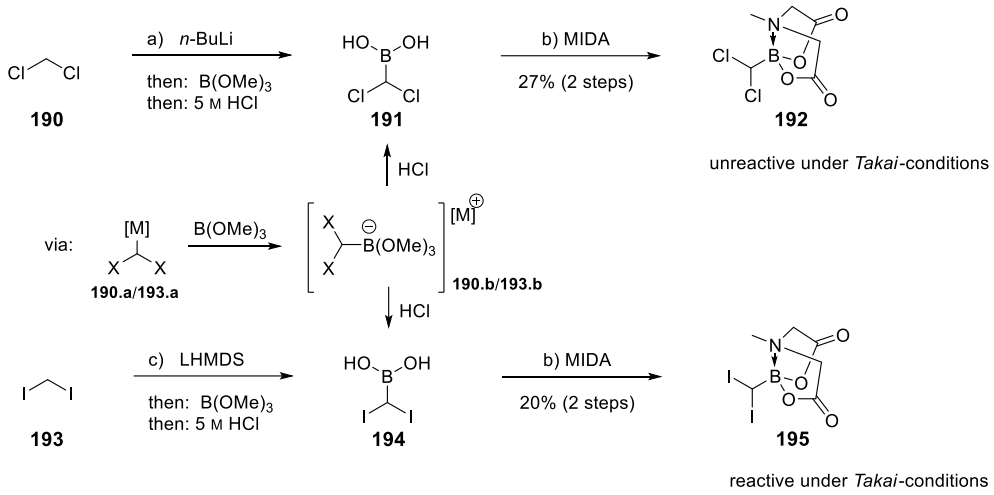

Scheme 44. Synthesis of MIDA-protected dihalomethylboronic acids **192** and **195**. Conditions: a) DCM (1.1 eq.), *n*-BuLi (1.0 eq.), THF, −100 °C, 1.5 h, then: $B(OMe)_3$ (1.1 eq.), 40 min, then: HCl 5 M, r.t., 1 h; b) MIDA (1.0 eq.), toluene/dmso 9:1, 120 °C, Dean-Stark, 27%; c) DIM (1.1 eq.), LHMDS (1.0 eq.), THF/Et_2O (2:1), −90 °C, 1.5 h, then: $B(OMe)_3$ (1.1 eq.), 40 min, then: HCl 5 M, r.t., 1 h; b) MIDA (2.0 eq.), toluene/dmso 9:1, 120 °C, Dean-Stark, 20%.

Next, aldehyde **184** was reacted with both Takai reagents **192** and **195** under *Takai* conditions using 8 equivalents of chromium dichloride in THF with additional 8 equivalents of lithium iodide in case of the dichloro-derivative to ensure the reported essential halogen-exchange.[57]

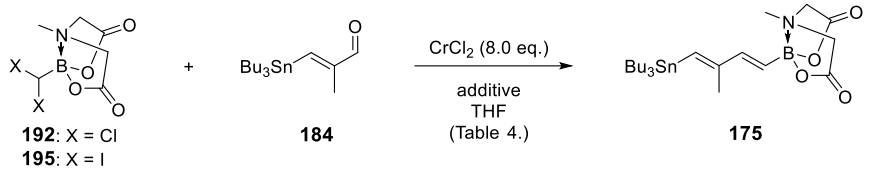

192: X = Cl
195: X = I

184

175

Table 4. Evaluation of reagents **192** and **195** in the boryl-*Takai* olefination for the synthesis of Sn-B(MIDA)-linchpin (**175**).

entry	halogen X, equivalents	additive, equivalents	T [°C]	t [h]	purification	yield/comment
1	Cl, (2.0 eq.)	LiI, (8.0 eq.)	r.t.	10	-	no reaction
2	Cl, (2.0 eq.)	LiI, (8.0 eq.)	r.t.	24	-	no reaction
3	I, (2.0 eq.)		r.t.	9	silica, 5% NEt_3	reaction proceeded
4	I, (2.0 eq.)		r.t.	12	RP C18 silica	25%
5	**I, (2.0 eq.)**		**0**	**24**	**RP C18 silica**	**49%**
6	I, (2.0 eq.)	TMEDA (8.0 eq.)	r.t.	12	-	no reaction
7	I, (2.0 eq.)		-3	65	-	no reaction
8	I, (2.0 eq.)		3	48	-	decomposition

As shown in table 4, *Takai* reactions with the dichlorocompound **192** did not provide any product. Instead, when the geminal diiodo compound **195** was reacted under the same conditions (table 4, entry 3) a color change from green to orange was visible within 30 minutes and product formation was confirmed by crude NMR analysis.

However, after silica chromatography no product was recovered. Subsequent, alteration of the purification procedure (entry 4) provided Sn-B(MIDA)-linchpin (**175**) with a yield of 25%. During this reaction, the formation of destannylated product was observed in accordance with literature reports of destannylation during *Takai* olefinations.[131] For that reason, a lower temperature (0 °C) in combination with a longer reaction time (24 h) was chosen to prevent excessive destannylation resulting in formation of **175** 49% isolated yield (entry 5). Addition of TMEDA,[143] lower temperatures and longer reaction times did not provide any product (entries 6-8).

As a halogen exchange was reported to be essential for *Takai* reactions, a control experiment for the unreactive dichloroderivative **192** was conducted (Scheme 45).

While a halogen-exchange for dichloromethylboronic acid pinacolester **196** to the diiodo-derivative **197** was reported in literature,[141] no halogen-exchange was observed for **192** when treated with sodium iodide in refluxing acetone for 48 hours.

This observation supports the argument of an essential halogen-exchange for the *Takai* reaction to proceed and the observed lack of reactivity under *Takai* conditions for **192**.

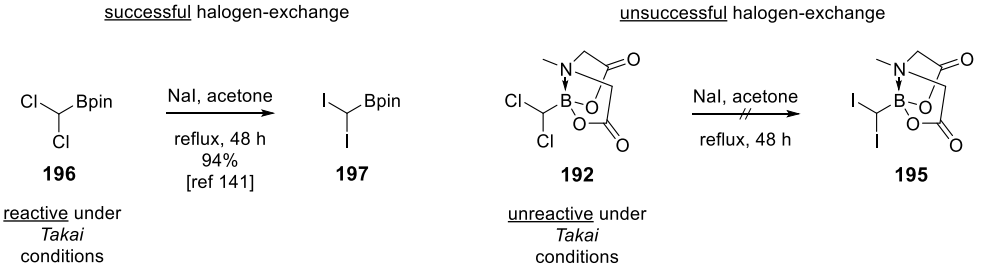

Scheme 45. Comparison of the halogen-exchange behavior of the two dichloromethylboronic acid derivatives **196** and **197** under *Finkelstein*-conditions.

With conditions in hand, the corresponding Sn-B(MIDA)-linchpin **175** was synthesized in three steps with an overall yield of 36% (Scheme 46) however, requiring an RP C18 silica column combined with a step-gradient H_2O/MeCN → MeCN to provide sufficiently pure material.

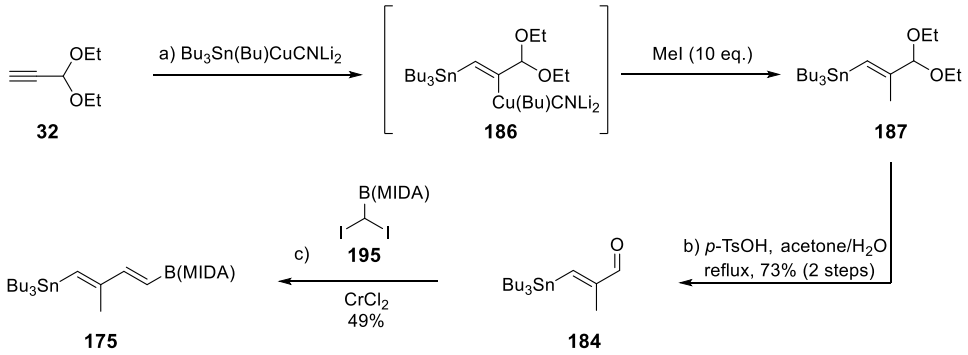

Scheme 46. Synthesis of Sn-B(MIDA)-linchpin **175**. Conditions: a) CuCN (1.2 eq.), *n*-BuLi (2.4 eq.), Bu_3SnH (2.4 eq.), −78 °C, 1 h, then: MeI (10 eq.), −78 °C to r.t., 5 h**;** b) *p*-TsOH (0.1 eq.), acetone/H_2O (15:1), reflux, 20 h, 73% (2 steps), c) $CHI_2B(MIDA)$ (2.0 eq.), $CrCl_2$ (8.0 eq.), THF, 0 °C, 24 h, 49%.

4.2.5 Synthesis of Sn-B(neop)-Linchpin 176

The last section of this chapter is the synthesis of the Sn-B(neop)-linchpin (**176**) (Scheme 47). The motivation behind the alteration of the boron nucleophile to a neopentylglycol ester were studies by *Denmark* demonstrating highly accelerated transmetalation rates compared to pinacolesters when reacted under anhydrous conditions.[144]

According to these studies, neopentylgylcol esters of boronic acids showed a good balance between high reactivity during the transmetalation step in *Suzuki* couplings and stability towards chromatography.

For the synthesis of Sn-B(neop)-linchpin (**176**) a *Snieckus* hydroboration[145] was chosen according to a modified protocol by *Roush*, who utilized this method for the synthesis of a Sn-B(pin)-linchpin (not shown).[128]

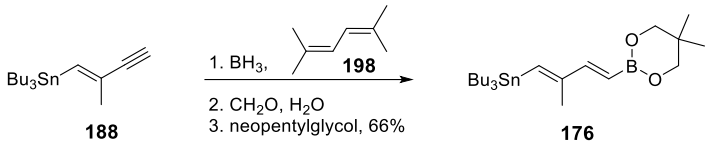

Scheme 47. Synthesis of Sn-B(neop)-linchpin (**176**) by *Snieckus* hydroboration of enyne **188** with *in-situ* formed di(*iso*propylprenyl)borane.

In this reaction, the active hydroboration reagent di(*iso*propylprenyl)borane (*i*PP_2BH) (**199**) is formed *in-situ* after double anti-*Markovnikov* hydroboration of the 2,5-dimethyl-2,4-hexadiene (**198**) (Scheme 48).[145]

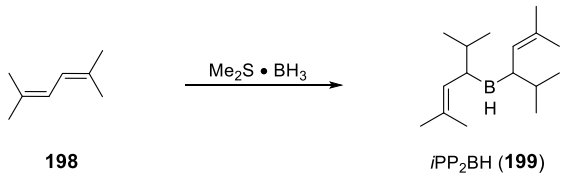

Scheme 48. Formation of the hydroboration reagent di(*iso*propylprenyl)borane (*i*PP_2BH) (**199**) by hydroboration of the 2,5-dimethyl-2,4-hexadiene (**198**). [145]

The initial hydroboration with BH_3 stops at the secondary borane due to steric hindrance which also results in good anti-*Markovnikov* selectivities upon further use of this reagent.

Then, after anti-*Markovnikov* addition (Scheme 49) to the the alkyne **188** the vinyl(bisallyl)boron complex **200** undergoes rapid protonolysis upon addition of water resulting in the formation of the borinic acid **203** and liberation of the alkene **202**.[145]

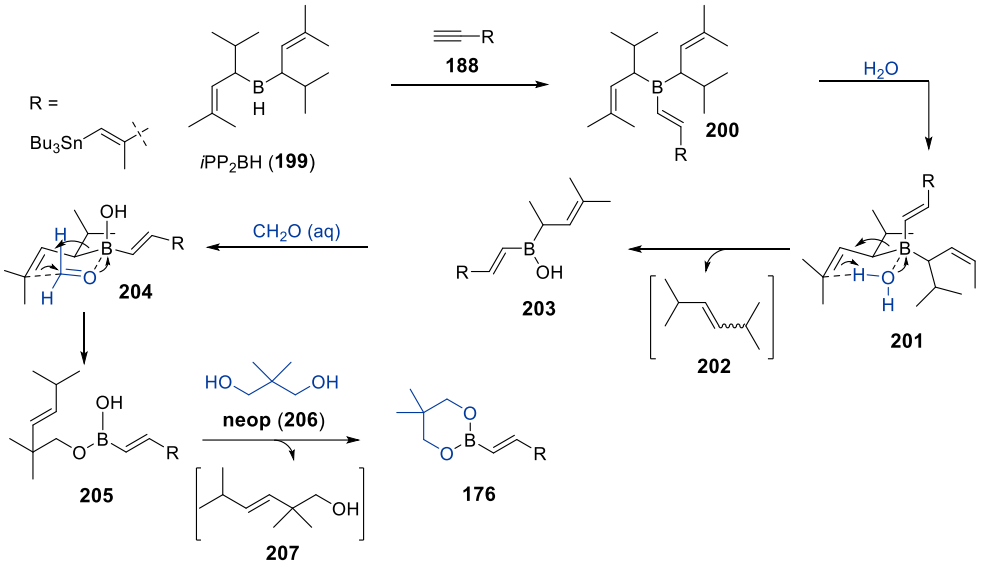

Scheme 49. Adapted mechanism for the formation of neopentylborane bearing Sn-B(neop)-linchpin **176** using the *Snieckus* hydroboration method.[145]

Subsequent addition of formaldehyde leads to formation of a hemiboronate (monoester) **205** via the *Zimmermann-Traxler*[146] transition state **204**. The resulting hemiboronate **205** is then transesterified with neopentylglycol (**206**) to the more stable cyclic diester liberating homoallyl alcohol **207** and the final product **176**.

Although, this mild hydroboration protocol proceeded with good yields, the obtained product **176** posed limited stabilities toward chromatography in accordance with the stabilities observed for the previously synthesized Sn-B(pin)-linchpins (**113**, **121**).

Again, purification with RP C18 silica using a step-gradient elution was the only method to obtain semi-pure product containing unidentified impurities. As this issue could not be addressed sufficiently, a subsequent utilization of the reagent with a potentially increased transmetalation acitivity in *Suzuki* couplings was unfortunately not further pursued.

Also, a ^{13}C-NMR of the compound was not recorded due to the presence of too many impurities.

Retrospectively, as at a later stage (4.2.3) the boryl-*Wittig* reaction in combination with a zero-chromatography purification protocol was developed for Sn-B(pin)-linchpin II (**121**), it is highly recommended to carry out the synthesis according to the suggested method (Scheme 50).

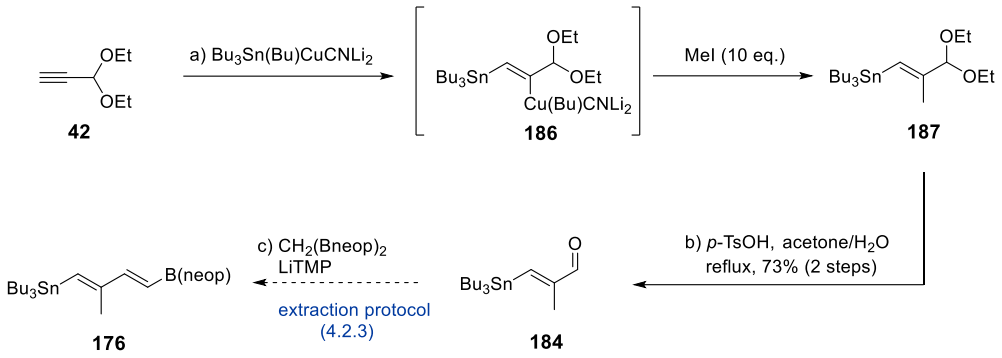

Scheme 50. Suggested method for an improved synthesis of Sn-B(neop)-linchpin (**176**) using the boryl-*Wittig* olefination in combination with a zero-chromatography purification protocol.

A literature known synthesis of bis[(neopentylglycolato)boryl]methane[147] $CH_2(Bneop)_2$, the fact that the boryl-*Wittig* reaction is not exclusive to pinacol analogs[137] and the larger steric demand[148] of the neopentylboronate compared to the pinacolboronate support the argument, that with a modified boryl-*Wittig* protocol Sn-B(neop)-linchpin **176** could be synthesized in high yields and purities.

Further studies on these types of linchpins should to be undertaken in the future to reveal their improved potential in anhydrous *Suzuki* couplings.

4.3 Synthesis of the eastern fragment

The synthesis of the eastern fragment (**119**) was one of the simpler challenges during this total synthesis project, as a complete literature procedure had already been established in the total synthesis of (−)-isodomoic acid B (**214**) by *Clayden* and co-workers[89] starting from the *S*-Roche ester (**208**) (Scheme 51).

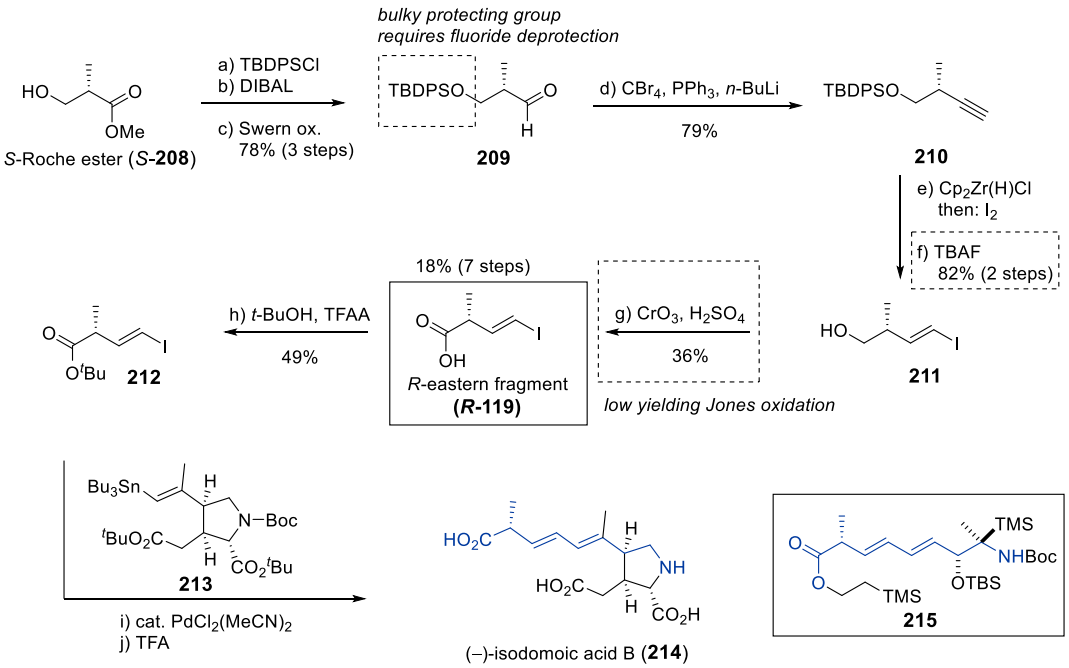

Scheme 51. Synthesis, protection and *Stille* coupling of the eastern fragment **119** in context of the total synthesis of (−)-isodomoic acid B (**214**) by *Clayden et al.*[89] Conditions: a) TBDPSCl (1.1 eq.), imidazole (1.05 eq.), DMF, 0 °C, 2 h, 98%; b) DIBAL (2.6 eq.), DCM, −15 °C, 2 h, 89%; c) oxalyl chloride (2.2 eq.), DMSO (2.8 eq.), Et_3N (5.0 eq.), DCM, −78 °C, 2 h, 89%; d) CBr_4 (2.7 eq.), Zn (2.7 eq.), PPh_3 (2.7 eq.), DCM, 0 °C, 4 h; then: *n*-BuLi (2.5 eq.), −78 °C, 1 h, 79%; e) $Cp_2Zr(H)Cl$ (1.2 eq.), DCM, r.t., 30 min; then: iodine (1.3 eq.), 30 min; f) TBAF (1.5 eq.), THF, 1 h, 82% (2 steps); g) Jones reagent (stoichiometry not reported), acetone, −10 °C, 1 h, 36%; h) TFAA (5.1 eq.), ^{t}BuOH, r.t., 1 h, 49%; i) **213** (1.0 eq.), **212** (1.5 eq.), $PdCl_2(MeCN)_2$ (2 mol-%), DMF, 50 °C, 48 h, 51%; j) TFA, DCM, r.t., 15 h, 100%.

In this sequence (Scheme 51), the Roche ester (*S*-**208**) was protected with a bulky TBDPS-group, subsequently reduced to the alcohol (not shown) and reoxidized to yield the protected aldehyde **209**. Then, a *Corey-Fuchs* reaction[149] yielded the homologated alkyne **210** which was stereoselectively transformed into the *E*-vinyl iodide **211** by a hydrozirconation using *Schwartz* reagent and subsequent electrophilic trapping of the alkenylzirconium intermediate (not shown) with iodine.[89]

After deprotection using TBAF in THF, the resulting homoallylic alcohol **211** was oxidized to the carboxylic acid and required eastern fragment (**119**) by a *Jones*[150] oxidation. The total synthesis of (−)-isodomoic acid B (**214**) proceeded with a subsequent protection of the carboxylic acid **119** by formation of the *tert*-butyl ester **212** followed by a *Stille* reaction with the vinyl stannane **213** and a final deprotection to yield the target natural product.[89] The endgame sequence of this literature synthesis was shown due to the similarity of **214** with the motif found in the revised eastern fragment II (**215**) (disscussed in chapter 7.2, Scheme 107).

Analysis of the literature sequence led to the identification of two major disadvantages. First, the use of a TBDPS-group introduces a bulky and highly stable silyl ether into the molecule, that requires fluoride for an effective cleavage.[151] Instead, the use of a TBS protecting group could circumvent unnecessary use of a fluoride source by simply using acid to facilitate the deprotection of the corresponding silylether.

Secondly, a more efficient oxidation protocol for the conversion of homoallyl alcohol **211** to the carboxylic acid **119** was desired, as the previously reported low yield of 36% would result in the loss of two-thirds of the valuable product at the sixth step of the synthetic sequence.

With this in mind, a modified synthetic procedure toward the eastern fragment (**119**) was developed (Scheme 52).

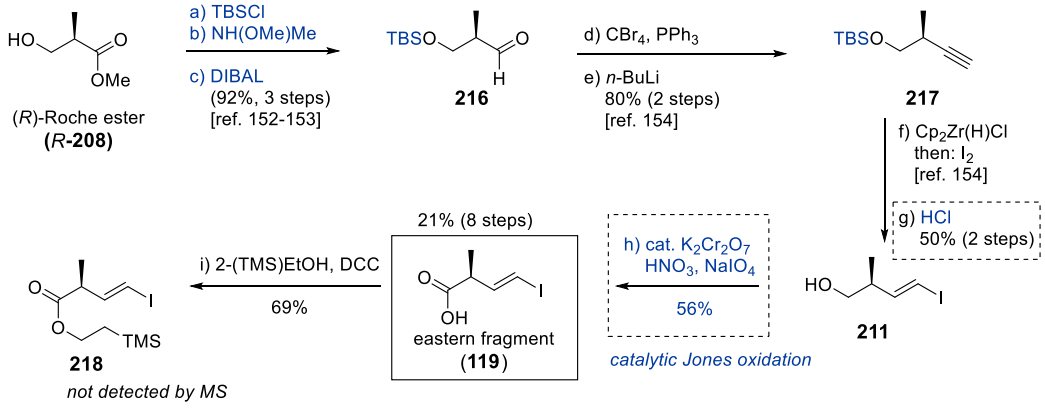

Scheme 52. Modified synthetic procedure and protection of the eastern fragment (**119**).[152-154] Conditions: a) TBSCl (1.1 eq.), imidazole (2.2 eq.), DCM, 0 °C, 3.5 h, 99%; b) *N*,*O*-dimetyhlhydroxylamine hydrochloride (1.6 eq.); ^{i}PrMgCl (3.0 eq.), −78 °C to r.t., 8 h, 94%; c) DIBAL (2.5 eq.), THF, −78 °C, 2 h, 99%; d) CBr_4 (2.0 eq.), PPh_3 (4.0 eq.), DCM, r.t., 1 h; e) *n*-BuLi (2.5 eq.), THF, −78 °C, 1 h, 80% (2 steps); f) $Cp_2Zr(H)Cl$ (1.2 eq.), DCM, r.t., 40 min; then: iodine (1.2 eq.), 1.5 h, 54% g) HCl (3 M in MeOH, 5.0 eq.), MeOH, r.t., 0.5 h, 93%; h) $K_2Cr_2O_7$ (6 mol-%), HNO_3 (aq. 65%, 0.5 eq.), $NaIO_4$ (2.5 eq.), H_2O, MeCN, 0 °C, 7 h then: 4 °C, 18 h, **56%**; i) 2-(TMS)EtOH (1.3 eq.), pyridine (2.0 eq.), DCC (1.1 eq.), MeCN, 0 °C, 5 h, **69%**.

First, a different literature approach[152] towards aldehyde **216** bearing the TBS-ether was followed using a TBS-protection of the *R*-Roche ester (*R*-**208**), followed by formation of the *Weinreb* amide and subsequent reduction with DIBAL giving the desired aldehyde **216** in an excellent yield of 92% over three steps.

Then, a *Corey-Fuchs*[149,154] reaction was carried out to obtain the desired alkyne **217** in 80% over two steps. Other than in the original literature, the corresponding dibromoalkene (not shown) was isolated and characterized. The alkyne **217** showed slightly volatile behavior and was consequently purified by *Kugelrohr* distillation (100 °C, 150 mbar). Subsequent hydrozirconation and electrophilic trapping with iodine to form **211** provided a yield of only 54% (lit: 66%)[154] in contrast to the >80% obtained for the TBDPS-protected derivative.[89] However, the intended acidic deprotection of the TBS ether proceeded with an excellent of 93%.

Completion of the eastern fragment (**119**) was obtained by a catalytic *Jones* oxidation investigated by *Johannes Herbst* during his master thesis.[155] Following this protocol gave the carboxylic acid **119** in an improved yield of 56% compared to the 36% achieved in the original protocol[89] (Scheme 51).

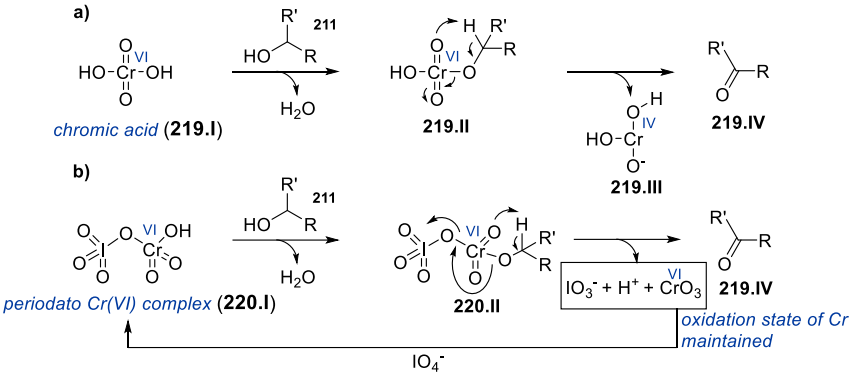

Scheme 53. Mechanistic key steps of the classic *Jones* oxidation[156] (a) and the periodate-mediated catalytic *Jones* oxidation (b).[157]

The main difference between the classic and the catalytic *Jones* oxidation (Scheme 53) is the formation of a periodato Cr(VI) complex (**220.I**) which acts as a highly reactive oxidant forming a periodato Cr(VI) alkoxy species (**220.II**) in analogy to the classical reaction (**219.II**).[157] After the subsequent β-elimination, the iodine is reduced from (VII) to (V) allowing chromium (VI) to maintain its oxidation state, which is afterwards transformed back into the periodato Cr(VI) complex (**220.I**) upon reaction with excess periodate.[157] As substoichiometric amounts of acid are used, this method renders particularly useful for the oxidation of acid labile substrates. Moreover, the use of stoichiometric amounts of toxic chromium is prevented.

In summary, the eastern fragment (**119**) was synthesized following a modified literature protocol. The steric hindrance of the silyl ether protecting group was reduced, enabling deprotection under acidic conditions instead of requiring a fluoride source.

A protection of the eastern fragment (**119**) with a TMSE group[158] was evaluated for the case, that a protection of the carboxylic acid would be required. Reaction of the eastern fragment (**119**) with 2-(TMS)ethanol and DCC[159] in presence of pyridine gave the protected eastern fragment **218** in 66% yield. While characterization via ^{1}H- and ^{13}C-NMR confirmed product formation, compound **218** remained undetectable by mass spectrometry.

The low-yielding *Jones* oxidation[89] was optimized by employing a periodate-mediated, chromium-catalyzed variant,[159] improving the yield from 36% to 56%. Despite this improvement, the overall yield increased only moderately from 18% to 22%, primarily due to a low yield in the hydrozirconation step, which remains an area for further optimization.

4.4 Synthesis of the central fragment III

For the bacillaene analogue (**7**), the synthesis of central fragment III (**132**) was planned. The retrosynthetic analysis of **132** (Scheme 54) resulted in the carboxylic acid fragment **129** and the MIDA sidechain **133**, for which suitable literature precedences were available.[107,139,160,161]

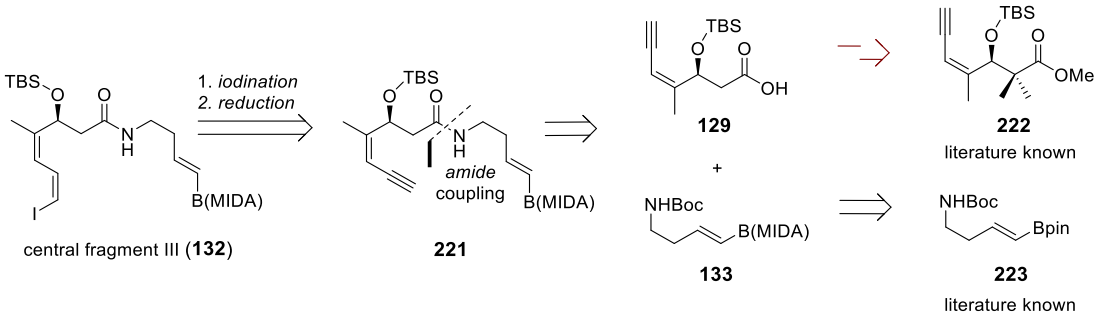

Scheme 54. Key disconnection of central fragment III (**132**) resulting in the carboxylic acid **129** and the MIDA side chain **133**.

4.4.1 Synthesis of the MIDA side chain (133)

The synthesis of the MIDA side chain (**133**) began with the preparation of the literature known pinacol analogue **223**,[160] which required the *Boc*-protected homopropargylamine **227**.

For the synthesis of **227**, homopropargyl alcohol (**224**) was first tosylated to **225**[162] and then reacted with sodium azide in an S_N2-reaction.[163] During this reaction, a blast shield was used during the reaction to ensure the highest possible safety. Since the resulting homopropargyl azide (not shown) has a C/N-ratio[126] of only 1.3:1, its isolation was omitted (as also reported in the literature),[163] and the subsequent *Staudinger*[123,163] reduction was carried out immediately after extraction to obtain **226**.

After successful *Boc*-protection forming **227**, the final literature known hydroboration of **227** using *Schwartz* reagent was carried out, achieving a yield of 85% smiliar to the reported one.[160]

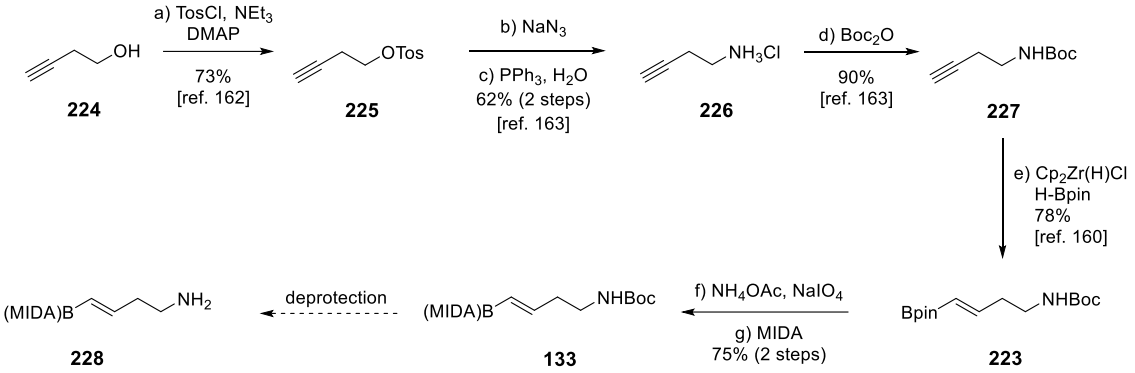

Scheme 55. Synthesis of the MIDA side chain (**133**). Conditions: a) TosCl (1.35 eq.), Et_3N (2.0 eq.), DMAP (0.15 eq.), DCM, 0 °C, 2 h, 73%; b-c) NaN_3 (2.5 eq.), DMF, 70 °C, 4 h, then: PPh_3 (1.0 eq.), Et_2O, 0 °C, 2 h, then: H_2O, r.t., 20 h, 60% (2 steps); d) Boc_2O (1.0 eq.), Et_3N (2.0 eq.),THF, r.t., 4 h, 90%; e) HBpin (2.0 eq.), $Cp_2Zr(H)Cl$ (0.12 eq.), Et_3N (0.12 eq.), DCM, 60 °C, 12 h, 85%; f-g) $NaIO_4$ (2.5 eq.), NH_4OAc (2.5 eq.), acetone/H_2O (1:1), r.t., 19 h, then: MIDA (2.0 eq.), toluene/dmso (10:1), 115 °C, 18 h, 74% (2 steps).

In the following step, the planned conversion of the pinacol boronic ester **223** to the MIDA boronate **133** was carried out. For this transformation, the $NH_4OAc/NaIO_4$ method[139] was used, which allows the transformation of pinacol esters into the corresponding boronic acids under mild conditions.

The obtained boronic acid (not shown) was then directly converted to **133**, following *Burke*'s conditions[46] (2.0 eq. MIDA, toluene/DMSO 10:1, *Dean-Stark*, reflux), yielding the resulting crude **133** with subsequent vapor diffusion crystallization[164] used as the purification method.

For this crystallization, the crude product **133** was dissolved in MeCN, and the *anti*-solvent diethyl ether was slowly diffused into the MeCN solution via gas-phase transfer. This gradually lowered the overall polarity of the solvent, inducing crystallization of the product. With an overall yield of 75% over two steps, this method proved to be highly efficient.

Next, the deprotection of **133** was carried out. Since the stability of MIDA boronates toward acidic conditions had been documented[47], acidic deprotection conditions were evaluated (Table 5).

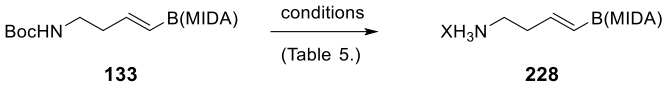

133 **228**

Table 5. Evaluation of deprotection conditions for **133**.

entry	conditions	*Boc*	MIDA
1	HCl (4 M in 1,4-dioxane)	deprotected	deprotected
2	HCl (1.25 M in EtOH)	deprotected	transesterification[a] to R-B(OEt)$_2$
3	TMSOTf, 2,6-Lutidine	no reaction	no reaction
4	TFA/DCM/0 °C	deprotected	ca. 10% deprotected
5	TFA/TFAA (20:1)/DCM/0 °C	deprotected	stable

[a]: determined from MS data.

During the evaluation of deprotection conditions, analysis of the crude NMR spectra revealed that the MIDA ligand was more sensitive to acidic conditions than initially expected.

The disappearance of the characteristic MIDA-signals at approximately 4.1 ppm was observed when using HCl in 1,4-dioxane as well as HCl in EtOH (Table 5, entries 1-2). Additionally, when using HCl in EtOH, the formation of a diethoxyboronate was detected via MS. The use of TMSOTf in combination with 2,6-lutidine[165] (entry 3) proved unsuccessful.

Good stabilities of the MIDA-ligand were observed when using TFA in DCM. However, partial deprotection of the MIDA ligand was observed presumably caused by the presence of water. To address this, a mixture of TFA/TFAA in a 20:1 ratio was prepared resulting in a “self-drying” reagent. With this mixture, deprotection was repeated, with no observed deprotection of the MIDA ligand. Whether the improved deprotection is due to the removal of water or if TFAA plays an additional role was not further investigated.

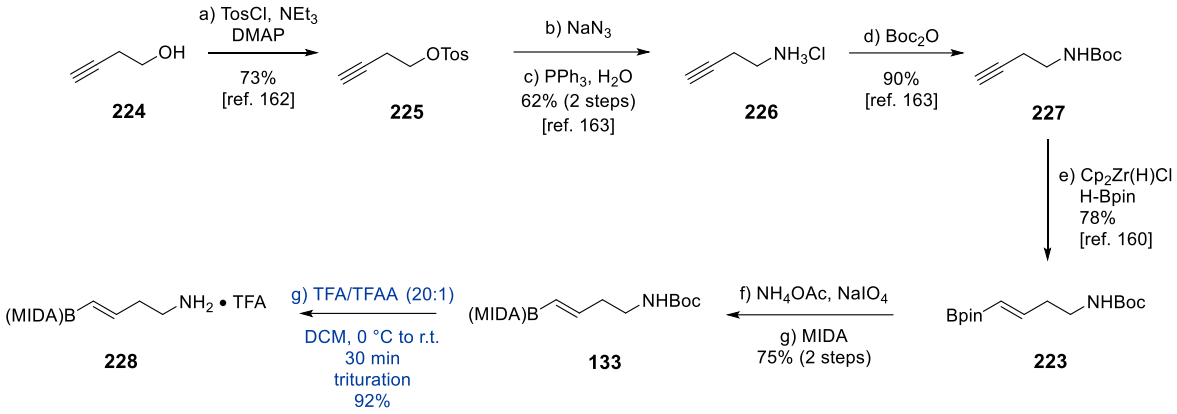

Scheme 56. Synthesis and deprotection of the MIDA side chain (**133**). Conditions: a) TosCl (1.35 eq.), Et_3N (2.0 eq.), DMAP (0.15 eq.), DCM, 0 °C, 2 h, 73%; b-c) NaN_3 (2.5 eq.), DMF, 70 °C, 4 h, then: PPh_3 (1.0 eq.), Et_2O, 0 °C, 2 h, then: H_2O, r.t., 20 h, 60% (2 steps); d) Boc_2O (1.0 eq.), Et_3N (2.0 eq.),THF, r.t., 4 h, 90%; e) HBpin (2.0 eq.), $Cp_2Zr(H)Cl$ (0.12 eq.), Et_3N (0.12 eq.), DCM, 60 °C, 12 h, 85%; f-g) $NaIO_4$ (2.5 eq.), NH_4OAc (2.5 eq.), acetone/H_2O (1:1), r.t., 19 h, then: MIDA (2.0 eq.), toluene/dmso (10:1), 115 °C, 18 h, 74% (2 steps); g) TFA/TFAA (20:1, 10 eq.), DCM, 0 °C, 30 min, 92%.

The obtained crude **228** was then dissolved in a small amount of acetonitrile and added to a stirred mixture of Et_2O/*n*-pentane, achieving effective purification via trituration. With this method, the TFA-salt of **228** was obtained with a yield of 92%. Overall, the MIDA side chain was synthesized with a total yield of 22% over seven steps.

Later, the synthesis was repeated using commercially available *Boc*-protected homopropargylamine, reducing the route to four steps and avoiding the hazardous amine synthesis involving sodium azide.

With the side-chain fragment in hand, the next step was to complete the new central fragment, which is described in the following pages.

4.4.2 Synthesis of the carboxylic acid 129 and completion of the central fragment III

As mentioned at the beginning of the chapter (4.4), the synthesis of carboxylic acid **129** was practically known from the synthesis of oxazolomycin A (**237**) by *Eto* and co-workers (Scheme 58).[107,161]

The key reaction in this sequence was a cinchona-catalyzed asymmetric cyclocondensation[166] of aldehyde **231** resulting in the formation of the β-lactone **233** with excellent enantiomeric and diastereomeric selectivities and a subsequent lactone-opening leading to the β-hydroxy ester **234**.

This product **234** closely corresponds to the desired compound **129** except for the α-methyl group in **234**. Therefore, the substitution of propionyl chloride with acetyl chloride in the key cyclocondensation reaction would yield the desired intermediate.

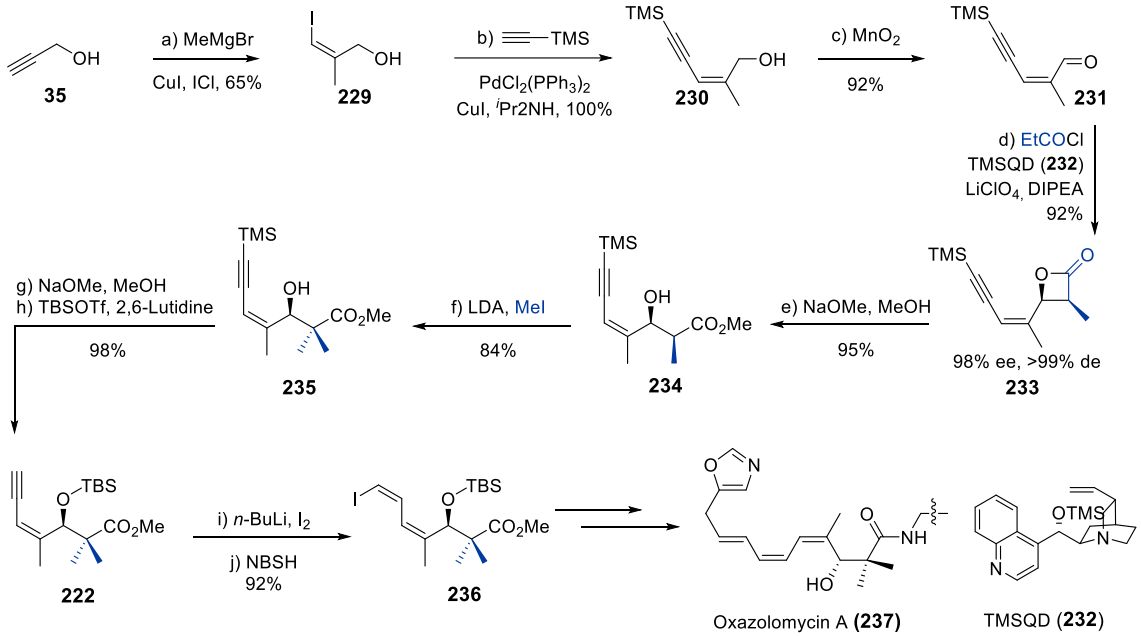

Scheme 57. Synthesis of α,α-dimethyl (blue) substituted iododiene **236** in the context of the total synthesis of oxazolomycin A (**237**).[107] Conditions: a) MeMgBr (2.0 eq.), CuI (1.0 eq.), Et_2O, −5 °C to r.t., 2 h, then: ICl (1.0 eq.), −5 °C to r.t., 16 h, 65%; b) TMS-acetylene (2.0 eq.), *i*Pr_2NH (7.5 eq.), $PdCl_2(PPh_3)_2$ (2 mol-%), CuI (8 mol-%), THF, r.t., 1 h, 100%; c) MnO_2 (15 eq.), *n*-hexane/DCM (1:1), r.t., 24 h, 92%; d) $LiClO_4$ (4.0 eq.), TMSQD (**232**) (0.2 eq.), DIPEA (2.5 eq.), EtCOCl (2.0 eq.), −78 °C, 22 h, 92%; e) NaOMe (0.01 eq.), MeOH, 0 °C, 30 min, 95%; f) LDA (4.0 eq.), −78 °C to −20 °C, MeI (10 eq.), −78 °C to −20 °C, 4 h, 84%; g) NaOMe (0.5 eq.), MeOH, 0 °C, 4 h, 98%; h) TBSOTf (2.0 eq.), 2,6-lutidine (4.0 eq.), DCM, 0 °C, 30 min, 100%; i) *n*-BuLi (1.1 eq.), THF, −78 °C, 1 h, then: I_2, −78 °C, 1 h, 99%; j) NBSH (2.0 eq.), Et_3N (1.3 eq.), THF/*i*PrOH (1:1), r.t., 40 h, dark, 93%.

In the reaction sequence (Scheme 58), the introduction of the second α-methyl group to form **235** follows, which can simply be skipped, followed by desilylation of the terminal alkyne and TBS protection of the β-hydroxy group yielding **222**.

The synthesis of the iododiene fragment **236** is completed by iodination of the terminal alkyne and subsequent diimide reduction.[101] The formation of the diimide occurs through aminolysis of 2-nitrobenzenesulfonylhydrazide (NBSH)[167] under very mild reaction conditions.

Derived from the preiously described sequence, the synthetic route for the central fragment III (**132**), was modeled as shown below (Scheme 59).

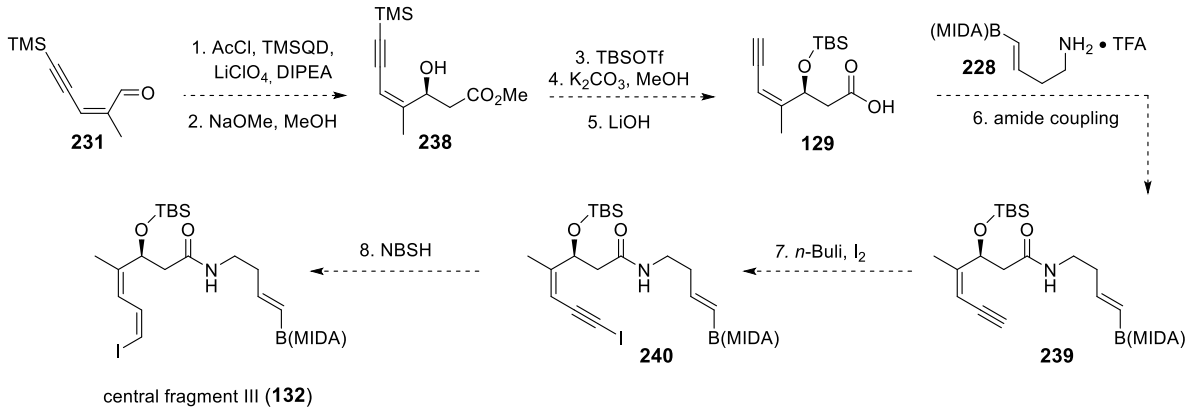

Scheme 58. Planned synthetic procedure for the central fragment III (**132**) based on the total synthesis of oxazolomycin A (**237**).[107]

Analogous to *Eto´*s synthesis[107] (Scheme 58), aldehyde **231** should be subjected to the cinchona-catalyzed cyclocondensation[166] with acetyl chloride instead of propionyl chloride to avoid substitution in α-position, followed by lactone-opening to form the ester **238**. Subsequent TBS protection, desilylation and saponification would yield the key intermediate **129**. After amide coupling with the MIDA side chain (**228**), the iodination and diimide reduction were to be performed analogously to the literature synthesis of **236** (Scheme 58).

Next, the preparation of aldehyde **231** was carried out (Scheme 60) according to the literature procedure,[161] with the reported yields being well reproducible. Only in the first step, *Duboudin´s anti*-carbomagnesation[168] of propargylic alcohol (**35**) iodine monochloride (ICl) was substituted with iodine (I_2), as it is easier to handle. The higher polarizability of ICl compared to I_2 is not required for the reaction, as indicated by the similarly high yields.

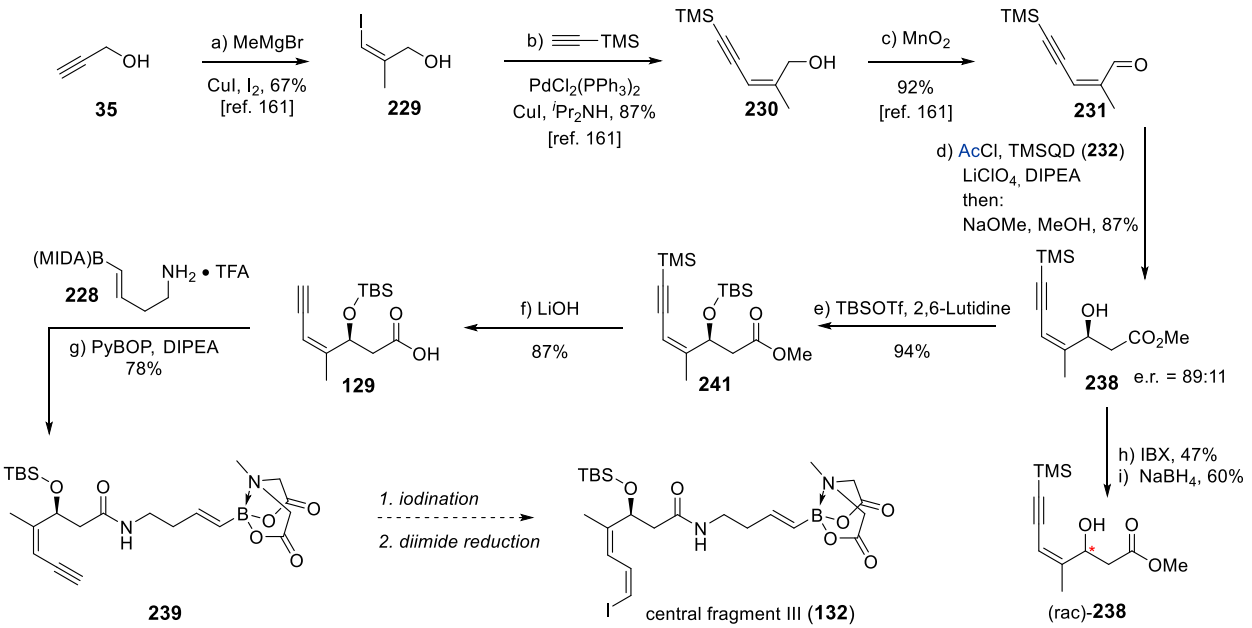

Scheme 59. Synthesis of carboxylic acid **129** and subsequent amide coupling with the MIDA side chain **228**. Conditions: a) MeMgBr (2.1 eq.), CuI (1.0 eq.), Et_2O, −5 °C to r.t., 2 h, then: I_2 (1.0 eq.), −5 °C to r.t., 12 h, 67%; b) TMS-acetylene (2.0 eq.), *i*Pr_2NH (9.0 eq.), $PdCl_2(PPh_3)_2$ (2 mol-%), CuI (10 mol-%), THF, r.t., 1.5 h, 87%; c) MnO_2 (16 eq.), DCM (1:1), r.t., 20 h, 78%; d) $LiClO_4$ (4.0 eq.), TMSQD (**232**) (0.2 eq.), DIPEA (2.5 eq.), AcCl (2.0 eq.), −78 °C, 10 h, then: NaOMe (1.3 eq.), MeOH, r.t., overnight 87%; e) TBSOTf (2.0 eq.), 2,6-lutidine (4.0 eq.), DCM, 0 °C, 30 min, 91%; f) LiOH (23 eq.), THF/H_2O (1:1), 60 °C, 12 h, 87%; g) **228** (1.1 eq.), **129** (1.0 eq.), PyBOP (1.4 eq.), DIPEA (10 eq.), DMF, r.t., overnight, 78%; h) IBX (2.1 eq.), EtOAc, 80 °C, 47%; i) $NaBH_4$ (2.2 eq.), MeOH, r.t., 30 min, 60%.

The asymmetric cyclocondensation[166] and lactone opening was carried out with acetyl chloride, followed by the addition of sodium methoxide in a one-pot procedure to convert the resulting lactone (not shown) into the β-hydroxy ester **238**. Under these conditions, prolonged stirring led to the formation of desilylated **238** (not shown).

Since a stereocenter is introduced, the absolute configuration of **238** was later determined by *Johannes Herbst* using *Mosher* ester analysis (see experimental section).[155] Additionally, a racemic standard was prepared to enable precise quantification of the enantiomeric ratio by HPLC. For the synthesis of the chiral standard, substrate **238** was first oxidized using IBX[169] and subsequently reduced to (*rac*)-**238** using sodium borohydride. Comparison of (*rac*)-**238** with **238** revealed an enantiomeric ratio (e.r. = 89:11) lower than the one reported from *Eto* (e.r. = 99:1, Scheme 58).[107]

Next, TBS protection of **238** provided **241** with excellent yield. The subsequent saponification of **241** to carboxylic acid **129** resulted in the simultaneous deprotection of the TMS-alkyne, which was desired at

this stage. After obtaining carboxylic acid **129**, the amide **239** was successfully synthesized using the previously described MIDA fragment **228** (4.4.1) and PyBOP as the coupling reagent.

The following step, was the intended iodination of the terminal alkyne **239**, followed by a *Z*-selective reduction of the resulting iodienyne **240** (Scheme 61).

Initially, attempts were made to deprotonate **239** with *n*-BuLi and subsequent reaction it with iodine, following the procedure of *Eto* (Scheme 58)[107]. However, in multiple attempts, a maximum crude yield of merely 38% was achieved.

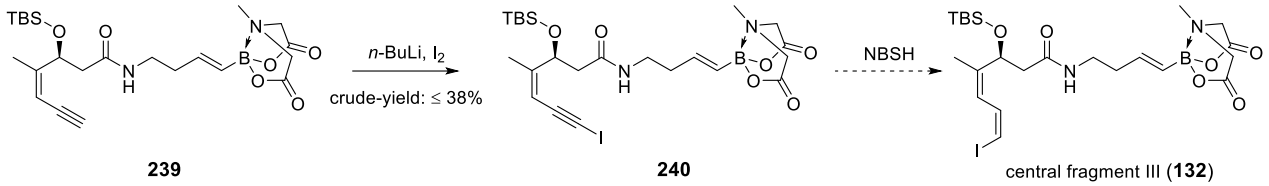

Scheme 60. Intended transformation of enyne **239** into the *Z,Z*-iododiene central fragment III (**132**).

Searching for alternative iodination methods, the silver-catalyzed iodination[170] using *N*-iodosuccinimide (NIS) was selected as a suitable approach. Since this reaction has been reported with various silver(I) sources, it was decided to evaluate the best catalyst through a screening process.

As five different silver(I) salts ($AgNO_3$, AgF, AgOTf, AgOAc, AgOBz) were available in stock, these salts were selected for the screening.

Next, a stock solution of **239** together with NIS (1.05 eq.) in acetone-d6 was prepared. The respective silver(I) salt (1.0 eq.) was weighed into NMR-tubes. After addition of the stock solution, a ^{1}H-NMR spectrum was recorded for each reaction (Scheme 62).

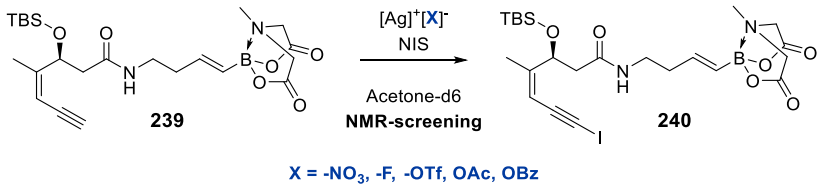

Scheme 61. Evaluation of silver(I) sources for the iodination of terminal alkyne **239**.

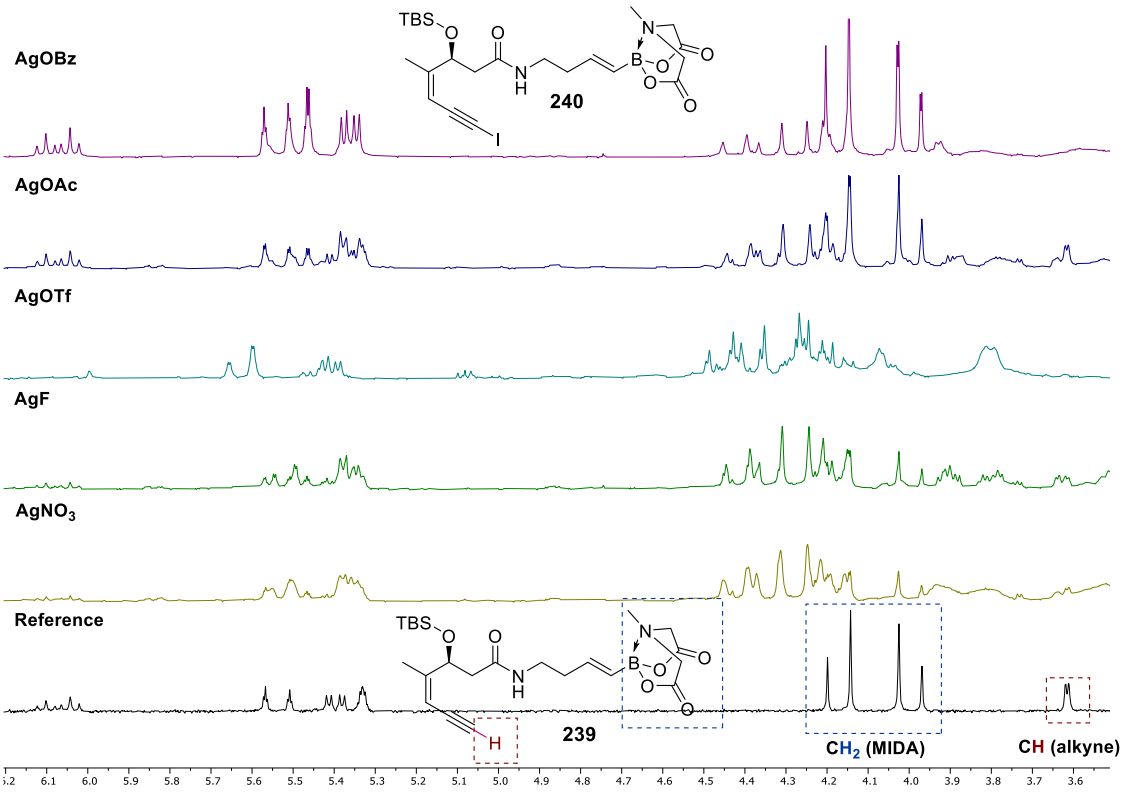

Figure 9. Results (excerpt of the ^{1}H-NMR spectra in acetone-d6, 300 MHz) of the evaluation of silver(I) sources for the iodination of terminal alkyne **239**. The important signals of the CH_2-protons of the MIDA group (blue) and the CH-proton (red) of the terminal alkyne are marked for the starting material **239**.

As visible in the NMR-spectra (Figure 10), the use of different silver(I) salts led to highly variable results. In the lower reference spectrum of the terminal alkyne **239**, the key signals are marked, corresponding to the CH- signal of the alkyne and the CH_2-signals of the MIDA boronate. A successful iodination of the alkyne **239** can be assumed if the CH-signal of the alkyne **239** vanishes while the CH_2-signals of the MIDA boronate remain largely unaffected.

It was observed that with all silver(I) sources except for AgOBz, either a doubling of the CH-alkyne signal and/or a disappearance of the MIDA CH_2-signals occurred, indicating at least partial decomposition of the MIDA boronate, often accompanied by incomplete iodination.

Only in the case of AgOBz the CH-signal completely vanished, along with a good retention of the integrity of the MIDA-signals. While performing very well, the question remains, why silver benzoate exhibited such a superior profile compared to the other silver(I) sources.

In the case of AgF, one could argue that the fluoride anion may react with the TBS protecting group and, due to its high affinity for boron, could tend to form numerous side products. However, this explanation does not apply to nitrate, acetate, or triflate.

A faster reaction of silver(I)-benzoate compared to other sources could be explained by the better solubility of the benzoate anion, which may act as a phase-transfer catalyst, improving the availability of silver ions in solution.

However, why the different salts lead to varying degrees of deprotection of the MIDA ligand remains to be elucidated.

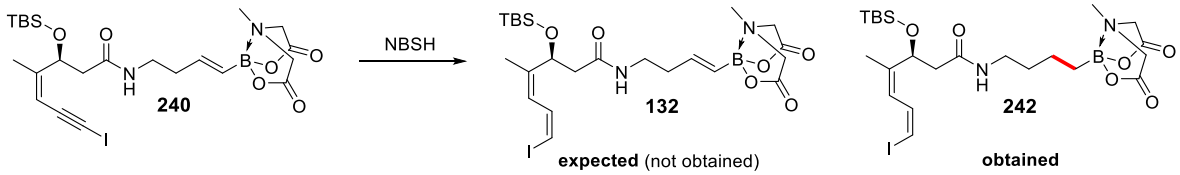

Scheme 62. Intended final diimide reduction of iodoenyne **240** to yield western fragment III (**132**). Instead, the overreduced product **242** was obtained.

The planned final step in completing the new central fragment was the diimide reduction[101] of the previously obtained iodoenyne **240** (Scheme 64). The reduction was intended to follow the same procedure as the reduction of **236** (Scheme 58) in the synthesis of oxazolomycin A.[107] However, at this stage, the over-reduced product **242** was obtained instead of **132**. This outcome was not entirely surprising, as the ability of diimide to reduce double bonds is well-documented.[171]

At this stage, one could have considered alternative reduction methods. Instead, it was decided to try this iodination- and reduction sequence with the carboxylic acid fragment **129**, which successfully yielded carboxylic acid **244** (Scheme 63).

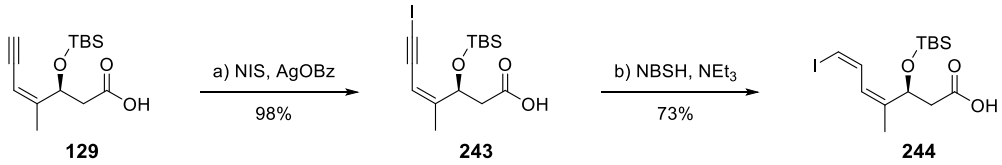

Scheme 63. Successful iodination- and reduction sequence of carboxylic acid **129** resulting in *Z,Z*-iododiene carboxylic acid **244**. Conditions: a) NIS (1.1 eq.), AgOBz (0.1 eq.), acetone, −78 °C to r.t., 30 min, 98%; b) NBSH (2.0 eq.), Et_3N (2.0 eq.), THF/*i*PrOH (1:1), 17 h, dark, 71%.

Notably, the NIS/AgOBz iodination of **129** proceeded in the presence of the free carboxylic acid with an excellenct yield of 98%.

Next, the final amide coupling (Scheme 64) between **244** and the MIDA chain **228** was facilitated with EDC and DMAP, resulting in an easier purification than the previously used PyBOP conditions.

Overall, the central fragment III (**129**) was obtained with a yield of 22% over 9 steps (LLS) with the lowest yielding step (67%) being the initial carbomagnesation of propargylalcohol (**35**).

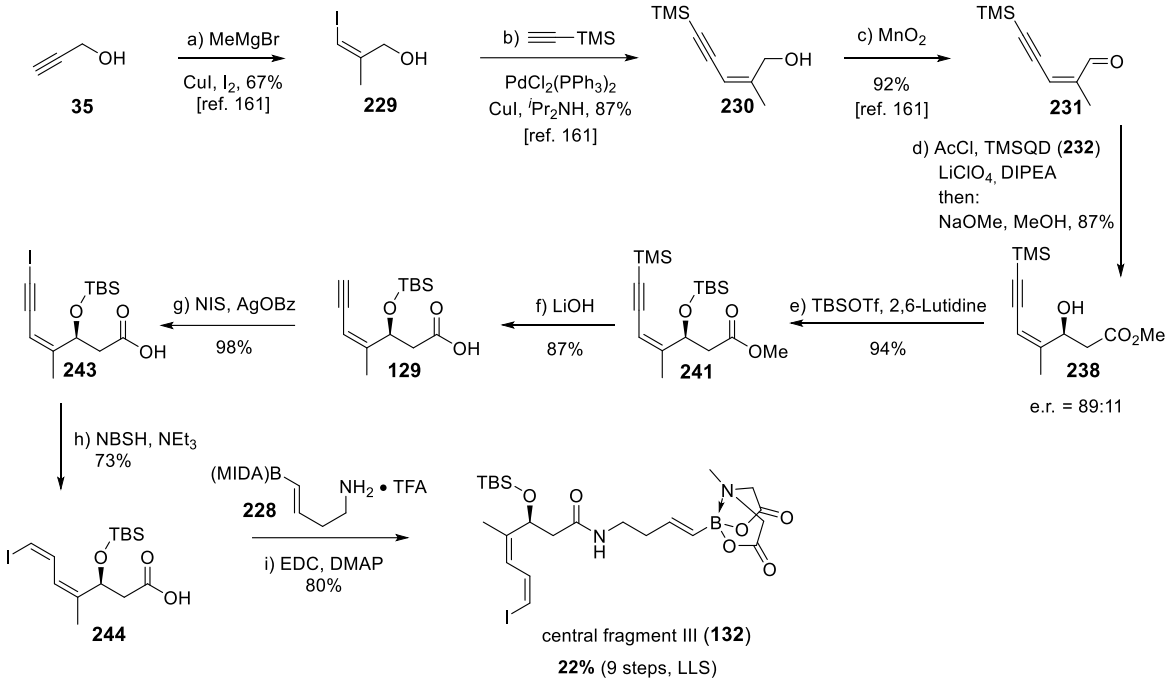

Scheme 64. Final successful synthetic sequence for the synthesis of central fragment III (**132**). Conditions: a) MeMgBr (2.1 eq.), CuI (1.0 eq.), Et_2O, −5 °C to r.t., 2 h, then: I_2 (1.0 eq.), −5 °C to r.t., 12 h, 67%; b) TMS-acetylene (2.0 eq.), *i*Pr_2NH (9.0 eq.), $PdCl_2(PPh_3)_2$ (2 mol-%), CuI (10 mol-%), THF, r.t., 1.5 h, 87%; c) MnO_2 (16 eq.), DCM (1:1), r.t., 20 h, 78%; d) $LiClO_4$ (4.0 eq.), TMSQD (**232**) (0.2 eq.), DIPEA (2.5 eq.), AcCl (2.0 eq.), −78 °C, 10 h, then: NaOMe (1.3 eq.), MeOH, r.t., overnight 87%; e) TBSOTf (2.0 eq.), 2,6-lutidine (4.0 eq.), DCM, 0 °C, 30 min, 91%; f) LiOH (23 eq.), THF/H_2O (1:1), 60 °C, 12 h, 87%; g) NIS (1.1 eq.), AgOBz (0.1 eq.), acetone, −78 °C to r.t., 30 min, 98%; h) NBSH (2.0 eq.), Et_3N (2.0 eq.), THF/*i*PrOH (1:1), 17 h, dark, 71%; i) **244** (1.0 eq.), **228** (1.05 eq.), EDC (1.4 eq.), DMAP (1.4 eq.), DCM, r.t., 13 h, 80%.

Part 3: Fragment union and endgame studies

5.1 Overview

In the previous chapters (4.1-4.4), the syntheses of the depicted fragments (Scheme 65) were discussed. Within the initial collaboration with *Reuter-Schniete*, central fragment IV **116** was successfully synthesized, while side-chain fragment **110** was still in progress. At that stage, first evaluations of iterative cross coupling strategies were undertaken. The overall goal was to synthesize bacillaene (**1**), and the availability of the three fragments (**112**, **113** and **116**) provided a foundation for these initial assessments.

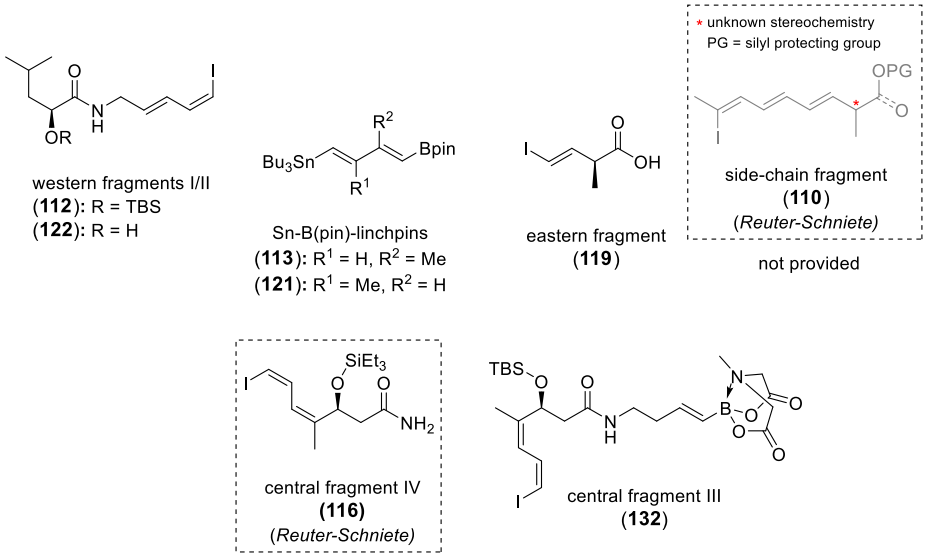

Scheme 65. Overview of the various fragments synthesized during this work and provided by *Reuter-Schniete*.

In contrast, the central fragment III (**132**) and Sn-B(pin)-linchpin (**121**) were synthesized later during this project, as initital coupling evaluations did not provide the desired coupling products in the required yield and, more importantly, not in the required quality and geometrical purity.

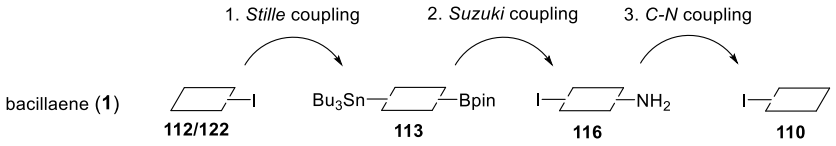

Scheme 66. Possible iterative cross-coupling sequence for the authentic natural product bacillaene (**1**) using the available fragments **112**/**122**, **113**, **116**, (**110**, not available).

5.1 Evaluated couplings for bacillaene (1)

5.1.1 Stille coupling of the western fragments and Sn-B(pin)-linchpin

The first coupling according to the previously described sequence was the *Stille* coupling between the protected or unprotected western fragments I/II (**112**/**122**) with the Sn-B(pin)-linchpin I (**113**) developed in this work.

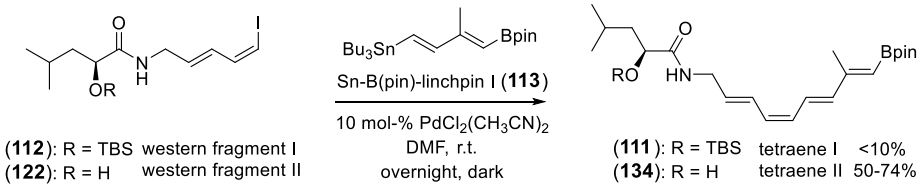

Scheme 67. Evaluated *Stille* couplings between the protected/unprotected western fragments I/II (**112**/**122**) with the Sn-B(pin)-linchpin I (**113**).

For the evaluation of the *Stille* coupling, both fragments **112** and **122** were reacted with **113** (1.5 eq.) under classical conditions[172] in a subdued light environment. For the TBS protected western fragment I (**112**) only traces of the product **111** could be detected via mass spectrometry, while for the unprotected fragment II (**122**) yields of up to 74% (semi-purified) were obtained for **134** under the same reaction conditions.

However, tetraene II (**134**) proved unstable toward silica. Analytical HPLC indicated a geometrical purity of 81% with an isomer ratio of 8.6/0.4/1 and absorption maxima (λ_{max} = 314 nm) in accordance with the formation of a conjugated tetraene system.[173] However, decomposition occurred during semi-preparative HPLC separation, resulting in complete loss of the product.

Purification was partly possible through manual RP-C18 column chromatography, however full structural assignment via NMR was not fully possible due to poorly resolved signals in the olefinic region. With this procedure, the tetraene II (**134**) was obtained in sufficient yield, although not completely isomerically pure. Nevertheless, it was subsequently used to explore the next coupling reaction.

5.1.2 Suzuki coupling between tetraene II and western fragment IV

Next, as part of the collaboration project, the subsequent *Suzuki* coupling of tetraene II (**134**) with the central fragment IV (**116**) to form the already advanced intermediate hexaene I (**117**) was evaluated (Scheme 68).

For the initial reaction conditions, $Pd(PPh_3)_4$ was selected as a suitable starting catalyst. Three equivalents of either cesium carbonate (Cs_2CO_3) or thallium ethoxide (TlOEt)[174] were evaluated as bases in a THF/water mixture.

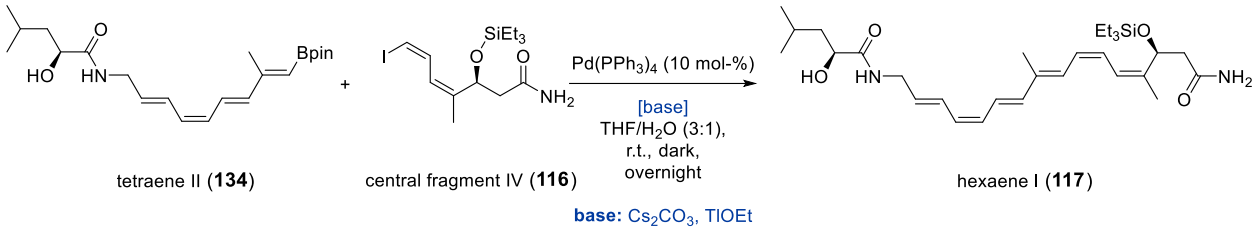

Scheme 68. Initial evaluation of the *Suzuki* coupling between tetraene II (**134**) and central fragment IV (**116**).

While TlOEt did not yield any product, the *Suzuki* coupling using cesium carbonate as a base showed better results. A small amount of hexaene I (**117**) was successfully isolated and identified as the desired compound through MS analysis. Additionally, a full NMR dataset was recorded, however the spectra suffered from low signal intensity and contained numerous unassignable peaks as well as significant overlap in the olefinic region. As previously observed with the tetraene II (**111**) signal assignment proved highly challenging.

At this stage, analytical HPLC would have been highly beneficial for determination of the number of isomers and geometrical purity. Furthermore, analytical HPLC could have provided additional confirmation of the conjugated hexaene scaffold through detection of the absorption band at $\lambda_{max} \approx 360$ nm.

To move forward, it would have been necessary to repeat the reaction, optimize the reaction conditions, and conduct analytical HPLC to determine the number of isomers present in the mixture and assess the feasibility of their separation. Unfortunately, at this stage the collaboration was terminated, with no more contributions to this synthetic sequence as *M. Reuter-Schniete* terminated her Ph.D. thesis.

5.2 Evaluated couplings for the bacillaene analogue (7)

Due to termination of the collaboration project toward the total synthesis of bacillaene (**1**) the alternative synthesis and evaluation of coupling conditions toward the bacillaene analogue (**7**) was pursued.

5.2.1 Initital coupling strategy

For the synthesis of **7**, a similar iterative cross-coupling strategy was initially pursued (Scheme 69), following the previously successful *Stille* coupling (Chapter 5.1.1) between **122** and **113**. This reaction yielded tetraene II (**134**) in sufficient quantities and acceptable purity.

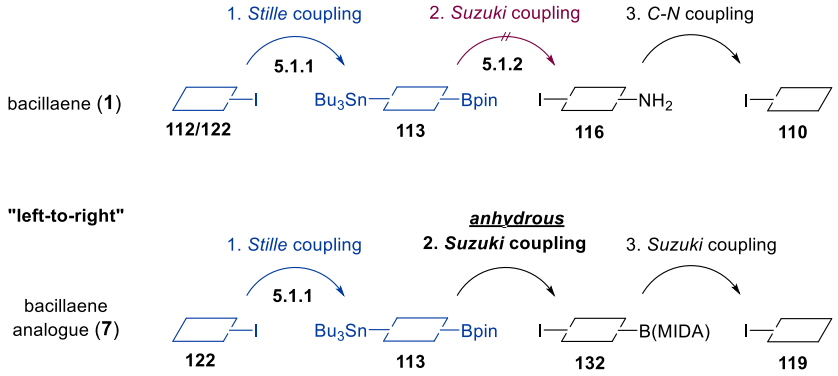

Scheme 69. Initital iterative cross coupling coupling strategy ("left-to-right") for the synthesis of the bacillaene analogue (**7**), following a similar coupling sequence as used in the synthesis of bacillaene (**1**).

As visible (Scheme 69), the obtained central fragment III (**132**) (Chapter 4.4) was now to be coupled with the tetraene II (**134**) in an anhydrous *Suzuki* coupling to form hexaene **131**. This step would represent the penultimate coupling in the sequence, with only the second aqueous *Suzuki* coupling remaining, followed by deprotection of the TBS group of the secondary alcohol.

5.2.2 Anhydrous Suzuki coupling of tetraene II with central fragment III

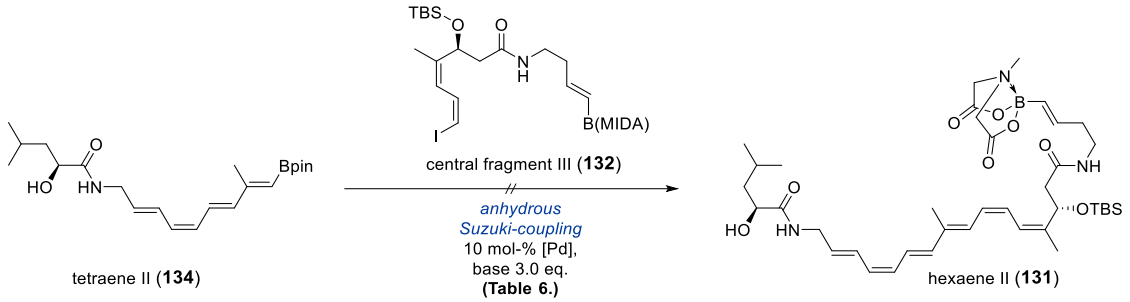

Scheme 70. Estimated fragment union of tetraene II (**134**) and central fragment III (**129**) for the synthesis of hexaene **131**.

For the the intended coupling (Scheme 70) between tetraene II (**134**) and central fragment III (**132**), it was decided to keep the base, solvent and temperature constant (3.0 eq. Cs_2CO_3, anhydrous THF, r.t.) while first identifying a suitable catalyst (Table 6).

To obtain a broad range of results, catalyst/ligand systems with varying steric and electronic properties were investigated. Electron-rich monodentate ligands such as XPhos and NHC (Umicore CX21) were tested, as well as electron-deficient ligands like P(2-furyl)$_3$ and $AsPh_3$. As a reference, $Pd(PPh_3)_4$ was also evaluated as the standard catalyst.

Table 6. Evaluated reaction conditions for the anhydrous Suzuki coupling between tetraene II (**134**) and central fragment III (**132**). No product was obtained for any of the listed reaction conditions.

entry	[Pd]	ligand	base	solvent	yield
1	$Pd(PPh_3)_4$	-	Cs_2CO_3	THF	-
2	$Pd(OAc)_2$	XPhos	Cs_2CO_3	THF	-
3	XPhos Pd G3	-	Cs_2CO_3	THF	-
4	Pd_2dba_3	P(2-furyl)$_3$	Cs_2CO_3	THF	-
5	$Pd(OAc)_2$	$AsPh_3$	Cs_2CO_3	THF	-
6	Umicore CX21	-	Cs_2CO_3	THF	-

Unfortunately, for all coupling attempts no formation of hexaene II (**131**) was observed, however no HPLC or LC/MS analyses were performed at this stage.

A comparison of this screening with the later successful couplings (Chapter 5.2.5-5.2.6) suggests that THF was an unsuitable solvent for this reaction and probably DMF would have resulted in successful conversions. Particularly under anhydrous conditions, THF does not sufficiently dissolve the base, whereas cesium carbonate exhibits significantly better solubility in DMF or DMSO.[175]

5.2.3 Alternative Stille coupling between central fragment III and Sn-B(pin)-linchpin I

With the first iterative cross coupling strategy failed, a potential second coupling strategy was evaluated. This time, it was tested whether an initial *Stille* coupling between the central fragment III (**132**) and Sn-B(pin)-linchpin I (**113**) would be more feasible.

To test this hypothesis, the western fragment III (**132**) and iododiene **245** were reacted with the corresponding Sn-B(pin)-linchpin I (**113**) accepting the fact, that the methyl group would be temporarily installed at the wrong position in the resulting tetraenes III/IV (**246**/**247**) chain (Scheme 72).

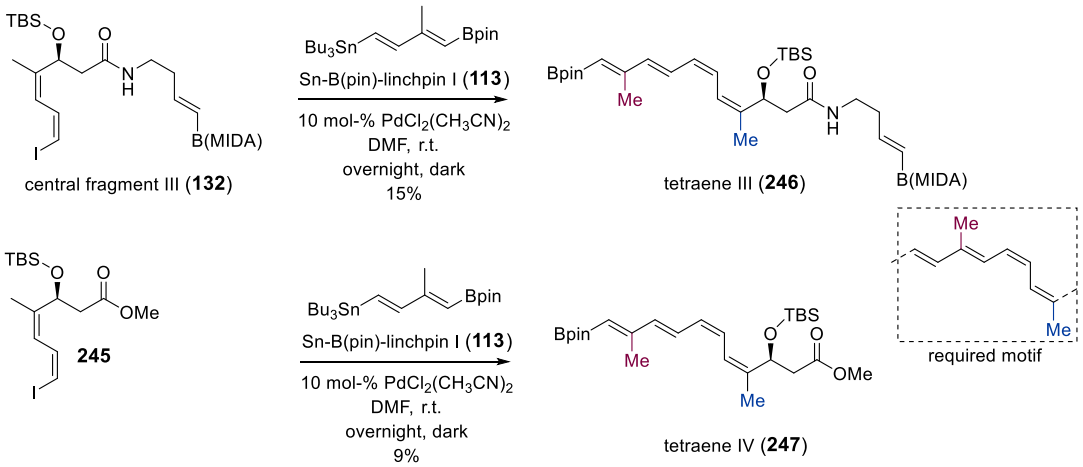

Scheme 71. Evaluation of alternative coupling orders and syntheses of tetraenes **246** and **247** via *Stille* coupling.

Both substrates **132** and **245** were to identical *Stille* coupling conditions as used earlier (Chapter 5.1.1). While both reactions yielded only low amounts of product, the resulting molecules exhibited improved stability toward silica column chromatography.

More importantly, their ^{1}H-NMR spectra featured a well-defined olefinic region, in contrast to the first tetraene II (**134**), as shown in the comparison of the NMR-spectra (Figure 11).

This finding was significant, as it allows for an unambiguous assignment of the olefinic signals and facilitates the interpretation of correlation spectra (COSY, NOESY, etc.).

For this reason, it was reasonable to temporarily accept the lower yields obtained in the *Stille* couplings of substrates **132** and **245**, as the improved stability of the resulting tetraenes III/IV (**246**, **247**) and spectral clarity were of greater importance at this stage.

Although not specifically quantified, it also appeared that the propensity toward isomerization of both new tetraenes III (**246**) IV (**247**) appeared to be lower compared to the previously synthesized tetraene II (**134**) (Chapter 5.1.1) despite possessing two thermodynamically less stable *Z*-configured double bonds compared to only one for tetraene II (**134**).

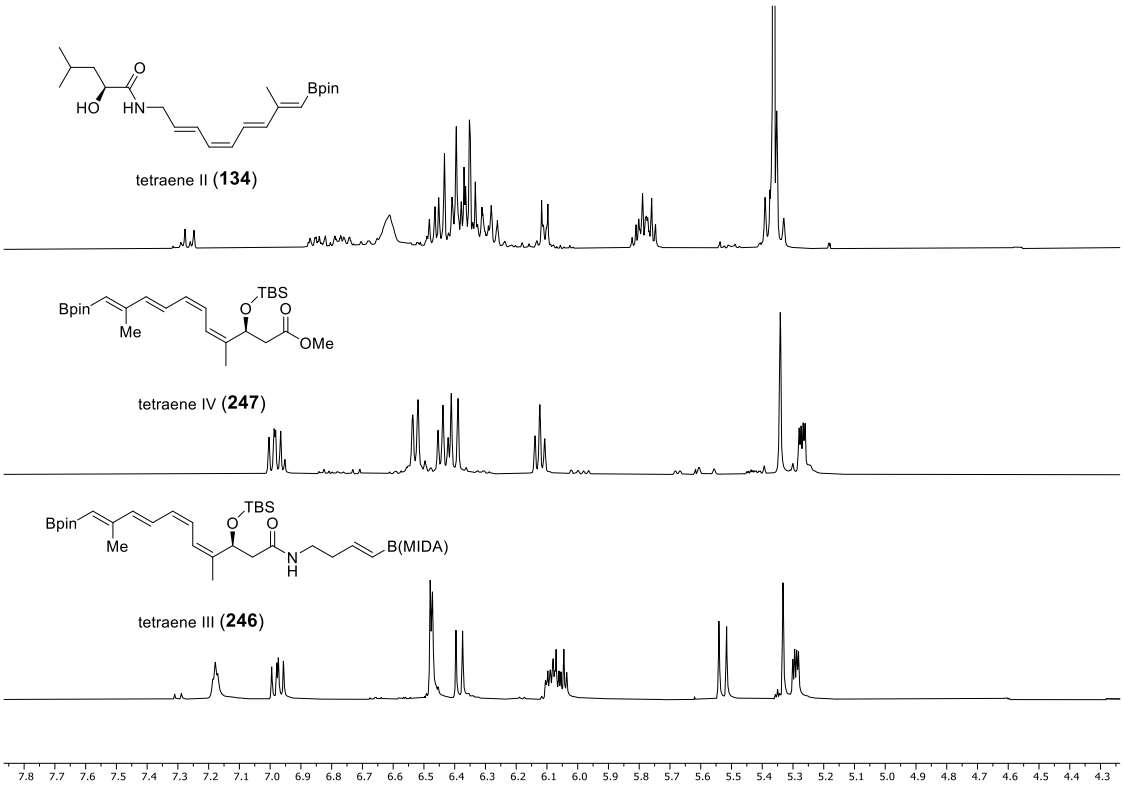

Figure 10. Comparison of the ^{1}H-NMRs (olefinic region) of tetraene II (**134**) (500 MHz, CD_2Cl_2; top), tetraene IV (**247**) (700 MHz, acetone-d6; mid) and tetraene III (**246**) (700 MHz, acetone-d6; bottom) with both tetraenes III (**246**) and IV (**247**) showing a well-defined olefinic region, in contrast to the upper tetraene II (**134**).

5.2.4 Revised coupling approach

Building on these new insights gained from the previously performed *Stille* couplings (Chapter 5.2.3), it was decided to first couple the central fragment III (**132**) with a new Sn-B(pin)-linchpin II (**121**) (Chapter 4.2.3), rather than proceeding with the initially planned coupling sequence (Scheme 72). The difference of the Sn-B(pin)-licnhpins I/II (**113**/**121**) lies in the position of the corresponding methyl group, which now needs to be in β-position to the tin.

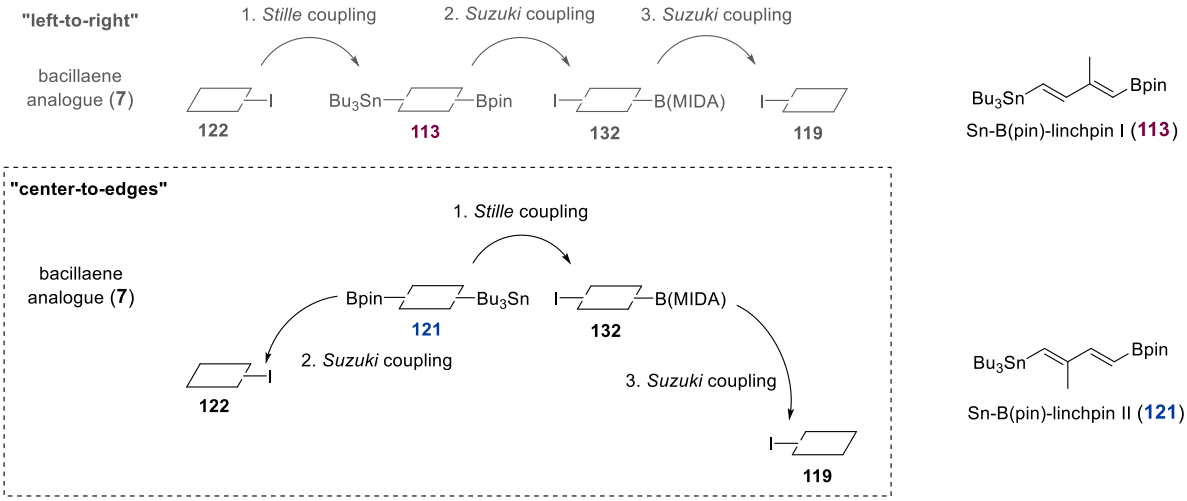

Scheme 72. Schematic representation of the revised synthetic approach for the synthesis of bacillaene analogue (**7**). As Indicated by the arrows, the old approach followed a “left-to-right” approach while the new synthetic approach follows an “inside-out” or “center-to-edges” scheme.

Notably, in contrast to the previous approaches, which followed a linear "left-to-right" approach, this revision introduced a new synthetic direction to build up the molecule from the "center-to-edges".

Here, following a successful *Stille* coupling of the central fragment III (**132**) with the Sn-B(pin)-linchpin II (**121**), an extended bis-boronate central fragment tetraene V (**135**) would be obtained.

Subsequently, the vinyliodide “edges” would be attached to the central tetraene V (**135**) through two sequential *Suzuki* couplings as indicated (Scheme 72). Similar to the previous approaches, a site-discrimination would be facilitated by the different hybridization states (sp^2 vs. sp^3) of the two boron centers bearing either a pinacol boronate or a MIDA-boronate.

5.2.5 Stille coupling between Sn-B(pin)-linchpin II and central fragment III

Next, the *Stille* coupling between the new Sn-B(pin)-linchpin II **(121)** and the central fragment III (**132**) was explored in hope that the high geometrical purity and the well-defined set of signals in the olefinic region of the ^{1}H-NMR, previously observed for the tetraenes III/IV (**246**/**247**) (Chapter 5.2.3), could also be achieved for the required tetraene V (**135**).

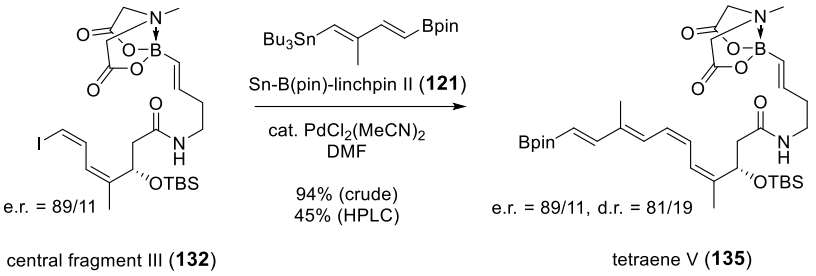

Scheme 73. Synthesis of tetraene V (**135**) via *Stille* coupling between central fragment III (132) with Sn-B(pin)-linchpin II (**121**). Conditions: **121** (2.2 eq.), $PdCl_2(MeCN)_2$ (0.1 eq.), DMF, r.t., 11 h, dark, 94% (crude yield), d.r. = 8.1/1.9, **45%** (isolated yield, semi-prep. HPLC).

When **132** and **121** were reacted under standard *Stille* coupling conditions, full conversion was observed after 11 hours of stirring in the dark. Following the usual work-up, the crude mixture was concentrated, and the residue was redissolved in acetonitrile before being washed several times with *n*-hexane.

The purpose of this secondary extraction was to remove excess Sn-B(pin)-linchpin II (**121**) as well as Bu_3Sn-I, often reported to be troublesome during purifications.[114] Since MIDA-boronates are reportedly insoluble in *n*-hexane[47], this organic/organic extraction provided a simple and effective pre-purification step, eliminating most of the organotin impurities before further purification.

Following this procedure 94% of prepurified crude product was obtained with a good geometrical purity of 81% determined by analytical HPLC. Chiral analytical HPLC also confirmed that the enantiopurity of 89% resulting from the synthesis of the central fragment III (**132**) (Chapter 4.4.2) did not alter during the course of the reaction.

5.2.5.1 Purification and characterization of tetraene-V

Next, purification was achieved by semi-preparative HPLC which gave the fully purified geometrically pure tetraene V (**135**) in 45% yield, followed by full characterization using 1D- and 2D-NMR.

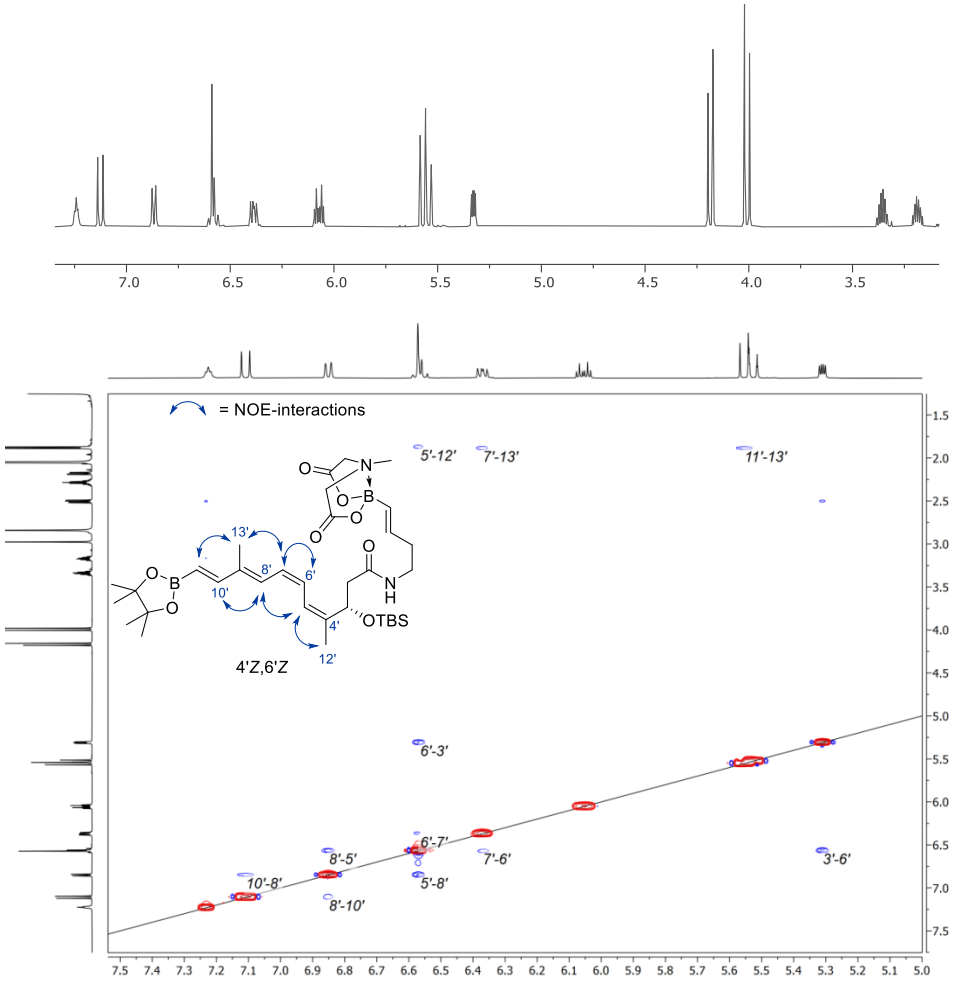

Figure 11. Excerpt of the ^{1}H-NMR spectrum (3.0–7.5 ppm) in acetone-d6 (700 MHz) demonstrating the exceptionally high geometrical purity and defined olefinic region for tetraene V (**135**) (top) and part of the NOESY-spectrum in acetone-d6 (700 MHz) of **135** with key-interactions annotated.

As shown in Figure 12, exceptionally high geometrical purity was achieved after HPLC separation, accompanied with a well-defined olefinic region in the ^{1}H-NMR spectrum, which enabled full characterization and structural assignment. With these well-resolved data in hand, the configuration of the tetraene core was unambiguously verified by NOESY-NMR, which showed well-matching *NOE*-interactions among all hydrogen atoms involved in the conjugated tetraene core.

With this well-working route to tetraene V (**135**) in hand and two remaining *Suzuki* coupling steps ahead, two key tasks had to be addressed:

1. Sufficient material of **135** had to be prepared to comfortably evaluate the upcoming *Suzuki* coupling steps, as they were expected to be challenging. The first coupling would form the sensitive hexaene core, while the second one would need to proceed in the presence of this delicate hexaene system.

2. The undesired enantiomer present in **135**, originating from the cyclocondensation reaction (Chapter 4.4.2), had to be removed prior to the first *Suzuki* coupling to prevent the formation of unwanted diastereoisomers upon introduction of the second stereocenter.

Accordingly, sufficient amounts of the central fragment III (**132**) and Sn-B(pin)-linchpin II (**121**) were resynthesized, and the previously reported *Stille* reaction was performed multiple times in succession to ensure a reliable supply of material and minimize the risk of failure during a single reaction.

Using this strategy, **392 mg** of pre-purified tetraene V (**135**) were synthesized, ready for bulk purification by semi-preparative HPLC.

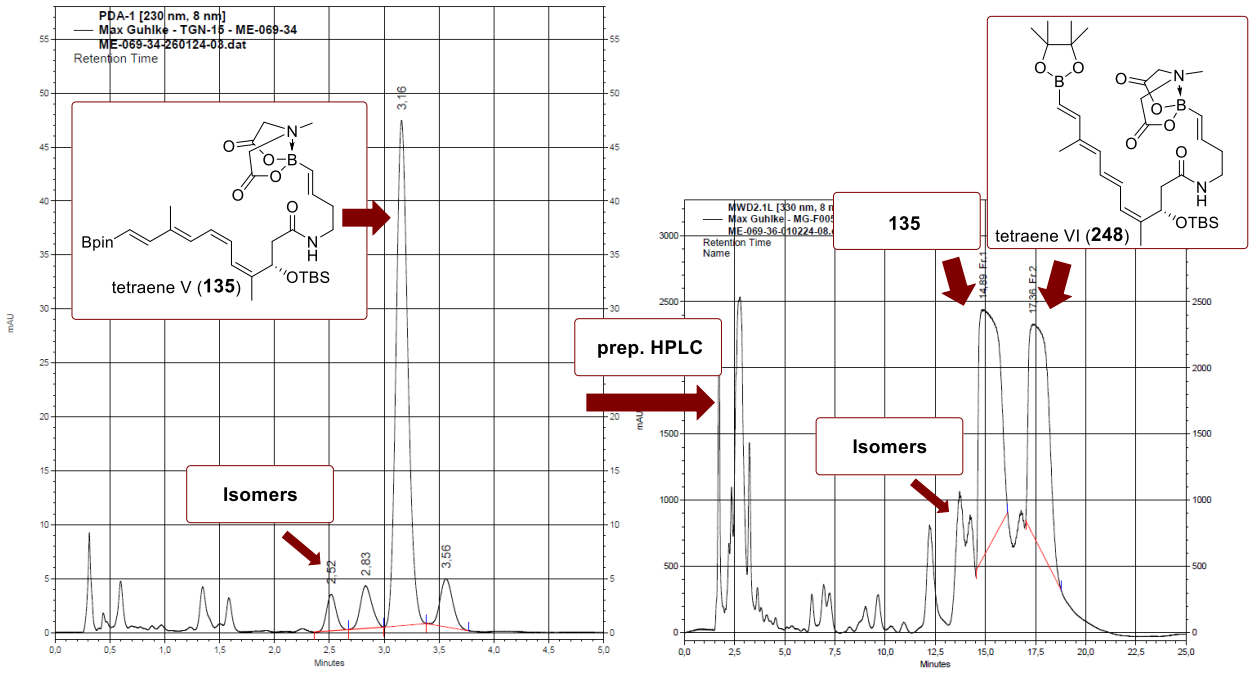

Figure 12. Analytical chromatogram of pre-purified tetraene V (**135**) with a geometrical purity of 80% (left) and chromatogram of the bulk-purification revealing the formation of a second major peak, which was characterized as the 4'*Z*,6'*E*-isomer tetraene VI (**248**).

As shown in Figure 13, significant isomer formation was observed during the bulk purification of tetraene V (**135**), as visible by the appearance of a second dominant peak in the chromatogram. Both major fractions were collected and subsequently analyzed.

The first eluting fraction was identified as the desired tetraene V (**135**), while the second fraction was characterized as the 4'*Z*,6'*E*-isomer tetraene VI (**248**), resulting from the isomerization of the *Z*-double bond to the *E*-double bond at *C*-6'. Similar to tetraene **135**, the isolated isomer **248** was fully characterized by 2D-NMR (Figure 14).

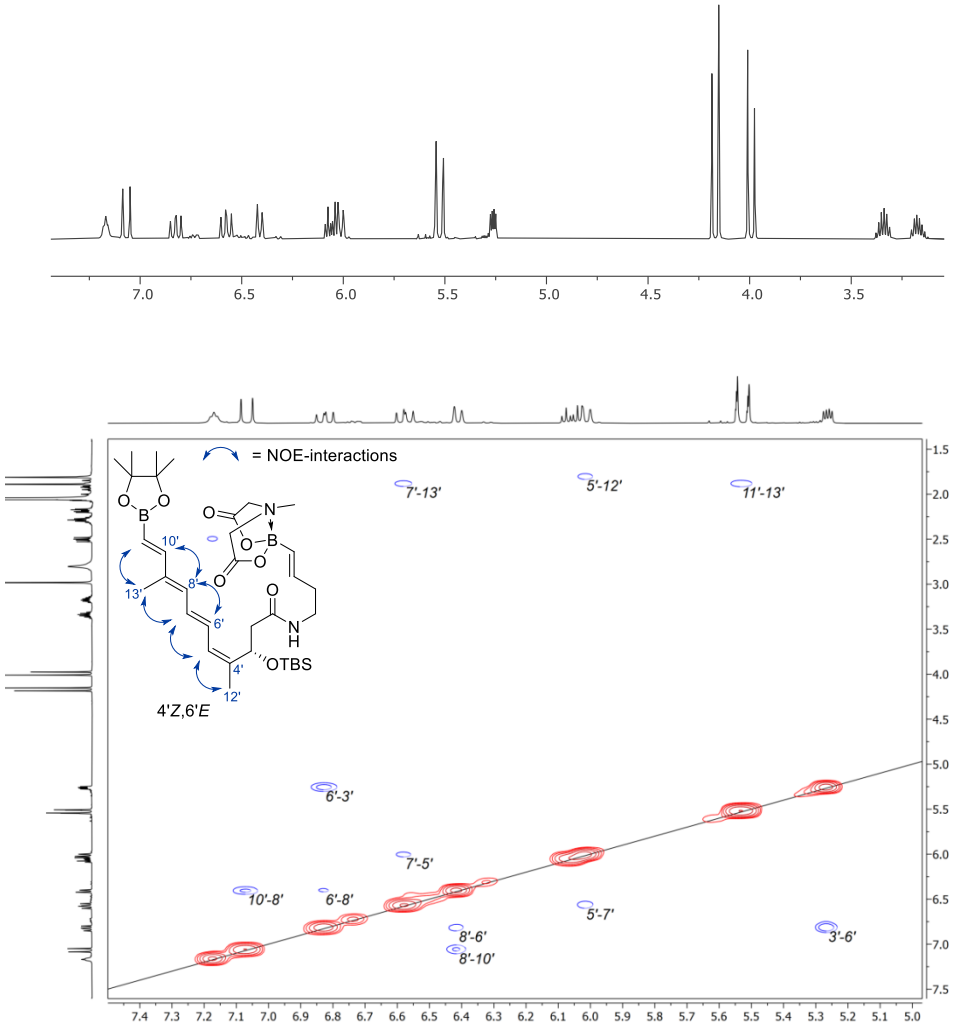

Figure 13. Excerpt of the ^{1}H-NMR spectrum (3.0–7.5 ppm) in acetone-d6 (500 MHz) of the 4'*Z*,6'*E*-isomer tetraene VI (**248**) (top) and part of the NOESY-spectrum in acetone-d6 (500 MHz) of tetraene VI (**248**) with key-interactions annotated.

5.2.5.2 Isolation of the *S*-enantiomer of tetraene-V

As stated at the beginning of this chapter, the undesired enantiomer *R*-**135**, originating from the cyclocondensation reaction (Chapter 4.4.2), had to be removed from the mixture, bearing an enantiomeric ratio (e.r. = 89:11). Given the previously observed isomerization during the bulk HPLC purification, performing a second chiral HPLC separation appeared to be a risky but unavoidable step.

In contrast, when the preparative chiral HPLC separation was conducted, no significant isomerization was observed. However, an early eluting unidentified peak appeared in the chromatogram (Figure 15). After successful isolation of the desired *S*-enantiomer *S*-**135**, a purity control experiment confirmed that the *S*-**135** had indeed been fully separated from *R*-**135**.

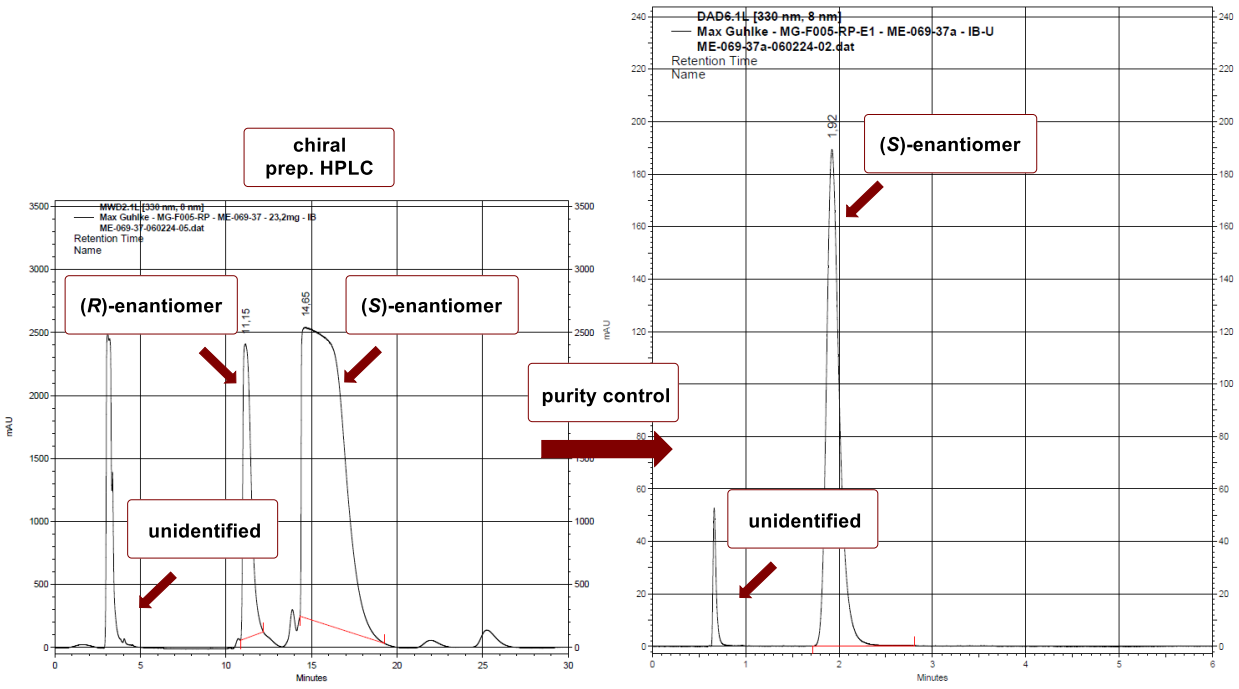

Figure 14. Chromatogram of the semi-preparative chiral HPLC conducted for the isolation of *S*-**135** (left) and chromatogram of the purity control experiment performed after the separation of *S*-**135**, revealing the presence of an early eluting unidentified peak.

Nonetheless, the reappearance of the early eluting unidentified peak in the purity control suggests that it results from degradation of **135**.

After performing the achiral and chiral HPLC purification steps, the initial 392 mg of pre-purified tetraene **135** were reduced to only 78 mg of remaining material (20%).

A confusing inconsistency was the isomerization behavior of **135**. While severe isomerization occurred during the semi-preparative bulk purification, no isomerization was observed during analytical HPLC runs or chiral semi-preparative HPLC runs.

To investigate potential factors influencing this behavior, the specifications of the individual HPLC runs were compiled into a table (Table 7.) and compared, aiming to identify possible conditions that may have triggered the isomerization.

Table 7. Comparison of the different HPLC conditions aiming to identify factors that may have contributed to the isomerization of **135**.

spezifications	analytical	semi-preparative	chiral semi-preparative
column	MACHEREY-NAGEL Nucleodur 100-3 Gravity C18	MACHEREY-NAGEL Nucleodur 100-5 Gravity C18	DAICEL Chiralpak IB
column material	C18 (RP18, ODS, octadecyl)	C18 (RP18, ODS, octadecyl)	modified cellulose; silica matrix
particle size	3 µm	5 µm	5 µm
solvent	MeCN/H_2O 3:1	MeCN/H_2O 3:1	*n*-hexane/EtOH 4:1
gradient	isocratic	isocratic	isocratic
pressure	173 bar	163 bar	107 bar
flow rate	0.5 mL/min	26 mL/min	18 mL/min
detector	UV	UV	UV
isomerization	**no**	**yes**	**no**

The most critical factor potentially influencing the isomerization of **135** is UV detection, as UV-induced isomerization of polyenes is a well-documented phenomenon.[176,177] However, since the collected and analyzed fractions exhibited excellent geometrical purity, the isomerization must have occurred prior to detection. If isomerization had taken place during detection, multiple isomers would have been present in the collected fractions, which was not observed. This suggests that a different factor, occurring at an earlier stage of the purification process, was indeed responsible for the isomerization.

The next critical parameter to consider is the stationary phase, which differed between the semi-preparative runs (RP vs. modified cellulose) but was identical in the analytical runs. Since no

isomerization was observed in the analytical runs, the stationary phase itself cannot be considered the trigger for isomerization.

In fact, none of the factors listed (Table 7) can clearly identify a single explicit cause for the observed isomerization. Therefore, together with my master student *Tra Giang Nguyen,* we decided to further investigate the factors causing isomerization of tetraene **135**.[178]

5.2.5.3 Stability studies of tetraene V

Based on the previous observations, an experiment was designed to determine which physicochemical parameters would have the greatest influence on the isomerization of tetraene V (**135**).

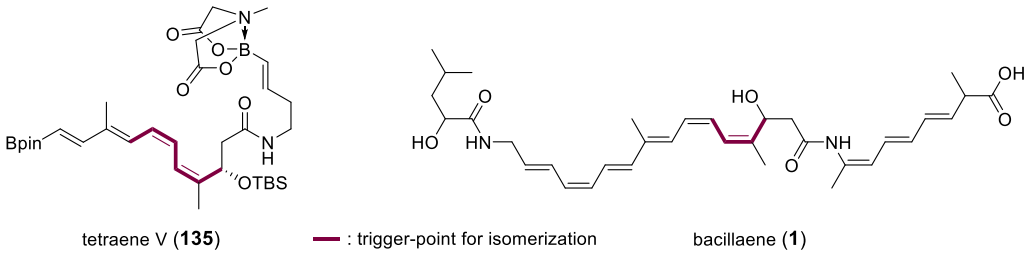

Figure 15. The identified trigger-point for isomerization for tetraene V (**135**), which matches the reported decomposition trigger-point of the natural product bacillaene (**1**).

Since bacillaene (**1**) has been reported to exhibit instability towards light, air, heat[13] and even a concentration-dependent degradation,[20] we decided to systematically investigate the influence of these parameters on the stability of tetraene V (**135**). To test this, an experiment was designed using a stock solution (75 µM) of tetraene **135** in degassed acetonitrile, which was then distributed into several vials and exposed to various physicochemical conditions (Table 8). After 1, 2, 4 and 24 hours of exposure, analytical HPLC was performed to assess whether isomer formation had occurred or if the compound remained stable under given conditions.

Table 8. List of physicochemical conditions to which the individual test vials of **135** were exposed.

Concentration	Irradiation wavelength	Tempterature	Oxygen
0.15 µM	310 nm	40 °C	atmospheric oxygen
1.5 µM	325 nm	60 °C	oxygen saturated solution
15 µM	365 nm	80 °C	
75 µM	white light (>400 nm)		

Unless stated otherwise for the concentration-dependent experiments (Table 8), all experiments were conducted at a concentration of 75 µM**.** All experiments were performed in the dark and irradiation experiments were conducted in the absence of other light sources.

Interestingly, no isomerization of **135** was detected when exposed to air, oxygen and temperatures up to 80 °C even after prolonged exposure of 24 hours. A decomposition threshold temperature was not determinded.

However, exposure to light within its absorption region at λ_{ex} = 310, 325 and 365 nm resulted in rapid isomerization, giving three additional isomers (Figure 17), corresponding to *E*/*Z*-isomerization of one or both *Z*-double bonds, in agreement with a previous report on bacillaene (**1**).[20] After 1 hour of irradiation, only 19-30% of original 4'*Z*,6'*Z*-isomer remained with complete decomposition after 24 hours of irradiation.

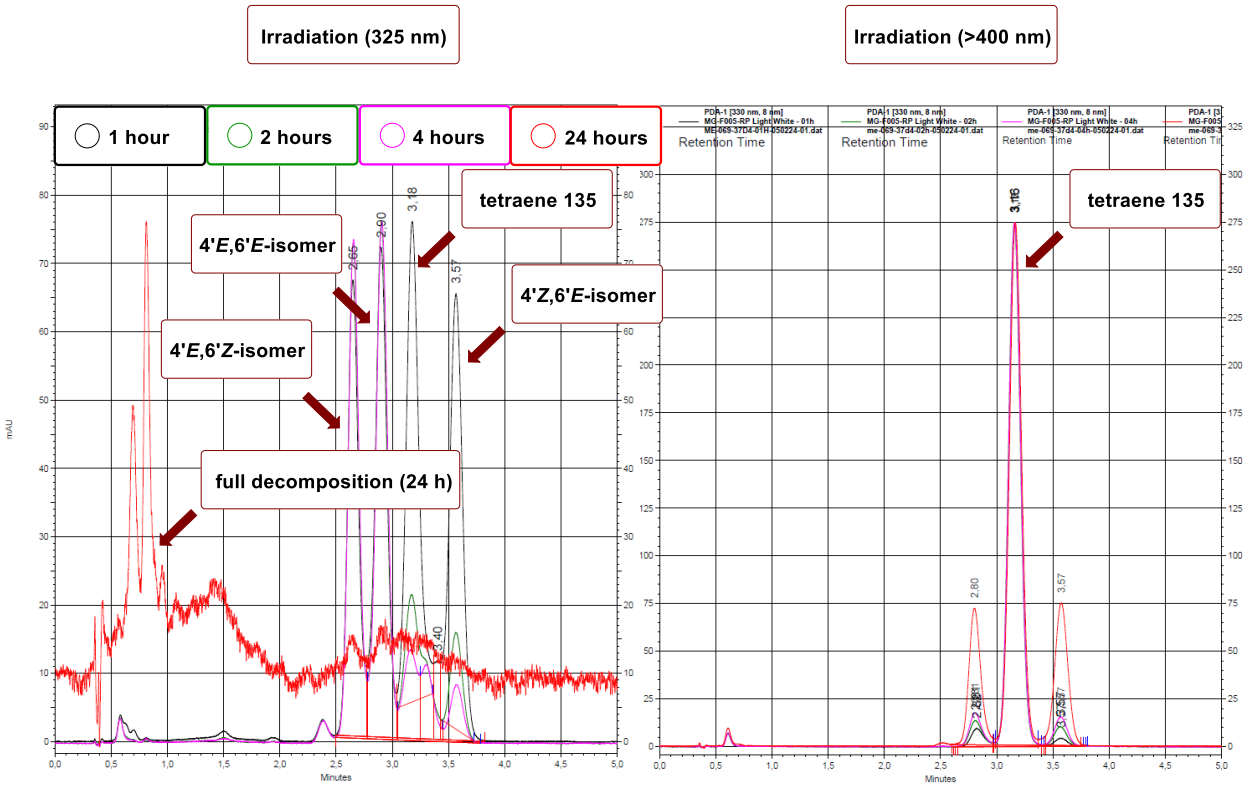

Figure 16. Superimposed chromatograms (analytical HPLC) obtained from the irradiation experiments of tetraene **135** after 1, 2, 4 and 24 hours using irradiation wavelengths λ_{ex} = 325 nm (*left*) and λ_{ex} > 400 nm (*right*).

While the original tetraene **135** and the 4'*Z*,6'*E*-isomer **248** had been fully characterized (Chapter 5.2.5.1), the two additional isomers observed at retention times of t_R = 2.65 min and t_R = 2.90 min were assigned without further analytical confirmation. This means that their assigned double bond configurations could either be incorrectly assigned (swapped) or even result from isomerization of other double bonds within the conjugated system. However, it can be assumed that the thermodynamically less stable *Z*-double bonds are indeed more prone to isomerization than the *E*-configured double bonds within this system.

A definitive structural assignment could have been achieved by irradiating **135** with a 325 nm light source for 4 hours, followed by semi-preparative HPLC separation of all isomers and subsequent NMR analysis. However, due to the limited availability of **135**, this approach was not further pursued.

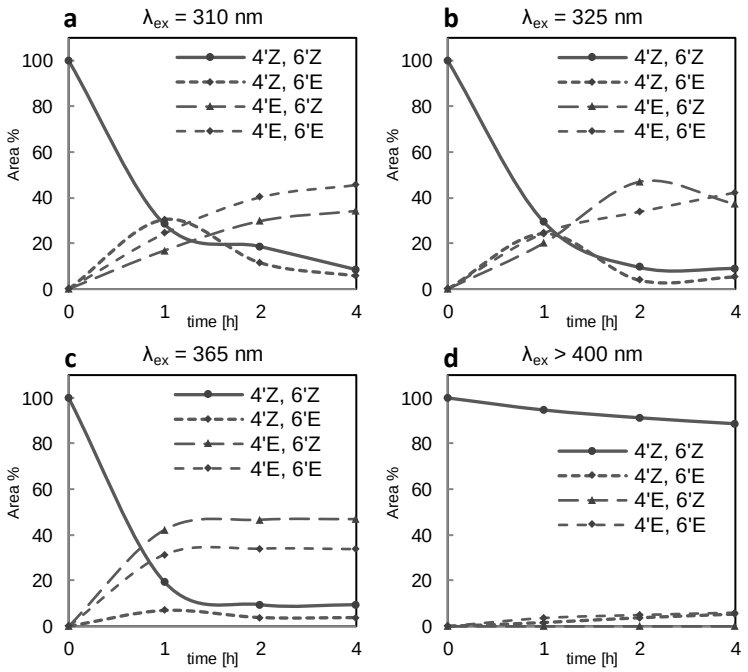

Figure 17. Isomeric profile of **135** (75 µM in MeCN) based on HPLC peak area percentages upon irradiation with various light sources: a) λ_{ex} = 310 nm; b) λ_{ex} = 325 nm; c) λ_{ex} = 365 nm; d) λ_{ex} > 400 nm (white light). For original chromatographic data see appendix.

The stability studies revealed that tetraene **135** is highly prone to isomerization under exposure of UV-light within its absorption band. Good stability was observed towards irradiation of longer wavelengths >400 nm outside the absorption band of **135**, exposure to oxygen, and temperatures up to 80 °C.

Moreover, the observed trigger-point for isomerization of tetraene **135** matches the reported one for bacillaene (**1**).[20]

While these experiments did not fully clarify the isomerization observed during semi-preparative HPLC purification, they provided valuable insights into the compound's stability. This knowledge is valuable for determining which physicochemical conditions should be avoided during handling of this compound and also reveals a safe operational window of conditions for further reactions such as temperature.

5.2.6 *Suzuki*-coupling between tetraene V and western fragment II

With a usable quantity of both highly (enantio)pure tetraene V (**135**) and western fragment II (**122**), the next major challenge was the formation of the sensitive hexaene core by a *Suzuki* cross-coupling. Besides the propensity towards isomerization, this step also presented a significant challenge due to the presence of two boron centers in the molecule, requiring carefully chosen reaction conditions to prevent deprotection and undesired coupling at the MIDA-bearing site.

A critical factor was the exclusion of water from the reaction mixture to avoid the formation of hydroxide ions, potentially triggering a hydrolysis of the MIDA-boronate. However, *Suzuki* couplings are known to proceed sluggishly under strictly anhydrous conditions, often due to the poor solubility of inorganic bases. To address this problem, suitable conditions were developed by *Burke* and coworkers using $Pd(dppf)Cl_2$ or XPhos Pd G2 with $NaHCO_3$ or Cs_2CO_3 in anhydrous DMSO providing good yields while preventing deprotection of the MIDA-boronates under these conditions.[49]

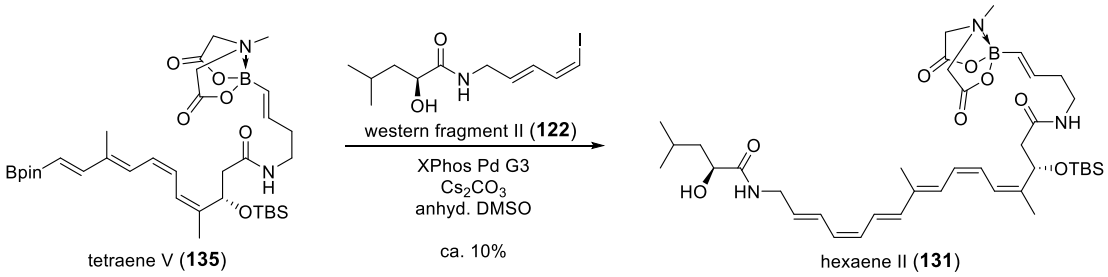

Scheme 74. Initial coupling tetraene V **135** with the western fragment II (**122**) using anhydrous reaction conditions devolped by *Burke* and co-workers. Low conversions and significant isomer formation was observed. Conditions: **122** (2.0 eq.), XPhos Pd G3 (0.1 eq.), Cs_2CO_3 (3.5 eq.), DMSO, r.t., 18 h.

However, when these conditions were applied to the given system, only low conversions were observed in combination with significant isomer formation after 18 hours of stirring in the dark (Scheme 75).

As the catalyst was assumed to be the most influential parameter for this reaction, the first priority was the identification of a suitable catalyst.

5.2.6.1 Catalyst screening

As outlined above, the primary goal of the catalyst screening was to identify a system capable of achieving high conversions in the *Suzuki* coupling while maintaining the stereochemical integrity of the double bonds (Scheme 76).

To achieve this, a screening protocol was designed that allowed for the efficient evaluation of catalysts, with subsequent analysis performed by analytical HPLC.

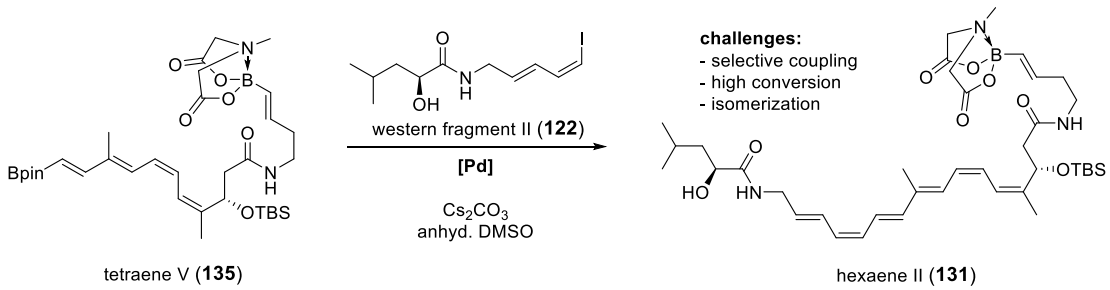

Scheme 75. The three major challenges faced during the Suzuki coupling between tetraene V (**135**) and western fragment II (**122**) (selectivity, conversion, and isomerization) intended to be addressed through a catalyst screening.

With a vinyl pinacolboronate as the nucleophile, slow transmetalation was one of the main concerns related to this reaction.[144] To address this, the catalyst selection not only included the (pre)catalysts used by *Burke* and co-workers (Xphos, SPhos, dppf) but also electron-poor catalysts such as JackiePhos[179] and P(o-Tol)$_3$, which has been reported to help retain the *Z*-geometry during *Suzuki* couplings.[180] As a reference, also Pd(PPh$_3$)$_4$ was added to the selection.

In order to obtain, high quality samples for HPLC analysis, a solid-phase extraction (SPE) protocol was developed to extract the organic content from the crude reaction mixture. This approach ensured a clean and reproducible sample preparation for subsequent HPLC analysis.

Next, a stock solution of **135** and **122** in anhydrous DMSO was prepared and distributed into reaction flasks containing pre-weighed catalyst (0.2 eq.) along with cesium carbonate (3.0 eq.). The reactions were stirred at 40 °C in the dark for 9 hours. Upon completion, the mixtures were quenched with a threefold volume of saturated NH_4Cl, loaded onto C18 SPE cartridges, washed with H_2O/MeOH (95:5), and eluted with pure acetonitrile. The collected fractions were then analyzed by HPLC (Scheme 77).

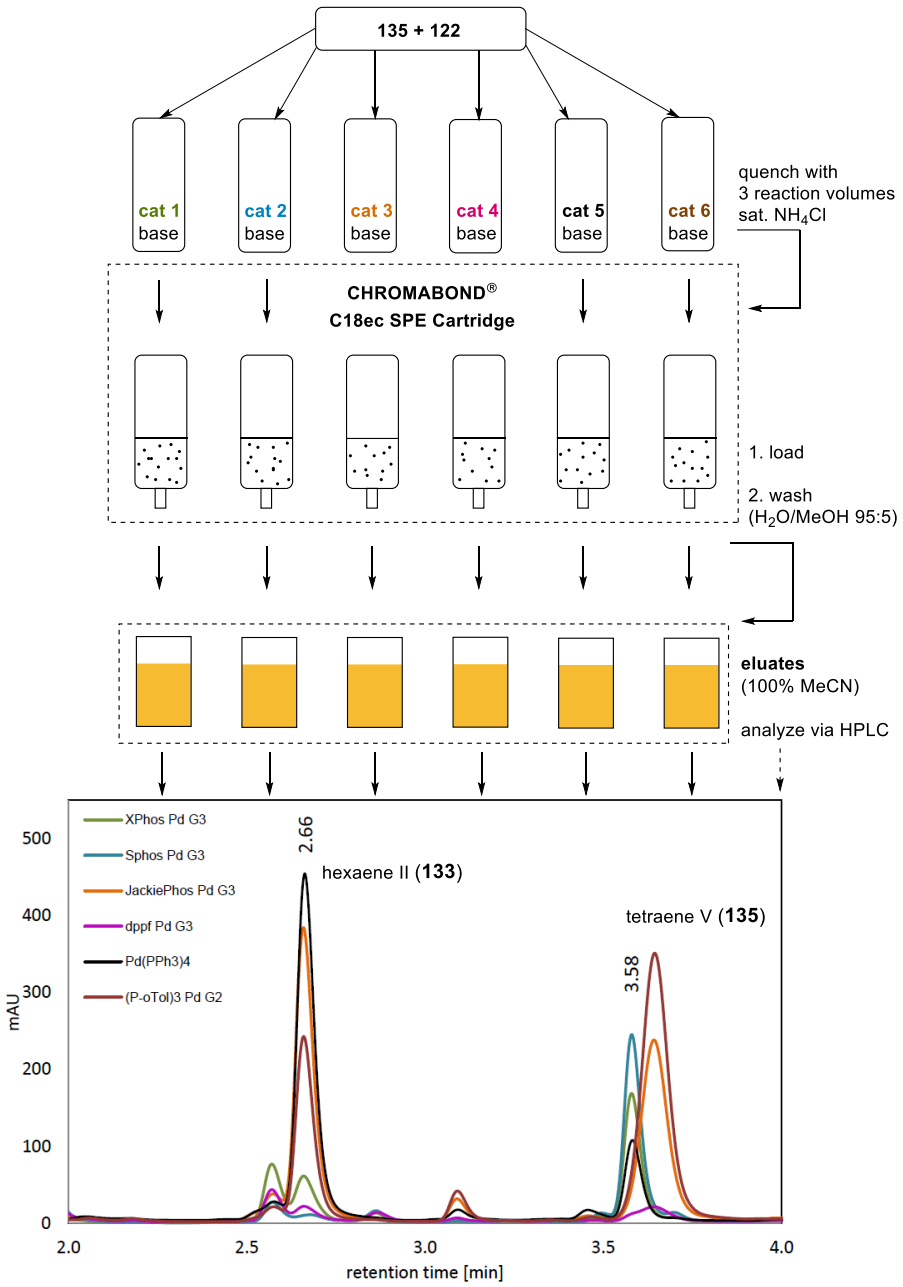

Scheme 76. Schematic illustration and results of the catalyst screening for the synthesis of hexaene II (**133**). XPhos Pd G3 (green), SPhos Pd G3 (blue), JackiePhos Pd G3 (orange), dppf Pd G3 (violet), $Pd(PPh_3)_4$ (black), $(P\text{-}o\text{-}Tol)_3$ Pd G2 (brown). The starting substrate tetraene V (**135**) appears at a retention time t_R = 3.58 min and the resulting hexaene II (**133**) at t_R = 2.66 min.

The screening revealed significant differences in catalyst performance. The biaryl-type ligands (SPhos, XPhos) and dppf resulted in low conversions and notable double bond isomerizations.

In contrast, electron-deficient ligands such as JackiePhos and $P(o\text{-}Tol)_3$ delivered better conversions, however with a shift in retention time of the starting material. The most promising outcome was

obtained with the classical $Pd(PPh_3)_4$ catalyst, which provided near-complete conversion and minimal isomerization, making it the best choice for the coupling step.

5.2.6.2 Base screening

With the optimal catalyst identified, the coupling reaction initially was scaled up to 10 mg. Despite careful handling, low conversions were observed prompting further optimization of the reaction conditions. The next key parameter to adjust was the base, as *Suzuki* couplings are known to proceed under a wide range of inorganic bases.

To efficiently track the conversion of tetraene V (**135**) to the corresponding hexaene II (**132**), a reliable analytical method was required. While an SPE-HPLC protocol was considered, similar to the one used during catalyst screening (5.2.6.1), it was deemed too time- and resource consuming for further reaction monitoring.

Since the UV/vis spectra of both compounds differed significantly, with an absorption maximum of λ_{max} = 328 nm for tetraene V (**135**) and λ_{max} = 363 nm for hexaene II (**132**), determined within previous HPLC analyses, the feasibility of UV/vis spectroscopy for reaction monitoring was explored.

A UV/vis monitoring would leverage the bathochromic shift that occurs as the conjugated polyene system extends, due to a decreasing gap between highest occupied molecular orbital (HOMO) and lowest unoccupied molecular orbital (LUMO) energies.[181]

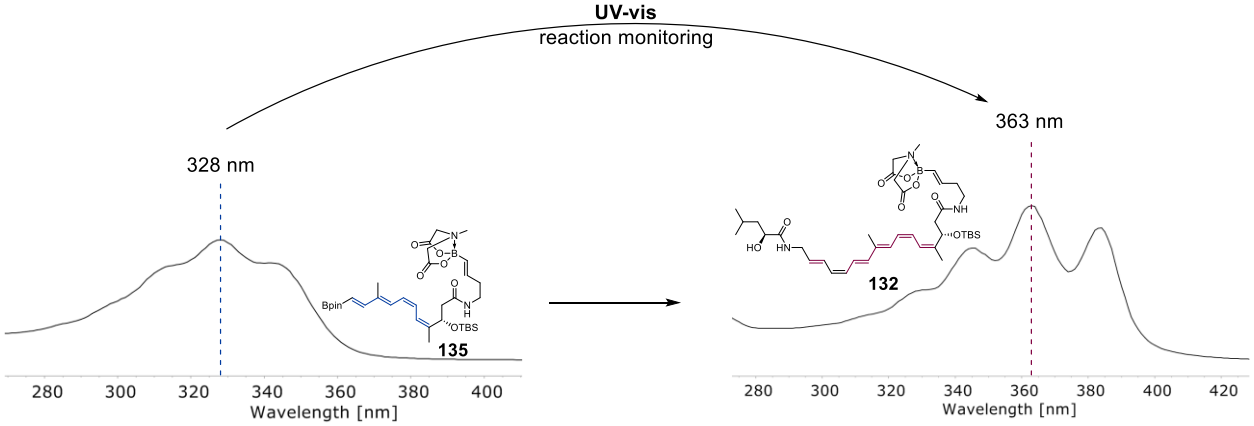

Scheme 77. Comparison of the UV/vis spectra and absorption maxima of tetraene V (**135**) (left) and hexaene II (**132**) (right), illustrating the bathochromic shift and the rationale for monitoring product conversion using UV/vis spectroscopy.

Initial concerns that the presence of palladium species in the reaction mixture might mask the polyene absorption bands due to overlapping charge-transfer transitions[182] proved unfounded. In fact, an initital

test coupling revealed that the expected absorption bands of the polyene systems of **135** and **132** remained clearly distinguishable in presence of the palladium catalyst.

Next, a selection of bases was prepared including standard inorganic bases, such as cesium carbonate (Cs_2CO_3) and potassium phosphate (K_3PO_4), as well as organic bases, such as sodium ethoxide (NaOEt) and potassium *tert*-butoxide (KO*t*Bu). Additionally, more "exotic" bases such as silver oxide (Ag_2O) and thallium carbonate (Tl_2CO_3) were tested. Furthermore, potassium trimethylsilanolate (KOTMS) was included in the screening, as it was reported by *Denmark et al.* to perform particularly well in anhydrous *Suzuki* couplings.[183]

For the screening, a stock-solution of tetraene V (**135**) and western fragment III (**122**) was prepared. A second stock solution containing the $Pd(PPh_3)_4$ catalyst was prepared separately. Next, both stock solutions were sequentially added to the flasks containing various pre-weighed bases. After 5 hours and 19 hours of reaction time, a small sample was drawn from the reaction mixtures, diluted with acetonitrile and analyzed by UV/vis spectroscopy.

Table 9. Measured absorbances and calculated conversions for the polyene iteration step from tetraene V (**135**) to hexaene II (**132**) with various bases after 5 hours and 19 hours; [a] decomposition was observed; [b] Formation of a new polyene-peak was observed with λ = 287 nm, 300 nm, 315 nm (indicative of triene) presumably due to coupling of **122** with the MIDA-bearing site.

Base	**$A_{328\ nm}$ [a.u.],** 5 hours	**$A_{383\ nm}$ [a.u.],** 5 hours	**conversion,** 5 hours	**$A_{328\ nm}$ [a.u.],** 19 hours	**$A_{383\ nm}$ [a.u.],** 19 hours	**conversion,** 19 hours
Cs_2CO_3	0.702	0.196	21%	0.344	0.155	26%
CsOAc	0.531	0	-	0.681	0	-
NaOEt	0.515	0.173	21%	0.231	0.114	28%
KOtBu	0[a]	0[a]	-	n.d.[a]	-	-
KOTMS	0[a]	0[a]	-	n.d.[a]	-	-
Tl_2CO_3	**0.494**	**0.635**	**51%**	**0**	**0.764**	**100%**
Ag_2O	0.640	0	-	n.d.	n.d.	-
K_3PO_4	0.465	0.425	-	0	0.885	100%[b]

A detailed instruction for the calculation of product conversions is provided in the Experimental Section.

As summarized in Table 9, the base screening revealed significant differences in conversion efficiency depending on the choice of base. While some bases, such as cesium acetate (CsOAc) and silver(I) oxide (Ag_2O), resulted in no conversion, the strong organic bases potassium *tert*-butoxide (KO*t*Bu) and potassium trimethylsilanolate (KOTMS) led to decomposition of the starting material.

This decomposition was likely caused by dehydrohalogenation, as a rapid reaction was observed even before addition of the catalyst stock solution, a phenomenon similar to that described in Chapter 6.3.4.

In contrast, full conversion was observed with potassium phosphate (K_3PO_4) and thallium carbonate (Tl_2CO_3). However, the use of potassium phosphate resulted in the appearance of a new polyene absorption peak. The UV/vis maxima of this peak (λ = 287 nm, 300 nm, 315 nm) suggested that it likely originated from a deprotection and reaction at the MIDA-bearing site, leading to the formation of a triene upon reaction with the western fragment II (**122**).

While the precise role of thallium in Suzuki couplings remains poorly understood, this screening once again confirmed the impact of the "thallium effect".[184,185] An older study suggested that thallium may form a supernucleophilic borate-thallium complex,[186] potentially accelerating the transmetalation step. More recent studies have highlighted the inhibitory effect of iodide in *Suzuki* couplings,[187] suggesting an alternative explanation. The observed rate enhancement may simply arise from the precipitation of insoluble thallium(I) iodide (TlI). Therefore, the thallium may act as an iodide scavenger.

5.2.6.3 Role of the solvent

With the optimized catalyst and base identified, the next step was to investigate the influence of the solvent on the reaction. This was again screened by tracking the conversion via UV/vis spectroscopy. For the reaction, three polar aprotic solvents were evaluated (DMSO, DMF, MeCN).

Although a *Suzuki* reaction using $Pd(PPh_3)_4$, Tl_2CO_3, and MeCN has been previously reported,[186] it was surprising that no conversion was observed under these conditions.

In contrast, reactions run in DMF proceeded slightly faster (17 h) compared to those in DMSO (19 h). Given its slightly faster reaction time, DMF was chosen as the preferred solvent for this coupling.

5.2.6.4 Purification, isolation and characterization of hexaene II

With the optimized reaction conditions established, the next step involved a careful upscaling to a 5-8 mg scale, while developing an efficient isolation protocol for this highly sensitive polyene **132**. Since direct injection into semi-preparative HPLC was ruled out, solid-phase extraction (SPE) was again considered as a purification strategy (Scheme 79).

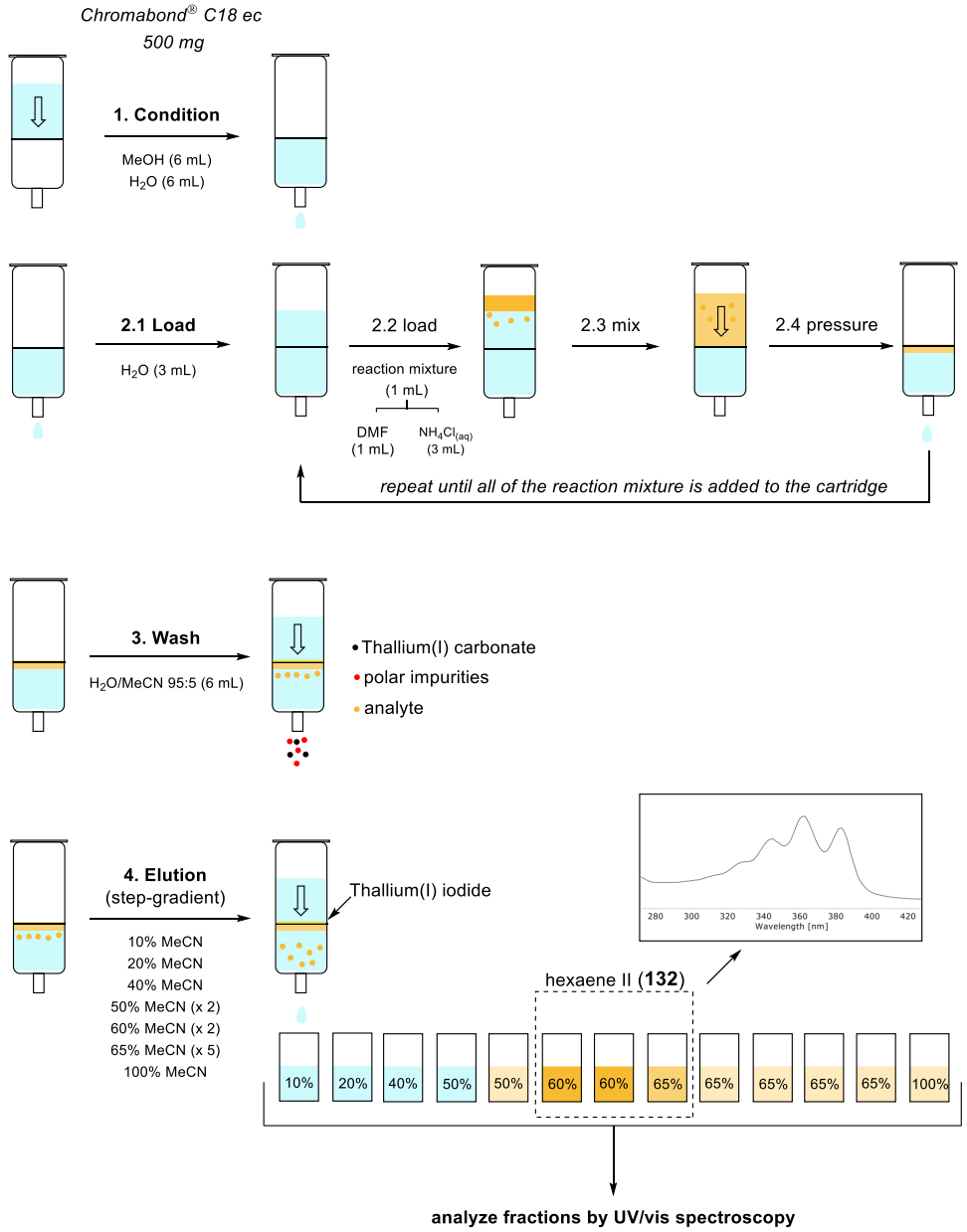

Scheme 78. SPE purification method for the isolation of hexaene II (**132**) from the reaction mixture. The procedure was conducted in a subdued-light environment to ensure minimal isomerization and delivered reproducible results. Additionally, the toxic thallium(I) iodide (TlI) was effectively immobilized on the cartridge, allowing its safe disposal after the process.

The idea was to load the crude reaction mixture, after quenching with saturated NH_4Cl, onto an RP-cartridge (500 mg bed size). After an initial washing step, the product should be eluted with a step-gradient of MeCN/water, gradually increasing the organic content.

An initial assessment of this method using tetraene V (**135**) revealed that **135** eluted at 70% MeCN. Given the higher polarity of hexaene II (**132**), elution of **132** was expected within the 50–65% MeCN range. However, to prevent analyte breakthrough during the loading steps, the quenched reaction mixture had to be further diluted with water. This, unfortunately, caused precipitation of the crude mixture, which disrupted loading and led to poor recoveries.

To overcome this issue, an alternative loading method was developed:

1. After initial conditioning, water (3 mL) was added to the headroom of the cartridge.
2. Next, a portion (1 mL) of the quenched reaction mixture was then carefully mixed with this previously added water and slowly loaded using positive pressure.
3. This step was repeated until the entire crude mixture was successfully loaded onto the cartridge.
4. After each loading step, the collected solvent was analyzed by UV/vis spectroscopy to detect any analyte breakthrough.

After two washing steps with MeCN/H_2O (5:95), the step-gradient elution was performed by gradually increasing the acetonitrile content. UV/vis analysis of the collected fractions confirmed that the 60-65% MeCN fractions showed the expected absorption spectrum of hexaene II (**132**).

Next, the collected fractions were evaporated, and the resulting pre-purified **132** was immediately submitted to analytical and semi-preparative HPLC (Figure 19). Analytical HPLC confirmed that the product had been successfully isolated with the SPE-method, with only minor isomeric impurities present.

Subsequent semi-preparative HPLC enabled the isolation of hexaene II (**132**) with a yield of 50% and an excellent geometrical purity of 96%, verified by a reinjection and analytical HPLC from the eluate.

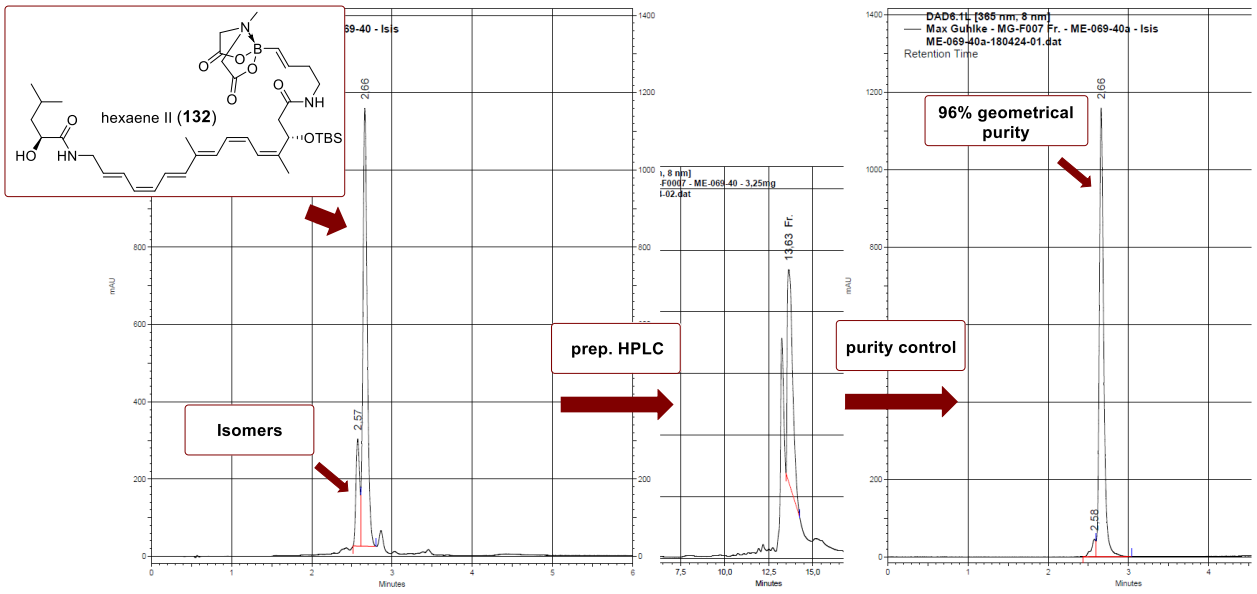

Figure 18. Chromatograms of the hexaene II (**132**) after the SPE-purification protocol (left), semi-preparative HPLC run (middle) and the purity control experiment revealing an excellent geometrical purity of 96% (right).

After purification by semi-preparative HPLC, the eluate was immediately evaporated, and the residue was dissolved in acetone-d6 for NMR analysis (Figure 20).

To obtain an NMR sample comparable to the published data for bacillaene (**1**), the coupling and purification sequence was repeated, and the sample was subsequently measured in MeOD. Unfortunately, on both experimental days, the high-resolution (700 MHz) NMR-spectrometer suffered from shimming issues, resulting in slightly distorted peak shapes in the spectra.

Additionally, the appearance of minor peaks in the olefinic region suggests that some isomerization had occurred between HPLC separation and NMR analysis, likely during solvent evaporation, despite this step being performed in the dark. To confirm this, an analytical HPLC run of the NMR sample prior to NMR measurements should have been conducted. Also either lyophilization or SPE-NMR[188] is recommended to prevent isomerization between HPLC purification and NMR data acquisition.

Nevertheless, the identity and stereochemistry of the hexaene II (**132**) were successfully assigned using 2D-NMR techniques. However, NOESY-NMR analysis was partially hindered by signal overlap, as indicated (Figure 20).

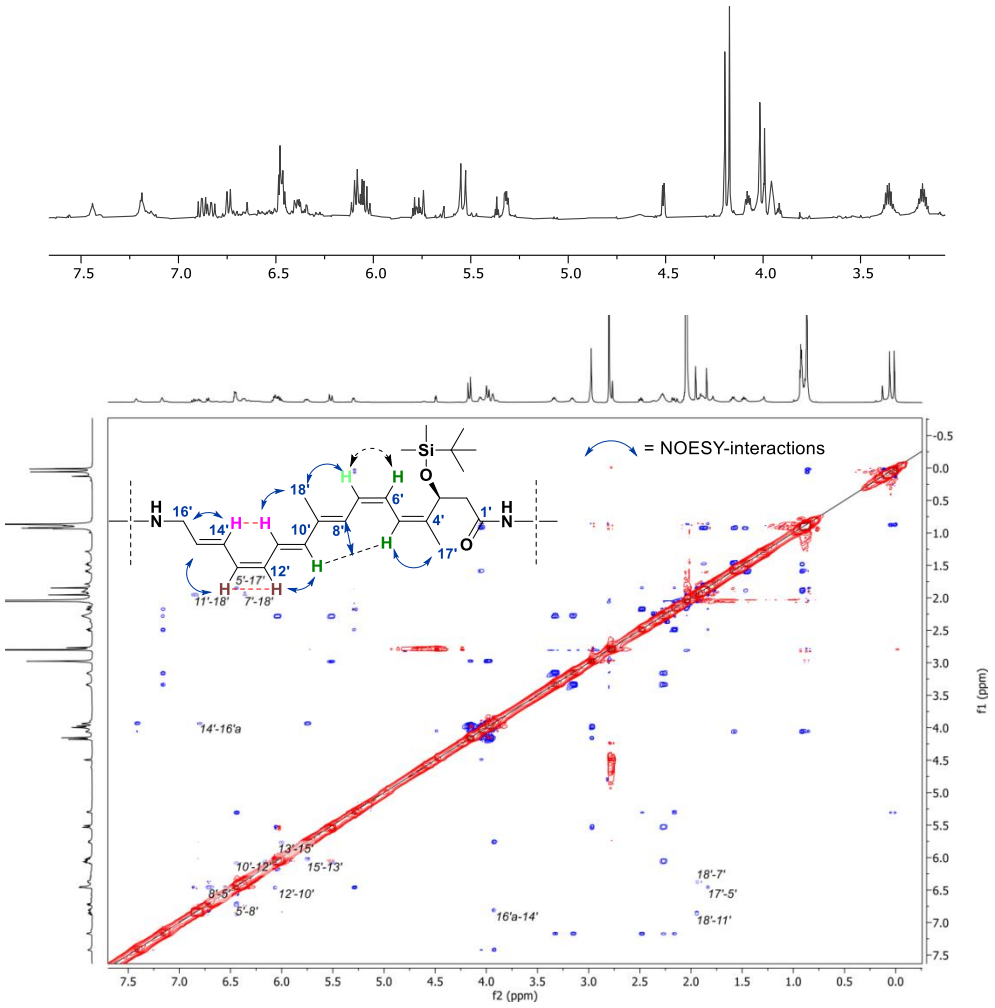

Figure 19. Excerpt of the ^{1}H-NMR spectrum (3.0–7.5 ppm) in acetone-d6 (700 MHz) of hexaene II (**132**) (top) and part of the NOESY-spectrum in acetone-d6 (700 MHz) of **132** with key-interactions annotated. Protons of the same color belong to the same multiplet; one single interaction of 8'-10' and 8'-5' is observed; interaction of 6'-7' is too close to the diagonal for an accurate detection.

The measurement of the second sample of **132** in MeOD-d4 demonstrated good agreement between the identical subunits of **132** and the published NMR-data for bacillaene (**1**) (see experimental section).

Notably, these measurements were the first direct acquisition of ^{13}C-NMR data for the hexaene core, whereas the previously published data for bacillaene (**1**) only provided ^{13}C-NMR shifts obtained from the extrapolation of HMBC cross-peaks.[22]

The largest deviations in the ^{1}H-NMR spectrum were observed in the *C1'–C3'* region, likely due to the presence of the TBS protecting group and the absence of the adjacent enamide structure in **132**.

Additionally, the opposite stereochemistry at *C*3' in **132**, compared to the bioinformatically predicted[16] configuration of *C*3' for bacillaene (**1**), suggests that these deviations may also arise from an incorrect stereocenter. However, the absolute confirmation of the stereochemistry may only be achieved through a total synthesis of the authentic natural product.

5.2.6.5 Summary of the hexaene synthesis

In summary, the highly challenging *Suzuki* coupling between tetraene V (**135**) and western fragment II (**122**) providing the hexaene core (**132**) of bacillaene (**1**) was accomplished with an isolated yield of 50% and a remarkable geometrical purity of 96%. The geometry of the hexaene scaffold of bacillaene (**1**) was confirmed by NMR-comparison with published data (see experimental section).

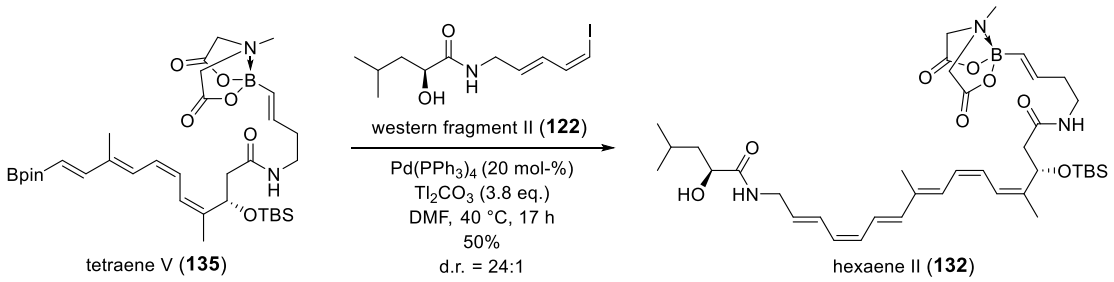

A catalyst screening (5.2.6.1) revealed that the stereochemical integrity of the double bonds is highly dependent on the nature of the catalyst/ligand system, contrary to the usually stereoretentive nature of sp^2-sp^2 couplings.

Next, reaction conversions were optimized through the evaluation of a suitable base and solvent by an innovative UV/vis screening method leveraging the bathochromic shift associated with increasing conjugation in the polyene system (5.2.6.2). This method allows a fast and resourcefriendly tracking of reaction conversions, however with limited information output, as the formation of isomers cannot be detected.

An SPE-HPLC isolation and purification method (5.2.6.3), which facilitated the isolation of this sensitive hexaene II (**132**) with a remarkable purity was described in detail.

Since polyene syntheses are often thwarted due to the instability and isomerization-prone nature of these conjugated scaffolds, the strategies (5.2.6.1-5.2.6.4) developed in this work may serve as a guide for future synthetic efforts in polyene synthesis and isolation.

5.3 Evaluation of the final Suzuki cupling

With the limited amount of hexaene II (**132**) left, the final *Suzuki* coupling of the MIDA-bearing site of **132** with the eastern fragment (**119**) and subsequent deprotection was explored. This sequence would indeed yield the first synthetic bacillaene analogue (**7**) (Scheme 81).

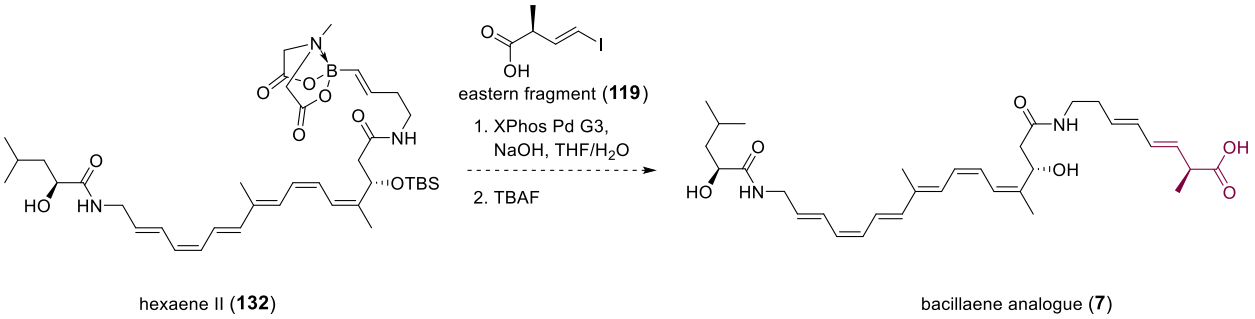

Scheme 79. Planned synthetic sequence for the formation of the bacillaene analogue (**7**) via *Suzuki* coupling followed by deprotection of the silyl ether.

Earlier during the synthetic work on this analogue **7**, the feasibility of this estimated *Suzuki* coupling was evaluated by *Johannes Herbst* during his master thesis.[155] Here, the *Boc*-protected fragment **133** was successfully coupled with the unprotected eastern fragment (**119**) and gave the desired diene **249** with a fair yield of 54% (Scheme 82).

Notably, the strategy of coupling the unprotected carboxylic acid was inspired by *Burke's* synthesis of β-parinaric acid[90] with the difference of a separate deprotection of the MIDA-boronate prior to the coupling.

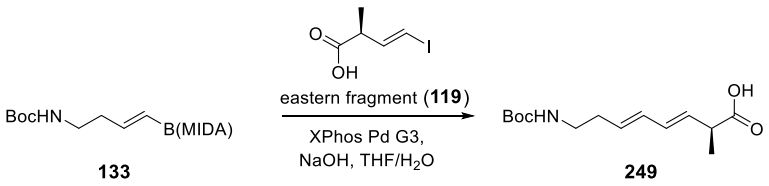

Scheme 80. Succesful *Suzuki* coupling of the *Boc*-protected fragment **133** with the eastern fragment (**119**) performed by *Johannes Herbst*. Conditions: **133** (1.0 eq.), **119** (1.03 eq.), XPhos Pd G3 (5 mol-%), NaOH (0.3 M in H_2O, 4.0 eq.), THF, r.t., overnight, 54%.[155]

However, when these conditions were applied to the authentic system, a plethora of peaks was visible in the analytical HPLC chromatograms, indicating not only isomerization but also the formation of other hexaene containing species as judged by the retention times and absorption spectra.

Next, the deprotection of **132** with three different bases after one hour at r.t. was evaluated and analyzed by LC-MS revealing that the presence of sodium hydroxide (NaOH) led to rapid deborylation of the starting hexaene II (**132**) while cesium carbonate (Cs_2CO_3) and potassium phosphate (K_3PO_4) resulted in a slower but detectable deborylation of the starting material.

As cesium carbonate showed the least abundance of protodeborated product **251**, a small catalyst screening (Scheme 83) was conducted on a 100 µg scale using three different catalysts (XPhos Pd G3, JackiePhos Pd G3, P(o-Tol)$_3$ Pd G2).

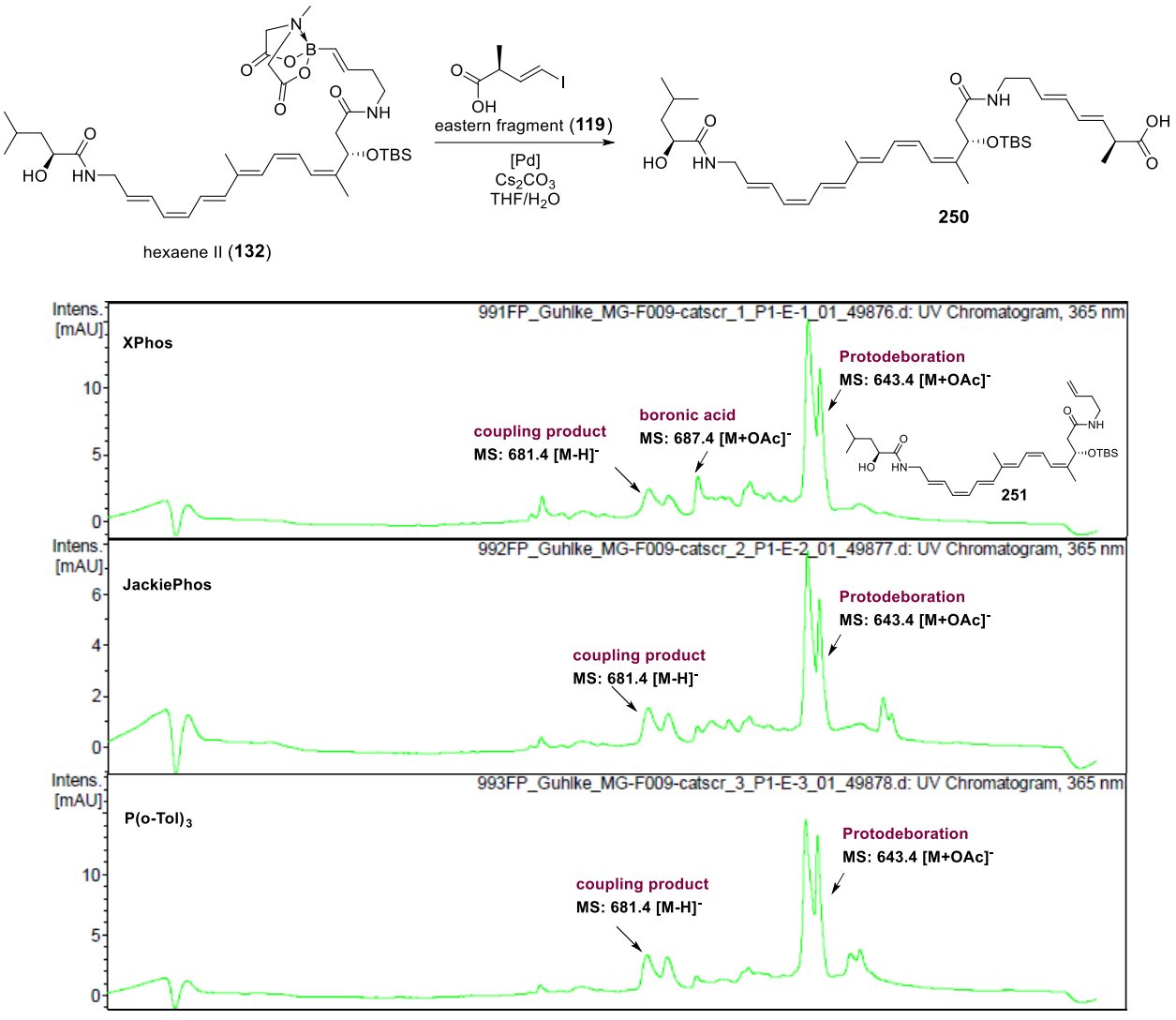

Scheme 81. Evaluation of the final *Suzuki* coupling using three different catalysts and LC-MS chromatograms recorded after work-up. Conditions: hexaene II (**132**) (1.0 eq.), eastern fragment (**119**) (3.5 eq.), Pd-catalyst (0.15 eq.), Cs_2CO_3 (8 eq.), 1,4-dixoane/H_2O (5:1), 55 °C, 9 h; (100 µg-scale).

As visible in the LC-MS chromatograms (Scheme 81), all three reactions resulted in the formation several isomers of the desired coupling product **250**. Moreover, all reactions resulted in formation of the protodeborated product **251** as the major product. Using XPhos as the catalyst, also a small amount of remaining boronic acid, resulting from the deprotection of **132**, was detected.

As the P(o-Tol)$_3$ Pd G2 catalyst showed an overall purer chromatogram compared to the other catalysts it was decided further evaluate the influence of the equivalents of added base while sticking to said catalyst. As protodeboration is pH-dependent[189] a strong influence was expected.

As two equivalents of the eastern fragment II (**129**) were present bearing a carboxylic acid and the MIDA-boronate required base mediated deprotection[190] prior to coupling, it was expected that a minimum of 5-6 equivalents of cesium carbonate (Cs_2CO_3) were required to drive the reaction to completion. Therefore, the reaction was evaluated using 3, 5, 7 and 9 equivalents of cesium carbonate (Cs_2CO_3).

Additionally, two reactions using 7 equivalents of cesium carbonate (Cs_2CO_3) were spiked with either 2 equivalents of neopentylglycol (neop) or 3,4-diethyl-hexane-3,4-diol (Epin).[191] These additives were considered potential stabilizers for the released boronic acid via complexation, although this effect was expected to be negligible considering the amount of water present in the reaction mixture.

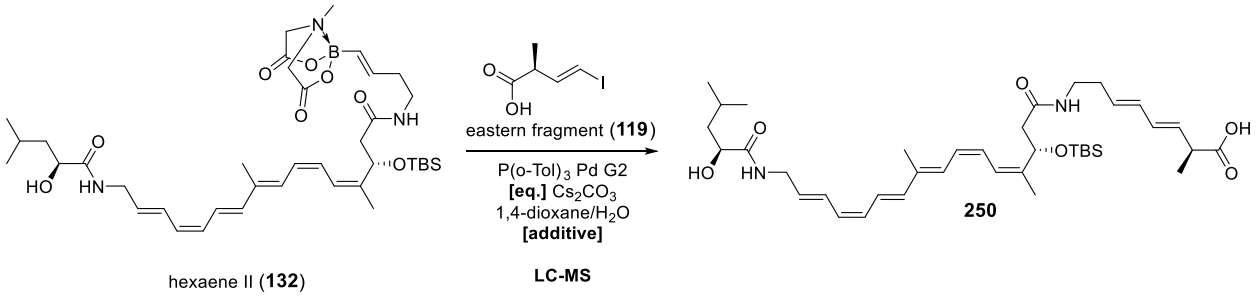

Scheme 82. Evaluation of base stoichiometry and the influence of additives on the final *Suzuki* coupling. Conditions: hexaene II (**132**) (1.0 eq.), eastern fragment (**129**) (2.0 eq.), P(o-Tol)$_3$ Pd G2 (0.15 eq.), Cs_2CO_3 [various eq.], 1,4-dixoane/H_2O (5:1), 50 °C, 9 h; (100 µg-scale).

As shown in the resulting LC-MS chromatograms (Figure 21), the use of 3 equivalents of cesium carbonate (Cs_2CO_3) led to nearly equal amounts of the desired product **250** and protodeborated product **251**, while the corresponding boronic acid (**252**, Scheme 83) was the dominant species. This suggests that by this stage, all the base had been consumed, preventing both the productive coupling and the unproductive base-mediated protodeboration.

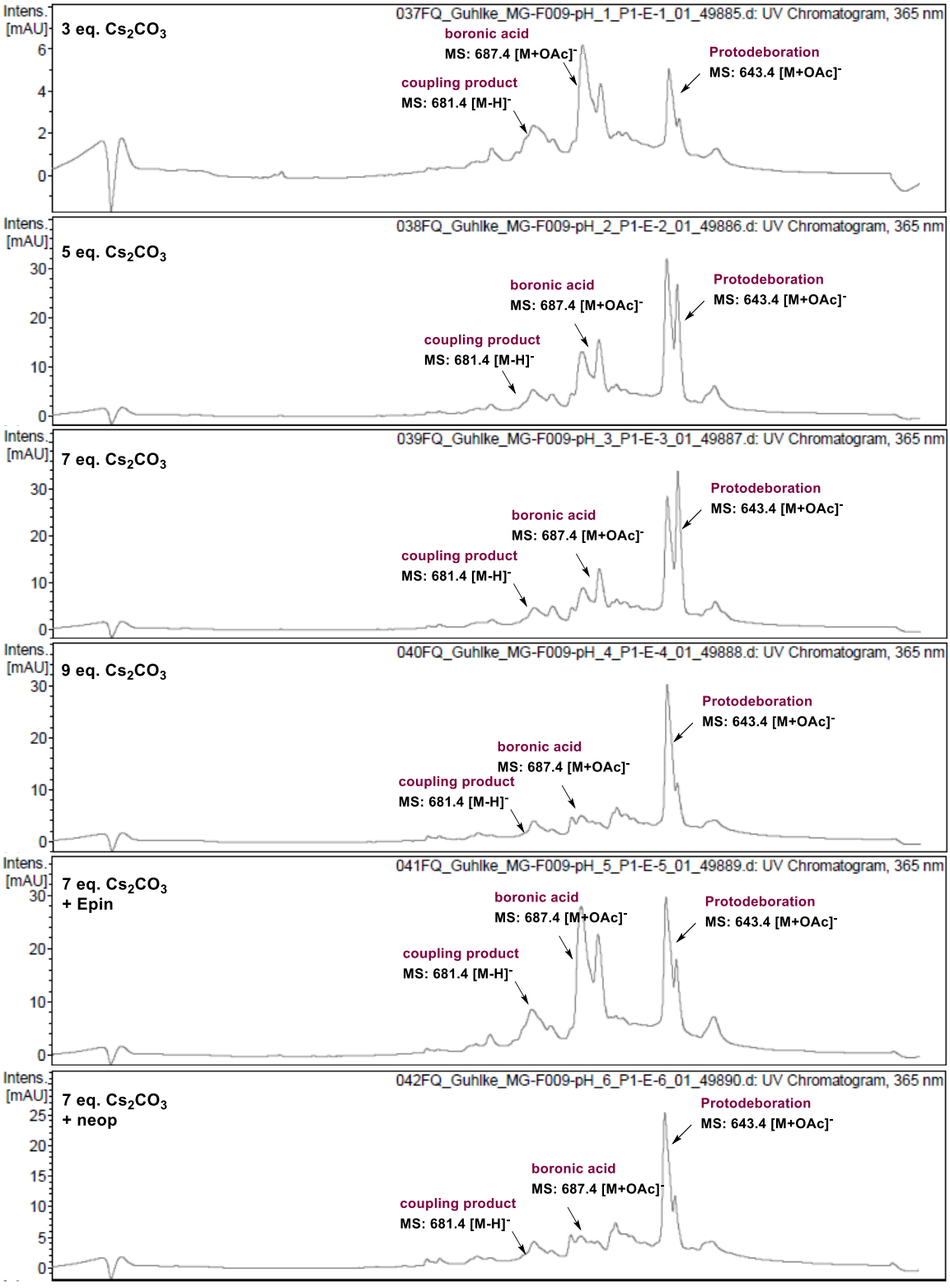

Figure 20. LC-MS chromatograms of the final *Suzuki*-coupling evaluating the influence of base stoichiometry and additives.

With an increasing base stoichiometry, the ratio of product **250** to protodeborated product **251** deteriorated, while the amount of free boronic acid simultaneously decreased, indicating that the unproductive protodeboration is accelerated with an increasing amount of base. Surprisingly, the addition of 3,4-diethyl-hexane-3,4-diol (Epin), showed a similar product distribution as for the reaction using 3 equivalents of cesium carbonate indicating a stabilizing effect.

As illustrated (Scheme 83), the boronic acid **252** appears to undergo two competing pathways upon formation of the "ate" complex[189] (**252.II**). The upper pathway represents the productive transmetalation via **252.III**[192] and **252.IV**, leading to the desired coupling product, while the lower pathway via **252.V** corresponds to the significantly faster protodeboration process resulting in the formation of **251**.

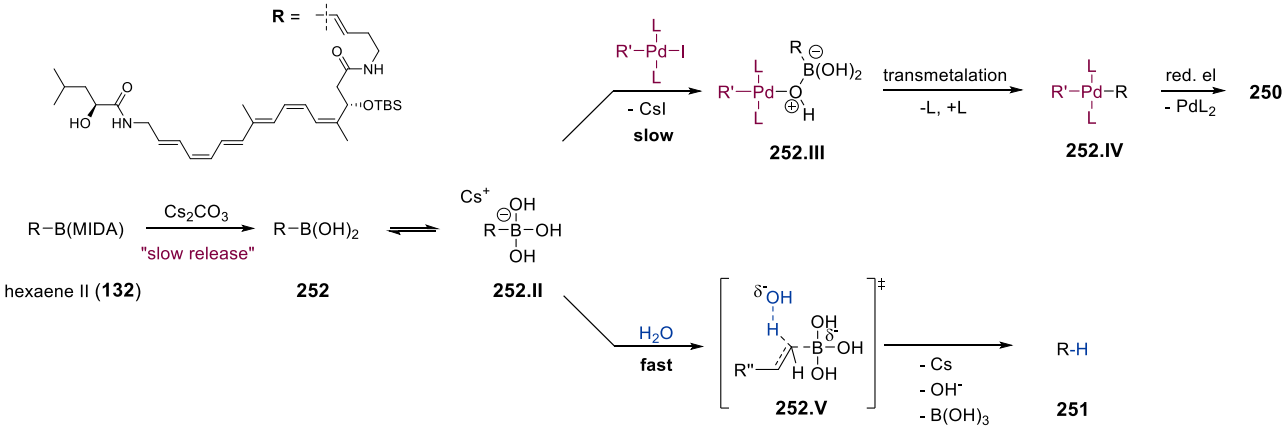

Scheme 83. The two competitive pathways after formation of the boron"ate" complex **252.II**.

Although the "slow-release" protocol[46,47] for MIDA-boronates, employing weak inorganic bases, was designed to circumvent the instabilities of boronic acids by enabling slow deprotection and immediate reaction of the gradually released boronic acid with the catalyst complex, it appears that this strategy fails to prevent the rapid protodeboration of the "ate"-complex (**252.II**) as suggested for this system.

Therefore, it appeared that either exclusion of water would prevent the observed protodeboration or the use of a highly electrophilic catalyst complex that would enable a large rate enhancement of the transmetalation. As water is required for the initial deprotection of the MIDA-ligand only the second option was feasible.

However by this time, the amount of available starting material **132** was extremely limited. Therefore, said optimization of the deprotection and coupling step needed to be carried out on a suitable test

system. As the *Boc*-proteced side chain **133** was successfully coupled (Scheme 80) even in the presence of aqueous sodium hydroxide (NaOH) it was deemed a non-suitable testsystem.

Therefore, a second test-system **254** was synthesized (Scheme 84) incorporating the TBS-protected β-hydroxyamide which exhibited a higher similarity to the authentic system **132**.

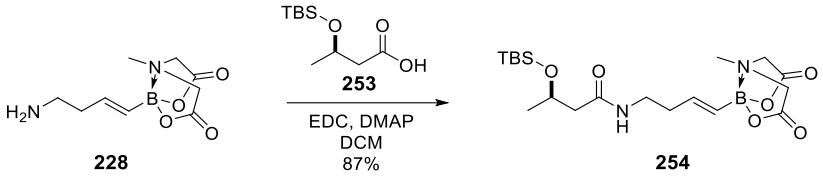

Scheme 84. Synthesis of the new test system **254**. Conditions: **228** (1.0 eq.), **253** (1.0 eq.), EDC-HCl (1.4 eq.), DMAP (1.3 eq.), DCM, r.t., 13 h, 87%.

Next, **254** was reacted with the eastern fragment (**119**) under the same conditions as the authentic system **132** and analyzed by LC-MS (Scheme 85) to evaluate if the protobeboration can be reproduced with **254**. For the base, three equivalents of cesium carbonate were chosen as this showed an equally distributed amount of all intermediates of interest in the original experiment (Figure 21).

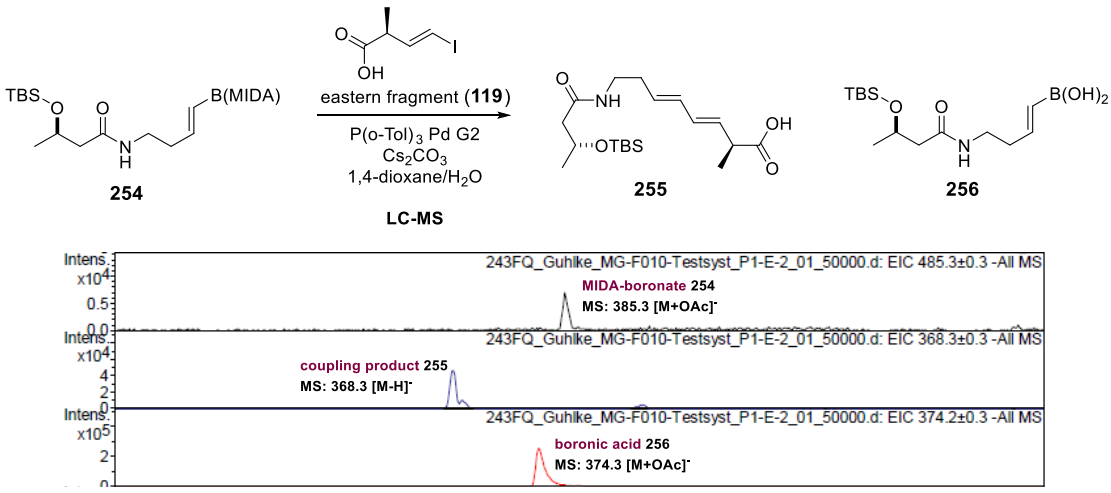

Scheme 85. Attempted error reproduction with the simplified testsystem **254** using the same coupling conditions as for **132**. No protodeborated product could be detected via LC-MS. Conditions: MIDA-boronate **254** (1.0 eq.), eastern fragment (**119**) (2.0 eq.), P(o-Tol)$_3$ Pd G2 (0.15 eq.), Cs_2CO_3 (3.0 eq.), 1,4-dixoane/H_2O (5:1), 50 °C, 9 h, (same concentration as for the authentic experiment).

As visible (Scheme 85), the starting material **254**, along with the corresponding coupling product **255** and the boronic acid **256** were successfully detected in the LC-MS run. However, no protodeborated product

was observed. This led to the conclusion, that the rapid protodeboration was in fact an intrinsic property of the authentic boronic acid **252**.

Retrospectively, a control experiment should have been conducted by synthesizing the protodeborated product of **254** by amide coupling of **253** with homoallylamine to rule out that the absence of protodeborated **254** was not caused by a "detection problem".

In conclusion, two test-systems **133** and **254** were successfully coupled with the eastern fragment (**129**). For the first system **133**, no LC-MS data were collected but the coupling proceeded in presence of a strong base (sodium hydroxide). If a similar protodeboration behavior would have been present for **133**, nearly no product would have been expected. The second test system **254**, containing the TBS-protected β-hydroxyamide motif was reacted under similar conditions as the authentic system **132**. In this case, no protodeborated **254** could be detected via LC-MS.

With these diverging experimental results for different systems, an optimization of the desired coupling reaction would have been feasible only with the authentic hexaene II (**132**). However, the amount of hexaene **132** left at this point was too low to continue with the optimization process. Moreover, the LC-MS chromatograms (Figure 21), indicate that at least four isomers of the coupling product **250** were present in the mixture. This isomerization would need to be addressed as well, if a full characterization and structure elucidation of **250** is desired.

Instead, one last experiment was conducted (Scheme 86), evaluating if a TBAF-deprotection of the coupling product **250** would yield the desired bacillaene analogue (**7**).

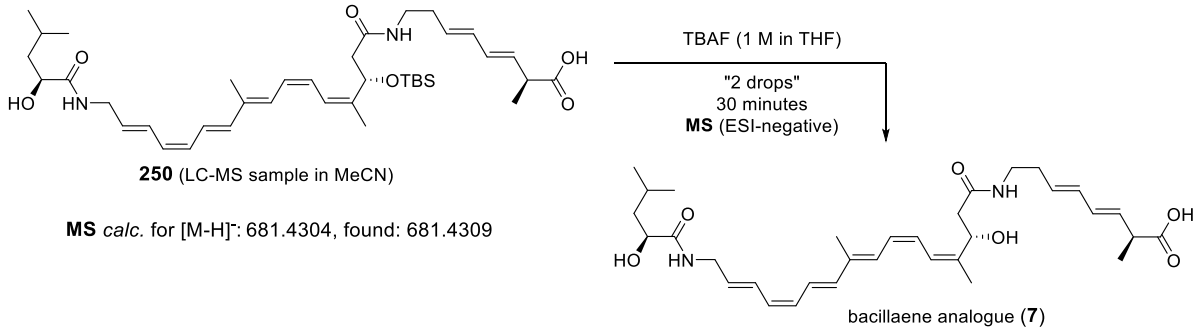

Scheme 86. Final deprotection of the coupling product **250** and detection of the desired bacillaene analogue (**7**) via mass spectrometry.

Indeed, when one of the LC-MS samples containing **250** was treated with 2 drops of TBAF (1 M in THF), analysis via mass spectrometry revealed the presence of the bacillaene analogue (**7**).

Unfortunately, both products **250** and **7** could not be isolated and fully characterized due to the previously mentioned problems. However, it shows that **250** is indeed stable towards TBAF allowing for a deprotection as the final step of a total synthesis.

As will be discussed in the outlook chapter (7.2), a total synthesis of bacillaene (**1**) and its analogue (**7**) appears possible if the eastern side-chain is incorporated into the molecule at an earlier step.

Part 4: Synthetic Routes to Enamide Fragments

6.1 Introduction

While the primary focus of this work was the synthesis of the simplified bacillaene analogue (**7**), which lacks the enamide structure, significant efforts were also dedicated to developing a synthetic pathway for the *Z*-enamide motif found in the authentic natural product bacillaene (**1**)**.**

Scheme 87. Structural comparison of the central fragment III (**132**) used in the synthesis of bacillaene analogue (**7**) (blue) and the enamide-containing central fragment II (**120**) required for the synthesis of authentic bacillaene (**1**) (red).

As the overall synthetic sequence for the bacillaene analogue (**7**) followed a modular design, an incorporation of the *Z*-enamide into the central fragment II (**120**) was pursued (Scheme 87). This approach would potentially enable the synthesis of authentic bacillaene (**1**) using the same iterative cross coupling strategy as for the analogue **7**.

Notably, the synthetic efforts described in this chapter were carried out simultaneously with those for the bacillaene analogue (**7**). As a result, key insights gained during the late stages of the synthesis of analogue **7** (Chapter 5.3), such as the realization that the side chain of **1** and **7** should ideally be synthesized prior to the hexaene core, were not incorporated during the initial planning of this fragment.

Among the various potentially suitable methods discussed in the introduction (Chapter 2.4), this work primarily focused on incorporating two key strategies (Scheme 88) into the attempted total synthesis of bacillaene (**1**).

The first strategy explored in this work was the *N*-acylation[86] (Chapter 2.4.5) of commercially available methyl 3-aminocrotonate **92**. This method did allow for the synthesis of a trisubstituted *Z*-enamide motif, however we will see that it suffers from low stereoselectivity. Furthermore, subsequent functionalizations of the resulting enamidoesters **94** proved challenging likely due to the stabilizing effect by hydrogen bonding.

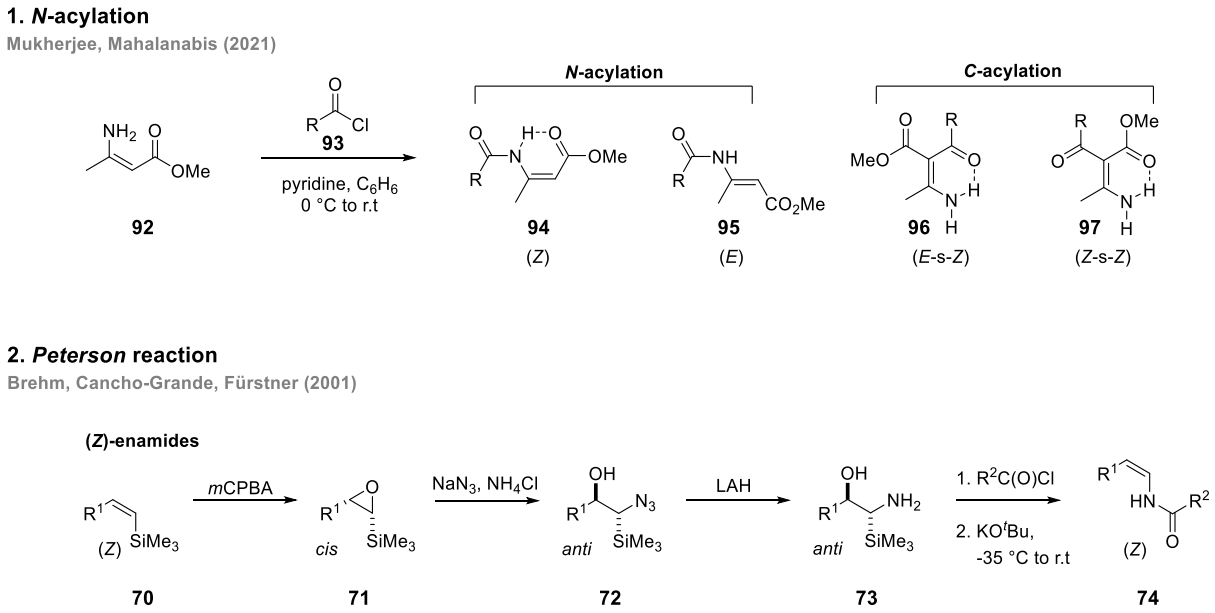

Scheme 88. Recap of the both strategies for enamide synthesis explored during this work. A deeper discussion is provided in chapters 2.4.3 (*Peterson*), and 2.4.5 (*N*-acylation).

The second strategy explored in this work was *Fürstner's Peterson* reaction manifold[79] (Chapter 2.4.3), which separates *C*-*N* bond formation and elimination/enamide-formation into two distinct steps, enabling a greater flexibility in synthetic route design and late-stage liberation of the sensitive enamide-functionality.[65] However, as we will see, the synthesis of the required building block **264** (Chapter 6.3.1-6.3.3) remains a significant challenge.

Nevertheless, a proof of concept demonstrates that the enamide motif can indeed be constructed using this approach.

6.2 Enamide synthesis by *N*-acylation of methyl 3-aminocrotonate

Methyl 3-aminocrotonate (**92**) is a highly versatile and commercially available substrate, frequently employed in dihydropyridine syntheses[193] and the production of β-amino acids[194]. Crotonate **92** is a stable *Z*-configured enamine, as the imine-enamine tautomerism[195] is suppressed by the stabilizing effect of the hydrogen bonding between the amino- and N_V-carbonyl group.

Systematic studies on the acylation of methyl 3-aminocrotonate (**92**) by *Mukherjee* and *Mahalanabis*[86] revealed that the selectivity of *N*-terminal acylation over *C*-terminal acylation is primarily influenced by the nature of the electrophile and the choice of base, with pyridine being identified as the preferred base for selective *N*-acylation.

Based on this set of information, an initial test reaction (Scheme 89) was performed after acid chloride formation from substrate **129** (Chapter 4.4.2).

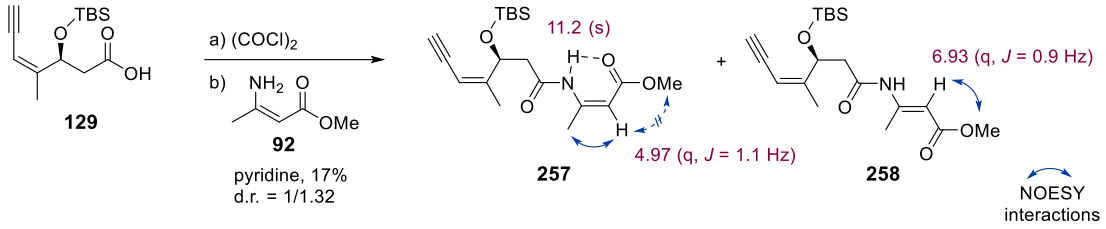

Scheme 89. Results of the initial *N*-acylation of **92** after acid chloride formation from carboxylic acid **129**. Conditions: a) **129** (1.0 eq.), $(COCl)_2$ (1.0 eq.), cat. DMF, DCM, r.t., 1.5 h; b) **92** (1.5 eq.), pyridine (4.5 eq.), DCM, 0 °C, 1 h, 17% (isolated yield for **257**), d.r. = 1:1.3 (determined from crude NMR).

While no *C*-acylated product was observed, the major product obtained from this reaction was the *E*-enamidoester **258**, which was isolated in 22% yield, while the desired *Z*-enamidoester **257** was obtained in only 17% yield. The *E*-enamidoester **258** exhibited significantly higher polarity than **257** on TLC, likely due to the absence of hydrogen bonding, resulting in stronger interactions of the polar amide and ester functional groups with the silica. While **258** was obtained as a colorless oil the *E*-isomer **257** was obtained as a white solid.

Structural differentiation between the two isomers by NMR was straightforward, as the strongly downfield-shifted signal of the hydrogen-bonded proton was clearly visible for **257**, along with the *NOE*-interaction between the enamide proton and the adjacent methyl group.

A significant difference of 2 ppm between the *Z*- and *E*-enamide protons was observed, consistent with literature-reported observations.[196] A NOESY-interaction between the enamide proton and the methyl ester was observed only for **258** indicating a slightly distorted geometry for **257** presumably caused by the hydrogen bonding, however the exact reason remains to be elucidated (preferably by X-ray crystallography).

Next, the simplified silyl protected β-hydroxyacid **253** was prepared and reacted under the same conditions to test the reproducibility of these initial observations (Scheme 90).

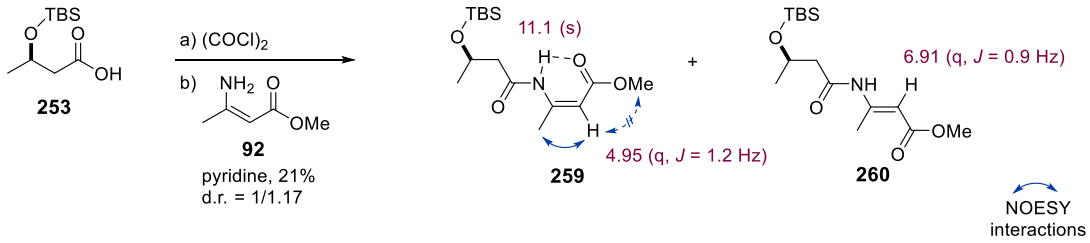

Scheme 90. Results of the *N*-acylation of **92** after acid chloride formation from simplified acid **253**. Conditions: a) **253** (1.0 eq.), $(COCl)_2$ (1.0 eq.), cat. DMF, DCM, r.t., 1.5 h; b) **92** (1.5 eq.), pyridine (4.5 eq.), DCM, 0 °C, 1 h, 21% (isolated yield for **259**), d.r. = 1/1.17 (determined from crude ^{1}H-NMR).

With the simplified system **253**, similar results were obtained with good accordance of the previously obtained results (Scheme 89). A slightly more favourable diastereomeric ratio (d.r. = 1:1.17) was observed for **259** in contrast to the previous reaction (d.r. = 1:1.32). In total, the similarity in reaction behavior was deemed sufficient to use **253** as a model system for the optimization of reaction conditions and further exploration of subsequent functionalization.

First, various methods for carboxylic acid activation were explored (Table 10) in hopes of achieving higher yields or improved diastereomeric selectivities compared to the initially used acid chloride. Therefore, pentafluorophenyl ester[197], CDI[198], HATU[199], HBTU[200] and the relatively new MYTsA (*N*-methyltoluenesulfonamide)[201] were tested as coupling agents. Among these, only HATU and HBTU facilitated product formation, though with poorer diastereomeric selectivities than initially achieved using the acid chloride.

Table 10. Evaluated coupling agents for the activation of **253** and subsequent *N*-acylation of **92**.

entry	active ester	yield (**259**)	d.r. (*Z*/*E*)
1	acid chloride	21	1/1.17[a]
2	R-O(C_6F_5)	-	-
3	HATU	not isolated	1/1.35[a]
4	CDI	-	-
5	MYTsA	-	-
6	HBTU		1/3.96[a]

[a] determined from crude NMR.

Given the unsatisfactory results from reaction optimization, it was decided to explore the subsequent functionalization of enamidoester **259** to determine whether further investment in reaction optimization would be justified.

Specifically, the reduction of **259** to the corresponding aldehyde **263** was investigated. To increase the chances of a successful reduction, the *Weinreb* amide **261** was also synthesized. While this reaction proceeded with 80% yield, it led to the formation of an inseparable side product **262**.

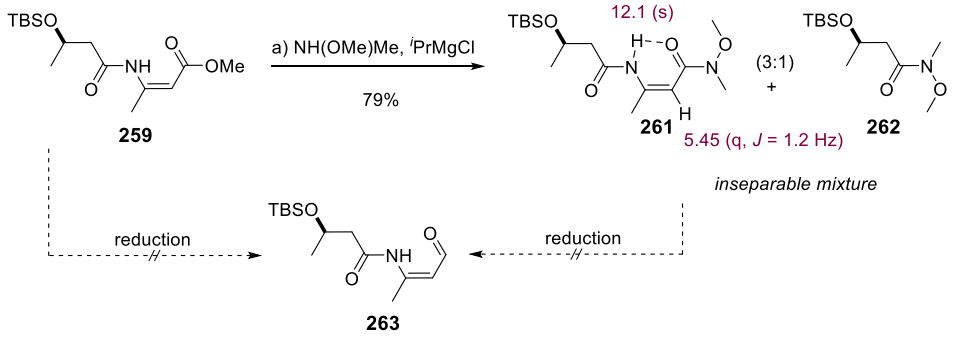

Scheme 91. Formation of the *Weinreb* amide **261** from *Z*-enamidoester **259** along with the formation of side-product **262** and intended reduction of both substrates **259** and **261** to the corresponding *Z*-enamidoaldehyde **263**. Conditions: a) *N*,*O*-dimethylhydroxylamine hydrochloride (3.1 eq.), ^{i}PrMgCl (6.3 eq.), THF, 0 °C to r.t., 5 h, 79%.

The results of the subsequent reductions are summarized in Table 11. For substrate **261**, aldehyde formation was observed upon reaction with DIBAL at both −78 °C and room temperature. However, analysis of the resulting crude products revealed significant decomposition, as indicated by a complex mixture of signals in the ^{1}H-NMR spectra. In contrast, treatment with the milder reducing agents LDBBA[202] and $LiBH_4$[203] resulted in no reaction, suggesting that the enamidoester **259** exhibits greater

stability compared to classical esters presumably due to the stabilizing effect caused by the hydrogen bonding.

Table 11. Explored reductions of the *Z*-enamidoester **259** and *Z*-enamidoamide **261**.

entry	substrate	reducing agent	solvent	temperature	aldehyde signal signal	comment
1	**259**	DIBAL	DCM	r.t.	observed	complex mixture
2	**259**	DIBAL	DCM	−78 °C	observed	complex mixture
3	**259**	LDBBA	THF	0 °C	-	no reaction
4	**259**	$LiBH_4$	THF	0 °C	-	no reaction
5	**261**	DIBAL	DCM	−78 °C	integral = 0.2	reduction product of **262**
6	**261**	LDBBA	THF	0 °C	-	no reaction
7	**261**	$LiBH_4$	THF	0 °C	-	no reaction
8	**261**	$Cp_2Zr(H)Cl$	THF	r.t.	integral = 0.2	reduction product of **262**

Treatment of the *Weinreb* amide **261** with LDBBA and $LiBH_4$ again resulted in no reaction. Similar to substrate **259**, reaction with DIBAL produced an aldehyde signal in the NMR spectrum. An almost identical spectrum was observed when **261** was treated with the *Schwartz* reagent, known for reducing *Weinreb* amides to their corresponding aldehydes.[204] However, analysis of the ^{1}H-NMR spectra suggested that the aldehyde signal originated from the reduction of the inseparable side-product **262**, rather than the desired enamidoaldehyde **263**.

Based on the obtained results, the synthesis of the enamide motif using this method appears unsuitable due to both the low yield and poor selectivity of the *N*-acylation of methyl 3-aminocrotonate (**92**) and, more importantly, the unsuccessful functionalization attempts of the resulting *Z*-enamidoester **259**. Apart from catalytic hydrogenations, there is unfortunately little literature precedent to guide further functionalization efforts.

However, the successful transformation of *Z*-enamidoester **259** to the *Weinreb* amide **261** showed that additions of magnesium amides[205] are tolerated suggesting that other additions of organometallic nucleophiles such as *Grignard* reagents are probably tolerated as well, opening a pathway to various functionalized *Z*-enamides. This area remains underexplored and should be investigated more systematically in future studies.

6.3 Enamide synthesis by *Peterson* olefination

Encountered with the rather poor results from the previous synthetic attempts via *N*-acylation (Chapter 6.2), a second strategy was explored, namely the enamide synthesis through a *Peterson* reaction manifold developed by *Fürstner*.[79]

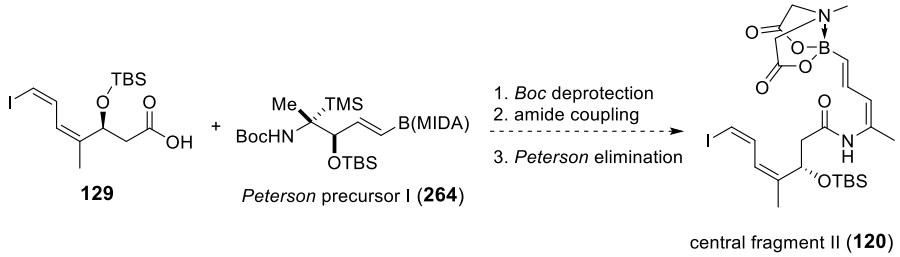

Scheme 92. Estimated synthetic sequence for the synthesis of central fragment II (**120**) via amide coupling of carboxylic **129** with the *Peterson* precursor I (**264**) after deprotection and subsequent elimination forming the *Z*-enamide.

While the *Fürstner* group had demonstrated this approach using synthetically simple precursors with only disubstituted double bonds in the starting vinylsilane, the required *Peterson* precursor I (**264**) (Scheme 92) presented a significantly greater challenge. The presence of both a quaternary center and a vinyl MIDA-boronate introduced considerable synthetic hurdles. The steric hindrance imposed by the quaternary center may not only complicate the formation of necessary precursors but might also perturbate the final elimination. Given these challenges, adapting *Fürstner's* methodology to this more complex system required careful reconsideration of reaction steps.

6.3.1 Retrosynthesis and synthesis of the starting alcohol

An initial retrosynthetic analysis (Scheme 93) revealed that fragment **264** could be accessed from the corresponding aminoalcohol **265**, which in turn would be obtained by epoxide opening of **266** using sodium azide, followed by reduction of the 1,2-azidoalcohol **265**.

However, MIDA-boronates are typically unstable toward LAH reductions,[47] while the olefin motif may interfere with catalytic hydrogenations. This significantly narrowed the range of viable reductions, making a *Staudinger*[123] reduction the most practical choice for this step.

Based on the experiences gained during the synthesis of the MIDA sidechain **133** (4.4.1) present in central fragment III (**132**), MIDA-boronate **266** could be derived from the vinylpinacolboronate precursor **267**, for which a boryl-*Wittig*[137] reaction again appeared to be a reasonable choice, leading to the epoxyaldehyde **268**.

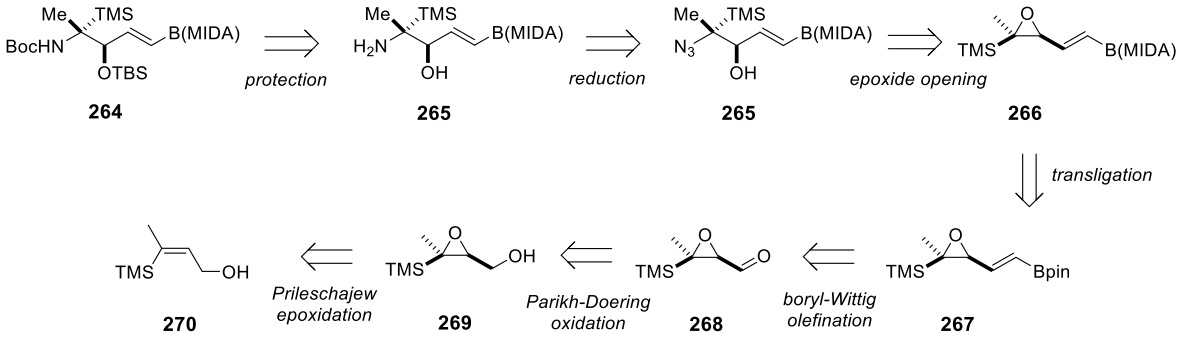

Scheme 93. Initial retrosynthetic analysis of the *Peterson* precursor I (**264**).

The oxidation of silylepoxyalcohol **269** to the corresponding aldehyde **268** offered numerous established protocols.[206,207,208] Given that enantioselectivity was not a concern due to the diastereoconvergent nature of the *Peterson* elimination,[81] a straightforward *m*CPBA epoxidation to form **269** was planned, leading to the starting alcohol **270**.

For alcohol **270** a single "footnote protocol"[209] was available which however turned out to be working very efficiently (Scheme 94). First, 2-butyne-1-ol (**271**) was reacted with RedAl® to form the corresponding metalla-dihydrofurane intermediate **272** which was subsequently treated with iodine to provide *Z*-iodoallylalcohol **273**[210] as a single isomer.

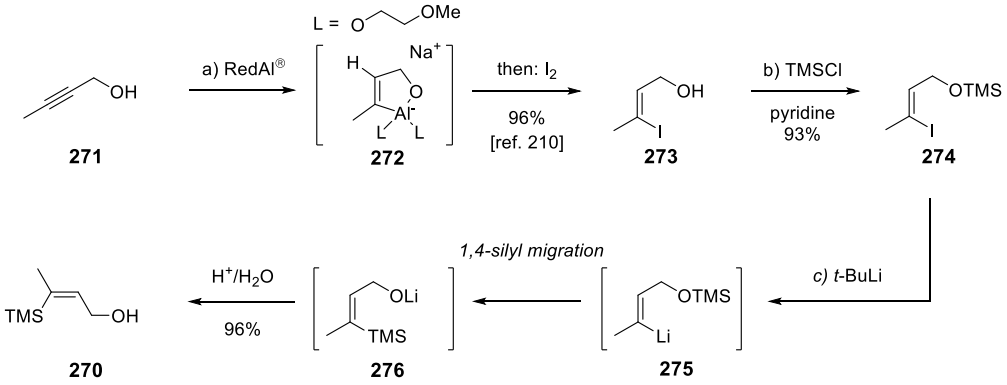

Scheme 94. Synthesis of the starting alcohol **270**. Conditions: a) RedAl (1.4 eq.), Et_2O, 0 °C to r.t., 4 h, then: I_2 (1.5 eq.), 0 °C to r.t., 14 h, dark, 96%; TMSCl (1.4 eq.), pyridine (2.2 eq.), DMF, 0 °C to r.t., overnight, 93%; c) *t*-BuLi (2.1 eq.), THF, –78 °C, 30 min, r.t., 30 min, 96%.

Next, the TMS-ether **274** was formed by treatment of **273** with TMS-chloride in the presence of pyridine. Notably, **274** exhibited the typical instability toward silica chromatography. However, an analytical sample of **274** was successfully obtained via column chromatography using a CN-modified silica phase.

For bulk preparation, crude TMS-ether **274** was subjected to two equivalents of *t*-BuLi, leading to the formation of alcohol **270** through a retro-*Brook* rearrangement.[211] In this sequence, an initial lithium-halogen exchange generates intermediate **275**, followed by a 1,4-migration of the silyl group forming the more stable oxygen-centered anion **276**. After hydrolysis, the alcohol **270** was obtained in excellent yield (86%, 3 steps) as a single isomer.

6.3.2 Synthetic attempts of the *Peterson* precursor I via boryl-*Wittig* olefination

With alcohol **270** in hand, a *Prileschajew* epoxidation[210] was carried out using *m*CPBA, delivering the *syn*-epoxide **269** in nearly quantitative yield (Scheme 95). Next, *Parikh-Doering*[213,206,207] oxidation was performed to obtain the desired epoxyaldehyde **268** which proved to be volatile, albeit to a controllable extent.

Subsequently, the planned boryl-*Wittig*[137] reaction was attempted, providing **267** in a poor yield of only 18% (maximum yield). While the initial olefination proceeded smoothly (TLC), the product exhibited unusual behavior on silica gel chromatography, with poor recovery, presumably due to epoxide opening caused by the silica. As a result, crude **267** was again purified using a CN-modified silica phase. However, co-elution with an impurity (due to epoxide opening as judged by ^{1}H-NMR) led to the isolation of only 18% of a semi-pure sample of **267**.

As an alternative a later introduction of the epoxide was tested (Scheme 95). Hence, starting alcohol **270** was first oxidized to the aldehyde **277**, followed by the boryl-*Wittig*[137] olefination which gave the diene **278** in a good yield of 68% (d.r. > 20:1) over two steps, despite the high volatility of intermediate **277**. Transligation from **278** Bpin → B(MIDA) **279** was achieved by the 2-step protocol using $NH_4OAc/NaIO_4$[139] via the boronic acid (not shown) and subsequent complexation with MIDA under *Dean-Stark* conditions[46] in 87% yield.

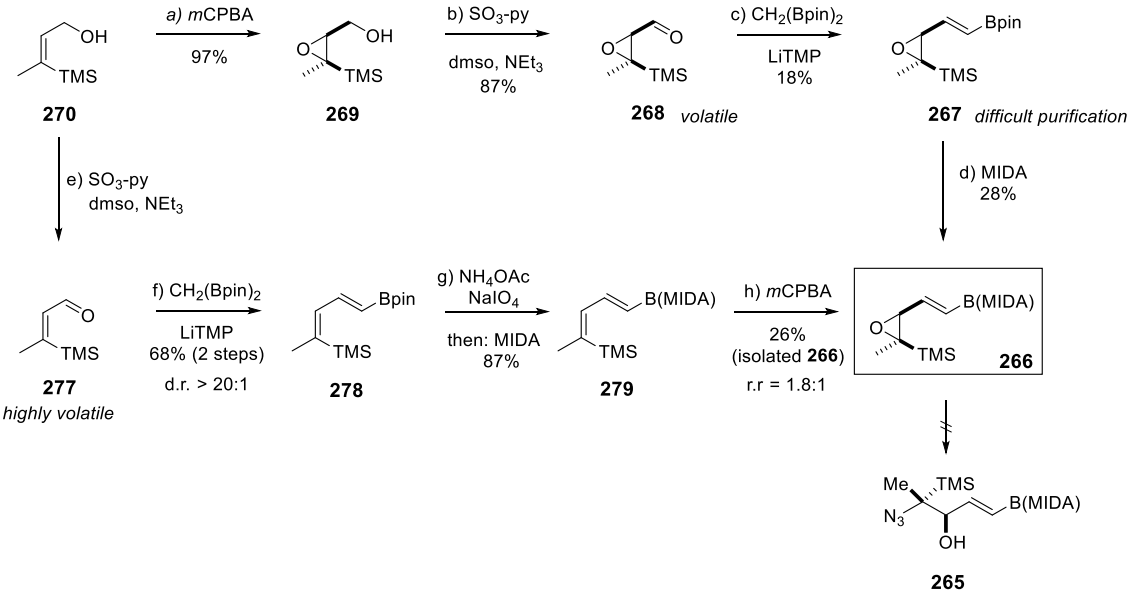

Scheme 95. Synthesis of key intermediate **266** by two different approaches. Conditions: a) *m*CPBA (1.2 eq.), DCM, 0 °C to r.t., 1 h, 97%; b) SO_3-pyridine complex (6.0 eq.), Et_3N (10 eq.), DMSO (20 eq.), DCM, 0 °C, 30 min, 87%; c) $CH_2(Bpin)_2$ (1.8 eq.), LiTMP (1.6 eq.), THF, 0 °C, 1.5 h, 18%; d) MIDA (6.0 eq.), $HC(OMe)_3$ (4.0 eq.), toluene/dmso (2:1), 110 °C, overnight, 28%; e-f) SO_3-pyridine complex (6.0 eq.), Et_3N (11 eq.), DMSO (20 eq.), DCM, 0 °C, 30 min; then: $CH_2(Bpin)_2$ (1.4 eq.), LiTMP (1.4 eq.), THF, 0 °C, 1.5 h, 68%, d.r. > 20/1; g) NH_4OAc (2.5 eq.), $NaIO_4$ (2.5 eq.), acetone/H_2O (1:1), r.t., 13 h; then: MIDA (2.0 eq.), toluene/dmso (2:1), 120 °C, 10 h, 87%; h) *m*CPBA (1.0 eq.) dropwise over 6 h, MeCN, r.t., 1 h, 26% (isolated **266**), r.r. = 1.8/1.

The subsequent epoxidation of **279** proved to be unselective, despite higher substitution of the targeted double bond. A reduced temperature of 0 °C completely suppressed product formation. The best regioisomeric ratio (r.r = 1.8:1) was achieved when *m*CPBA was added dropwise at r.t. over six hours. However, the isolated yield of **266** remained low at only 26%, primarily due to the formation of numerous mixed fractions during chromatographic purification. An attempt at HPLC separation of **266** was carried out, but unfortunately led to decomposition of the product.

After encountering repeated failures in the epoxide opening of **266**, this step was repositioned earlier in the reaction sequence (Scheme 96), prior to the installation of the vinyl boronate motif.

Accordingly, the starting alcohol **270** was first protected with a PMB group to form **280**, followed by a quantitative epoxidation resulting in the *syn*-epoxide **281** (Scheme 96). Silicon directed epoxide opening[80] was then carried out using reported conditions, successfully affording the desired *anti*-1,2-azidoalcohol **282** in an excellent 80% yield as a single regioisomer.

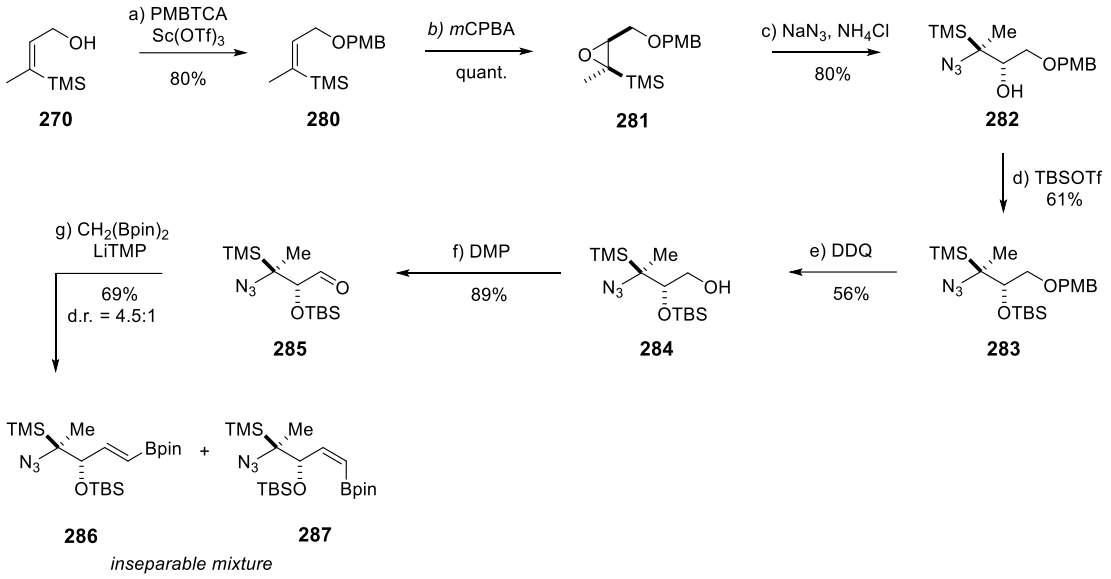

Scheme 96. Synthesis of boronic ester **286**. Conditions: a) PMBTCA (1.1 eq.), $Sc(OTf)_3$ (0.03 eq.), toluene, 0 °C to r.t., 1 h, 80%; b) *m*CPBA (1.3 eq.), DCM, 0 °C to r.t., 1 h, quant.; c) NaN_3 (6.5 eq.), NH_4Cl (2.5 eq.), MeOH/H_2O 8:1, 45 °C, 40 h, 80%; d) TBSOTf (1.9 eq.), 2,6-lutidine (3.7 eq.), DCM, r.t., 45 min, 61%; e) DDQ (1.5 eq.), DCM/pH 7-buffer (8:1), r.t., 4 h, 56%; f) DMP (1.1 eq.), DCM, r.t., 3 h, 89%; g) $CH_2(Bpin)_2$ (2.0 eq.), LiTMP (1.8 eq.), THF, −78 °C to r.t., 12 h, 69%, d.r. = 4.5:1.

Next, the obtained secondary alcohol **282** was protected with a TBS-group and the orthogonal PMB-ether of **283** was cleaved using DDQ. These two protection/deprotection steps resulted in a product loss of 66%, which is hardly tolerable given the length of this sequence.

Formation of the PMP-acetal of **282** followed by reduction of the azide, *Boc*-protection and reductive ring-opening[214] had been considered, however studies on similar systems had shown that these types of acetals preferably open towards the secondary alcohol instead of the expected primary alcohol.[215]

Alcohol **284** was subsequently oxidized to aldehyde **285** with an excellent yield of 89% using DMP followed by the boryl-*Wittig* olefination that yielded **286** and the *Z*-isomer **287** as an inseparable mixture (d.r. = 4.5:1). Notably, at this stage the skeleton of the desired *Peterson* precursor I (**264**) was already complete, merely requiring a reduction of the corresponding azide and a MIDA-protection of the boron center.

However, follow-up transformations of the obtained intermediate **286** failed (Scheme 97). First the transligation to the MIDA-boronate **288** was explored. However, reaction with MIDA in a mixture of toluene and DMSO resulted in no reaction at 75 °C, while at 100 °C formation of a MIDA-boronate was observed, however with no olefinic signals present in ^{1}H-NMR indicating decomposition of

compound **288**. Alternatively, formation of the MIDA-boronate via the boronic acid was explored using the $NH_4OAc/NaIO_4$-method. While the initial hydrolysis of the pinacolester succeeded (TLC), decomposition was observed during the MIDA-protection step.

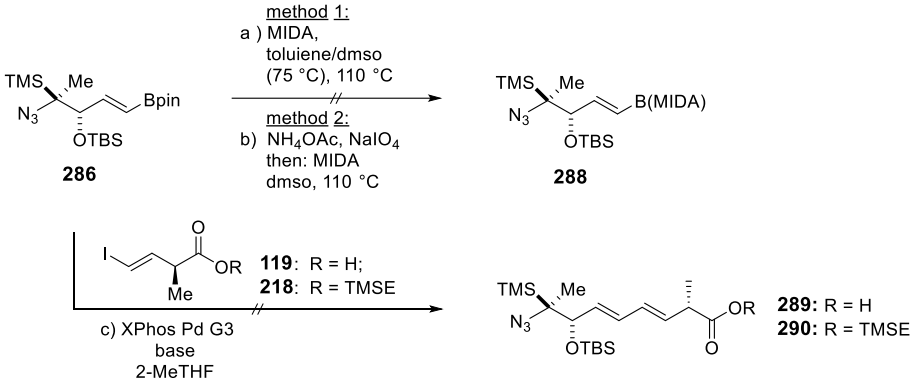

Scheme 97. Explored transformations of intermediate **286**. Conditions: a) MIDA (5.0 eq.), toluene/dmso (2:1), 110 °C, *Dean-Stark*, overnight; b) NH_4OAc (6.0 eq.), $NaIO_4$ (2.5 eq.) acetone/H_2O (1:1); then: MIDA (5.0 eq.), toluene/dmso (2:1), 110 °C, *Dean-Stark*, overnight; c) Fragment X or X (1.1 eq.), XPhos Pd G3 (5 mol-%), base = K_2CO_3 or NaOH (2.5 eq.), 2-MeTHF, overnight.

With a pinacolboronate present in fragment **286**, a *Suzuki*-coupling with the protected and unprotected eastern fragments **119** and **218** was explored using XPhos Pd G3 in 2-MeTHF with either aqueous potassium carbonate (K_2CO_3) or sodium hydroxide (NaOH) as the base.

However, no product formation was observed in any of these trials, and further experiments were not pursued due to a shortage of the pinacol fragment **286**.

Since the azide group was suspected of causing the decomposition observed during attempts to form the MIDA-boronate **288**, its reduction was repositioned to an earlier stage in the reaction sequence. Therefore, a reduction and *Boc*-protection was planned immediately after the epoxide opening, followed by the same sequence of steps previously employed (Scheme 98).

Accordingly, after epoxide opening the *anti*-1,2-azidoalcohol **282** was subjected to LAH reduction which gave the desired 1,2-aminoalcohol **291** in an excellent yield of 94%. However, the subsequent *Boc*-protection of **291** provided the protected intermediate **292** in a poor yield of only 25%.

Moreover, attempted TBS-protection to form **293** using either TBSCl/imidazole or the more reactive TBSOTf/2,6-lutidine proved unsuccessful. This lack of reactivity appears to be due to a combination of factors. First, the sterically demanding environment around the quaternary center likely hinders the approach of the bulky protecting agents. Additionally, there may be an intramolecular hydrogen bond in

292 between the alcohol and the adjacent carbonyl oxygen of the carbamate, which could reduce the nucleophilicity of the hydroxyl group however, such an interaction was not confirmed by ^{1}H-NMR. Retrospectively, the introduction of a sterically less demanding TES-protecting group should have been evaluated.

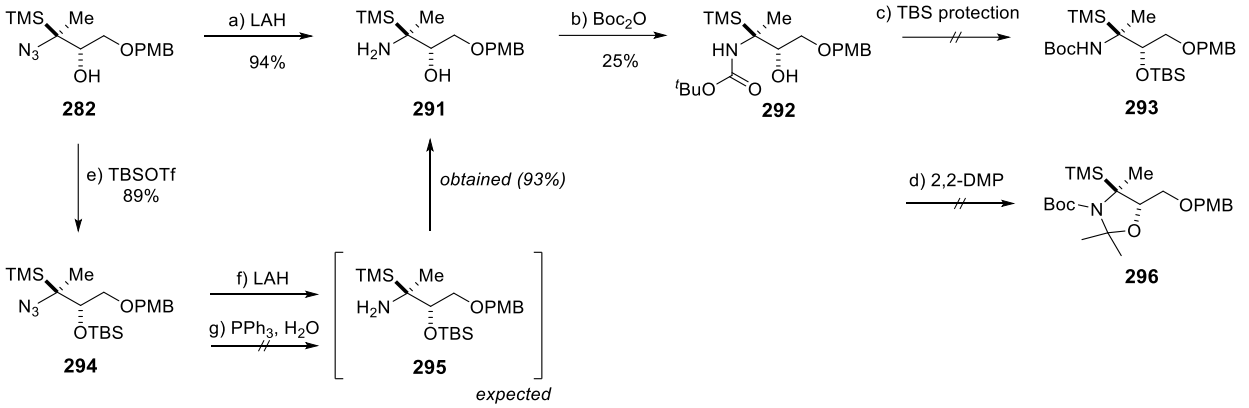

Scheme 98. Explored transformations of intermediate **282**. Conditions: a) LAH (2.0 eq.), Et_2O, r.t., 3 h, 94%; b) Boc_2O (2.0 eq.), Et_3N (2.0 eq.), cat. DMAP, THF, r.t., 12 h, 25%; c) 1. TBSOTf (2.5 eq.), 2,6-lutidine (5.0 eq.), DCM, r.t., no reaction; 2. TBSOTf (2.5 eq.), 2,6-lutidine (5.0 eq.), DCM, r.t., no reaction; 3. TBSCl (2.5 eq.), imidazole (5.0 eq.), DMF, r.t., no reaction; d) 2,2-DMP (8.0 eq.), *p*-TsOH (0.2 eq.), r.t., 20 h, no reaction; e) TBSOTf (2.0 eq.), 2,6-lutidine (4.0 eq.), DCM, 0 °C, 45 min, 89%; f) LAH (2.0 eq.), Et_2O, r.t., 6 h, 93% (**291**); g) PPh_3 (2.0 eq.), THF, r.t., 1 h; then: H_2O, r.t., overnight; no product isolated.

An alternative strategy involving protection of **292** as an *N*,*O*-acetal (**296**) (1,3-oxazolidine)[215] using 2,2-DMP remained unsuccessful. Moreover, this method among other strategies for the protection of 1,2-aminoalcohols typically require acidic conditions for deprotection. Such acidic environments are problematic as they can potentially trigger the *Peterson* elimination, which not only proceeds under acidic conditions but also results in a stereochemically reversed *anti*-elimination under these conditions.[81]

Instead, a TBS-protection of **282** prior to the LAH-reduction was tested providing compound **294** in 89% yield. This showed that one the one hand, the silylating reagent, which previously failed in the synthesis of **293**, was indeed sufficiently reactive. On the other hand, it demonstrated the smaller steric demand of the azide group within the adjacent quarternary center, resulting in an overall higher accessibility of the electrophile. Although, hydrogen bonding interactions with azides have been observed,[216] they seem to have a smaller impact (**282**) on the nucleophilicity of the hydroxyl group compared to the *Boc*-group in **292**.

Unfortunately, the subsequent LAH reduction of **294** resulted in formation of aminoalcohol **291** rather than **295**. This unexpected deprotection of the TBS-group closed a loop at an unfavorable position within this reaction sequence.

6.3.3 Synthetic attempts of the *Peterson* precursor I via cross metathesis

Given the previously described difficulties during the boryl-*Wittig* approach (Chapter 6.3.2) an alternative metathesis reaction was chosen to install the corresponding vinyl MIDA boronate (Scheme 99). This strategy was supported by numerous successful examples reported in the literature.[217] To evaluate the intended cross-metathesis reaction the terminal alkene **297** needed to be synthesized first.

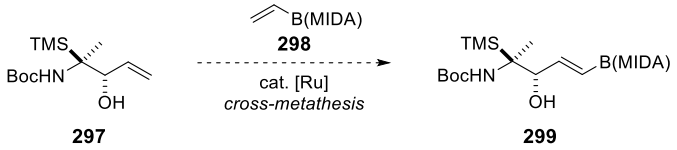

Scheme 99. Intended synthesis of the *Peterson*-fragment **299** by a cross-metathesis reaction.

Accordingly, the required vinyloxirane **300** was synthesized from the corresponding epoxyaldehyde **268** and subjected to epoxide opening (Scheme 100). After a reaction time of 21 hours, two distinct products **301** and **302** were isolated in a ratio of 2.8:1. Their structures were unambiguously confirmed using 2D-NMR. While the desired product **301** arises from the silicon-directed attack at the silyl-bearing carbon of the epoxide, the second product **302** likely forms via an S_N2'-reaction[218,219] involving an attack at the terminal vinyl carbon. Notably, the product **302** obtained from the S_N2'-pathway is significantly more polar than **301**, a difference that is most likely caused by an intramolecular hydrogen bonding interaction associated with the 1,2-azidoalcohol motif as mentioned earlier in this chapter.

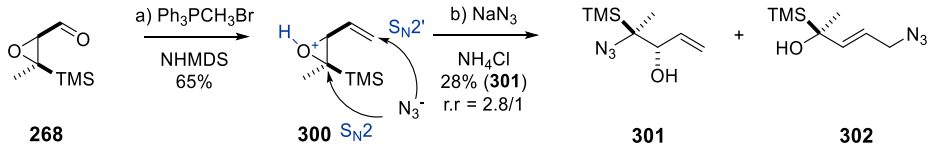

Scheme 100. Synthesis and epoxide opening of vinyloxirane **300**. Conditions: a) Ph_3PCH_3Br (1.5 eq.), NHMDS (1.45 eq.), THF, r.t., 1 h, **65%**; b) NaN_3 (5.0 eq.), NH_4Cl (2.5 eq.), MeOH/H_2O (6:1), 50 °C, 21 h; 28% (**300**), 10% (**302**) (initial and best attempt).

To investigate the influence of the temperature on the regioselectivity of the epoxide opening, a stock solution of **300** was prepared and the reaction was carried out at three different temperatures (40, 50

and 60 °C) and 48 hours of stirring as the initial 21 hours resulted in only incomplete conversion. Afterwards the reactions were subjected to work-up and crude NMR´s were recorded.

Table 12. Influence of the temperature on product distribution for the epoxide opening of **300**.

entry	T [°C]	reaction time [h]	epoxide **300**	1,2-product **301**	1,4-product **302**
1	40	48	0.55	1.0	0.08
2	50	48	0.37	1.0	0.06
3	60	48	0.73	1.0	0.05

As visible (Table 12), longer reaction times led to nearly no detection of the S_N2'-product **302**. A temperature increase from 40 °C to 50 °C significantly increased the ratio of **301**/**300** while a further increase to 60 °C led to the opposite result.

These inititally unintuitive results can be explained by thermal instabilities of **301** and **302**. According to these data, allylic azide **302** poses the least thermal stability showing nearly full decomposition after 48 hours of reaction time, regardless of the temperature. The desired compound **301** shows good stabilities towards temperatures of up to 50 °C.

More precise insights into the thermal decomposition behavior of **301** and **302** could have been obtained by conducting separate experiments to investigate the stability of the isolated compounds under controlled conditions.

However, these observations do give an explanation why complexation with the MIDA-ligand for compound **286** (Chapter 6.3.2) failed, as even higher temperatures are required while similar thermal stabilities can be considered for compound **286**.

A slightly different approach was followed when epoxyaldehyde **268** was transformed into the dibromovinyloxirane **303** as a potential alkyne precursor (Scheme 101).

Here, the initial *Wittig* reaction showed complete conversion of the starting aldehyde **268** but only 25% could be isolated with a good purity due to very close elution of compound **303** and unreacted triphenylphosphane (TPPO).

The subsequent epoxide opening is debatable as a single product **304** was observed in the crude NMR along with minor impurities indicating that the S_N2'-reaction resulting in **305** is prevented due to steric hindrance caused by the geminal dibromide.

On the other hand, as only 31% of product **304** (from 46% crude) was isolated after column chromatography, one could argue that the other half of the starting material **303** indeed reacted at the dibromovinyl terminus resulting in a presumably highly unstable allylic dibromo azide **305** (no such compounds are described in literature) followed by a decomposition cascade.

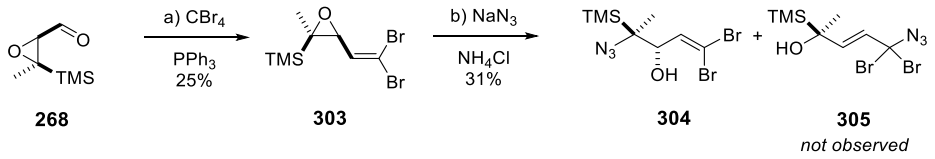

Scheme 101. Synthesis and epoxide opening of dibromovinyloxirane **303**. Conditions: a) Ph_3P (4.9 eq.), CBr_4 (2.0 eq.), DCM, 0 °C, 45 min, 25%; b) NaN_3 (5.0 eq.), NH_4Cl (2.4 eq.), MeOH/H_2O (6:1), 45 °C, 44 h; 31%.

Further transformations of this compound were not pursued due to the low yields obtained during both steps.

With a portion of the vinyl-1,2-azidoalcohol **301** in hand, an LAH reduction was carried out, successfully yielding the corresponding vinyl-1,2-aminoalcohol **306** in an excellent yield of 90% (Scheme 102). Subsequent *Boc*-protection of the resulting amine proceeded smoothly, affording the *N*-protected metathesis precursor **297**. This outcome stood in contrast to the PMB-protected diol (**292**, Scheme 98) for which the *Boc*-protection proceeded with a significantly lower yield of only 25%.

To ensure a protected version of **297** was available, the corresponding *N*,*O*-acetal **307** was also synthesized using 2,2-DMP. For this molecule, a TBS-protection was deliberately omitted, as the large steric bulk of the TBS group could potentially interfere with the metathesis reaction.

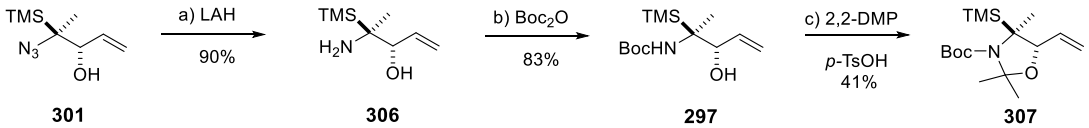

Scheme 102. Synthesis of the metathesis precursors **297** and **307**. Conditions: a) LAH (2.0 eq.), Et_2O, r.t., 3 h, 90%; b) Boc_2O (1.1 eq.), Et_3N (1.1 eq.), DCM, r.t., 12 h, 83%; c) 2,2-DMP (7.0 eq.), *p*-TsOH (0.1 eq.), toluene, 100 °C, 9 h, 41%.

Next, the planned cross-metathesis between fragment **297** and vinyl MIDA boronate (**298**) was explored. According to literature, vinyl MIDA boronate (**298**) behaves as a type III olefin[217] in accordance with *Grubbs*' general model for selectivity in cross-metathesis reactions[220]. Typically, secondary allylic alcohols such as **297** are classified as type II olefins under this model, indicating moderate reactivity in metathesis. However, in this case, the high steric demand imposed by the adjacent quaternary center likely alters the behavior of **297**, causing it to act more like a type III or even type IV olefin, which are known to react significantly more slowly in metathesis reactions. This slow reactivity could pose a challenge for efficient product formation. To test this hypothesis, several conditions for the cross metathesis were explored (Table 13).

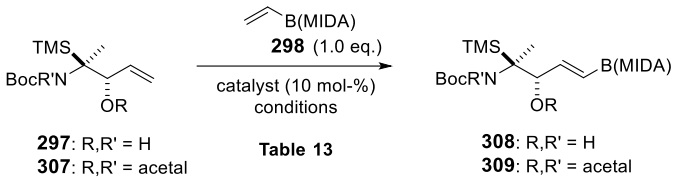

297: R,R' = H
307: R,R' = acetal

Table 13

308: R,R' = H
309: R,R' = acetal

Table 13. Explored conditions for the cross metathesis between **297**/**307** and vinyl MIDA-boronate (**298**).

entry	substrate	catalyst	conditions	yield	comment
1	**297**	Grubbs II	DCE, r.t., overnight	-	
2	**297**	Grubbs II	DCE, 50 °C, overnight	traces	MS: $[M+Cl^-]^-$
3	**297**	Grubbs II	toluene, 95 °C, 10 h	traces	MS: $[M+Cl^-]^-$
4	**297**	Stewart-Grubbs	toluene, 100 °C, overnight	-	
5	**297**	Nitro-Grela	DCM, 60 °C, overnight	-	pressure tube
6	**307**	Nitro-Grela	DCM, 60 °C, overnight	-	pressure tube

Indeed, when a 1:1 mixture of **297** and **298** was reacted with *Grubbs* II catalyst at room temperature, no reaction was observed (entry 1). At higher temperatures (entries 2–3), only traces of the desired product **308** could be detected via MS (ESI negative), appearing as a rather exotic $[M+Cl^-]^-$ adduct.

To address the previously mentioned steric interferences, a switch was made to the sterically less demanding *Stewart-Grubbs* catalyst[221] under forcing conditions (toluene, 100 °C, overnight) (entry 4), however no product formation was observed. Similarly, when the highly active Nitro-*Grela* catalyst[222] was employed, the reaction of both starting materials **297** and **307** again failed to yield any detectable products **308**/**309**.

Due to a shortage of material, further trials were not conducted. However, these results strongly suggest that, owing to the high steric demand of the quaternary center, **297** indeed behaves like a type III or even type IV olefin, leading to very slow conversions, even under forcing conditions. Given the limited remaining material, it was decided to redirect efforts towards feasibility studies of the *Peterson* olefination, rather than investing further resources into this challenging cross-metathesis.

6.3.4 Feasibility studies of the *Peterson* elimination

With some remaining unprotected 1,2-aminoalcohol **306** in hand, it was investigated whether the intended *Peterson* olefination would be a suitable strategy for constructing the *Z*-enamide motif found in the authentic natural product bacillaene (**1**). To assess the feasibility of this approach, **306** was subjected to an amide coupling with carboxylic acid fragment **244** (Chapter 4.4.2).

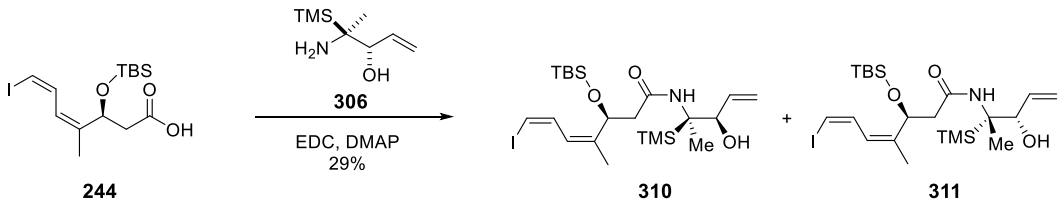

Scheme 103. Successful synthesis of α-silyl-β-hydroxyamides **310**/**311** by amide coupling of fragment **244** with 1,2-aminoalcohol **306**. Conditions: **306** (1.5 eq.), EDC•HCl (1.5 eq.), DMAP (1.5 eq.), DCM, r.t., overnight, **29%**.

When the reaction was performed in the presence of EDC and DMAP (unoptimized procedure), the expected α-silyl-β-hydroxyamides **310**/**311** were successfully isolated as a mixture of diastereoisomers. This outcome was anticipated, given the racemic nature of **306**. However, since the subsequent *Peterson* elimination is known to proceed in a diastereoconvergent manner,[81] this diastereomeric mixture was indeed expected to converge into a single stereodefined product after elimination.

However, as expected, the formation of two diastereomers complicated both the isolation and characterization of the obtained intermediates.

Next, the mixture of **310** and **311** was dissolved in THF, cooled to −41 °C, and reacted with of KO*t*Bu (1.3 eq.) following *Fürstner's* conditions.[79] Initially, no reaction was observed after 45 minutes, prompting the addition of a second portion (1.3 eq.) of KO*t*Bu. Upon warming to room temperature, two new product spots were detected by TLC.

After work-up, the reaction mixture was cautiously purified using a C18 SPE-cartridge to prevent potential decomposition by normal phase silica. Other than expected, the obtained product

(Scheme 104) was identified as the corresponding double-elimination product **313**, resulting from the intended *Peterson* elimination along with an additional undesired elimination of hydrogen iodide from the iododiene.

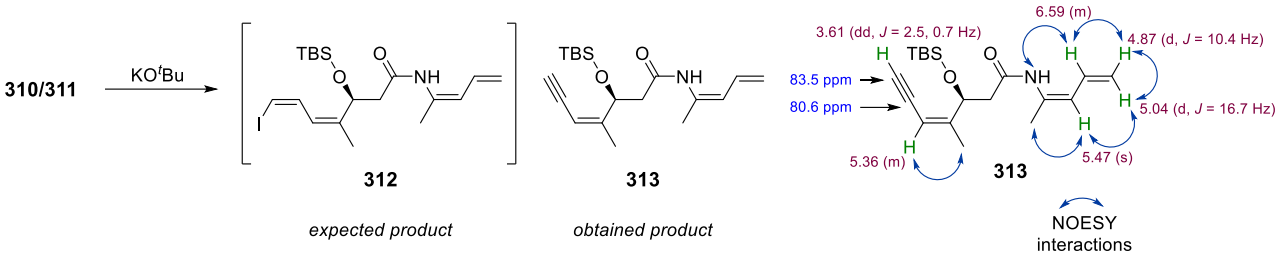

Scheme 104. Reaction of the α-silyl-β-hydroxyamides **310**/**311** with KO*t*Bu in the intended *Peterson* olefination. 2D-NMR analysis identified the obtained product as the double-elimination product **313**.

The presence of an alkyne was confirmed by ^{13}C-NMR analysis, which displayed two characteristic signals in the 80 ppm region. Furthermore, in the ^{1}H-NMR spectrum, a proton signal at 3.61 ppm (alkyne) exhibited two long-range *J*-couplings (over four and six bonds) to both the olefinic hydrogen and the adjacent methyl group, as confirmed by COSY-NMR.

The formation of the trisubstituted *Z*-configured dienamide was unambiguously verified by NOESY-NMR, which showed perfectly matching *NOE*-interactions among all hydrogen atoms involved in the conjugated *Z*-enamide system, providing clear structural confirmation. The terminal hydrogens of the conjugated dienamide system could be distinguished due to a difference in chemical shifts and their corresponding *cis*- or *trans*-coupling constants (10.4 Hz, 16.7 Hz).

As only a small sample of **313** was obtained from this reaction, all material was submitted for NMR analysis, and neither the yield nor the optical rotation was determined. However, based on the obtained results, it is evident that *Fürstner's Peterson* olefination approach is indeed a viable strategy for the synthesis of bacillaene's (**1**) trisubstituted *Z*-enamide motif.

Moreover, although the amide synthesis forming **310/311** and the subsequent elimination reaction had not been optimized, the desired *Z*-enamide found in **313** was successfully obtained in a single experiment. The observed double elimination can likely be avoided by strategically repositioning this reaction within the overall synthetic sequence, as will be discussed in chapter 7.2.

7. Conclusion and Outlook

7.1 Conclusion

During this work, the total synthesis of the unstable polyketide and polyene antiobiotic bacillaene (**1**) as well as the synthesis of a structurally simplified analogue (**7**) was explored. The key motivation was to establish a modular, iterative cross coupling strategy based on the use of hetero bimetallic linchpin reagents along with MIDA-protected haloboronic esters that would allow for a rapid assembly of the extended polyene framework through iterative cross coupling. The bacillaene analogue (**7**) was designed as a synthetically more accessible model system, lacking the sensitive *Z*-enamide moiety of bacillaene (**1**), yet retaining the essential core polyene backbone of bacillaene (**1**).

In Part 2, several retrosynthetic approaches (3.1-3.2) for bacillaene (**1**) and its analogue (**7**) were discussed, followed by the successful syntheses of all fragments required for the synthesis of the analogue (**7**). For the western fragment II (**122**), several approaches were tested to achieve the highest possible purity of the *Z*,*E*-iododieneamine (**152**). However, the most efficient approach was one of the earlier developed ones (4.1.2). A highlight were the syntheses of several homo- and heterobimetallic 1,4-difunctionalized isoprene derivatives (4.2.1-4.2.5) providing highly efficient routes to methyl-branched linchpin dienes. A MIDA-derivative was synthesized by an unprecedented MIDA-boryl *Takai* olefination for which reagent **195** was developed (4.2.4).

Part 3 dealt with the formation of the higher conjugated polyene systems via iterative cross-coupling of the previously synthesized fragments. Here, it was shown that the coupling order of the individual fragments had a significant impact on the success of the individual coupling reactions and on the stability of the resulting intermediates. The initially planned synthetic sequence following a “left-to-right” approach was experimentally revised to a “center-to-edges” approach (5.2.4), in which the geometrically defined central tetraene V (**135**) was established first, and the molecular scaffold was then extended in both directions. The isomerization behavior of tetraene V (**135**) toward various physicochemical conditions was deeply investigated and its isomerization behavior mimicked that of the natural product bacillaene (**1**) confirming its previously identified “triggerpoint for isomerization”.[20]

A critical milestone was the successful synthesis, isolation, and purification of the hexaene II (**131**) with a confirmed geometrical purity of 96% (5.2.6). For the synthesis of the geometrically defined hexaene system, several catalysts were explored and it was shown that the catalyst/ligand systems have a

significant impact on the stereochemistry of the conjugated system, contrary to the usually reported stereoretentive nature of the *Suzuki-Miyaura* coupling.

To evaluate the influence of other reaction parameters on reaction progress, a UV-vis based screening method was developed to monitor reaction conversions, leveraging the bathochromic shift that occurs upon formation of a larger conjugated system. This method allowed for a fast- and resourcefriendly assessment of reaction conditions without the need for full sample preparation and HPLC analysis for every reaction.

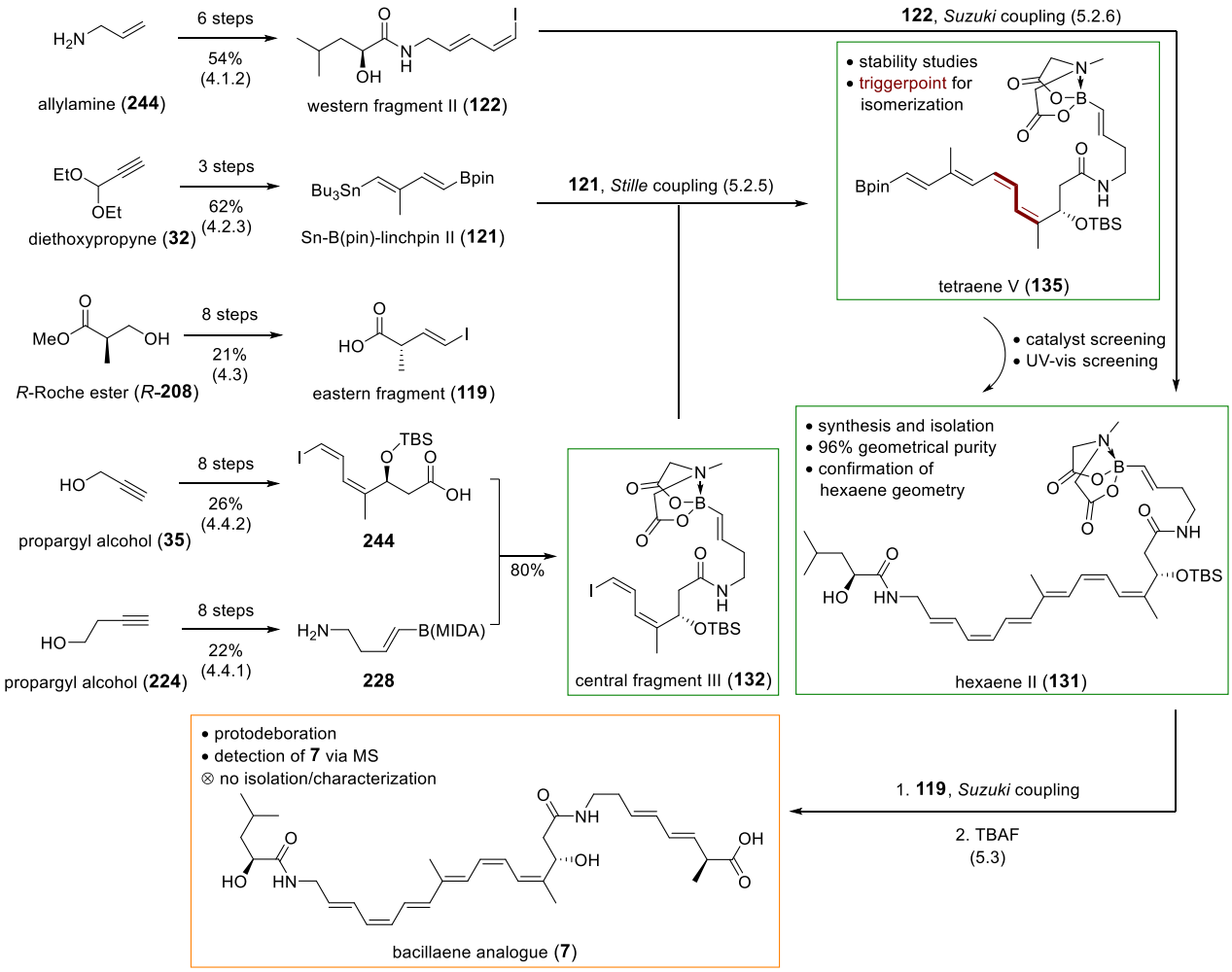

Scheme 105. The so far most successful synthetic route towards a first bacillaene analogue (**7**) developed during this work.

The final *Suzuki*-coupling (5.3) of hexaene II (**131**) with the eastern fragment (**119**) was investigated showing that protodeboration was a significant side reaction within this step. Two simplified model systems did not show similar protodeboration during this coupling step indicating that the severe

protodeboration of **131** is an intrinsic property of this unstable molecule. Due to this behavior, the coupling product **250** could not be synthesized in sufficient quantities to allow for an isolation and full characterization. However, it was demonstrated that treatment of **250** with TBAF was tolerated and indeed resulted in the formation of the desired bacillaene analogue (**7**), which was detected via mass spectrometry. These results indicate that the formation of the hexaene system should be positioned at a later stage of the coupling sequence and lead to a final revised synthetic approach (7.2).

In parallel (Part 4), multiple strategies (6.2-6.3) were explored to facilitate the introduction of the enamide motif into the synthetic sequence providing a pathway for the authentic natural product bacillaene (**1**). The synthesis of the enamide motif via *N*-aclyation (6.2) of methyl 3-aminocrotonate (**92**), a stable *Z*-configured enamine was explored first. However, *N*-aclyations proceeded with low yield and poor diastereomeric selectivties. Moreover, further functionalizations of the resulting enamidoesters proved difficult and require a more systematic evaluation of these underexplored compounds in the future.

Next, *Fürstner's Peterson*-olefination approach (6.3) was investigated requiring the highly functionalized *Peterson*-precursor I (**264**). Several pathways (6.3.1-6.3.3) for the synthesis of **264** were explored, however none of them yielded the desired fragment **264**. Nevertheless, with a simplified vinyl system **306**, the feasibility of the *Peterson*-approach (6.3.4) could be successfully confirmed by the synthesis of the *Z*-configured dieneamide **313**. This outcome suggests that the *Peterson*-approach, when strategically positioned within the synthetic sequence, is indeed a viable method, particularly as it enables an early C-N bond formation combined with a late-stage elimination and formation of the unstable enamide-system.

In conclusion, significant progress was made toward the total synthesis of the highly unstable natural product bacillaene (**1**) and its analogue (**7**). The hexaene core has been synthesized with an excellent geometrical purity and it has been shown that a total synthesis of this molecule is indeed possible, if the problems faced during the final coupling step are correctly addressed.

7.2 Outlook

Building on the results obtained during this work, revised synthetic approaches for both bacillaene (**1**) and its structurally simplified analogue (**7**) are proposed. These new routes are based on key insights gained throughout this work, particularly the observation that further elaboration at the MIDA-bearing site after formation of the hexaene intermediate II (**132**, see Chapter 5.3) should be avoided. Therefore, the construction of the fully conjugated hexaene should be positioned closer to the end of the synthetic sequence, necessitating earlier incorporation of the complete side chain.

For the bacillaene analogue (**7**), the test system **249,** previously used for evaluating *Suzuki* coupling conditions (5.3), was successfully synthesized by *Johannes Herbst*.[155] Further *C*-protection and *N*-deprotection steps would yield amine **314**, which could be coupled with carboxylic acid **244** (4.4.2) to form the central eastern fragment (**315**). Based on bioinformatic predictions provided by *Dickschat*,[16] the preparation of *R*-**244** should be considered.

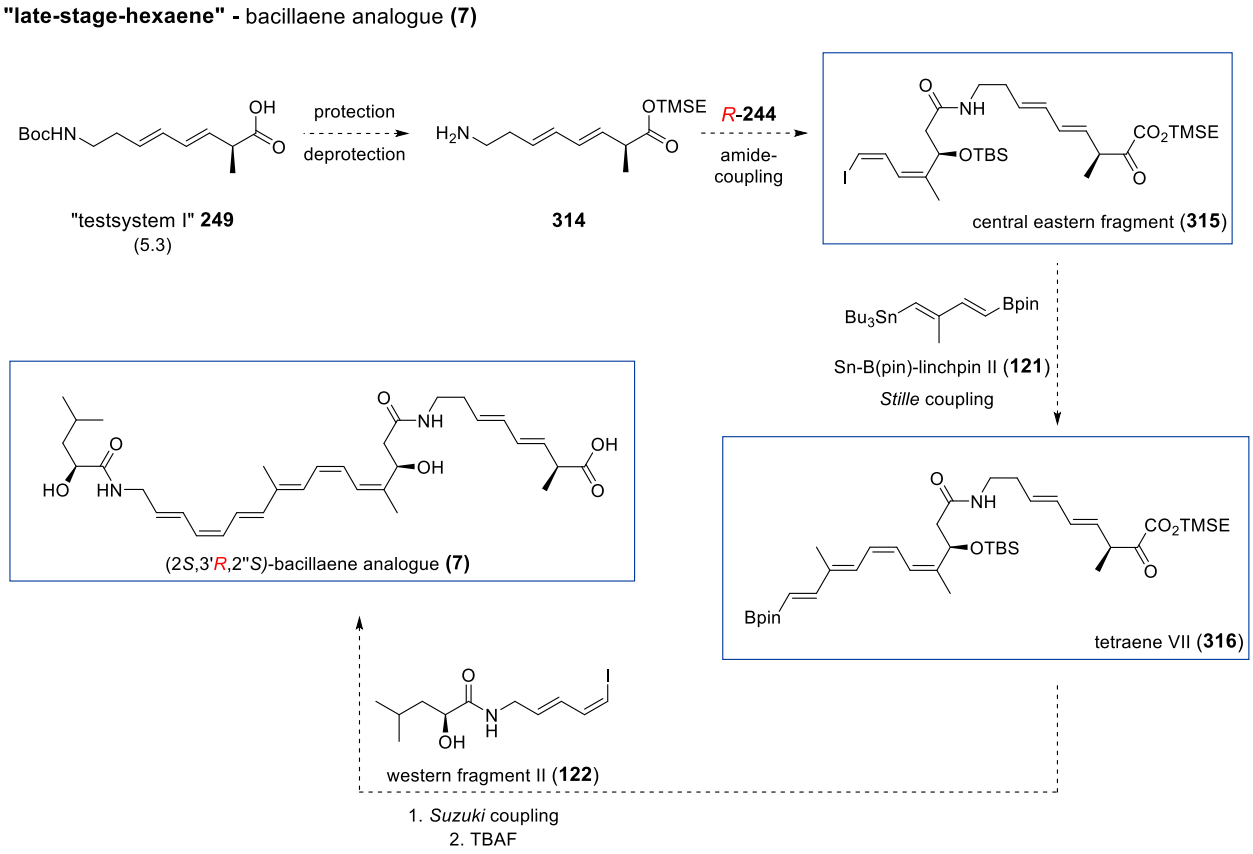

Scheme 106. Suggested synthetic pathway for the bacillaene analogue (**7**).

A subsequent *Stille* coupling between **315** and the Sn-B(pin)-linchpin II (**121**) would generate the tetraene VII (**316**), containing the same polyene backbone as the previously synthesized and characterized tetraene V (**135**, see 5.2.5). A final *Suzuki* coupling, analogous to the reaction described in Chapter 5.2.6, would then yield the conjugated hexaene framework, followed by global deprotection to afford the bacillaene analogue (**7**).

For the authentic natural product bacillaene (**1**), a similar route is envisioned (Scheme 107), incorporating a late-stage *Peterson* elimination to install the sensitive *Z*-enamide. This procedure is supported by the feasibility studies described in Chapter 6.3.4. In analogy to the test system **249**, the eastern fragment II (**215**), bearing a TBS-protected β-hydroxy silane moiety, could be coupled with carboxylic acid **244** to generate the central eastern fragment II (**318**). Again, the use of *R*-**244** should be considered.

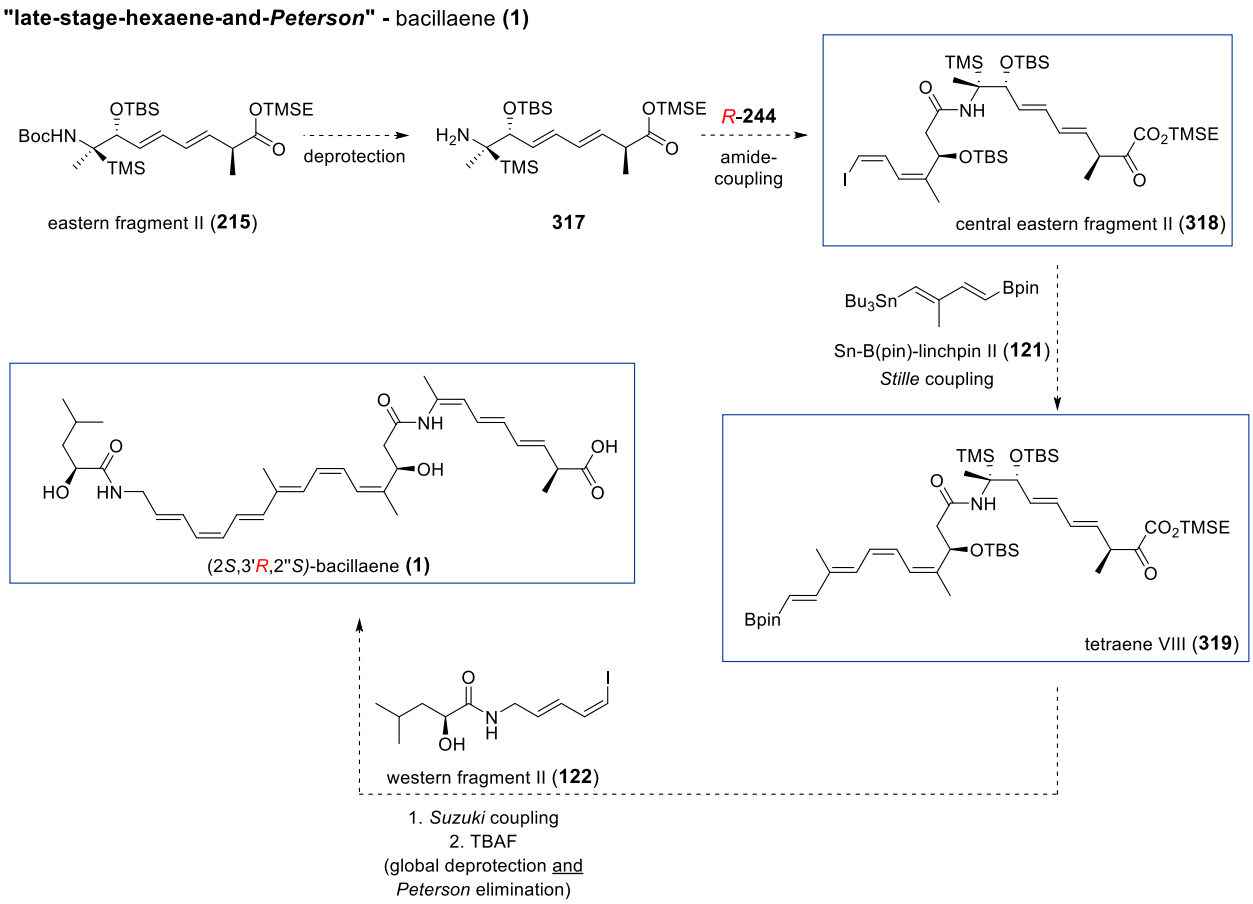

Scheme 107. Suggested synthetic pathway for the authentic natural product bacillaene (**1**) incorporating the late-stage global deprotection/*Peterson* elimination.

A *Stille* coupling between **318** and the Sn-B(pin)-linchpin II (**121**) would yield tetraene VIII (**319**), again featuring the same polyene backbone as tetraene V (**135**). Synthesis of the hexaene system via *Suzuki* coupling and global deprotection would then be followed by TBAF-mediated *Peterson* elimination to deliver bacillaene (**1**), as previously demonstrated in the total synthesis of (+)-crocacin A (2.4.3).[65]

Unlike the test system **249**, for which a *Suzuki* coupling was successfully performed, a *Stille* coupling is recommended for the synthesis of fragment **215**. This is suggested due to the difficulties encountered during the synthesis of the *Peterson* precursor I (**264**, see 6.3.1–6.3.3), as well as the successful *Stille* coupling of **218**-(CO_2tBu) in the total synthesis of (–)-isodomoic acid B (**214**, see 4.3).[89]

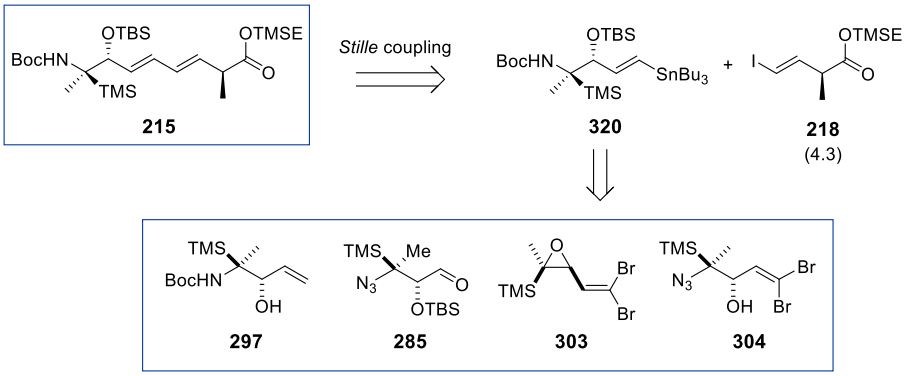

Scheme 108. Retrosynthesis of the eastern fragment II (**215**) resulting in the vinyl stannane **320** (top) along with possible precursors to **320** synthesized within this work.

Possible precursors for vinyl stannane **320,** required for the preparation of fragment **215**, are provided in Scheme 108 and were partially synthesized during this work (blue box). However, due to difficulties faced during attempts to synthesize the *Peterson* precursor **264**, a fully defined route toward **320** is not proposed at this stage.

These synthetic routes provide a revised approach for the total synthesis of bacillaene (**1**) and its analogue (**7**), based on experimentally gained insights with these highly delicate polyene systems.

8. Experimental Section

8.1 General Methods

Reaction Conditions

All reagents were purchased from commercial suppliers (Sigma Aldrich, TCI, Acros, Alfa Aesar, abcr, Carbolution) in the highest purity grade available and used without further purification. Anhydrous solvents (THF, toluene, CH_2Cl_2, MeCN) were obtained from a solvent drying system MB SPS-800 (MBraun) and stored over molecular sieves (4 Å).

The reactions in which dry solvents were used were performed under an argon atmosphere in flame-dried glassware, which had been flushed with argon unless stated otherwise. The reactants were handled using standard Schlenk techniques. Temperatures above r.t. (23 °C) refer to oil bath temperatures which were controlled by a temperature modulator. For cooling, the following baths were used: acetone/dry ice (−78 °C), acetonitrile/dry ice (−40 °C), water/ice (0 °C). For cooling overnight an immersion cooler was used (Huber, TC100E-F).

TLC monitoring was performed with silica gel 60F254 pre-coated polyester sheets (0.2 mm silicagel, Macherey-Nagel) and for reversed phase TLC silica gel 60 RP-18 F254S pre-coated aluminum sheets (Merck). For highly acid sensitive compounds TLC sheets coated with Alox (Macherey-Nagel) were used. The spots were visualized using UV light and stained with a solution of CAM (1.0 g $Ce(SO_4)_2$), 2.5 g $(NH_4)_6Mo_7O_{24}$, 8 mL conc. H_2SO_4 in 100 mL H_2O) and subsequent heating.

Purification Methods

For column chromatography, silica gel (pore size 60 Å, 40-63 µm) obtained from Merck or Sigma Aldrich was used. For reversed phase column chromatography C18-reversed phase silica gel (pore size 90 Å) from Sigma Aldrich or Carl Roth was used. Compounds were eluted using the stated mixtures under a positive pressure of argon or air. Solvents for column chromatography were distilled prior to use.

SPE purifications were carried out with Chromabond C18 ec cartridges, 45 µm particle size, 500 mg bed size, fitted with a suitable syringe adapter under manual positive pressure. Collected fractions were analyzed by UV-VIS spectroscopy using 5-10 µL of the eluate diluted with 0.5 mL MeCN.

Semi-preparative and analytical HPLC analyzes were performed on *Knauer Wissenschaftliche Geräte GmbH* systems by *Andreas J. Schneider*. The solvents for HPLC were purchased in HPLC grade. The chromatograms were recorded by UV-detection with Agilent OpenLab version A.04.10 software.

Table 14. HPLC-systems from *Knauer Wissenschaftliche Geräte GmbH* used by *Andreas J. Schneider.*

System (analytical)	**A**	**B**	**C**
series	PLATINblue/Azura	PLATINblue/Azura	Azura
pumps (from 03/24)	binary, HPG P1, 5 mL (binary, HPG P 6.1L, 5 mL)	binary, HPG P1, 5 mL (quarternary, LPG P 6.1L, 5 mL)	binary, HPG P 6.1L, 10 mL
pressure	1000	1000	700
autosampler (from 03/24)	AS1 with 10 µL injection loop (AS 6.1L with 10 µL injection loop)	AS1 with 10 µL injection loop	3950 with 100 µL injection loop
mixing chamber	static, 100 µL	static, 100 µL	static mixing chamber, 100 µL
column heater	T-1	T-1	CT-2.1
detection type (from 03/24)	PDA UV/VIS detection PDA1, D_2/Hg halogen lamps, 190-1000 nm (PDA UV/VIS detection DAD 6.1L, D_2/Hg halogen lamps, 190-1020 nm)	PDA UV/VIS detection PDA1, D_2/Hg halogen lamps, 190-1000 nm PDA UV/VIS detection DAD 2.1L, D_2-lamps, 190-700 nm	PDA UV/VIS detection DAD 2.1, D_2-lamps, 190-1020 nm
degasser	analytical 2-channel-online-degasser	analytical 4-channel-online-degasser	analytical 2-channel-online-degasser
System (preparative)	**D**	**E**	**F**
series	Azura	Azura	Azura
pumps	binary, P 2.1L, 100 mL	P 2.1L, 100 mL, ternary LPG-block	binary, HPG P 6.1L, 50 mL
pressure	400	400	200/300
autosampler	ASM 2.2L with feed pump P 4.1S	manual injection valve V 4.1S (6 port)	ASM 2.1L with feed pump P 2.1S
mixing chamber	static, SmartMix 350 µL	static, SmartMix 350 µL	integrated static mixing chamber, 200 µL
detection type	MWL 2.1L with D_2 lamp (190-700 nm) with 3 mm (2 µL) flow cell	MWL 2.1L with D_2 lamp (190-700 nm) with 3 mm (2 µL) flow cell	MWL 2.1L with D_2 lamp (190-700 nm) with 3 mm (2 µL) flow cell
degasser	preparative 2-channel-online-degasser	preparative 2-channel-online-degasser	preparative 2-channel-online-degasser DG 2.1S

Analytical Methods

All NMR spectra were recorded on Bruker spectrometers at the University Bonn under supervision of Dr. Senada Nozinovic with operating frequencies of 100 (^{13}C), 125 (^{13}C), 175 (^{13}C), 400 (^{1}H), 500 (^{1}H), and 700 MHz (^{1}H) in deuterated solvents obtained from Deutero, Carl Roth or Sigma Aldrich. Spectra were measured at room temperature unless stated otherwise and chemical shifts are reported in ppm relative to $(Me)_4Si$ (δ = 0.00 ppm) and were calibrated to the residual signal of undeuterated solvents. Data for ^{1}H-NMR spectra are reported as follows: chemical shift (multiplicity, coupling constants, number of hydrogens, assignment). Abbreviations used are: s (singlet), d (doublet), t (triplet), q (quartet), m (multiplet), br (broad).

Mass spectra (MS) and High-resolution-mass spectra (HRMS) were recorded on the documented systems in Table 15 at the University Bonn under supervision of Dr. *Marianne Engeser*.

Table 15. Used MS systems for MS and HRMS.

System	Manufacturer	Measurements
microTOF-Q	Bruker Daltonik (Bremen)	ESI, APCI, nano-ESI MS/MS, LC/MS, DC/MS
Orbitrap XL	Thermo Fisher Scientific (Bremen)	ESI, APCI, APPI, nano-ESI
Apex IV FT-ICR	Bruker Daltonik (Bremen)	ESI, nano-ESI, MALDI, EI, CI

UV-vis spectroscopy was carried out using an Agilent Cary 60 UV-vis spectrometer and Brand single use UV cuvettes (Cat. No. 759200) with suitable covers (Cat. No. 759242).

Irradiation experiments

Irradiation experiments were carried out using Prizmatrix fiber collimated LEDs.

Table 16. Light output of used LEDs.

λ [nm]	310	325	365	white
Output power (1 m optical fiber) [mW]	1	8.6	170	74

8.2 Syntheses of Fragments

8.2.1 Syntheses of the western fragments I/II

(*S*)-2-hydroxy-4-methylpentanoic acid (137)

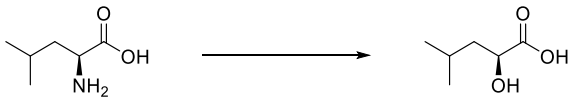

$C_6H_{12}O_3$
M = 132.16 g/mol

The synthesis was carried out according to a known literature procedure:[92]

To a solution of *L*-Leucine (9.63 g, 73.4 mmol, 1.00 eq.) in H_2O (120 mL) was added a 2 M solution of H_2SO_4 (45 mL, 90 mmol, 1.2 eq.) at 0 °C. The resulting solution was stirred at 0 °C and a solution of $NaNO_2$ (11.5 g, 167 mmol, 2.30 eq.) in H_2O (20 mL) was added over one hour. The resulting mixture was stirred overnight at room temperature. After full conversion, the crude mixture was diluted with ethyl acetate (100 mL). Phases were separated and the aqueous phase was extracted with EtOAc (4 × 100 mL). The combined organic layers were dried over $MgSO_4$, filtered and the solvent was evaporated under reduced pressure. The resulting crude product was recrystallized twice from Et_2O/*n*-hexane (1:10) and once from Et_2O/*n*-hexane (1:1) to obtain the compound **137** as a white crystalline solid (6.57 g, 49.7 mmol, 68%). $\mathbf{R_f}$ = 0.36 (CH/EtOAc, 1:1); $\boldsymbol{\alpha_D^{20}}$ = −12.8 (c = 1.0, EtOH); **^{1}H-NMR** (400 MHz, $CDCl_3$) δ = 0.97 (m, 6H), 1.63 (ddd, *J* = 9.0 Hz, *J* = 5.3, *J* = 3.0 Hz, 2H), 1.91 (m, 1H), 4.29 (m, 2H); **^{13}C-NMR** (101 MHz, $CDCl_3$) δ = 21.6, 23.3, 24.6, 43.4, 69.1, 180.7; **MS (ESI)** m/z: 271.132 [$(2M-OH+Na)^+$, 100]. The spectroscopic data were in agreement with those previously pulished.[92]

(*S*)-2-((*tert*-butyldimethylsiliyl)oxy)-4-methylpentanoic acid (138)

$C_{12}H_{26}O_3Si$
M = 246.42 g/mol

The synthesis was carried out according to a known literature procedure:[92]

To a solution of *S*-2-hydroxy-4-methylpentanoic acid (1.50 g, 11.4 mmol, 1.00 eq.) in DMF (10 mL) was added *tert*-butyldimethylsilyl chloride (4.35 g, 28.9 mmol, 2.54 eq.) and imidazole (3.71 g, 54.5 mmol, 4.78 eq.). The resulting mixture was stirred for 16 hours. Afterwards, the reaction mixture was diluted with EtOAc and toluene (1:1, 10 mL) and acidified to pH 3 with citrate buffer solution (150 mL). Phases

were separated and the organic layer was washed with conc. aq. $NaHCO_3$ (100 mL), H_2O (100 mL) and brine (100 mL), dried over $MgSO_4$, filtered and the solvent was removed under reduced pressure. The resulting crude product was purified by flash column chromatography (Silica, CH/EtOAc 5:1) to yield the desired product **138** as a colorless oil (1.43 g, 5.80 mmol, 51 %). $\mathbf{R_f}$ = 0.25 (CH/EA, 5:1); $\boldsymbol{\alpha_D^{20}}$ = −28.0 (c = 1.0, EtOH); **^{1}H-NMR** (500 MHz, $CDCl_3$) δ = 0.05 (s, 3H), 0.08 (s, 3H), 0.93 (m, 6H), 0.94 (s, 9H), 1.48 (ddd, *J* = 13.3 Hz, *J* = 8.7 Hz, *J* = 4.3 Hz, 1H), 1.62 (ddd, *J* = 13.6 Hz, *J* = 8.6 Hz, *J* = 5.2 Hz, 1H), 1.79 (m, *J* = 13.4 Hz, *J* = 8.8 Hz, *J* = 6.8 Hz, *J* = 5.1 Hz, 1H), 4.16 (dd, *J* = 8.5 Hz, *J* = 4.3 Hz, 1H); **^{13}C-NMR** (126 MHz, $CDCl_3$) δ = -5.3, -4.8, 22.0, 23.5, 24.4, 25.9, 44.4, 71.7, 174.7. **HRMS (ESI)** *m/z*: calc. for $[M+H]^+$: 245.1567; found: 245.1552. The spectroscopic data were in agreement with those previously pulished.[92]

(*S*)-*N*-allyl-2-((*tert*-butyldimethylsiliyl)oxy)-4-methylpentanamide (139)

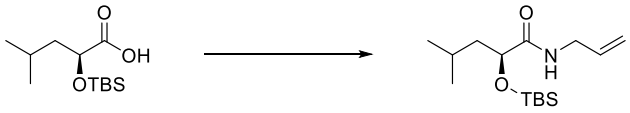

$C_{15}H_{31}NO_2Si$
M = 285,50 g/mol

This synthesis was carried out during my master thesis:[91]

To a solution of (*S*)-2-*tert*-butyldimethylsiliyloxy-4-methylpentanoic acid (0.50 g, 2.03 mmol, 1.00 eq.), PyBOP (1.27 g, 2.44 mmol, 1.20 eq.), HOBt (0.330 g, 2.44 mmol, 1.20 eq.) in anhydrous DCM (9 mL) and dry DMF (0.5 mL) was added allylamine (0.20 mL, 2.7 mmol, 1.3 eq.) and DIPEA (0.50 mL, 2.9 mmol, 1.4 eq.). The resulting mixture was stirred under argon overnight. After complete conversion, the mixture was diluted with H_2O (10 mL). Phases were separated and the organic layer was washed with water (3 × 10 mL). The aqueous phase was extracted with DCM and the pooled organic layers were dried over $MgSO_4$, filtered and the solvent was evaporated. The resulting brown crude product was purified by flash column chromatography (Silica, CH/EtOAc 3:1) to yield the amide **139** as a colorless oil (328.4 mg, 1.15 mmol, 57%). $\mathbf{R_f}$ = 0.50 (CH/EtOAc, 2:1); $\boldsymbol{\alpha_D^{20}}$ = −52.1 (c = 1.1, DCM); **^{1}H-NMR** (500 MHz, $CDCl_3$) δ = 0.07 (s, 3H), 0.10 (s, 3H), 0.92 (m, 15H), 1.58 (m, 2H), 1.79 (m, *J* = 8.3 Hz, *J* = 6.7 Hz, *J* = 5.3 Hz, 1H), 3.88 (m, 2H), 4.15 (dd, *J* = 7.2 Hz, *J* = 4.6 Hz, 1H), 5.15 (m, 2H), 5.83 (ddt, *J* = 17.2 Hz, *J* = 10.3 Hz, *J* = 5.7 Hz, 1H), 6.60 (bs, 1H); **^{13}C-NMR** (126 MHz, $CDCl_3$) δ = −5.0, −4.7, 18.2, 22.5, 23.6, 24.2, 25.9, 41.4, 45.0, 72.8, 116.7, 134.2, 174.3; **HRMS** (ESI) m/z: calc. for $[M+H]^+$: 286.2197; found: 286.2197.

(*S*)-*N*-(2'-oxoethyl)-2-((*tert*-butyldimethylsiliyl)oxy)-4-methylpentanamide (140)

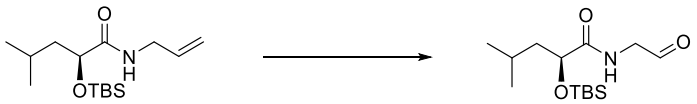

$C_{14}H_{29}NO_3Si$
M = 287.48 g/mol

This synthesis was carried out during my master thesis:[91]

S-*N*-allyl-2-*tert*-butyldimethylsiliyloxy-4-methylpentanamide **139** (77.7 mg, 0.27 mmol, 1.0 eq.) and osmium (VIII)oxide (2.5 wt−% in *t*-BuOH, 200 mg, 25 µmol, 0.03 eq.) were dissolved in 1,4-dioxane (2 mL). Subsequently, water (2 mL) was added, resulting in a black solution. $NaIO_4$ (200 mg, 0.94 mmol, 3.5 eq.) was added over 15 minutes, resulting in a decoloration of the mixture and formation of a yellow-white precipitate. After three hours, the reaction mixture was diluted with water (2 mL), EtOAc (2 mL) and filtered over celite. Phases were separated and the aqueous phase was extracted with EtOAc (3 x 20 mL). The combined organic layers were dried over $MgSO_4$, filtered and concentrated. The resulting black crude product was purified by column chromatography (Silica, CH/EtOAc 2:1) to yield the desired aldehyde **140** (66.5 mg, 0.23 mmol, 85%) as a colorless oil. $\mathbf{R_f}$ = 0.15 (CH/EtOAc 2:1); $\boldsymbol{\alpha_D^{20}}$ = −56.3 (c = 1, DCM); **^{1}H-NMR** (500 MHz, $CDCl_3$) δ = 0.09 (s, 3H), 0.11 (s, 3H), 0.92 (t, *J* = 6.8 Hz, 6H), 0.96 (s, 9H), 1.59 (m, 2H), 1.80 (m, *J* = 8.3 Hz, *J* = 6.7 Hz, *J* = 5.3 Hz, 1H), 4.18 (m, 2H), 4.28 (dd, *J* = 20.6 Hz, *J* = 5.4 Hz, 1H), 9.69 (s, 1H); **^{13}C-NMR** (126 MHz, $CDCl_3$) δ = −5.0, −4.7, 18.2, 22.5, 23.5, 24.2, 25.9, 45.0, 50.0, 72.6, 175.0, 195.9; **HRMS** (ESI) m/z: calc. for $[M+H]^+$: 288.1989; found: 288.1988.

***N*-allyl-*tert*-butylcarbamate (145)**

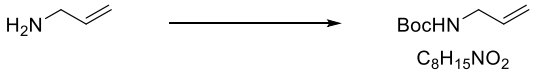

$C_8H_{15}NO_2$
M = 157.21 g/mol

The synthesis was carried out according to a known literature procedure:[106]

To a solution of allylamine (1.88 mL, 25.0 mmol, 1.00 eq.) and DMAP (20.0 mg, 0.16 mmol, 0.6 mol–%) in DCM (50 mL) at 0 °C was added a solution of Boc_2O (6.00 g, 27.5 mmol, 1.10 eq.) in DCM (50 mL) over 30 minutes. After the addition, the resulting solution was stirred for one hour. The reaction was quenched by addition of water and stirred for 10 minutes. Phases were separated and the aqueous layer was extracted with DCM (3 × 20 mL). The combined organic layers were washed with brine, dried over $MgSO_4$, filtered and concentrated. The resulting crude product was purified by column chromatography (Silica, CH/EtOAc 9:1) to yield the product **145** (3.78 g, 24.1 mmol, 96%) as a colorless crystalline solid. $\mathbf{R_f}$ = 0.30 (CH/EtOAc 9:1); **^{1}H-NMR** (400 MHz, $CDCl_3$) δ = 1.44 (s, 9H), 3.74 (t, *J* = 5.8 Hz, 2H), 4.59 (s, 1H),

5.10 (dq, *J* = 20.2 Hz, *J* = 1.5 Hz, 1H), 5.17 (dq, *J* = 17.2 Hz, J = 1.6 Hz, 1H), 5.84 (ddq, *J* = 17.1 Hz, *J* = 10.6 Hz, *J* = 5.2 Hz, 1H). **^{13}C-NMR** (101 MHz, $CDCl_3$) δ = 28.2, 43.2, 79.5, 115.8, 135.1, 155.9. **MS** (ESI) m/z: 158.118 ([M+H]$^+$, 100). The spectroscopic data were in agreement with those previously pulished.[106]

(9H-fluoren-9-yl)methyl allylcarbamate (146)

The synthesis was carried out according to a known literature procedure:[107]

To a solution of allyamine (1.0 mL, 13 mmol, 1.5 eq.) in 1,4-dioxane (80 mL) were added $NaHCO_3$ (2.5 g, 30 mmol, 3.0 eq.) and 9-fluorenylmethyl chloroformate (2.5 g, 9.7 mmol, 1.0 eq.) at 0 °C. After 20 hours, the solvent was removed and the residue was dissolved in EtOAc (150 mL), followed by addition of sat. NH_4Cl (50 mL). Phases were separated and the organic layer was washed with 1 M HCl (50 mL), brine (50 mL), dried over $MgSO_4$, filtered and concentrated. The product **146** (2.55 g, 9.66 mmol, 94%) was obtained as a white solid, which was used in the next step without further purification. $\mathbf{R_f}$ = 0.28 (CH/EtOAc 9:1); **^{1}H-NMR** (500 MHz, acetone-d6) δ = 3.75–3.82 (m, 2H), 4.23 (t, *J* = 7.1 Hz, 1H), 4.34 (d, *J* = 7.2 Hz, 2H), 5.05 (dq, *J* = 10.3, 1.7 Hz, 1H), 5.18 (dq, *J* = 17.1, 1.8 Hz, 1H), 5.80–5.96 (m, 1H), 6.62 (s, 1H), 7.32 (td, *J* = 7.5, 1.2 Hz, 2H), 7.41 (tt, *J* = 7.5, 0.9 Hz, 2H), 7.68–7.72 (m, 2H), 7.86 (dt, *J* = 7.6, 1.0 Hz, 2H); **^{13}C-NMR** (126 MHz, acetone-d6) δ = 43.9, 48.1, 66.9, 115.4, 120.8, 126.1, 127.9, 128.5, 136.4, 142.1, 145.2, 157.1; **HRMS** (ESI) m/z: calc. for [M+H]$^+$: 280.1332; found: 280.1332. The spectroscopic data were in agreement with those previously pulished.[107]

***N*-(2-oxoethyl)-*tert*-butylcarbamate (147)**

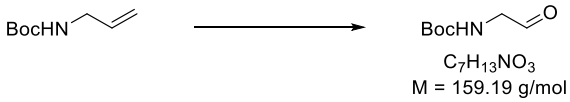

This synthesis was carried out during my master thesis:[91]

N-allyl-*tert*-butylcarbamate (1.00 g, 6.36 mmol, 1.00 eq.) and osmium(VIII)oxide (2.5−wt-% in *t*-BuOH, 500 mg, 44.5 µmol, 0.7 mol−%) were dissolved in 1,4-dioxane (12 mL). Subsequently, water (12 mL) was added, resulting in a brown solution. $NaIO_4$ (4.10 g, 19.2 mmol, 3.02 eq.) was added over 15 minutes, resulting in a decoloration of the solution while a yellow-white precipitate formed. After three hours, the reaction mixture was diluted with water and EtOAc and filtered over celite. Phases were separated and the aqueous phase was extracted with EtOAc (3 × 30 mL). The combined organic layers were dried over

$MgSO_4$, filtered and concentrated. The resulting black crude product was purified by flash column chromatography (Silica, CH/EtOAc 1:1) to yield the desired aldehyde **147** (743 mg, 4.67 mmol, 73%) as a yellow oil. $\mathbf{R_f}$ = 0.20 (CH/EA 1:1); **^{1}H-NMR** (400 MHz, $CDCl_3$) δ = 1.45 (s, 9H), 4.07 (m, 2H), 5.18 (s, 1H), 1.59 (m, 2H), 9.65 (s, 1H); **^{13}C-NMR** (101 MHz, $CDCl_3$) δ = 28.4, 51.6, 80.3, 155.8, 197.2; **MS (ESI)** m/z: 319.186 $[2M+H]^+$, 100). The spectroscopic data were in agreement with those previously pulished.[103]

(*E*)-*N*-boc-4-amino-ethyl-but-2-enoate (148)

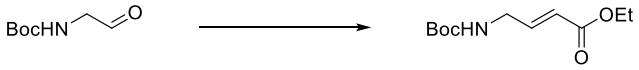

$C_{11}H_{19}NO_4$
M = 229.28 g/mol

This synthesis was carried out during my master thesis:[91]

To a solution of triethylphosphonoacetate (5.80 g, 25.9 mmol, 1.15 eq.) and LiCl (500 mg, 11.8 mmol, 0.52 eq.) in a mixture of DME (100 mL) and THF (50 mL) was added *n*-BuLi (2.5 M in hexane, 10 mL, 25 mmol, 1.1 eq.) at −78 °C. The resulting solution was stirred for 15 minutes at −78 °C and 30 minutes at room temperature. Then, *N*-boc-2-amino acetaldehyde (**147**) (3.58 g, 22.5 mmol, 1.00 eq.) was added over 15 minutes. The resulting solution was stirred for four hours followed by addition of water (10 mL). The solvent was evaporated and the crude product was dissolved in Et_2O, washed with sat. $NaHCO_3$-solution, water and neutralized with sat. $KHSO_4$ solution. Phases were separated and the aqueous layer was extracted with DCM (3 x 50 mL). The pooled organic layers were dried over $MgSO_4$, filtered and concentrated. The resulting crude product was purified by flash column chromatography (Silica; DCM/EtOAc 9:1) to yield compound **148** (2.67 g, 11.7 mmol, 52%) as a colorless oil, which crystallized overnight. $\mathbf{R_f}$ = 0.30 (DCM/EA 9:1); **^{1}H-NMR** (500 MHz, $CDCl_3$) δ = 1.28 (td, *J* = 7.1 Hz, *J* = 0.9 Hz, 3H), 1.45 (s, 9H), 3.92 (t, *J* = 5.4 Hz, 2H), 4.19 (qd, *J* = 7.2 Hz, *J* = 0.9 Hz, 2H), 4.69 (s, 1H), 5.93 (ddd, *J* = 15.7 Hz, *J* = 2.4 Hz, *J* = 1.4 Hz, 1H), 6.90 (dt, *J* = 15.7 Hz, *J* = 4.8 Hz, 1H); **^{13}C-NMR** (126 MHz, $CDCl_3$) δ = 14.4, 28.5, 41.5, 60.6, 80.0, 121.5, 144.9,155.7, 166.2; **MS (ESI)** *m/z:* 230.140 ($[M+H]^+$, 100). The spectroscopic data were in agreement with those previously reported.[105]

(*E*)-*N*-boc-4-amino-but-2-enol (149)

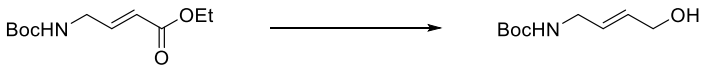

$C_{11}H_{19}NO_4$
M = 229.28 g/mol

This synthesis was carried out during my master thesis:[91]

A solution of *N*-boc-4-amino-ethyl-but-2-enoate (**148**) (500 mg, 2.18 mmol, 1.00 eq.) in DCM (10 mL) at −78 °C was treated with DIBAL-H (1.1 M in hexane, 8.7 mL, 7.9 mmol, 3.6 eq.) for two hours, followed by *Fieser* workup. The resulting crude product was purified by column chromatography (Silica, CH/EtOAc 1:3) to yield compound **149** (231 mg, 1.24 mmol, 58%) as a clear oil. $\mathbf{R_f}$ = 0.30 (CH/EA 1:3); **^{1}H-NMR** (500 MHz, $CDCl_3$) δ = 1.45 (s, 9H), 3.76 (t, J = 5.4 Hz, 2H), 4.14 m, 2H), 4.60 (s, 1H), 5.77 (m, 2H); **^{13}C-NMR** (126 MHz, $CDCl_3$) δ = 28.5, 42.1, 63.1, 79.6, 128.6, 130.8, 155.9; **HRMS** (ESI) m/z: calc. for $[M\text{-}CH_3]^+$: 172.0979; found:172.0975. The spectroscopic data were in agreement with those previously reported.[105]

(*E*)-*N*-Boc-4-amino-but-2-enal (150)

$C_9H_{15}NO_3$
M = 185.22 g/mol

To a refluxing solution of *N*-allyl-*tert*-butylcarbamate (**145**) (900 mg, 5.72 mmol, 1.00 eq.) and freshly distilled crotonaldehyde (5.0 mL, 60.4 mmol, 10.6 eq.) in DCM (25 mL) at 50 °C was added nitro-Grela's catalyst (400 mg, 0.06 mmol, 1 mol-%). The resulting solution was refluxed for two hours, followed by addition of another portion of nitro-Grela's catalyst (400 mg, 0.06 mmol, 1 mol-%). After two hours, the solvent was evaporated under reduced pressure and the residue was purified by flash column chromatography (Silica, CH/EtOAc 2:1) to yield the compound **150** (861 mg, 4.65 mmol, 81%) as a green oil. $\mathbf{R_f}$ = 0.20 (CH/EtOAc 2:1); **^{1}H-NMR** (400 MHz, CD_2Cl_2) δ = 1.44 (s, 9H), 3.99 (d, *J* = 5.8 Hz, 2H), 4.86 (bs, 1H), 6.17 (ddt, *J* = 15.8, 7.8, 1.9 Hz, 1H) 6.81 (dt, *J* = 15.7 Hz, 4.6 Hz, 1H), 9.56 (d, *J* = 7.8 Hz, 1H); **^{13}C-NMR** (101 MHz, CD_2Cl_2) δ = 28.6, 42.2, 80.3, 132.1, 154.6, 156.1, 193.6; **HRMS** (EI) m/z: calc. for $[M+H]^+$: 186.1125; found: 186.1124; The reported instability[106] of aldehyde **150** was not observed. Instead, when stored under argon at -80 °C the purified aldehyde was stable for several weeks.

(9H-fluoren-9-yl)methyl (*E*)-(4-oxobut-2-en-1-yl)carbamate (151)

To a solution of **146** (2.00 g, 7.16 mmol, 1.0 eq.) in dry toluene (80 mL) was added freshly distilled crotonaldehyde (6.0 mL, 72 mmol, 10 eq.) and BHT (157 mg, 716 µmol, 0.10 eq.). The mixture was degassed by freeze pump (3 cycles), Grubbs II (122 mg, 143 µmol, 0.02 eq.) was added and the mixture was allowed to stir at 65 °C for 21 hours. Afterwards, all volatiles were removed *in vacuo* (50 °C bath temperature) and the obtained crude red oil was dissolved in hot toluene (65 °C, ca. 40 mL). Once, a clear solution was obtained, *n*-heptane was added until the solution became slightly cloudy. Then, the flask was allowed to cool down, sealed and stored in a freezer for overnight to complete crystallization. The obtained crystals were washed with *n*-heptane and dried *in vacuo* to yield the desired compound **151** as an orange crystalline solid (2.04 g, 6.64 mmol, 93%). $\mathbf{R_f}$ = 0.33 (CH/EtOAc 2:1); **^{1}H-NMR** (300 MHz, acetone-d6) δ = 4.10 (d, *J* = 5.7 Hz, 2H), 4.26 (d, *J* = 6.9 Hz, 1H), 4.40 (d, *J* = 7.0 Hz, 2H), 6.16 (dd, *J* = 15.8, 7.7 Hz, 1H), 6.89 (s, 1H), 6.98 (dt, *J* = 15.8, 4.5 Hz, 1H), 7.33 (td, *J* = 7.4, 1.2 Hz, 2H), 7.39–7.45 (m, 3H), 7.67–7.74 (m, 2H), 7.87 (dt, *J* = 7.5, 1.1 Hz, 2H), 9.59 (d, *J* = 7.8 Hz, 1H); **HRMS** (APCI) m/z: calc. for $[M+H]^+$: 308.1281; found: 308.1281. The spectroscopic data were in agreement with those previously pulished.[107]

(1*Z*),(3*E*)-*N*-Fmoc-4-amino-1-iodopenta-1,3-diene (153)

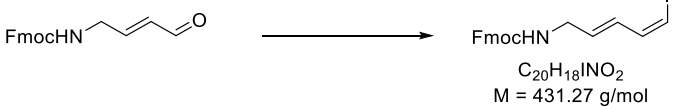

To a suspension of iodomethyl triphenylphosphonium iodide (904 mg, 1.71 mmol, 1.05 eq.) in THF (10 mL) was added NaHMDS (1 M in THF, 1.5 mL, 1.5 mmol, 0.95 eq.). The resulting mixture was stirred at r.t for 5 minutes and then cooled to −78 °C. This mixture was added added via syringe pump to a solution of aldehyde **151** in THF (15 mL) over 4 hours. After 45 minutes, the mixture was quenched with a saturated solution of NH_4Cl (10 mL). The mixture was extracted with Et_2O (3 x 20 mL) and the combined organic layers were washed with brine, dried over $MgSO_4$, filtered and concentrated. Purification by column chromatography (Silica, CH/EtOAc 4:1) yielded the desired compound **153** as a white solid that degrades over time (135 mg, 313 µmol, 19%). $\mathbf{R_f}$ = 0.20 (CH/EtOAc 4:1); **^{1}H-NMR** (500 MHz, acetone-d6) δ = 3.88 (t, *J* = 5.8 Hz, 2H), 4.25 (t, *J* = 7.3 Hz, 1H), 4.35 (d, *J* = 7.2 Hz, 2H), 6.11 (dt, *J* = 15.5, 5.7 Hz, 1H), 6.38 (q, *J* = 8.9 Hz, 2H), 6.80 (s, 1H), 6.85 (dd, *J* = 9.9, 7.6 Hz, 1H), 7.33 (td, *J* = 7.5, 1.2 Hz, 2H), 7.41 (tt, *J* = 7.5, 1.0 Hz, 2H), 7.72 (d, *J* = 7.6 Hz, 2H), 7.86 (dt, *J* = 7.5, 0.9 Hz, 2H); **^{13}C-NMR** (126 MHz, acetone-d6)

δ = 48.1, 82.3, 120.8, 126.1, 128.0, 128.5, 131.3, 139.0, 142.1, 145.2 [due to low concentration, the carbonyl signal was not observed.], **HRMS** (ESI) m/z: calc. for $[M+H]^+$: 432.0452; found: 432.0455.

(1*Z*),(3*E*)-*N*-Boc-4-amino-1-iodopenta-1,3-diene (152)

$C_{10}H_{16}INO_2$
M = 309.15 g/mol

To a suspension of iodomethyl triphenylphosphonium iodide (0.76 g, 1.43 mmol, 1.15 eq.) in THF (3.5 mL) and DMI (0.5 mL) was added sodium hexamethyldisilazane (1 M in THF, 1.4 mL, 1.4 mmol, 1.1 eq.). After 5 minutes, the obtained orange solution was cooled to -78 °C and aldehyde **150** (230 mg, 1.24 mmol, 1.00 eq.) in THF (1 mL) was added over 20 minutes. After 3 hours, the reaction was quenched with a saturated NH_4Cl-solution (5 mL), filtered over a pad of Celite and rinsed with DCM (3 × 20 mL). Phases were separated and the aqueous phase was extracted with DCM (3 × 20 mL). The combined organic layers were dried over $MgSO_4$, filtered and concentrated. The resulting crude product was purified by column chromatography (Silica, CH/EtOAc 5:1) to yield the vinyl iodide **152** (262 mg, 847 µmol, 68%) as a yellow oil with 90% 1*Z*, 3*E* isomeric purity determined by ^{1}H-NMR. $\mathbf{R_f}$ = 0.30 (CH/EtOAc 5:1); **^{1}H-NMR** (500 MHz, CD_2Cl_2) δ = 1.44 (s, 9H), 3.79 (d, *J* = 6.2 Hz, 2H), 4.74 (s, 1H), 6.00 (ddt, *J* = 15.3 Hz, *J* = 5.7 Hz, 1H), 6.33 (ddt, *J* = 7.6 Hz, *J* = 0.9 Hz, 1H), 6.33 (ddd, *J* = 15.2 Hz, *J* = 9.8 Hz, *J* = 1.5 Hz, 1H), 6.74 (ddt, *J* = 9.9 Hz, *J* = 7.6 Hz, *J* = 0.8 Hz, 1H); **^{13}C-NMR** (126 MHz, CD_2Cl_2) δ = 28.7, 42.8, 79.3, 82.4, 131.2, 136.3, 138.2, 156.1; **HRMS** (ESI) m/z: calc. for $[M+H]^+$: 310.0298; found: 310.0297.

(2*E*,4*Z*)-5-iodopenta-2,4-dien-1-amine HCl-salt (154)

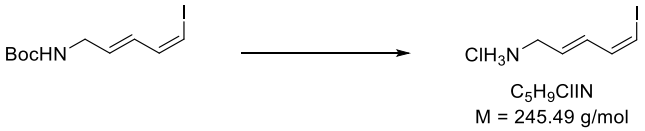

C_5H_9ClIN
M = 245.49 g/mol

Protected diene **152** (500 mg, 1.62 mmol, 1.00 eq.) was added to a flask and HCl (1.25 M in EtOH, 6.5 mL, 8.1 mmol, 5.0 eq.) was added. The resulting mixture was stirred at 50 °C for 2 hours. Then, all volatiles were removed under reduced pressure and the obtained brown crude product **154** was washed with diethylether (10 mL) and used in the subsequent step without further purification (405 mg, 1.62 mmol,

quant.). Repeated recrystallization from *i*-PrOH was conducted to provide an analytical sample of **154** with 98% 1*Z*, 3*E* isomeric purity determined by ^{1}H-NMR. **^{1}H-NMR** (500 MHz, D_2O) δ = 3.74 (dd, *J* = 6.7, 1.4 Hz, 2H), 6.11 (dtt, *J* = 15.3, 6.7, 0.8 Hz, 1H), 6.56–6.65 (m, 2H), 6.90 (dd, *J* = 9.9, 7.8 Hz, 1H); **^{13}C-NMR** (126 MHz, D_2O) δ = 40.8, 85.7, 128.0, 135.9, 137.2; **HRMS (ESI)** m/z: calc. for $[M+H]^+$: 209.9774; found: 209.9773.

(*S*)-2-hydroxy-*N*-((2*E*,4*Z*)-5-iodopenta-2,4-dien-1-yl)-4-methylpentanamide (122)

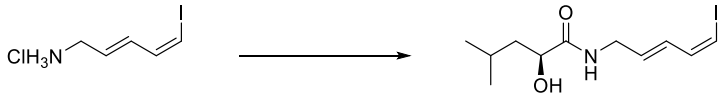

$C_{11}H_{18}INO_2$
M = 323.17 g/mol

Amine · HCl **154** (400 mg, 1.63 mmol, 1.00 eq.), hydroxyacid **137** (258 mg, 1.96 mmol, 1.20 eq.), PyBOP (1.0 g, 1.9 mmol, 1.2 eq.) and HOBt-hydrate (264 mg, 1.96 mmol, 1.20 eq.) were dissolved in anhydrous DMF (12 mL) under argon atmosphere. Then, DIPEA (1.4 mL, 8.2 mmol, 5.0 eq.) was added and the resulting solution was stirred at r.t for three hours. Afterwards, the mixture was diluted with EtOAc (50 mL) and water (50 mL). Phases were separated and the aqueous phase was extracted with EtOAc (3 × 20 mL). The combined organic layers were washed with sat. NH_4Cl (20 mL) and brine (20 mL). After drying over $MgSO_4$ and filtration, the solvent was evaporated under reduced pressure. Purification by column chromatography (Silica, CH/EtOAc 3:5 → 1:3) yielded the desired western fragment II (**122**) as a yellow solid (483 mg, 1.49 mmol, 92%) with 90% 1*Z*, 3*E* isomeric purity determined by ^{1}H-NMR. Further purification was achieved by semi-preparative HPLC (column: KNAUER Eurospher II 100-5 C18P; 5 µm; 250 x 20 mm, eluent: A: H_2O, B:MeCN, gradient: 45% A, 55% B → 25% A, 75% B (0–20 min), 45% A, 55% B (20–21 min), 45% A, 55% B (21–25 min), flowrate: 24.0 mL/min, detection wavelengths: λ_1 = 215 nm, λ_2 = 250 nm, λ_3 = 270 nm) which increased the isomeric purity to ≥ 98% 1*Z*, 3*E* determined by ^{1}H-NMR. The obtained product **122** is light-sensitive and degrades over time upon storage in an aluminum wrapped flask at –30 °C under argon. $\mathbf{R_f}$ = 0.40 (EtOAc); $\boldsymbol{\alpha_D^{20}}$ = –31.7 (c = 1.0, MeCN); **^{1}H-NMR** (500 MHz, Acetone-d6) δ = 0.93 (dd, *J* = 6.7, 2.2 Hz, 6H), 1.53 (ddd, *J* = 13.8, 9.6, 4.9 Hz, 1H), 1.62 (ddd, *J* = 13.8, 9.1, 3.6 Hz, 1H), 1.85-1.96 (m, 1H), 3.87-4.01 (m, 2H), 4.08 (ddd, *J* = 9.4, 5.6, 3.6 Hz, 1H), 4.48 (d, *J* = 5.6 Hz, 1H), 6.08 (dtt, *J* = 15.3, 5.6, 0.7 Hz, 1H), 6.29-6.38 (m, 2H), 6.81–6.86 (m, 1H), 7.51 (s, 1H); **^{13}C-NMR** (126 MHz, Acetone) δ = 21.9, 23.9, 25.2, 40.9, 45.1, 71.1, 82.1, 131.3, 137.1, 139.0, 175.1; **HRMS** (ESI) m/z: calc. for $[M+H]^+$: 324.0455; found: 324.0453.

(*S*)-*N*-((4*Z*),(2*E*)-5-iodopenta-2,4-dienyl)-2-((*tert*-butyldimethylsiliyl)oxy)-4-methylpentanamide (112)

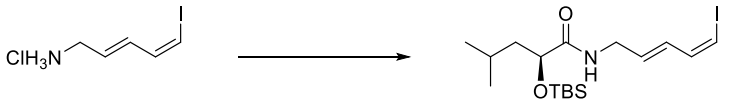

Chemical Formula: $C_{17}H_{32}INO_2Si$
Molecular Weight: 437,44

To a solution of **154** (21 mg, 0.10 mmol, 1.0 eq.) and acid **138** (25 mg, 0.10 mmol, 1.0 eq.) in DCM/DMF (1:1, 4 mL) were sequentially added PyBOP (58 mg, 0.11 mmol, 1.1 eq.), HOBt (15 mg, 0.11 mmol, 1.1 eq.) and DIPEA (0.16 mL, 0.92 mmol, 9.2 eq.) The resulting solution was stirred for 1.5 hours. Afterwards, the solution was poured into water, phases were separated and the aqueous phase was extracted with DCM (3 x 10 mL). The pooled organic layers were washed with brine, dried over $MgSO_4$, filtered and concentrated *in vacuo*. The obtained crude product was purified by column chromatography (Silica, CH/EtOAc 3:1) to yield the amide **112** as a yellow oil (27.2 mg, 0.062 mmol, 62%). $\mathbf{R_f}$ = 0.40 (CH/EtOAc 3:1); $\boldsymbol{\alpha_D^{20}}$ = 9.2 (c = 1.05, DCM); **^{1}H-NMR** (500 MHz, CD_2Cl_2) δ = 0.10 (s, 3H), 0.12 (s, 3H), 0.90–0.95 (m, 15H), 1.51-1.66 (m, 2H), 1.81 (ddtd, *J* = 13.4 Hz, *J* = 8.4 Hz, *J* = 6.7 Hz, *J* = 5.3 Hz, 1H), 3.87-4.00 (m, 2H), 4.15 (dd, *J* = 7.4 Hz, *J* = 4.5 Hz, 1H), 5.94–6.03 (m, 1H), 6.28 (dt, *J* = 7.9 Hz, *J* = 0.9 Hz, 1H), 6.34 (ddd, *J* = 15.3 Hz, *J* = 9.9 Hz, *J* = 1.5 Hz, 1H), 6.63-6.71 (m, 1H), 6.75 (dd, *J* = 9.9 Hz, *J* = 7.6 Hz, 1H); **^{13}C-NMR** (126 MHz, CD_2Cl_2) δ = -4.7, -4.5, 18.5, 22.8, 23.8, 24.6, 26.2, 40.8, 45.5, 73.2, 82.6, 131.8,135.3, 138.2, 174.4; **HRMS** (ESI) m/z: calc. for $[M+H]^+$: 438.1320; found: 438.1318.

***tert*-butyl prop-2-yn-1-ylcarbamate (156)**

$C_8H_{13}NO_2$
M = 155.20 g/mol

To a solution of propargyl amine (4.96 g, 90.0 mmol, 1.00 eq.) in anhydrous DCM (100 mL) at 0 °C was added a solution of Boc_2O (23.0 g, 105 mmol, 1.17 eq.) in anhydrous DCM (20 mL) over 5 minutes. The resulting solution was allowed to warm to r.t. while being stirred overnight (8 h). Then, the solvent was evaporated and the crude product was dissolved in Et_2O (100 mL). The solution was left in the freezer (−28 °C) overnight, resulting in precipitation of the product. The obtained crystals were washed with *n*-heptane and dried *in vacuo* yielding the carbamate **156** as a white crystalline solid (6.95 g, 44.8 mmol, 50%). $\mathbf{R_f}$ = 0.65 (CH/EtOAc 2:1); **^{1}H-NMR** (500 MHz, $CDCl_3$) δ = 1.45 (s, 9H), 2.22 (t, *J* = 2.5 Hz, 1H), 3.92 (d, *J* = 4.7 Hz, 2H), 4.69 (s, 1H); **^{13}C-NMR** (126 MHz, $CDCl_3$) δ 28.3, 30.4, 71.2, 80.0, 80.0, 155.2; **HRMS** (APCI) m/z: calc. for $[M+H]^+$: 156.1019; found: 156.1019. The spectroscopic data were in agreement with those previously reported.[109]

***tert*-butyl (*E*)-(3-(tributylstannyl)allyl)carbamate (157)**

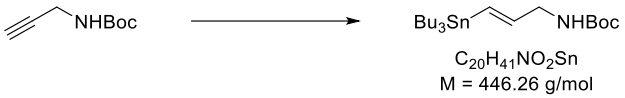

The synthesis was carried out according to a known literature procedure:[108]

To a suspension of copper(I) cyanide (2.65 g, 29.6 mmol, 1.00 eq.) in anhydrous THF (70 mL) at −78 °C was added *n*-BuLi (2.5 M in hexanes, 25 mL, 62.5 mmol, 2.1 eq.) leading to a clear pale yellow solution within 15 minutes. Then, tributyltin hydride (17 mL, 63 mmol, 2.1 eq.) was added dropwise over 15 minutes. Finally, alkyne **156** (4.60 g, 29.6 mmol, 1.00 eq.) in THF (15 mL) was added over 15 minutes and the resulting mixture was stirred for further 30 minutes. Afterwards, MeOH (10 mL) was slowly added over 10 minutes followed by addition of water (10 ml) and 15 minutes of stirring at 0 °C and finally addition of water (10 mL) and stirring at r.t. Then, Et_2O (100 mL) was added, phases were separated and the aqueous layer was extracted with Et_2O (3 × 50 mL). The combined organic layers were washed with brine, dried over $MgSO_4$, filtered and concentrated. The resulting crude product was purified by column chromatography (Silica, CH/EtOAc 20:1) to yield the desired compound **157** as a colorless oil (9.59 g, 21.5 mmol, 72%). $\mathbf{R_f}$ = 0.29 (CH/EtOAc 20:1); **^{1}H-NMR** (700 MHz, $CDCl_3$) δ = 0.82–0.94 (m, 15H), 1.24–1.37 (m, 6H), 1.46–1.52 (m, 6H), 3.79 (s, 2H), 4.59 (s, 1H), 5.96 (dt, *J* = 19.0, 5.0 Hz, 1H), 6.02–6.16 (m, 1H); **^{13}C-NMR** (176 MHz, $CDCl_3$) δ = 9.6, 13.8, 27.4, 28.6, 29.2, 46.2, 79.4, 129.3, 144.4, 155.9; **HRMS** (ESI) m/z: calc. for $[M+H]^+$: 448.2236; found: 448.2230. The spectroscopic data were in agreement with those previously pulished.[108]

***tert*-butyl (*E*)-(3-iodoallyl)carbamate (158)**

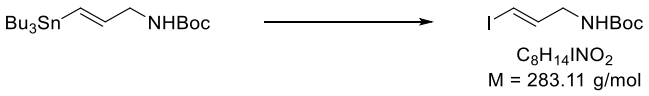

The synthesis was carried out according to a known literature procedure:[108]

A solution of vinyl tin compound **157** (9.10 g, 20.4 mmol, 1.00 eq.) in anhydrous DCM (100 mL) was cooled to 0 °C. In a second flask, iodine (5.70 g, 22.5 mmol, 1.10 eq.) was dissolved in anhydrous DCM (50 mL) and transferred to the first flask via cannula. A rapid decoloration of the iodine solution was observed. The remaining iodine was rinsed with DCM (2 × 20 mL) and Et_2O (2 × 20 mL) and added to the solution until a red color change was observable in the reaction mixture. Then, a saturated solution of

$Na_2S_2O_3$ (200 mL) was added and phases were separated. The aqueous layer was extracted with Et_2O (3 × 100 mL) and the combined organic layers were washed with brine (100 mL), dried over $MgSO_4$, filtered and concentrated. Purification by column chromatography (Silica, CH/EtOAc 20:1) yielded the compound **158** as a colorless oil, contaminated with tributyltin iodide, which crystallized overnight in the freezer (−28 °C). Therefore, the product was recrystallized from *n*-heptane/Et_2O and the obtained crystals were washed with *n*-heptane and dried *in vacuo*, yielding the desired compound **158** as a white crystalline solid (5.13 g, 18.1 mmol, 89%). $\mathbf{R_f}$ = 0.16 (CH/EtOAc 20:1); **^{1}H-NMR** (700 MHz, CD_2Cl_2) δ = 1.42 (s, 9H), 3.66 (d, *J* = 6.3 Hz, 2H), 4.73 (s, 1H), 6.27 (dt, *J* = 14.5, 1.6 Hz, 1H), 6.55 (dt, *J* = 14.5, 5.9 Hz, 1H); **^{13}C-NMR** (176 MHz, CD_2Cl_2) δ = 28.6, 45.2, 77.6, 79.9, 143.5, 155.9; **HRMS** (ESI) m/z: calc. for $[M+H]^+$: 284.0142; found: 284.0142. The spectroscopic data were in agreement with those previously pulished.[108]

***tert*-butyl (*E*)-(5-(trimethylsilyl)pent-2-en-4-yn-1-yl)carbamate (S-1)**

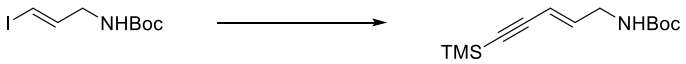

$C_{13}H_{23}NO_2Si$
M = 253.42 g/mol

The synthesis was carried out according to a known literature procedure:[108]

To a flask, charged with copper(I) iodide (345 mg, 1.81 mmol, 0.10 eq.) and $Pd(PPh_3)_2Cl_2$ (180 mg, 544 µmol, 0.03 eq.) was added a solution of vinyl iodide **158** (5.13 g, 18.1 mmol, 1.00 eq.) in anhydrous THF (100 mL). Then, a solution of TMS-acetylene (**159**) (2.14 g, 21.7 mmol, 1.20 eq.) in THF (100 mL) was added and cooled to −78 °C. The resulting mixture was degassed, followed by addition of DIPEA (38 mL, 0.21 mol, 12 eq.). The mixture was stirred at −78 °C for 15 minutes and two hours at room temperature. Then, the reaction was diluted with Et_2O (200 mL) a saturated solution of NH_4Cl (100 mL) and phases were separated. The aqueous phase was extracted with Et_2O (3 × 100 mL) and the combined organic layers were washed with brine (150 mL), dried over $MgSO_4$, filtered and concentrated. Purification by column chromatography (Silica, CH/EtOAc 8:1) yielded the compound **S-1** as a yellow oil (4.04 g, 15.9 mmol, 88%). $\mathbf{R_f}$ = 0.25 (CH/EtOAc 8:1); **^{1}H-NMR** (500 MHz, Acetone-d6) δ = 0.79 (s, 9H), 2.05 (s, 9H), 4.39 (td, *J* = 5.8, 1.9 Hz, 2H), 6.31 (dt, *J* = 16.0, 1.8 Hz, 1H), 6.80 (dt (bs), *J* = 15.9, 5.5 Hz, 2H); **^{13}C NMR** (126 MHz, Acetone-d6) δ = 0.0, 42.6, 78.9, 94.5, 104.4, 110.7, 143.3, 156.5. **HRMS** (ESI) m/z: calc. for $[M+Na]^+$: 276.1390; found: 276.1386. The spectroscopic data were in agreement with those previously pulished.[108]

***tert*-butyl (*E*)-pent-2-en-4-yn-1-ylcarbamate (160)**

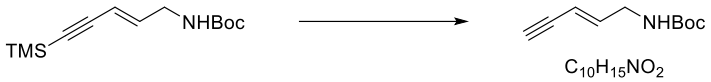

$C_{10}H_{15}NO_2$
M = 181.24 g/mol

The synthesis was carried out according to a known literature procedure:[108]

To a solution of TMS-alkyne **S-1** (4.59 g, 18.1 mmol, 1.00 eq.) in MeOH (150 mL) was added K_2CO_3 (2.50 g, 18.1 mmol, 1.00 eq.) and the resulting mixture was stirred at r.t. for 1 hour. Afterwards, the solvent was evaporated and to the residue was added a saturated solution of NH_4Cl (50 mL) and Et_2O (100 mL). Phases were separated and the aqueous layer was extracted with Et_2O (3 × 50 mL). The combined layers were washed with brine, dried over $MgSO_4$, filtered and concentrated. The residue was filtered over a large plug of Silica (CH/EtOAc 4:1) and after evaporation of the solvent the obtained residue was recrystallized from *n*-heptane/Et_2O to yield the desired compound **160** as an off-white solid (1.87 g, 10.3 mmol, 57%). $\mathbf{R_f}$ = 0.31 (CH/EtOAc 5:1); **^{1}H-NMR** (500 MHz, $CDCl_3$) δ = 1.44 (s, 9H), 2.86 (dd, *J* = 2.3, 0.8 Hz, 1H), 3.80 (t, *J* = 5.9 Hz, 2H), 4.60 (s, 1H), 5.60 (dq, *J* = 16.0, 1.9 Hz, 1H), 6.21 (dt, *J* = 16.0, 5.7 Hz, 1H); **^{13}C-NMR** (126 MHz, $CDCl_3$) δ = 28.5, 42.3, 77.8, 79.9, 81.5, 110.1, 141.9, 155.7; **HRMS** (ESI) m/z: calc. for $[M-{}^t\text{Bu}+H]^+$: 126.0550; found: 126.0549. The spectroscopic data were in agreement with those previously pulished.[108]

***tert*-butyl (*E*)-(5-iodopent-2-en-4-yn-1-yl)carbamate (161)**

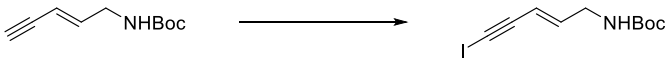

$C_{10}H_{14}INO_2$
M = 307.13 g/mol

To a solution of alkyne **160** (100 mg, 552 µmol, 1.00 eq.) in acetone (4 mL) was sequentially added NIS (174 mg, 773 µmol, 1.20 eq.) and AgOBz (18.0 mg, 78.6 µmol, 0.14 eq.) and the resulting mixture was stirred in the dark for 30 minutes. Then, the solvent was removed and the residue was dissolved in a mixture of Et_2O (5 mL) and water (5 mL). Phases were separtated and the aqueous phase was extracted with Et_2O (3 × 5 mL). The combined layers were washed with brine, dried over $MgSO_4$, filtered and concentrated. The residue was filtered over a short plug of Silica (CH/EtOAc 5:1) and after evaporation of the solvent, compound **161** was obtained as a white solid (159 mg, 518 µmol, 94%). $\mathbf{R_f}$ = 0.25 (CH/EtOAc 5:1); **^{1}H-NMR** (500 MHz, acetone-d6) δ = 1.41 (s, 9H), 3.75 (td, *J* = 5.7, 1.8 Hz, 2H), 5.76 (dt, *J* = 15.9,

1.8 Hz, 1H), 6.16 (dt, *J* = 15.9, 5.5 Hz, 1H, bs, 1H); **HRMS** (ESI) m/z: calc. for $[M+H]^+$: 308.0142; found: 308.0140.

***tert*-butyl (*E*)-(5-(tributylstannyl)pent-2-en-4-yn-1-yl)carbamate (162)**

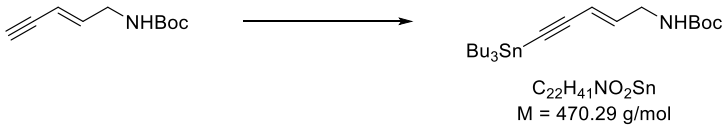

$C_{22}H_{41}NO_2Sn$
M = 470.29 g/mol

To a solution of **160** (50.0 mg, 276 µmol, 1.00 eq.) in THF (1 mL) at −78 °C was added *n*-BuLi (2.5 M in hexanes, 165 µL, 414 µmol, 1.5 eq.) and the resulting solution was stirred for 30 minutes. Then, neat dry tributyltin chloride (150 µL, 553 µmol, 2.0 eq.) was added at −78 °C. The ice bath was removed and the resulting solution was stirred at r.t. for 1 hour followed by addition of a saturated solution of NH_4Cl (5 mL) and Et_2O (5 mL). Phases were separated and the aqueous layer was extracted with Et_2O (3 × 5 mL). The combined organic layers were washed with brine (10 mL), dried over $MgSO_4$, filtered and concentrated. Purification by column chromatography (Silica/K_2CO_3 9:1, CH/EtOAc 10:1 + 5% NEt_3) yielded the desired stannylenyne **162** (100 mg, 213 µmol, 77%) as a pale yellow oil. **^{1}H-NMR** (400 MHz, $CDCl_3$) δ = 0.90 (t, *J* = 7.4 Hz, 9H), 0.92–1.11 (m, 6H), 1.27–1.41 (m, 6H), 1.44 (s, 9H), 1.49–1.68 (m, 6H), 3.78 (s, 2H), 4.54 (s, 1H), 5.65 (dt, *J* = 15.8, 1.7 Hz, 1H), 6.09 (dt, *J* = 15.9, 5.9 Hz, 1H); **HRMS** (ESI) m/z: calc. for $[M+H]^+$: 472.2236; found: 472.2233.

(*Z*)-ethyl 3-iodacrylate (165)

$C_5H_7IO_2$
M = 226.01 g/mol

The synthesis was carried out according to a known literature procedure:[116]

To a solution of ethyl propiolate (**164**) (5.51 g, 56.2 mmol, 1.00 eq.) in acetic acid (30 mL) sodium iodide (16.85 g, 112.4 mmol, 2.00 eq.) was added. The solution was stirred at 70 °C for 22 h. The reaction was then diluted with Et_2O and 1 M NaOH was added (3 mL). The aqueous layer was extracted with Et_2O, and the combined organics layers carefully washed with saturated K_2CO_3 and $NaHCO_3$ solutions, then dried ($MgSO_4$) and the solvent evaporated by reduced pressure. The crude product was purified by flash column chromatography (Silica; CH/Et2O 9:1) to yield compound **165** (13.55 g, 43.78 mmol, 78%). $\mathbf{R_f}$ = 0.31 (CH/ Et2O 9:1); **^{1}H-NMR** (500 MHz, $CDCl_3$) δ = 1.32 (t, *J* = 7.1 Hz, 3H), 4.25 (q, *J* = 7.1 Hz, 2H),

6.89 (d, *J* = 8.9 Hz, 1H), 7.44 (d, *J* = 8.9 Hz, 1H); **^{13}C-NMR** (126 MHz, $CDCl_3$) δ = 14.3, 61.9, 94.7, 130.1, 164.7; **HRMS** (ESI) m/z: calc. for $[M+H]^+$: 226.9564; found: 226.9489. The spectroscopic data were in agreement with those previously pulished.[116]

(2*E*,4*Z*)-ethyl 5-iodopenta-2,4-dienoate (167)

$C_7H_9IO_2$
M = 252.05 g/mol

The synthesis was carried out according to a known literature procedure:[118]

To a solution of (*Z*)-ethyl 3-iodacrylate (**165**) (2.26 g, 10 mmol, 1.00 eq.) in anhydrous DCM (20 mL) was added dropwise DIBAL-H (1 M in hexane, 10.5 ml, 10.5 mmol, 1.05 eq.) at −78 °C. The solution was stirred at −78 °C for 5 min. Then, MeOH (5 mL) was slowly added. Immediately after this addition, saturated potassium sodium tartrate solution (30 mL) was. The mixture was warmed to room temperature and stirred for 30 min and extracted with DCM (30 mL). The combined organic layers were washed with brine, filtered and rinsed with THF. Afterwards, DCM was carefully (!) removed under reduced pressure to yield a solution of (*Z*)-3-iodacrolein (**166**) in THF which was immediately used for the next step without further purification.

To a solution of triethyl phosphonoacetate (**141**) (3.36 g, 15.0 mmol, 1.50 eq.) in THF (20 mL) at −78 °C was added *n*-BuLi (2.5 M in hexanes, 6.0 mL, 15 mmol, 1.5 eq.). The solution was stirred at −78 °C for 30 min and a solution of the above prepared (*Z*)-3-iodoacrolein (**166**) (ca. 10 mmol, 1.0 equiv.) in THF (10 mL) was added via cannula at −78 °C under dark. The reaction mixture was stirred at −78 °C for 30 min and allowed to warm to r.t. overnight. Then, the reaction was diluted with ether and water (20 mL) was added. After separation of the organic layer, the aqueous phase was extracted with ether (4 x 20 mL). The combined organic layers were washed with brine (20 mL), dried over $MgSO_4$, filtered and the solvent was evaporated under reduced pressure. The crude product was purified by column chromatography (Silica, CH/EtOAc 19:1) to yield the compound **167** (1.92 g, 7.62 mmol, 76%) as an orange oil. $\mathbf{R_f}$ = 0.31 (CH/Et2O 9:1); **^{1}H-NMR** (500 MHz, $CDCl_3$) δ = 1.32 (t, *J* = 7.1 Hz, 3H), 4.24 (q, *J* = 7.1 Hz, 2H), 6.13 (dt, *J* = 0.8 Hz, 15.5 Hz, 1H), 6.82 (dt, *J* = 0.8 Hz, 7.8 Hz, 1H), 6.90 (ddd, *J* = 0.8 Hz, 7.8 Hz, 10.4 Hz, 1H), 7.40 (ddd, *J* = 0.98 Hz, 10.4 Hz, 15.5 Hz, 1H); **^{13}C-NMR** (126 MHz, $CDCl_3$) δ = 14.4, 60.8, 92.0, 125.9, 136.8, 143.1, 166.6; **HRMS** (ESI) m/z: calc. for $[M+H]^+$: 252.9720; found: 252.9701. The spectroscopic data were in agreement with those previously pulished.[118]

(2*E*,4*Z*)-5-iodopenta-2,4-dien-1-ol (168)

C_5H_7IO
M = 210.01 g/mol

The synthesis was carried out according to a known literature procedure:[120]

Ester **167** (3.00 g, 11.9 mmol, 1.00 eq) was dissolved in anhydrous DCM (100 mL), and cooled to 0 °C. DIBAL (1.0 M in hexanes, 30 mL, 30 mmol, 2.5 eq.) was added dropwise. After 45 minutes at 0 °C, the reaction was quenched by the addition of saturated aqueous Rochelle's salt (50 mL) and subsequently diluted with Et_2O (50 mL). Layers were separated, the aqueous layer was extracted with Et_2O (3 x 40 mL) and the combined organic layers were washed with aqueous $NaHCO_3$ (3 x 30 mL), brine (30 mL), dried over $MgSO_4$, filtered and concentrated to afford the alcohol **168** as a yellow oil which was used in the next step without further purification (2.14 g, 10.2 mmol, 86%). $\mathbf{R_f}$ = 0.29 (CH/EtOAc 3:1); **^{1}H-NMR** (400 MHz, acetone-d6) δ 3.97 (t, *J* = 5.6 Hz, 1H), 4.14–4.20 (m, 2H), 6.20 (dtt, *J* = 15.3, 4.8, 0.7 Hz, 1H), 6.33 (dp, *J* = 7.6, 0.9 Hz, 1H), 6.45 (ddtd, *J* = 15.3, 10.0, 1.9, 1.1 Hz, 1H), 6.82–6.88 (m, 1H); **^{13}C-NMR** (126 MHz, acetone-d6) δ = 62.5, 81.6, 129.6, 139.2, 140.5; **HRMS** (ESI) m/z: calc. for $[M-H_2O+H]^+$: 192.9509; found: 192.9506. The spectroscopic data were in agreement with those previously reported.[120]

(1*Z*,3*E*)-5-bromo-1-iodopenta-1,3-diene (169)

C_5H_6BrI
M = 272.91 g/mol

A solution of (2*E*,4*Z*)-5-iodopenta-2,4-dien-1-ol (**168**) (1.00 g, 4.76 mmol, 1.00 eq.) and carbon tetrabromide (3.49 g, 10.5 mmol, 2.21 eq.) in DCM (20 mL) was cooled to 0 °C. Triphenylphosphane (2.50 g, 9.52 mmol, 2.00 eq.) was added in 5 portions over 30 min with vigorous stirring. Cyclohexane (200 mL) was poured into the reaction solution and the resulting suspension was filtered over a Celite pad. The filtrate was concentrated under reduced pressure. The filtration procedure was repeated twice to give (1*Z*,3*E*)-5-bromo-1-iodopenta-1,3-diene (**169**) as a brown oil (1.30 g, yield is not representative due to contamination with TPPO). $\mathbf{R_f}$ = 0.61 (CH); **^{1}H-NMR** (400 MHz, acetone-d6) δ = 4.23 (dd, *J* = 7.7, 1.0 Hz, 2H), 6.30 (dtt, *J* = 15.0, 7.8, 0.7 Hz, 1H), 6.47–6.58 (m, 2H), 6.91 (ddd, *J* = 10.0, 7.6, 0.7 Hz, 1H); **^{13}C-NMR** (101 MHz, acetone-d6) δ = 32.2, 84.4, 128.5, 134.0, 137.5; **MS (EI**): m/z calculated for [M-HBr]: 192.9; found: 192.9. Due to the instability of the compound, a high resolution mass spectrum could not be obtained.

(1*Z*,3*E*)-5-azido-1-iodopenta-1,3-diene (170)

$C_5H_6IN_3$
M = 235.03 g/mol

Sodium azide (780 mg, 11.9 mmol, 2.50 eq.) was added in batches over one minute to a well-stirred solution of (1*Z*,3*E*)-5-bromo-1-iodopenta-1,3-diene (**169**) (1.30 g, 4.76 mmol, 1.00 eq.) in DMF (15 mL). The reaction was heated to 60 °C and stirred for 3 h. A blast shield was placed in front of the reaction during this time. The reaction mixture was allowed to cool to r.t. and poured into water (50 mL). The resulting mixture was extracted with Et_2O (3 x 50 mL) (do not use chlorinated solvents with NaN_3). The combined organic layers were washed with water (3 x 50 mL), dried over $MgSO_4$, filtered and concentrated. The crude brown oil was used in the next step without further purification. $\mathbf{R_f}$ = 0.26 (CH); **^{1}H-NMR** (500 MHz, acetone-d6) δ = 3.98–4.04 (m, 2H), 6.12–6.20 (m, 1H), 6.46–6.55 (m, 2H), 6.92 (dd, *J* = 10.0, 7.6 Hz, 1H); **^{13}C-NMR** (126 MHz, acetone-d6) δ = 52.8, 84.4, 132.7, 134.2, 138.5; **HRMS** (ESI) m/z: calc. for $[M-N_2+H]^+$: 207.9616; found: 207.9618.

(2*E*,4*Z*)-5-iodopenta-2,4-dienenitrile (172)

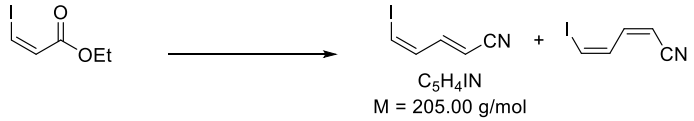

The synthesis was carried out according to a known literature procedure:[119]

To a solution of (*Z*)-ethyl 3-iodacrylate (**165**) (2.26 g, 10 mmol, 1.00 eq.) in anhydrous DCM (20 mL) was added dropwise DIBAL-H (1 M in hexane, 10.5 mL, 10.5 mmol, 1.05 eq.) at −78 °C. The solution was stirred at −78 °C for 5 min. Then, MeOH (5 mL) was slowly added. Immediately after this addition, saturated potassium sodium tartrate solution (30 mL) was. The mixture was warmed to room temperature and stirred for 30 min and extracted with DCM (30 mL). The combined organic layers were washed with brine, filtered and rinsed with THF. Afterwards, DCM was carefully (!) removed under reduced pressure to yield a solution of (*Z*)-3-iodacrolein (**166**) in THF which was immediately used for the next step without further purification.

To a solution of diethyl cyanomethylphosphonate (**171**) (2.66 g, 15.0 mmol, 1.50 eq.) in THF (20 mL) at −78 °C was added *n*-BuLi (2.5 M in hexanes, 6.0 mL, 15 mmol, 1.5 eq.). The solution was stirred at −78 °C for 30 min and a solution of the above prepared (*Z*)-3-iodoacroleine (**166**) (ca. 10 mmol, 1.0 equiv.) in THF (10 mL) was added via cannula at −78 °C under dark. The reaction mixture was stirred at −78 °C for 30 min and allowed to warm to r.t. overnight. Then, the reaction was diluted with ether and water (20 mL) was added. After separation of the organic layer, the aqueous phase was extracted with ether (4 x 20 mL). The combined organic layers were washed with brine (20 mL), dried over $MgSO_4$, filtered and the solvent was evaporated under reduced pressure. Purification of the crude product by column chromatography (Silica, CH/Et_2O 5:1) yielded the desired (2*E*,4*Z*)-**172** (435 mg, 2.12 mmol, 21%) as an orange oil and (2*Z*,4*Z*)-**172** (486 mg, 2.37 mmol, 24%) as a white solid. *(2E,4Z)-Isomer:* $\mathbf{R_f}$ = 0.15 (CH/Et_2O 5:1); **^{1}H-NMR** (500 MHz, $CDCl_3$) δ = 5.62 (dt, *J* = 16.0, 0.8 Hz, 1H), 6.89 (ddd, *J* = 10.3, 7.9, 0.8 Hz, 1H), 6.96 (dt, *J* = 7.9, 0.8 Hz, 1H), 7.18 (ddd, *J* = 16.1, 10.3, 0.9 Hz, 1H); **^{13}C-NMR** (126 MHz, $CDCl_3$) δ = 94.0, 103.3, 117.6, 136.0, 149.5; *(2Z,4Z)-Isomer:* $\mathbf{R_f}$ = 0.40 (CH/Et_2O 5:1); **^{1}H-NMR** (500 MHz, $CDCl_3$) δ = 5.51 (dt, *J* = 11.3, 1.1 Hz, 1H), 7.00–7.07 (m, 2H), 7.29 (ddd, *J* = 10.5, 8.0, 1.0 Hz, 1H); **^{13}C NMR** (126 MHz, $CDCl_3$) δ = 94.7, 101.7, 116.2, 134.8, 148.3; **HRMS** (ESI) m/z: calc. for $[M+H]^+$: 205.9461; found: 205.9458. The spectroscopic data were in agreement with those previously pulished.[119]

(2*E*,4*Z*)-5-iodopenta-2,4-dienoic acid (S-2)

$C_5H_5IO_2$
M = 224.00 g/mol

To a solution of (2*E*,4*Z*) ethyl 5-iodopenta-2,4-dienoate (**167**) (500 mg, 1.98 mmol, 1.0 eq.) in THF (30 mL) was added a solution of LiOH (361 mg, 15.1 mmol, 7.6 eq.) in water (15 mL) and stirred at room temperature for 6 h. The reaction mixture was cooled down to 0 °C acidified with 1M HCl (aq.) and the aqueous phase was extracted with Et_2O (3 x 10 mL). Combined organic layers were washed with brine (50 mL), dried over $MgSO_4$, filtered and the solvent was evaporated under reduced pressure to give the product **S-2** as an off-white solid (354.8 mg, 1.58 mmol, 80%). $\mathbf{R_f}$ = 0.5 (MeOH); **^{1}H-NMR** (500 MHz, MeOD) δ = 6.19 (d, *J* = 15.3 Hz, 1H), 7.00 (m, 2H), 7.42 (ddd, *J* = 15.4 Hz, 7.6 Hz, 1.8 Hz, 1H); **^{13}C-NMR** (126 MHz, MeOD) δ = 92.6, 127.0, 137.8, 144.7, 169.8; **HRMS** (ESI) m/z: calc. for $[M-H]^-$: 222.9251; found: 222.9264.

(2*E*,4*Z*)-5-iodopenta-2,4-dienamide (173)

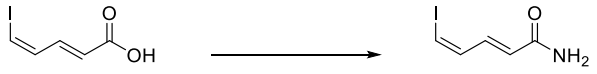

C_5H_6INO
M = 223.01 g/mol

Acid **S-2** (558 mg, 2.49 mmol, 1.00 eq.) was dissolved in anhydrous DCM (15 mL) under argon. A few drops of DMF were added, followed by dropwise addition of oxalyl chloride (0.20 mL, 2.3 mmol, 0.94 eq.) via syringe over a period of 5 min. Stirring continued for 1 h at r.t. to ensure full conversion to the acid chloride. The resulting solution was then transferred to a solution of ammonia in (2 M in *i*PrOH, 10 mL, 20 mmol, 6.0 eq.) at 0 °C and the mixture was stirred for 30 min. The organic layer was extracted with Et_2O and washed with brine (10 mL), dried with $MgSO_4$ and filtered. The solvent was removed under reduced pressure to give the product **173** as a white solid (508 mg, 2.49 mmol, 91%). $\mathbf{R_f}$ = 0.30 (EtOAc); **^{1}H-NMR** (400 MHz, MeOD) δ = 6.35 (dt, *J* = 0.8 Hz, 15.1 Hz, 1H), 6.91 (dt, *J* = 0.8 Hz, 7.8 Hz, 1H), 6.98 (ddd, *J* = 10.1 Hz, 7.8 Hz, 0.8 Hz, 1H), 7.36 (ddd, *J* = 0.8 Hz, 10.2 Hz, 15.2 Hz, 1H); **^{13}C-NMR** (101 MHz, MeOD) δ = 91.25, 129.07, 137.90, 141.48, 170.31; **HRMS** (ESI) m/z: calc. for $[M+H]^+$: 223.9567; found: 223.9569.

8.2.2 Syntheses of bimetallic linchpins

(*E*)-3-(tributylstannyl)prop-2-en-1-ol (36)

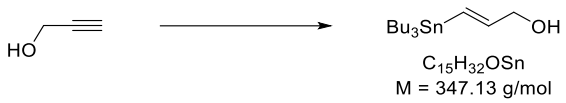

The synthesis was carried out according to a known literature procedure:[58]

Pd_2dba_3 (184 mg, 178 µmol, 0.5 mol−%), tricyclohexylphosphonium tetrafluoroborate (262 mg, 730 µmol, 2.0 mol−%) and diisopropylethylamine (184 mg, 1.42 mmol, 4 mol−%) were added successively to dry DCM (200 mL) and the resulting mixture was stirred at room temperature for 10 minutes. Propargyl alcohol **35** (2.00 g, 35.6 mmol, 1.00 eq.) was added and the reaction mixture was cooled to 0 °C. Then, tributyltinhydride (12.46 g, 42.8 mmol, 1.20 eq.) was added dropwise via a syringe over 5 minutes. The reaction was then stirred at 0 °C for 2 hours. The reaction mixture was concentrated under reduced pressure and purified by column chromatography (Silica, CH/EtOAc 9:1) to afford the corresponding vinylstannane **36** as a yellow oil (7.43 g, 21.4 mmol, 60%). $\mathbf{R_f}$ = 0.15 (CH/EtOAc 9:1); **^{1}H-NMR** (500 MHz, CD_2Cl_2) δ = 0.81–0.99 (m, 15H), 1.31 (h, *J* = 7.3 Hz, 6H), 1.46–1.60 (m, 6H), 4.09–4.16 (m, 2H), 6.09–6.28 (m, 2H); **^{13}C-NMR** (126 MHz, CD_2Cl_2) δ = 9.9, 14.0, 27.9, 29.6, 66.7, 128.3, 148.0; **MS** (EI): m/z: 291.0 ([M]−$C_4H_9^+$, 100). The spectroscopic data were in agreement with those previously reported.[58]

(*E*)-3-(tributylstannyl)prop-2-en-1-al (33)

The synthesis was carried out according to a known literature procedure:[58]

Activated MnO_2 (Alfa Aesar) previously dried in an oven at 80 °C overnight (13.5 g, 155 mmol, 20 eq.) was suspended in DCM (90 mL). Vinylstannane **36** (2.69 g, 7.75 mmol, 1.0 eq.) in DCM (10 mL) was added at room temperature and the mixture was stirred overnight. The mixture was filtered through Celite® and rinsed with DCM (40 mL) and EtOAc (40 mL). The solvent was evaporated under reduced pressure and the resulting residue was purified by column chromatography (Silica, CH/EtOAc 20:1) to afford the corresponding aldehyde **33** (2.39 g, 6.94 mmol, 90%) as a pale yellow oil. $\mathbf{R_f}$ = 0.55 (CH/EtOAc 20:1); **^{1}H-NMR** (500 MHz, CD_2Cl_2) δ = 5.31 (t, *J* = 7.3 Hz, 9H), 5.37–5.52 (m, 6H), 5.73 (h, *J* = 7.3 Hz, 6H), 5.86–

6.03 (m, 6H), 10.90–11.12 (m, 1H), 12.06–12.32 (m, 1H), 13.80 (d, *J* = 7.5 Hz, 1H); **^{13}C-NMR** (126 MHz, CD_2Cl_2) δ = 10.3, 14.0, 27.8, 29.5, 148.2, 163.6, 194.0; **HRMS** (APCI) m/z: calc. for $[M+H]^+$: 347.1391; found: 347.1390. The spectroscopic data were in agreement with those previously reported.[58]

(*E*)-tributyl(but-1-en-3-yn-1-yl)stannane (180)

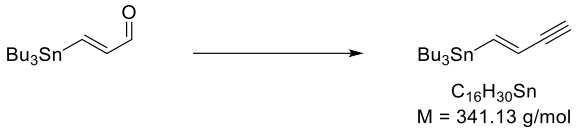

To a −78 °C solution of trimethylsilyldiazomethane (2 M in hexanes, 0.82 mL, 1.6 mmol, 1.5 eq.) was added *n*-BuLi (2.5 M in hexanes, 0.57 mL, 1.4 mmol, 1.3 eq.). After being stirred for 30 min, a solution of aldehyde **33** (375 mg, 1.09 mmol, 1.00 eq.) in THF (2 mL) was added. The mixture was stirred for 1 h at −78 °C, 1 h at 0 °C and then quenched with saturated aqueous solution of NH_4Cl (4 mL). The aqueous phase was extracted with DCM (3 x 20 mL). The combined organic phases were washed with brine, dried over anhydrous $MgSO_4$, filtered and concentrated. Purification of the crude product by column chromatography (Silica, CH + 2% NEt_3) afforded alkyne **180** (319 mg, 0.94 mmol, 85%) as a pale yellow oil. $\mathbf{R_f}$ = 0.60 (CH + 2% NEt_3); **^{1}H-NMR** (500 MHz, CD_2Cl_2) δ = 5.34 (dt, *J* = 24.0, 7.7 Hz, 15H), 5.74 (h, *J* = 7.3 Hz, 6H), 5.85–6.03 (m, 6H), 7.35 (d, *J* = 2.1 Hz, 1H), 10.27–10.47 (m, 1H), 11.30–11.51 (m, 1H); **^{13}C-NMR** (126 MHz, CD_2Cl_2) δ = 9.5, 13.4, 27.2, 28.9, 75.2, 83.9, 124.4, 149.6; **HRMS (ESI)** m/z: calc. for $[M+H]^+$: 343.1445; found: 343.1439.

tributyl((1*E*,3*E*)-3-methyl-4-(4,4,5,5-tetramethyl-1,3,2-dioxaborolan-2-yl)buta-1,3-dien-1-yl)-stannane (113)

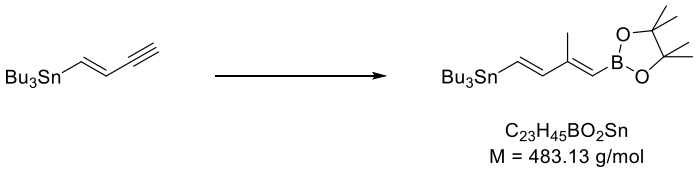

Zirconocene dichloride (263 mg, 900 µmol, 0.3 eq.) was dissolved in anhydrous DCM (20 mL) and cooled to –78 °C. Then, MMAO-12 (10% in toluene, 1.0 mL) and trimethyl aluminium (2.0 M in toluene, 3.0 mL, 6.0 mmol, 2.0 eq.) was added and the resulting mixture was stirred at –78 °C for 10 minutes. Then, neat enyne **25**[23] (1.00 g, 3.00 mmol, 1.00 eq.) was added and the reaction was allowed to warm to r.t. over

the course of 10 hours in the dark, during which the solution takes on a typical red-brown color. Then, the solution was cooled to –40 °C and *iso*propyl pinacolborate (1.0 mL, 4.9 mmol, 1.6 eq.) was added over 10 seconds. The resulting mixture was stirred at that temperature for 15 minutes and at r.t. for another 20 minutes. After that time, the mixture was again cooled to –40 °C and slowly quenched with water (5 × 0.2 mL). After being stirred for 10 minutes another addition of water (1 mL) was performed, the ice bath was removed and after 10 minutes a final addition of water (1 mL) was performed. Then, Na_2SO_4 (ca. 10 g) was added and the mixture was filtered over a plug of Florisil®, rinsed with Et_2O and the filtrate was evaporated under reduced pressure. The residue was dissolved in CH+2% Et_3N (20 mL), filtered over a plug of deactivated Silica (50 g, dissolved in CH, with Et_3N added while stirring until pH = 8) and rinsed with CH+2% Et_3N (150 mL). After evaporation of the solvent, compound **113** was obtained as an orange-green oil (1.14 g, 2.36 mmol, 79%). $\mathbf{R_f}$ = 0.45 (CH/EtOAc 50:1); **^{1}H-NMR** (500 MHz, CD_2Cl_2) δ = 0.85–1.01 (m, 15H), 1.25 (s, 12H), 1.29 (s, 6H), 1.47–1.56 (m, 6H), 2.06 (d, *J* = 0.9 Hz, 3H), 5.24 (dt, *J* = 1.5, 0.8 Hz, 1H), 6.46 (d, *J* = 19.2 Hz, 1H), 6.64 (dd, *J* = 19.4, 0.8 Hz, 1H); **^{13}C NMR** (126 MHz, CD_2Cl_2) δ = 10.0, 14.0, 16.1, 25.2, 27.9, 29.7, 83.4, 133.0, 152.8, 156.7 [note: the carbon attached to boron was not observed due to quadrupole broadening caused by the ^{11}B nucleus]; **HRMS (ESI)** m/z: calc. for $[M+H]^+$: 485.2616; found: 485.2610.

(*E*)-tributyl(3,3-diethoxyprop-1-en-1-yl)stannane (S-3)

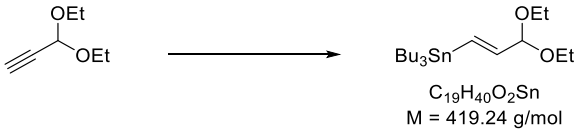

The synthesis was carried out according to a known literature procedure:[45]

To a cooled (−78 °C) solution of CuCN (2.10 g, 23.4 mmol, 1.20 eq.) in dry THF (50 mL) *n*-BuLi (2.5 M in hexanes, 18.7 mL, 46.8 mmol, 2.40 eq.) was added dropwise and the resulting grey mixture was stirred at r.t for 20 min. The temperature was cooled down again to −78 °C and *n*-Bu_3SnH (12.4 mL, 46.8 mmol, 2.40 eq.) was added. After stirring for 30 min, 3,3-diethoxyprop-1-yne (**32**) (2.50 g, 19.5 mmol, 1.00 eq.) was added and the reaction was stirred at −78 °C for 30 min. Dry MeOH (10 mL) was added dropwise while stirring, keeping the temperature at −78 °C for 30 min. Then, water (20 mL) was added, the mixture was warmed to r.t and stirred for further 15 minutes. The reaction mixture was diluted with Et_2O (200 mL) and water (200 mL). Phases were separated and the organic layer was washed with brine

(3 x 100 mL). The organic layer was dried over $MgSO_4$ and filtered over a plug of silica. After evaporation of the solvent, the crude product was received as a yellow oil (11.80 g). An aliquant of 100 mg was purified by column chromatography (Silica, CH/EtOAc 50:1) to obtain an analytical sample of **S-3** (yellow oil) and the remaining crude product **S-3** was used in the next step without further purification. $\mathbf{R_f}$ = 0.25 (CH/EtOAc 50:1); **^{1}H-NMR** (500 MHz, $CDCl_3$) δ = 0.83–0.99 (m, 15H), 1.23 (t, *J* = 7.1 Hz, 6H), 1.30 (h, *J* = 7.3 Hz, 6H), 1.42–1.57 (m, 6H), 3.50 (dq, *J* = 9.5, 7.1 Hz, 2H), 3.64 (dq, *J* = 9.5, 7.1 Hz, 2H), 4.78–4.84 (m, 1H), 5.87–6.07 (m, 1H), 6.23–6.46 (m, 1H); **^{13}C-NMR** (126 MHz, $CDCl_3$) δ = 9.6, 13.8, 15.4, 27.4, 29.2, 61.1, 103.4, 133.1, 144.9; **HRMS** (ESI) m/z: calc. for $[M+Na]^+$: 443.1946; found: 443.1949. The spectroscopic data were in agreement with those previously reported.[45]

(*E*)-3-(tributylstannyl)prop-2-en-1-al (33) – alternative synthesis

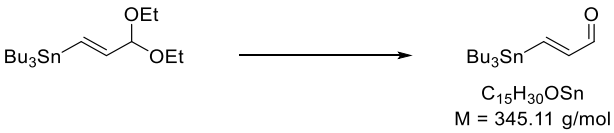

The synthesis was carried out according to a known literature procedure:[45]

Crude **S-3** was dissolved in acetone (150 mL) and water (10 mL), *p*-toluenesulfonic acid (0.74 g, 3.9 mmol, 0.20 eq.) was added and the resulting mixture was stirred at 100 °C for 24 h. When completion was judged by TLC analysis, the reaction was quenched by addition of a saturated aqueous solution of $NaHCO_3$. The aqueous layer was extracted with Et_2O (3 x 100 mL) and the combined organic layers were washed with brine (2 x 50 mL), dried over $MgSO_4$ and solvent was evaporated. The residue was purified by column chromatography (Silica, CH/EtOAc 20:1) to afford (*E*)-(3-tributylstannyl)acrylaldehyde (**33**) (5.60 g, 16.2 mmol, 83%) as a yellow oil. $\mathbf{R_f}$ = 0.55 (CH/EtOAc 20:1); **^{1}H-NMR** (500 MHz, CD_2Cl_2) δ = 5.31 (t, *J* = 7.3 Hz, 9H), 5.37–5.52 (m, 6H), 5.73 (h, *J* = 7.3 Hz, 6H), 5.86–6.03 (m, 6H), 10.90–11.12 (m, 1H), 12.06–12.32 (m, 1H), 13.80 (d, *J* = 7.5 Hz, 1H); **^{13}C-NMR** (126 MHz, CD_2Cl_2) δ = 10.3, 14.0, 27.8, 29.5, 148.2, 163.6, 194.0; **HRMS** (APCI) m/z: calc. for $[M+H]^+$: 347.1391; found: 347.1390. The spectroscopic data were in agreement with those previously reported.[45]

((1*E*,3*E*)-2-methylbuta-1,3-diene-1,4-diyl)bis(tributylstannane) (174)

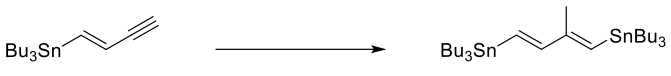

$C_{29}H_{60}Sn_2$
M = 646.22 g/mol

To a cooled (–78 °C) solution of CuCN (110 mg, 1.23 mmol, 1.20 eq.) in anhydrous THF (5 mL) *n*-BuLi (1.0 mL, 2.5 M in hexanes, 2.5 mmol, 2.5 eq.) was added dropwise and the resulting grey mixture was stirred at r.t for 20 min, which turns into a clear pale yellow solution during that time. The temperature was cooled down again to –78 °C and *n*-Bu_3SnH (0.66 mL, 2.5 mmol, 2.5 eq.) was added during which the color immediately turns into an intense yellow. After stirring for 30 min, enyne **180** (350 mg, 1.03 mmol, 1.00 eq.) in THF (2 mL) was added and the reaction was stirred at –78 °C for 1 hour. Iodomethane (0.50 mL, 8.0 mmol, 8.0 eq.) was added over 30 seconds at –78 °C. The reaction was allowed to stir overnight, while slowly warming up to room temperature. Then, the mixture was quenched with a saturated solution of NH_4Cl (5 mL) and diluted with Et_2O (20 mL). Phases were separated and the organic layer was washed with a saturated aqueous solution of NH_4Cl (2 × 20 mL), water (20 mL) and brine (20 mL), dried over $MgSO_4$, filtered over Celite and concentrated. Purification was achieved by semi-preparative HPLC (column: KNAUER Eurospher II 100-5 C18P; 5 µm; 250 x 20 mm, eluent: A: MeCN, B: Chloroform (stab. EtOH), isocratic: 65% A, 35% B (0–28 min), flowrate: 28.0 mL/min, detection wavelengths: λ_1 = 260 nm). After evaporation of the solvent, the obtained purified product **174** was received as a colorless oil (423 mg, 655 µmol, 64%). $\mathbf{R_f}$ = 0.75 (CH); **^{1}H-NMR** (400 MHz, $CDCl_3$) δ = 0.87–0.94 (m, 30H), 1.26–1.38 (m, 15H), 1.43–1.58 (m, 15H), 1.87–1.92 (m, 3H), 5.91 (s, 1H), 6.06–6.14 (m, 1H), 6.59–6.67 (m, 1H); **^{13}C-NMR** (126 MHz, acetone-d6) δ = 10.0, 10.7, 14.0, 20.3, 28.0, 127.1, 132.7, 152.8, 153.0. [note: the compound **174** degrades in chloroform, therefore the ^{13}C-NMR was recorded in acetone-d6; product **174** was <u>not detected</u> by mass spectrometry].

(*E*)-tributyl(3,3-diethoxy-2-methylprop-1-en-1-yl)stannane (187)

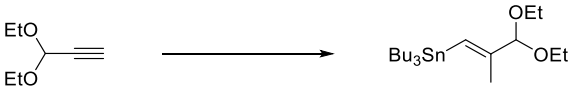

$C_{20}H_{42}O_2Sn$
M = 433.26 g/mol

To a cooled (–78 °C) solution of CuCN (1.68 g, 18.7 mmol, 1.20 eq.) in anhydrous THF (50 mL) *n*-BuLi (15 mL, 2.5 M in hexanes, 37 mmol, 2.4 eq.) was added dropwise and the resulting grey mixture was

stirred at r.t for 20 min, which turns into a clear pale yellow solution during that time. The temperature was cooled down again to –78 °C and *n*-Bu_3SnH (10 mL, 37 mmol, 2.4 eq.) was added during which the color immediately turns into an intense yellow. After stirring for 30 min, 3,3-diethoxyprop-1-yne (**32**) (2.00 g, 15.6 mmol, 1.00 eq.) was added and the reaction was stirred at –78 °C for 1 hour. Iodomethane (10 mL, 156 mmol, 10 eq.) was added over 30 seconds at –78 °C. The reaction was allowed to stir for 5 hours, while slowly warming up to room temperature. Then, the mixture was filtered over a large plug of Silica/K_2CO_3 (9:1) and rinsed with Et_2O (3 × 50 mL). [note: this procedure does not remove tetraalkyltin byproducts formed during the reaction but is rather used to compensate the acidity of silica.] The filtrate was evaporated under reduced pressure and the obtained liquid was redissolved in Et_2O (100 mL), washed with a saturated aqueous solution of NH_4Cl (2 × 50 mL), water (50 mL) and brine (50 mL), dried over $MgSO_4$ and filtered. Evaporation of the solvent yielded crude (*E*)-(3-tributylstannyl)methacroleine-diethylacetal (**187**) as a yellow oil, which was used in the following step without further purification. An aliquant of 100 mg was purified by column chromatography (Silica, CH/EtOAc 50:1) to provide an analytical sample of **187**, which was obtained as a colorless to pale yellow oil. $\mathbf{R_f}$ = 0.25 (CH/EtOAc 50:1); **^{1}H-NMR** (500 MHz, Acetone-d6) δ = 0.89 (t, *J* = 7.4 Hz, 9H), 0.95–1.04 (m, 6H), 1.15 (t, *J* = 7.1 Hz, 6H), 1.34 (dt, *J* = 14.7, 7.3 Hz, 6H), 1.49–1.62 (m, 6H), 1.73–1.77 (m, 3H), 3.41 (dq, *J* = 9.5, 7.0 Hz, 2H), 3.55 (dq, *J* = 9.5, 7.0 Hz, 2H), 4.68 (d, *J* = 0.9 Hz, 1H), 5.86–6.02 (t, $J_{Sn\text{-}H}$ = 34.9 Hz, 1H); **^{13}C-NMR** (126 MHz, Acetone-d6) δ = 10.6, 14.0, 15.6, 19.6, 27.9, 61.9, 106.6, 126.1, 152.1; **HRMS** (ESI) m/z: calc. for $[M–EtOH+H]^+$: 389.1861; found: 389.1861.

(*E*)-(3-tributylstannyl)methacrylaldehyde (184)

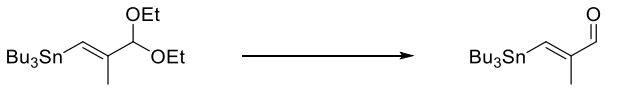

$C_{16}H_{32}OSn$
M = 359.14 g/mol

Crude acetal **187** was dissolved in acetone (150 mL) and water (25 mL), *para*-toluenesulfonic acid (269 mg. 1.56 mmol, 0.1 eq.) was added and the resulting mixture was stirred at 110 °C for 20 h. The reaction mixture was cooled to r.t. and quenched by addition of a saturated aqueous solution of $NaHCO_3$ (20 mL). The aqueous layer was extracted with Et_2O (3 × 100 mL) and the combined organic layers were washed with brine (50 mL), dried over $MgSO_4$, filtered and concentrated. After purification by column chromatography (Silica, CH/EtOAc 30:1) the product **184** was obtained as a pale yellow oil (4.10 g, 15.6 mmol, 73% over 2 steps). $\mathbf{R_f}$ = 0.49 (CH/EtOAc 30:1); **^{1}H-NMR** (500 MHz, Acetone-d6) δ = 0.90 (d,

J = 7.4 Hz, 9H), 1.04–1.18 (m, 6H), 1.31–1.39 (m, 6H), 1.46-1.75 (m, 6H), 1.86–1.89 (m, 3H), 7.41 (q, *J* = 0.9 Hz, 1H), 9.46 (s, 1H); **^{13}C-NMR** (126 MHz, Acetone-d6) δ = 10.7, 13.9, 16.3, 19.1, 27.9, 155.2, 157.3, 194.0; **HRMS (APCI)** m/z: calc. for $[M+H]^+$: 361.1548; found: 361.1548. The spectroscopic data were in agreement with those previously reported.[131]

(*E*)-tributyl(2-methylbuta-1,3-dien-1-yl)stannane (185)

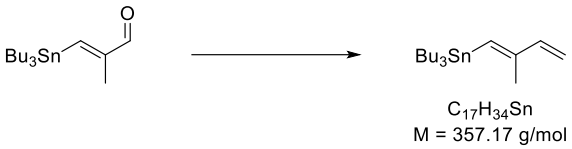

The synthesis was carried out according to a known literature procedure:[131]

To a stirred suspension of methyltriphenylphosphonium bromide (894 mg, 2.50 mmol, 1.30 eq.) in anhydrous THF (10 mL) at 0 ºC was added *n*-BuLi (2.5 M in hexanes, 1.00 mL, 2.5 mmol, 1.30 eq.) and stirring was continued for 1 h at room temperature. Then, a solution of aldehyde **184** in THF (5 mL) was added dropwise to the above mixture at 0 °C and the resulting solution was stirred at r.t. for one hour. After completion, the reaction was quenched with saturated aqueous NH_4Cl (5 mL) and the resulting mixture was extracted with Et_2O (2 x 20 mL). The combined extracts were washed with brine (20 mL), dried over $MgSO_4$, filtered and concentrated. Purification by column chromatography (Silica, CH + 1% NEt_3) yielded the desired compound **185** as a colorless oil (180 mg, 504 µmol; 26%) [note: the low yield results from a flask, which fell over]. $\mathbf{R_f}$ = 0.65 (CH + 1% NEt_3); **^{1}H-NMR** (500 MHz, acetone-d6) δ = 0.89 (t, *J* = 7.3 Hz, 9H), 0.94–1.06 (m, 6H), 1.28–1.39 (m, 6H), 1.47–1.64 (m, 6H), 1.90–1.94 (m, 3H), 4.92–5.02 (m, 1H), 5.08–5.16 (m, 1H), 5.96 (p, *J* = 0.7 Hz, 1H), 6.40–6.56 (m, 1H); **^{13}C-NMR** (126 MHz, acetone-d6) δ = 10.7, 13.9, 20.3, 27.9, 112.3, 133.8, 143.3, 151.9 [note: one carbon signal is masked by the solvent signal]; **HRMS (APCI)** m/z: calc. for $[M+H]^+$: 357.1599; found: 357.1596. The spectroscopic data were in agreement with those previously reported.[131]

(*E*)-tributyl(2-methylbut-1-en-3-yn-1-yl)stannane (188)

$C_{17}H_{32}Sn$
M = 355.15 g/mol

To a –78 ºC solution of trimethylsilyldiazomethane (2 M in Et_2O, 2.0 mL, 4.0 mmol, 1.4 eq.) was added *n*-BuLi (2.5 M in hexanes, 1.50 mL, 1.45 eq.) and the resulting mixture was stirred for 30 min. Then, a solution of aldehyde **184** (1.00 g, 2.78 mmol, 1.00 eq.) in anhydrous THF (5 mL) was added. The mixture was stirred for 30 minutes at –78 ºC, 30 min at 0 ºC and then quenched with saturated aqueous solution of NH_4Cl (20 mL). The aqueous phase was extracted with Et_2O (3 × 30 mL). The combined organic phases were washed with brine (20 mL), dried over $MgSO_4$, filtered and concentrated. Purification of the crude product by column chromatography (Silica, CH + 2% Et_3N) afforded alkyne **188** as a pale yellow oil (657 mg, 1.85 mmol, 66%); $\mathbf{R_f}$ = 0.45 (CH); **^{1}H-NMR** (700 MHz, Acetone-d6) δ = 0.89–0.91 (m, 9H), 0.99–1.06 (m, 6H), 1.32–1.36 (m, 6H), 1.50–1.62 (m, 5H), 1.94–1.96 (m, 3H), 3.36 (s, 1H), 6.43 (s, 1H); **^{13}C-NMR** (176 MHz, Acetone) δ = 10.7, 13.9, 19.3, 25.8, 27.9, 76.0, 87.1, 135.1, 141.2; **HRMS (APCI)** m/z: calc. for $[M+H]^+$: 357.1602; found: 357.1598.

tributyl((1*E*,3*E*)-2-methyl-4-(4,4,5,5-tetramethyl-1,3,2-dioxaborolan-2-yl)buta-1,3-dien-1-yl) stannane (121)

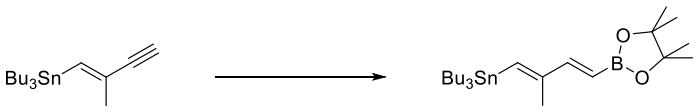

$C_{23}H_{45}BO_2Sn$
M = 483.13 g/mol

To a solution of alkyne **188** (270 mg, 0.76 mmol, 1.00 eq.) in anhydrous DCM (5 mL) was added pinacolborane (0.2 mL, 1.4 mmol, 1.8 eq.) and Schwartz-reagent (98 mg, 0.38 mmol, 0.50 eq.). The mixture was stirred at r.t. for 18 hours. Then, water (10 mL) and Et_2O (10 mL) were added and the mixture was stirred until gas evolution ceased. Phases were separated and the aqueous layer was extracted with Et_2O (3 × 10 mL). The combined organic layers were washed with brine (10 mL), dried over $MgSO_4$, filtered and concentrated. After evaporation of the solvent, the crude product was purified by column chromatography (RP-Silica C18, 10 g). After loading, the column was rinsed with MeCN/H_2O (2:1, 150 mL) and eluted with MeCN/Et_2O (1:1, 15 × 4 mL). The collected fractions were TLC checked on normal phase TLC (CH/EtOAc 50:1). Fractions 3-12 showed product spots on TLC (several spots were

observed due to instability on normal phase silica). The fractions were collected and the solvent was evaporated to yield the desired pure compound **121** as a yellow-green oil (295 mg, 0.61 mmol, 80%); R_f = 0.35 (CH/EtOAc 50:1); **^{1}H-NMR** (700 MHz, Acetone-d6) δ = 0.88–0.91 (m, 9H), 0.95–1.07 (m, 6H), 1.25 (s, 12H), 1.32–1.35 (m, 6H), 1.49–1.60 (m, 6H), 1.93–1.95 (m, 3H), 5.36–5.42 (m, 1H), 6.17–6.28 (m, 1H), 7.04 (dt, *J* = 18.0, 1.1 Hz, 1H); **^{13}C-NMR** (176 MHz, Acetone-d6) δ = 10.7, 13.9, 20.3, 25.1, 27.9, 83.8, 138.8, 152.7, 155.1, [note: the carbon attached to boron was not observed due to quadrupole broadening caused by the ^{11}B nucleus]; **HRMS (APCI)** m/z: calc. for $[M+H]^+$: 485.2616; found: 485.2608.

Synthesis of 121 via Boryl-Wittig olefination:

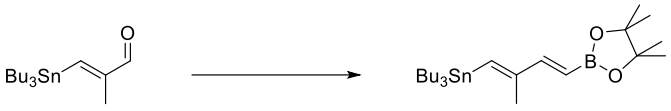

$C_{23}H_{45}BO_2Sn$
M = 483.13 g/mol

To a solution of 1,1-bis[(pinacolato)boryl]methane (1.41 g, 5.25 mmol, 2.00 eq.) in anhydrous THF (10 mL) at –78 °C was added a solution of lithium tetramethylpiperidide (676 mg, 4.59 mmol, 1.75 eq.) in anhydrous THF (10 mL) resulting in a brown cloudy mixture. The ice bath was removed and the mixture was stirred at r.t. for 10 minutes. Then, the solution was again cooled to –78 °C and a solution of aldehyde **184** (945 mg, 2.63 mmol, 1.00 eq.) in anhydrous THF (10 mL) was added. The mixture was allowed to slowly warm to r.t. over the course of 20 hours. After the indicated time, the mixture was diluted with Et_2O (50 mL) and and poured into phosphate buffer (pH 7, 80 mL). Phases were separated and the aqueous phase was extracted with Et_2O (50 mL). The combined organic layers were washed with water (50 mL) and brine (30 mL), dried over $MgSO_4$, filtered and concentrated The obtained residue was dissolved in *n*-pentane (100 mL) and washed with MeCN (2 × 75 mL), MeOH/H_2O 10:3 (65 mL) and MeOH/H_2O 1:1 (60 mL). The *n*-pentane layer was dried over $MgSO_4$ and filtered. After evaporation, the product (1.3 g, ca. 100%) was obtained with remaining traces of pinacol byproducts. Therefore, it was again dissolved in *n*-pentane (100 mL) and washed with MeCN (3 × 50 mL). After the final washing step, the pure product **121** was obtained as an orange-green oil (1.08 g, 2.24 mmol, 85%). The spectroscopic data matched with those reported above.

tributyl((1*E*,3*E*)-2-methyl-4-(1,3,6,2-dioxazaborocane-4,8-dione-2-yl)buta-1,3-dien-1-yl) stannane (175)

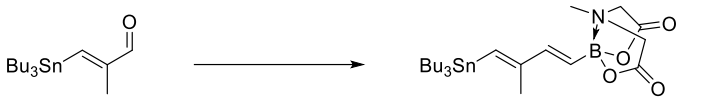

Chemical Formula: $C_{22}H_{40}BNO_4Sn$
Molecular Weight: 512,09

Anhydrous $CrCl_2$ (274 mg, 2.23 mmol, 8.0 eq.) and MIDA-reagent **195** (235 mg, 560 µmol, 2.0 eq.) were added to a dry flask, followed by anhydrous THF (10 mL). The resulting mixture was sonicated for 10 minutes and afterwards cooled to 0 °C. Aldehyde **184** (100 mg, 278 µmol, 1.00 eq.) was added and the resulting mixture was stirred at 0 °C for 24 hours. Then, brine (10 mL) and EtOAc (10 mL) were added and phases were separated. The aqueous layer was extracted with EtOAc (3 × 10 mL) and the combined organic layers were washed with brine, dried over $MgSO_4$, filtered and concentrated. After purification by column chromatography (RP-Silica C18, gradient: 50% H_2O/MeCN → 100% MeCN) the product **175** was obtained as a yellow gum (69.4 mg, 136 µmol, 49%). **^{1}H-NMR** (500 MHz, Acetone-d6) δ = 0.89 (t, *J* = 7.3 Hz, 9H), 0.94–1.07 (m, 6H), 1.30–1.39 (m, 6H), 1.46–1.64 (m, 6H), 1.93–1.98 (m, 3H), 3.01 (s, 3H), 4.04 (d, J = 16.8 Hz, 2H), 4.21 (d, *J* = 16.8 Hz, 2H), 5.60 (d, *J* = 17.9 Hz, 1H), 6.02 (d, J = 0.8 Hz, 1H), 6.60–6.76 (m, 1H); **^{13}C-NMR** (126 MHz, Acetone-d6) δ = 10.7, 13.9, 20.8, 28.0, 30.0, 47.4, 62.3, 134.3, 148.3, 152.9, 169.1; [note: the carbon attached to boron was not observed due to quadrupole broadening caused by the ^{11}B nucleus; One carbon signal overlaps with the solvent signal at δ = 30.0 ppm].**HRMS (APCI)** m/z: calc. for $[M+H]^+$: 514.2153; found: 514.2152.

2-(Dichloromethyl)-1,3,6,2-dioxazaborocane-4,8-dione (192)

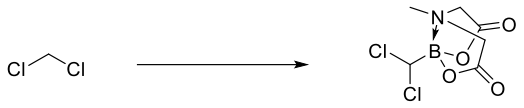

Chemical Formula: $C_6H_8BCl_2NO_4$
Molecular Weight: 239,84

Anhydrous DCM (3.5 mL, 55 mmol, 1.1 eq.) was added to anhydrous THF (100 mL). The mixture was cooled to –100 °C (EtOH/N_2), then *n*-BuLi (2.5 M in hexane, 19.9 mL, 49.8 mmol, 1.00 eq.) was added dropwise *via* an syringe pump over 45 min. The reaction was stirred for 40 min at this temperature, then trimethylborate (6.2 mL, 55 mmol, 1.1 eq.) was added in one portion and the reaction was stirred another 40 min at –100 °C. The reaction was quenched with 5 N HCl solution (10 mL), the coooling bath was removed and the mixture was stirred at room temperature for 1 h. Then, the mixture was extracted with ether (3 × 50 mL), the organic layers were combined, washed with brine, dried over magnesium sulfate, filtered and concentrated in vacuum to provide the crude boronic acid. The crude product was dissolved in anhydrous toluene (30 mL) and anhydrous DMSO (8 mL) and MIDA (7.31 g, 49.7 mmol, 1.00 eq.) was added. The resulting solution was refluxed under *Dean-Stark* conditions at 120 °C overnight. After the indicated time, all volatiles were removed *in vacuo* and the residue was dissolved in EtOAc (150 mL). After addition of water (100 mL), phases were separated and the organic layer was washed with water (3 × 50 mL) and brine (50 mL). $MgSO_4$ was added and the resulting mixture was filtered. After removal of the solvent, the crude product was dissolved in a minimum amount of MeCN and triturated with Et_2O. The obtained solid was washed with Et_2O and finally dried to obtain the desired MIDA-ester **192** as an off-white solid (3.18 g, 13.3 mmol, 27%). $\mathbf{R_f}$ = 0.25 (Et_2O/MeCN 2:10); **^{1}H-NMR** (500 MHz, Acetone-d6) δ = 3.37 (s, 3H), 4.24 (d, *J* = 17.0 Hz, 2H), 4.45 (d, *J* = 17.0 Hz, 2H), 5.81 (s, 1H); **^{13}C-NMR** (126 MHz, Acetone-d6) δ = 46.8, 64.3, 168.0; [note: the carbon attached to boron was not observed due to quadrupole broadening caused by the ^{11}B nucleus]; **HRMS (ESI-)** m/z: calc. for $[M-H]^-$: 237.9852; found: 237.9850.

2-(Diiodomethyl)-1,3,6,2-dioxazaborocane-4,8-dione (195)

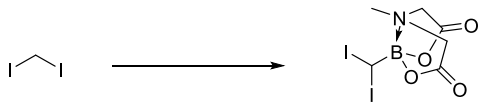

Chemical Formula: $C_6H_8BI_2NO_4$
Molecular Weight: 422,75

To a solution of LHMDS (1 M in THF, 20 mL, 20 mmol, 1.0 eq.) in THF (40 mL) and Et_2O (20 mL) at –78 °C was added a solution of diiodomethane (1.8 mL, 22 mmol, 1.1 eq.) in THF (10 mL) over 5 minutes under the exclusion of light. After 30 minutes, the mixture was cooled to –90 °C. When this temperature was reached, triisopropylborate (5.0 mL, 22 mmol, 1.1 eq.) was added in one portion and the cooling unit was turned off. The resulting solution was stirred over 1.5 hours during which the ice bath gradually warmed to –40 °C. The reaction was quenched with 5 M HCl solution (20 mL), the ice bath was removed and the resulting mixture was stirred for 45 minutes. The mixture was extracted with Et_2O (3 × 50 mL) and the combined layers were washed with brine (50 mL). Toluene (100 mL) and $MgSO_4$ were added, followed by filtration. The volatile solvents (Et_2O and THF) were removed under reduced pressure and to the remaining crude mixture of diiodomethylboronic acid in toluene was added DMSO (10 mL) and MIDA (6.0 g, 41 mmol, 2.0 eq. based on max. yield). The resulting mixture was heated under Dean-Stark conditions (115 °C) for 16 hours. After the indicated time, all volatiles were removed *in vacuo.* EtOAc (350 mL) and 5% NaCl (150 mL) were added and the mixture was sonicated for 10 minutes. Phases were separated and the organic layer was washed with water (3 × 50 mL). The aqueous phase was backextracted with EtOAc (3 × 50 mL), followed by washing steps with sat. $Na_2S_2O_3$ (2 × 100 mL) and brine (50 mL). $MgSO_4$ was added and the resulting mixture was filtered. After removal of the solvent, the crude product was dissolved in MeCN (40 mL) and triturated with Et_2O (600 mL). The resulting suspension was stored in a freezer (12 h, –32 °C) and subsequently decanted. The remaining yellow solid was washed with Et_2O (2 × 100 mL) and filtered through a fritted funnel. The residual solids were dissolved in MeCN (100 mL), followed by evaporation of the solvent. The product **195** was obtained as a yellow solid (1.69 g, 4.00 mmol, 20%). $\mathbf{R_f}$ = 0.25 (Et_2O/MeCN 1:5); **^{1}H-NMR** (500 MHz, Acetone-d6) δ = 3.37 (s, 3H), 4.29 (d, *J* = 16.9 Hz, 2H), 4.45 (d, *J* = 16.9 Hz, 2H), 4.97 (s, 1H); **^{13}C-NMR** (126 MHz, Acetone-d6) δ = 45.1, 64.2, 166.4; [note: the carbon attached to boron was not observed due to quadrupole broadening caused by the ^{11}B nucleus]; **HRMS (ESI-)** m/z: calc. for $[M-H]^-$: 421.8564; found: 421.8566.

tributyl((1*E*,3*E*)-4-(5,5-dimethyl-1,3,2-dioxaborinan-2-yl)-2-methylbuta-1,3-dien-1-yl)stannane (176)

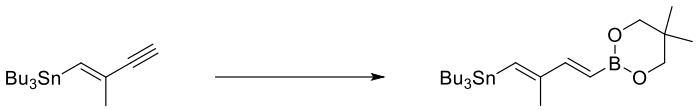

$C_{22}H_{43}BO_2Sn$
M = 469.10 g/mol

To a solution of 2,5-dimethyl-2,4-hexadiene (300 µL, 2.11 mmol, 3.00 eq.) in THF (1 mL) at 0 °C was dropwise added BH_3 SMe_2 (80 µL, 0.84 mmol, 1.2 eq.) over 5 minutes. The solution was stirred for 3 h at 0 °C and then a solution of alkyne **188** (250 mg, 704 µmol, 1.00 eq.) in THF (1 mL) was added dropwise. The reaction mixture was stirred at 0 °C for 1 h and was then allowed to warm to room temperature. Water (100 µL, 5.63 mmol, 8.00 eq.) was added, the reaction mixture was stirred for 30 min and then treated with an aqueous solution of formaldehyde (37%, 50 µL, 704 µmol, 1.00 eq). After the mixture was stirred for 1 h, neopentylglycol (110 mg, 1.06 mmol, 1.50 eq.) and $MgSO_4$ (1 g) were added and the resulting suspension was vigorously stirred overnight. After 12 hours, the mixture was filtered and the solvent was removed. After evaporation of the solvent, the crude product loaded onto an RP-column (10 g), rinsed with MeCN/H_2O (2:1, 150 mL) and eluted with MeCN/Et_2O (15 x 4 mL). After evaporation of the solvent the semi-purified compound **176** was obtained as a yellow oil (218 mg, 465 µmol, 66%). $\mathbf{R_f}$ = 0.42 (CH/EtOAc 50:1), **^{1}H-NMR** (300 MHz, acetone-d6) δ = 0.86–0.96 (m, 15H), 1.29–1.35 (m, 6H), 1.50–1.60 (m, 6H), 1.90–1.94 (m, 3H), 3.65 (s, 6H), 5.33 (dd, *J* = 18.0, 0.6 Hz, 1H), 6.15 (d, *J* = 0.8 Hz, 1H), 6.93–7.06 (m, 1H); **HRMS (APCI)** m/z: calc. for $[M+H]^+$: 471.2459; found: 471.2448.

8.2.3 Synthesis of the eastern fragment 129

methyl (*R*)-3-((*tert*-butyldimethylsilyl)oxy)-2-methylpropanoate (S-4)

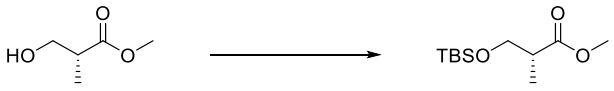

$C_{11}H_{24}O_3Si$
M = 232.40 g/mol

The synthesis was carried out according to a known literature procedure:[152]

To a solution of *R*-Roche ester (*R*-**208**) (6.9 g, 58 mmol, 1.0 eq.) in anhydrous DCM (90 mL) was added imidazole (8.75 g, 129 mmol, 2.22 eq.) at r.t. and a solution of TBSCl (9.68 g, 64.2 mmol, 1.11 eq.) in DCM (20 mL) was added dropwise at 0 °C over 1 h. The reaction mixture was stirred for 2.5 hours at r.t. followed by evaporation of the solvent. The residue was redissolved in EtOAc (100 mL) and washed with

aqueous saturated NH_4Cl (50 mL), $NaHCO_3$ (50 mL) and dried over $MgSO_4$. Purification of the crude product by column chromatography (Silica, CH/EtOAc, 20:1) yielded the product **S-4** (13.5 g, 58.1 mmol, 99%) as a colorless oil. Rf = 0.40 (CH/EtOAc 20:1); $\boldsymbol{\alpha_D^{20}}$ = –24.6 (c = 1.0, MeCN); 1H-NMR (500 MHz, acetone-d6) δ = 0.04 (s, 3H), 0.05 (s, 3H), 0.87 (s, 9H), 1.09 (d, J = 7.0 Hz, 3H), 2.62 (td, J = 7.0, 5.6 Hz, 1H), 3.63 (s, 3H), 3.71 (dd, J = 9.7, 5.6 Hz, 1H), 3.76 (dd, J = 9.7, 6.8 Hz, 1H); **^{13}C-NMR** (126 MHz, Acetone-d6) δ = –5.4, –5.4, 13.7, 18.7, 26.1, 43.1, 51.6, 66.0, 175.4; HRMS (**ESI**) m/z: calc. for $[M+H]^+$: 233.1567; found: 233.1566. The spectroscopic are in agreement with those previously reported.[152]

(*R*)-3-((*tert*-Butyldimethylsilyl)oxy)-*N*-methoxy-*N*,2-dimethylpropanamide (S-5)

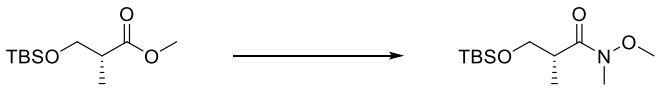

$C_{12}H_{27}NO_3Si$
M = 261.44 g/mol

The synthesis was carried out according to a known literature procedure:[152]

A mixture of Ester **S-4** (6.20 g, 26.7 mmol, 1.00 eq.) and *N*,*O*-dimethylhydroxylamine hydrochloride (4.03 g, 41.4 mmol, 1.55 eq.) was cooled to –78 °C followed by addition of ^{i}PrMgCl (2 M in THF, 40 mL, 80 mmol, 3.0 eq.) dropwise over 10 minutes. The resulting solution was allowed to warm to r.t. over the course of 8 hours. Then, the reaction was quenched by addition of a saturated solution of NH_4Cl (100 mL) followed by extraction with Et_2O (3 × 200 mL). The combined organic layers were washed with brine (50 mL), dried over $MgSO_4$, filtered and concentrated. Purification of the crude product by column chromatography (Silica, CH/EtOAc 4:1) yielded the product **S-5** (6.53 g, 25.0 mmol, 94%) as a colorless oil. $\mathbf{R_f}$ = 0.29 (CH/EtOAc 4:1); $\boldsymbol{\alpha_D^{20}}$ = –16.5 (c = 1.0, MeCN); **^{1}H-NMR** (500 MHz, Acetone-d6) δ = 0.04 (s, 3H), 0.05 (s, 3H), 0.87 (s, 9H), 1.00 (d, *J* = 6.9 Hz, 3H), 3.13 (s, 3H), 3.53 (dd, *J* = 9.4, 5.9 Hz, 1H), 3.73 (s, 3H), 3.80 (dd, *J* = 9.5, 8.2 Hz, 1H); **^{13}C-NMR** (126 MHz, Acetone-d6) δ = -5.3, -5.3, 14.0, 18.8, 26.2, 32.2, 38.8, 61.9, 66.4, 176.2; **HRMS (ESI)** m/z: calc. for $[M+H]^+$: 262.1833; found: 262.1830; The spectroscopic are in agreement with those previously reported.[152]

(2*R*)-3-(*tert*-Butyldimethylsilyl)oxy-2-methylpropanal (216)

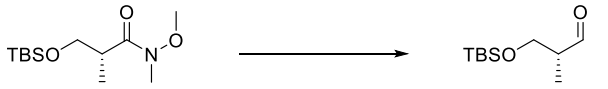

$C_{10}H_{22}O_2Si$
M = 202.37 g/mol

The synthesis was carried out according to a known literature procedure:[153]

Weinrebamide **S-5** (5.33 g, 20.4 mmol, 1.00 eq.) was dissolved in anhydrous THF (40 mL). The mixture was cooled to –78 °C DiBAL-H (1 M in hexanes, 40.8 mL, 40.8 mmol, 2.00 eq.) was added and the mixture was stirred for 2.5 h at this temperature. Afterwards, the mixture was pured into a saturated aqueous Rochelle salt solution (250 mL) followed by vigorous stirring for 1 h. Phases were separated and the aqueous phase was extracted with Et_2O (3 × 150 mL). The combined organic phases were dried over $MgSO_4$, filtered, and concentrated. The crude product was purified by column chromatography (Silica, CH/EtOAc 15:1) affording the product **216** as a colorless oil (4.09 g, 20.2 mmol, 99%). $\mathbf{R_f}$ = 0.35 (CH/EtOAc 15:1); $\boldsymbol{\alpha_D^{20}}$ = –41.6 (c = 1.0, MeCN); **^{1}H-NMR** (500 MHz, Acetone-d6) δ = 0.07 (s, 6H), 0.88 (s, 9H), 1.05 (d, *J* = 7.0 Hz, 3H), 3.86 (dd, *J* = 10.3, 6.0 Hz, 1H), 3.97 (dd, *J* = 10.3, 4.8 Hz, 1H), 9.70 (d, *J* = 1.5 Hz, 1H); **^{13}C-NMR** (126 MHz, Acetone-d6) δ = –5.4, –5.4, 10.4, 18.8, 26.1, 49.4, 64.0, 204.5; **HRMS (ESI)** m/z: calc. for $[M+H]^+$: 203.1462; found: 203.1462; The spectroscopic data are in agreement with those previously reported.[153]

(2*S*)-1-(*tert*-Butyldimethylsilyloxy)-4,4-dibromo-2-methylbut-3-ene (S-6)

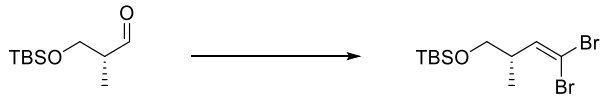

$C_{11}H_{22}Br_2OSi$
M = 358.19 g/mol

The synthesis was carried out according to a known literature procedure:[154]

To a cooled 0 °C solution of aldehyde **216** (3.01 g, 14.9 mmol, 1.00 eq.) and triphenyl phosphine (15.6 g, 59.5 mmol, 3.99 eq.) in anhydrous DCM (70 mL) was added carbon tetrabromide (9.87 g, 29.8 mmol, 2.00 eq.) portionwise over 5 min. After stirring the brown suspension for 1 hour at ambient temperature, the solvent was removed and the residue was suspended in cyclohexane (300 mL), filtered over a large plug of Silica and rinsed with CH/Et_2O (1:1, 3 × 150 mL). Further purification by column chromatography (Silica, CH/Et_2O 100:1) afforded the desired dibromide **S-6** as a colorless oil; $\mathbf{R_f}$ = 0.50 (CH/Et_2O 100:1);

α_D^{20} = +10.9 (c = 1.0, MeCN); **^{1}H-NMR** (500 MHz, Acetone-d6) δ = 0.07 (s, 5H), 0.91 (s, 9H), 1.02 (d, *J* = 6.8 Hz, 3H), 2.64 (ddtd, *J* = 12.8, 9.3, 6.8, 6.0 Hz, 1H), 3.58 (dd, *J* = 6.0, 2.7 Hz, 2H), 6.41 (d, *J* = 9.3 Hz, 1H); **^{13}C-NMR** (126 MHz, Acetone-d6) δ = –5.3, –5.2, 15.4, 18.8, 26.2, 42.1, 66.7, 88.5, 143.0; **HRMS (APCI)** m/z: calc. for $[M+H]^+$: 358.9859; found: 358.9858.

(2*S*)-1-(*tert*-Butyldimethylsilyl)oxy-2-methylbut-3-yne (217)

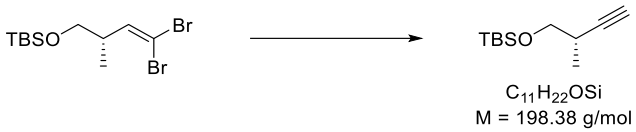

$C_{11}H_{22}OSi$
M = 198.38 g/mol

The synthesis was carried out according to a known literature procedure:[154]

Dibromoalkene **S-6** (2.85 g, 7.96 mmol, 1.00 eq.) was dissolved in anhydrous THF (10 mL) and cooled to −78 °C. Then, *n*-BuLi (2.5 M in THF, 8.0 mL, 20 mmol, 2.5 eq.) was added and the mixture was stirred for 1 h at –78 °C. The reaction was quenched with saturated aqueous solution of $NaHCO_3$ (30 mL). Phases were separated and the aqueous phase was extracted with Et_2O (2 × 20 mL). The combined organic layers were washed with brine (20 mL), dried over $MgSO_4$, filtered, and concentrated. The crude residue was purified by *Kugelrohr* distillation (50 mbar, 95 °C) to provide the product **217** as a colorless oil (1.27 g, 6.40 mmol, 80%). R_f = 0.41 (CH/Et_2O 50:1); α_D^{20} = –7.6 (c = 1.0, MeCN); **^{1}H-NMR** (500 MHz, Acetone-d6) δ = 0.08 (s, 6H), 0.91 (s, 9H), 1.15 (d, *J* = 6.9 Hz, 3H), 2.43 (d, *J* = 2.4 Hz, 1H), 2.51–2.60 (m, 1H), 3.50 (dd, *J* = 9.6, 7.4 Hz, 1H), 3.69 (dd, *J* = 9.6, 5.7 Hz, 1H); **^{13}C-NMR** (126 MHz, Acetone-d6) δ = –5.2, –5.2, 17.6, 18.9, 26.2, 67.8, 70.6, 87.0 [one carbon signal overlaps with the solvent signal]; **HRMS (APCI)** m/z: calc. for $[M+H]^+$: 199.1513; found: 199.1510. The spectroscopic data are in agreement with those previously reported.[154]

(2*S*, 3*E*)-1-(*tert*-Butyldimethylsilyl)oxy-4-iodo-2-methylbut-3-ene (S-7)

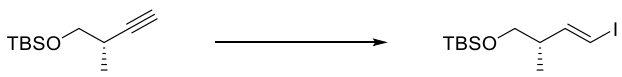

$C_{11}H_{23}IOSi$
M = 326.29 g/mol

The synthesis was carried out according to a known literature procedure:[154]

To a solution of alkyne **217** (1.04 g, 5.04 mmol, 1.00 eq.) in anhydrous DCM (15 mL) at room temperature was added *Schwartz* reagent (1.56 g, 6.08 mmol, 1.16 eq.) and the solution was stirred for 40 min. Then, iodine (1.64 g, 6.45 mmol, 1.23 eq.) was added and the reaction was stirred for 1.5 hours before being

quenched with saturated aqueous Na_2SO_3 (15 mL). Phases were separated and the aqueous layer was extracted twice with DCM (2 × 20 mL). The combined organic phases were washed with brine (15 mL), dried over $MgSO_4$, and concentrated under reduced pressure. Purification of the crude product by column chromatography (Silica, CH/Et_2O 9:1) yielded **S-7** as an orange oil (929 mg, 2.85 mmol, 54%); $\mathbf{R_f}$ = 0.17 (CH); $\boldsymbol{\alpha_D^{20}}$ = –32.4 (c = 1.0, MeCN); **^{1}H-NMR** (500 MHz, Acetone-d6) δ = 0.06 (s, 6H), 0.90 (s, 9H), 1.00 (d, *J* = 6.8 Hz, 3H), 2.40 (dddd, *J* = 13.0, 7.4, 6.2, 1.0 Hz, 1H), 3.52 (d, *J* = 6.2 Hz, 2H), 6.21 (dd, *J* = 14.5, 1.1 Hz, 1H), 6.54 (dd, *J* = 14.5, 7.7 Hz, 1H); **^{13}C-NMR** (126 MHz, Acetone-d6) δ = –5.2, –5.2, 15.8, 18.8, 26.2, 43.9, 67.5, 75.7, 150.3; **HRMS (APCI)** m/z: calc. for $[M+H]^+$: 327.0636; found: 327.0634. The spectroscopic data are in agreement with those previously reported.[154]

(2*S*,3*E*)-4-Iodo-2-methyl-3-buten-1-ol (211)

C_5H_9IO
M = 212.03 g/mol

To a solution of **S-7** (1.48 g, 4.54 mmol, 1.00 eq.) in MeOH (2 mL) was added HCl (3 M in MeOH, 7.5 mL, 23 mmol, 5.0 eq) and the resulting solution was stirred for 30 minutes. All volatiles were removed under reduced pressure and the dark green residue was purified by column chromatography (Silica, CH/EtOAc 3:1). The product **211** was obtained as a pale yellow oil (894 mg, 4.22 mmol, 93%). $\mathbf{R_f}$ = 0.26 (CH/EtOAc 3:1); $\boldsymbol{\alpha_D^{20}}$ = –20.6 (c = 1.0, MeCN); **^{1}H-NMR** (500 MHz, Acetone-d6) δ = 1.00 (d, *J* = 6.9 Hz, 3H), 2.37 (dtdd, *J* = 7.8, 6.8, 6.1, 1.1 Hz, 1H), 3.37–3.48 (m, 2H), 3.77 (d, *J* = 5.6 Hz, 1H), 6.19 (dd, *J* = 14.5, 1.1 Hz, 1H), 6.56 (dd, *J* = 14.5, 7.6 Hz, 1H); **^{13}C-NMR** (126 MHz, Acetone-d6) δ = 16.0, 44.0, 44.0, 66.5, 66.6, 75.4, 150.7; **HRMS (APCI)** m/z: calc. for $[M+H]^+$: 212.9771; found: 212.9767; The spectroscopic data are in agreement with those previously reported.[89]

(2*S*, 3*E*)-4-Iodo-2-methyl-3-butenoic acid (119)

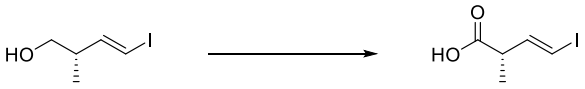

$C_5H_7IO_2$
M = 226.01 g/mol

Reproduced with permission from *Johannes Herbst*.[155]

A solution of $K_2Cr_2O_7$ (36.7 mg, 123 µmol, 6 mol–%), 65% aq. HNO_3 (80 µL, 1.1 mmol, 0.54 eq.) and $NaIO_4$ (1.12 g, 5.22 mmol, 2.55 eq.) in H_2O (12 mL) was prepared and MeCN (20 mL) and homoallylalcohol **211** (435 mg, 2.05 mmol, 1.00 eq.) were added at 0°C. At this temperature the reaction mixture was stirred for 7 h and left overnight without stirring at 4 °C for 18 h. Inorganic salts were filtered off and washed with Et_2O. The organic phase was separated and the aqueous phase was extracted with Et_2O (3 × 40 mL). The combined organic phases were dried over $MgSO_4$ and the solvent was evaporated *in vacuo*. The residue was diluted with aqueous NaOH (1 M, 10 mL) and subsequently extracted with Et_2O (3 × 30 mL). To the aqueous phase was added HCl (1 M, 11 mL) and the aqueous phase subsequently extracted with Et_2O (3 × 40 mL). The combined organic phases were dried over $MgSO_4$, filtered and the solvents were removed *in vacuo*. The crude product was purified via flash column chromatography (Silica, CH/EtOAc 7:3). The product **119** was obtained as an off-white solid (261 mg, 1.15 mmol, 56%); $\mathbf{R_f}$ = 0.54 (CH/EtOAc 7:3); $\boldsymbol{\alpha_D^{20}}$ = +22.0 (c = 1.0, MeOH); **^{1}H-NMR** (500 MHz, Acetone-d6) δ = 1.25 (d, *J* = 7.0 Hz, 3H), 3.24 (ddd, *J* = 8.1, 7.1, 1.1 Hz, 1H), 6.43 (dd, *J* = 14.6, 1.1 Hz, 1H), 6.68 (dd, *J* = 14.6, 8.0 Hz, 1H); **^{13}C-NMR** (126 MHz, Acetone-d6) δ = 16.8, 46.2, 77.6, 145.9, 174.0; **HRMS (APCI)** m/z: calc. for $[M+H]^+$: 226.9563; found: 226.9562. The spectroscopic data are in agreement with those previously reported.[89]

2-(trimethylsilyl)ethyl (*S*,*E*)-4-iodo-2-methylbut-3-enoate (218)

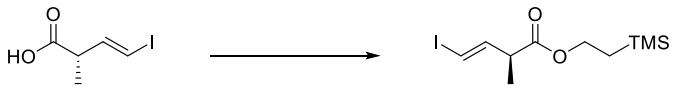

$C_{10}H_{19}IO_2Si$
M = 326.25 g/mol

A solution of carboxylic acid **119** (84.0 mg, 372 µmol, 1.00 eq.), 2-(trimethylsilyl)ethanol (70 µL, 0.48 mmol, 1.3 eq.) and pyridine (60 µL, 0.74 mmol, 2.0 eq.) in MeCN (1 mL) was cooled to 0 °C followed by addition of DCC (1 M in DCM, 0.40 mL, 0.40 mmol, 1.1 eq.). The ice bath was removed and the

resulting solution was stirred for 5 hours. The reaction mixture was diluted with EtOAc and loaded onto Celite®. Purification by column chromatogrpahy (Silica, CH/EE 30:1) yielded the desired ester **218** as a clear liquid (83.5 mg, 256 µmol, 69%). $\mathbf{R}_f$ = 0.25 (CH/EtOAc 30:1); $\boldsymbol{\alpha}_D^{20}$ = +1.5 (c = 0.2, MeCN); **^{1}H-NMR** (500 MHz, acetone-d6) δ = 0.06 (s, 9H), 0.97–1.03 (m, 2H), 1.24 (d, *J* = 7.0 Hz, 3H), 3.20–3.28 (m, 1H), 4.13–4.21 (m, 2H), 6.42 (dd, *J* = 14.6, 1.1 Hz, 1H), 6.64 (dd, *J* = 14.6, 8.0 Hz, 1H); **^{13}C-NMR** (126 MHz, acetone-d6) δ = -1.4, 16.8, 17.8, 46.6, 63.5, 77.9, 145.7, 173.1; [note: the product was not detected by mass spectrometry].

8.2.4 Synthesis of the central fragment III (132)

but-3-yn-1-yl 4-methylbenzenesulfonate (225)

The synthesis was carried out according to a modified literature procedure.[162]

To a solution of 3-butyn-1-ol (**224**) (5.00 g, 71.3 mmol, 1.00 eq.), DMAP (1.31 g, 10.7 mmol, 0.15 eq.) and triethylamine (20 mL, 0.14 mol, 2.0 eq.) in DCM (30 mL) at 0 °C was added dropwise a solution of tosyl chloride (18.4 g, 96.3 mmol, 1.35 eq.). The solution was allowed to warm to r.t. and stirred for 2 h. Water (30 mL) was added and the reaction was stirred for 20 min. Afterwards, the organic layer was separated and the aqueous layer was extracted (DCM, 5 x 40 mL). The combined extracts were dried over $MgSO_4$, filtered and concentrated. Purification by column chromatography (Silica, CH/EtOAc 9:1) yielded the compound **225** as a yellow oil (11.6 g, 51.8 mmol, 73%). $\mathbf{R}_f$ = 0.35 (CH/EtOAc 9:1); **^{1}H-NMR** (500 MHz, $CDCl_3$) δ = 1.97 (t, *J* = 2.7 Hz, 1H), 2.46 (s, 3H), 2.56 (td, *J* = 7.1, 2.7 Hz, 2H), 4.11 (t, *J* = 7.0 Hz, 2H), 7.35 (d, *J* = 8.0 Hz, 2H), 7.78-7.84 (m, 2H); **^{13}C-NMR** (126 MHz, $CDCl_3$) δ = 19.6, 21.8, 67.6, 70.9, 78.5, 128.1, 130.0, 133.0, 145.1. The spectroscopic data are in agreement with those previously reported.[162]

but-3-yn-1-amine hydrochloride (226)

The synthesis was carried out according to a modified literature procedure.[163]

To a solution of but-3-yn-1-yl-tosylate (**225**) (10.0 g, 44.6 mmol, 1.00 eq.) in DMF (50 mL) was added sodium azide (7.25 g, 111 mmol, 2.5 eq.) in batches over 5 minutes. The reaction was heated to 70 °C and stirred for 4 hours. A blast shield was placed in front of the reaction during this time. Afterwards, the reaction mixture was poured into water (50 mL) and the resulting solution was extracted with Et_2O (3 x 100 mL). The combined organic extracts were washed with water (2 x 100 mL), dried over $MgSO_4$, filtered and concentrated. The solvent removal was not pursued to completion due to the volatility of the product. This mixture of Et_2O, DMF, and but-3-yn-1-azide was taken directly to the reduction step. A solution of but-3-yn-1-azide from above in Et_2O (100 mL, degassed by the passage of Ar gas) was cooled to 0 °C. Triphenylphosphane (12 g, 46 mmol, 1.0 eq.) was added and the reaction was stirred at 0 °C for two hours. Afterwards, water (8 mL) was added to the mixture and the reaction mixture was stirred for further 20 hours at room temperature. The reaction mixture was poured into 10% $HCl_{(aq)}$ (25 mL) and layers were separated. The aqueous layer was washed with DCM (3 x 50 mL) and then concentrated to dryness under high vacuum, to give but-3-yn-1-amine hydrochloride (**226**) (2.84 g, 26.9 mmol, 60%) as an off-white solid. **^{1}H-NMR** (500 MHz, D_2O) δ = 2.53 (tt, *J* = 2.7, 0.8 Hz, 1H), 2.66 (tdd, *J* = 6.5, 2.7, 1.0 Hz, 2H), 3.20 (td, *J* = 6.6, 1.0 Hz, 2H); **^{13}C-NMR** (126 MHz, D_2O) δ = 16.8, 38.1, 72.5, 79.4; **HRMS (EI)**: m/z calc. for $[M]^+$: 69.0578; found: 69.0579. The spectroscopic data are in agreement with those previously reported.[163]

***tert*-butyl but-3-yn-1-ylcarbamate (227)**

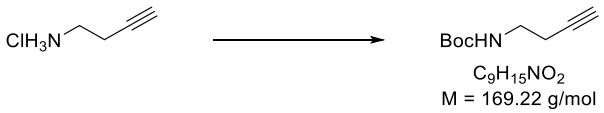

The synthesis was carried out according to a modified literature procedure.[163]

Triethylamine (6.6 mL, 47 mmol, 2.0 eq.) was added to a mixture of **226** (2.50 g, 23.7 mmol, 1.00 eq.) and Boc_2O (5.17 g, 23.7 mmol, 1.00 eq.) in dry THF (150 mL). The mixture was stirred at r.t. for 4 h after which time the solvent was removed. The crude product was partitioned between a biphasic mixture of water (100 mL) and DCM (100 mL). The aqueous layer was extracted with DCM (3 × 50 mL). The combined organic layers were dried over $MgSO_4$, filtered and concentrated to give the crude product as a yellow oil. Purification by column chromatography (Silica, CH/EtOAc 9:1) yielded the desired compound **227** as a colorless oil (3.61 g, 21.3 mmol, 90%). $\mathbf{R_f}$ = 0.20 (CH/EtOAc 9:1), **^{1}H-NMR** (500 MHz, acetone-d6) δ = 1.40 (s, 9H), 2.31–2.38 (m, 3H), 3.20 (td, *J* = 7.1, 5.2 Hz, 2H), 6.08 (s, 1H); **^{13}C-NMR** (126 MHz, $CDCl_3$) δ = 20.1, 28.5, 39.4, 70.0, 79.6, 81.8, 155.9; **HRMS (ESI)**: m/z calc. for $[M+H]^+$: 170.1176; found: 170.1174. The spectroscopic data are in agreement with those previously reported.[163]

***tert*-Butyl (*E*)-(4-(4,4,5,5-tetramethyl-1,3,2-dioxaborolan-2-yl)but-3-en-1-yl)carbamate (223)**

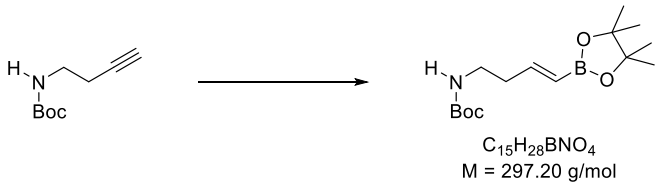

The synthesis was carried out according to a known literature procedure.[160]

To a solution of Carbamate **227** (5.30 g, 31.3 mmol, 1.00 eq.) in anhydrous DCM (60 mL) was added pinacolborane (9.0 mL, 62 mmol, 2.0 eq.) followed by Schwartz reagent (1.00 g, 3.88 mmol, 0.12 eq.) and triethylamine (0.52 mL, 3.8 mmol, 0.12 eq.). The mixture was stirred at 60 °C for 12 h. Then, the reaction mixture was cooled to room temperature and concentrated *in vacuo*. Purification by column chromatography (Silica, CH/EtOAc: 3:1) afforded the desired product **223** as a colorless oil, which solidified upon cooling (7.95 g, 26.8 mmol, 85%). $\mathbf{R_f}$ = 0.25 (CH/EtOAc 3:1); **^{1}H-NMR** (500 MHz, Acetone-d6): δ = 1.22 (s, 12H), 1.39 (s, 9H), 2.33 (qd, *J* = 6.9, 1.6 Hz, 2H), 3.16 (td, *J* = 7.0, 5.8 Hz, 2H), 5.42 (dt, *J* = 17.9, 1.6 Hz, 1H), 5.93 (s, 1H), 6.55 (dt, *J* = 17.9, 6.6 Hz, 1H); **^{13}C-NMR** (126 MHz, Acetone-d6):

δ = 25.1, 28.6, 37.0, 40.1, 78.4, 83.6, 151.8, 156.6 [note: the carbon attached to boron was not observed due to quadrupole broadening caused by the ^{11}B nucleus]; **HRMS (ESI)**: m/z calc. for $[M+Na]^+$: 320.2006; found: 320.2009. The spectroscopic data are in agreement with those previously reported.[160]

***tert*-butyl (*E*)-(4-(1,3,6,2-dioxazaborocane-4,8-dione-2-yl)but-3-en-1-yl)carbamate (133)**

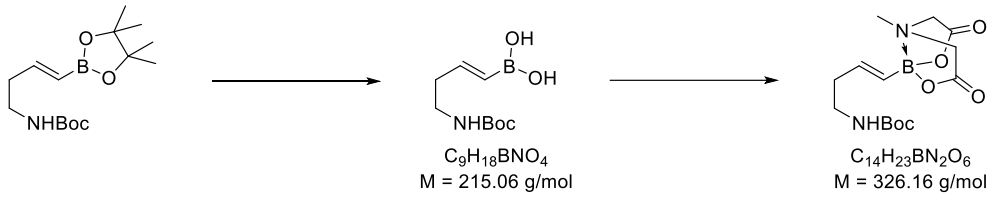

$C_9H_{18}BNO_4$
M = 215.06 g/mol

$C_{14}H_{23}BN_2O_6$
M = 326.16 g/mol

Boronic ester **223** (2.37 g, 7.97 mmol, 1.00 eq.) was dissolved in acetone/H_2O (1:1, 20 mL). Sodium periodate (4.26 g, 19.9 mmol, 2.50 eq.) and ammonium acetate (1.54 g, 19.9 mmol, 2.50 eq) were added. The resulting mixture was purged with argon and allowed to stir for 19 hours at room temperature. The suspension was filtered over Celite® and rinsed with EtOAc (50 mL). The organic solvents were removed under reduced pressure and the remaining aqueous solution was diluted with water (10 mL) and Et_2O (50 mL). The organic layer was separated and the aqueous layer was extracted with Et_2O (2 × 50 mL). The combined organic layers were washed with brine (20 mL), dried over sodium sulfate, filtered into a 500 mL Schlenk flask, concentrated (colorless oil) and used immediately.

MIDA (2.34 g, 15.9 mmol, 1.99 eq.) was added, followed by anhydrous toluene (100 mL) and anhydrous DMSO (10 mL). The flask was fitted with a *Dean-Stark* trap, purged with argon and heated to reflux (115 °C). After 18 hours, the mixture was cooled to room temperature and the solvent was removed under reduced pressure (60 °C bath temperature). The crude product was loaded onto Celite® and added to a large plug of Silica. The plug was sequentially rinsed with Et_2O (300 mL), EtOAc (200 mL) and eluted with MeCN (200 mL). The MeCN eluate was concentrated under reduced pressure. The residue was dissolved in EtOAc (200 mL) and H_2O (200 mL) was added. Phases were separated and the organic layer was washed with H_2O (3 × 100 mL) and brine (50 mL), dried over $MgSO_4$, filtered and concentrated to obtain the desired product as an off-white solid. Further purification was obtained by vapor diffusion crystallization (solvent: MeCN, anti-solvent: Et_2O) which yielded the desired compound **133** as a colorless crystalline solid (1.91 g, 5.86 mmol, 74%). Boronic acid (**S-8**): **^{1}H-NMR** (500 MHz, DMSO-d6) δ = 1.34 (s, 9H), 2.16 (q, *J* = 7.0 Hz, 2H), 2.89–3.03 (m, 2H), 5.33 (dd, *J* = 17.9, 1.5 Hz, 1H), 6.34 (dt, *J* = 17.9, 6.5 Hz, 1H), 6.70 (t, *J* = 5.8 Hz, 1H), 7.62 (s, 2H); **^{13}C-NMR** (126 MHz, DMSO-d6) δ = 28.7, 36.0, 78.2, 147.6, 156.2. [note: the carbon attached to boron was not observed due to quadrupole broadening caused by the ^{11}B-nucleus]; **HRMS (ESI)**: m/z calc. for $[M+H]^+$: 216.1403; found: 216.1397. MIDA-boronate **133**: **^{1}H-NMR**

(500 MHz, acetone-d6): δ = 1.39 (s, 9H), 2.25–2.34 (m, 2H), 3.00 (s, 3H), 3.15 (q, *J* = 6.6 Hz, 2H), 3.99 (d, *J* = 16.8 Hz, 2H), 4.17 (d, *J* = 16.8 Hz, 2H), 5.54 (dt, *J* = 17.6, 1.5 Hz, 1H), 5.97 (s, 1H), 6.06 (dt, *J* = 17.6, 6.6 Hz, 1H); **^{13}C-NMR** (126 MHz, Acetone-d6): δ = 8.7, 36.8, 40.7, 47.3, 62.1, 78.4, 143.1, 156.6, 169.1 [note: the carbon attached to boron was not observed due to quadrupole broadening caused by the ^{11}B nucleus]; **HRMS (ESI)**: m/z calc. for $[M+NH_4]^+$: 344.1987; found: 344.2002.

***tert*-butyl (*E*)-(4-(1,3,6,2-dioxazaborocane-4,8-dione-2-yl)but-3-en-1-yl)ammonium trifluoroacetate (228)**

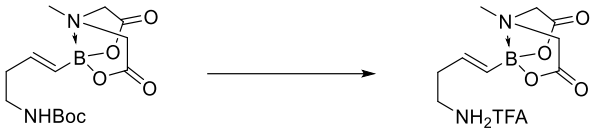

$C_{11}H_{15}BF_3N_2O_5$
M = 323.06 g/mol

To a suspension of **133** (2.69 g, 8.25 mmol, 1.00 eq.) in anhydrous DCM (60 mL) at 0 °C was added a mixture of TFA/TFAA (20:1, 6.3 mL, 82 mmol, 10 eq.) resulting in a rapid dissolution of the starting material. The solution was stirred at r.t. for 30 minutes, followed by evaporation of all volatiles (50°C bath temperature). MeCN (20 mL) was added to the residue with stirring until the crude resin was fully dissolved. Then, a mixture of Et_2O/*n*-heptane (1:1, 100 mL) was slowly added with vigorous stirring. The mixture was carefully decanted and washed twice with Et_2O/*n*-heptane (1:1, 100 mL). After the final decantation, the remaining residual solvents were removed under reduced pressure and the obtained solid was dried in high vacuum. The product **228** was obtained as a white solid (2.57 g, 7.58 mmol, 92%). **^{1}H-NMR** (500 MHz, Acetone-d6): δ = 2.48–2.57 (m, 2H), 2.62 (qd, *J* = 6.9, 1.5 Hz, 2H), 3.00 (s, 3H), 3.87 (t, *J* = 6.9 Hz, 2H), 4.06 (d, *J* = 16.8 Hz, 2H), 4.17 (d, *J* = 16.8 Hz, 2H), 5.65 (dt, *J* = 17.7, 1.4 Hz, 1H), 6.05 (dt, *J* = 17.7, 6.6 Hz, 1H); **^{13}C-NMR** (126 MHz, Acetone-d6): δ = 34.1, 47.1, 47.2, 62.2, 140.4, 169.1; [note: the carbon attached to boron was not observed due to quadrupole broadening caused by the ^{11}B nucleus]: **HRMS (ESI):** m/z calc. for $[M+H]^+$: 227.1199; found: 227.1202.

(*Z*)-3-Iodo-2-methylprop-2-en-ol 229

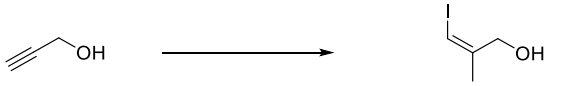

C_4H_7IO
M = 198,00 g/mol

The synthesis was carried out according to a modified literature procedure.[161]

To a suspension of propargyl alcohol (**35**) (5.0 mL, 87 mmol, 1.0 eq.) and CuI (16.5 g, 86.7 mmol, 1.00 eq.) in anhydrous Et_2O (600 mL) was added MeMgBr (21.7 g, 182 mmol, 2.09 eq.) at –5 °C. The mixture was gradually allowed to warm to r.t. and stirred for 2 h. After the indicated time, iodine (22 g, 87 mmol, 1.0 eq.) was added at –5 °C. The mixture was gradually allowed to warm to room temperature and stirring was continued for additional 12 h. The reaction was quenched with saturated NH_4Cl (200 mL) at 0 °C. The reaction mixture was filtered through a Celite pad and the filtrate was extracted with Et_2O (3 × 100 mL). The extract was washed with sat. NH_4Cl until blue coloration of the aqueous phase ceased and subsequently washed with brine (100 mL). The combined organic layers were dried over $MgSO_4$ and activated charcoal was added. The resulting suspension was filtered over a short plug of silica, rinsed with Et_2O and the solvent was removed. The crude product was purified by column chromatography (Silica, CH/EtOAc 20:1 → 5:1) to give the compound **229** (10.9 g, 55.2 mmol, 67%) as a yellow oil. $\mathbf{R_f}$ = 0.26 (CH/EtOAc 5:1); **^{1}H-NMR** (500 MHz, CD_2Cl_2) δ = 1.63 (t, *J* = 6.2 Hz, 1H, -OH), 1.96 (s, 3H), 4.22 (dd, *J* = 6.2, 0.8 Hz, 2H), 5.98 (s, 1H); **^{13}C-NMR** (126 MHz, CD_2Cl_2) δ = 21.8, 68.6, 74.8, 147.1; **HRMS** (EI): m/z calc for $[M]^+$: 197.9542; found: 197.9538. The spectroscopic data are in agreement with those previously reported.[161]

(*Z*)-2-Methyl-5-(trimethylsilyl)pent-2-en-4-yn-1-ol (230)

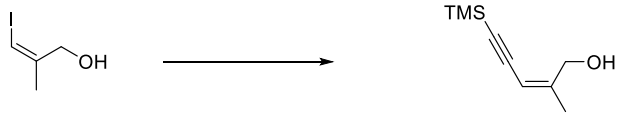

$C_9H_{16}OSi$
M = 168.31 g/mol

The synthesis was carried out according to a known literature procedure.[161]

To a solution of (*Z*)-3-iodo-2-methylprop-2-en-ol (**229**) (8.0 g, 40 mmol, 1.0 eq.) in anhydrous degassed THF (300 mL) was added (trimethylsilyl)acetylene (11.5 mL, 80.8 mmol, 2.02 eq.), ^{i}Pr$_2$NH (50 mL, 0.36 mol, 9.0 eq.), $PdCl_2(PPh_3)_2$ (567 mg, 808 µmol, 0.02 eq.), and CuI (769 mg, 4.04 mmol, 0.10 eq.) at room temperature. After being stirred at room temperature for 1.5 h under sonication, the solvent was removed and the residue was dissolved in Et_2O (200 mL), washed with saturated $NaHCO_3$ (100 mL) and saturated aqueous NH_4Cl (2 × 100 mL). The organic layer was dried over $MgSO_4$. Activated charcoal was added, the resulting suspension was filtered over a pad of silica and the solvent was removed. The obtained crude product was purified by column chromatography (Silica CH/EtOAc 10:1 → 5:1) to afford the desired compound **230** (2.95 g, 17.5 mmol, 87%) as an orange oil. $\mathbf{R_f}$ = 0.17 (CH/EtOAc 5:1); **^{1}H-NMR** (500 MHz, $CDCl_3$) δ = 0.19 (s, 9H), 1.88 (d, *J* = 1.6 Hz, 3H), 4.36 (s, 2H), 5.42 (s, 1H); **^{13}C-NMR** (126 MHz,

$CDCl_3$) δ = 0.11, 20.4, 64.3, 98.7, 101.7, 106.8, 151.9; **HRMS (APCI)**: m/z calc for $[M+H]^+$: 169.1043; found: 169.1042. The spectroscopic data are in agreement with those previously reported.[161]

(2*Z*)-2-Methyl-5-(trimethylsilyl)pent-2-en-4-ynal (231)

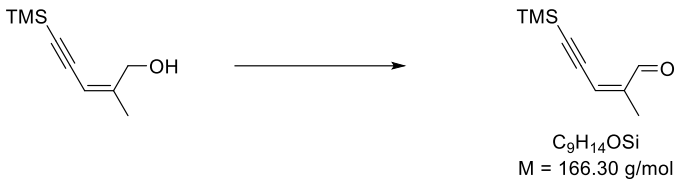

The synthesis was carried out according to a known literature procedure.[161]

Activated MnO_2 (24.6 g, 282 mmol, 15.7 eq.) was suspended in a solution of alcohol **230** (3.02 g, 17.9 mmol, 1.00 eq.) in anhydrous DCM (120 mL) at room temperature. The reaction mixture was stirred for 20 h at room temperature, filtered through a Celite® pad and concentrated *in vacuo*. The product **231** was obtained as a slightly volatile orange oil (2.32 g, 13.9 mmol, 78%) and used in the subsequent reaction without further purification. $\mathbf{R_f}$ = 0.59 (CH/EtOAc 5:1); **^{1}H-NMR** (500 MHz, acetone-d6): δ = 0.22 (s, 9H), 1.81 (d, *J* = 1.7 Hz, 3H), 6.75 (q, *J* = 1.6 Hz, 1H), 10.22 (s, 1H, H-7); **^{13}C-NMR** (126 MHz, Acetone-d6) δ = –0.4, 14.9, 99.9, 106.1, 125.7, 148.3, 191.9; **HRMS (APCI)**: m/z calc. for $[M+H]^+$: 167.0877; found: 167.0877. The spectroscopic data are in agreement with those previously reported.[161]

methyl (4*Z*,3*S*)-3-hydroxy-4-methyl-hept-4-en-6-ynoate (S-9)

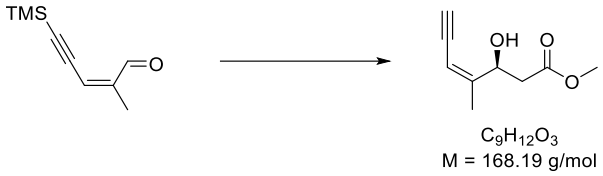

To a stirred solution of $LiClO_4$ (5.12 g, 48.1 mmol, 4.00 eq.) and TMSQD (954 mg, 2.41 mmol, 0.20 eq.) in DCM/Et_2O (1:1, 40 mL) at –78 °C were added aldehyde **231** (2.00 g, 12.0 mmol, 1.00 eq.) and *N*,*N*-di*iso*propylethylamine (5.2 mL, 30 mmol, 2.5 eq.). Then, acetyl chloride (1.7 mL, 24 mmol, 2.0 eq.) in DCM (8 mL) was added to the mixture at –78 °C with a syringe pump over 2 h. After being stirred at −78 °C for 8 h, MeOH (20 mL) was added, followed by NaOMe (5.4 M, 3.0 mL, 16 mmol, 1.3 eq.). The resulting solution was allowed to warm to r.t. overnight. Afterwards, the reaction mixture was cooled to 0 °C and the pH was adjusted to pH 7 by dropwise addition of conc. HCl, followed by evaporation of the organic solvents. EtOAc (100 mL) and water (100 mL) were added, phases were separated and the

aqueous phase was extracted with EtOAc (3 x 100 mL).The combined organic layers were washed with a solution of saturated NH_4Cl (50 mL) and brine (50 mL), dried over $MgSO_4$, filtered and concentrated. The organe-brown crude product was dissolved in dry MeOH (40 mL) and K_2CO_3 (830 mg, 6.0 mmol, 0.5 eq.) was added. The resulting suspension was stirred for 6 h followed by filtration over a plug of silica (rinsed with EtOAc). Purification by column chromatography (Silica, CH/EtOAc Gradient: 15:1→5:1) yielded the desired product **S-9** (1.26 g, 7.52 mmol, 63%) as an orange oil. $\mathbf{R_f}$ = 0.23 (CH/EtOAc 8:3), $\boldsymbol{\alpha_D^{20}}$ = −4.7 (c = 1.0, DCM), **^{1}H-NMR** (500 MHz, $CDCl_3$) δ = 5.36 (s, 1H), 5.25 (dd, *J* = 9.3, 3.3 Hz, 1H), 3.73 (s, 3H), 3.12 (d, *J* = 2.3 Hz, 1H), 2.65 (dd, *J* = 16.2, 9.8 Hz, 1H), 2.53 (dd, *J* = 16.2, 3.4 Hz, 1H), 1.84 (d, *J* = 1.5 Hz, 3H); **^{13}C-NMR** (126 MHz, $CDCl_3$) δ = 172.9, 153.4, 105.7, 82.4, 79.7, 68.5, 52.1, 39.3, 17.5; **HRMS (APCI)**: m/z calc for $[M+H]^+$: 169.0859; found: 169.0859.

methyl (4*Z*,3*S*)-3-hydroxy-4-methyl-7-(trimethylsilyl)hept-4-en-6-ynoate (238)

$C_{12}H_{20}O_3Si$
M = 240.37 g/mol

TMS-quinidine (896 mg, 2.42 mmol, 0.20 eq.) and $LiClO_4$ (5.18 g, 48.7 mmol, 3.98 eq.) were dissolved in CH_2Cl_2/Et_2O (2:3, 50 mL) and cooled to –78 °C. Aldehyde **231** (2.04 g, 12.2 mmol, 1.00 eq.) was added, followed by DIPEA (5.2 mL, 30 mmol, 4.0 eq.). A solution of acetyl chloride (1.8 mL, 26 mmol, 2.1 eq.) in anhydrous DCM (16 mL) was added dropwise via syringe pump over 3 h. Afterwards MeOH (16 mL) and NaOMe (5.4 M in MeOH, 6 mL, 32.4 mmol, 2.7 eq.) were added and the resulting solution was allowed to warm to r.t. over 18 hours under stirring. The reaction was quenched with saturated aqueous NH_4Cl (40 mL) and the pH was adjusted to pH 4 by addition of saturated aqueous citric acid (10 mL). All volatiles were removed *in vacuo* and EtOAc (60 mL) was added. Phases were separated and the aqueous phase was extracted with ethyl acetate (3 × 40 mL). The combined organic layers were washed with brine (20 mL), dried over $MgSO_4$, filtered, and concentrated in vacuo. Purification of the crude product via column chromatography (Silica, CH/EtOAc 5:1) yielded the product **238** as an orange oil (2.60 g, 12.3 mmol, 88%, e.r = 89:11). $\mathbf{R_f}$ = 0.23 (CH/EtOAc 5:1); $\boldsymbol{\alpha_D^{20}}$ = +33.3 (c = 1.0, MeCN); **^{1}H-NMR** (500 MHz, $CDCl_3$) δ = 0.18 (s, 9H), 1.83 (d, *J* = 1.6 Hz, 3H), 2.56 (dd, *J* = 15.9, 3.6 Hz, 1H), 2.63 (dd, *J* = 16.0, 9.5 Hz, 1H), 2.93 (bs, H-O*H*), 3.73 (s, 3H), 5.22 (dd, *J* = 9.4, 3.6 Hz, 1H), 5.37 (qd, *J* = 1.6, 0.7 Hz, 1H); **^{13}C-NMR** (126 MHz, $CDCl_3$) δ = 0.02, 17.7, 39.4, 52.0, 68.9, 100.2, 101.3, 106.5, 153.3, 172.9; **HRMS (ESI)**: m/z calc for $[M+H]^+$: 241.1254; found: 241.1255.

methyl (*Z*)-4-methyl-3-oxo-7-(trimethylsilyl)hept-4-en-6-ynoate (S-10)

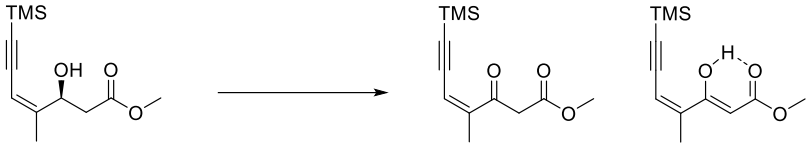

$C_{12}H_{18}O_3Si$
M = 238.36 g/mol

IBX (171 mg, 0.612 mmol, 2.11 eq.) was added to a solution of **238** (70 mg, 0.29 mmol, 1.00 eq.) in anhydrous EtOAc (8 mL), and the solution was stirred at 80 °C until TLC indicated complete conversion. The solvent was removed and the residue was suspended in CH/EtOAc (12:1), followed by filtration over a silica (4 cm) and Celite® (2 cm) pad. The filtrate was concentrated under reduced pressure to afford the crude ketoester as a yellow oil. The crude product was purified by column chromatography (Silica, CH/EtOAc 20:1) and afforded the compound **S-10** (32.6 mg, 137 µmol, 47%) as a yellow oil. $\mathbf{R_f}$ = 0.36 (CH/EtOAc 10:1). Keto-tautomer: **^{1}H-NMR** (700 MHz, acetone-d6) δ = 0.22 (s, 9H), 1.93 (d, *J* = 1.6 Hz, 3H), 3.68 (s, 3H), 4.08 (s, 2H), 6.36 (q, *J* = 1.6 Hz, 1H); **^{13}C-NMR** (176 MHz, acetone-d6) δ = –0.5, 19.6, 48.7, 52.2, 102.6, 106.8, 116.9, 148.3, 168.6, 194.9; Enol-tautomer: **^{1}H-NMR** (700 MHz, acetone-d6) δ = 0.19 (s, 9H), 1.99 (d, *J* = 1.6 Hz, 3H), 3.77 (s, 3H), 5.93 (q, *J* = 1.6 Hz, 1H), 6.00 (s, 1H), 12.25 (s, 1H); **^{13}C-NMR** (176 MHz, acetone-d6) δ = –0.3, 20.0, 51.9, 91.9, 103.3, 104.7, 112.9, 143.2, 174.4; **HRMS (ESI)**: m/z calc for $[M+H]^+$: 239.1098; found: 239.1100.

(*rac*)-methyl (4*Z*)-3-hydroxy-4-methyl-7-(trimethylsilyl)hept-4-en-6-ynoate (*rac*-238)

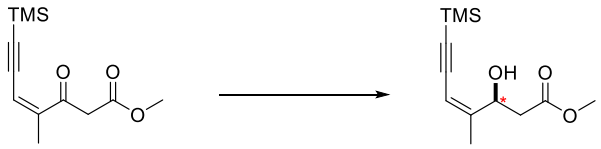

$C_{12}H_{20}O_3Si$
M = 240.37 g/mol

Ketoester **S-10** (32.0 mg, 134 µmol, 1.00 eq.) was dissolved in dry MeOH (2 mL) and $NaBH_4$ (11.2 mg, 295 µmol, 2.20 eq.) was added as a solid at room temperature. After 30 minutes, acetone (5 mL) was added and the solvents were evaporated. Purification by column chromatography (Silica, CH/EtOAc 5:1) yielded the racemic standard (*rac*-**238**) as a yellow oil (22.0 mg, 91.5 µmol, 68%). $\mathbf{R_f}$ = 0.16 (CH/EtOAc 8:1); **^{1}H-NMR** (500 MHz, $CDCl_3$) δ = 1.84 (d, *J* = 1.5 Hz, 3H), 2.53 (dd, *J* = 16.2, 3.4 Hz, 1H), 2.65 (dd, *J* = 16.2, 9.8 Hz, 1H), 3.12 (d, *J* = 2.3 Hz, 1H), 3.73 (s, 3H), 5.25 (dd, *J* = 9.3, 3.3 Hz, 1H), 5.36 (s, 1H); **^{13}C-NMR** (126 MHz, $CDCl_3$) δ = 17.5, 39.3, 52.1, 68.5, 79.7, 82.4, 105.7, 153.4, 172.9; **HRMS (ESI)**: m/z calc for

$[M+H]^+$: 241.1254; found: 241.1255. The spectroscopic data are in agreement with those reported for **238**.

Determination of enantiomeric ratio:

Enantiomeric ratio of **238** was determined by HPLC (column: DAICEL Chiralpak IB-U, 1.6 µm: 3.0 × 100 mm (IBU0CK-VB007), eluent: A: *n*-hexane, B: *iso*-propanol; isocratic: 95% A, 5% B, flowrate: 0.85 mL/min, detection wavelengths: λ = 190–600 nm); e.r = 89:11.

Determination of absolute configuration:

methyl (4*Z*,3*S*)-4-methyl-3-((2*S*)-3,3,3-trifluoro-2-methoxy-2-phenylpropanoyl)oxy-7-trimethylsilylhept-4-en-6-ynoate (*S*)-238-M

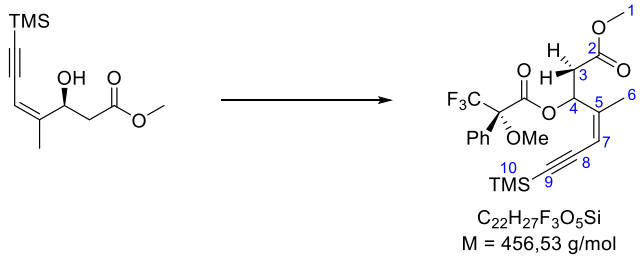

Reproduced with permission from *Johannes Herbst*.[155]

β-Hydroxy ester **238** (33.0 mg, 137 µmol, 1.00 eq.) and anhydrous pyridine (32 µL, 0.39 mmol, 2.9 eq.) was transferred to an argon flushed 2 mL screwcap-vial and were dissolved in anhydrous DCM (1.0 mL). *R*-(-)-MTPA-Cl (30.0 µL, 165 µmol, 1.20 eq.) was added and the mixture was stirred at room temperature for 18 h. The reaction mixture was partitioned between DCM (3 mL) and water (1 mL). The organic layer was separated and the aqueous phase was extracted with DCM (3 × 3 mL). The combined organic layers were washed with saturated aqueous NH_4Cl (2 mL), water (2 mL), saturated aqueous $NaHCO_3$ (2 mL) and brine (2 mL). The organic phase was dried over $MgSO_4$, filtered, and concentrated in vacuo. The crude product was purified via column chromatography (Silica, CH/EtOAc 4:1). The product ***S*-238-M** was obtained as colorless oil (43.3 mg, 94.9 µmol, 69%). $\mathbf{R_f}$ = 0.51 (CH/EtOAc 4:1); $[\alpha]_D^{20}$ = +39.0 (c = 1.0, MeCN); **^{1}H-NMR** (700 MHz, $CDCl_3$): δ = 0.20 (s, 9H, H-10) 1.76 (d, J = 1.6 Hz, 3H, H-6), 2.66 (dd, J = 15.5, 4.4 Hz, 1H, H-3''), 2.86 (dd, J = 15.5, 9.6 Hz, 1H, H-3'), 3.50 (s, 3H, OMe), 3.62 (s, 3H, H-1), 5.51–5.48 (m, 1H, H-7), 6.47 (dd, J = 9.6, 4.4 Hz, 1H, H-4), 7.43–7.37 (m, 3H, 3 × CH-Ph), 7.54–7.48 (m, 2H, 2 × CH-Ph); **^{13}C-NMR** (176 MHz, $CDCl_3$): δ = –0.1 (C-10), 18.0 (C-6), 37.5 (C-3), 52.1 (C-1), 55.5 (OMe), 73.4 (C-4), 84.9

(q, J = 27.6 Hz, C_q-Mosher), 100.3 (C-9), 101.8 (C-8), 109.8 (C-7), 123.4 (q, J = 287.0 Hz, CF3), 127.8 (CH-Ph), 128.5 (CH-Ph), 129.7 (CH-Ph), 132.0 (C_q-Ph), 147.3 (C-5), 165.4 (C=O-Mosher), 169.7 (C-2); **HRMS (ESI+)**: m/z calc for $[M+Na]^+$: 479.1472; found: 479.1471.

methyl (4*Z*,3*S*)-4-methyl-3-((2*R*)-3,3,3-trifluoro-2-methoxy-2-phenylpropanoyl)oxy-7-trimethylsilylhept-4-en-6-ynoate (*R*)-238-M

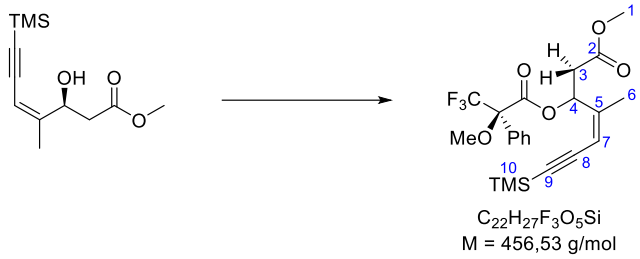

$C_{22}H_{27}F_3O_5Si$
M = 456,53 g/mol

Reproduced with permission from *Johannes Herbst*.[155]

β-Hydroxy ester **238** (33.0 mg, 137 µmol, 1.00 eq.) and anhydrous pyridine (32.0 µL, 398 µmol, 2.91 eq.) was transferred to an argon flushed 2 mL vial with screwcap and were dissolved in anhydrous DCM (1 mL). *S*-(+)-MTPA-Cl (45.0 µL, 247 µmol, 1.80 eq.) was added and the mixture was stirred at room temperature for 18 h. The reaction mixture was partitioned between DCM (3 mL) and water (1 mL). The organic layer was separated and the aqueous phase was extracted with DCM (3 × 3 mL). The combined organic layers were washed with saturated aqueous NH_4Cl (2 mL), water (2 mL), saturated aqueous $NaHCO_3$ (2 mL) and brine (2 mL). The organic phase was dried over $MgSO_4$, filtered, and concentrated *in vacuo*. The crude product was purified via flash column chromatography (Silica, CH/EtOAc 4:1). The product ***R*-238-M** was obtained as colorless oil (50.2 mg, 110 µmol, 80%); $\mathbf{R_f}$ = 0.51 (CH/EtOAc 4:1); $[\boldsymbol{\alpha}]_{\mathbf{D}}^{\mathbf{20}}$ = +95.0 (c = 1.0, MeCN); **^{1}H-NMR** (700 MHz, $CDCl_3$): δ = 0.21 (s, 9H, H-10), 1.58 (d, *J* = 1.7 Hz, 3H, H-6), 2.66 (dd, *J* = 15.8, 3.6 Hz, 1H, H-3''), 2.86 (dd, *J* = 15.8, 10.2 Hz, 1H, H-3'), 3.54 (s, 3H, OMe), 3.67 (s, 3H, H-1), 5.46–5.44 (m, 1H, H-7), 6.48 (dd, *J* = 10.2, 3.6 Hz, 1H, H-4), 7.42–7.36 (m, 3H, 3 × CH-Ph), 7.55–7.49 (m, 2H, 2 × CH-Ph); **^{13}C-NMR** (176 MHz, $CDCl_3$): δ = 0.0 (C-10), 17.4 (C-6), 37.5 (C-3), 52.1 (C-1), 55.7 (OMe), 73.4 (C-4), 84.6 (q, J = 27.8 Hz), 100.3 (C-9), 101.8 (C-8), 109.4 (C-7), 123.4 (q, *J* = 289.6 Hz, CF_3), 127.5 (CH-Ph), 128.5 (CH-Ph), 129.7 (CH-Ph), 132.3 (C_q-Ph), 147.5 (C-5), 165.4 (C=O-Mosher), 170.0 (C-2); **HRMS (APCI)**: m/z calc for $[M+Na]^+$: 479.1472; found: 479.1473.

Mosher's ester analysis of absolute configuration at C-4

The absolute configuration was determined and confirmed by the model for the analysis of the *Mosher* ester.[223] For this purpose the ^{1}H-NMR data of both esters *(S)*-**238-M** and *(R)*-**238-M** were collected and analyzed as shown in table 17. The difference between each signal led to the absolute configuration depicted (Figure 22).

Table 17. NMR-data for *Mosher*'s ester analysis of allyl alcohol **238**.

Position	δ (*S*)-Ester [ppm]	δ (*R*)-Ester [ppm]	$\Delta\delta^{SR}$ [ppm]	$\Delta\delta^{SR}$ [Hz]
H-6	1.76	1.58	0.18	126.07
H-7	5.50	5.45	0.05	35.02
H-3'	2.87	2.86	0.00	0.00
H-3''	2.66	2.66	0.00	0.00
CH_3-TMS	0.20	0.21	-0.01	-7.00
H-4	6.47	6.49	-0.01	-7.00
H-1	3.62	3.68	-0.05	-35.02

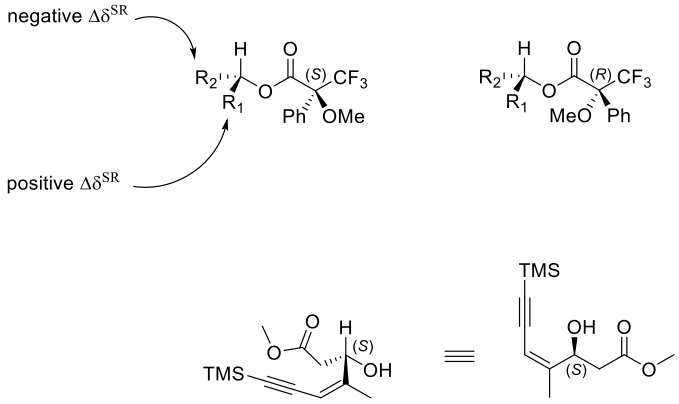

Figure 21. Proposed conformation according to the *Mosher*'s ester analysis.

methyl (4*Z*,3*S*)-3-((*tert*-butyldimethylsilyl)oxy)-4-methyl-hept-4-en-6-ynoate (S-11)

$C_{15}H_{26}O_3Si$
M = 282.46 g/mol

To a solution of alcohol **S-9** (1.26 g, 7.49 mmol, 1.00 eq.) in anhydrous DCM (30 mL) was added 2,6-lutidine (3.5 mL, 30 mmol, 4.00 eq.) and TBSOTf (3.2 mL, 15 mmol, 2.0 eq.) at 0 °C. After being stirred at room temperature for 0.5 h, the mixture was quenched with a saturated solution of NH_4Cl (10 mL) at 0 °C and extracted with DCM. The extract was washed with brine, dried over $MgSO_4$, filtered and concentrated. The crude product was purified by column chromatography (Silica, CH/EtOAc 100:1) to give the compound **S-11** (1.93 g, 6.83 mmol, 91%) as a colorless oil. $\mathbf{R_f}$ = 0.12 (CH/EtOAc 100:1) $\boldsymbol{\alpha_D^{20}}$ = +41.6 (c = 1.0, DCM); **^{1}H-NMR** (700 MHz, $CDCl_3$) δ = 5.34 (dd, *J* = 9.4, 4.3 Hz, 1H), 5.30−5.28 (m, 1H), 3.68 (s, 3H), 3.12 (dd, *J* = 2.4, 0.7 Hz, 1H), 2.61 (dd, *J* = 14.1, 9.4 Hz, 1H), 2.39 (dd, *J* = 14.1, 4.3 Hz, 1H), 1.79 (dd, *J* = 1.6, 0.7 Hz, 3H), 0.86 (s, 9H), 0.08 (s, 3H), 0.03 (s, 3H); **^{13}C-NMR** (126 MHz, $CDCl_3$) δ = 171.3, 154.2, 105.2, 81.9, 79.9, 69.6, 51.7, 41.4, 25.8, 18.1, 16.8, −4.9, −5.3; **HRMS (APCI):** m/z calc for $[M+H]^+$: 283.1724; found: 283.1722.

methyl (4*Z*,3*S*)-3-((*tert*-butyldimethylsilyl)oxy)-4-methyl-7-(trimethylsilyl)-hept-4-en-6-ynoate (241)

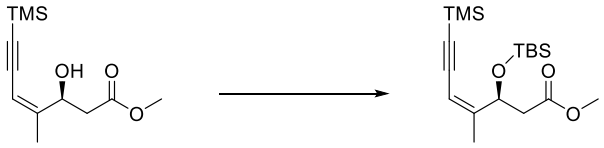

$C_{18}H_{34}O_3Si_2$
M = 354.64 g/mol

2,6-Lutidine (4.0 mL, 34 mmol, 4.1 eq.) and TBSOTf (4.0 mL, 18 mmol, 2.2 eq.) were added to a solution of β-hydroxy ester **238** (2.02 g, 8.39 mmol, 1.00 eq.) in anhydrous DCM (40 mL) at 0 °C. The reaction mixture was stirred for 1.5 h at 0 °C and afterwards diluted with saturated aqueous NH_4Cl (20 mL). Phases were separated and the aqueous layer was extracted with DCM (2 × 20 mL). The combined organic layers were washed with brine (20 mL), dried over $MgSO_4$, filtered, and concentrated. The crude product was purified by column chromatography (Silica, *n*-pentane/EtOAc 50:1) to afford the product **241** as a colorless oil (2.79 g, 7.87 mmol, 94%). $\mathbf{R_f}$ = 0.21 (CH/EtOAc 100:1); $\boldsymbol{\alpha_D^{20}}$ = +73.1 (c = 1.0, MeCN); **^{1}H-NMR** (500 MHz, $CDCl_3$) δ = 0.03 (s, 3H), 0.07 (s, 3H), 0.20 (d, *J* = 0.5 Hz, 9H), 0.86 (d, *J* = 0.5 Hz, 9H), 1.77 (d, *J* = 1.6 Hz, 3H), 2.37 (dd, *J* = 13.9, 4.0 Hz, 1H), 2.60 (dd, *J* = 14.0, 9.6 Hz, 1H), 3.68 (d, *J* = 0.6 Hz,

3H), 5.32–5.27 (m, 1H), 5.38 (dd, *J* = 9.6, 4.0 Hz, 1H); **^{13}C-NMR** (126 MHz, $CDCl_3$) δ = –5.2, –4.8, 0.1, 16.7, 18.1, 25.8, 41.4, 51.7, 69.8, 99.1, 101.5, 106.3, 153.9, 171.3; **HRMS (ESI):** m/z calc for $[M+H]^+$: 355.2119; found: 355.2118.

(S,Z)-3-((tert-butyldimethylsilyl)oxy)-4-methylhept-4-en-6-ynoic acid (129)

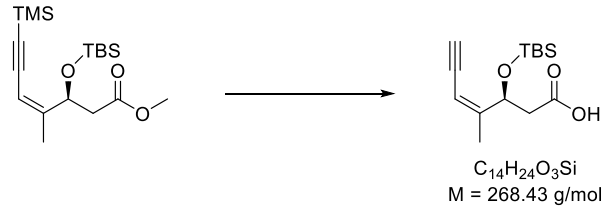

$C_{14}H_{24}O_3Si$
M = 268.43 g/mol

To a solution of ester **241** (1.10 g, 3.10 mmol, 1.00 eq.) in THF/H_2O (1:1, 15 mL) was added LiOH (2.99 g, 71.3 mmol, 23.0 eq.) and the resulting mixture was stirred at 65 °C for 12 hours. Afterwards, the mixture was concentrated and the residue was diluted with water, washed with cyclohexane (2 × 10 mL) and acidified to pH4, followed by extraction with Et_2O (3 × 30 mL). The organic layer was washed with brine (10 mL), dried over $MgSO_4$, filtered and concentrated. After evaporation of the solvent, the product **129** was obtained as a yellow solid (675 mg, 2.51 mmol, 81%). $\mathbf{R_f}$ = 0.12 (CH/EtOAc 5:1); $\boldsymbol{\alpha_D^{20}}$ = +87.9 (c = 1.0, MeCN); **^{1}H-NMR** (700 MHz, $CDCl_3$) δ = 0.05 (s, 3H), 0.10 (s, 3H), 0.87 (s, 9H), 1.80 (dd, *J* = 1.5, 0.7 Hz, 3H), 2.44 (ddd, *J* = 14.6, 3.9, 1.0 Hz, 1H), 2.64 (dd, *J* = 14.6, 9.3 Hz, 1H), 3.14 (dd, *J* = 2.4, 0.7 Hz, 1H), 5.31 (dq, *J* = 3.5, 1.7 Hz, 1H), 5.35 (dd, *J* = 9.3, 3.9 Hz, 1H); **^{13}C-NMR** (176 MHz, $CDCl_3$) δ = –5.2, –4.9, 16.9, 18.1, 25.8, 41.0, 69.4, 79.7, 82.3, 105.5, 153.8, 175.8; **HRMS (APCI):** m/z calc for $[M+H]^+$: 269.1567; found: 269.1563.

(*S*,4*Z*)-3-((*tert*-butyldimethylsilyl)oxy)-4-methyl-*N*-((*E*)-4-(1,3,6,2-dioxazaborocane-4,8-dione-2-yl)but-3-en-1-yl)hepta-4-en-6-ynamide (239)

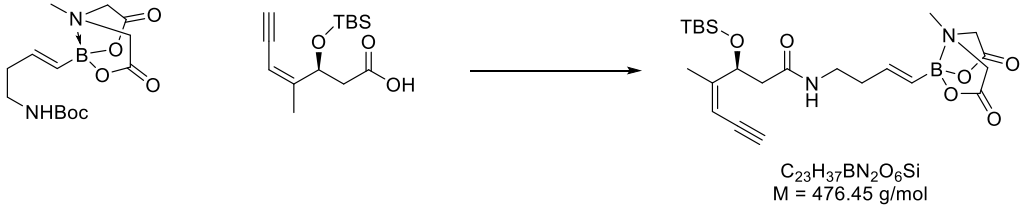

$C_{23}H_{37}BN_2O_6Si$
M = 476.45 g/mol

MIDA-boronate **133** (400 mg, 1.20 mmol, 1.09 eq.) was suspended in DCM (20 mL). The mixture was cooled to 0 °C and a freshly prepared mixture of TFA/TFAA (20:1, 0.5 mL) was added, resulting in a rapid dissolution of the boronate. The ice bath was removed and the resulting solution was vigorously stirred.

After 30 minutes, the solvent and excess TFA were removed *in vacuo*. The residue was dissolved in DMF (20 mL) and cooled to 0 °C. DIPEA (1.9 mL, 11 mmol, 10 eq.) was added, followed by carboxylic acid **129** (300 mg, 1.10 mmol, 1.00 eq.). Finally, PyBOP (785 mg, 1.50 mmol, 1.36 eq.) was added to the flask and the resulting mixture was allowed to stir overnight. The solvent was evaporated (50 °C bath temperature) and the residue was dissolved in MeCN (5 mL) and loaded onto Celite. After evaporation of the solvent, the solid was loaded onto a Silica column (packed with Et_2O), rinsed with Et_2O (250 mL) and eluted with neat EtOAc. The desired compound was obstained as a white crystalline solid (273 mg, 571 µmol, 51%). $\mathbf{R_f}$ = 0.19 (Et_2O/MeCN 10:3); $\boldsymbol{\alpha_D^{20}}$ = +41.7 (c = 1.0, DCM); **^{1}H-NMR** (500 MHz, acetone-d6) δ = 0.05 (s, 3H), 0.08 (s, 3H), 0.86 (s, 9H), 1.79 (dd, *J* = 1.6, 0.7 Hz, 3H), 2.11 (dd, *J* = 13.5, 3.5 Hz, 1H), 2.24–2.37 (m, 2H), 2.47 (dd, *J* = 13.5, 9.7 Hz, 1H), 2.99 (s, 3H), 3.12–3.21 (m, 1H), 3.33–3.42 (m, 1H), 3.62 (dd, *J* = 2.4, 0.7 Hz, 1H), 4.00 (dd, *J* = 16.9, 1.0 Hz, 2H), 4.17 (d, *J* = 16.8 Hz, 2H), 5.33 (ddt, *J* = 2.6, 1.6, 0.8 Hz, 1H), 5.40 (dd, *J* = 9.6, 3.5 Hz, 1H), 5.54 (dt, *J* = 17.7, 1.5 Hz, 1H), 6.07 (dt, *J* = 17.7, 6.6 Hz, 1H), 7.16 (s, 1H); **^{13}C-NMR** (126 MHz, acetone-d6) δ = −4.8, −4.8, 17.1, 18.6, 26.1, 36.5, 39.6, 43.7, 47.3, 62.1, 70.7, 80.7, 83.4, 105.3, 143.2, 155.5, 169.2, 169.2, 170.0; **HRMS (ESI)**: m/z calc. for $[M+H]^+$: 477.2591; found: 477.2581.

(*S*,4*Z*)-3-((*tert*-butyldimethylsilyl)oxy)-7-iodo-4-methyl-*N*-((*E*)-4-(1,3,6,2-dioxazaborocane-4,8-dione-2-yl)but-3-en-1-yl)hepta-4-en-6-ynamide (240)

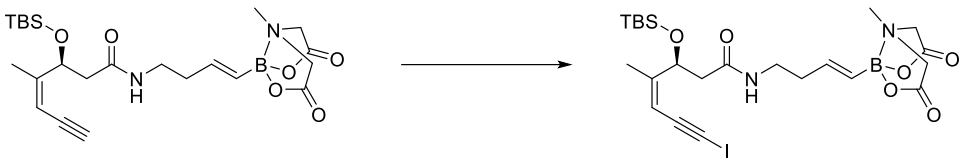

$C_{23}H_{36}BIN_2O_6Si$
M = 602.35 g/mol

Starting alkyne **239** (120 mg, 252 µmol, 1.00 eq.) was dissolved in acetone and cooled to −78 °C, followed by addition of NIS (62.0 mg, 277 µmol, 1.10 eq.) as a solid. The mixture was stirred for 5 minutes, followed by addition of AgOBz (11.5 mg, 50.4 µmol, 0.20 eq.). The resulting solution was stirred in the dark at −78 °C for 5 minutes and at r.t for further 10 minutes. Then, Celite was added and the solvent was evaporated. Purification by column chromatography (Silica, EtOAc) yielded the desired haloalkyne **240** as a white crystalline solid (136 mg, 226 µmol, 89%). $\mathbf{R_f}$ = 0.27 (Et_2O/MeCN 10:3); $\boldsymbol{\alpha_D^{20}}$ = +24.9 (c = 1.0, MeCN); **^{1}H-NMR** (500 MHz, acetone-d6) δ = 0.06 (s, 3H), 0.09 (s, 3H), 0.86 (s, 9H), 1.79 (d, *J* = 1.6 Hz, 3H), 2.12 (ddd, *J* = 13.5, 3.8, 1.1 Hz, 1H), 2.24–2.37 (m, 2H), 2.48 (dd, *J* = 13.6, 9.4 Hz, 1H), 2.99 (s, 3H), 3.12–3.22 (m, 1H), 3.32–3.41 (m, 1H), 4.00 (dd, *J* = 16.9, 2.2 Hz, 2H), 4.17 (d, *J* = 16.8 Hz, 2H), 5.36

(dd, *J* = 9.4, 3.8 Hz, 1H), 5.46 (q, *J* = 1.6 Hz, 1H), 5.54 (dt, *J* = 17.7, 1.5 Hz, 1H), 6.07 (dt, *J* = 17.6, 6.5 Hz, 1H), 7.17 (s, 1H); **^{13}C-NMR** (126 MHz, acetone-d6) δ = −4.8, −4.7, 13.6, 16.8, 18.7, 26.2, 36.4, 39.5, 39.6, 43.6, 43.7, 47.3, 62.1, 70.7, 91.0, 106.7, 143.1, 156.1, 169.2, 169.2, 169.9, 206.3; **HRMS (ESI)**: m/z calc. for $[M+H]^+$: 603.1558; found: 603.1559.

methyl (*S*,*Z*)-3-((*tert*-butyldimethylsilyl)oxy)-7-iodo-4-methylhept-4-en-6-ynoate (S-12)

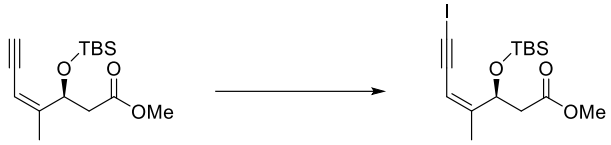

$C_{15}H_{25}IO_3Si$
M = 408.35 g/mol

Alkyne **S-11** (255 mg, 903 µmol, 1.00 eq.) was dissolved in acetone (5 mL) and cooled to 0 °C, followed by addition of NIS (223 mg, 993 µmol, 1.10 eq.) and AgOBz (20 mg, 90 µmol, 0.1 eq.). The resulting mixture was stirred in the dark for 15 minutes at 0 °C and another 15 minutes at room temperature. Afterwards, Celite was added and the solvent was removed. Purification by column chromatography (Silica, CH/EtOAc 20:1) yielded the desired compound **S-12** as a pale yellow oil (365 mg, 894 µmol, 99%). $\mathbf{R_f}$ = 0.27 (CH/EtOAc 20:1); $\boldsymbol{\alpha_D^{20}}$ = +83.4 (c = 0.9, MeCN); **^{1}H-NMR** (500 MHz, C_6D_6) δ = 0.14 (s, 3H), 0.21 (s, 3H), 0.95 (s, 9H), 1.51 (d, *J* = 1.6 Hz, 3H), 2.19 (dd, *J* = 14.4, 4.1 Hz, 1H), 2.56 (dd, *J* = 14.4, 9.4 Hz, 1H), 3.37 (s, 3H), 5.10–5.24 (m, 1H), 5.57 (dd, *J* = 9.4, 4.1 Hz, 1H); **^{13}C-NMR** (126 MHz, C_6D_6) δ = −5.0, −4.8, 10.5, 16.3, 18.3, 25.9, 41.4, 51.2, 69.9, 90.8, 106.8, 155.1, 170.5; **HRMS (ESI):** m/z calc for $[M+H]^+$: 409.0690; found: 409.0692.

methyl (4*Z*,6*Z*,3*S*)-3-((*tert*-Butyldimethylsilyl)oxy)-7-iodo-4-methyl-hept-4,6-dienoate (245)

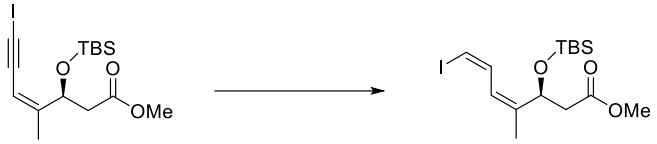

$C_{15}H_{27}IO_3Si$
M = 410.37 g/mol

To a solution of **S-11** (134 mg, 328 µmol, 1.00 eq.) in THF/^{i}PrOH (1:1, 8 mL) was added NBSH (285 mg, 1.31 mmol, 4.00 eq.) and triethylamine (90 µL, 0.65 mmol, 2.0 eq.). The flask was sealed and the resulting solution was stirred in the dark for 17 hours. Then, Celite® was added and all volatiles were

removed *in vacuo*. Purification by column chromatography (Silica, CH/EtOAc 50:1) yielded a mixture of products which was further purified by semi-preparative HPLC (column: MACHEREY-NAGEL Nucleodur 110-5 Gravity C18; 5 µm, eluent: A: MeCN, B: H_2O, isocratic: 90% A, 10% B, flowrate: 15 mL/min, detection wavelength: λ_1 = 240 nm). Yield: (96 mg, 234 µmol, 71%) pale yellow oil. $\mathbf{R_f}$ = 0.28 (CH/EtOAc 20:1), $\boldsymbol{\alpha_D^{20}}$ = +17.3 (c = 1.0, MeCN); **^{1}H-NMR** (700 MHz, acetone-d6) δ = 0.02 (s, 3H), 0.07 (s, 3H), 0.87 (s, 9H), 1.85 (dt, *J* = 1.3, 0.6 Hz, 3H), 2.43 (dd, *J* = 14.6, 4.5 Hz, 1H), 2.65 (dd, *J* = 14.6, 9.0 Hz, 1H), 3.62 (s, 3H), 5.17 (dd, *J* = 9.0, 4.5 Hz, 1H), 5.94–6.05 (m, 1H), 6.46 (ddq, *J* = 7.6, 1.5, 0.8 Hz, 1H), 7.18 (dd, *J* = 10.5, 7.6 Hz, 1H); **^{13}C-NMR** (176 MHz, acetone-d6) δ = −5.1, −4.8, 18.6, 26.0, 26.0, 42.2, 51.7, 69.9, 84.0, 126.9, 133.8, 145.5, 171.3; **HRMS (ESI)**: m/z calc. for $[M+H]^+$: 411.0847; found: 411.0845.

(*S*,*Z*)-3-((*tert*-butyldimethylsilyl)oxy)-7-iodo-4-methylhept-4-en-6-ynoic acid (243)

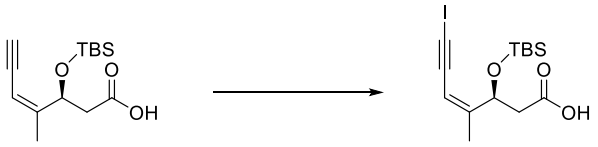

$C_{14}H_{23}IO_3Si$
M = 394.32 g/mol

Carboxylic acid **129** (233 mg, 868 µmol, 1.00 eq.) was dissolved in acetone (8 mL) and cooled to –78 °C, followed by addition of NIS (215 mg, 955 µmol, 1.10 eq.). The resulting mixture was stirred for 5 minutes, followed by addition of AgOBz (20 mg, 87 µmol, 0.1 eq.). The ice bath was removed and the resulting solution was stirred for 30 minutes. Celite® was added and the solvent was removed. Purification of the crude product by column chromatography (Silica, CH/EA 5:1) yielded carboxylic acid **243** as an off-white solid (334 mg, 847 µmol, 98%). $\mathbf{R_f}$ = 0.16 (CH/EtOAc 5:1); $\boldsymbol{\alpha_D^{20}}$ = +69.3 (c = 1.0, MeCN); **^{1}H-NMR** (500 MHz, acetone-d6) δ = 0.07 (s, 3H), 0.12 (s, 3H), 0.87 (s, 9H), 1.82 (d, *J* = 1.6 Hz, 3H), 2.33 (dd, *J* = 14.7, 3.6 Hz, 1H), 2.58 (dd, *J* = 14.7, 9.6 Hz, 1H), 5.37 (dd, *J* = 9.6, 3.6 Hz, 1H), 5.49–5.54 (m, 1H); **^{13}C-NMR** (126 MHz, acetone-d6) δ = –5.0, –4.7, 13.9, 16.6, 18.6, 26.1, 41.5, 70.3, 90.9, 107.1, 155.6, 171.8; **HRMS (APCI):** m/z calc for $[M+H]^+$: 395.0534; found: 395.0532.

(4*Z*,6*Z*,3*S*)-3-((*tert*-Butyldimethylsilyl)oxy)-7-iodo-4-methyl-hept-4,6-dienoic acid (244)

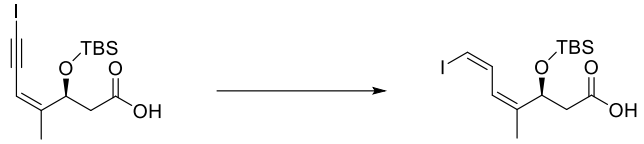

$C_{14}H_{25}IO_3Si$
M = 396.34 g/mol

Carboxylic acid **243** (534 mg, 1.35 mmol, 1.00 eq.) was dissolved in THF/^{i}PrOH (1:1, 12 mL) and triethylamine (290 µL, 2.07 mmol, 1.53 eq.) and NBSH[X] (750 mg, 3.45 mmol, 2.55 eq.) were added. The reaction flask was flushed with Argon for 5 min and the reaction mixture was stirred at room temperature for 27 h while protected from light. Celite® was added and all volatiles were removed. The residue was purified by column chromatography (Silica, *n*-pentane/EtOAc 4:1 → 1:1) to afford the desired diene **244** as a yellow solid (392 mg, 989 µmol, 73%); $\mathbf{R_f}$ = 0.21 (CH/EtOAc 5:1); $\boldsymbol{\alpha_D^{20}}$ = +12.2 (c = 1.0, MeCN); **^{1}H-NMR** (500 MHz, Acetone-d6): δ = 0.03 (s, 3H), 0.08 (s, 3H), 0.88 (s, 9H), 1.87 (s, 3H), 2.42 (dd, *J* = 14.9, 4.5 Hz, 1H), 2.63 (dd, *J* = 14.9, 8.7 Hz, 1H), 5.19 (dd, *J* = 8.8, 4.6 Hz, 1H), 6.00 (d, *J* = 10.5 Hz, 1H), 6.44 (d, *J* = 7.6 Hz, 1H), 7.19 (dd, *J* = 10.5, 7.6 Hz, 1H); **^{13}C-NMR** (126 MHz, Acetone-d6): δ = –5.0, –4.7, 18.7, 26.1, 42.1, 69.9, 83.9, 126.9, 134.0, 145.8, 171.8; **HRMS (APCI)**: m/z calc. for $[M+H]^+$: 397.0690; found: 397.0694.

(*S*,4*Z*,6*Z*)-3-((*tert*-butyldimethylsilyl)oxy)-7-iodo-4-methyl-*N*-((*E*)-4-(1,3,6,2-dioxazaborocane-4,8-dione-2-yl)but-3-en-1-yl)hepta-4,6-dienamide (132, western fragment III)

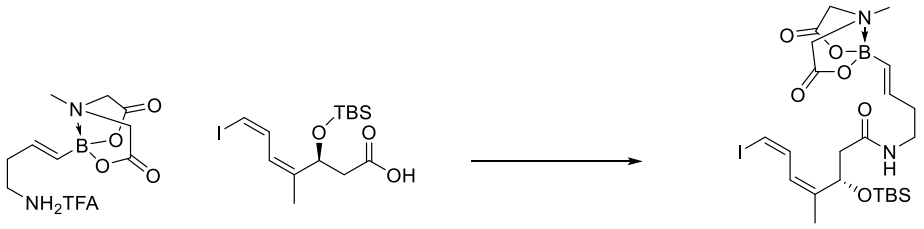

$C_{23}H_{38}BIN_2O_6Si$
M = 604.36 g/mol

To a solution of Carboxylic acid **244** (290 mg, 732 µmol, 1.0 eq.) in anhydrous DCM (10 mL) were sequentially added amine-TFA-salt **228** (261 mg, 768 µmol, 1.05 eq.), DMAP (125 mg, 1.02 mmol, 1.39 eq.) and EDC-HCl (196 mg, 1.02 mmol, 1.39 eq.). The resulting suspension was stirred at room temperature for 13 hours. Afterwards, EtOAc (50 mL) was added and the mixture was transferred to a sep funnel. Water (40 mL) was added, phases were separated and the aqueous layer was extracted with EtOAc (2 × 30 mL). The combined organic layers were washed with water (2 × 40 mL), saturated aqueous NH_4Cl (2 × 40 mL) and brine (40 mL), dried over $MgSO_4$, filtered and concentrated. Purification by column chromatography (Silica, EtOAc/MeCN 9:1) afforded the desired product as a white solid (355 mg, 587 µmol, 80%). $\mathbf{R_f}$ = 0.31 (EtOAc/MeCN 9:1); $\boldsymbol{\alpha_D^{20}}$ = –1.8 (c = 0.5, MeCN); **^{1}H-NMR** (500 MHz, acetone-d6): δ = 0.03 (s, 3H), 0.07 (s, 3H), 0.89 (s, 9H), 1.81–1.88 (m, 3H), 2.23 (dd, *J* = 13.7, 4.9 Hz, 1H), 2.29 (qdd, *J* = 6.9, 4.1, 1.5 Hz, 2H), 2.50 (dd, *J* = 13.7, 8.4 Hz, 1H), 3.00 (s, 2H), 3.18 (ddd, *J* = 13.3, 7.1, 1.5 Hz, 1H), 3.30–3.38 (m, 1H), 4.01 (dd, *J* = 16.8, 0.9 Hz, 2H), 4.19 (d, *J* = 16.8 Hz, 2H), 5.20 (dd, *J* = 8.4, 4.8 Hz, 1H), 5.55 (dt, *J* = 17.6, 1.5 Hz, 1H), 5.93–6.00 (m, 1H), 6.07 (dt, *J* = 17.6, 6.6 Hz, 1H), 6.41 (dt, *J* = 7.6, 0.9 Hz, 1H), 7.18 (dd, *J* = 10.4, 7.6 Hz, 1H), 7.22 (s, 1H); **^{13}C-NMR** (126 MHz, acetone-d6): δ = –5.8, –5.7, 17.8, 18.0, 25.2, 35.5, 38.6, 43.5, 46.4, 61.2, 69.5, 82.4, 125.5, 133.4, 142.2, 145.6, 168.2, 169.0 [note: the carbon attached to boron was not observed due to quadrupole broadening caused by the ^{11}B nucleus]; **HRMS (ESI)**: m/z calc. for $[M+H]^+$: 605.1714; found: 605.1712.

(*S*,4*Z*,6*Z*)-3-hydroxy-7-iodo-4-methyl-*N*-((*E*)-4-(1,3,6,2-dioxazaborocane-4,8-dione-2-yl)but-3-en-1-yl)hepta-4,6-dienamide (S-13)

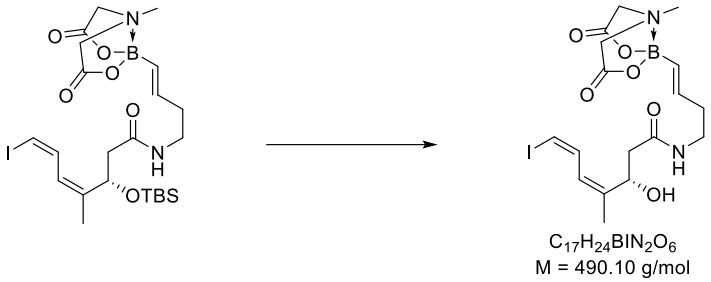

To a solution of **132** (105 mg, 174 µmol, 1.00 eq.) in THF (3 mL) was added HF-pyridine complex (0.20 mL, 2.2 mmol, 13 eq.). The resulting solution was stirred for 6 hours at r.t in the dark. Then, water (2 mL) was added followed by stepwise addition of $NaHCO_3$ (ca. 1 g). The mixture was stirred for 10 min until no futher gas evolution was observed. MeCN (4 mL) was added and the resulting mixture was azeotropically dried by coevaporation with MeCN (2 x 4 mL). The reulting mixture was absorbed onto Celite® from acetone and loaded onto a short (1 cm) plug of silica which was pretreated with Et_2O and covered with sand. The plug was rinsed with Et_2O (25 mL) and eluted with MeCN (25 mL). After evaporation of the solvent, the product **S-13** was obtained as a white solid (85.6 mg, 174 µmol, 100%) which was further purified by HPLC (column: KNAUER Eurospher II 100-5 C18P; 5 µm; 250 × 16 mm; eluent: A: MeCN, B: H_2O, isocratic: 25% A, 75% B, flowrate: 16.0 mL/min, detection wavelength: λ_1 = 205 nm). $\mathbf{R_f}$ = 0.30 (Et_2O/MeCN 1:1); $\boldsymbol{\alpha_D^{20}}$ = +19.7 (c = 1.0, MeCN); **^{1}H-NMR** (500 MHz, acetone-d6) δ = 1.79–1.85 (m, 3H), 2.22–2.32 (m, 3H), 2.42–2.50 (m, 1H), 3.00 (s, 3H), 3.28 (td, *J* = 6.7, 5.7 Hz, 2H), 4.00 (dd, *J* = 16.9, 4.2 Hz, 2H), 4.17 (dd, *J* = 16.9, 0.7 Hz, 2H), 5.04 (dd, *J* = 9.2, 4.1 Hz, 1H), 5.55 (dt, *J* = 17.6, 1.5 Hz, 1H), 5.91–5.98 (m, 1H), 6.05 (dt, *J* = 17.7, 6.6 Hz, 1H), 6.34 (dt, *J* = 7.6, 0.9 Hz, 1H), 7.11–7.19 (m, 1H), 7.31 (s, 1H); **^{13}C-NMR** (126 MHz, acetone-d6) δ = 19.0, 36.3, 39.3, 42.1, 47.3, 62.1, 68.8, 83.0, 126.5, 134.4, 143.1, 146.9, 169.1, 169.2, 171.7; [note: the carbon attached to boron was not observed due to quadrupole broadening caused by the ^{11}B nucleus]; **HRMS (ESI)**: m/z calc. for $[M+Na]^+$: 513.0667; found: 513.0668.

8.3 Fragment Couplings

8.3.1 Synthesis of Tetraenes

methyl (*S*,4*Z*,6*Z*,8*E*,10*E*)-3-((*tert*-butyldimethylsilyl)oxy)-4,10-dimethyl-11-(4,4,5,5-tetramethyl-1,3,2-dioxaborolan-2-yl)undeca-4,6,8,10-tetraenoate (134, tetraene II)

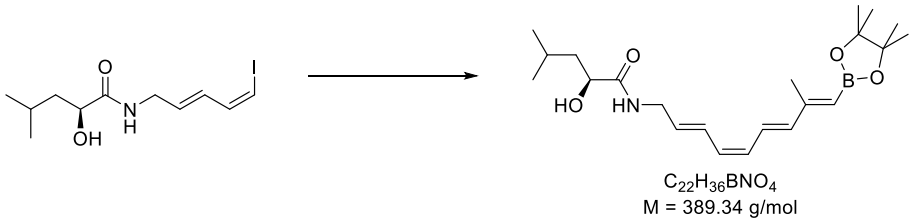

Western fragment II (**122**) (154 mg, 477 µmol, 1.00 eq.) and Sn-B(pin)-linchpin I (**113**) (342 mg, 708 µmol, 1.49 eq.) were dissolved in dry degassed DMF (5 mL). Then, bis(acetonitrile)palladiumdichloride (25 mg, 95 µmol, 0.2 eq.) was added and the resulting mixuture was stirred at 50 °C in the dark overnight (10 hours). After the indicated time, water (10 mL) and EtOAc (10 mL) was added. Phases were separated and the aqueous layer was extracted with EtOAc (3 × 10 mL). The organic layer was washed with a saturated solution of NH_4Cl (10 mL) and brine (10 mL). The organic layer was dried over $MgSO_4$, filtered and concentrated. Purification by column chromatography (RP-Silica, MeCN/H_2O 1.5 : 1) yielded the desired compound as a mixture of isomers (d.r. = 8.1/1.5/0.4) determined by analytical HPLC. Decomposition of the compound was observed during a semi-preparative HPLC separation (column: DAICEL Chiralpak IB; 5 µm; 250 x 20 mm, eluent: A: MeOH, B: H_2O, isocratic: 65% A, 35% B, flowrate: 18.0 mL/min, detection wavelength: λ_1 = 330 nm) **^{1}H-NMR** (500 MHz, CD_2Cl_2) δ = 0.94–0.98 (m, 6H), 1.24–1.28 (m, 12H), 1.47–1.56 (m, 1H), 1.57–1.66 (m, 1H), 1.79–1.89 (m, 1H), 1.96–2.16 (m, 3H), 3.90–4.00 (m, 2H), 4.11 (d, *J* = 9.6 Hz, 1H), 5.28–5.32 (m, 1H), 5.74 (ddt, *J* = 14.5, 10.0, 6.3 Hz, 1H), 5.97–6.15 (m, 1H), 6.19–6.46 (m, 4H), 6.57 (s, 1H); **^{13}C-NMR** (126 MHz, CD_2Cl_2) δ = 16.7, 21.8, 23.8, 25.1, 25.2, 41.3, 44.6, 71.3, 83.4, 130.6, 131.5, 132.6, 133.6, 133.8, 139.6, 155.6, 174.5; [note: the carbon attached to boron was not observed due to quadrupole broadening caused by the ^{11}B nucleus]; **HRMS (APCI)**: m/z calc. for $[M+H]^+$: 390.2814; found: 390.2812.

(*S*,4*Z*,6*Z*,8*E*,10*E*)-3-((*tert*-butyldimethylsilyl)oxy)-4,10-dimethyl-11-(4,4,5,5-tetramethyl-1,3,2-dioxaborolan-2-yl)-*N*-((*E*)-4-(1,3,6,2-dioxazaborocane-4,8-dione-2-yl)undeca-4,6,8,10-tetraenamide (246, tetraene III)

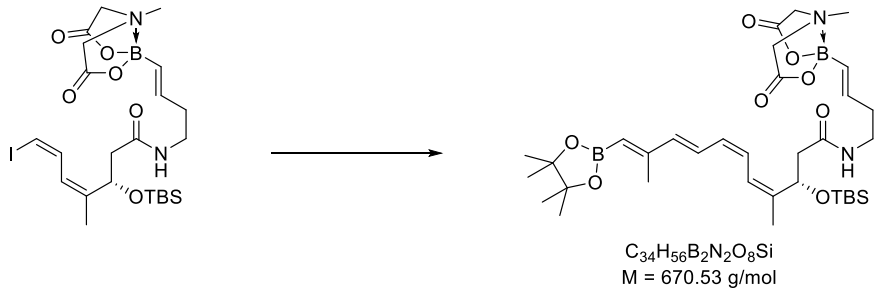

Central fragment III (**132**) (20.0 mg, 33.1 µmol, 1.00 eq.) and Sn-B(pin)-linchpin I (**113**) (20.8 mg, 43.0 µmol, 1.30 eq.) were dissolved in dry degassed DMF (1 mL). Then, bis(acetonitrile)-palladiumdichloride (0.86 mg, 3.3 µmol, 0.10 eq.) was added and the resulting mixuture was stirred in the dark for 13 hours. After the indicated time, a saturated aqueous solution of NH_4Cl (2 mL) and EtOAc (5 mL) was added. Phases were separated and the aqueous layer was extracted with EtOAc (3 × 5 mL). The organic layer was washed with H_2O (4 × 2 mL) and brine (2 mL). The organic layer was dried over $MgSO_4$, filtered and concentrated. Purification by column chromatography (Silica, EtOAc) yielded the desired tetraene III (**246**) as an off-white solid (3.60 mg, 5.37 µmol, 16%). $\mathbf{R_f}$ = 0.15 (EtOAc); $\boldsymbol{\alpha_D^{20}}$ = 98.9 (c = 0.01, MeCN), **^{1}H-NMR** (700 MHz, acetone-d6) δ = 0.02 (s, 3H), 0.06 (s, 3H), 0.87 (s, 9H), 1.26 (s, 12H), 1.85 (s, 3H), 2.15 (d, *J* = 0.9 Hz, 3H), 2.16–2.19 (m, 1H), 2.23–2.33 (m, 2H), 2.50 (dd, *J* = 13.7, 8.8 Hz, 1H), 2.98 (s, 3H), 3.13–3.21 (m, 1H), 3.29–3.37 (m, 1H), 3.99 (dd, *J* = 16.8, 3.0 Hz, 2H), 4.17 (d, *J* = 16.8 Hz, 2H), 5.29 (dd, *J* = 8.7, 4.3 Hz, 1H), 5.33 (s, 1H), 5.53 (dt, *J* = 17.6, 1.5 Hz, 1H), 6.02–6.12 (m, 2H), 6.39 (d, *J* = 15.1 Hz, 1H), 6.48 (d, *J* = 5.0 Hz, 2H), 6.98 (dd, *J* = 15.2, 11.5 Hz, 1H), 7.17 (d, *J* = 5.9 Hz, 1H); **^{13}C-NMR** (176 MHz, acetone-d6) δ = −4.8, −4.7, 16.7, 18.7, 18.9, 25.2, 25.2, 26.2, 36.5, 39.6, 44.4, 47.3, 62.1, 69.0, 83.5, 122.0, 126.4, 127.1, 129.4, 140.3, 142.7, 143.2, 156.2, 169.1, 170.2; [note: both carbons attached to borons were not observed due to quadrupole broadening caused by the ^{11}B nucleus]; **HRMS (APCI)**: m/z calc. for $[M+H]^+$: 671.4077; found: 671.4077.

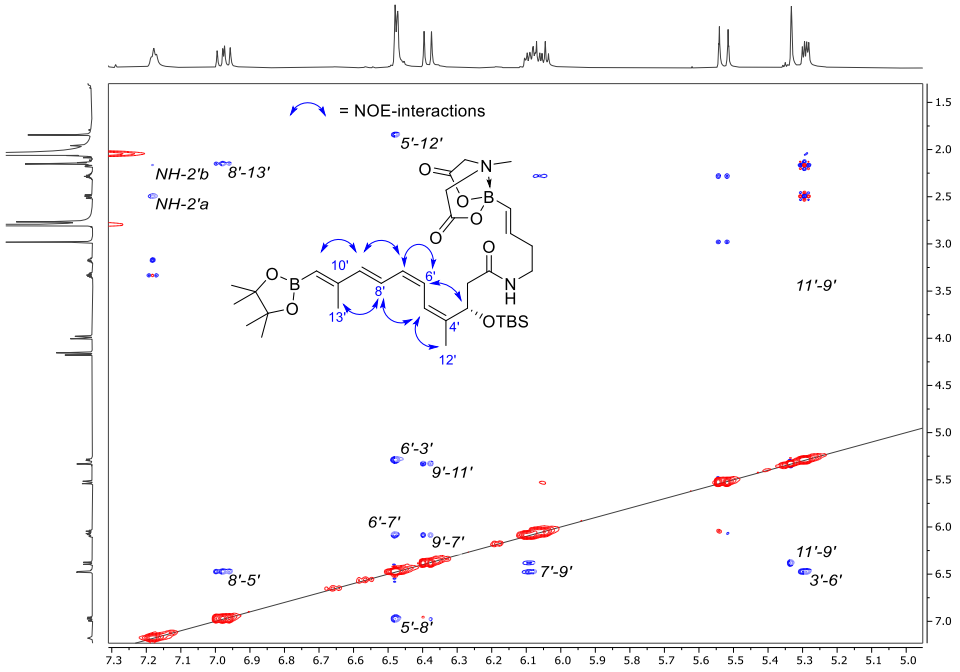

Figure 22. Part of the NOESY-spectrum in acetone-d6 (700 MHz) of tetraene III **246** with key-interactions annotated.

methyl (*S*,4*Z*,6*Z*,8*E*,10*E*)-3-((*tert*-butyldimethylsilyl)oxy)-4,10-dimethyl-11-(4,4,5,5-tetramethyl-1,3,2-dioxaborolan-2-yl)undeca-4,6,8,10-tetraenoate (247, tetraene IV)

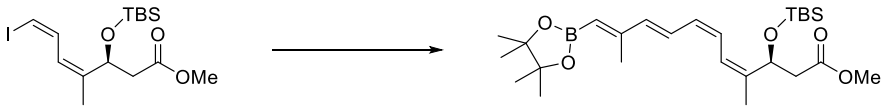

$C_{26}H_{45}BO_5Si$
M = 476.54 g/mol

Diene **245** (10 mg, 24 µmol, 1.0 eq.) and Sn-B(pin)-linchpin II (**121**) (15 mg, 31 µmol, 1.3 eq.) were dissolved in dry degassed DMF (1 mL). Then, bis(acetonitrile)palladiumdichloride (0.63 mg, 2.4 µmol, 0.10 eq.) was added and the resulting mixuture was stirred in the dark overnight. After the indicated time, a saturated aqueous solution of NH_4Cl (2 mL) and EtOAc (5 mL) was added. Phases were separated and the aqueous layer was extracted with EtOAc (3 × 5 mL). The organic layer was washed with H_2O (4 × 2 mL) and brine (2 mL). The organic layer was dried over $MgSO_4$, filtered and concentrated. Purification by column chromatography (Silica, CH/EtOAc 20:1) yielded the desired tetraene IV (**247**) as a yellow oil (3.0 mg, 6.3 µmol, 26%). $\mathbf{R_f}$ = 0.13 (CH/EtOAc 20:1); $\boldsymbol{\alpha_D^{20}}$ = 38.7 (c = 0.3, MeCN), **^{1}H-NMR** (700 MHz, acetone-d6) δ = 0.02 (d, *J* = 1.5 Hz, 3H), 0.06–0.08 (m, 3H), 0.87 (d, *J* = 1.3 Hz, 9H), 1.26 (d, *J* = 1.5 Hz, 12H), 1.86 (d, *J* = 1.8 Hz, 3H), 2.15 (t, *J* = 1.2 Hz, 3H), 2.39 (ddd, *J* = 14.4, 4.3, 1.5 Hz, 1H), 2.65

(ddd, *J* = 14.4, 9.2, 1.5 Hz, 1H), 3.63 (d, *J* = 1.4 Hz, 3H), 5.27 (dd, *J* = 9.2, 4.3 Hz, 1H), 5.34 (s, 1H), 6.12 (t, *J* = 11.1 Hz, 1H), 6.40 (d, *J* = 15.2 Hz, 1H), 6.44 (t, *J* = 11.5 Hz, 1H), 6.53 (d, *J* = 12.4 Hz, 1H), 6.98 (dd, *J* = 15.2, 11.5 Hz, 1H); ^{13}C-NMR (176 MHz, acetone-d6) δ = −5.0, −4.7, 16.7, 18.6, 25.1, 26.0, 42.3, 51.7, 68.5, 83.5, 122.5, 125.8, 126.9, 129.9, 140.6, 141.6, 156.1, 171.6; [note: the carbon attached to boron was not observed due to quadrupole broadening caused by the ^{11}B nucleus]; **HRMS (APCI)**: m/z calc. for $[M+H]^+$: 477.3207; found: 477.3202.

(*S*,4*Z*,6*Z*,8*E*,10*E*)-3-((*tert*-butyldimethylsilyl)oxy)-4,9-dimethyl-11-(4,4,5,5-tetramethyl-1,3,2-dioxaborolan-2-yl)-*N*-((*E*)-4-(1,3,6,2-dioxazaborocane-4,8-dione-2-yl)undeca-4,6,8,10-tetraenamide (135, tetraene V)

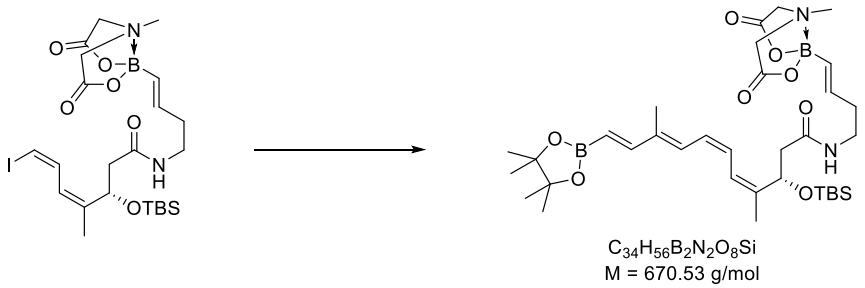

$C_{34}H_{56}B_2N_2O_8Si$
M = 670.53 g/mol

Central fragment III (**132**) (30.0 mg, 49.6 µmol, 1.00 eq.) and Sn-B(pin)-linchpin II (**122**) (52.8 mg, 109 µmol, 2.20 eq.) were added to a schlenk flask and azeotropically dried with MeCN (3 × 2 mL). In a second flask, bis(acetonitrile)palladiumdichloride (5.0 mg, 19 µmol, 0.39 eq.) was dissolved in anhydrous DMF (4 mL) and freeze-pump-thaw degassed (3 cycles). Then, the catalyst solution (2.0 mL, 9.6 µmol, 0.20 eq.) was added to the flask containing MIDA-boronate and bimetallic linker. The resulting mixuture was stirred in the dark for 11 hours. After the indicated time, a saturated aqueous solution of NH_4Cl (4 mL) and EtOAc (20 mL) was added. Phases were separated and the aqueous layer was extracted with EtOAc (2 × 6 mL). The organic layer was washed with brine/H_2O (1:1, 5 × 8 mL) and the solvent was removed. The residue was dissolved in MeCN (10 mL) and washed with *n*-hexane (3 × 4 mL). The combined hexane-layers were backextracted with MeCN (2 × 4 mL) and the combined MeCN-layers were dried over $MgSO_4$, filtered and concentrated to yield the sufficiently pure crude tin-free product as an orange resin (31.3 mg, 46.7 µmol, 94%). Further purification of cumulated crude or semi-purified (Silica or RP-column) products was achieved by semi-preparative HPLC (column: MACHEREY-NAGEL Nucleodur 100-5 Gravity C18; 5 µm, eluent: A: H_2O, B: MeCN, isocratic: 75% A, 25% B, flowrate: 26.0 mL/min, detection wavelengths: λ_1 = 230 nm, λ_2 = 330 nm). [note: during this HPLC-run isomerization of the

compound was observed, which led to a diminished yield of 29% and isolation of the 4'*Z*,6'*E*-isomer tetraene VI (**248**).] Separation of the (*R*)-enantiomer *R*-**135** was achieved by chiral semi-preparative HPLC (column: DAICEL Chiralpak IB; 5 µm; 250 × 20 mm, eluent: A: *n*-hexane, B:EtOH, isocratic: 80% A, 20% B, flowrate: 18.0 mL/min, detection wavelengths: λ_1 = 300 nm, λ_2 = 330 nm, λ_3 = 345 nm). Total yield from 392 mg crude product: 78.0 mg, 116 µmol, 18% (white solid). (4'*Z*,6'*Z*)-Isomer (tetraene V, **135**): $\mathbf{R_f}$ = 0.15 (EtOAc); $\boldsymbol{\alpha_D^{20}}$ = –1.1 (c = 0.35, MeCN); **^{1}H-NMR** (700 MHz, acetone-d6) δ = 0.02 (s, 3H), 0.06 (s, 3H), 0.87 (s, 9H), 1.25 (s, 12H), 1.87 (d, *J* = 1.3 Hz, 3H), 1.89 (d, *J* = 1.2 Hz, 3H), 2.18 (dd, *J* = 13.6, 4.4 Hz, 1H), 2.29 (dqd, *J* = 8.3, 6.8, 1.5 Hz, 2H), 2.51 (dd, *J* = 13.6, 8.8 Hz, 1H), 2.98 (s, 3H), 3.17 (dtd, *J* = 13.1, 7.0, 5.4 Hz, 1H), 3.30–3.38 (m, 1H), 3.99 (d, *J* = 16.8 Hz, 2H), 4.17 (dd, *J* = 16.9, 0.8 Hz, 2H), 5.31 (dd, *J* = 8.7, 4.4 Hz, 1H), 5.51–5.54 (m, 1H), 5.55 (d, *J* = 18.2 Hz, 1H), 6.06 (dt, *J* = 17.6, 6.5 Hz, 1H), 6.35–6.39 (m, 1H), 6.57 (d, *J* = 8.1 Hz, 2H), 6.85 (d, *J* = 12.1 Hz, 1H), 7.11 (dd, *J* = 18.1, 0.8 Hz, 1H), 7.23 (s, 1H); **^{13}C-NMR** (176 MHz, acetone-d6) δ = –4.8, –4.7, 11.8, 18.9, 25.1, 25.1, 26.2, 36.4, 39.5, 44.4, 47.3, 62.1, 62.1, 69.0, 83.7, 122.0, 124.9, 127.1, 130.5, 137.3, 143.1, 143.1, 143.3, 154.8, 169.1, 169.1, 170.3 [note: both carbons attached to borons were not observed due to quadrupole broadening caused by the ^{11}B nucleus]; **HRMS (ESI)**: m/z calc. for $[M+H]^+$: 671.4077; found: 671.4067; **UV/Vis**: (MeCN, nm ($mol^{-1}dm^3cm^{-1}$)): λ_{max} (ε) = 313 (20976), 328 (27074), 343 (21829). (4'*Z*,6'*E*)-Isomer (tetraene VI, **248**): $\mathbf{R_f}$ = 0.15 (EtOAc); $\boldsymbol{\alpha_D^{20}}$ = –3.1 (c = 1.0, MeCN); **^{1}H-NMR** (500 MHz, acetone-d6) δ = 0.07 (d, *J* = 3.0 Hz, 3H), 0.87 (d, *J* = 0.7 Hz, 9H), 1.25 (s, 12H), 1.83–1.91 (m, 3H), 2.13–2.22 (m, 1H), 2.29 (qdd, *J* = 7.2, 5.7, 1.5 Hz, 2H), 2.45–2.55 (m, 1H), 2.98 (d, *J* = 1.4 Hz, 3H), 3.17 (dtd, *J* = 13.1, 6.9, 5.4 Hz, 1H), 3.29–3.40 (m, 1H), 3.99 (d, *J* = 16.7 Hz, 2H), 4.17 (d, *J* = 16.9 Hz, 2H), 5.27 (dt, *J* = 8.7, 4.8 Hz, 1H), 5.49–5.57 (m, 2H), 6.06 (dd, *J* = 17.6, 6.6 Hz, 1H), 6.41 (d, *J* = 11.5 Hz, 1H), 6.58 (dd, *J* = 14.4, 11.4 Hz, 1H), 7.07 (dd, *J* = 18.0, 0.8 Hz, 1H), 7.18 (d, *J* = 6.0 Hz,1H); **^{13}C-NMR** (126 MHz, acetone-d6) δ = –4.8, –4.7, 1.1, 12.2, 18.7, 18.9, 25.1, 25.1, 26.2, 36.5, 39.6, 44.4, 47.3, 62.1, 69.4, 83.7, 127.6, 129.4, 131.5, 136.1, 136.7, 142.3, 143.2, 154.4, 169.1, 170.2; 3 [note: both carbons attached to borons were not observed due to quadrupole broadening caused by the ^{11}B nucleus]; **HRMS (ESI)**: m/z calc. for $[M+H]^+$: 671.4077; found: 671.4077.

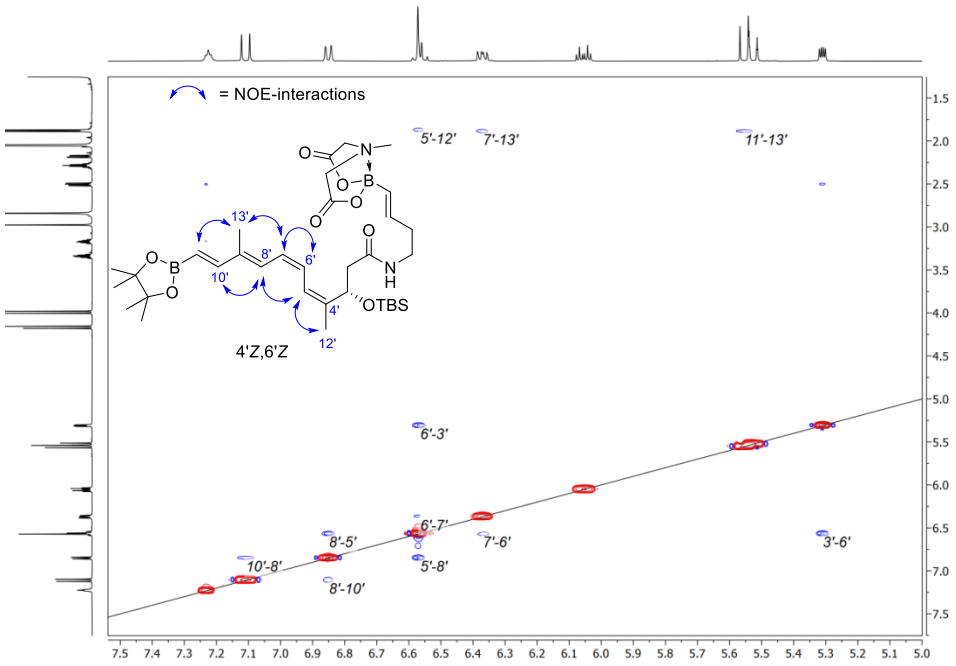

Figure 23. Part of the NOESY-spectrum in acetone-d6 (700 MHz) of tetraene V (**135**) with key-interactions annotated.

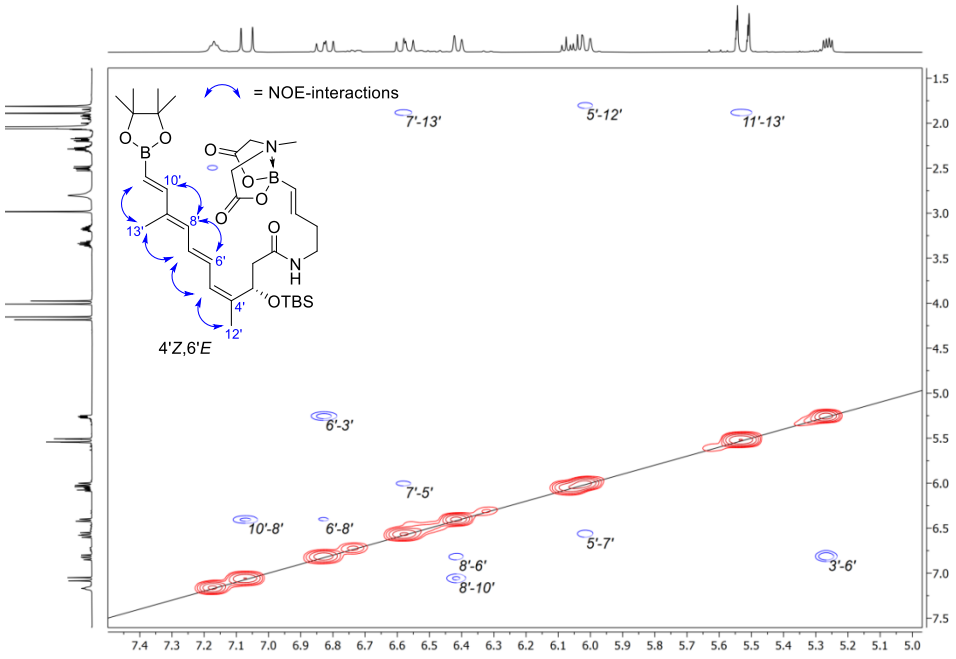

Figure 24. Part of the NOESY-spectrum in acetone-d6 (700 MHz) of 4*Z*,6*E*-isomer, tetraene VI (**248**) with key-interactions annotated.

8.3.2 Stability studies of tetraene V (135)

Tetraene V (**135**) (1.00 mg, 1.49 µmol) was dissolved in degassed MeCN (20 mL) to provide a 50 µg/mL (75 µM) solution. The resulting solution was transferred to septum vials (6 × 1 mL/vial) or pressure tubes for temperature experiments (3 × 5 mL/pressure tube). The resulting solutions were exposed to conditions noted in table 18. Each sample was examined by analytical HPLC after 1 h, 2 h, 4 h and 24 h (column: MACHEREY-NAGEL Nucleodur 100-3 Gravity C18; 3 µm; 2.0 × 100 mm, eluent: A: H_2O, B: MeCN, isocratic: 75% A, 25% B, flowrate: 0.5 mL/min, detection wavelengths: λ = 190-600 nm).

Table 18. Conditions for stability studies of **135**.

Irradiation	Temperature	Oxygen
310 nm	40 °C, dark[a]	pure oxygen, dark[a]
325 nm	60 °C, dark[a]	atmospheric oxygen, dark[a]
365 nm	80 °C, dark[a]	
white light (>400 nm)		

[a] no isomerization was observed under these conditions.

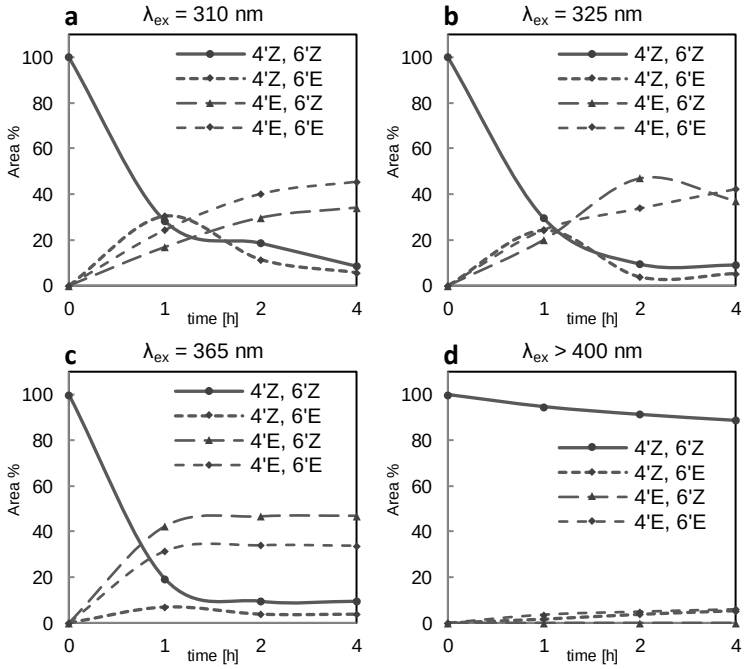

Figure 25. Isomeric profile of **135** (75 µM in MeCN) based on HPLC peak area percentages upon irradiation with various light sources: a) λ_{ex} = 310 nm; b) λ_{ex} = 325 nm; c) λ_{ex} = 365 nm; d) λ_{ex} > 400 nm (white light). For original chromatographic data see appendix.

8.3.3 Optimized synthetic procedure for hexaene II (131)

(*S*,4*Z*,6*Z*,8*E*,10*E*,12*Z*,14*E*)-3-((*tert*-butyldimethylsilyl)oxy)-16-((*S*)-2-hydroxy-4-methyl pentanamido)-4,9-dimethyl-*N*-((*E*)-4-(1,3,6,2-dioxazaborocane-4,8-dione-2-yl)but-3-en-1-yl) hexadeca-4,6,8,10,12,14-hexaenamide (131, hexaene II)

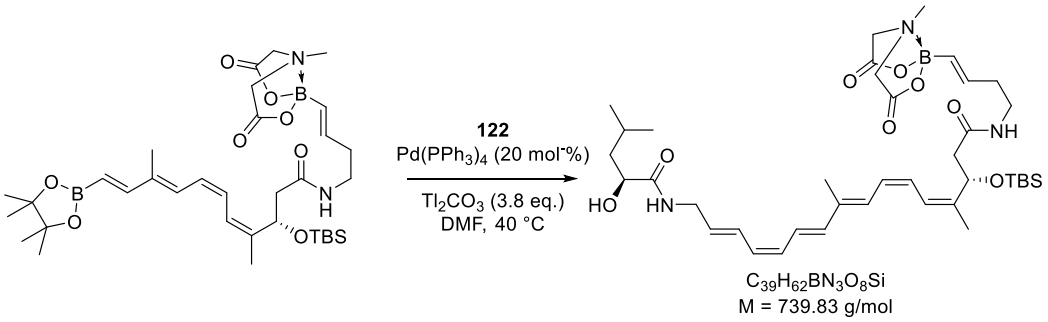

A mixture of tetraene V (**135**) (9.5 mg, 14.2 µmol, 1.0 eq.) and western fragment II (**122**) (6.87 mg, 25.2 µmol, 1.5 eq.) was azeotropically dried by co-evaporation with MeCN (3 × 2 mL). Subsequently, the

Figure 26. Isomeric profile of **135** (75 µM in MeCN) based on HPLC peak area percentages upon irradiation with various light sources: a) λex = 310 nm; b) λex = 325 nm; c) λex = 365 nm; d) λex > 400 nm (white light). For original chromatographic data see appendix.

residue was dissolved in anhydrous DMF (1.0 mL). In a second flask, thallium carbonate (25 mg, 54 µmol, 3.8 eq.) was added. In a third flask, a solution of $Pd(PPh_3)_4$ (6.50 mg, 5.62 µmol, 0.4 eq.) in anhydrous DMF (1.0 mL) was prepared. Then, the solution of starting materials was added to the base containing flask, followed by the catalyst solution (0.5 mL, 20 mol-%) and the resulting mixture was stirred at 40 °C in the dark. After 17 hours, the mixture was cooled to 0 °C and quenched by addition of a solution of sat NH_4Cl (3 mL). The resulting mixture was loaded onto a CHROMABOND C18 ec, 45 µm, 500 mg SPE-cartridge (conditioned: 6 mL MeOH, 6 mL H_2O) the following way: Water (3 mL) was added to the cartridge, the reaction mixture (1 mL) was mixed in the headroom of the cartridge and then slowly eluted. This procedure was repeated four more times. The reaction flask was rinsed with MeCN (0.5 mL) and mixed with water (4 mL) in the headroom of the cartridge (2 ×). The fully loaded cartridge was washed with MeCN/H_2O (5:95; 6 mL). Then, the cartridge was eluted with a gradient of MeCN/H_2O (3 mL) each: 10%; 20%; 40%; 50%; 50%; **60%; 60%;** 60%; 60%; 60%; 65%; 65%; 65%; 100%. The obtained fractions were analyzed by UV-vis spectroscopy (approx. 10 µL in 0.5 mL MeCN) with the first 60%-fractions showing the typical hexane absorptions. After evaporation of the solvent, the obtained pre-purified sample was further purified by semi-preparative HPLC (column: KNAUER Eurospher II 100-5 C18P; 5 µm; 250 × 16 mm; eluent: A: MeCN, B: H_2O, gradient: 50% A, 50% B → 100% A, (0–20 min), 100% A, (20–25 min), flowrate: 15.0 mL/min, detection wavelengths: λ_1 = 230 nm, λ_2 = 330 nm, λ_3 = 360 nm)

which yielded the hexaene II (**131**) (5.50 mg, 14.9 µmol, 50%) as a yellow amorphous solid with a geometrical purity of 96% determined by analytical HPLC.

R_f = 0.22 (EtOAc/MeCN 10:1).

$\boldsymbol{\alpha_D^{20}}$ = -13.0 (c = 1.0, MeCN).

^{1}H-NMR (700 MHz, acetone-d6) δ = 0.01 (s, 3H), 0.06 (s, 3H), 0.87 (s, 10H), 0.92 – 0.95 (m, 6H), 1.49 (ddd, *J* = 14.1, 9.8, 4.7 Hz, 1H), 1.55–1.63 (m, 1H), 1.85 (s, 3H), 1.86–1.93 (m, 2H), 2.14–2.20 (m, 1H), 2.24–2.33 (m, 2H), 2.49 (dd, *J* = 13.6, 8.6 Hz, 1H), 2.98 (s, 2H), 3.14–3.18 (m, 1H), 3.34 (dq, *J* = 13.4, 6.8 Hz, 1H), 3.94 (s, 2H), 3.99 (dd, *J* = 16.8, 2.3 Hz, 2H), 4.06 (ddd, *J* = 9.4, 5.7, 3.4 Hz, 1H), 4.17 (d, *J* = 16.9 Hz, 3H), 4.50 (d, *J* = 5.6 Hz, 1H), 5.30 (dd, *J* = 8.6, 4.6 Hz, 1H), 5.52 (dt, *J* = 17.6, 1.5 Hz, 1H), 5.76 (dt, *J* = 15.2, 6.1 Hz, 1H), 5.99–6.11 (m, 3H), 6.37 (d, *J* = 8.4 Hz, 1H), 6.45 (dt, *J* = 13.7, 5.9 Hz, 3H), 6.73 (d, *J* = 12.3 Hz, 1H), 6.78–6.86 (m, 1H), 6.83–6.89 (m, 1H), 7.17 (d, *J* = 6.2 Hz, 1H), 7.42 (s, 1H).

^{13}C-NMR (176 MHz, acetone-d6) δ = -4.8, -4.7, 12.6, 18.7, 18.9, 21.8, 23.9, 25.2, 26.2, 36.4, 39.6, 41.1, 44.4, 44.9, 47.3, 62.1, 69.0, 71.1, 122.1, 124.7, 125.2, 125.4, 127.7, 128.1, 129.6, 130.6, 132.4, 137.0, 139.5, 142.6, 143.2, 169.1, 169.1, 170.2, 174.9 [note: the carbon attached to boron was not observed due to quadrupole broadening caused by the ^{11}B nucleus].

HRMS (APCI): m/z calc. for $[M+H]^+$: 740.4479; found: 740.4466.

UV/Vis: (MeCN, nm ($mol^{-1}dm^3cm^{-1}$)): λ_{max} (ε) = 328 (18052), 345 (28784), 363 (39510), 383 (34041).

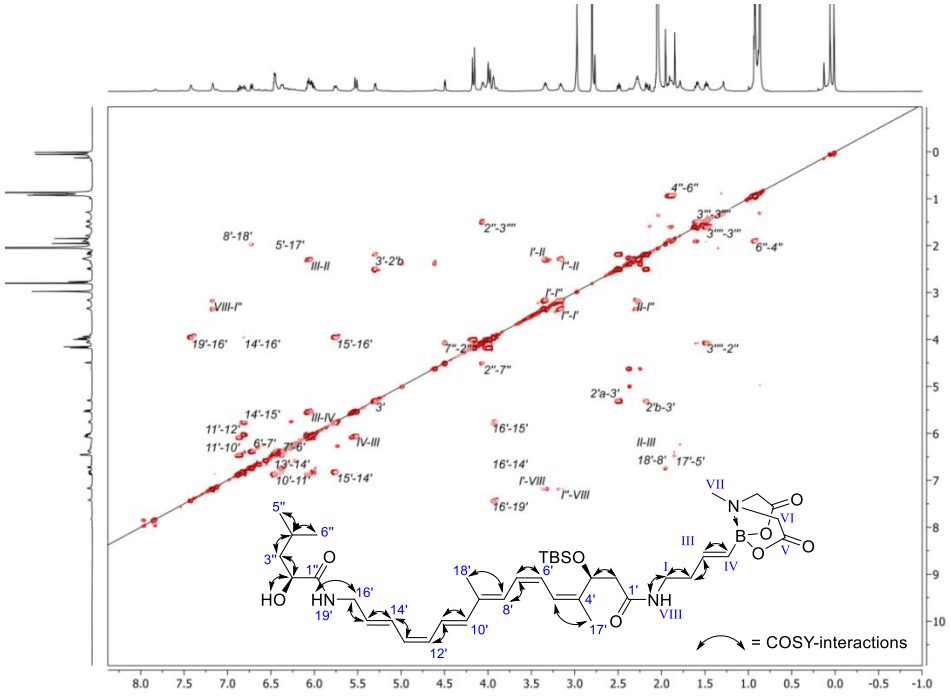

Figure 27. COSY-spectrum in acetone-d6 (700 MHz) of hexaene II (**131**) with key-interactions annotated.

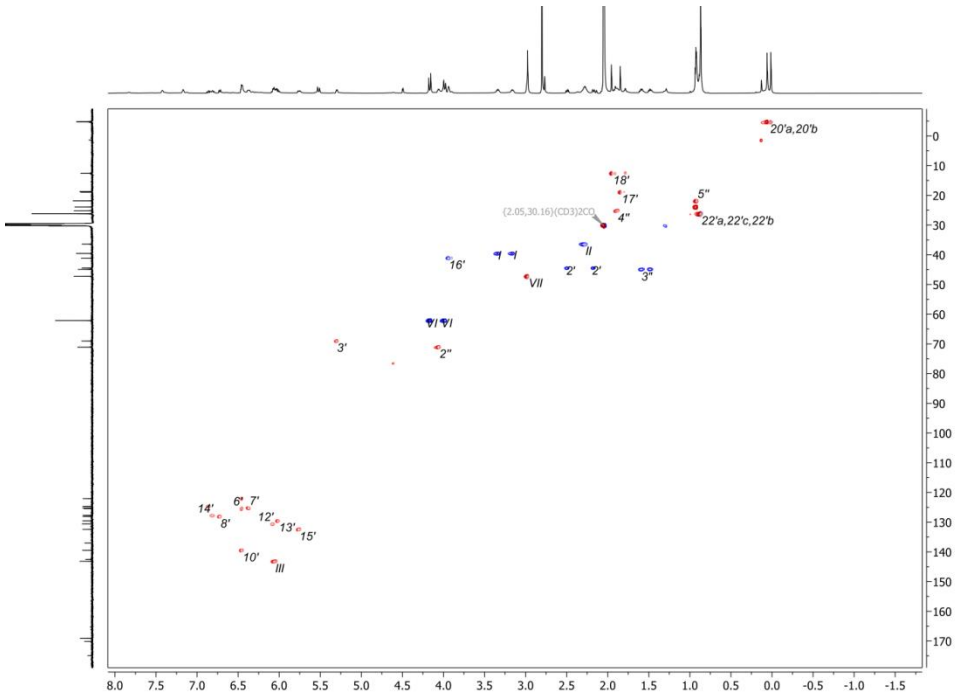

Figure 28. HSQC-spectrum in acetone-d6 (700 MHz) of hexaene II (**131**) with key-interactions annotated.

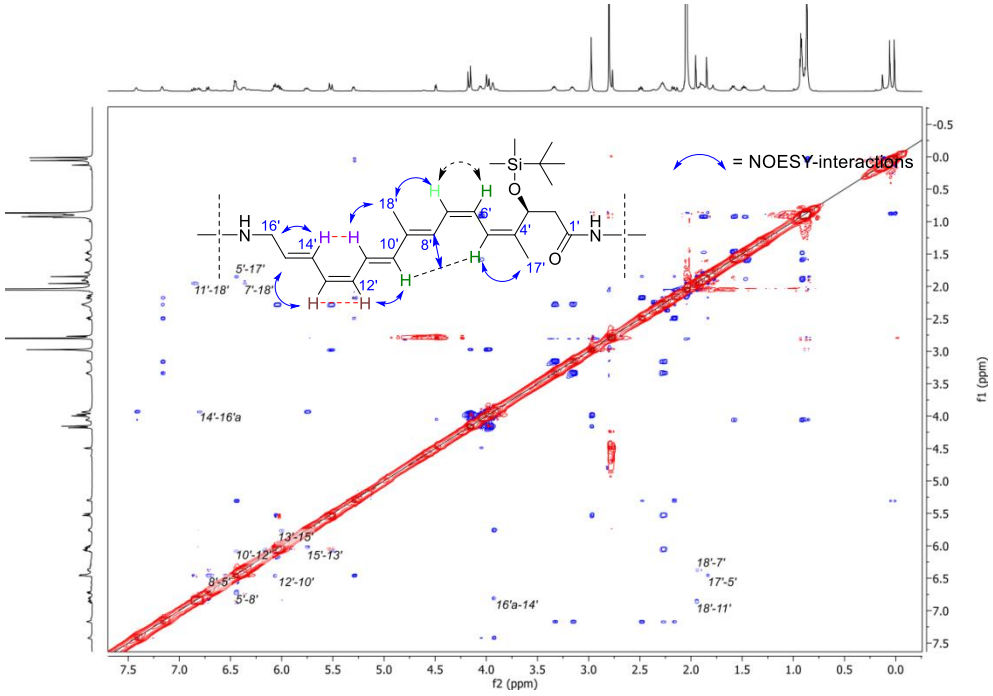

Figure 29. NOESY-spectrum in acetone-d6 (700 MHz) of hexaene II (**131**) with key-interactions annotated. Protons of the same color belong to the same multiplet; one single interaction of 8'-10' and 8'-5' is observed; interaction of 6'-7' is too close to the diagonal for an accurate detection.

8.3.4 Catalyst-screening for the Synthesis of Hexaene II (131)

A mixture of tetraene V (**135**) (7.0 mg, 10 µmol, 1.0 eq.) and western fragment II (**122**) (4.72 mg, 14.6 ymol, 1.4 eq.) was azeotropically dried by co-evaporation with MeCN (3 × 2 mL). Subsequently, the residue was dissolved in anhydrous DMSO (0.7 mL). In a second flask, cesium carbonate (12.5 mg, 38.4 µmol, 3.7 eq.) was dissolved in anhydrous DMSO (1.4 mL). Then, to each of pre-weighed catalysts (0.2 eq./reaction) in DMSO (0.3 mL) was added 0.1 mL of tetraene containing solution and 0.2 mL of base-solution. The resulting solutions were stirred at 40 °C for 8 hours, quenched with a 1 M solution of NH_4Cl (2 mL). These mixtures were loaded onto CHROMABOND C18 ec, 45 µm, 500 mg SPE-cartridges (conditioned: 6 mL MeOH, 6 mL H_2O), washed with MeCN/H_2O (5:95) and eluted with MeCN (3 × 3 mL). The resulting eluates (first MeCN-fraction) were subsequently analyzed by analytical HPLC (column: KNAUER Eurospher II 100-3 C18P; 3 µm; 2.0 × 100 mm eluent: A: MeCN, B: H_2O, gradient: 50% A, 50% B → 100% A,(0–4 min), 100% A, (4-6 min), flowrate: 0.5 mL/min, detection wavelengths: λ = 190-600 nm). The results of the screening are illustrated in figure 30, with $Pd(PPh_3)_4$ being identified as the most suitable catalyst, showing highest conversion and the best isomerization profile.

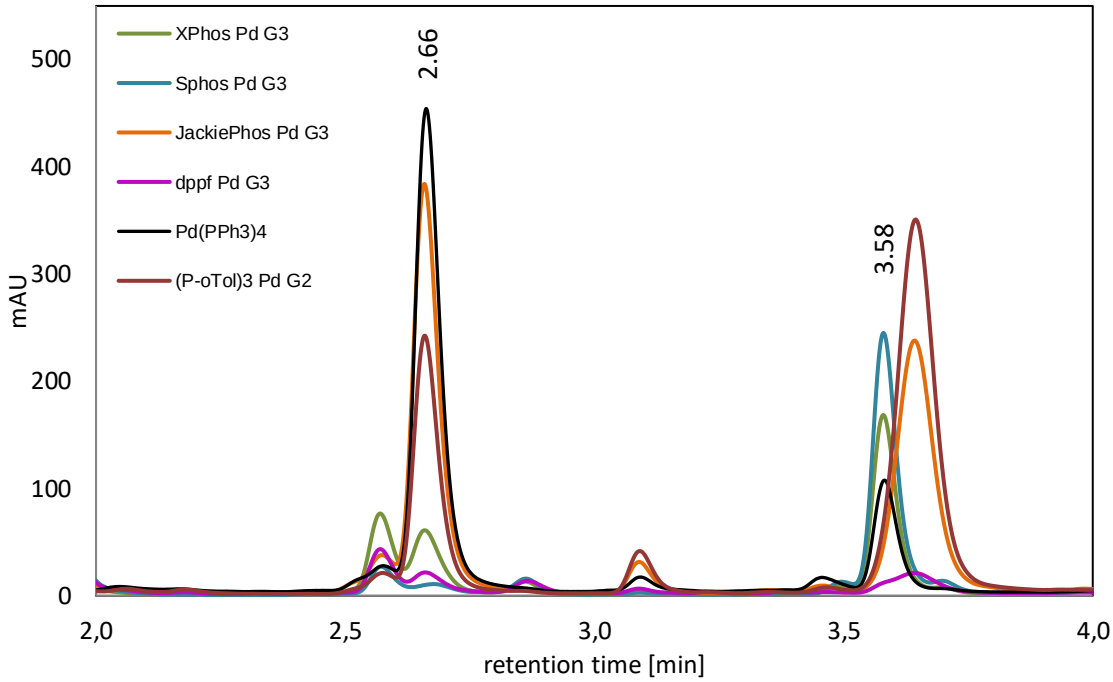

Figure 30. Results and comparison of catalyst screening for the synthesis of hexaene II (**131**). XPhos Pd G3 (green), SPhos Pd G3 (blue), JackiePhos Pd G3 (orange), dppf Pd G3 (violet), $Pd(PPh_3)_4$ (black), $(P\text{-}o\text{-}Tol)_3$ Pd G2 (brown). The starting substrate tetraene V (**135**) appears at a retention time t_R = 3.58 min and the resulting hexaene II (**131**) at t_R = 2.66 min.

8.3.5 Base-screening for Synthesis of Hexaene II (131)

A mixture of tetraene V (**135**) (8.0 mg, 12 µmol, 1.0 eq.) and western fragment II (**122**) (5.8 mg, 18 µmol, 1.5 eq.) was azeotropically dried by co-evaporation with MeCN (3 × 2 mL). Subsequently, the residue was dissolved in anhydrous DMSO (2.4 mL). In a second flask, $Pd(PPh_3)_4$ (2.76 mg, 2.39 µmol, 0.20 eq.) was dissolved in anhydrous DMSO (0.8 mL). Then, to each of pre-weighed bases (3.0 eq./reaction) was added 0.3 mL of tetraene containing solution (1.0 mg, 1.5 µmol, 1.0 eq.) and 0.1 mL of catalyst-solution (0.35 µg, 0.30 µmol, 0.2 eq.). The resulting solutions were stirred at 40 °C.

After 5 hours a small sample of the reaction mixture was drawn via syringe and approx. 5-10 µL of this crude reaction mixture in DMSO was diluted with MeCN (0.5 mL) and analyzed by UV-vis spectroscopy. The analysis was repeated after 19 hours.

Table 19. Measured absorbances and calculated conversions for the polyene iteration step from tetraene V (**135**) to hexaene II (**131**) with various bases after 5 hours and 19 hours; a: Decomposition was observed; b: Formation of a new polyene-peak was observed with λ = 287 nm, 300 nm, 315 nm (indicative of triene) presumably due to coupling of diene **122** with the MIDA-bearing site.

Base	$A_{328\ nm}$ [a.u.], 5 hours	$A_{363\ nm}$ [a.u.], 5 hours	conversion 5 hours	$A_{328\ nm}$ [a.u.], 19 hours	$A_{363\ nm}$ [a.u.], 19 hours	conversion 19 hours
Cs_2CO_3	0.702	0.196	21%	0.344	0.155	26%
CsOAc	0.531	0	-	0.681	0	-
NaOEt	0.515	0.173	21%	0.231	0.114	28%
KO*t*Bu	0[a]	0[a]	-	n.d.[a]	-	-
KOTMS	0[a]	0[a]	-	n.d.[a]	-	-
Tl_2CO_3	0.494	0.635	51	0	0.764	100%
Ag_2O	0.640	0	-	n.d.[b]	n.d.[b]	-
K_3PO_4	0.465	0.425	42%	0	0.885	100%[c]

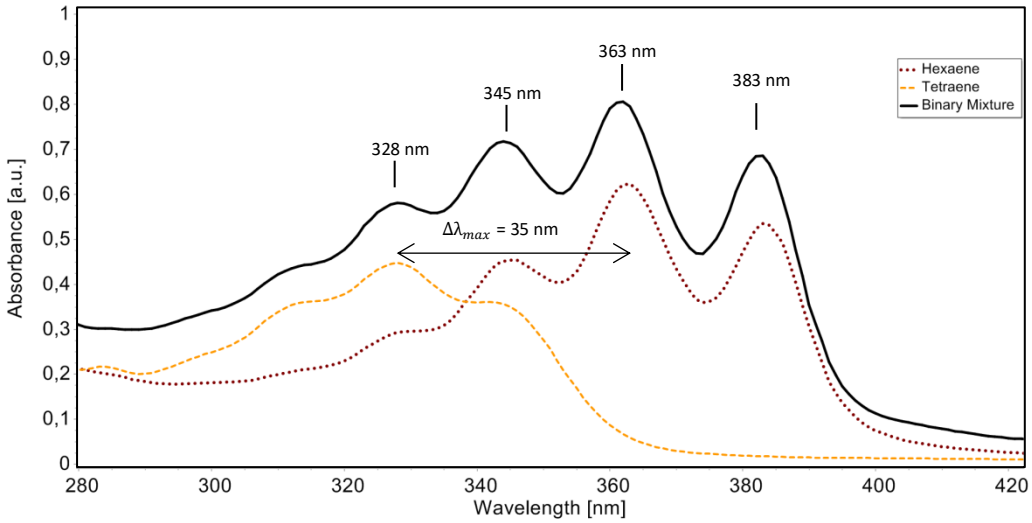

Figure 31. Example of an observed UV-vis spectrum of an incomplete reaction composed of a binary mixture of tetraene V (**135**) and hexane II (**131**) (solid line) superimposed with the spectra of the individual compounds. Key absorbance peaks are noted at λ = 328 nm; 345 nm; 363 nm and 383 nm.

Calculation of product conversions:

The measured absorbance A_{obs} at a given wavelength is the sum of the individual contributions of all compounds absorbing at this wavelength.

(1) $$A_{obs}^{\lambda\,[nm]} = A_{tetraene}^{\lambda\,[nm]} + A_{hexaene}^{\lambda\,[nm]}$$

This represents the sum of the absorbances from both tetraene and hexaene.

Next, applying Lambert-Beer's law, the individual absorbance contributions at specific wavelengths λ = 328 nm and λ = 383 nm) can be written as:

(2) $$A_{obs}^{328} = l \cdot c_{tetraene} \cdot \varepsilon_{tetraene}^{328} + l \cdot c_{hexaene} \cdot \varepsilon_{hexaene}^{328}$$

(3) $$A_{obs}^{383} = l \cdot c_{tetraene} \cdot \varepsilon_{tetraene}^{383} + l \cdot c_{hexaene} \cdot \varepsilon_{hexaene}^{383}$$

Since the extinction coefficient for tetraene **135** at λ = 383 nm is negligible ($\varepsilon_{tetraene}^{383} = 0$), equation (3) simplifies to:

(4) $$A_{obs}^{383} = l \cdot c_{hexaene} \cdot \varepsilon_{hexaene}^{383}$$

This allows us to calculate the concentration of hexaene **131**:

(5) $$c_{hexaene} = \frac{A_{obs}^{383}}{l \cdot \varepsilon_{hexaene}^{383}}$$

We can now substitute this expression for $c_{hexaene}$ back into the equation for the absorbance at λ = 328 nm, which results in:

(6) $$A_{obs}^{328} = l \cdot c_{tetraene} \cdot \varepsilon_{tetraene}^{328} + l \cdot \left(\frac{A_{obs}^{383}}{l \cdot \varepsilon_{hexaene}^{383}}\right) \cdot \varepsilon_{hexaene}^{328}$$

Rearranging this equation allows us to solve for $c_{Tetraene}$:

(7) $$c_{Tetraene} = \frac{A_{obs}^{328} - \left(\frac{A_{obs}^{383}}{\varepsilon_{hexaene}^{383}} \cdot \varepsilon_{hexaene}^{328}\right)}{l \cdot \varepsilon_{tetraene}^{328}}$$

Now that we have expressions for both $c_{Tetraene}$ and $c_{hexaene}$, we can calculate the percentage conversion of tetraene **135** to hexaene **131** using the following formula:

(8) $$\text{conversion}\ (\%) = \frac{c_{Hexaene}}{c_{Tetraene} + c_{Hexaene}} \cdot 100$$

Substituting the expressions for $c_{Tetraene}$ and $c_{hexaene}$ into the conversion formula, we get:

(9) $$\text{conversion} = \frac{\frac{A_{obs}^{383}}{l \cdot \varepsilon_{hexaene}^{383}}}{\left(\left(\frac{A_{obs}^{328} - \left(\frac{A_{obs}^{383}}{\varepsilon_{hexaene}^{383}} \cdot \varepsilon_{hexaene}^{328}\right)}{l \cdot \varepsilon_{tetraene}^{328}}\right) + \frac{A_{obs}^{383}}{l \cdot \varepsilon_{hexaene}^{383}}\right)} \cdot 100$$

8.3.6 Determination of molar absorptivities

HPLC-purified polyenes **135** or **131** were dissolved in MeCN to provide a 1.0 mM stock solution. From this stock solution the following solutions were prepared: 0.05 mM, 0.04 mM, 0.025 mM, 0.0125 mM and 0.01 mM. The solutions were measured by UV-vis spectroscopy and the measured absorbance was plotted against concentration. The extinction coefficients were calculated by $\varepsilon(\lambda) = (dA(\lambda)/dc)/l$ (l = 1.25 cm) according to *Lambert-Beer*'s law.

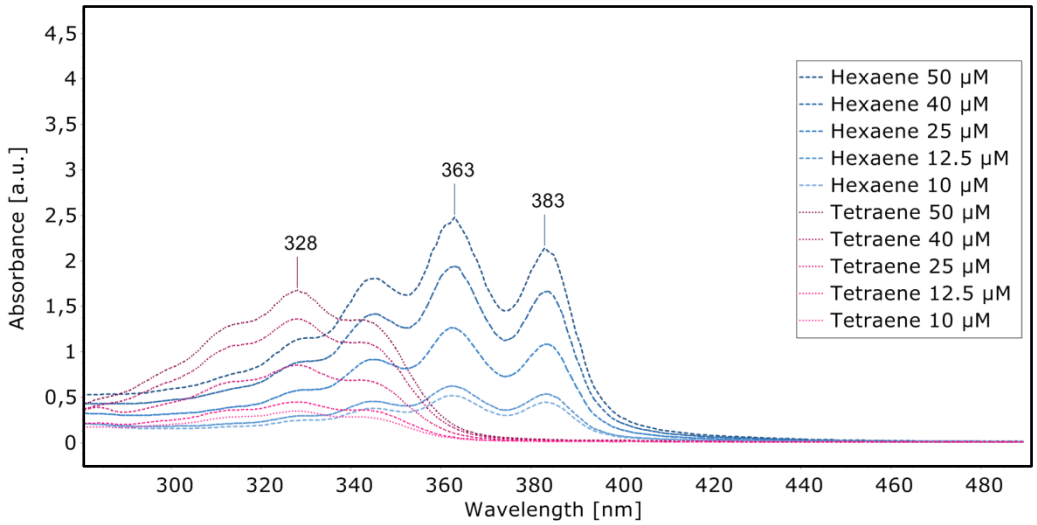

Figure 30. Consolidated UV-vis spectra of the dilution series of tetraene V (**135**) (red dotted lines) and hexaene II (**131**) (blue dashed lines) at concentrations varying from 10 µM to 50 µM.

Table 20. Measured absorbances [a.u.] of the dilution series of tetraene V (**135**) at λ = 328 nm and hexaene II (**131**) at λ = 328 nm and 383 nm at concentrations varying from 10 µM to 50 µM and calculated extinction coefficients (bottom row).

c [µM]	A_{328} nm (tetraene)	A_{328} nm (hexaene)	A_{383} nm (hexaene)
50	1.67	1.14	2.14
40	1.36	0.879	1.66
25	0.852	0.575	1.08
12.5	0.448	0.292	0.535
10	0.350	0.240	0.445
ε [L mol^{-1} cm^{-1}]	**27074**	**18052**	**39510**

8.3.7 Comparison of hexaene II NMR-data with published data of bacillaene

Table 21. Comparison of ^{1}H- and ^{13}C-chemical shifts for the 1′-18′ and 1′′-6′′ identical structural units of bacillaene (**1**)[14] (600 MHz) and hexaene II (**131**) in MeOD (700 MHz).

	Bacillaene (**1**) (MeOD)		**131** (MeOD)	
position	δ_C, type	δ_H	δ_C, type, (Δδ)	δ_H, (Δδ)
1′	170.2, C		172.9, C, (**2.7**)	
2′	41.8, CH_2	2.69	44.5, CH_2, (**2.7**)	2.41, (**0.28**)
		2.45		2.21, (**0.24**)
3′	66.0, CH	5.27	69.4, CH, (**3.4**)	5.25, (0.02)
4′	140.3, C		142.1, C, (**1.8**)	
5′	122.1, CH	6.56	123.0, CH, (0.9)	6.43 (0.13)
6′	123.9, CH	6.44	125.4, CH, (1.5)	6.43, (0.01)
7′	124.3, CH	6.36	125.7, CH (1.4)	6.35, (0.01)
8′	127.0, CH	6.69	128.2, CH (1.2)	6.64, (0.05)
9′	136.1, C		137.6, C, (1.5)	
10′	138.4, CH	6.45	139.9, CH, (1.5)	6.44, (0.01)
11′	123.4, CH	6.82	124.9, CH, (1.5)	6.81 (0.01)
12′	129.8, CH	6.11	131.2, CH, (1.4)	6.08, (0.03)
13′	128.0, CH	6.02	129.5, CH, (1.5)	5.99, (0.03)
14′	126.8, CH	6.78	128.4, CH, (1.6)	6.76, (0.02)
15′	129.7, CH	5.74	131.2, CH, (1.5)	5.71, (0.03)
16′	40.1, CH_2	3.94	41.6, CH_2, (1.5)	3.92, (0.02)
17′	17.2, CH_3	1.96	18.7, CH_3, (1.5)	1.88, (0.08)
18′	11.2, CH_3	1.95	12.6, CH_3, (1.4)	1.95, (0.00)
1′′	176.7, C		177.8, C, (1.1)	
2′′	69.8, CH	4.08	71.5, CH, (1.7)	4.05, (0.03)
3′′	43.4, CH_2	1.55	45.0, CH_2, (1.6)	1.54, (0.01)
4′′	24.0, CH	1.88	25.6, CH, (1.6)	1.80, (0.08)
5′′	20.2, CH_3	0.98	21.8, CH_3, (1.6)	0.95, (0.03)
6′′	22.7, CH_3	0.97	24.0, CH_3, (1.3)	0.95, (0.02)

8.3.8 Testsystems for the final *Suzuki* coupling

(2*S*,3*E*,5*E*)-8-((*tert*-butyl)oxycarbonylamino)-2-methylocta-3,5-dienoic acid (249)

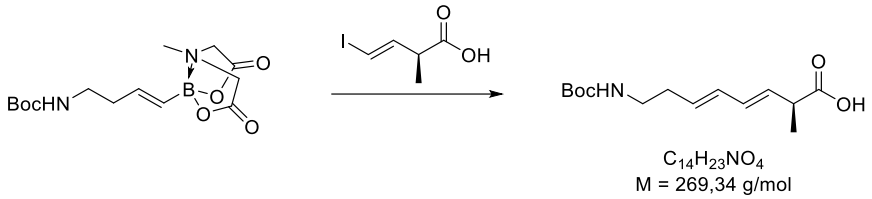

$C_{14}H_{23}NO_4$
M = 269,34 g/mol

Reproduced with permission from *Johannes Herbst*.[155]

Eastern fragment (**119**) (10.3 mg, 45.6 µmol, 1.00 eq.), MIDA boronate **133** (18.3 mg, 56.1 µmol, 1.23 eq.), and XPhos Pd G3 (2.0 mg, 2.3 µmol, 5 mol-%) were added to a schlenk flask under ambient conditions. The vial was sealed and was placed under Ar atmosphere. The solids were suspended in a solution of NaOH (0.4 M in THF/H_2O 5:1, 650 µL, 270 µmol, 6.00 eq.). The reaction mixture was stirred overnight at room temperature. Then, the mixture was transferred to a separatory funnel and was diluted with saturated aqueous NH_4Cl (5 mL). Et_2O (15 mL) was added, the phases were separated and the aqueous phase was extracted with Et_2O (3 × 15 mL). The combined organic layers were washed with brine (20 mL), dried over $MgSO_4$, filtered, and concentrated *in vacuo.* The crude residue was purified by column chromatography (Silica, CH/EtOAc 7:3) to yield the product **249** as a colorless solid. $\mathbf{R_f}$ = 0.30 (CH/EtOAc 7:3); $\boldsymbol{\alpha_D^{20}}$ = +21.0 (c = 1.0, MeOH); **^{1}H-NMR** (500 MHz, acetone-d6) δ = 1.22 (d, *J* = 7.0 Hz, 3H), 1.38 (s, 9H), 2.29–2.21 (m, 2H), 3.20-3.08 (m, 3H), 5.75–5.59 (m, 2H), 5.93 (s, 1H), 6.18–6.05 (m, 2H); **^{13}C-NMR** (126 MHz, acetonde-d6) δ = 17.6, 28.6, 34.0, 40.8, 43.0, 78.4, 131.7, 132.0, 132.0, 132.4, 156.6, 175.5; **HRMS** (ESI): m/z calc for $[M+Na]^+$: 292.1519; found: 292.1517.

(rac,*E*)-3-((*tert*-butyldimethylsilyl)oxy)-*N*-(4-(6-methyl-1,3,6,2-dioxazaborocane-4,8-dione-2-yl)but-3-en-1-yl)butanamide (254)

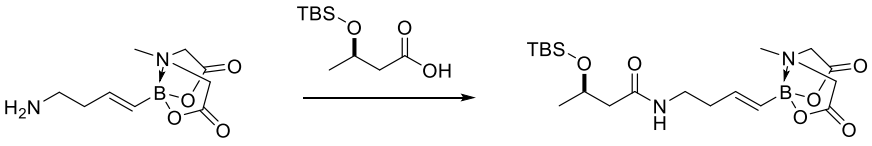

$C_{19}H_{35}BN_2O_6Si$
M = 426,39 g/mol

To a solution of Carboxylic acid **253** (300 mg, 1.37 mmol, 1.01 eq.) in anhydrous DCM (10 mL) was sequentially added amine-TFA-salt **228** (472 mg, 1.39 mmol, 1.01 eq.), DMAP (218 mg, 1.79 mmol, 1.30 eq.) and finally EDC-HCl (369 mg, 1.92 mmol, 1.40 eq.). The resulting suspension was stirred at r.t. for 13 hours. Afterwards, EtOAc (50 mL) was added and the mixture was transferred to a sep funnel.

Water (50 mL) was added, phases were separated and the organic layer was washed with water (2 × 50 mL), sat. NH_4Cl (2 × 50 mL) and brine (50 mL), dried over $MgSO_4$, filtered and concentrated. The obtained colorless solid (511 mg, 1.20 mmol, 87%) was used in the subsequent step without further purification. $\mathbf{R_f}$ = 0.20 (EtOAc); **^{1}H-NMR** (500 MHz, acetone-d6) δ = 0.06 (d, *J* = 10.6 Hz, 6H), 0.87 (s, 9H), 1.15 (d, *J* = 6.1 Hz, 3H), 2.16–2.23 (m, 1H), 2.25–2.34 (m, 3H), 2.99 (s, 3H), 3.14–3.25 (m, 1H), 3.33 (dq, *J* = 13.4, 6.9 Hz, 1H), 4.00 (dd, *J* = 16.9, 2.0 Hz, 2H), 4.17 (dd, *J* = 16.8, 0.7 Hz, 2H), 4.23–4.35 (m, 1H), 5.54 (dt, *J* = 17.7, 1.5 Hz, 1H), 6.06 (dt, *J* = 17.7, 6.6 Hz, 1H), 7.09 (s, 1H); **^{13}C-NMR** (126 MHz, acetonde-d6) δ = −5.6, −5.3, 17.7, 23.4, 25.3, 35.6, 38.5, 46.3, 46.5, 61.2, 66.2, 142.3, 168.2, 170.0; [note: the carbon attached to boron was not observed due to quadrupole broadening caused by the ^{11}B nucleus]; **HRMS** (ESI): m/z calc for $[M+H]^+$: 427.2443; found: 427.2434.

8.4 Synthetic procedures for the enamide fragments

8.4.1 *N*-acylation approach

methyl (*Z*)-3-((*S*,*Z*)-3-((tert-butyldimethylsilyl)oxy)-4-methylhept-4-en-6-ynamido)but-2-enoate (257)

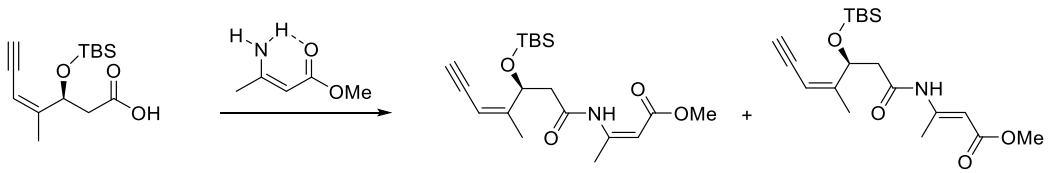

$C_{19}H_{31}NO_4Si$
M = 365.55 g/mol

$C_{19}H_{31}NO_4Si$
M = 365.55 g/mol

Acid **129** (50.0 mg, 186 µmol, 1.00 eq.) was dissolved in anhydrous DCM (5 mL) under argon and five drops of DMF were added, followed by dropwise addition of oxalyl chloride (2 M in DCM, 90 µL, 100 µmol, 0.97 eq.) via syringe. Stirring continued for 1 h at r.t. to ensure full conversion to the acid chloride. The resulting solution was then transferred to a solution of methyl 3-aminocrotonate (**92**) (32 mg, 0.28 mmol, 1.5 eq.) and pyridine (68 µL, 0.84 mmol, 4.5 eq.) in DCM (2 mL) at 0 °C and the mixture was stirred for 30 min. Then, the reaction was quenched by addition of water (5 mL) and diluted with EtOAc. Phases were separated and aqueous layer was extracted with EtOAc (3 × 10 mL). The combined organic layers were washed with 0.5 M HCl (2 × 5 mL), sat. $NaHCO_3$ (2 × 5 mL) and brine (2 × 5 mL), dried with $MgSO_4$ and filtered. After evaporation of the solvent, the crude product was purified by column chromatography (Silica, CH/EtOAc 9:1), the desired (*Z*)-enamide (**257**) was obtained as a colorless oil (11.8 mg, 41.1 µmol, 22%) and the (*E*)-enamide side-product **258** was isolated as a white solid (22.0 mg, 77 µmol, 41%). (*Z*)-enamide (**257**): $\mathbf{R_f}$ = 0.43 (CH/EtOAc 9:1); $\boldsymbol{\alpha_D^{20}}$ = +74.8 (c = 1.0, MeCN); **^{1}H-NMR** (500 MHz, acetone-d6) δ = 0.06 (d, *J* = 5.4 Hz, 6H), 0.85 (s, 9H), 1.86 (dd, *J* = 1.7, 0.7 Hz, 3H), 2.37

(d, *J* = 1.1 Hz, 3H), 2.37–2.41 (m, 1H), 2.60 (dd, *J* = 13.6, 9.9 Hz, 1H), 3.67 (s, 4H), 4.97 (q, *J* = 1.1 Hz, 1H), 5.41 (s, 1H), 5.43 (d, *J* = 3.3 Hz, 1H), 11.16 (s, 1H); **^{13}C-NMR** (126 MHz, acetone-d6) δ = −5.1, −4.8, 16.9, 18.5, 22.0, 26.0, 45.9, 51.3, 71.0, 80.3, 84.0, 96.4, 105.8, 154.8, 155.9, 169.6, 170.0; **HRMS** (APCI): m/z calc for $[M+H]^+$: 366.2095; found: 366.2096; (*E*)-enamide (**258**): $\mathbf{R_f}$ = 0.05 (CH/EtOAc 9:1); $\boldsymbol{\alpha_D^{20}}$ = +21.2 (c = 0.5, MeCN); **^{1}H-NMR** (500 MHz, acetone-d6) δ = 0.06 (d, *J* = 6.3 Hz, 6H), 0.86 (s, 9H), 1.80 (dd, *J* = 1.6, 0.7 Hz, 3H), 2.27 (dd, *J* = 13.6, 3.2 Hz, 1H), 2.32 (d, *J* = 0.9 Hz, 3H), 2.70 (dd, *J* = 13.6, 10.0 Hz, 1H), 3.60 (s, 3H), 3.66–3.68 (m, 1H), 5.38 (dtd, *J* = 3.3, 1.6, 0.8 Hz, 1H), 5.42 (dd, *J* = 10.0, 3.2 Hz, 1H), 6.93 (q, *J* = 0.9 Hz, 1H), 8.79 (s, 1H); ^{13}C NMR (126 MHz, acetone-d6) δ = −5.0, −4.8, 17.0, 18.1, 18.6, 26.1, 44.8, 50.7, 70.8, 80.4, 83.8, 101.5, 105.7, 151.1, 154.8, 169.1, 170.5; **HRMS** (APCI): m/z calc for $[M+H]^+$: 366.2095; found: 366.2096.

(rac)-methyl 3-((*tert*-butyldimethylsilyl)oxy)butanoate (S-14)

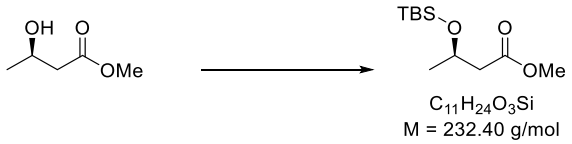

The synthesis was carried out according to a known literature procedure:[224]

Methyl-3-hydroxybutyrat (2.86 g, 24.2 mmol, 1.00 eq.), imidazole (2.52 g, 37.1 mmol, 1.50 eq.) and *tert*-butyldimethylsilylchlorid (4.45 g, 29.2 mmol, 1.20 eq.) were dissolved in anhydrous DMF (50 mL). The reaction mixture was stirred at r.t. for 16 h. Then the solvent was removed pressure, to the residue was added saturated $NaHCO_3$ (20 mL) and the mixture was extracted with Et_2O (3 x 20 mL). The combined organic layers were washed with saturated aqueous NH_4Cl (10 mL), brine (10 mL), dried over anhydrous $MgSO_4$, filtered and concentrated to yield the product **S-14** as a colorless oil, which was used in the subsequent step without further purification (3.18 g, 13.8 mmol, 57%). $\mathbf{R_f}$ = 0.32 (CH/EtOAc 20:1); **^{1}H-NMR** (500 MHz, $CDCl_3$) δ = 0.04 (s, 3H), 0.06 (s, 3H), 0.86 (s, 9H), 1.19 (d, *J* = 6.1 Hz, 3H), 2.37 (dd, *J* = 14.5, 5.2 Hz, 1H), 2.48 (dd, *J* = 14.5, 7.7 Hz, 1H), 3.66 (s, 3H), 4.17–4.41 (m, 1H); **^{13}C-NMR** (126 MHz, $CDCl_3$) δ = −4.9, −4.4, 18.1, 24.1, 25.9, 44.9, 51.6, 66.0, 172.2; **HRMS (APCI)**: m/z calc for $[M+H]^+$: 233.1567; found: 233.1566. The spectroscopic are in agreement with those previously reported.[224]

(*rac*)-3-((*tert*-butyldimethylsilyl)oxy)butanoic acid (253)

$C_{10}H_{22}O_3Si$
M = 218.37 g/mol

The synthesis was carried out according to a known literature procedure:[225]

Compound **S-13** (2.51 g, 10.8 mmol, 1.00 eq.) was dissolved in MeOH (100 mL) and aqueous NaOH (1 M, 55 mL, 55 mmol, 5.1 eq.) was added. The reaction mixture was stirred at r.t. for 72 h. Then, the MeOH was removed under reduced pressure and the obtained residue was washed with Et_2O (2 x 15 mL). The aqueous layer was acidified with aqueous HCl (2.5 M, 17 mL) to pH 1 and subsequently extracted with Et_2O (3 x 15 mL). The combined organic layers were dried over anhydrous $MgSO_4$, filtered and the solvent was removed under reduced pressure to yield the product **253** as a colorless oil (1.56 g, 7.14 mmol, 66%). $\mathbf{R_f}$ = 0.34 (CH/EtOAc 4:1); **^{1}H-NMR** (500 MHz, acetone-d6) δ = 0.07 (s, 3H), 0.09 (s, 3H), 0.87 (s, 9H), 1.20 (d, *J* = 6.2 Hz, 3H), 2.36–2.44 (m, 2H), 4.30 (dp, *J* = 6.9, 6.1 Hz, 1H), 10.52 (s, 1H); **^{13}C-NMR** (126 MHz, acetone-d6) δ = −4.8, −4.4, 18.5, 24.2, 26.2, 45.0, 66.7, 172.5; **HRMS (ESI)**: m/z calc for $[M+H]^+$: 219.1411; found: 219.1414. The spectroscopic are in agreement with those previously reported.[225]

(rac)-methyl (*Z*)-3-(3-((*tert*-butyldimethylsilyl)oxy)butanamido)but-2-enoate (259)

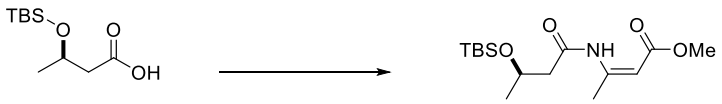

$C_{15}H_{29}NO_4Si$
M = 315.49 g/mol

Carboxylic acid **253** (5.70 g, 26.1 mmol, 1.00 eq.) was dissolved in anhydrous DCM (120 mL) under argon. DMF (0.10 mL, 1.29 mmol, 0.05 eq.) was added, followed by dropwise addition of oxalyl chloride (2.35 mL, 27.4 mmol, 1.05 eq.) via syringe over 5 minutes. Stirring continued for 30 minutes at r.t. to ensure full conversion to the acid chloride. The resulting solution was then transferred to a solution of methyl-3-aminocrotonate (**92**) (4.96 g, 43.1 mmol, 1.65 eq.) and pyridine (10.1 mL, 125 mmol, 4.80 eq.) in anhydrous DCM (50 mL) at 0 °C. The solution was stirred for 60 minutes. The crude product was loaded onto Celite® and purified by column chromatography (Silica, CH/EA 10:1) to give the product **259** as a pale yellow oil (1.75 g, 5.55 mmol, 21%). $\mathbf{R_f}$ = 0.27 (CH/EtOAc 10:1); **^{1}H-NMR** (500 MHz, acetone-d6) δ = 0.03 (s, 3H), 0.08 (s, 3H), 0.85 (s, 9H), 1.23 (d, *J* = 6.1 Hz, 3H), 2.35 (d, *J* = 1.1 Hz, 3H), 2.36–2.40 (m, 1H), 2.48 (dd, *J* = 13.8, 4.0 Hz, 1H), 3.66 (s, 3H), 4.32 (dqd, *J* = 8.6, 6.1, 4.0 Hz, 1H), 4.95 (q, *J* = 1.2 Hz, 1H),

11.11 (s, 1H); **^{13}C-NMR** (126 MHz, acetone-d6) δ = −4.9, −4.4, 18.5, 22.0, 24.4, 26.1, 49.5, 51.2, 67.2, 96.2, 156.0, 170.0, 170.5; **HRMS (ESI)**: m/z calc for $[M+H]^+$: 316.1939; found: 316.1943.

(rac)-(*Z*)-3-(3-((*tert*-butyldimethylsilyl)oxy)butanamido)-*N*-methoxy-*N*-methylbut-2-enamide (261)

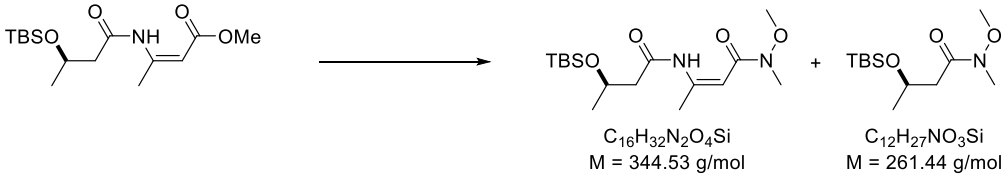

Enamidoester **259** (150 mg, 475 µmol, 1.00 eq.) and *N*,*O*-dimethylhydroxylammonium hydrochloride (144 mg, 1.47 mmol, 3.10 eq.) were dissolved in anhydrous THF (2 mL) and cooled to 0 °C, followed by dropwise addition of *iso*propylmagnesium chloride (2 M in THF, 1.50 mL, 3.00 mmol, 6.30 eq.). The resulting solution was allowed to warm to r.t. while stirring continued for 5 hours. After addition of a saturated aqueous solution of NH_4Cl (5 mL) and EtOAc (10 mL), phases were separated and the aqueous layer was extracted with EtOAc (2 x 10 mL). The combined organic layers were washed with 5 M aqueous HCl (10 mL) and brine (10 mL), dried over $MgSO_4$, filtered and concentrated. The crude product was purified by column chromatography (CH/EtOAc 7:2) to afford the desired compound **261** with the coeluting side product **262** as a colorless oil (130 mg, 377 µmol, 79%). $\mathbf{R_f}$ = 0.32 (CH/EtOAc 3:1); **^{1}H-NMR** (500 MHz, acetone-d6) δ = 0.03–0.09 (m, 9H), 0.85 (s, 9H), 1.22 (d, *J* = 6.1 Hz, 3H), 2.30–2.36 (m, 1H), 2.36 (d, *J* = 1.2 Hz, 3H), 2.41 (dd, *J* = 13.8, 4.2 Hz, 1H), 3.15 (s, 3H), 3.70 (s, 3H), 4.32 (ddq, *J* = 12.3, 8.5, 4.7 Hz, 1H), 5.45 (q, *J* = 1.2 Hz, 1H), 12.11 (s, 1H); **^{13}C-NMR** (126 MHz, acetone-d6) δ = −5.8, −5.3, 17.6, 21.6, 23.5, 25.2, 31.1, 48.7, 61.0, 66.3, 93.5, 153.1, 169.2, 169.4; **HRMS (ESI)**: m/z calc for $[M+H]^+$: 345.2204; found: 345.2200.

8.4.2 *Peterson* elimination approach

(*Z*)-3-iodobut-2-en-1-ol (273)

C_4H_7IO
M = 198.00 g/mol

The synthesis was carried out according to a known literature procedure:[210]

To a solution of Red-Al® in toluene (60 wt-%, 34.0 mL, 105 mmol, 1.40 eq.) in Et_2O (150 mL) was added 2-butyne-1-ol (**271**) (5.60 mL, 74.9 mmol, 1.00 eq.) at 0 °C. The resulting reaction mixture was stirred at r.t. for 4 hours. Then, the solution was recooled to 0 °C and EtOAc (20 mL) and iodine (28.0 g, 110 mmol, 1.5 eq.) were added to the mixture under dark. The resulting solution was stirred in the dark for further 14 hours before being quenched with a saturated solution of $Na_2S_2O_3$ (100 mL). The emulsion was diluted with 2.5 M HCl (100 mL), layers were separated and the aqueous layer was extracted with EtOAc (3 x 100 mL). The combined organic layers were washed with brine (100 mL), dried over $MgSO_4$, filtered over a plug of silica and concentrated. After removal of the solvent, the crude product **273** (14.23 g, 71.87 mmol, 96%) was received as a yellow oil, which was used in the next step without further purification. An aliquant (150 mg) was purified by column chromatography (Silica, CH/EtOAc 4:1) to provide an analytical sample. $\mathbf{R_f}$ = 0.22 (CH/EtOAc 4:1); **^{1}H-NMR** (500 MHz, acetone-d6) δ = 2.50 (q, *J* = 1.5 Hz, 3H), 3.91 (t, *J* = 5.6 Hz, 1H), 4.06 (tq, *J* = 5.6, 1.5 Hz, 2H), 5.76 (tq, *J* = 5.5, 1.6 Hz, 1H); **^{13}C-NMR** (126 MHz, acetone-d6) δ = 33.7, 67.7, 99.4, 137.1; ; **HRMS (EI)**: m/z calc for $[M]^{+\cdot}$: 197.9542; found: 197.9535. The spectroscopic are in agreement with those previously reported.[210]

(*Z*)-((3-iodobut-2-en-1-yl)oxy)trimethylsilane (274)

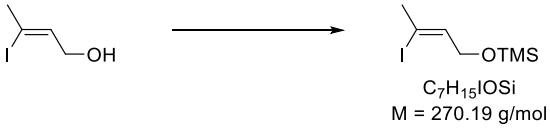

$C_7H_{15}IOSi$
M = 270.19 g/mol

To a solution of allyl alcohol **273** (14.8 g, 74.8 mmol, 1.00 eq.) in anhydrous DMF (60 mL) was added pyridine (13.0 mL, 160 mmol, 2.15 eq.) and the resulting solution was cooled to 0 °C. Then, chlorotrimethylsilane (13.0 mL, 103 mmol, 1.37 eq.) was added over 2 minutes and the resulting mixture was stirred overnight. After the indicated time, the reaction mixture was diluted with Et_2O (150 mL) and cooled to 0 °C, followed by addition of phosphate buffer (pH 7, 100 mL). Phases were separated and the

aqueous layer was extracted with Et_2O (2 x 200 mL). The combined organic layers were washed with water (4 x 100 mL) and brine (100 mL), dried over $MgSO_4$, filtered and concentrated. After evaporation of the solvent, the crude product **274** was obtained as a red-brown oil (18.9 g, 70.0 mmol, 93%). An aliquant (100 mg) was purified by column chromatography (CN-Phase, Cyclohexane) [note: the compound is unstable on silica] and yielded pale yellow oil. $\mathbf{R_f}$ = 0.67 (CH/EtOAc 4:1), 0.58 (CN-phase, CH); **^{1}H-NMR** (500 MHz, acetone-d6) δ = 0.11 (s, 9H), 2.51 (q, *J* = 1.5 Hz, 3H), 4.15 (dq, *J* = 5.6, 1.4 Hz, 2H), 5.73 (tq, *J* = 5.6, 1.6 Hz, 1H); **^{13}C-NMR** (126 MHz, acetone-d6) δ = −0.3, 33.7, 68.4, 99.9, 136.2; **HRMS (APCI)**: m/z calc for $[M+H]^+$: 271.0010; found: 271.0010.

(*Z*)-3-(trimethylsilyl)but-2-en-1-ol (270)

To a solution of TMS-ether **271** (13.0 g, 48.1 mmol, 1.00 eq.) in anhydrous THF (250 mL) at −78 °C was added *t*-BuLi (1.7 M in pentane, 58.0 mL, 98.6 mmol, 2.05 eq.) and the resulting solution was stirred at −78 °C for 30 minutes and at room temperature for 30 minutes. The reaction was diluted with Et_2O (200 mL) and quenched with saturated solution of NH_4Cl (150 mL). Layers were separated and the aqueous layer was extracted with Et_2O (2 x 150 mL). The combined organic layers were washed with brine (100 mL), dried over $MgSO_4$, filtered and concentrated. After evaporation of the solvent, the crude product was purified by *Kugelrohr* distillation (b.p. =110 °C, 167 mbar) and the product was received as a colorless liquid (6.64 g, 46.0 mmol, 96%). $\mathbf{R_f}$ = 0.35 (CH/EtOAc 3:1), **^{1}H-NMR** (500 MHz, acetone-d6) δ = 0.13 (s, 9H), 1.78 (q, *J* = 1.4 Hz, 3H), 3.54 (t, *J* = 5.4 Hz, 1H), 4.10 (ddq, *J* = 6.7, 5.4, 1.2 Hz, 2H), 6.13 (tq, *J* = 6.7, 1.7 Hz, 1H); **^{13}C-NMR** (126 MHz, acetone-d6) δ = −0.1, −0.1, 24.7, 61.9, 137.0, 143.5; **HRMS (ESI)**: m/z calc for $[M+H]^+$: 145.1043; found: 145.1044.

(2*S,3*R**)-3-methyl-3-(trimethylsilyl)oxiran-2-yl)methanol (269)**

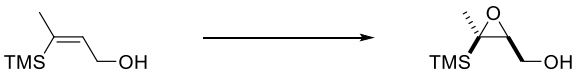

$C_7H_{16}O_2Si$
M = 160.29 g/mol

To a solution of allyl alcohol **270** (633 mg, 4.39 mmol, 1.00 eq.) in DCM (12 mL) was added *m*CPBA (75 wt-%, 1.20 g, 5.26 mmol, 1.20 eq.) at 0 °C. The ice bath was removed and the resulting solution was stirred at r.t for one hour. Then, the solvent was removed and EtOAc (20 mL) was added. A saturated solution of $Na_2S_2O_3$ (10 mL) was added and the mixture was stirred for further 20 minutes. Phases were separated and the aqueous phase was extracted with EtOAc (2 x 20 mL). The combined organic layers were washed with a saturated solution of $NaHCO_3$ (3 x 20 mL) and brine (20 mL), dried over $MgSO_4$, filtered and concentrated. The crude product **269** was obtained as a colorless oil (680 mg, 4.24 mmol, 97%) and used in the next step without further purification. An analytical sample was obtained by column chromatography (Silica, CH/EtOAc 3:1). $\mathbf{R_f}$ = 0.24 (CH/EtOAc 3:1); **^{1}H-NMR** (500 MHz, acetone-d6) δ = 0.10 (s, 9H), 1.20 (s, 3H), 2.84 (dd, *J* = 6.8, 4.2 Hz, 1H), 3.52 (ddd, *J* = 11.8, 6.8, 5.1 Hz, 1H), 3.70 (ddd, *J* = 11.8, 6.3, 4.2 Hz, 1H), 3.91 (dd, *J* = 6.3, 5.1 Hz, 1H); **^{13}C-NMR** (126 MHz, acetone-d6) δ = −1.8, 22.9, 53.7, 62.9, 66.7, 66.7; **HRMS (ESI)**: m/z calc for $[M+H]^+$: 161.0995; found: 161.0992.

(2*S,3*R**)-3-Methyl-3-(trimethylsilyl)oxirane-2-carbaldehyde (268)**

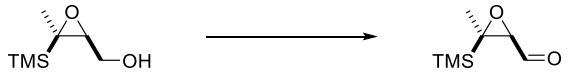

$C_7H_{14}O_2Si$
M = 158.27 g/mol

To a stirred mixture of the epoxy alcohol **269** (400 mg, 2.50 mmol, 1.00 eq.) in DCM (3.5 mL), DMSO (3.5 mL, 50 mmol, 20 eq.) and triethylamine (3.5 mL, 25 mmol, 10 eq.) was added SO_3-pyridine complex (2.4 g, 15 mmol, 6.0 eq.) in two portions at 0 °C. After the resulting solution had been stirred for 30 minutes, it was diluted with Et_2O/*n*-pentane (1:1, 30 mL). The organic layer was washed successively with water (10 mL), 1 M aqueous HCl (10 mL), and saturated $NaHCO_3$ (10 mL). After drying over $MgSO_4$ and careful removal of the solvent under reduced pressure [30 °C bath temperature due to volatility], the obtained crude product **268** was obtained as a yellow oil and used in the next step without further purification. Full conversion was judged by ^{1}H-NMR analysis. $\mathbf{R_f}$ = 0.41 (CH/EtOAc 9:1), **^{1}H-NMR** (400 MHz, acetone-d6) δ = 0.18 (s, 9H), 1.43 (s, 3H), 2.55 (s, 1H), 9.12 (s, 1H).

trimethyl((2*R,3*S**)-2-methyl-3-((*E*)-2-(4,4,5,5-tetramethyl-1,3,2-dioxaborolan-2-yl)vinyl)oxiran-2-yl)silane (267)**

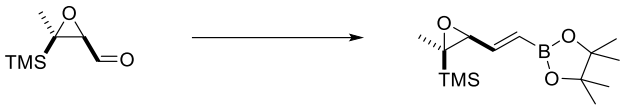

$C_{14}H_{27}BO_3Si$
M = 282.26 g/mol

To a solution of bis(pinacolato)boryl methane (1.17 g, 4.37 mmol, 1.75 eq.) in anhydrous THF (15 mL) at 0 °C was added a solution of LiTMP (569 mg, 3.87 mmol, 1.55 eq.) in THF (10 mL) resulting in a brown cloudy mixture. The ice bath was removed and the mixture was stirred at r.t. for 15 minutes. Then, the solution was cooled to 0 °C and a solution of aldehyde **268** (395 mg, 2.50 mmol, 1.00 eq.) in THF (5 mL) was added. The ice bath was removed and the resulting solution was stirred at r.t. for 1.5 hours. The reaction was quenched by addition of water (30 mL) and Et_2O (20 mL). Phases were separated and the aqueous layer was extracted with Et_2O (3 x 30 mL). The combined organic layers were washed with brine (20 mL), dried over $MgSO_4$, filtered and concentrated. After removal of the solvent, the crude product was purified by column chromatography (CN-Silica, CH/EtOAc 20:1) and was received as a colorless oil (129 mg, 457 µmol, 18%). [note: as most of the product is lost during the purification due to coelution, one should consider performing the organic/organic extraction as carried out for Sn-B(pin)-licnhpin II (**121**). This purification protocol was not yet developed during the synthesis of this compound and could drastically enhance this synthetic procedure.] $\mathbf{R_f}$ = 0.25 (CH/EtOAc 20:1), **^{1}H-NMR** (500 MHz, acetone-d6) δ = 0.10 (s, 9H), 1.23 (d, *J* = 1.4 Hz, 12H), 1.25 (d, *J* = 2.3 Hz, 3H), 3.21 (dd, *J* = 7.7, 1.0 Hz, 1H), 5.81 (dd, *J* = 18.0, 0.9 Hz, 1H), 6.41 (dd, *J* = 18.1, 7.7 Hz, 1H); **^{13}C-NMR** (126 MHz, acetone-d6) δ = −1.8, 22.8, 25.0, 25.1, 57.7, 66.3, 84.0, 151.2; [note: the product was <u>not detected</u> by mass spectrometry].

(*Z*)-3-(trimethylsilyl)but-2-en-1-al (277)

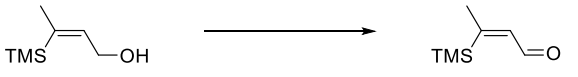

$C_7H_{14}OSi$
M = 142.27 g/mol

To a stirred mixture of allyl alcohol **270** (500 mg, 3.47 mmol, 1.00 eq.) in DCM (5 mL), DMSO (5 mL) and triethylamine (5.0 mL, 36 mmol, 11 eq.) was added SO_3-pyridine complex (3.31 g, 20.8 mmol, 6.00 eq.) in two portions at 0 °C. After the resulting solution had been stirred for 30 minutes, it was diluted with Et_2O/*n*-pentane (1:1, 20 mL). The organic layer was washed successively with water (10 mL), 1 M HCl (10 mL), a saturated solution of $NaHCO_3$ (10 mL) and brine (10 mL). After drying over $MgSO_4$ and removal of most of the solvent on a rotary evaporator [30 °C bath temperature, the product is highly volatile], the

residual oil was used without further purification. Full conversion to the aldehyde **277** was confirmed by ^{1}H-NMR analysis. **^{1}H-NMR** (300 MHz, acetone-d6) δ = 0.31 (s, 9H), 2.11 (d, *J* = 1.6 Hz, 3H), 6.37–6.49 (m, 1H), 9.89 (d, *J* = 8.3 Hz, 1H).

trimethyl((2*Z*,4*E*)-5-(4,4,5,5-tetramethyl-1,3,2-dioxaborolan-2-yl)penta-2,4-dien-2-yl)silane (278)

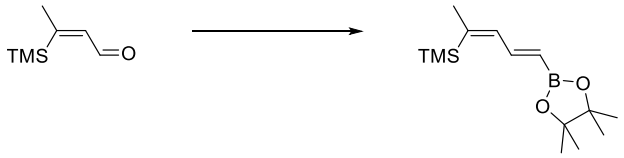

$C_{14}H_{27}BO_2Si$
M = 266.26 g/mol

To a solution of bis(pinacolato)boryl methane (2.60 mg, 9.70 mmol, 1.40 eq.) in anhydrous THF (15 mL) at 0 °C was added a solution of LiTMP (1.43 g, 9.70 mmol, 1.40 eq.) in anhydrous THF (10 mL) resulting in a brown cloudy mixture. The ice bath was removed and the mixture was stirred at room temperature for 15 minutes. Then, the solution was cooled to 0 °C and a solution of aldehyde **277** (986 mg, 6.93 mmol, 1.00 eq.) in anhydrous THF (5 mL) was added. The ice bath was removed and the resulting solution was stirred at r.t. for 1.5 hours. The reaction was quenched by addition of water (30 mL) and Et_2O (20 mL). Phases were separated and the aqueous layer was extracted with Et_2O (3 x 30 mL). The combined organic layers were washed with brine (20 mL), dried over $MgSO_4$, filtered and concentrated. The crude product **278** was purified by column chromatography (Silica, CH/EtOAc 30:1) and was obtained as a yellow oil (1.26 g, 4.73 mmol, 68%). $\mathbf{R_f}$ = 0.29 (CH/EtOAc 30:1); **^{1}H-NMR** (500 MHz, acetone-d6) δ = 0.18 (s, 9H), 1.27 (s, 12H), 1.97 (d, *J* = 1.3 Hz, 3H), 5.59 (dd, *J* = 18.0, 0.6 Hz, 1H), 5.79 (tt, *J* = 1.5, 0.8 Hz, 1H), 7.38 (d, *J* = 18.0 Hz, 1H); **^{13}C-NMR** (126 MHz, acetone-d6) δ = −0.4, 21.7, 24.2, 82.9, 135.9, 150.2, 150.6, [note: the carbon attached to boron was not observed due to quadrupole broadening caused by the ^{11}B-nucleus]; **HRMS (APCI)**: m/z calc for $[M+H]^+$: 267.1945; found: 267.1949.

trimethyl((2*Z*,4*E*)-5-(1,3,6,2-dioxazaborocane-4,8-dione-2-yl)penta-2,4-dien-2-yl)silane (279)

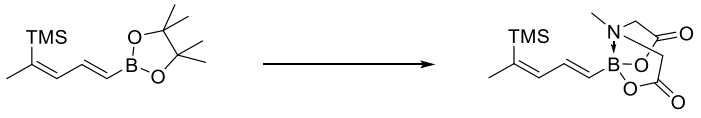

$C_{13}H_{22}BNO_4Si$
M = 295.22 g/mol

Boronic ester **278** (1.00 g, 3.76 mmol, 1.00 eq.) was dissolved in acetone/water (1:1, 20 mL). Then, sodium periodate (2.00 g, 9.35 mmol, 2.50 eq.) and ammonium acetate (724 mg, 9.39 mmol, 2.50 eq) were added. The resulting mixture was purged with argon and allowed to stir for 13 hours at room temperature. Afterwards, the suspension was filtered over Celite®, rinsed with acetone and the solvents

were removed under reduced pressure. The residue was dissolved in water (15 mL) and EtOAc (20 mL) was added. Phases were separated and the aqueous layer was extracted with EtOAc (3 x 10 mL). The combined organic layers were washed with brine (10 mL), dried over $MgSO_4$, filtered, concentrated and used immediately. Toluene (6 mL), DMSO (3 mL) and methyliminodiacetic acid (243 mg, 1.65 mmol, 2.00 eq.) were added, the resulting mixture was purged with argon and refluxed under *Dean-Stark* conditions overnight at 120 °C. After 10 h, the flask was cooled to room temperature and the solvents were removed under reduced pressure (80 °C bath temperature). To the remaining liquid was added EtOAc (300 mL) and water (100 mL). Phases were separated and the aqueous phase was extracted with EtOAc (3 x 100 mL). The combined organic layers were washed with water (5 x 100 mL) and brine (100 mL), dried over $MgSO_4$, filtered and concentrated to obtain the crude product as an off-white amorphous solid. The obtained crude product was purified by vapor diffusion crystallization (solvent: MeCN, anti-solvent: Et_2O) which yielded the desired compound **279** as a colorless crystalline solid (962 mg, 3.26 mmol, 87%). $\mathbf{R_f}$ = 0.31 (EtOAc); **^{1}H-NMR** (500 MHz, acetone-d6) δ = 0.13 (s, 9H), 1.97 (d, *J* = 1.3 Hz, 3H), 3.01 (s, 3H), 4.01 (d, *J* = 16.9 Hz, 2H), 4.24 (d, *J* = 16.9 Hz, 2H), 5.61 (d, *J* = 1.6 Hz, 1H), 5.80 (d, *J* = 17.8 Hz, 1H), 6.98 (d, *J* = 17.8 Hz, 1H); **^{13}C-NMR** (126 MHz, acetone-d6) δ = 0.6, 23.0, 47.3, 62.2, 133.4, 144.4, 151.7, 169.0; **HRMS (ESI)**: m/z calc for $[M+H]^+$: 296.1487; found: 296.1482.

trimethyl((2*Z*,4*E*)-5-(1,3,6,2-dioxazaborocane-4,8-dione-2-yl)vinyl)oxiran-2-yl)silane (266)

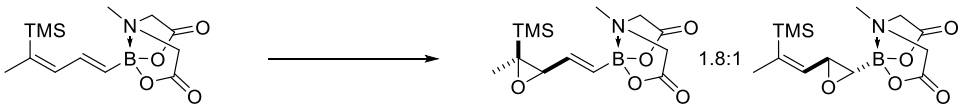

$C_{13}H_{22}BNO_5Si$
M = 311.22 g/mol

To a solution of MIDA-diene **279** (309 mg, 1.05 mmol, 1.00 eq.) in MeCN (20 mL) was added a solution of *m*CPBA (75 wt-%, 241 mg, 1.05 mmol, 1.00 eq.) in DCM (10 mL) dropwise over 6 hours. After complete addition, stirring was continued for 1 hour. EtOAc (50 mL) and a saturated solution of $NaHCO_3$ (20 mL) was added, phases were separated and the organic layer was washed with $NaHCO_3$ (2 x 20 mL).The combined organic layers were washed with brine (20 mL), dried over $MgSO_4$, filtered and concentrated. Crude NMR indicated formation of the desired product and formation of a regioisomer in a ratio of 1.8:1. Purification by column chromatography (Silica, EtOAc/MeOH 20:1) yielded the desired compound **266** as a white solid with a regioisomeric ratio of 30:1, however with diminished yield (85.0 mg, 273 µmol, 26%) due to the occurrence of several mixed fractions. $\mathbf{R_f}$ = 0.38 (EtOAc/MeOH 20:1), 0.33 (regioisomer); **^{1}H-NMR** (500 MHz, acetone-d6) δ = 0.10 (s, 9H), 1.23 (s, 3H), 3.04 (s, 3H), 3.18 (dd, *J* = 6.3, 1.0 Hz, 1H),

4.03 (dd, *J* = 28.6, 16.9 Hz, 2H), 4.24 (dd, *J* = 16.9, 7.0 Hz, 2H), 5.92–6.03 (m, 2H); **^{13}C-NMR** (126 MHz, acetone-d6) δ = −1.7, 22.8, 47.4, 57.0, 62.3, 62.4, 66.8, 143.1, 168.9, 168.9; **HRMS (ESI)**: m/z calc for $[M+H]^+$: 312.1436; found: 312.1432.

trimethyl((2*Z*,4*E*)-5-(1,3,6,2-dioxazaborocane-4,8-dione-2-yl)vinyl)oxiran-2-yl)silane (266)

$C_{13}H_{22}BNO_5Si$
M = 311.22 g/mol

To a solution of **267** (34.0 mg, 121 µmol, 1.00 eq.) in DMSO (1 mL) and toluene (2 mL) was added trimethoxymethane (52.7 µL, 481 µmol, 4.00 eq.) and MIDA (106 mg, 723 µmol, 6.00 eq.). The resulting solution was heated to 110 °C and stirred for 24 hours. Then, the mixture was diluted with EtOAc (5 mL) and water (5 mL). Phases were separated and the aqueous phase extracted with EtOAc (3 x 5 mL). The combined organic layers were washed with water (3 x 10 mL) and brine (10 mL), dried over $MgSO_4$, filtered and concentrated. The resulting crude product was loaded onto Celite® and purified via column chromatography (Silica, EtOAc) which yielded the compound as a white solid (10.4 mg, 33.4 µmol, 28%). **R_f** = 0.17 (EtOAc); **^{1}H-NMR** (500 MHz, acetone-d6) δ = 0.10 (s, 9H), 1.23 (s, 3H), 3.04 (s, 3H), 3.18 (dd, *J* = 6.3, 1.0 Hz, 1H), 4.03 (dd, *J* = 28.6, 16.9 Hz, 2H), 4.24 (dd, *J* = 16.9, 7.0 Hz, 2H), 5.92–6.03 (m, 2H); **^{13}C-NMR** (126 MHz, acetone-d6) δ = −1.7, 22.8, 47.4, 57.0, 62.3, 62.4, 66.8, 143.1, 168.9, 168.9; **HRMS (ESI)**: m/z calc for $[M+H]^+$: 312.1436; found: 312.1432.

(*Z*)-(4-((4-methoxybenzyl)oxy)but-2-en-2-yl)trimethylsilane (280)

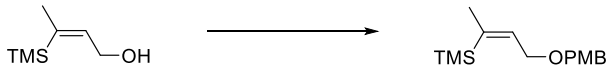

$C_{15}H_{24}O_2Si$
M = 264.44 g/mol

To a solution of allylalcohol **270** (1.60 g, 11.1 mmol, 1.00 eq.) in anhydrous toluene (30 mL) at 0 °C was added 4-methoxybenzyl-2,2,2-trichloroacetimidate (2.40 mL, 11.6 mmol, 1.05 eq.) and scandium triflate (164 mg, 333 µmol, 0.03 eq.). The ice bath was removed and the resulting solution was stirred at r.t for 1 hour. Then, a saturated solution of $NaHCO_3$ (10 mL) was added and the mixture was extracted with EtOAc (2 x 50 mL). The combined organic layers were washed with brine (10 mL), dried over $MgSO_4$, filtered and concentrated. After evaporation of the solvent, the crude product was purified by column

chromatogrqaphy (Silica, CH/EtOAc 20:1) to obtain the product **280** as a colorless oil (2.09 g, 7.90 mmol, 71%). $\mathbf{R_f}$ = 0.35 (CH/EtOAc 20:1), **^{1}H-NMR** (500 MHz, acetone-d6) δ = 0.10 (s, 9H), 1.80 (q, *J* = 1.4 Hz, 3H), 3.78 (s, 3H), 4.02 (dq, *J* = 6.6, 1.3 Hz, 2H), 4.42 (s, 2H), 6.13 (tq, *J* = 6.6, 1.7 Hz, 1H), 6.87–6.94 (m, 2H), 7.24–7.31 (m, 2H); **^{13}C-NMR** (126 MHz, acetone-d6) δ = −0.2, 24.8, 55.5, 69.6, 72.4, 114.4, 130.1, 131.8, 139.6, 139.8, 160.2; **HRMS (ESI)**: m/z calc for $[M+H]^+$: 265.1618; found: 265.1614.

((2*R,3*S**)-3-(((4-methoxybenzyl)oxy)methyl)-2-methyloxiran-2-yl)trimethylsilane (281)**

$C_{15}H_{24}O_3Si$
M = 280.44 g/mol

To a solution of PMB-ether **280** (2.09 g, 7.90 mmol, 1.00 eq.) in DCM (20 mL) was added *m*CPBA (2.36 g, 10.3 mmol, 1.30 eq.) at 0 °C. The ice bath was removed and the resulting solution was stirred at r.t for 1 hour. A saturated solution of $Na_2S_2O_3$ (10 mL) was added and the mixture was stirred for further 10 minutes. Then, EtOAc (20 mL) and saturated $NaHCO_3$ (5 mL) were added and phases were separated. The aqueous layer was extracted with EtOAc (3 x 10 mL) and the combined organic layers were washed with saturated $NaHCO_3$ (2 x 10 mL), brine (10 mL), dried over $MgSO_4$, filtered and concentrated. After purification by column chromatography (Silica, CH/EtOAc 12:1) the compound **281** was received as a colorless oil (2.21 g, 7.88 mmol, 100%). $\mathbf{R_f}$ = 0.17 (CH/EtOAc 12:1), **^{1}H-NMR** (500 MHz, acetone-d6) δ = 0.07 (s, 9H), 1.20 (s, 3H), 2.92 (dd, *J* = 6.9, 3.8 Hz, 1H), 3.41 (dd, *J* = 10.9, 6.9 Hz, 1H), 3.67 (dd, *J* = 10.9, 3.9 Hz, 1H), 3.79 (s, 3H), 4.43–4.57 (m, 2H), 6.87–6.95 (m, 2H), 7.23–7.33 (m, 2H); **^{13}C-NMR** (126 MHz, acetone-d6) δ = −1.9, 22.8, 53.3, 55.5, 64.4, 70.6, 73.1, 114.5, 130.2, 131.4, 160.3; **HRMS (ESI)**: m/z calc for $[M+Na]^+$: 303.1387; found: 303.1380.

(2*R,3*R**)-3-azido-1-((4-methoxybenzyl)oxy)-3-(trimethylsilyl)butan-2-ol (282)**

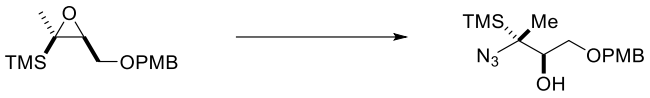

$C_{15}H_{25}N_3O_3Si$
M = 323.47 g/mol

A solution of epoxide **281** (2.20 g, 7.84 mmol, 1.00 eq.), sodium azide (3.3 g, 51 mmol, 6.5 eq.), NH_4Cl (1.05 g, 19.6 mmol, 2.5 eq.) in MeOH/H_2O (8:1, 72 mL) was stirred at 45 °C for 40 hours. Then, the solution was diluted with EtOAc (50 mL) and water (50 mL). Phases were separated and the aqueous

layer was extracted with EtOAc (3 x 50 mL). The combined organic layers were washed with water (3 x 100 mL), brine (50 mL), dried over $MgSO_4$, filtered and concentrated. The crude product was purified by column chromatography (CH/EtOAc 8:1) and the azidoalcohol **282** was obtained as a colorless oil (2.03 g, 6.28 mmol, 80%). $\mathbf{R_f}$ = 0.26 (CH/EtOAc 8:1), **^{1}H-NMR** (500 MHz, acetone-d6) δ = 0.14 (s, 9H), 1.27 (s, 3H), 3.48 (dd, *J* = 9.9, 7.5 Hz, 1H), 3.69 (dd, *J* = 9.8, 3.3 Hz, 1H), 3.79 (s, 3H), 3.88 (ddd, *J* = 7.6, 4.3, 3.4 Hz, 1H), 4.12 (d, *J* = 4.3 Hz, 1H), 4.48 (s, 2H), 6.88–6.94 (m, 2H), 7.25–7.33 (m, 2H); **^{13}C-NMR** (126 MHz, acetone-d6) δ = −2.1, 16.5, 55.5, 58.3, 72.2, 73.4, 76.3, 114.5, 130.1, 131.4, 160.3; **HRMS (ESI)**: m/z calc for $[M+Na]^+$: 346.1557; found: 346.1555.

(((2*R,3*R**)-3-azido-1-((4-methoxybenzyl)oxy)-3-(trimethylsilyl)butan-2-yl)oxy)(*tert*-butyl) dimethylsilane (283)**

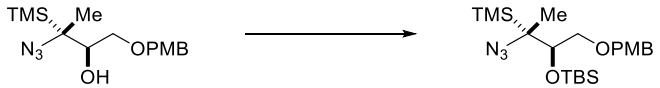

$C_{21}H_{39}N_3O_3Si_2$
M = 437.73 g/mol

To a solution of azido-alcohol **282** (143 mg, 442 µmol, 1.00 eq.) in anhydrous DCM (3 mL) was sequentially added 2,6-lutidine (0.2 mL, 1.8 mmol, 4.0 eq.) and TBSOTf (0.2 mL, 0.9 mmol, 2.0 eq.) at 0 °C. The resulting solution was stirred at 0 °C for 45 minutes, then diluted with Et_2O (10 mL) and quenched with a saturated solution of NH_4Cl (10 mL). Phases were separated and the aqueous layer was extracted with Et_2O (3 x 5 mL). The combined organic layers were washed with brine (10 mL), dried over $MgSO_4$, filtered and concentrated. The solvent was removed and the residue was purified by column chromatography (*n*-heptane/Et_2O 40:1). The product **283** was received as a colorless oil (172 mg, 394 µmol, 89%). $\mathbf{R_f}$ = 0.30 (CH/EtOAc 30:1); **^{1}H-NMR** (500 MHz, acetone-d6) δ = 0.09 (s, 9H), 0.10 (s, 3H), 0.13 (s, 3H), 0.92 (s, 9H), 1.35 (s, 3H), 3.36 (dd, *J* = 10.1, 6.2 Hz, 1H), 3.55 (dd, *J* = 10.1, 3.1 Hz, 1H), 3.79 (s, 3H), 3.87 (dd, *J* = 6.2, 3.1 Hz, 1H), 4.40–4.50 (m, 2H), 6.90–6.93 (m, 2H), 7.27–7.30 (m, 2H); **^{13}C-NMR** (126 MHz, acetone-d6) δ = −4.6, −4.0, -2.4, 14.5, 18.9, 55.5, 58.6, 65.3, 73.3, 78.1, 114.5, 128.5, 130.3, 131.1, 160.3; **HRMS (ESI)**: m/z calc for $[M+Na]^+$: 460.2422; found: 460.2413.

(2*R,3*R**)-3-azido-2-((*tert*-butyldimethylsilyl)oxy)-3-(trimethylsilyl)butan-1-ol (284)**

$C_{13}H_{31}N_3O_2Si_2$
M = 317.58 g/mol

To a solution of **283** (827 mg, 1.89 mmol, 1.00 eq.) in DCM/pH 7 buffer (8:1, 9 mL) was added DDQ (643 mg, 2.83 mmol, 1.50 eq.) at r.t and the resulting solution was stirred for 4 hours. After full conversion, the reaction was quenched with a saturated solution of $NaHCO_3$, diluted with H_2O and extracted with Et_2O (3 x 50 mL). The combined organic layers were washed with brine (50 mL), dried over $MgSO_4$, filtered and concentrated. After purification by column chromatography (Silica, *n*-pentan/Et_2O 4:1) the compound **284** was obtained as a colorless oil (335 mg, 1.05 mmol, 56%). $\mathbf{R_f}$ = 0.19 (CH/EtOAc 20:1); **^{1}H-NMR** (500 MHz, acetone-d6) δ = 0.14 (s, 9H), 0.16 (s, 6H), 0.94 (s, 9H), 1.36 (s, 3H), 3.43–3.51 (m, 1H), 3.65–3.72 (m, 1H), 3.78 (ddd, *J* = 9.0, 6.0, 4.3 Hz, 2H); **^{13}C-NMR** (126 MHz, acetone-d6) δ = −4.6, −3.9, −2.3, 14.2, 19.0, 26.4, 58.7, 65.0, 79.8; **HRMS (ESI)**: m/z calc for $[M+-N_2+H]^+$: 290.1959; found: 290.1966.

(2*R,3*R**)-3-azido-2-((*tert*-butyldimethylsilyl)oxy)-3-(trimethylsilyl)butanal (285)**

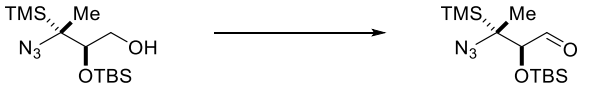

$C_{13}H_{29}N_3O_2Si_2$
M = 315.56 g/mol

To a solution of DMP (228 mg, 537 µmol, 1.10 eq.) in wet DCM (1 mL) was added alcohol **284** (155 mg, 488 µmol, 1.00 eq.) and the resulting solution was stirred at r.t. for 3 hours. Then, Celite® was added and the solvent was removed. The remaining solid was loaded onto a short plug of silica and eluted with 10 volumes of *n*-pentane/EtOAc (20:1). Afterwards, the solvent was removed under reduced pressure and the product **285** (138 mg, 437 µmol, 89%) was obtained as a colorless oil. $\mathbf{R_f}$ = 0.32 (CH/EtOAc 100:1); **^{1}H-NMR** (500 MHz, acetone-d6) δ = 0.09 (s, 3H), 0.12–0.17 (m, 12H), 0.97 (d, *J* = 0.9 Hz, 9H), 1.43 (d, *J* = 0.9 Hz, 3H), 4.18 (dd, *J* = 2.3, 0.9 Hz, 1H), 9.71 (dd, *J* = 2.3, 0.9 Hz, 1H); **^{13}C-NMR** (126 MHz, acetone-d6) δ = −4.7, −4.4, −2.5, 16.0, 18.9, 26.2, 57.9, 83.6, 202.4; **HRMS (ESI)**: m/z calc for $[M-N_2+H]^+$: 288.1810; found: 288.1812.

(((3*R,4*R**,*E*)-4-azido-1-(4,4,5,5-tetramethyl-1,3,2-dioxaborolan-2-yl)-4-(trimethylsilyl)pent-1-en-3-yl)oxy)(*tert*-butyl)dimethylsilane (286)**

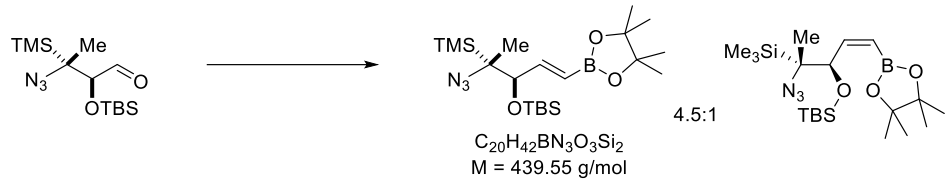

$C_{20}H_{42}BN_3O_3Si_2$
M = 439.55 g/mol

To a solution of bis(pinacolato)boryl methane (234 mg, 875 µmol, 2.00 eq.) in anhydrous THF (4 mL) at −78 °C was added a solution of LiTMP (116 mg, 787 µmol, 1.80 eq.) in anhydrous THF (4 mL) resulting in a brown cloudy mixture. The ice bath was removed and the mixture was stirred at r.t for 10 minutes. Afterwards, the solution was cooled to −78 °C and a solution of aldehyde **285** (138 mg, 437 µmol, 1.00 eq.) in THF (4 mL) was added. The mixture was allowed to slowly warm to r.t. overnight. After 12 hours, the mixture was diluted with Et_2O (10 mL) and quenched with a saturated solution of NH_4Cl (10 mL). Phases were separated and the aqueous phase was extracted with Et_2O (3 x 10 mL). The combined organic layers were washed with brine, dried over $MgSO_4$, filtered and concentrated. Purification by column chromatography (Silica, CH/EtOAc 30:1) yielded the desired compound **286** (132 mg, 300 µmol, 69%) as a mixture of isomers with an *E*/*Z*-ratio of 4.5:1 determined by ^{1}H-NMR. *E*-Isomer (**286**): $\mathbf{R_f}$ = 0.33 (CH/EtOAc 25:1); **^{1}H-NMR** (700 MHz, acetone-d6) δ = 0.04 (s, 3H), 0.12 (s, 9H), 0.14 (s, 3H), 0.94 (s, 9H), 1.23–1.25 (m, 12H), 1.27 (s, 3H), 4.32 (dd, *J* = 6.6, 1.3 Hz, 1H), 5.70 (dd, *J* = 17.9, 1.3 Hz, 1H), 6.54 (dd, *J* = 17.9, 6.6 Hz, 1H); **^{13}C-NMR** (176 MHz, acetone-d6) δ = −4.6, −3.9, −2.5, 13.8, 18.8, 24.9, 25.1, 26.4, 59.2, 80.5, 84.0, 152.3, [note: the carbon attached to boron was not observed due to quadrupole broadening caused by the ^{11}B nucleus]; *Z*-Isomer (**287**): $\mathbf{R_f}$ = 0.33 (CH/EtOAc 25:1); **^{1}H-NMR** (700 MHz, acetone-d6) δ = 0.09 (s, 3H), 0.15 (s, 8H), 0.16 (s, 2H), 0.92 (s, 9H), 1.22 (s, 3H), 1.28 (s, 12H), 5.09 (dd, *J* = 9.8, 0.8 Hz, 1H), 5.55 (dd, *J* = 13.7, 0.8 Hz, 1H), 6.39 (dd, *J* = 13.7, 9.8 Hz, 1H); **^{13}C-NMR** (176 MHz, acetone) δ = −3.9, −3.3, −1.9, 14.3, 20.8, 25.2, 25.3, 26.5, 77.4, 84.2, 153.0, [note: the carbon attached to boron was not observed due to quadrupole broadening caused by the ^{11}B nucleus]; **HRMS (APCI)**: m/z calc for $[M\text{-}N_2+H]^+$: 412.2873; found: 412.2873.

(2*R,3*R**)-3-amino-1-((4-methoxybenzyl)oxy)-3-(trimethylsilyl)butan-2-ol (291)**

$C_{15}H_{27}NO_3Si$
M = 297.47 g/mol

To a solution of silylazidoalcohol **282** (152 mg, 470 µmol, 1.00 eq.) in anhydrous Et_2O (7 mL) was slowly added lithium aluminium hydride (1 M in Et_2O, 0.94 mL, 0.94 mmol, 2.0 eq.). The reaction mixture was stirred at room temperature for 3 hours, and then sodium hydroxide (2.5 M, 10 mL) was added. Phases were separated and the aqueous layer was extracted with Et_2O (3 x 10 mL). The combined extracts were dried over $MgSO_4$ and concentrated to give the silylaminoalcohol **291** as a white solid (131 mg, 440 µmol, 94%). $\mathbf{R_f}$ = 0.38 (EtOAc/MeOH 7:1 + 2.5% NEt_3); **^{1}H-NMR** (500 MHz, acetone-d6) δ = 0.02 (s, 9H), 0.99 (s, 3H), 3.51 (dd, *J* = 9.6, 7.1 Hz, 1H), 3.61–3.68 (m, 2H), 3.79 (s, 3H), 4.45 (s, 2H), 6.87–6.94 (m, 2H), 7.25–7.32 (m, 2H); **^{13}C-NMR** (126 MHz, acetone-d6) δ = −2.8, 21.3, 45.3, 55.5, 72.3, 73.4, 75.9, 114.4, 130.0, 131.7, 160.2; **HRMS (APCI)**: m/z calc for $[M+H]^+$: 298.1833; found: 298.1830.

Product **291** was also obtained from the following reaction:

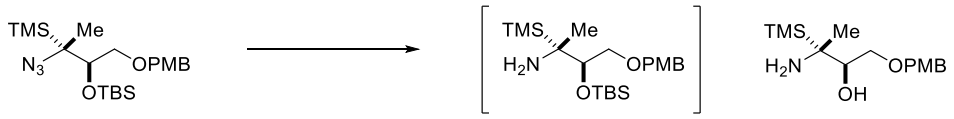

not obtained

$C_{21}H_{41}NO_3Si_2$
M = 411.73 g/mol

$C_{15}H_{27}NO_3Si$
M = 297.47 g/mol

To a solution of TBS-protected silylazidoalcohol **283** (75.0 mg, 171 µmol, 1.00 eq.) in anhydrous Et_2O (3 mL) was slowly added lithium aluminium hydride (1 M in Et_2O, 0.34 mL, 0.34 mmol, 2.0 eq.). The reaction mixture was stirred at room temperature for 6 hours, and then sodium hydroxide (2.5 M, 10 mL) was added. Phases were separated and the aqueous layer was extracted with Et_2O (3 x 10 mL). The combined extracts were dried over $MgSO_4$ and concentrated to give the silylaminoalcohol **291** as a white solid (47.5 mg, 160 µmol, 93%). $\mathbf{R_f}$ = 0.38 (EtOAc/MeOH 7:1 + 2.5% NEt_3); **^{1}H-NMR** (500 MHz, acetone-d6) δ = 0.02 (s, 9H), 0.99 (s, 3H), 3.51 (dd, *J* = 9.6, 7.1 Hz, 1H), 3.61–3.68 (m, 2H), 3.79 (s, 3H), 4.45 (s, 2H), 6.87–6.94 (m, 2H), 7.25–7.32 (m, 2H); **^{13}C-NMR** (126 MHz, acetone-d6) δ = −2.8, 21.3, 45.3, 55.5, 72.3, 73.4, 75.9, 114.4, 130.0, 131.7, 160.2; **HRMS (APCI)**: m/z calc for $[M+H]^+$: 298.1833; found: 298.1830.

tert-butyl ((2*R,3*R**)-3-hydroxy-4-((4-methoxybenzyl)oxy)-2-(trimethylsilyl)butan-2-yl)carbamate (292)**

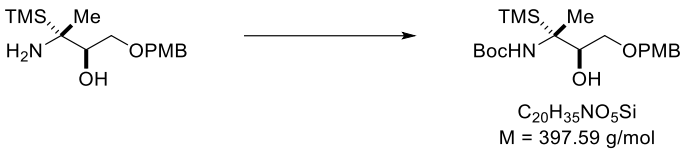

$C_{20}H_{35}NO_5Si$
M = 397.59 g/mol

To a solution of silylaminoalcohol **291** (125 mg, 420 µmol, 1.00 eq.) in anhydrous THF (3 mL) was added Boc_2O (183 mg, 840 µmol, 2.00 eq.), NEt_3 (110 µL, 840 µmol, 2.00 eq.), DMAP (one small crystal) and the resulting solution was stirred at r.t. for 12 hours. Then, Celite® was added and all volatiles were removed under reduced pressure, followed by purification with column chromatography (Silica, CH/EtOAc 5:1). The product **292** (42.5 mg, 107 µmol, 25%) was obtained as a white solid. $\mathbf{R_f}$ = 0.30 (CH/EtOAc 4:1); **^{1}H-NMR** (700 MHz, acetone-d6) δ = 0.16 (s, 9H), 1.35 (s, 3H), 1.52 (s, 9H), 3.68–3.75 (m, 2H), 3.81 (s, 3H), 4.46–4.59 (m, 2H), 6.90–6.95 (m, 2H), 7.28–7.34 (m, 2H); **^{13}C-NMR** (176 MHz, acetone-d6) δ = −3.4, 14.2, 27.3, 53.2, 54.6, 68.5, 72.5, 72.5, 78.9, 82.6, 113.6, 129.3, 130.1, 151.3, 159.4; **HRMS (ESI)**: m/z calc for $[M+H]^+$: 398.2357; found: 398.2356.

trimethyl((2*R,3*S**)-2-methyl-3-vinyloxiran-2-yl)silane (300)**

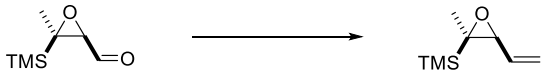

$C_8H_{16}OSi$
M = 156.30 g/mol

To a suspension of methyltriphenylphosphonium bromide (1.3 g, 3.6 mmol, 1.5 eq.) in THF (10 mL) at r.t was added NHMDS (1 M in THF, 3.50 mL, 3.50 mmol, 1.45 eq.). The solution was stirred at r.t for 15 minutes. Then, a solution of aldehyde **268** (380 mg, 2.40 mmol, 1.00 eq.) in THF (2 mL) was added and the resulting solution was stirred at room temperature for 1 hour. Then, a solution of saturated NH_4Cl (5 mL) and water (5 mL) were added and layers were separated. The aqueous layer was extracted with Et_2O (3 x 10 mL) and the combined organic layers were washed with brine, dried over $MgSO_4$ and filtered. The solvent was carefully removed and the remaining residue was purified by column chromatography (Silica, *n*-pentane/Et_2O 25:1) to afford the desired compound **300** as a colorless oil (96 mg, 0.61 mmol, 65%). $\mathbf{R_f}$ = 0.25 (CH/EtOAc 50:1); **^{1}H-NMR** (500 MHz, acetone-d6) δ = 0.10 (s, 9H), 1.23 (s, 3H), 3.15 (dt, *J* = 8.0, 0.9 Hz, 1H), 5.26 (ddd, *J* = 10.4, 1.7, 0.9 Hz, 1H), 5.47 (ddd, *J* = 17.2, 1.7, 0.8 Hz, 1H), 5.74 (ddd, *J* = 17.2, 10.4, 8.0 Hz, 1H); **^{13}C-NMR** (126 MHz, acetone-d6) δ = −1.8, 22.7, 56.7, 65.8, 119.5, 137.3; **HRMS (APCI)**: m/z calc for $[M+H]^+$: 157.1043; found: 157.1039.

(3*R,4*R**)-4-azido-4-(trimethylsilyl)pent-1-en-3-ol (301)**

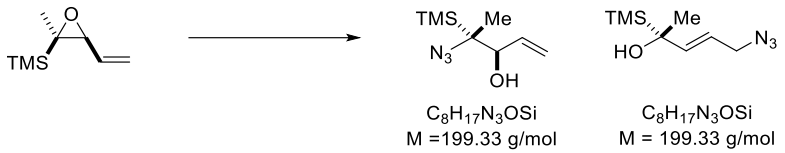

$C_8H_{17}N_3OSi$
M =199.33 g/mol

$C_8H_{17}N_3OSi$
M = 199.33 g/mol

To a round bottom flask, containing sodium azide (595 mg, 9.16 mmol, 5.30 eq.) was added a solution of vinyloxirane **300** (270 mg, 1.73 mmol, 1.00 eq.) in MeOH (4 mL), followed by addition of an aqueous solution of NH_4Cl (2.3 M, 1.1 mL, 2.5 eq.). The flask was sealed and heated to 50 °C in a sand bath for 48 hours. After the indicated time, a saturated solution of $NaHCO_3$ (10 mL) and EtOAc (10 mL) were added, followed by water until the mixture became a clear solution. Phases were separated and the aqueous layer was extracted with EtOAc (4 x 10 mL). The combined organic layers were washed with water (2 x 10 mL) and brine (20 mL). The organic layer was dried over $MgSO_4$, filtered and concentrated. Purification by column chromatography (Silica, CH/EtOAc 10:1) yielded the desired product **301** as a colorless oil (75.0 mg, 376 µmol, 22%) and the regioisomer **302** (S_N2'-product) as a colorless oil (26.8 mg, 134 µmol, 8%). $\mathbf{R_f}$ = 0.29 (CH/EtOAc 10:1), **^{1}H-NMR** (500 MHz, acetone-d6) δ = 0.15 (s, 9H), 1.21 (s, 3H), 4.16 (ddt, *J* = 7.0, 4.8, 1.1 Hz, 1H), 4.25 (dd, *J* = 4.8, 0.6 Hz, 1H), 5.21 (ddd, *J* = 10.4, 2.0, 1.0 Hz, 1H), 5.31 (ddd, *J* = 17.2, 2.0, 1.2 Hz, 1H), 5.97 (ddd, *J* = 17.3, 10.4, 7.0 Hz, 1H); **^{13}C-NMR** (126 MHz, acetone-d6) δ = −2.2, 16.1, 59.1, 78.9, 117.5, 138.5; **HRMS (APCI)**: m/z calc for $[M+N_2+H]^+$: 172.1152; found: 172.1152. regioisomer (**302**): $\mathbf{R_f}$ = 0.19 (CH/EtOAc 10:1); **^{1}H-NMR** (500 MHz, acetone-d6) δ = 0.03 (s, 9H), 1.30 (s, 3H), 3.24 (d, *J* = 0.4 Hz, 1H), 3.73–3.86 (m, 2H), 5.61 (dt, *J* = 15.3, 6.9 Hz, 1H), 6.00 (dt, *J* = 15.3, 1.2 Hz, 1H); **^{13}C-NMR** (126 MHz, acetone-d6) δ = −4.3, 24.9, 53.3, 68.0, 118.7, 144.5 [note: the signal intensity for the quaternary carbon of **302** is very low and was determined from HMBC correlations]; **HRMS (APCI)**: m/z calc for $[M+H]^+$: 200.1214; found: 200.1215.

((2*R,3*S**)-3-(2,2-dibromovinyl)-2-methyloxiran-2-yl)trimethylsilane (303)**

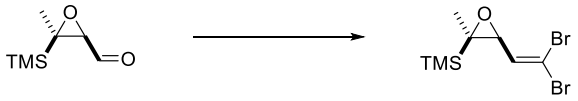

$C_8H_{14}Br_2OSi$
M = 314.09 g/mol

To a solution of aldehyde **268** (530 mg, 3.35 mmol, 1.00 eq.) and triphenylphosphane (3.51 g, 13.4 mmol, 4.90 eq.) in anhydrous DCM (15 mL) at 0 °C was added carbon tetrabromide (2.22 g, 6.70 mmol, 2.00 eq.)

portionwise over 5 minutes. After stirring the brown suspension for 45 minutes at room temperature, cyclohexane (30 mL) was added and the suspension was filtered through Celite®. The filter cake was thoroughly washed with cyclohexane and the filtrate was concentrated to yield a light-brown solid containing the desired product and PPh_3 side-products. Purification by column chromatography (Silica, CH/EE 50:1) followed by a second column (Silica, CH/EE 100:1) provided the desired compound **303** as a yellow liquid (266 mg, 847 µmol, 25%). $\mathbf{R_f}$ = 0.30 (CH/EtOAc 50:1), 0.25 (CH/EtOAc 100:1); **^{1}H-NMR** (500 MHz, acetone-d6) δ = 0.12 (s, 9H), 1.29 (s, 3H), 3.30 (d, *J* = 5.8 Hz, 1H), 6.47 (d, *J* = 5.9 Hz, 1H); **^{13}C-NMR** (126 MHz, acetone-d6) δ = −2.3, 22.2, 57.4, 64.1, 91.9, 138.0; **HRMS (EI)**: m/z calc for $[M]^+$: 311.9181; found: 311.9171.

(3*R,4*R**)-4-azido-1,1-dibromo-4-(trimethylsilyl)pent-1-en-3-ol (304)**

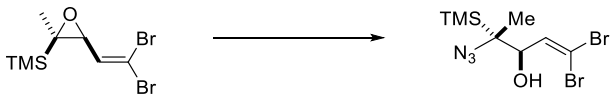

$C_8H_{15}Br_2N_3OSi$
M = 357.12 g/mol

To a round bottom flask, containing sodium azide (118 mg, 1.81 mmol, 5.00 eq.) was added a solution of oxirane **303** (114 mg, 0.363 mmol, 1.00 eq.) in MeOH (2 mL), followed by addition of an aqueous solution of NH_4Cl (2.5 M 0.35 mL, 2.4 eq.). The flask was sealed and heated to 45 °C in a sand bath for 44 hours. After the indicated time, the pH was adjusted to pH 8 by addition of a saturated solution of $NaHCO_3$ (2 mL). Then, MeOH was removed under reduced pressure and to the residue was added water (5 mL) and EtOAc (5 mL). Phases were separated and the aqueous layer was extracted with EtOAc (3 x 5 mL) and the combined organic layers were washed with brine (5 mL), dried over $MgSO_4$, filtered and concentrated. The obtained crude product was purified by column chromatography (Silica, CH/EtOAc 12:1) which yielded the desired product **304** as an off-white solid (40.0 mg, 112 µmol, 31%). $\mathbf{R_f}$ = 0.33 (CH/EtOAc 12:1); **^{1}H-NMR** (500 MHz, acetone-d6) δ = 0.18 (s, 9H), 1.26 (s, 3H), 4.40 (dd, *J* = 9.1, 5.2 Hz, 1H), 4.89 (d, *J* = 5.2 Hz, 1H), 6.66 (d, *J* = 9.1 Hz, 1H); **^{13}C-NMR** (126 MHz, acetone-d6) δ = −2.3, 16.2, 59.2, 77.8, 139.0; **HRMS (APCI)**: m/z calc for $[M+H]^+$: 329.9341; found: 329.9335.

(3*R,4*R**)-4-amino-4-(trimethylsilyl)pent-1-en-3-ol (306)**

$C_8H_{19}NOSi$
M = 173.33 g/mol

To a solution of silylazidoalcohol **301** (75 mg, 376 µmol, 1.00 eq.) in anhydrous Et_2O (3 mL) was slowly added lithium aluminium hydride (1 M in Et_2O, 0.75 mL, 0.75 mmol, 2.0 eq.). The reaction mixture was stirred at room temperature for 3 hours, and then sodium hydroxide (2.5 M, 10 mL) was added. Phases were separated and the aqueous layer was extracted with Et_2O (3 x 10 mL). The combined extracts were dried over $MgSO_4$ and concentrated to give the silylaminoalcohol **306** as a white solid (58.6 mg, 338 µmol, 90%). **^{1}H-NMR** (500 MHz, acetone-d6) δ = 0.04 (s, 9H), 0.91 (s, 3H), 3.97 (dt, *J* = 6.6, 1.2 Hz, 1H), 5.11–5.25 (m, 2H), 5.95 (ddd, *J* = 17.1, 10.5, 6.5 Hz, 1H); **^{13}C-NMR** (126 MHz, acetone-d6) δ = −2.7, 21.2, 46.0, 78.7, 116.2, 139.1; **HRMS (ESI)**: m/z calc for $[M+H]^+$: 174.1309; found: 174.1307.

***tert*-butyl ((2*R**,3*R**)-3-hydroxy-2-(trimethylsilyl)pent-4-en-2-yl)carbamate (297)**

$C_{13}H_{27}NO_3Si$
M = 273.45 g/mol

To a solution of amine **306** (58.0 mg, 335 µmol, 1.00 eq.) in anhydrous DCM (2 mL) was added Boc_2O (80 mg, 368 µmol, 1.10 eq.) as a solid and NEt_3 (50 µL, 0.37 mmol, 1.1 eq.). The resulting solution was stirred at r.t. overnight. After 12 hours, Celite® was added and all volatiles were removed under reduced pressure, followed by column chromatography (Silica, CH/EA 8:1). The product **297** (75.8 mg, 277 µmol, 83%) was received as a white crystalline solid. $\mathbf{R_f}$ = 0.28 (CH/EtOAc 8:1); **^{1}H-NMR** (500 MHz, acetone-d6) δ = 0.14 (s, 9H), 1.14 (s, 3H), 1.39 (s, 9H), 4.02 (ddt, *J* = 7.9, 6.2, 1.3 Hz, 1H), 5.12–5.29 (m, 3H), 5.58 (s, 1H), 5.92–6.04 (m, 1H); **^{13}C-NMR** (126 MHz, acetone-d6) δ = −1.1, 20.6, 28.6, 51.7, 78.6, 79.1, 116.4, 138.7, 157.7; **HRMS (ESI)**: m/z calc for $[M+Na]^+$: 296.1652; found: 296.1650.

***tert*-butyl (4*R**,5*R**)-2,2,4-trimethyl-4-(trimethylsilyl)-5-vinyloxazolidine-3-carboxylate (307)**

$C_{16}H_{31}NO_3Si$
M = 313.51 g/mol

In a pressure tube, to a solution of protected aminoalcohol **297** (32.0 mg, 117 µmol, 1.00 eq.) in anhydrous toluene (1.5 mL) was added 2,2-dimethoxypropane (0.10 mL, 0.82 mmol, 7.0 eq.) and *p*-TsOH (1.81 mg, 10.5 µmol, 0.09 eq.). The tube was purged with argon during the addition and later sealed. The mixture was heated to 100 °C for 9 hours. Afterwards, the mixture was allowed to cool to room temperature and Celite was added. All volatiles were removed under reduced pressure, the mixture was purified by column chromatography (Silica, CH/EtOAc 40:1) and the desired compound **307** was obtained as a colorless oil (14.9 mg, 47.5 µmol, 41%). $\mathbf{R_f}$ = 0.24 (CH/EtOAc 40:1); **^{1}H-NMR** (500 MHz, acetone-d6) δ = 0.10 (s, 9H), 1.12 (s, 3H), 1.46 (s, 3H), 1.48 (s, 9H), 1.58 (s, 3H), 4.51 (dt, *J* = 5.4, 1.3 Hz, 1H), 5.24–5.29 (m, 1H), 5.41–5.47 (m, 1H), 5.80–5.90 (m, 1H); **^{13}C-NMR** (126 MHz, acetone-d6) δ = −1.1, 16.7, 25.6, 28.6, 29.1, 55.8, 79.7, 80.0, 92.5, 119.1, 134.2, 152.8; **HRMS (APCI)**: m/z calc for $[M+H]^+$: 314.2150; found: 314.1590 [note: the difference of calculated and measured mass is too high, however ^{1}H- and ^{13}C-NMR clearly indicate formation of the desired product.]

8.4.3 *Peterson* elimination feasibility attempts:

(*S*,4*Z*,6*Z*)-3-((*tert*-butyldimethylsilyl)oxy)-*N*-((2*R,3*R**)-3-hydroxy-2-(trimethylsilyl)pent-4-en-2-yl)-7-iodo-4-methylhepta-4,6-dienamide (310, 311)**

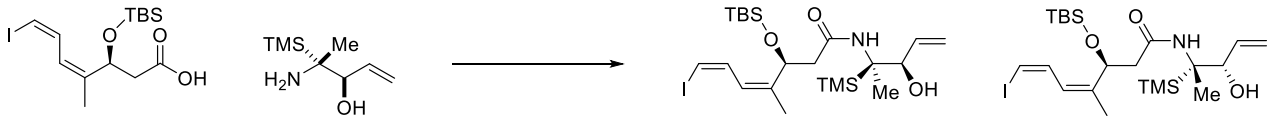

$C_{22}H_{42}INO_3Si_2$
M = 551.66 g/mol

$C_{22}H_{42}INO_3Si_2$
M = 551.66 g/mol

To a solution of carboxylic acid **244** (30.0 mg, 75.7 µmol, 1.00 eq.) in anhydrous DCM (1.5 mL) was sequentially added amine **306** (19.7 mg, 114 µmol, 1.50 eq.), DMAP (13.9 mg, 114 µmol, 1.50 eq.) and finally EDC-HCl (21.8 mg, 114 µmol, 1.50 eq.). The resulting solution was stirred at room temperature overnight. Afterwards, EtOAc (10 mL) and pH 7 buffer (10 mL) were added and the mixture was transferred to a separation funnel. Phases were separated and the aqueous phase was extracted with

EtOAc (2 x 10 mL). The combined organic layers were washed with water (10 mL), a saturated solution of NH_4Cl (10 mL) and brine (10 mL), dried over $MgSO_4$, filtered and concentrated. Purification by column chromatography (Silica, CH/EtOAc 5:1) yielded the desired compound as a mixture of diastereoisomers **310** and **311** (12.0 mg, 21.8 µmol, 29%). $\mathbf{R_f}$ = 0.15 (0.18) (CH/EtOAc 5:1); **HRMS (ESI)**: m/z calc for $[M+K]^+$: 590.1379; found: 590.1369.

(*S*,4*Z*,6*Z*)-3-((*tert*-butyldimethylsilyl)oxy)-*N*-((2*R,3*R**)-3-hydroxy-2-(trimethylsilyl)pent-4-en-2-yl)-7-iodo-4-methylhepta-4,6-dienamide (313)**

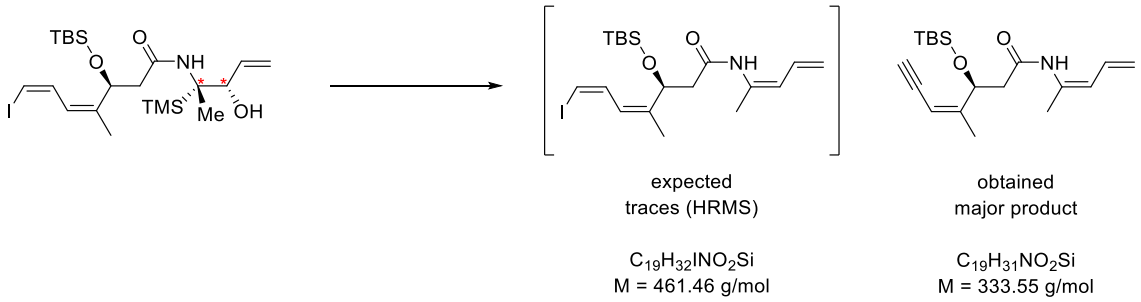

To a solution of both α-silyl-β-hydroxyamides **310** and **311** (10.0 mg, 18.1 µmol, 1.00 eq.) in anhydrous THF (0.3 mL) at −41 °C (dry ice, MeCN) was added a solution of KO*t*Bu (209 µmol/mL in THF, 0.10 mL, 21 µmol, 1.2 eq.). After 30 minutes at −41 °C the mixture was warmed to room temperature, as no reaction was observed (TLC). After 1 hour, a second portion of KO*t*Bu (209 µmol/mL in THF, 0.05 mL, 10 µmol, 0.5 eq.). After 1 hour of stirring, the mixture was quenched by addition of pH 7 buffer (4 mL) and the mixture was extracted with EtOAc (3 x 5 mL). The organic layer was washed with brine (10 mL), dried over $MgSO_4$, filtered and concentrated. The residue was dissolved in acetone/water (1:1, 1 mL) and loaded onto a CHROMABOND C18 ec, 45 µm, 200 mg SPE-cartridge (conditioned: MeCN 2 x 3 mL, H_2O: 3 mL). Then, the cartridge was eluted with a step-gradient of MeCN/H_2O (2 mL each): 9:1; 8:1; 6:1; 2:1; 1:1; 1:2; 1:4; 1:6. The obtained fractions were analyzed by TLC with the 1:2 and 1:4-fractions containing the estimated product. After evaporation of the solvent, the obtained product was dissolved in acetone-d6 and analyzed by NMR (yield not determined). $\mathbf{R_f}$ = 0.25 (0.29) (CH/EtOAc 5:1); <u>alkyne</u> (**313**): **^{1}H-NMR** (700 MHz, acetone-d6) δ = 1.83 (dd, *J* = 1.7, 0.7 Hz, 3H), 2.12 (s, 3H), 2.26 (dd, *J* = 13.8, 3.6 Hz, 1H), 2.74 (dd, *J* = 6.2, 1.8 Hz, 1H), 3.61 (dd, *J* = 2.5, 0.7 Hz, 1H), 4.87 (d, *J* = 10.4 Hz, 1H), 5.04 (d, *J* = 16.7 Hz, 1H), 5.34–5.38 (m, 1H), 5.45 (dd, *J* = 9.6, 3.4 Hz, 1H), 5.47 (s, 1H), 6.57–6.63 (m, 1H), 8.38 (s, 1H); **^{13}C-NMR** (176 MHz, acetone-d6) δ = 17.1, 21.8, 44.0, 70.8, 70.8, 80.6, 83.5, 105.5, 114.2, 118.2, 132.7, 135.3, 155.4; **HRMS (APCI)**: m/z calc for $[M+H]^+$: 334.2196; found: 334.2197; <u>iodo-diene</u> (**312**) [traces]: **HRMS (APCI)**: m/z calc for $[M+H]^+$: 462.1320; found: 462.1320.

8.5 Other syntheses not discussed within this work

(*E*)-3-((2*S,3*R**)-3-methyl-3-(trimethylsilyl)oxiran-2-yl)acrylaldehyde (S-15)**

$C_9H_{16}O_2Si$
M = 184.31 g/mol

A solution of epoxy aldehyde **268** (20 mg, 126 µmol, 1.00 eq.) and (triphenylphosphoranylidene) acetaldehyde (58.0 mg, 0.19 mmol, 1.5 eq.) in MeCN (1 mL) was refluxed for 1 hour. Then, Celite® was added and the solvent was removed. Purification by column chromatography (Silica, CH/EtOAc 9:1) yielded the desired product **S-15** as a pale yellow oil (12.7 mg, 68.9 µmol, 55%). $\mathbf{R_f}$ = 0.24 (CH/EtOAc 9:1); **^{1}H-NMR** (500 MHz, acetone-d6) δ = 0.14 (s, 9H), 1.32 (s, 3H), 2.80 (s, 1H), 3.49 (dd, *J* = 7.5, 0.9 Hz, 1H), 6.41 (ddd, *J* = 15.7, 7.8, 0.9 Hz, 1H), 6.82 (dd, *J* = 15.8, 7.4 Hz, 1H), 9.62 (d, *J* = 7.8 Hz, 1H); **^{13}C-NMR** (126 MHz, acetone-d6) δ = −1.8, 22.9, 59.4, 63.6, 135.4, 154.2, 193.3; **HRMS (APCI)**: m/z calc for $[M+H]^+$: 185.0992; found: 185.0986.

methyl (S)-2-methyl-3-((1-phenyl-1H-tetrazol-5-yl)thio)propanoate (S-16)

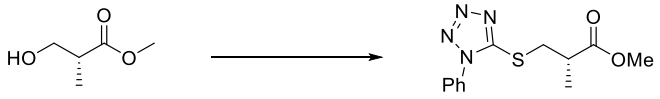

$C_{12}H_{14}N_4O_2S$
M = 278.33 g/mol

The synthesis was carried out according to a known literature procedure:[226]

To a solution of *S*-Roche-Ester (*S*-**208**) (1.00 g, 8.47 mmol, 1.00 eq.) and triphenylphosphane (3.33 g, 12.7 mmol, 1.50 eq.) in anhydrous THF (15 mL) was added a solution of 1-phenyl-1H-tetrazole-5-thiol (2.26 g, 12.7 mmol, 1.50 eq.) and DIAD (2.50 mL, 12.7 mmol, 1.50 eq.) in THF (20 mL) dropwise over one hour via syringe pump. The resulting mixture was stirred overnight. Afterwards, the mixture was diluted with Et_2O (100 mL) and water (40 mL). Phases were separated and the aqueous layer was extracted with Et_2O (2 x 50 mL). The combined organic layers were washed with brine (50 mL), dried over $MgSO_4$, filtered and concentrated. Purification by column chromatography (Silica, CH/EtOAc 5:2) yielded the desired product **S-16** as a colorless oil (2.36 g, 8.47 mmol, quant.). $\mathbf{R_f}$ = 0.33 (CH/EtOAc 5:2); $\boldsymbol{\alpha_D^{20}}$ = -21.8

(c = 1.0, MeCN); **^{1}H-NMR** (500 MHz, acetone-d6) δ = 1.29 (d, *J* = 7.1 Hz, 3H), 3.07 (td, *J* = 7.4, 5.8 Hz, 1H), 3.54 (dd, *J* = 13.6, 5.8 Hz, 1H), 3.58–3.63 (m, 1H), 3.64 (s, 3H), 7.62–7.73 (m, 5H); **^{13}C-NMR** (126 MHz, acetone-d6) δ = 16.9, 36.4, 40.2, 52.2, 125.3, 130.8, 131.3, 134.7, 155.1, 175.1; **HRMS (ESI)**: m/z calc for $[M+Na]^+$: 301.0730; found: 301.0726. The spectroscopic data were in agreement with those previously reported.[226]

(*S*)-2-methyl-3-((1-phenyl-1H-tetrazol-5-yl)thio)propanoIc acid (S-17)

$C_{11}H_{12}N_4O_2S$
M = 264.30 g/mol

To a stirred solution of thioether (**S-16**) (360 mg, 1.29 mmol, 1.00 eq.) in toluene (5 mL) was added TBTO (1.3 mL, 2.59 mmol, 2.00 eq.). The mixture was refluxed at 145 °C for 16 hours in a pressure tube. Then, a solution of 5% $NaHCO_3$ (10 mL) was added and the organic solvent was removed under reduced pressure at 45 °C. Afterwards, Et_2O was added and the organic layer was extracted with 5% $NaHCO_3$ (3 x 5 mL). The combined aqueous layers were washed with Et_2O (10 mL) and acidified to pH 4 by dropwise addition of 5 M HCl, during which the solution turns into a white cloudy mixture. After extraction with EtOAc (3 x 10 mL), the combined organic layers were washed with brine (15 mL) and dried over $MgSO_4$, filtered and concentrated. The product **S-17** was received as a white solid (118 mg, 446 µmol, 34%). $\boldsymbol{\alpha_D^{20}}$ = -27.7 (c = 1.0, MeCN); **^{1}H-NMR** (500 MHz, acetone-d6) δ = 1.33 (d, *J* = 7.1 Hz, 3H), 3.06 (pd, *J* = 7.2, 5.7 Hz, 1H), 3.55 (dd, *J* = 13.5, 5.7 Hz, 1H), 3.62 (dd, *J* = 13.5, 7.8 Hz, 1H), 7.58–7.77 (m, 5H), 10.98 (s, 1H); **^{13}C-NMR** (126 MHz, acetone-d6) δ = 16.1, 35.5, 39.2, 124.4, 129.9, 130.4, 133.8, 154.4; **HRMS (ESI)**: m/z calc for $[M+Na]^+$: 287.0573; found: 287.0570.

2-(trimethylsilyl)ethyl (*S*)-2-methyl-3-((1-phenyl-1H-tetrazol-5-yl)thio)propanoate (S-18)

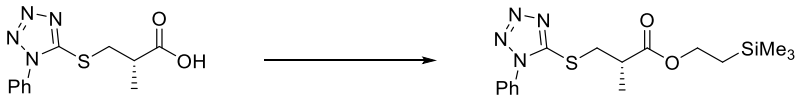

$C_{16}H_{24}N_4O_2SSi$
M = 364.54 g/mol

A solution of carboxylic acid **S-17** (107 mg, 405 µmol, 1.00 eq.), 2-(trimethylsilyl)ethanol (100 µL, 698 µmol, 1.70 eq.) and pyridine (65 µL, 0.81 mmol, 2.0 eq.) in MeCN (3 mL) was cooled to 0 °C followed by addition of DCC (1 M in DCM, 0.50 mL, 0.50 mmol, 1.2 eq.). The ice bath was removed and the

resulting solution was stirred for 5 hours. The reaction mixture was filtered, rinsed with MeCN and loaded onto Celite. Purification by column chromatogrpahy (Silica, CH/EE 12:1) yielded the desired ester **S-18** as a clear liquid (118 mg, 324 µmol, 80%). $\mathbf{R_f}$ = 0.28 (CH/EtOAc 12:1); $\boldsymbol{\alpha_D^{20}}$ = -21.6 (c = 1.0, MeCN); **^{1}H-NMR** (500 MHz, acetone-d6) δ = 0.04 (s, 9H), 0.95–1.01 (m, 2H), 1.29 (d, *J* = 7.2 Hz, 3H), 2.99–3.09 (m, 1H), 3.53–3.63 (m, 2H), 4.11–4.21 (m, 2H), 7.63–7.74 (m, 5H); **^{13}C-NMR** (126 MHz, acetone-d6) δ = -1.5, -1.4, 17.0, 17.9, 36.4, 40.5, 63.5, 125.3, 130.8, 131.3, 134.7, 155.1, 174.7; **HRMS (ESI)**: m/z calc for $[M+Na]^+$: 387.1281; found: 387.1294.

2-(trimethylsilyl)ethyl (*S*)-2-methyl-3-((1-phenyl-1H-tetrazol-5-yl)sulfonyl)propanoate (S-19)

$C_{16}H_{24}N_4O_4SSi$
M = 396.54 g/mol

To a solution of thioether **S-18** (100 mg, 274 µmol, 1.00 eq.) in DCM (2 mL) at 0 °C was added mCPBA (141 mg, 631 µmol, 2.30 eq.) in three portions. After stirring for 5 minutes, the ice bath was removed and the mixture was stirred for 24 hours. Then, a saturated solution of $Na_2S_2O_3$ (4 mL) was added and the mixture was stirred for 10 minutes. After dilution with EtOAc (20 mL), layers were separated and the organic layer was washed with a saturated solution of $NaHCO_3$ (4 x 6 mL) and brine (10 mL). The organic layer was dried over $MgSO_4$, filtered and concentrated to afford the crude product as a red-brown gum. After purification by column chromatography (Silica, CH/EtOAc 4:1), the desired product **S-19** was obtained as a colorless resin (68 mg, 0.17 mmol, 63%). $\mathbf{R_f}$ = 0.32 (CH/EtOAc 4:1); $\boldsymbol{\alpha_D^{20}}$ = -8.2 (c = 1.0, MeCN); **^{1}H-NMR** (500 MHz, acetone-d6) δ = 0.06 (s, 9H), 0.95–1.03 (m, 2H), 1.36 (d, *J* = 7.3 Hz, 3H), 3.18 (dqd, *J* = 8.2, 7.3, 4.5 Hz, 1H), 3.87 (dd, *J* = 15.1, 4.6 Hz, 1H), 4.09–4.20 (m, 3H), 7.67–7.75 (m, 3H), 7.76–7.81 (m, 2H); **^{13}C-NMR** (126 MHz, acetone-d6) δ = −1.5, 17.6, 17.7, 27.5, 35.7, 59.2, 64.1, 127.1, 130.4, 132.4, 134.4, 173.7; **HRMS (ESI)**: m/z calc for $[M+Na]^+$: 419.1180; found: 419.1178.

methyl (*S*)-3-bromo-2-methylpropanoate (S-20)

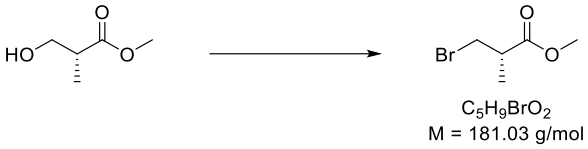

$C_5H_9BrO_2$
M = 181.03 g/mol

The synthesis was carried out according to a known literature procedure:[227]

To a solution of CBr_4 (5.61 g, 16.9 mmol, 2.00 eq.) in anhydrous DCM (20 mL) was added *R*-Roche ester (*R*-**208**) (1.00 g, 8.47 mmol, 1.00 eq.). The resulting solution was cooled to 0 °C, followed by addition of triphenylphosphane (2.50 g, 9.73 mmol, 1.15 eq.) over 10 minutes. The mixture was slowly warmed to r.t. over the course of 4 hours. Then, the mxiture was diluted with *n*-pentane (150 mL) and filtered over Celite®. The obtained filtrate was stored at -30 °C for 30 minutes and afterwards filtered for a second time to yield a clear colorless solution. After evaporation of the solvent a mixture of a colorless liquid and a crystalline solid was obtained. All soluble (*n*-pentane) material was loaded onto a silica column and eluted with a step gradient (*n*-pentane/Et_2O), (100:0, 100 mL), (100:2, 102 mL), (100:4, 104 mL), (100:10, 110 mL) (100:20, 3 x 120 mL) and (50:50, 100 mL). As the compound does not stain and is not UV-active, all fractions were collected, the solvents were evaporated and the obtained products were analyzed by NMR. Early fractions (1-4) mostly contained CBr_4 and bromoform. Pure product **S-20** was obtained from the 20% fractions as a yellow liquid (1.12 g, 6.19 mmol, 73%). $\boldsymbol{\alpha_D^{20}}$ = -15.8 (c = 1.0, DCM); **^{1}H-NMR** (500 MHz, acetone-d6) δ = 1.24 (d, *J* = 7.0 Hz, 3H), 2.95 (pd, *J* = 6.9, 5.5 Hz, 1H), 3.60–3.65 (m, 2H), 3.68 (s, 3H); **^{13}C-NMR** (126 MHz, acetone-d6) δ = 16.3, 35.5, 42.6, 52.1, 174.0; **HRMS (APCI)** m/z: calc. for $[M+H]^+$: 182.9839; found: 182.9839. The spectroscopic data were in agreement with those previously pulished.[227]

methyl (*S*)-3-bromo-2-methylpropanoic acid (S-21)

$C_4H_7BrO_2$
M = 167,00 g/mol

The synthesis was carried out according to a known literature procedure:[228]

To a stirred solution of TBTO (1.71 g, 2.87 mmol, 2.0 eq.) in toluene (20 mL) was added methyl 3-bromo-2-methylpropionate (**S-20**) (260 mg, 1.44 mmol, 1.0 eq.). The mixture was refluxed at 130 °C for 60 hours and the solvent evaporated *in vacuo*. The resulting oil was dissolved in EtOAc (30 mL) and extracted with 5% aqueous $NaHCO_3$ (4 x 12 mL). The aqueous layer was washed with Et_2O (1 x 20 mL) acidified to pH 2 with 1 M HCl and extracted with EtOAC (3 x 20 mL). The organic layer was washed with brine (1 x 20 mL), dried over $MgSO_4$, filtered and concentrated to afford **S-21** (166 mg, 994 µmol, 69%) as a colorless oil. $\boldsymbol{\alpha_D^{20}}$ = -10.1 (c = 1.0, MeCN); **^{1}H-NMR** (500 MHz, acetone-d6) δ = 1.26 (d, *J* = 7.0 Hz, 3H), 2.87–2.98 (m, 1H), 3.58–3.70 (m, 2H); **^{13}C-NMR** (126 MHz, acetone-d6) δ = 16.4, 35.7, 42.4, 174.4. **HRMS (ESI)** m/z: calc. for $[M.H]^-$: 166.9535; found: 166.9537. The spectroscopic data were in agreement with those previously pulished.[228]

2-(dichloromethyl)-4,4,5,5-tetramethyl-1,3,2-dioxaborolane (S-22)

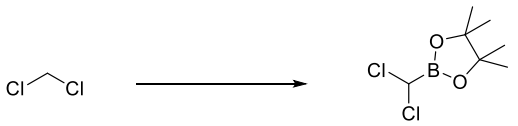

$C_7H_{13}BCl_2O_2$
M = 210.89 g/mol

The compound was synthesized according to a *modified* literature procedure.[141]

Anhydrous DCM (3.5 mL, 55 mmol, 1.1 eq.) was added to anhydrous THF (100 mL). The mixture was cooled to –100 °C ($EtOH/N_2$), then *n*-BuLi (2.5 M in hexane, 19.9 mL, 49.8 mmol, 1.00 eq.) was added dropwise *via* an syringe pump over 45 min. The reaction was stirred for 40 min at this temperature, then trimethylborate (6.2 mL, 55 mmol, 1.1 eq.) was added in one portion and the reaction was stirred another 40 min at –100 °C. The reaction was quenched with 5 N HCl solution (10 mL), the coooling bath was removed and the mixture was stirred at room temperature for 1 h. Then, the mixture was extracted with ether (3 × 50 mL), the organic layers were combined, washed with brine, dried over magnesium

sulfate, filtered and concentrated in vacuum to provide the crude boronic acid. The residue was dissolved in anhydrous DCM (40 mL), pinacol (6.19 g, 52.4 mmol, 1.05 eq.) and anhydrous $MgSO_4$ were added and the resulting mixture was stirred for 16 hours. Afterwards, the mixture was filtered and the solvent was removed. The crude product **S-22** was purified by double vacuum distillation (b.p. = 57 °C, 1.2 mbar) and yielded the compound as a colorless oil (4.80 g, 22.8 mmol, 45%). **^{1}H-NMR** (500 MHz, acetone-d6) δ = 1.31 (s, 12H), 5.66 (s, 1H); **^{13}C-NMR** (126 MHz, acetone-d6) δ = 23.8, 85.5; [note: the carbon attached to boron was not observed due to quadrupole broadening caused by the ^{11}B nucleus]; **HRMS (ESI-)** m/z: calc. for $[M+F^-]^-$: 229.0376; found: 229.0380. The spectroscopic data were in agreement with those previously pulished.[141]

2-(dichloromethyl)-5,5-dimethyl-1,3,2-dioxaborinane (S-23)

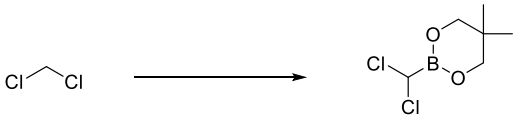

$C_6H_{11}BCl_2O_2$
M: 196.86 g/mol

The compound was synthesized according to a *modified* literature procedure.[141,229]

Anhydrous DCM (3.5 mL, 55 mmol, 1.1 eq.) was added to anhydrous THF (100 mL). The mixture was cooled to –100 °C (EtOH/N_2), then *n*-BuLi (2.5 M in hexane, 19.9 mL, 49.8 mmol, 1.00 eq.) was added dropwise *via* an syringe pump over 45 min. The reaction was stirred for 40 min at this temperature, then trimethylborate (6.2 mL, 55 mmol, 1.1 eq.) was added in one portion and the reaction was stirred another 40 min at –100 °C. The reaction was quenched with 5 M HCl solution (10 mL), the coooling bath was removed and the mixture was stirred at room temperature for 1 h. Then, the mixture was extracted with ether (3 × 50 mL), the organic layers were combined, washed with brine, dried over magnesium sulfate, filtered and concentrated in vacuum to provide the crude boronic acid. The residue was dissolved in anhydrous DCM (40 mL), neopentylglycol (5.19 g, 49.9 mmol, 1.00 eq.) and anhydrous $MgSO_4$ were added and the resulting mixture was stirred for 16 hours. Afterwards, the mixture was filtered and the solvent was removed. The crude product was purified by vacuum distillation (b.p. = 100 °C, 3.2 mbar) and yielded the compound **S-23** as a colorless oil (5.73 g, 29.1 mmol, 58%). **^{1}H-NMR** (500 MHz, $CDCl_3$) δ = 1.02 (s, 6H), 3.74 (s, 4H), 5.25 (s, 1H); **^{13}C-NMR** (126 MHz, $CDCl_3$) δ = 21.7, 32.1, 73.0, 127.8; **HRMS (EI)** m/z: calc. for $[M(^{10}B)]^+$: 195.0265; found: 195.0266. The spectroscopic data were in agreement with those previously pulished.[229]

9. Copies of NMR-spectra

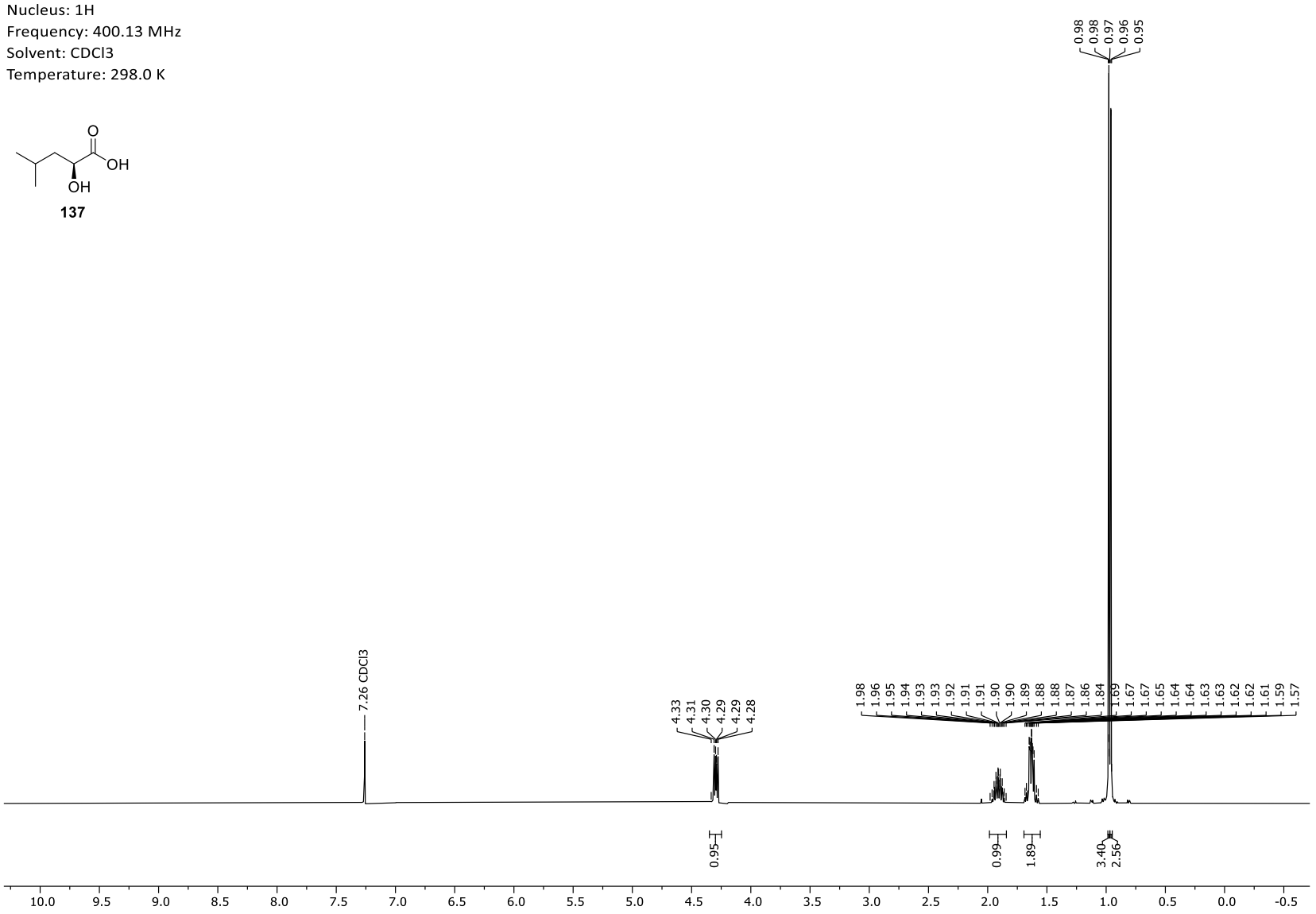

Appendix 1. ^{1}H-NMR spectrum of (*S*)-2-hydroxy-4-methylpentanoic acid (**137**).

Nucleus: 13C
Frequency: 100.63 MHz
Solvent: CDCl3
Temperature: 298.0 K

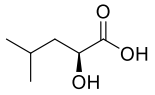

137

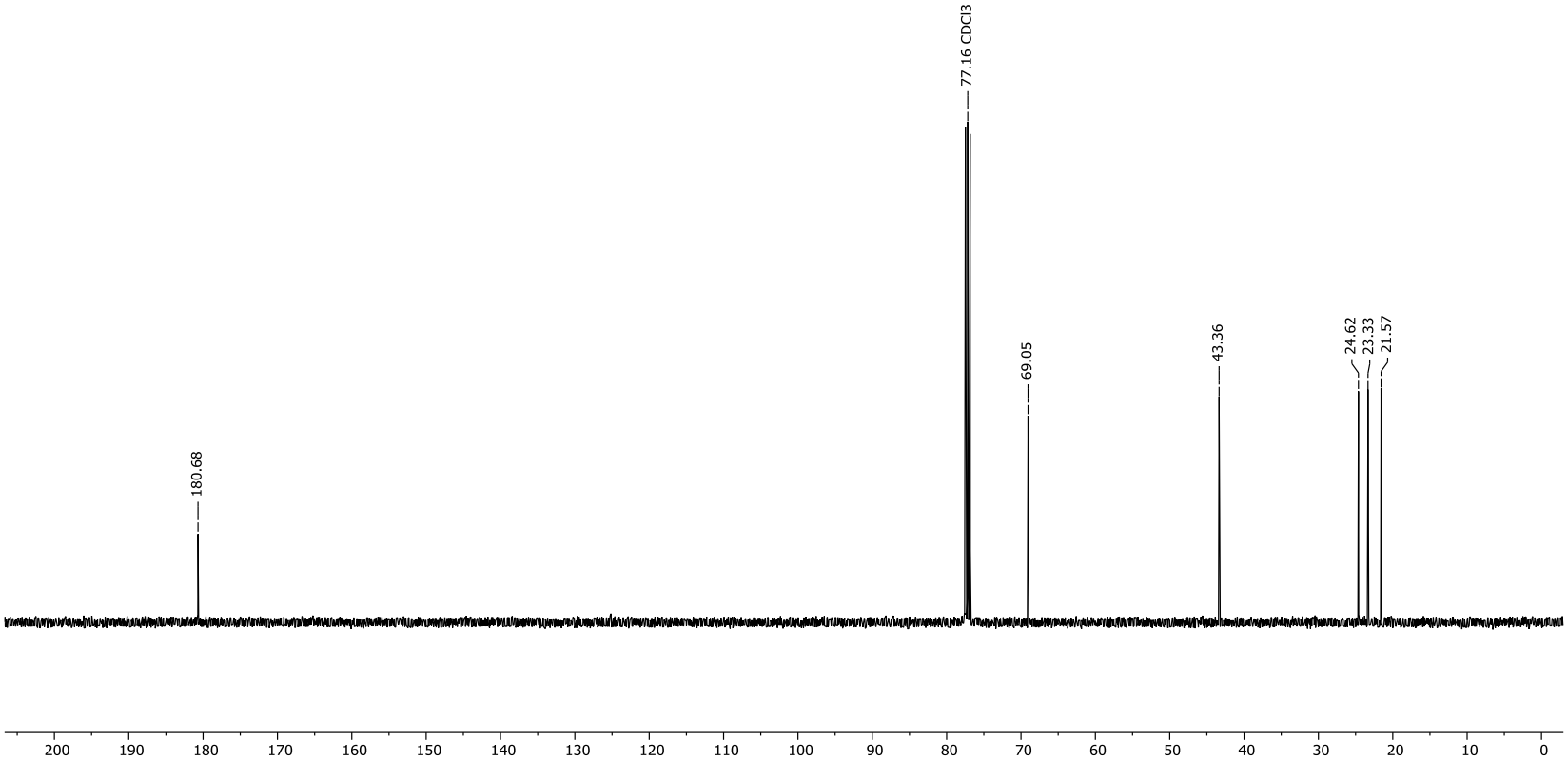

Appendix 2. ^{13}C-NMR spectrum of (*S*)-2-hydroxy-4-methylpentanoic acid (**137**).

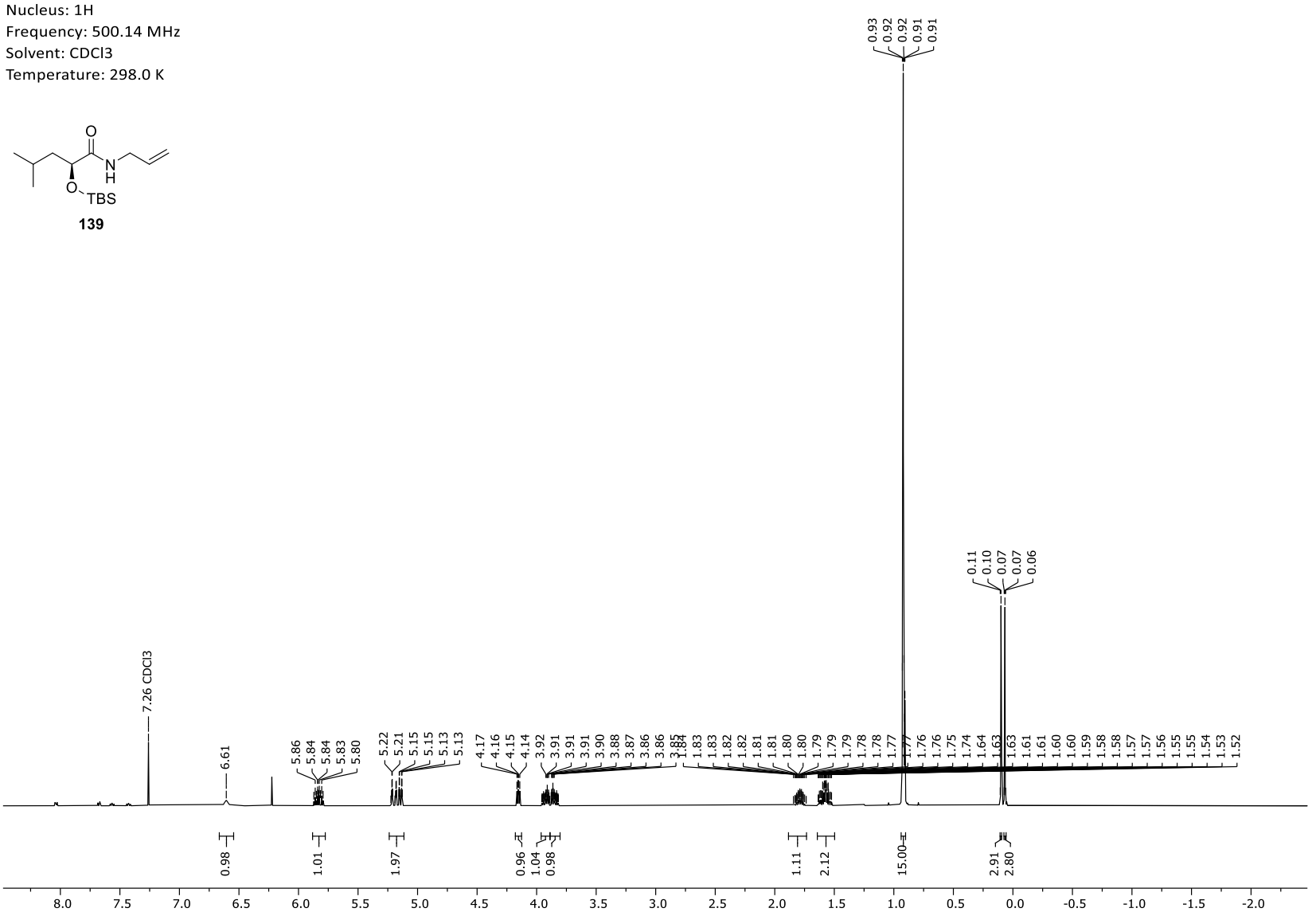

Appendix 3. ^{1}H-NMR spectrum of (*S*)-*N*-allyl-2-((*tert*-butyldimethylsiliyl)oxy)-4-methylpentanamide (**139**).

Nucleus: 13C
Frequency: 125.78 MHz
Solvent: CDCl3
Temperature: 298.0 K

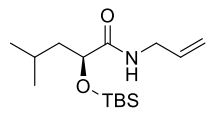

139

Appendix 4. ^{13}C-NMR spectrum of (*S*)-*N*-allyl-2-((*tert*-butyldimethylsiliyl)oxy)-4-methylpentanamide (**139**).

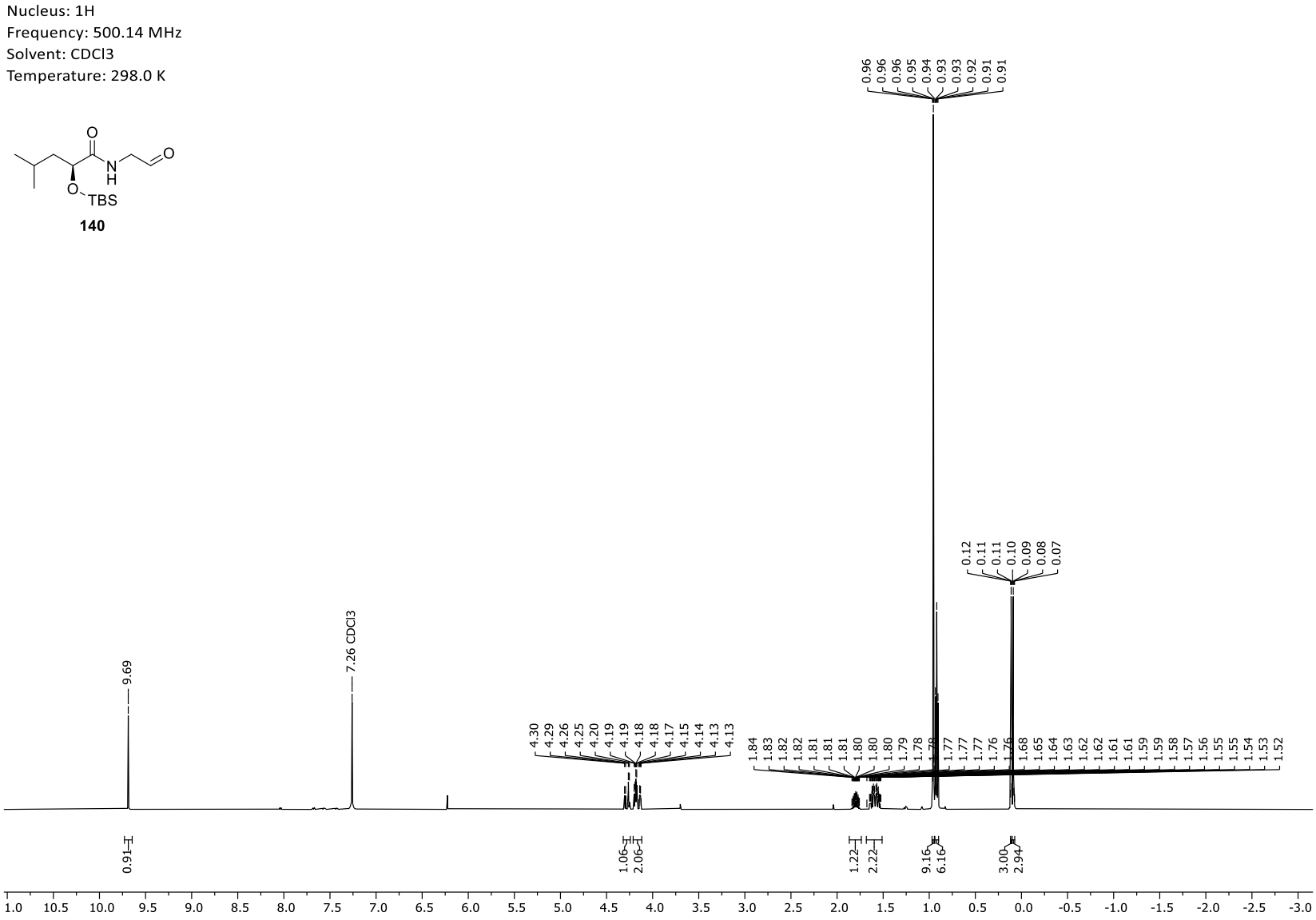

Appendix 5. ^{1}H-NMR spectrum of (*S*)-*N*-(2'-oxoethyl)-2-((*tert*-butyldimethylsiliyl)oxy)-4-methylpentanamide (**140**).

Nucleus: 13C
Frequency: 125.78 MHz
Solvent: CDCl3
Temperature: 298.0 K

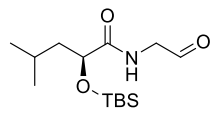

140

Appendix 6. ^{13}C-NMR spectrum of (*S*)-*N*-(2'-oxoethyl)-2-((*tert*-butyldimethylsiliyl)oxy)-4-methylpentanamide (**140**).

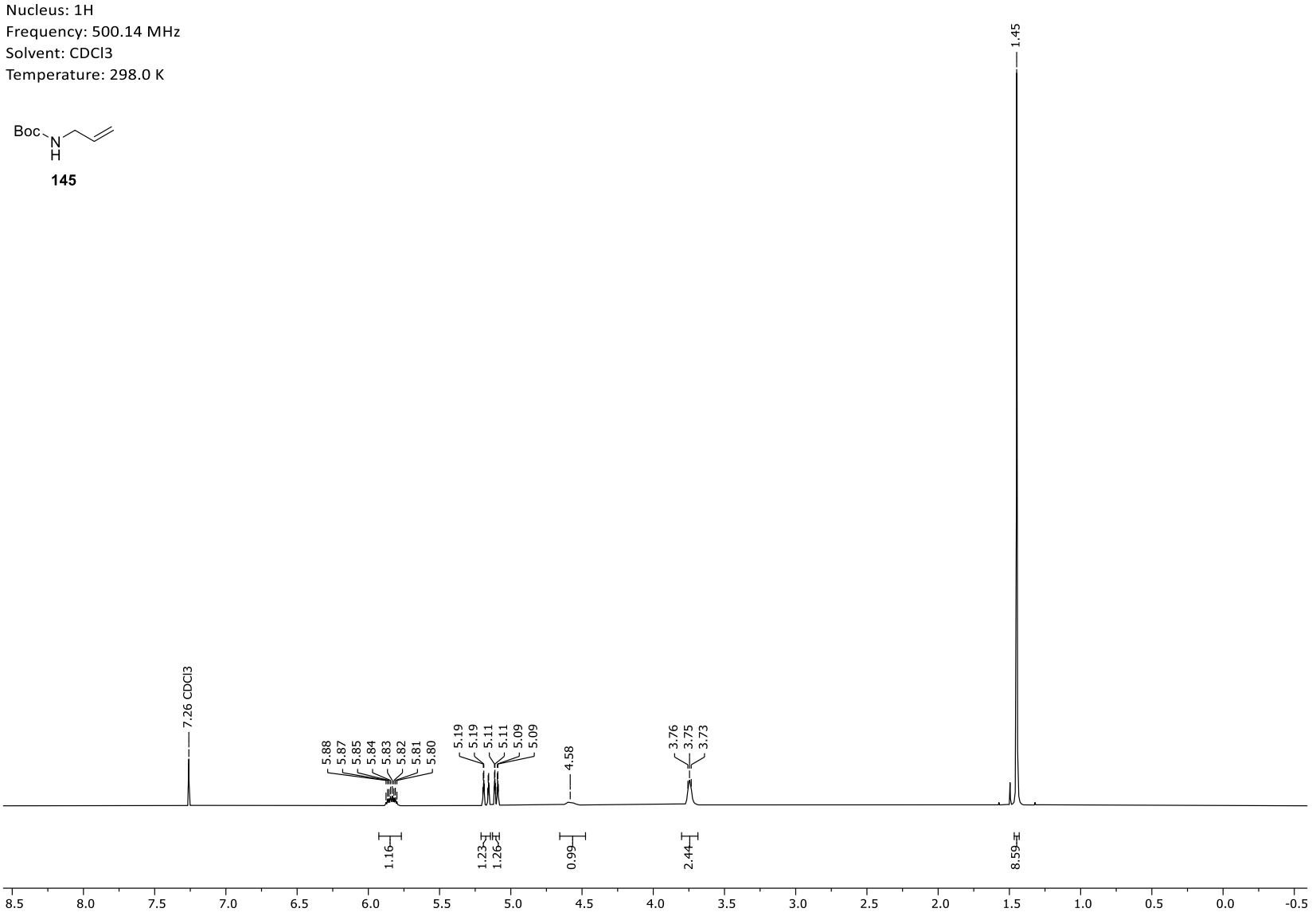

Appendix 7. ^{1}H-NMR spectrum of *N*-allyl-tert-butylcarbamate (**145**).

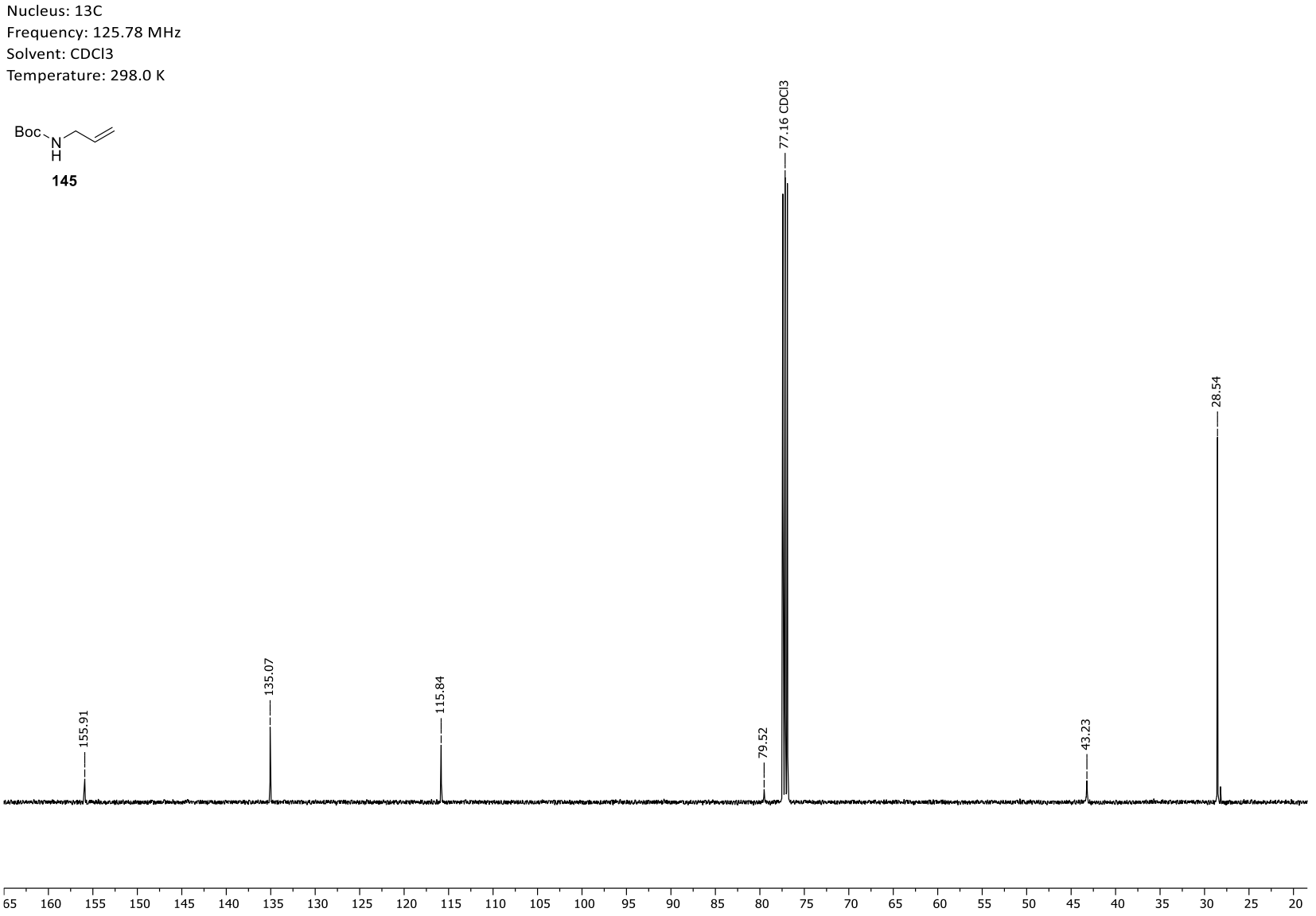

Appendix 8. ^{13}C-NMR spectrum of *N*-allyl-tert-butylcarbamate (**145**).

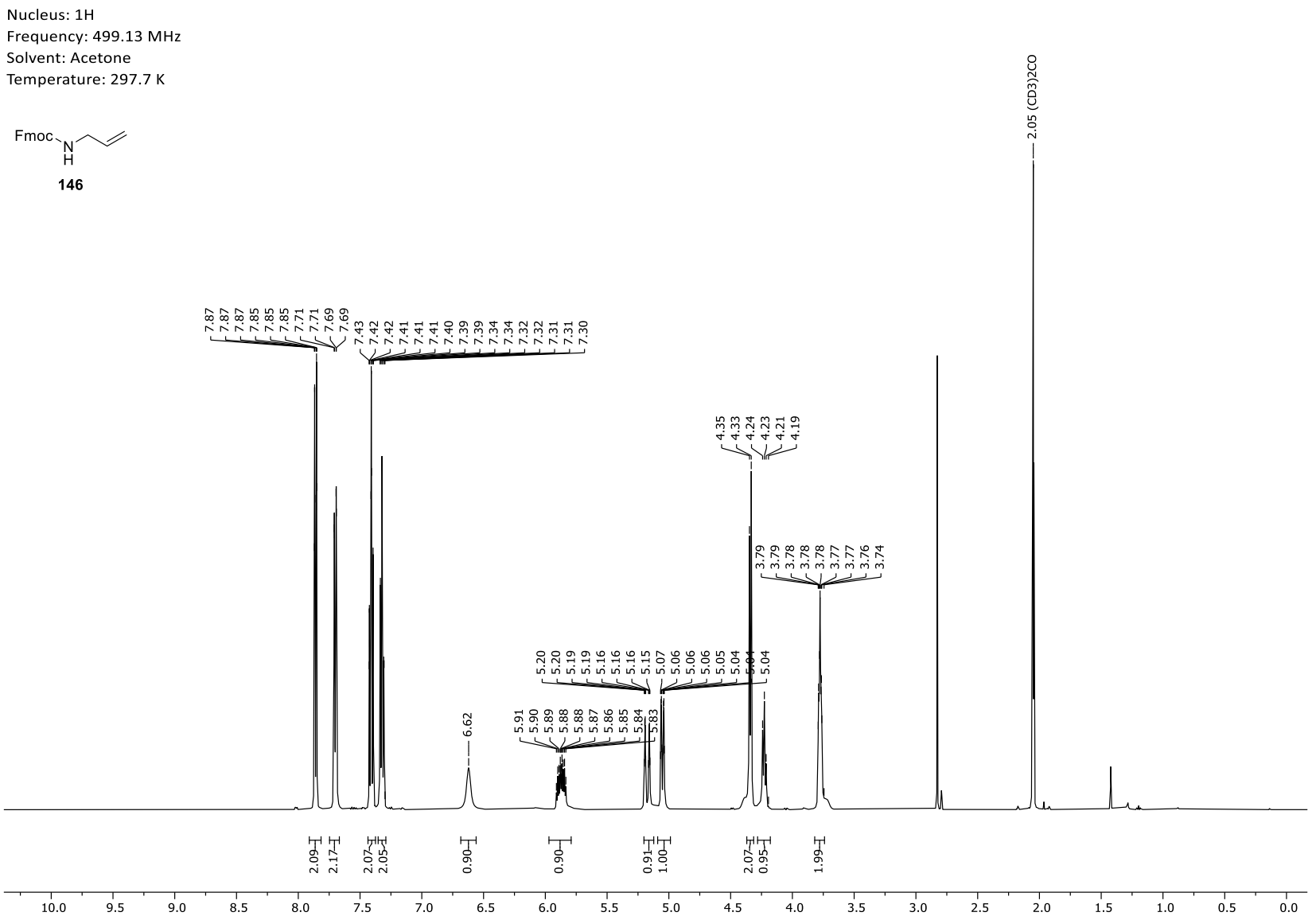

Appendix 9. ^{1}H-NMR spectrum of (9H-fluoren-9-yl)methyl allylcarbamate (**146**).

Nucleus: 13C
Frequency: 125.52 MHz
Solvent: Acetone
Temperature: 298.6 K

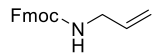

146

Appendix 10. ^{13}C-NMR spectrum of (9H-fluoren-9-yl)methyl allylcarbamate (**146**).

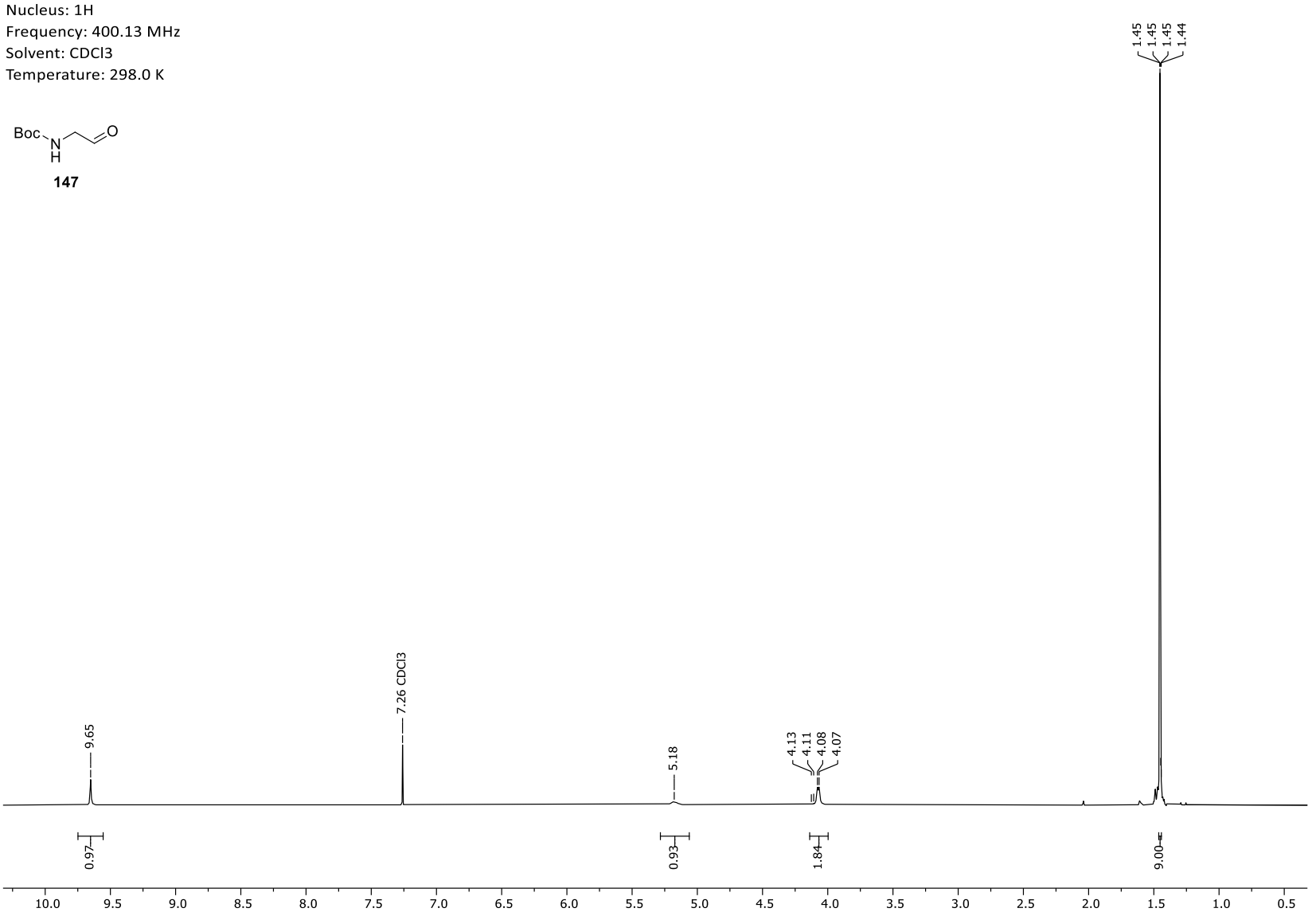

Appendix 11. ^{1}H-NMR spectrum of *N*-(2-oxoethyl)-*tert*-butylcarbamate (**147**).

Nucleus: 13C
Frequency: 100.63 MHz
Solvent: CDCl3
Temperature: 298.0 K

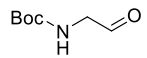

147

Appendix 12. ^{13}C-NMR spectrum of *N*-(2-oxoethyl)-*tert*-butylcarbamate (**147**).

Nucleus: 1H
Frequency: 700.41 MHz
Solvent: Acetone
Temperature: 298.0 K

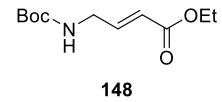

148

Appendix 13. ^{1}H-NMR spectrum of (*E*)-*N*-boc-4-amino-ethyl-but-2-enoate (**148**).

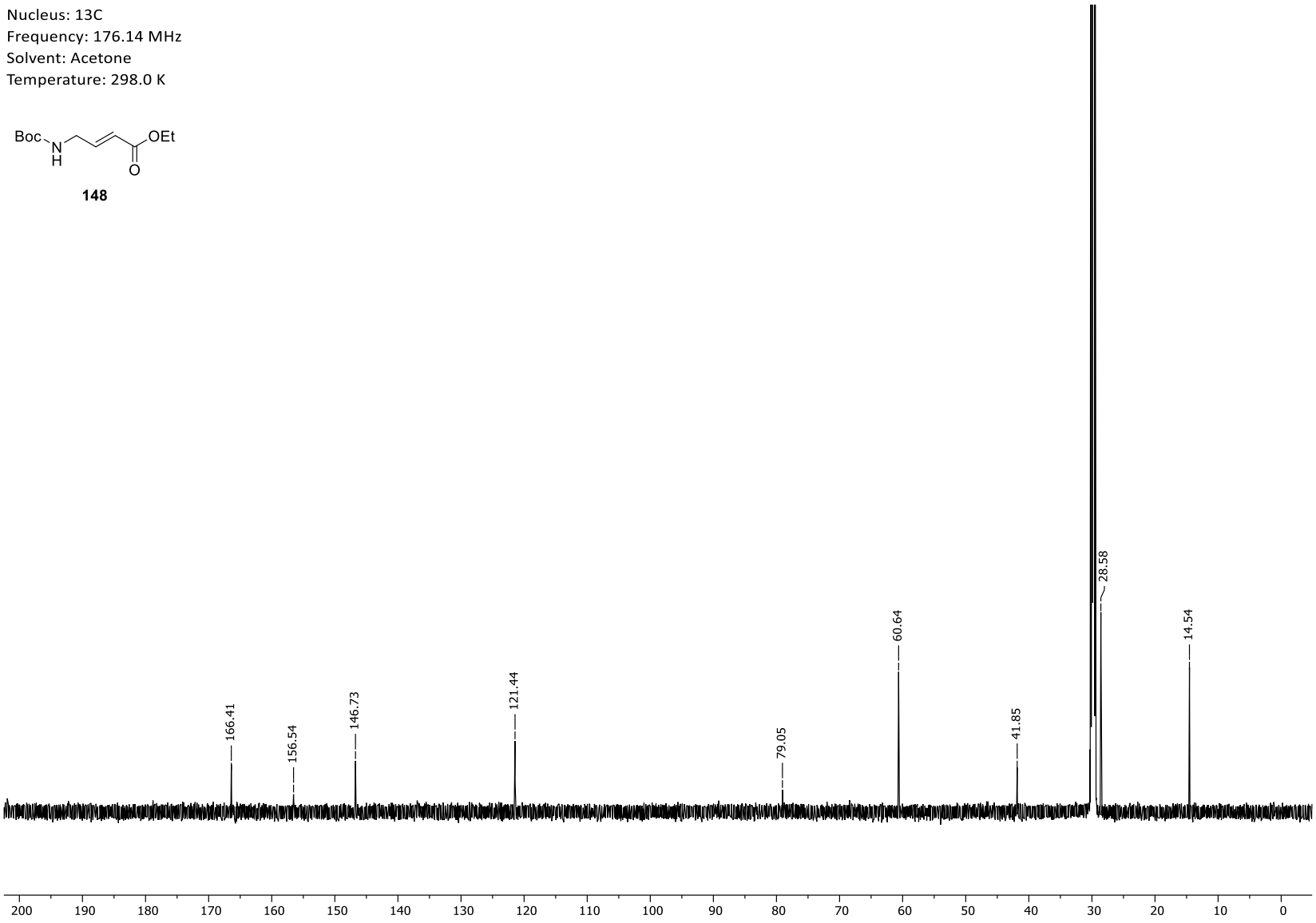

Appendix 14. ^{13}C-NMR spectrum of (*E*)-*N*-boc-4-amino-ethyl-but-2-enoate (**148**).

Nucleus: 1H
Frequency: 499.13 MHz
Solvent: CDCl3
Temperature: 298.0 K

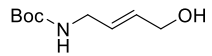

149

Appendix 15. ^{1}H-NMR spectrum of (*E*)-*N*-boc-4-amino-but-2-enol (**149**).

Nucleus: 13C
Frequency: 125.52 MHz
Solvent: CDCl3
Temperature: 297.9 K

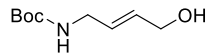

149

Appendix 16. ^{13}C-NMR spectrum of (*E*)-*N*-boc-4-amino-but-2-enol (**149**).

Nucleus: 1H
Frequency: 400.13 MHz
Solvent: CD2Cl2
Temperature: 298.0 K

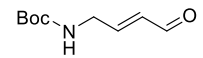

150

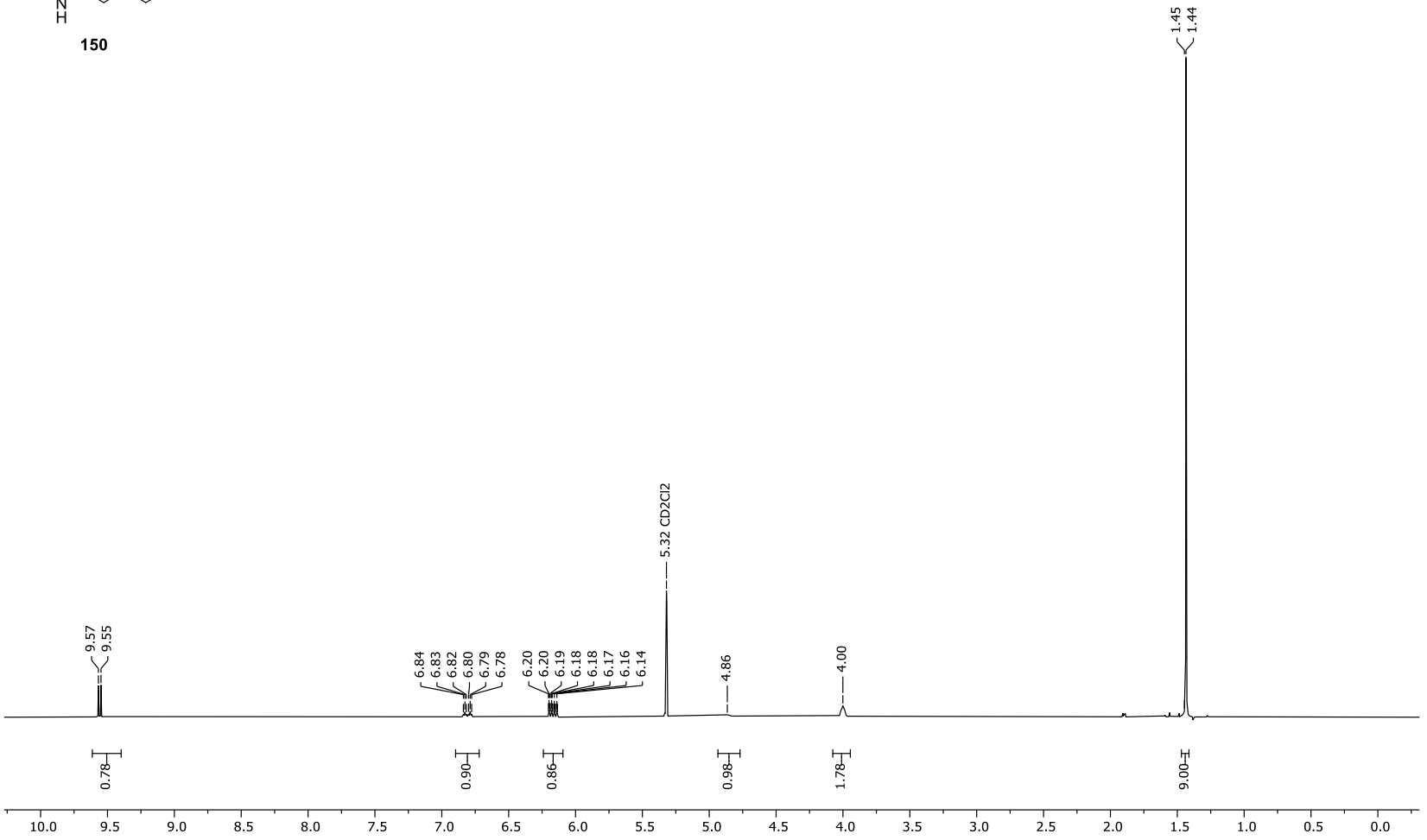

Appendix 17. ^{1}H-NMR spectrum of (*E*)-*N*-Boc-4-amino-but-2-enal (**150**).

Nucleus: 13C
Frequency: 100.63 MHz
Solvent: CD2Cl2
Temperature: 298.0 K

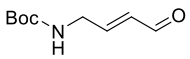

150

Appendix 18. ^{13}C-NMR spectrum of (*E*)-*N*-Boc-4-amino-but-2-enal (**150**).

Nucleus: 1H
Frequency: 300.13 MHz
Solvent: Acetone
Temperature: 298.0 K

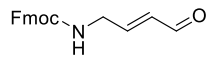

151

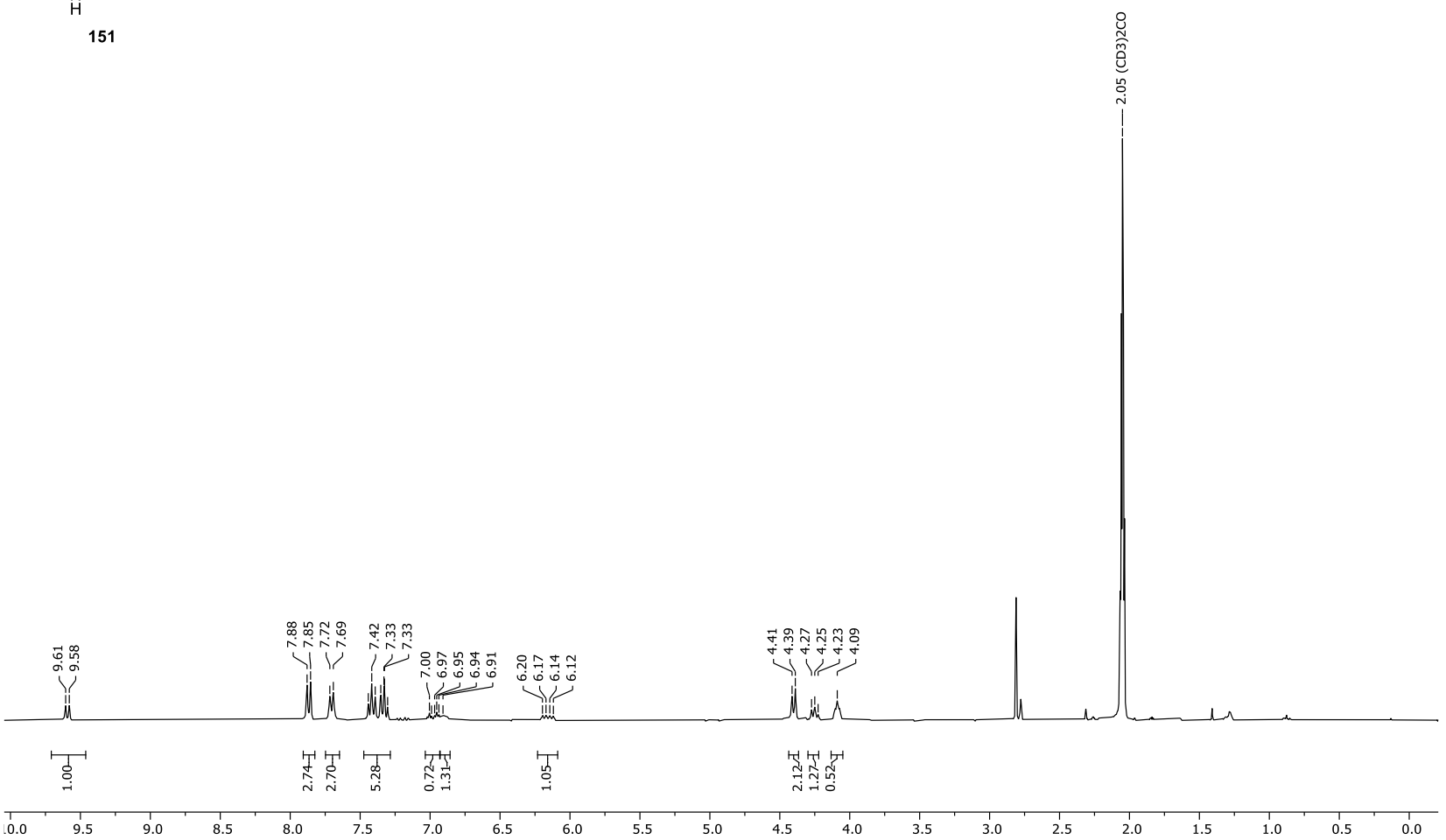

Appendix 19. ^{1}H-NMR spectrum of (9H-fluoren-9-yl)methyl (*E*)-(4-oxobut-2-en-1-yl)carbamate (**151**).

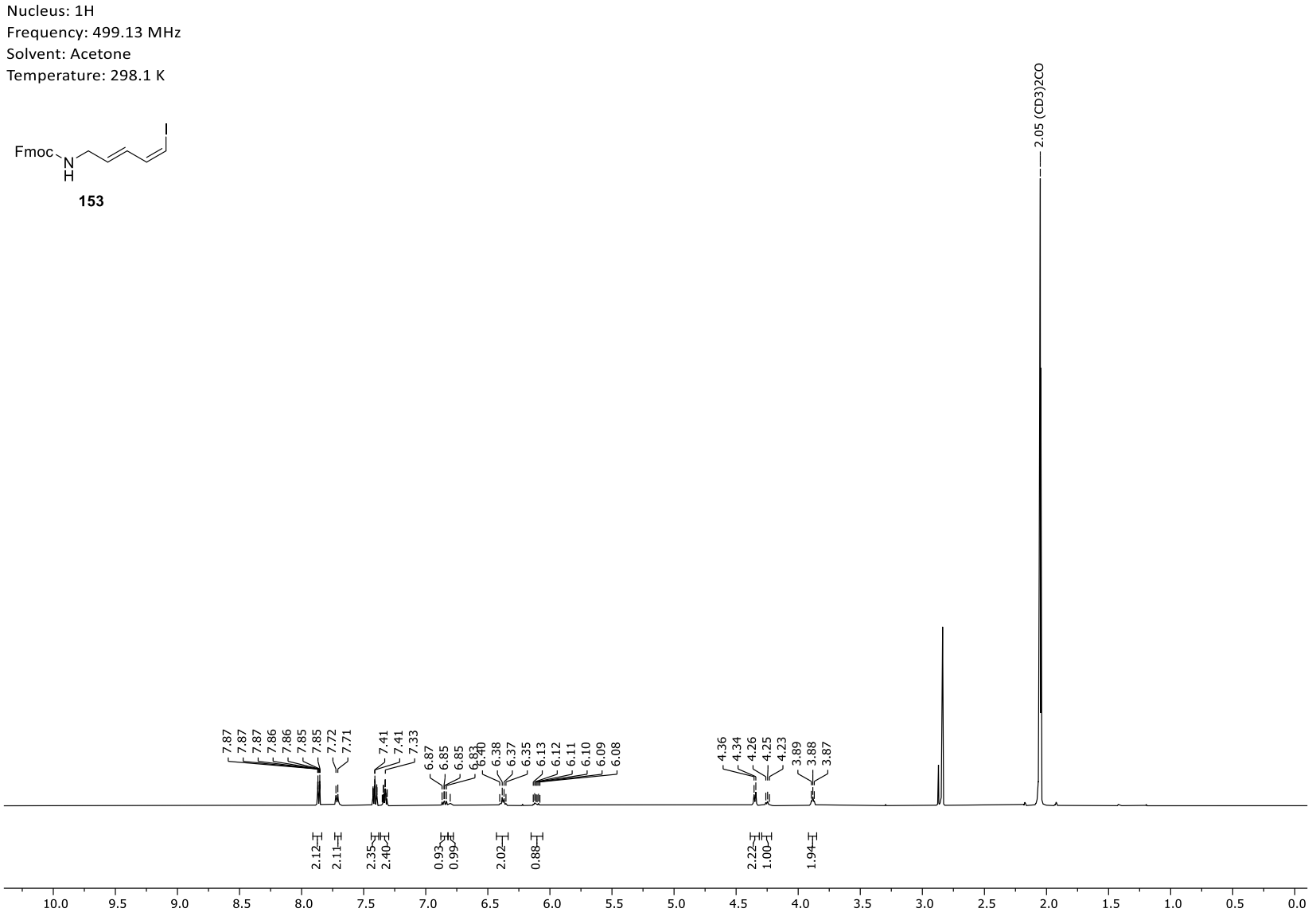

Appendix 20. ^{1}H-NMR spectrum of (1*Z*,3*E*)-*N*-Fmoc-4-amino-1-iodopenta-1,3-diene (**153**).

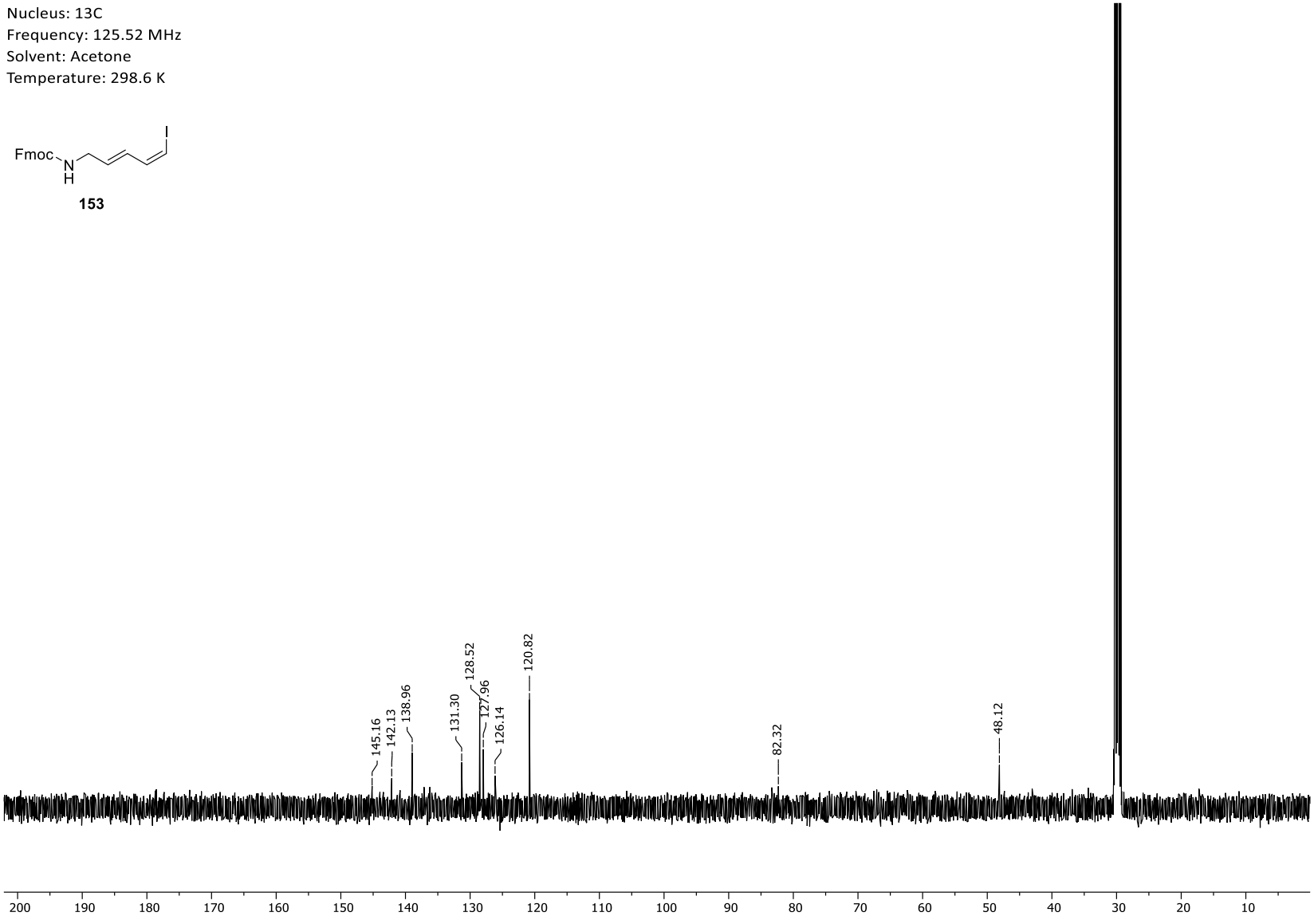

Appendix 21. ^{13}C-NMR spectrum of (1*Z*,3*E*)-*N*-Fmoc-4-amino-1-iodopenta-1,3-diene (**153**).

Nucleus: 1H
Frequency: 499.13 MHz
Solvent: CD2Cl2
Temperature: 298.1 K

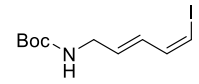

152

Appendix 22. ^{1}H-NMR spectrum of (1*Z*,3*E*)-*N*-Boc-4-amino-1-iodopenta-1,3-diene (**152**).

Nucleus: 13C
Frequency: 125.52 MHz
Solvent: CD2Cl2
Temperature: 298.1 K

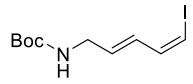

152

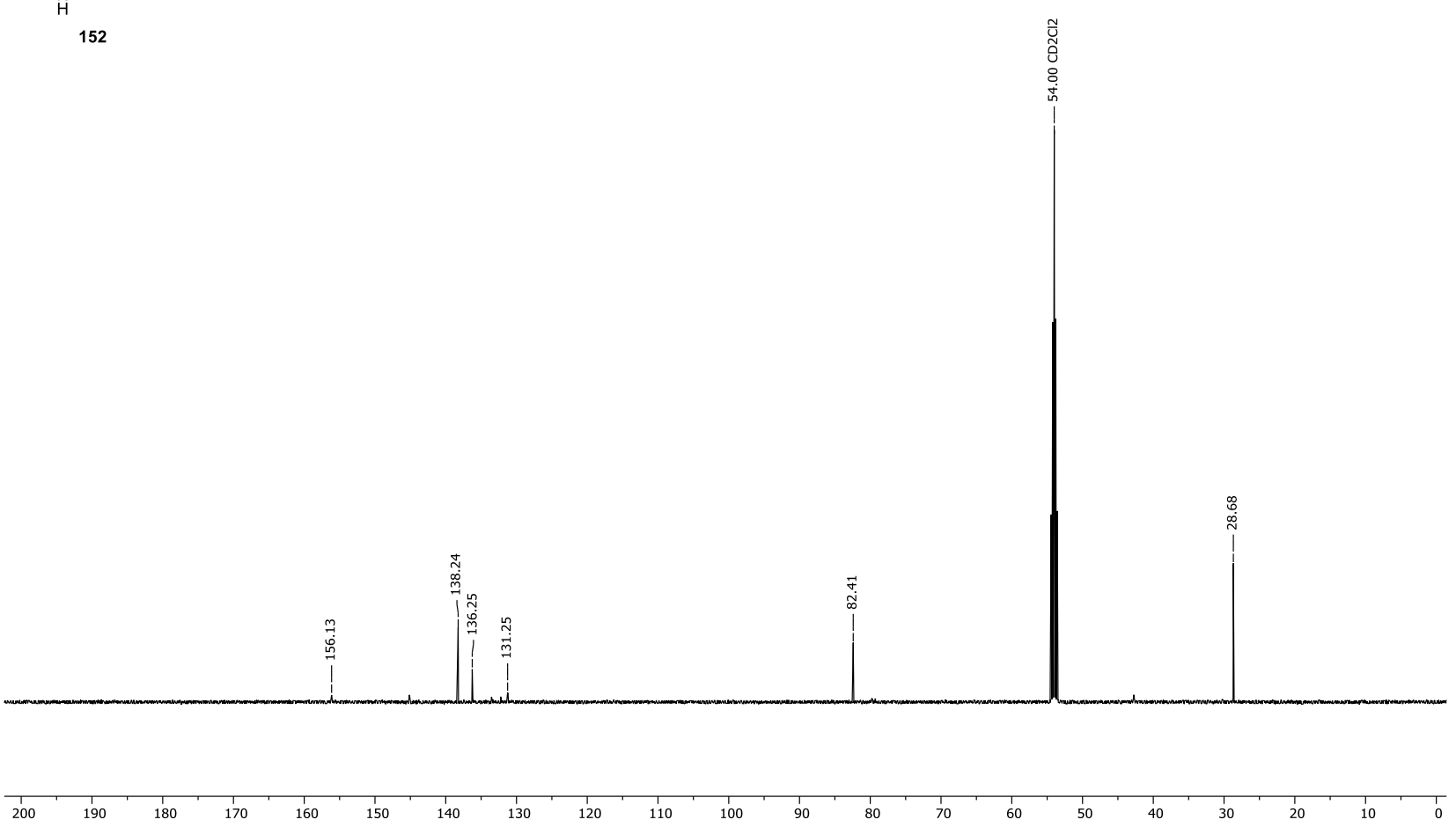

Appendix 23. ^{13}C-NMR spectrum of (1*Z*,3*E*)-*N*-Boc-4-amino-1-iodopenta-1,3-diene (**152**).

Nucleus: 1H
Frequency: 500.14 MHz
Solvent: D2O
Temperature: 298.0 K

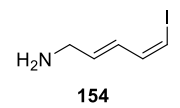

154

Appendix 24. ^{1}H-NMR spectrum of (2*E*,4*Z*)-5-iodopenta-2,4-dien-1-amine (**154**).

Nucleus: 13C
Frequency: 125.78 MHz
Solvent: D2O
Temperature: 298.0 K

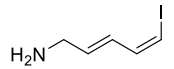

154

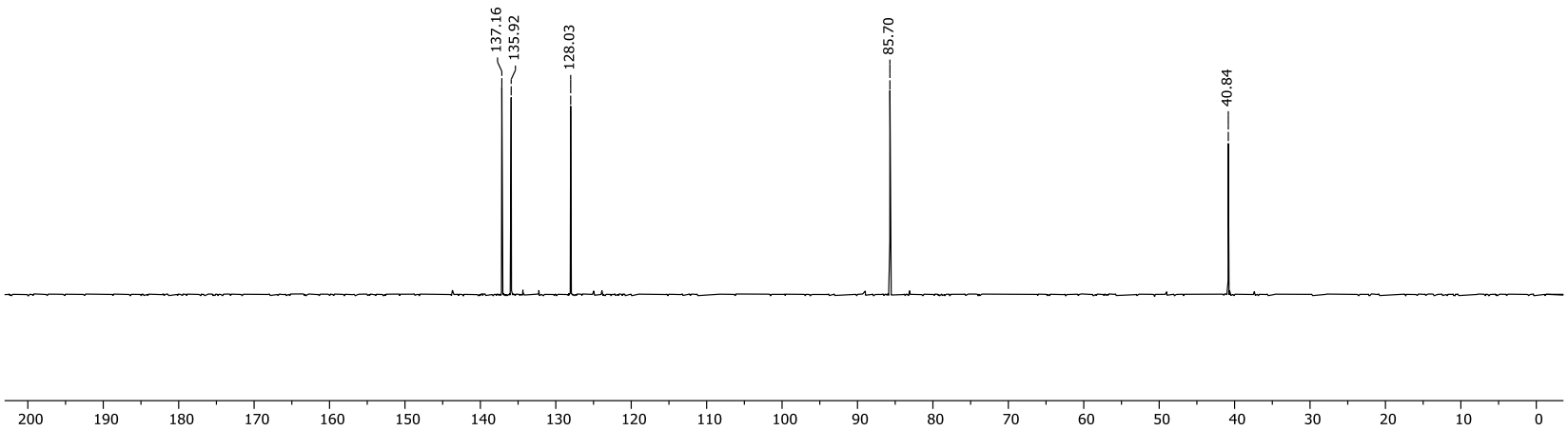

Appendix 25. ^{13}C-NMR spectrum of (2*E*,4*Z*)-5-iodopenta-2,4-dien-1-amine (**154**).

Nucleus: 1H
Frequency: 500.18 MHz
Solvent: Acetone
Temperature: 298.0 K

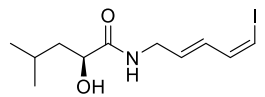

122

Appendix 26. ^{1}H-NMR spectrum of (*S*)-2-hydroxy-*N*-((2*E*,4*Z*)-5-iodopenta-2,4-dien-1-yl)-4-methylpentanamide (**122**).

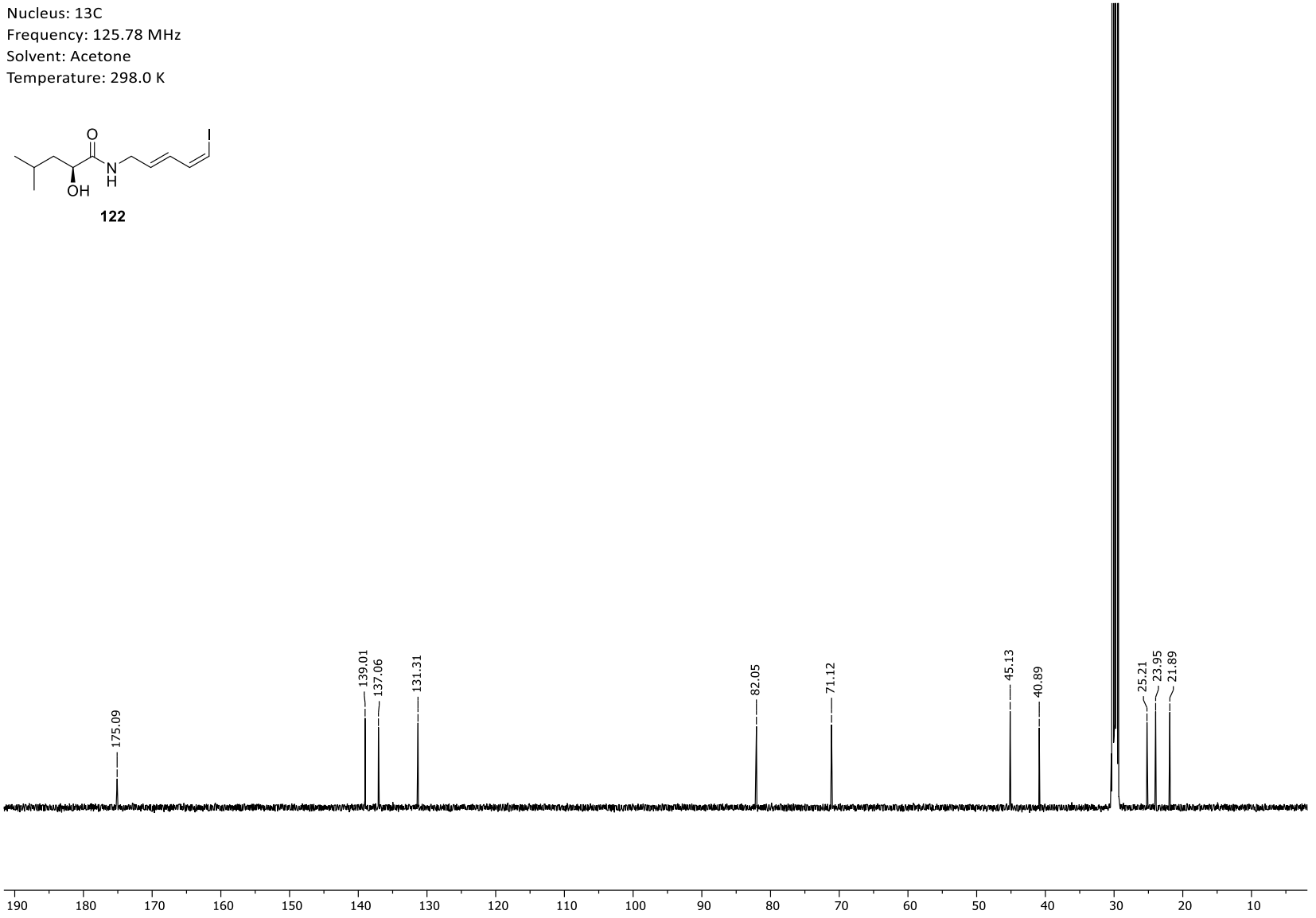

Appendix 27. ^{13}C-NMR spectrum of (*S*)-2-hydroxy-*N*-((2*E*,4*Z*)-5-iodopenta-2,4-dien-1-yl)-4-methylpentanamide (**122**).

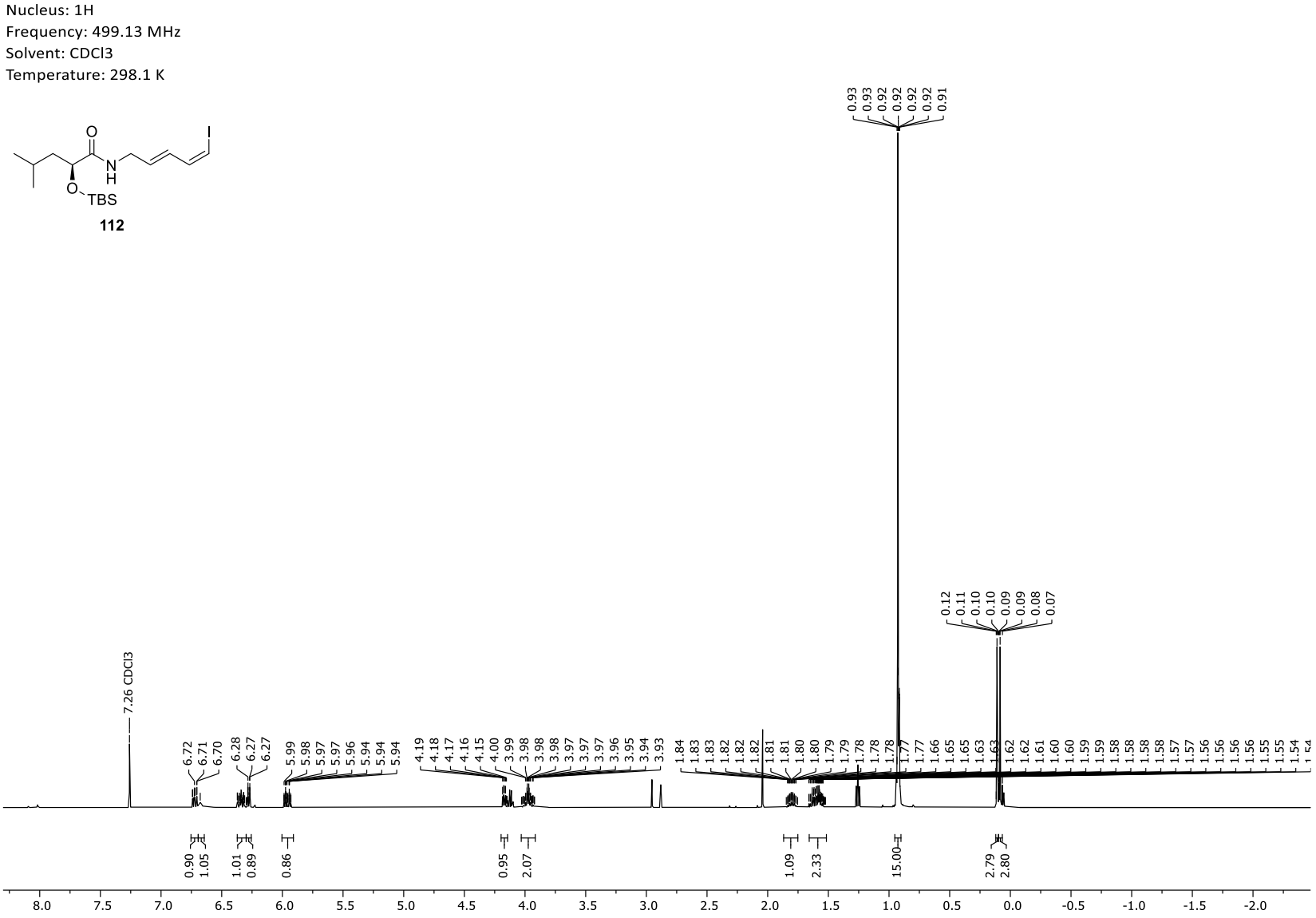

Appendix 28. ^{1}H-NMR spectrum of (*S*)-*N*-((4*Z*),(2*E*)-5-iodopenta-2,4-dienyl)-2-((*tert*-butyldimethylsiliyl)oxy)-4-methylpentanamide (**112**).

Nucleus: 13C
Frequency: 125.52 MHz
Solvent: CDCl3
Temperature: 298.1 K

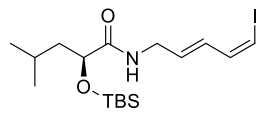

112

Appendix 29. ^{13}C-NMR spectrum of (*S*)-*N*-((4*Z*),(2*E*)-5-iodopenta-2,4-dienyl)-2-((*tert*-butyldimethylsiliyl)oxy)-4-methylpentanamide (**112**).

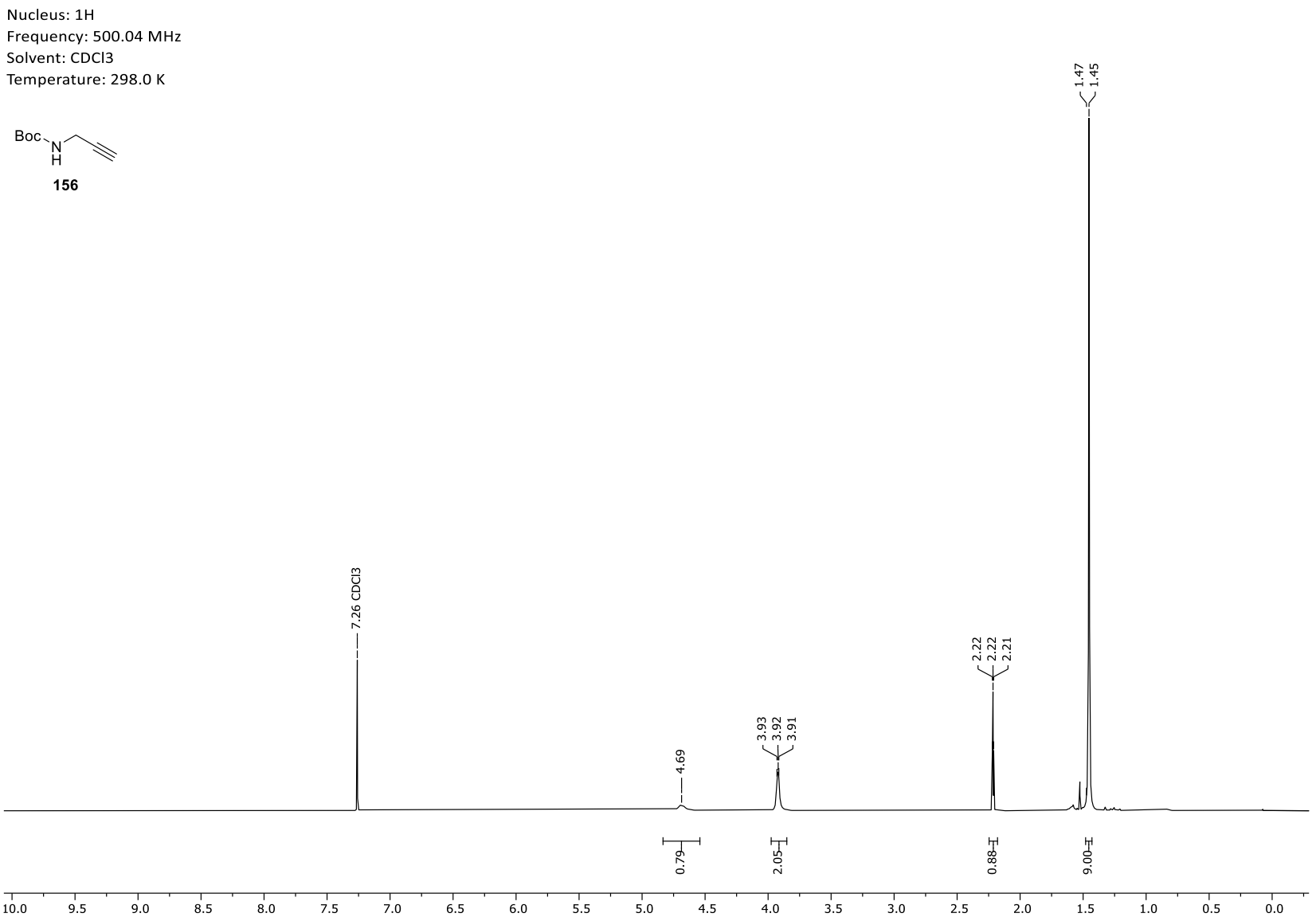

Appendix 30. ^{1}H-NMR spectrum of *tert*-butyl prop-2-yn-1-ylcarbamate (**156**).

Nucleus: 13C
Frequency: 125.75 MHz
Solvent: CDCl3
Temperature: 298.0 K

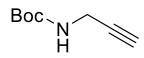

156

Appendix 31. ^{13}C-NMR spectrum of *tert*-butyl prop-2-yn-1-ylcarbamate (**156**).

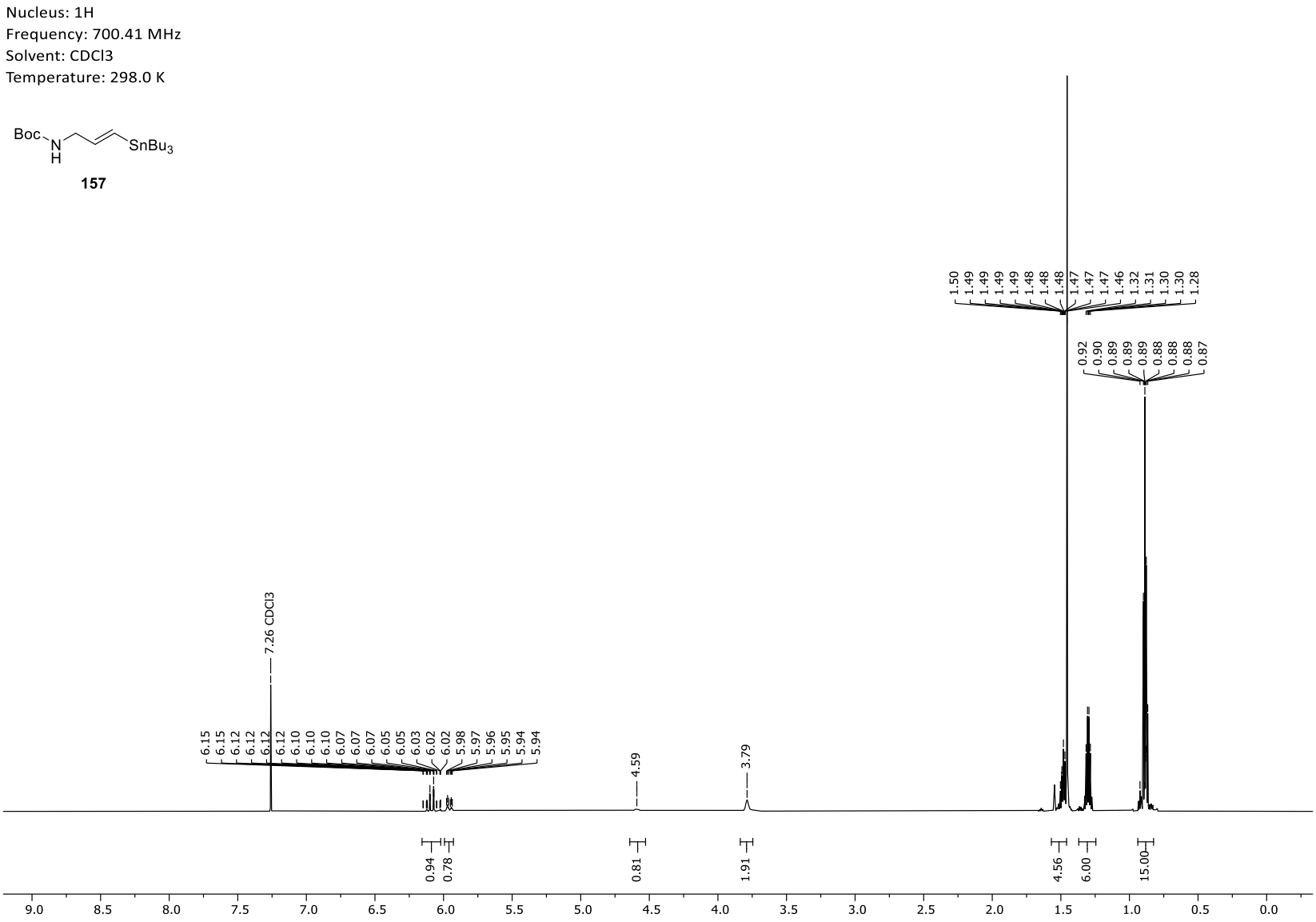

Appendix 32. ^{1}H-NMR spectrum of *tert*-butyl (*E*)-(3-(tributylstannyl)allyl)carbamate (**157**).

Nucleus: 13C
Frequency: 176.14 MHz
Solvent: CDCl3
Temperature: 298.0 K

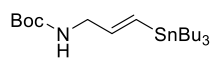

157

Appendix 33. ^{13}C-NMR spectrum of *tert*-butyl (*E*)-(3-(tributylstannyl)allyl)carbamate (**157**).

Nucleus: 1H
Frequency: 700.41 MHz
Solvent: CD2Cl2
Temperature: 298.0 K

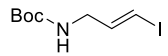

158

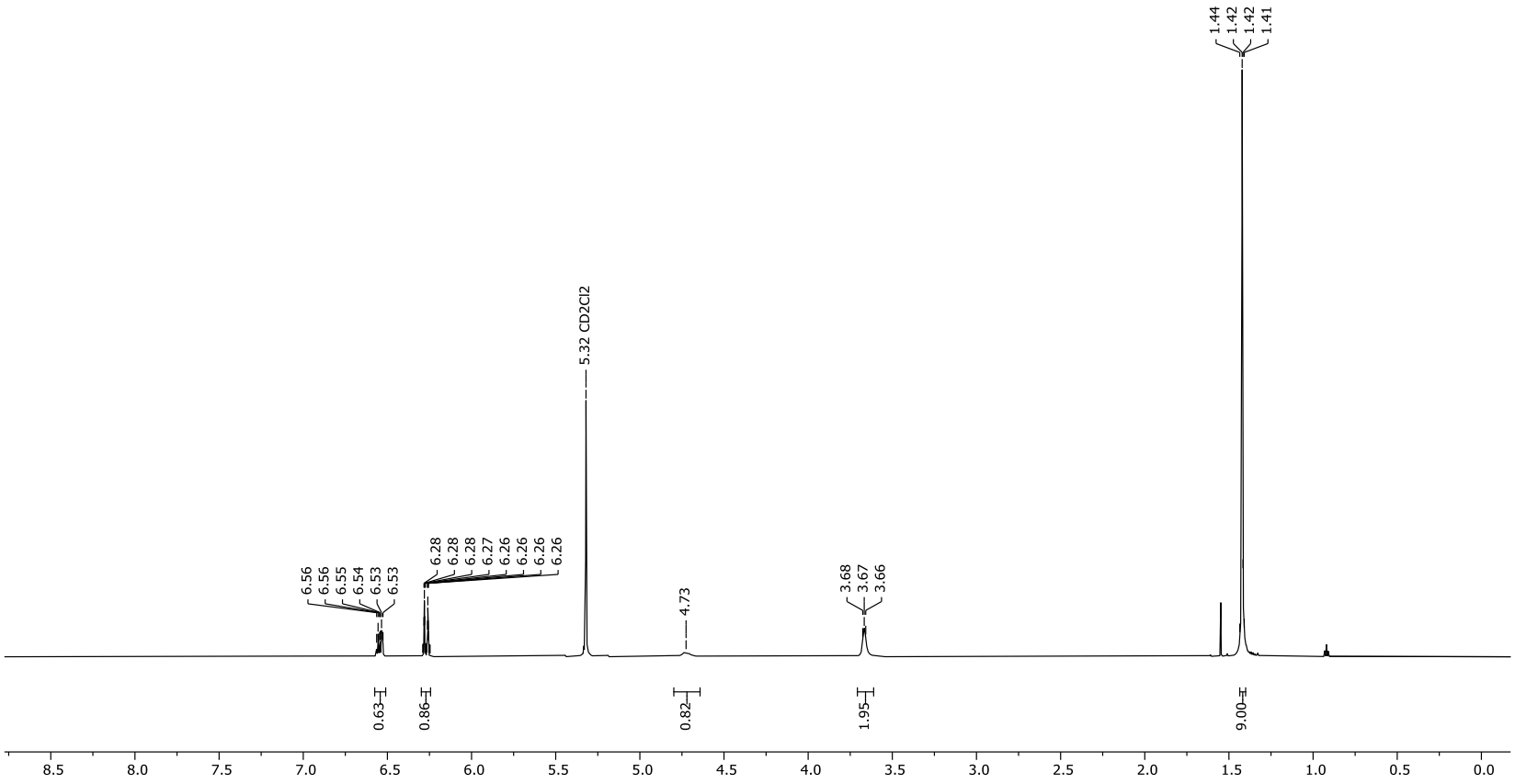

Appendix 34. ^{1}H-NMR spectrum of *tert*-butyl (*E*)-(3-iodoallyl)carbamate (**158**).

Nucleus: 13C
Frequency: 176.14 MHz
Solvent: CD2Cl2
Temperature: 298.0 K

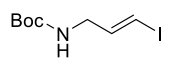

158

Appendix 35. ^{13}C-NMR spectrum of *tert*-butyl (*E*)-(3-iodoallyl)carbamate (**158**).

Nucleus: 1H
Frequency: 499.13 MHz
Solvent: Acetone
Temperature: 298.0 K

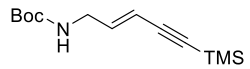

S-1

Appendix 36. ^{1}H-NMR spectrum of *tert*-butyl (*E*)-(5-(trimethylsilyl)pent-2-en-4-yn-1-yl)carbamate (**S-1**).

Nucleus: 13C
Frequency: 125.52 MHz
Solvent: Acetone
Temperature: 297.8 K

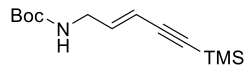

S-1

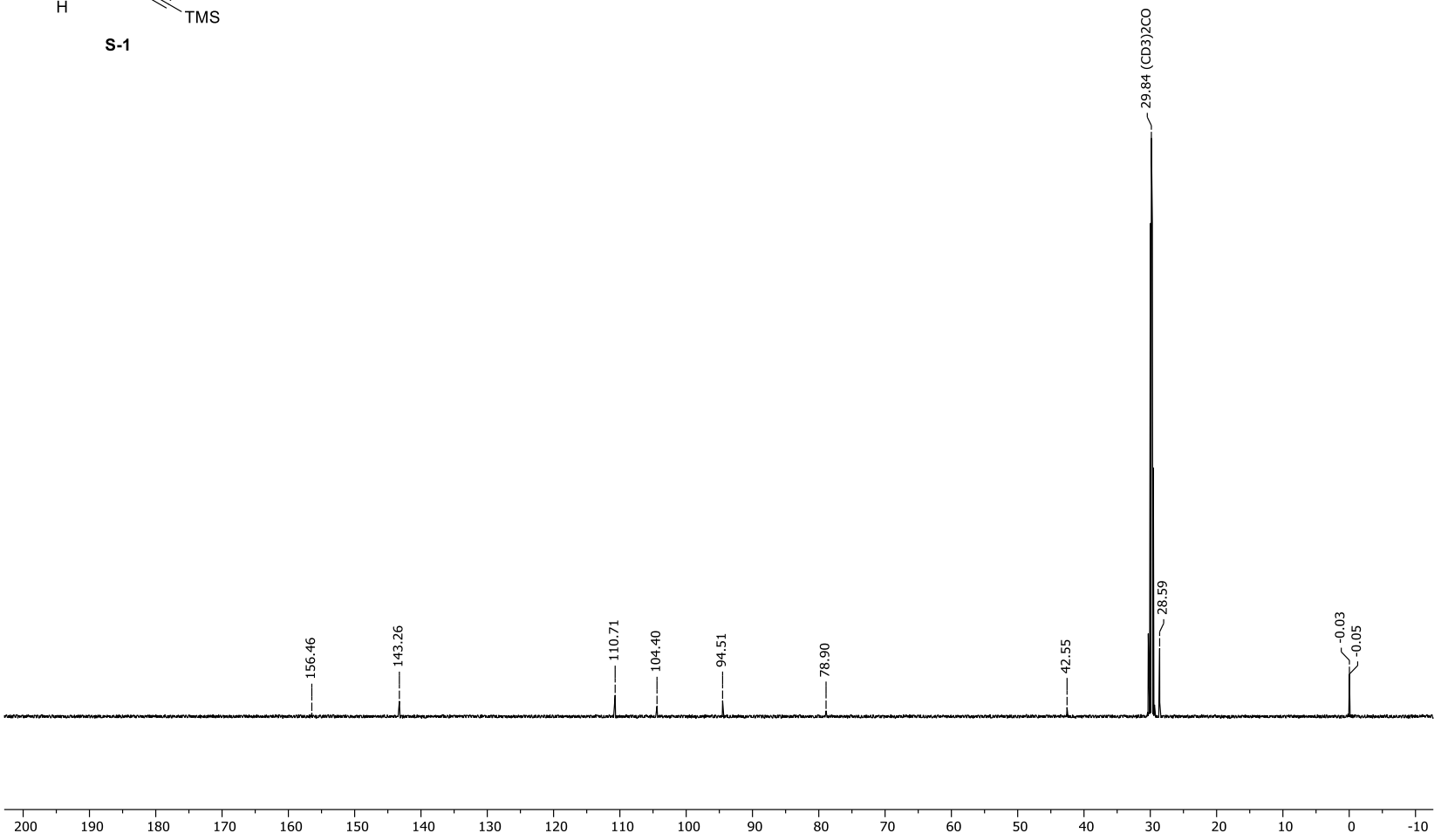

Appendix 37. ^{13}C-NMR spectrum of *tert*-butyl (*E*)-(5-(trimethylsilyl)pent-2-en-4-yn-1-yl)carbamate (**S-1**).

Nucleus: 1H
Frequency: 500.04 MHz
Solvent: CDCl3
Temperature: 298.0 K

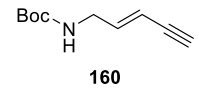

160

Appendix 38. ^{1}H-NMR spectrum of *tert*-butyl (*E*)-pent-2-en-4-yn-1-ylcarbamate (**160**).

Nucleus: 13C
Frequency: 125.75 MHz
Solvent: CDCl3
Temperature: 298.0 K

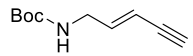

160

Appendix 39. ^{13}C-NMR spectrum of *tert*-butyl (*E*)-pent-2-en-4-yn-1-ylcarbamate (**160**).

Nucleus: 1H
Frequency: 300.13 MHz
Solvent: Acetone
Temperature: 298.0 K

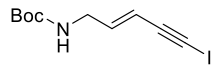

161

Appendix 40. *tert*-butyl (*E*)-(5-iodopent-2-en-4-yn-1-yl)carbamate (**161**).

Nucleus: 1H
Frequency: 400.13 MHz
Solvent: CDCl3
Temperature: 298.0 K

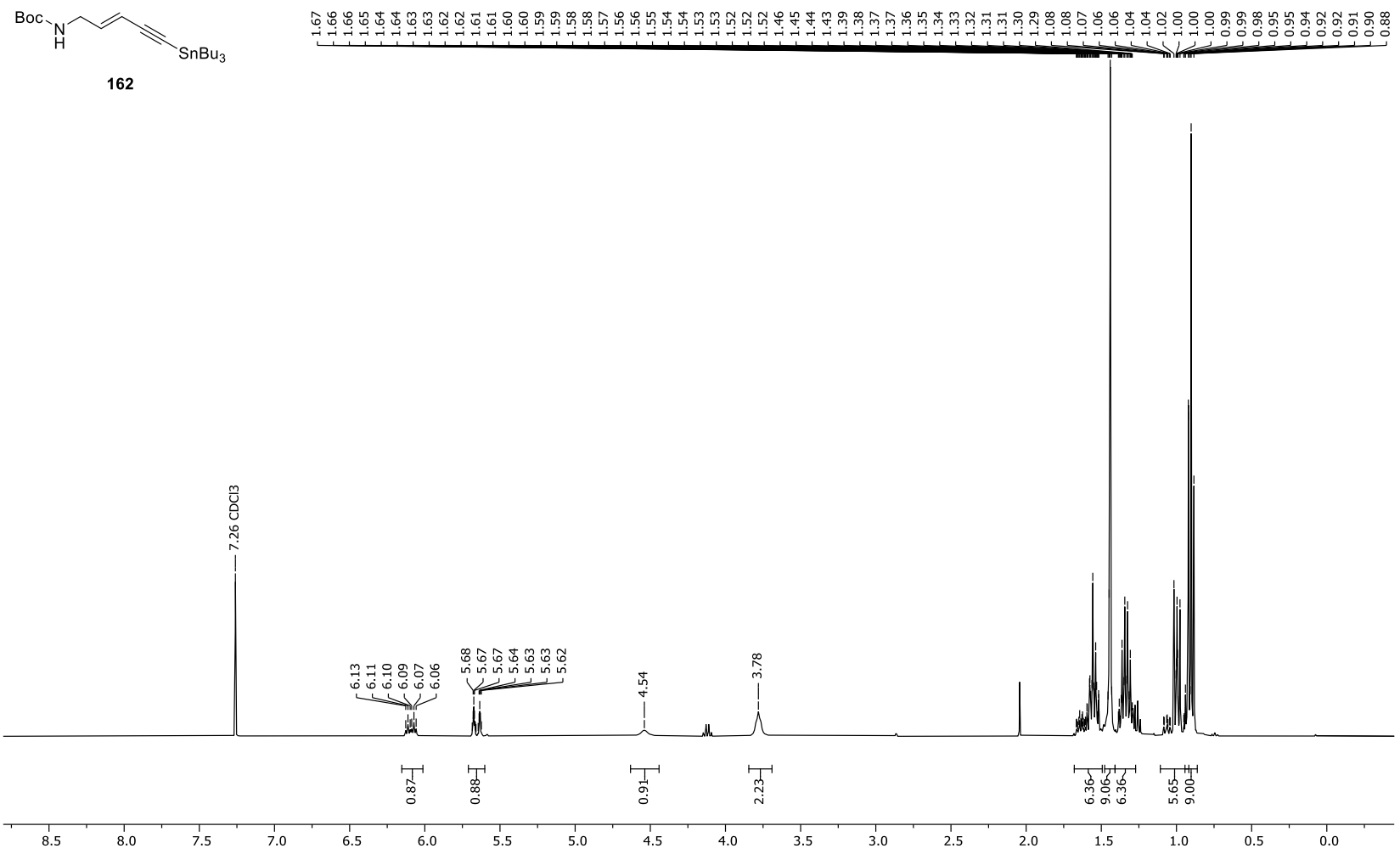

Appendix 41. ^{1}H-NMR spectrum of *tert*-butyl (*E*)-(5-(tributylstannyl)pent-2-en-4-yn-1-yl)carbamate (**162**).

Nucleus: 1H
Frequency: 500.14 MHz
Solvent: CDCl3
Temperature: 298.0 K

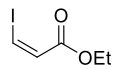

165

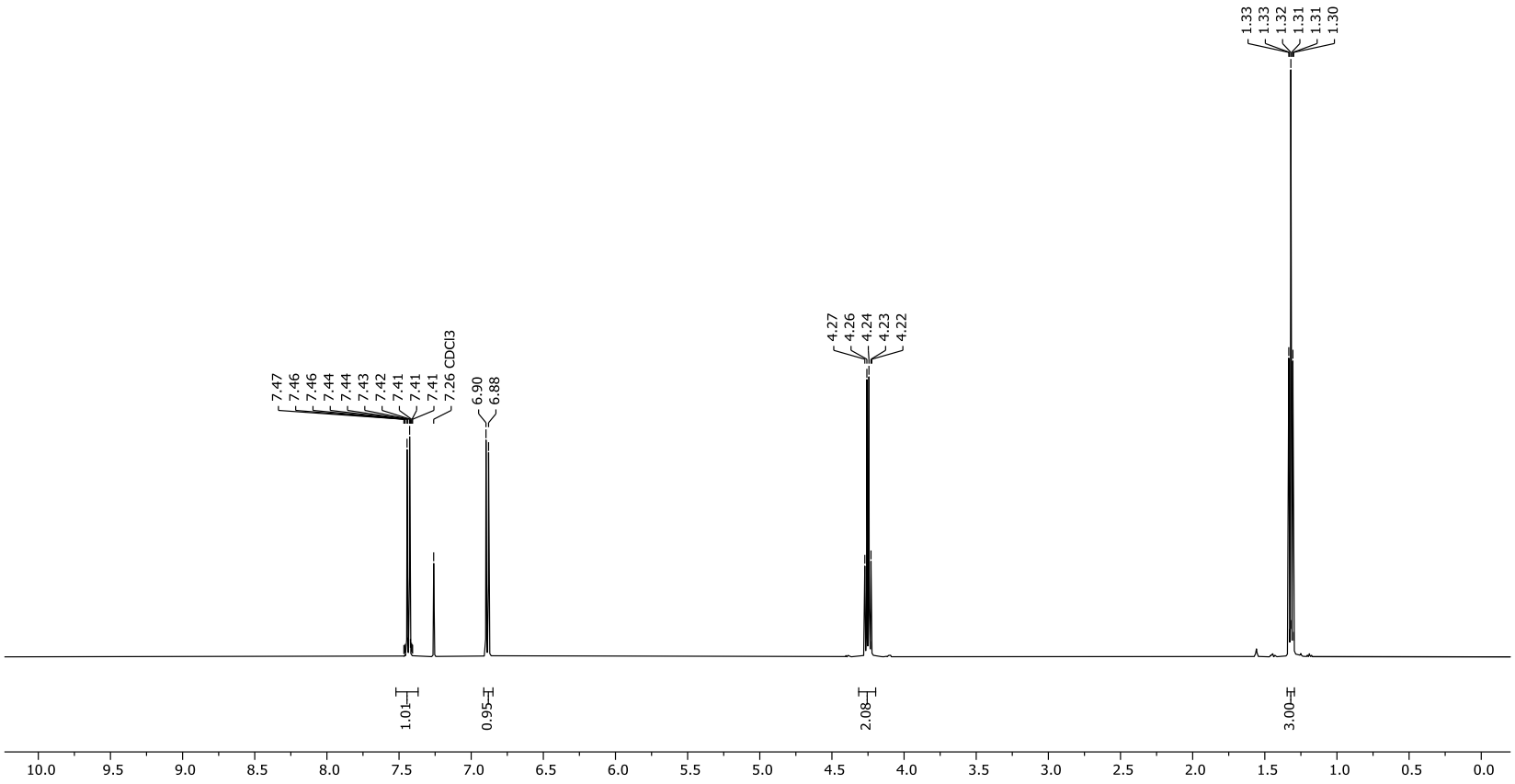

Appendix 42. ^{1}H-NMR spectrum of (*Z*)-ethyl 3-iodacrylate (**165**).

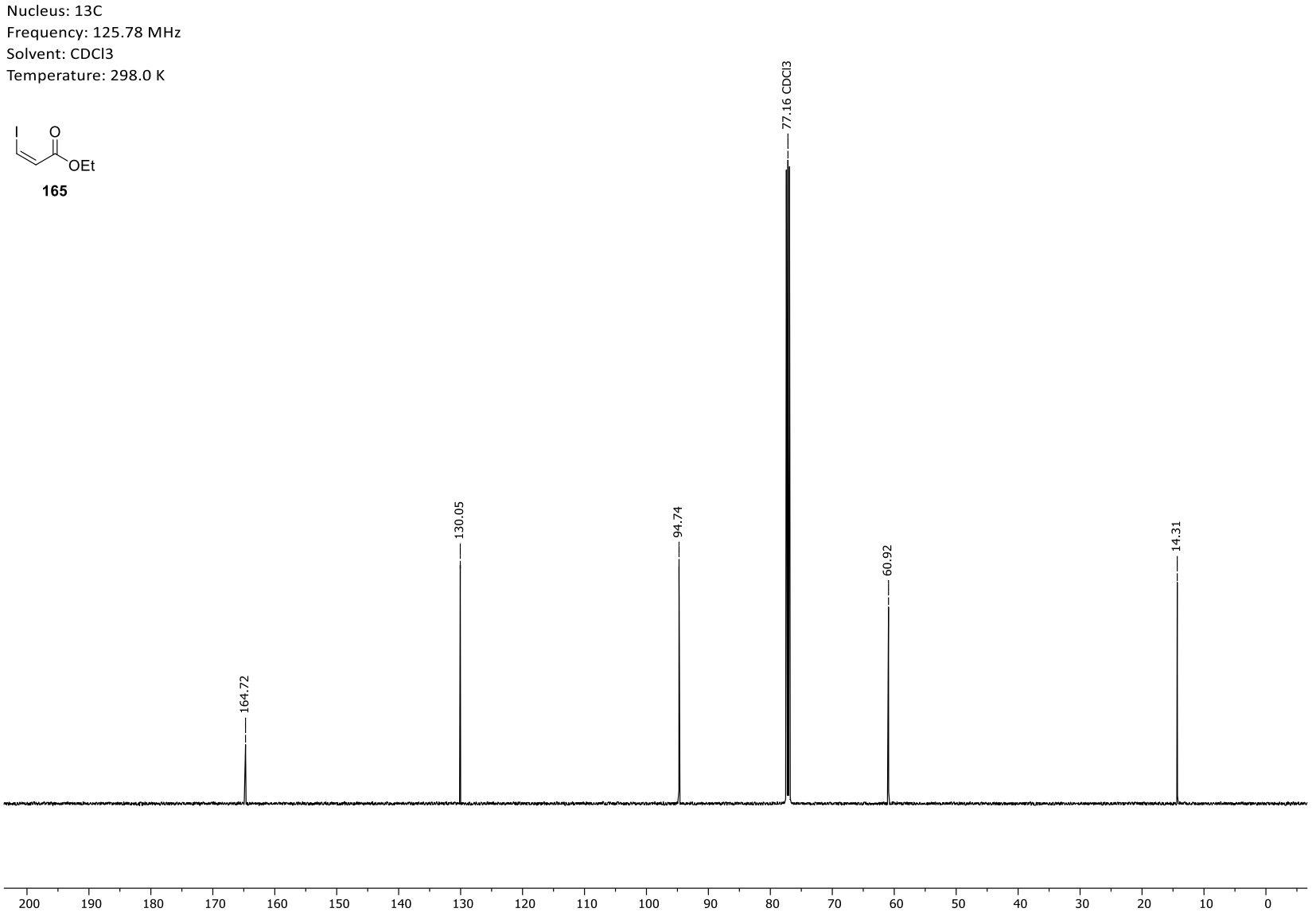

Appendix 43. ^{13}C-NMR spectrum of (*Z*)-ethyl 3-iodacrylate (**165**).

Nucleus: 1H
Frequency: 499.13 MHz
Solvent: CDCl3
Temperature: 298.0 K

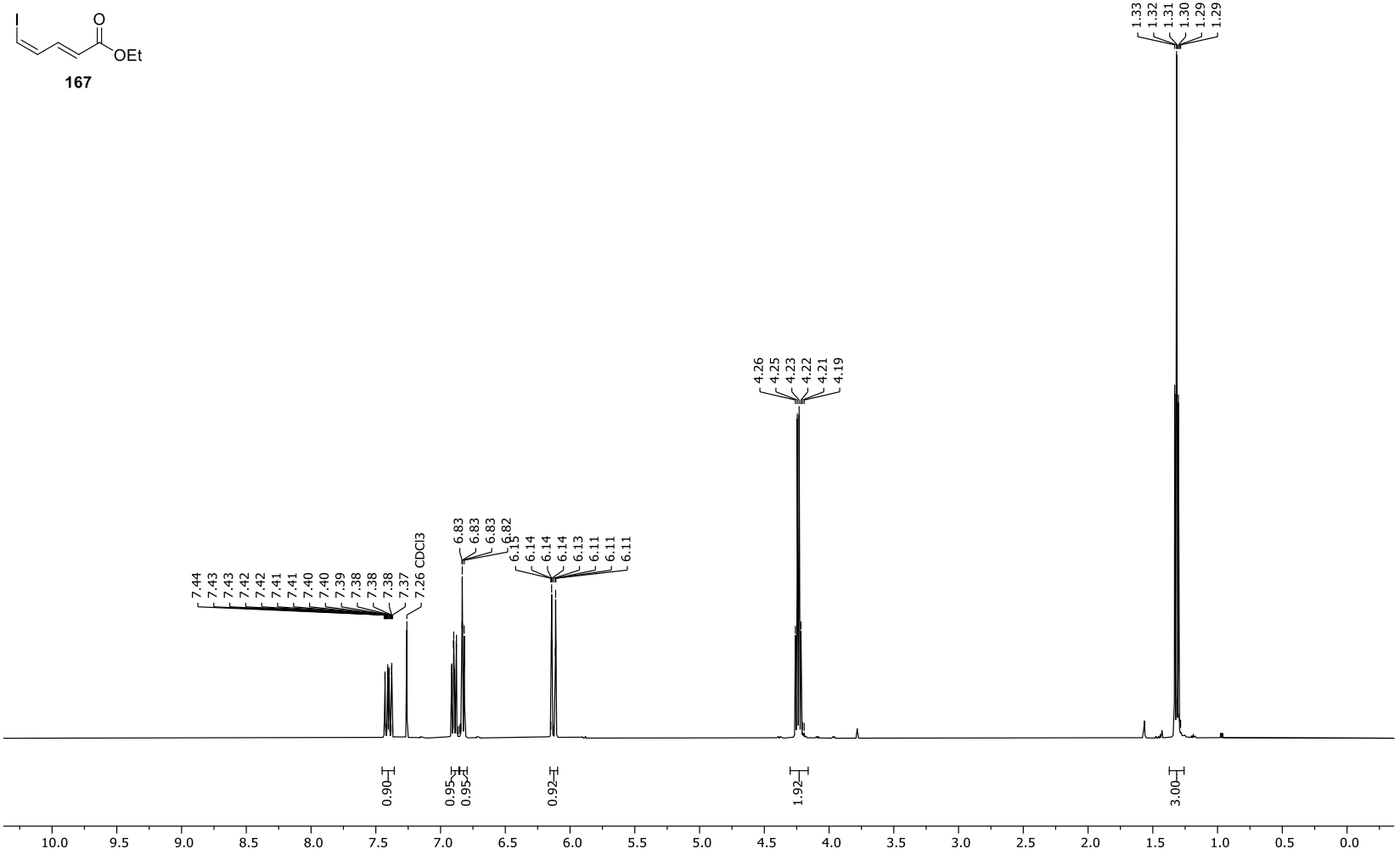

Appendix 44. ^{1}H-NMR spectrum of (2*E*,4*Z*)-ethyl 5-iodopenta-2,4-dienoate (**167**).

Nucleus: 13C
Frequency: 125.52 MHz
Solvent: CDCl3
Temperature: 297.9 K

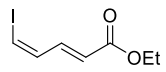

167

Appendix 45. ^{13}C-NMR spectrum of (2*E*,4*Z*)-ethyl 5-iodopenta-2,4-dienoate (**167**).

Nucleus: 1H
Frequency: 400.13 MHz
Solvent: Acetone
Temperature: 298.0 K

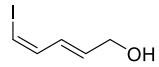

168

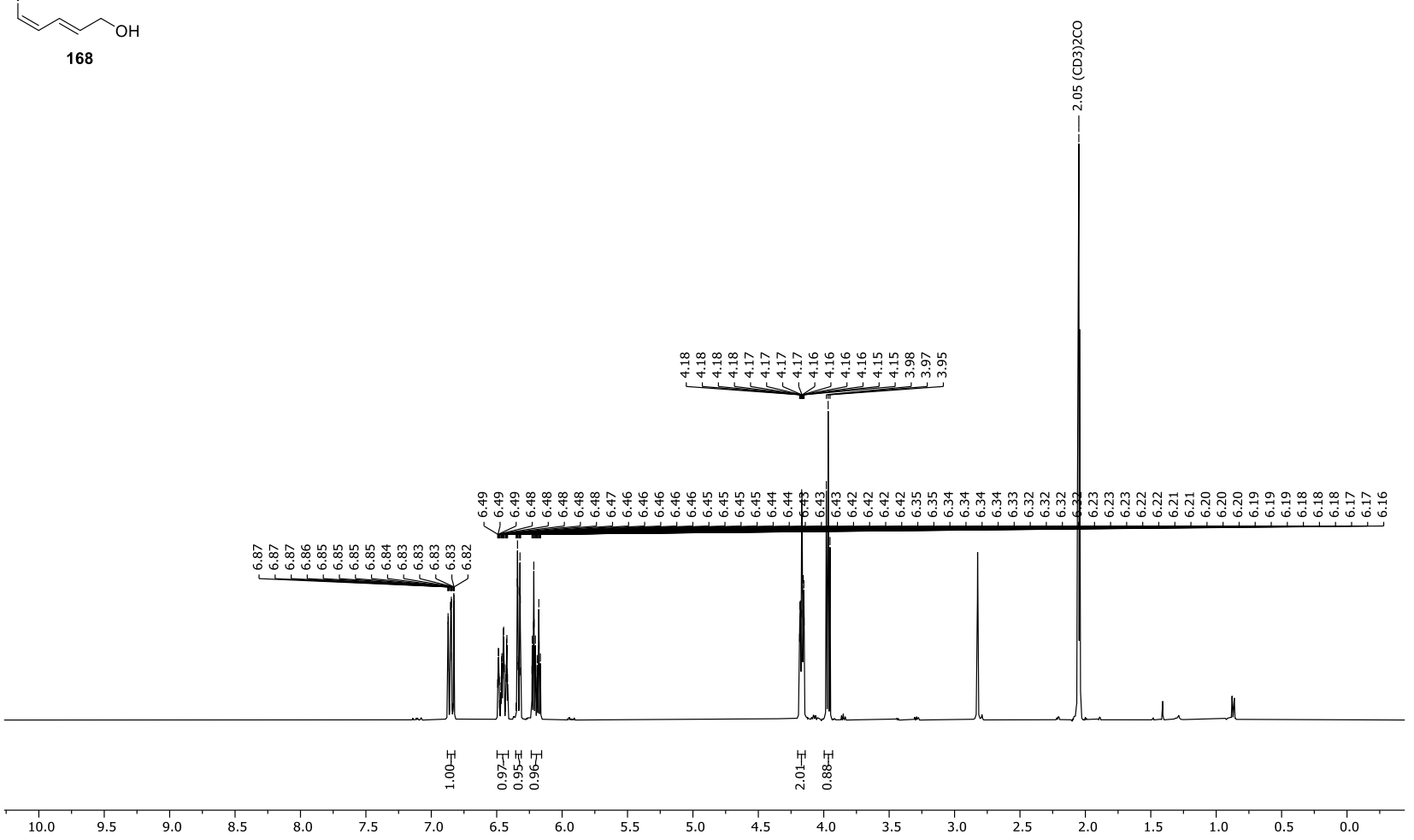

Appendix 46. ^{1}H-NMR spectrum of (2*E*,4*Z*)-5-iodopenta-2,4-dien-1-ol (**168**).

Nucleus: 13C
Frequency: 100.63 MHz
Solvent: Acetone
Temperature: 298.0 K

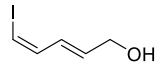

168

Appendix 47. ^{13}C-NMR spectrum of (2*E*,4*Z*)-5-iodopenta-2,4-dien-1-ol (**168**).

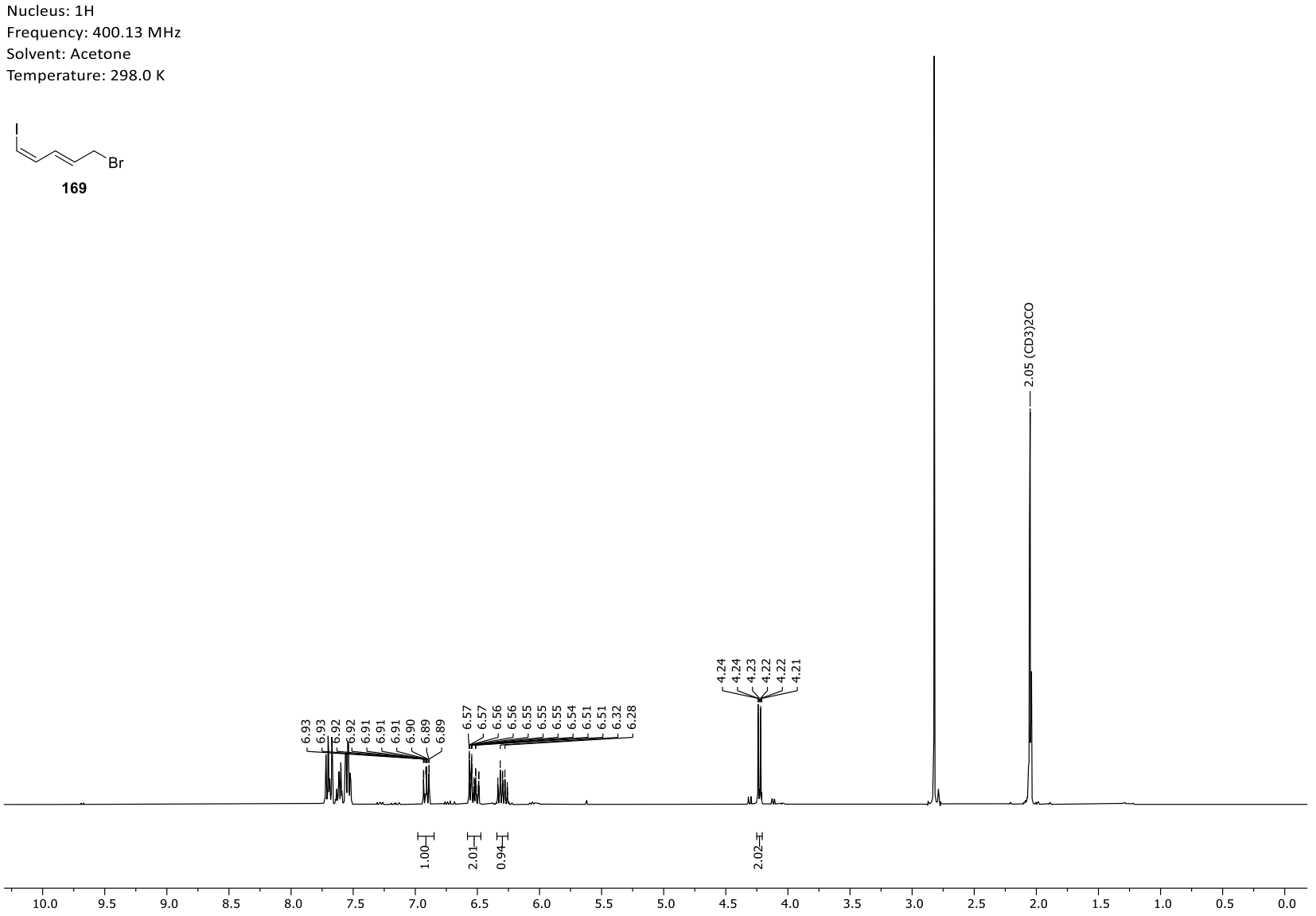

Appendix 48. ^{1}H-NMR spectrum of (1*Z*,3*E*)-5-bromo-1-iodopenta-1,3-diene (**169**).

Nucleus: 13C
Frequency: 100.63 MHz
Solvent: Acetone
Temperature: 298.0 K

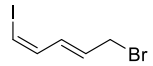

169

Appendix 49. ^{13}C-NMR spectrum of (1*Z*,3*E*)-5-bromo-1-iodopenta-1,3-diene (**169**).

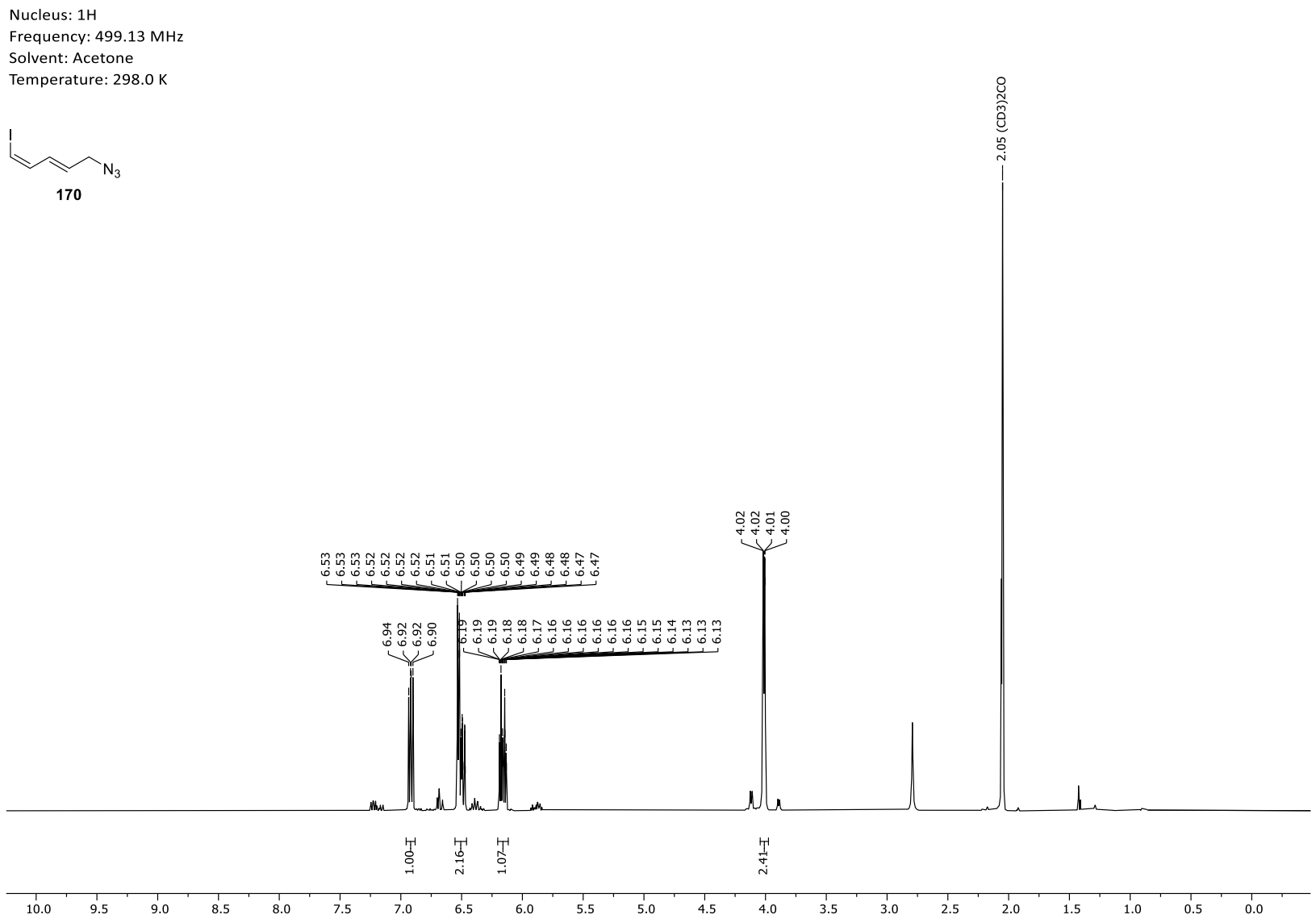

Appendix 50. ^{1}H-NMR spectrum of (1*Z*,3*E*)-5-azido-1-iodopenta-1,3-diene (**170**).

Nucleus: 13C
Frequency: 125.52 MHz
Solvent: Acetone
Temperature: 298.0 K

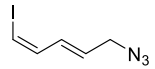

170

Appendix 51. ^{13}C-NMR spectrum of (1*Z*,3*E*)-5-azido-1-iodopenta-1,3-diene (**170**).

Nucleus: 1H
Frequency: 499.13 MHz
Solvent: CDCl3
Temperature: 298.2 K

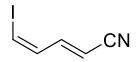

172

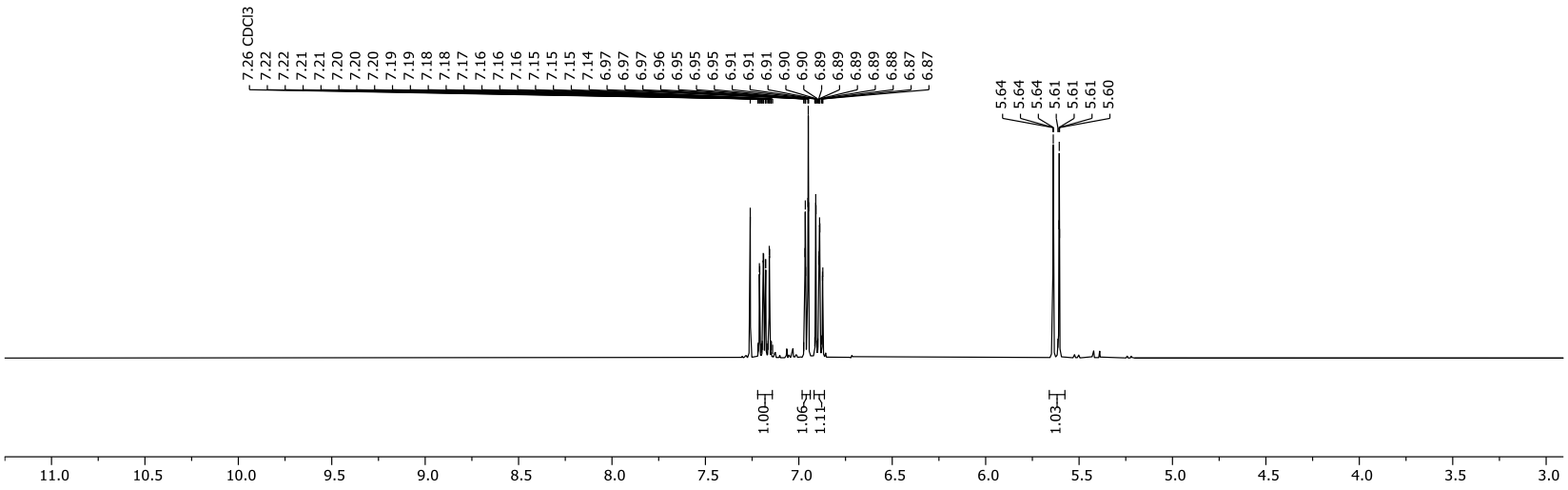

Appendix 52. ^{1}H-NMR spectrum of (2*E*,4*Z*)-5-iodopenta-2,4-dienenitrile (**172**).

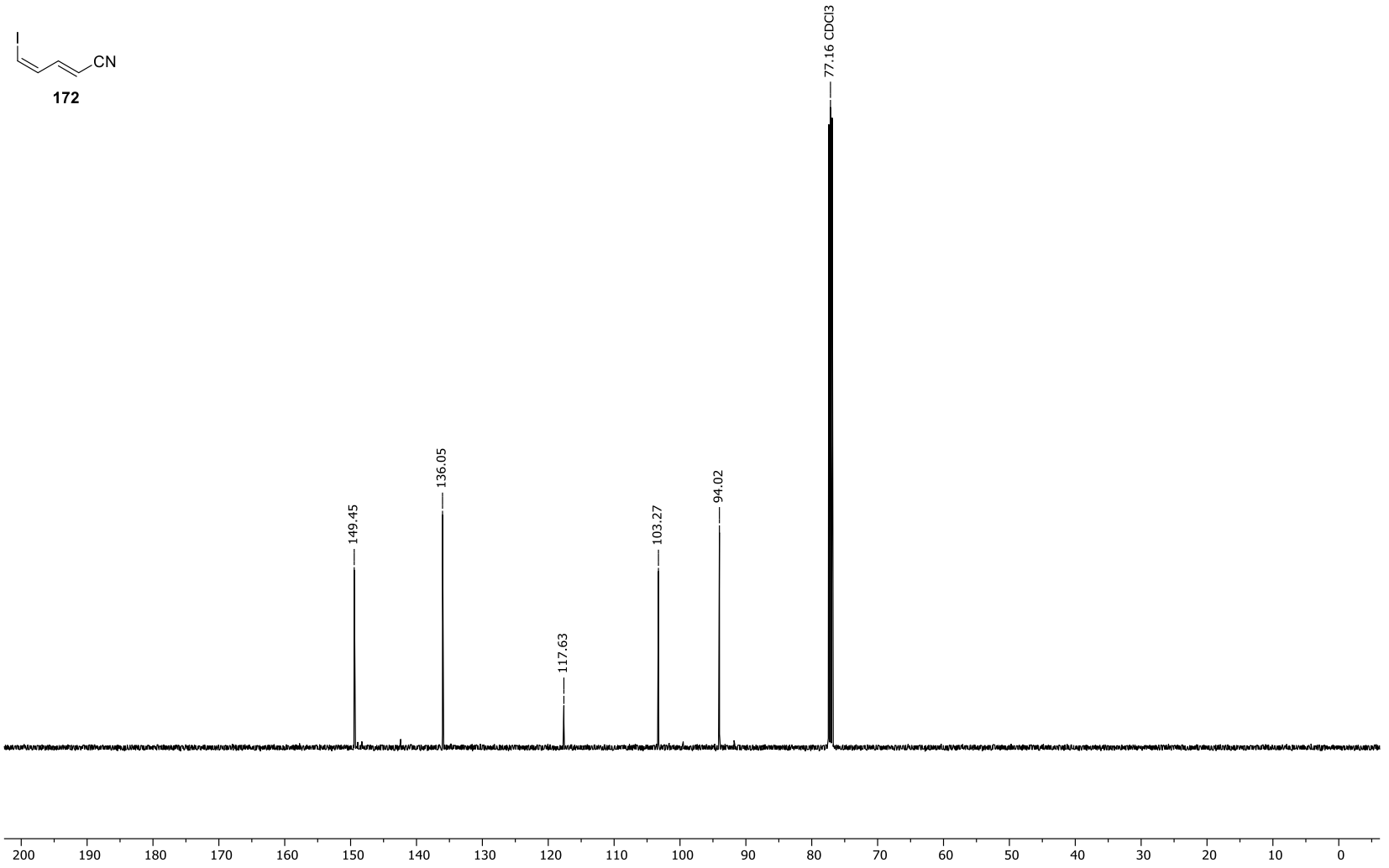

Appendix 53. ^{13}C-NMR spectrum of (2*E*,4*Z*)-5-iodopenta-2,4-dienenitrile (**172**).

Nucleus: 1H
Frequency: 499.13 MHz
Solvent: MeOD
Temperature: 298.0 K

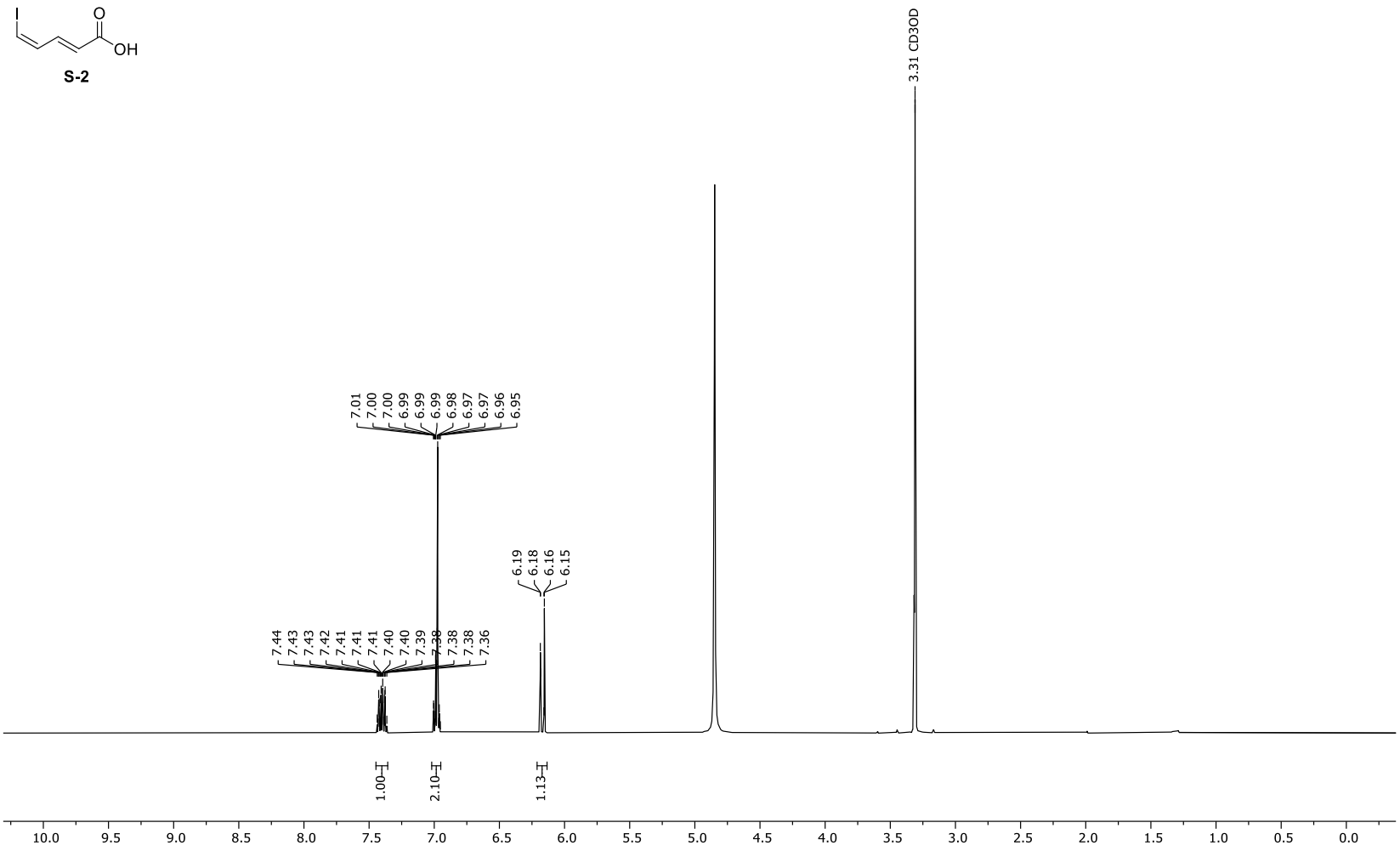

Appendix 54. ^{1}H-NMR spectrum of (2*E*,4*Z*)-5-iodopenta-2,4-dienoic acid (**S-2**).

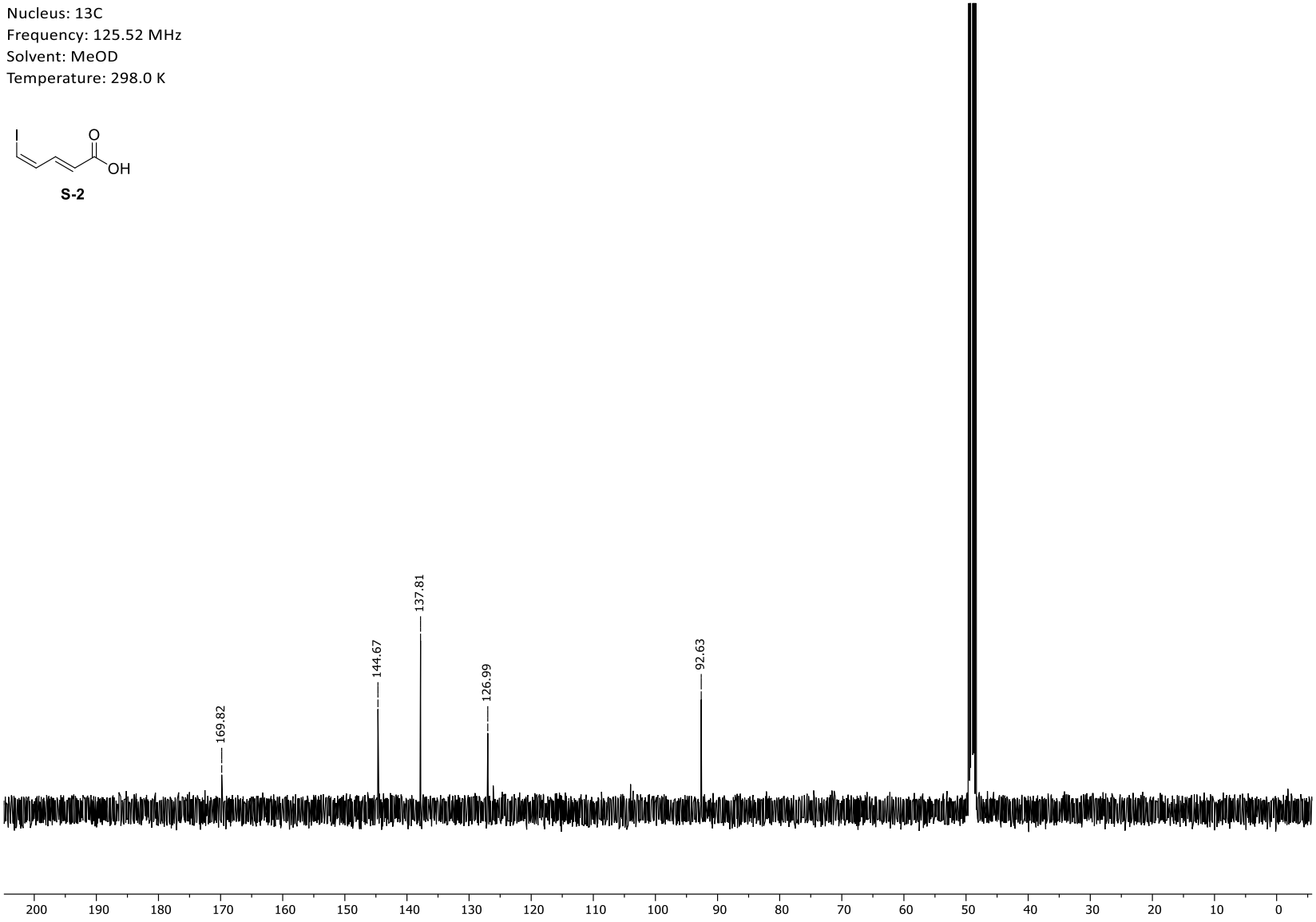

Appendix 55. ^{13}C-NMR spectrum of (2*E*,4*Z*)-5-iodopenta-2,4-dienoic acid (**S-2**).

Nucleus: 1H
Frequency: 400.13 MHz
Solvent: MeOD
Temperature: 298.0 K

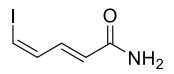

173

Appendix 56. ^{1}H-NMR spectrum of (2*E*,4*Z*)-5-iodopenta-2,4-dienamide (**173**).

Nucleus: 13C
Frequency: 100.63 MHz
Solvent: MeOD
Temperature: 298.0 K

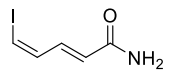

173

Appendix 57. ^{13}C-NMR spectrum of (2*E*,4*Z*)-5-iodopenta-2,4-dienamide (**173**).

Nucleus: 1H
Frequency: 500.14 MHz
Solvent: CD2Cl2
Temperature: 298.0 K

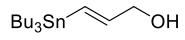

36

Appendix 58. ^{1}H-NMR spectrum of (*E*)-3-(tributylstannyl)prop-2-en-1-ol (**36**).

Nucleus: 13C
Frequency: 125.78 MHz
Solvent: CD2Cl2
Temperature: 298.0 K

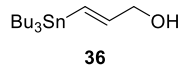

36

Appendix 59. ^{13}C-NMR spectrum of (*E*)-3-(tributylstannyl)prop-2-en-1-ol (**36**).

Nucleus: 1H
Frequency: 500.14 MHz
Solvent: CD2Cl2
Temperature: 298.0 K

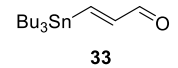

33

Appendix 60. ^{1}H-NMR spectrum of (*E*)-3-(tributylstannyl)prop-2-en-1-al (**33**).

Nucleus: 13C
Frequency: 125.78 MHz
Solvent: CD2Cl2
Temperature: 298.0 K

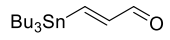

33

Appendix 61. ^{13}C-NMR spectrum of (*E*)-3-(tributylstannyl)prop-2-en-1-al (**33**).

Nucleus: 1H
Frequency: 500.14 MHz
Solvent: CD2Cl2
Temperature: 298.0 K

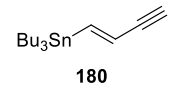

180

Appendix 62. ^{1}H-NMR spectrum of (*E*)-tributyl(but-1-en-3-yn-1-yl)stannane (**180**).

Nucleus: 13C
Frequency: 125.78 MHz
Solvent: CD2Cl2
Temperature: 298.0 K

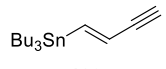

180

Appendix 63. ^{13}C-NMR spectrum of (*E*)-tributyl(but-1-en-3-yn-1-yl)stannane (**180**).

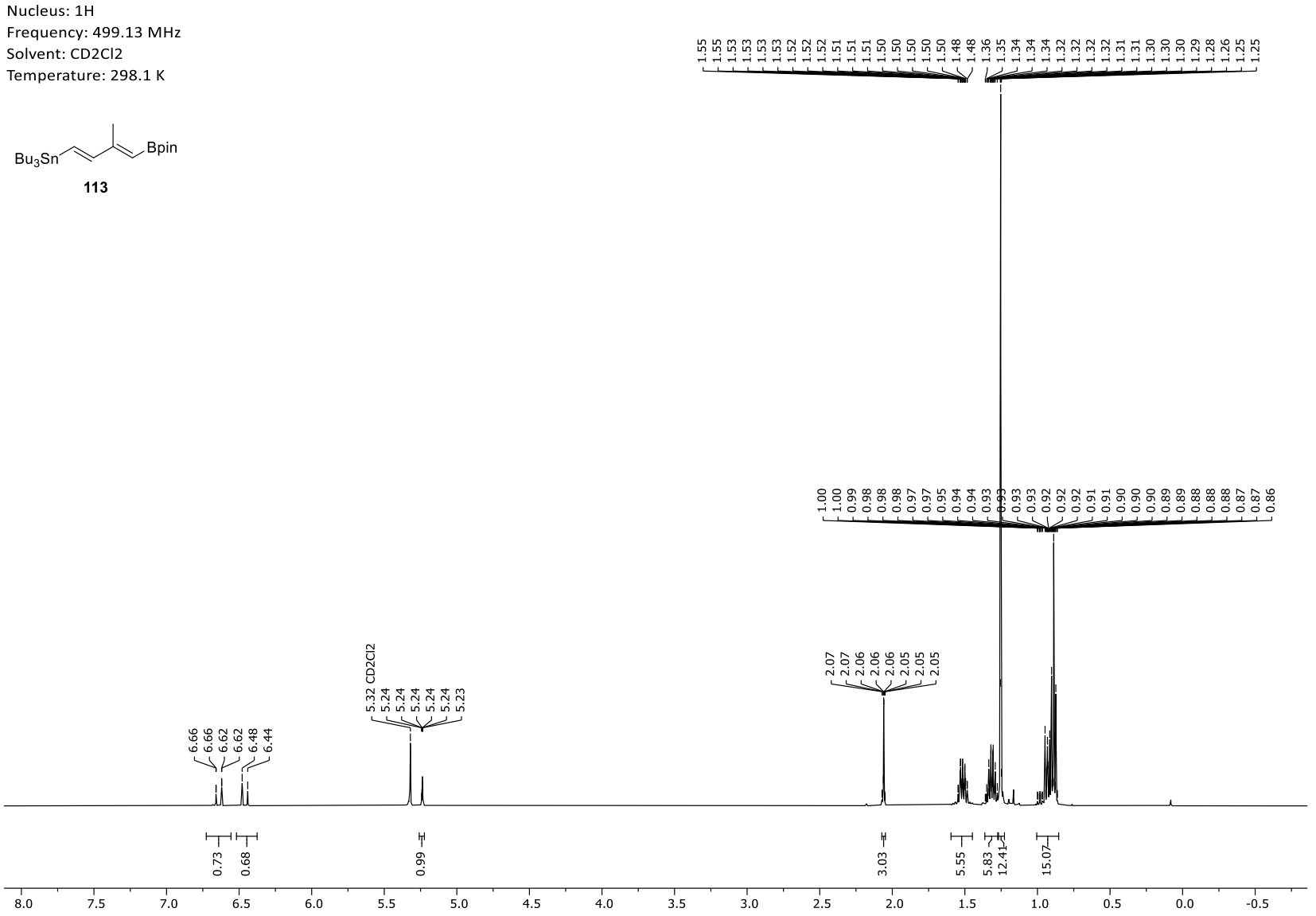

Appendix 64. ^{1}H-NMR spectrum of tributyl((1*E*,3*E*)-3-methyl-4-(4,4,5,5-tetramethyl-1,3,2-dioxaborolan-2-yl)buta-1,3-dien-1-yl)-stannane (**113**).

Nucleus: 13C
Frequency: 125.52 MHz
Solvent: CD2Cl2
Temperature: 298.2 K

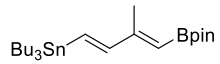

113

Appendix 65. ^{13}C-NMR spectrum of tributyl((1*E*,3*E*)-3-methyl-4-(4,4,5,5-tetramethyl-1,3,2-dioxaborolan-2-yl)buta-1,3-dien-1-yl)-stannane (**113**).

Nucleus: 1H
Frequency: 499.13 MHz
Solvent: CDCl3
Temperature: 297.9 K

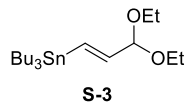

S-3

Appendix 66. ^{1}H-NMR spectrum of (*E*)-tributyl(3,3-diethoxyprop-1-en-1-yl)stannane (**S-3**).

Nucleus: 13C
Frequency: 125.52 MHz
Solvent: CDCl3
Temperature: 298.0 K

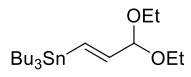

S-3

Appendix 67. ^{13}C-NMR spectrum of (*E*)-tributyl(3,3-diethoxyprop-1-en-1-yl)stannane (**S-3**).

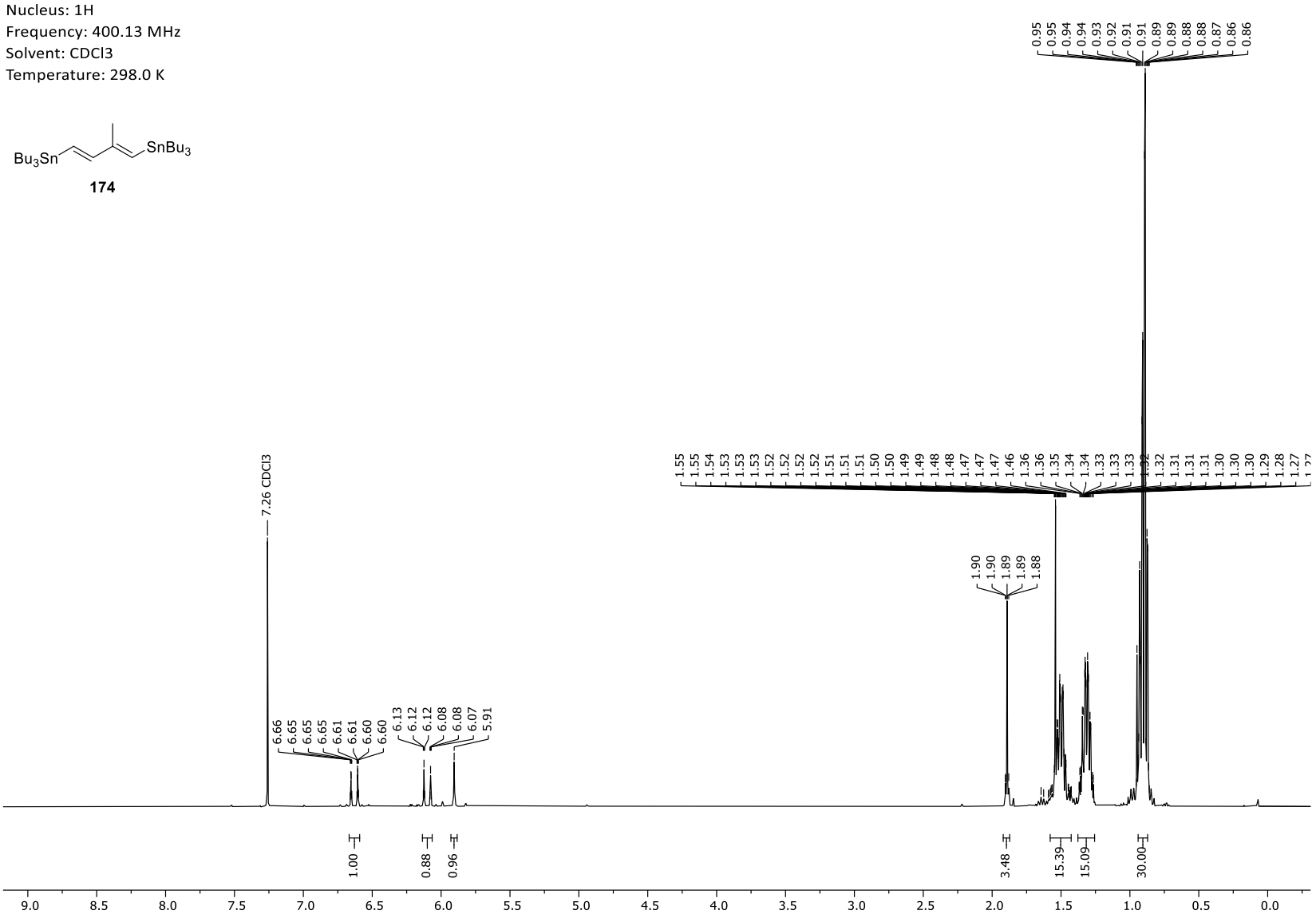

Appendix 68. ^{1}H-NMR spectrum of ((1*E*,3*E*)-2-methylbuta-1,3-diene-1,4-diyl)bis(tributylstannane) (**174**).

Nucleus: 13C
Frequency: 125.52 MHz
Solvent: Acetone
Temperature: 298.0 K

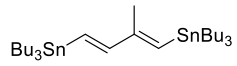

174

Appendix 69. ^{13}C-NMR spectrum of ((1*E*,3*E*)-2-methylbuta-1,3-diene-1,4-diyl)bis(tributylstannane) (**174**).

Nucleus: 1H
Frequency: 499.13 MHz
Solvent: Acetone
Temperature: 297.9 K

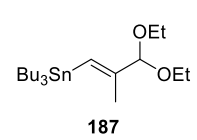

187

Appendix 70. ^{1}H-NMR spectrum of (*E*)-tributyl(3,3-diethoxy-2-methylprop-1-en-1-yl)stannane (**187**).

Nucleus: 13C
Frequency: 125.52 MHz
Solvent: Acetone
Temperature: 298.0 K

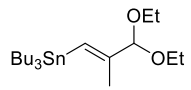

187

Appendix 71. ^{13}C-NMR spectrum of (*E*)-tributyl(3,3-diethoxy-2-methylprop-1-en-1-yl)stannane (**187**).

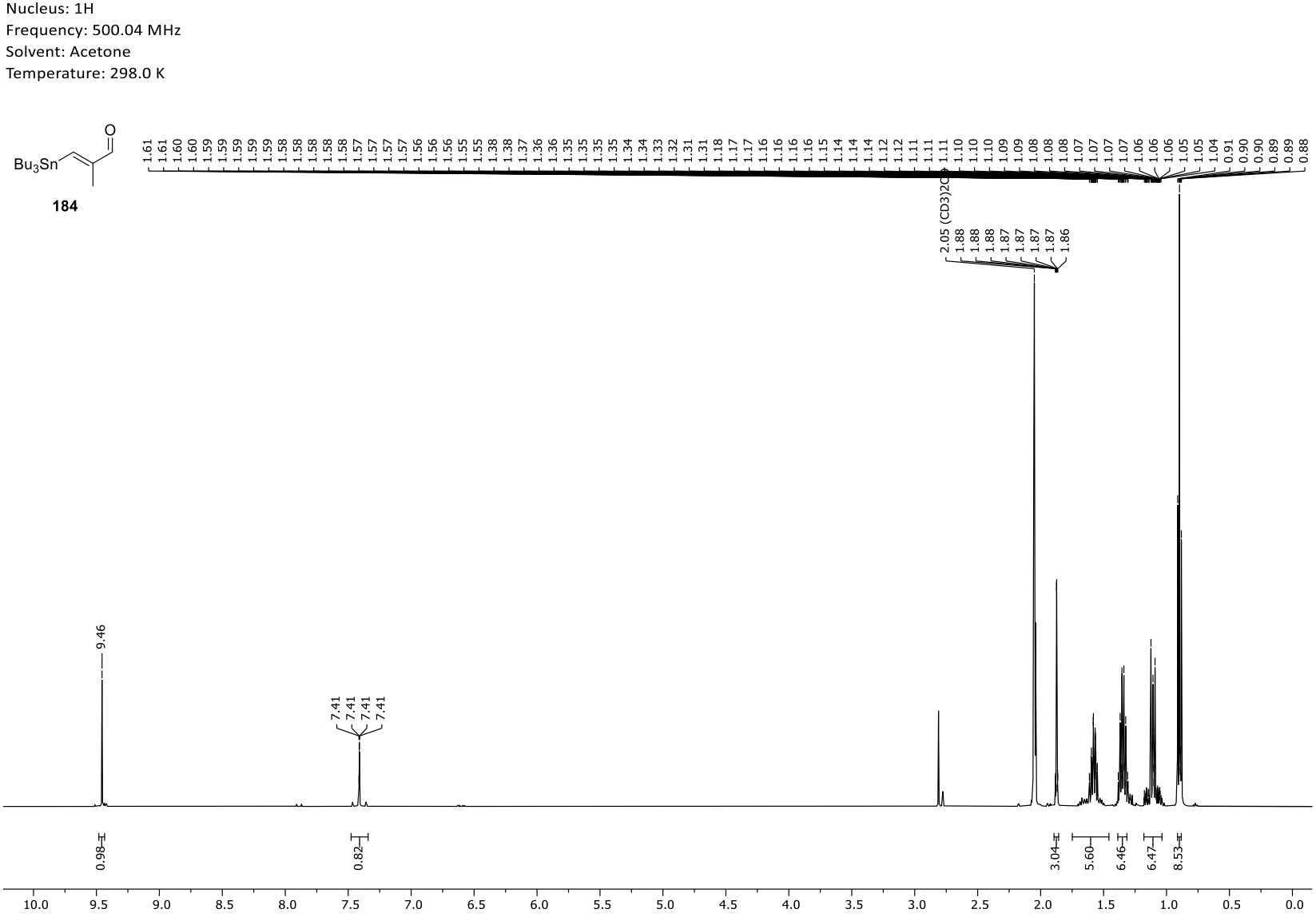

Appendix 72. ^{1}H-NMR spectrum of (*E*)-(3-tributylstannyl)methacrylaldehyde (**184**).

Nucleus: 13C
Frequency: 125.75 MHz
Solvent: Acetone
Temperature: 298.0 K

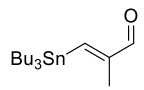

184

Appendix 73. ^{13}C-NMR spectrum of (*E*)-(3-tributylstannyl)methacrylaldehyde (**184**).

Nucleus: 1H
Frequency: 499.13 MHz
Solvent: Acetone
Temperature: 298.0 K

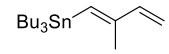

185

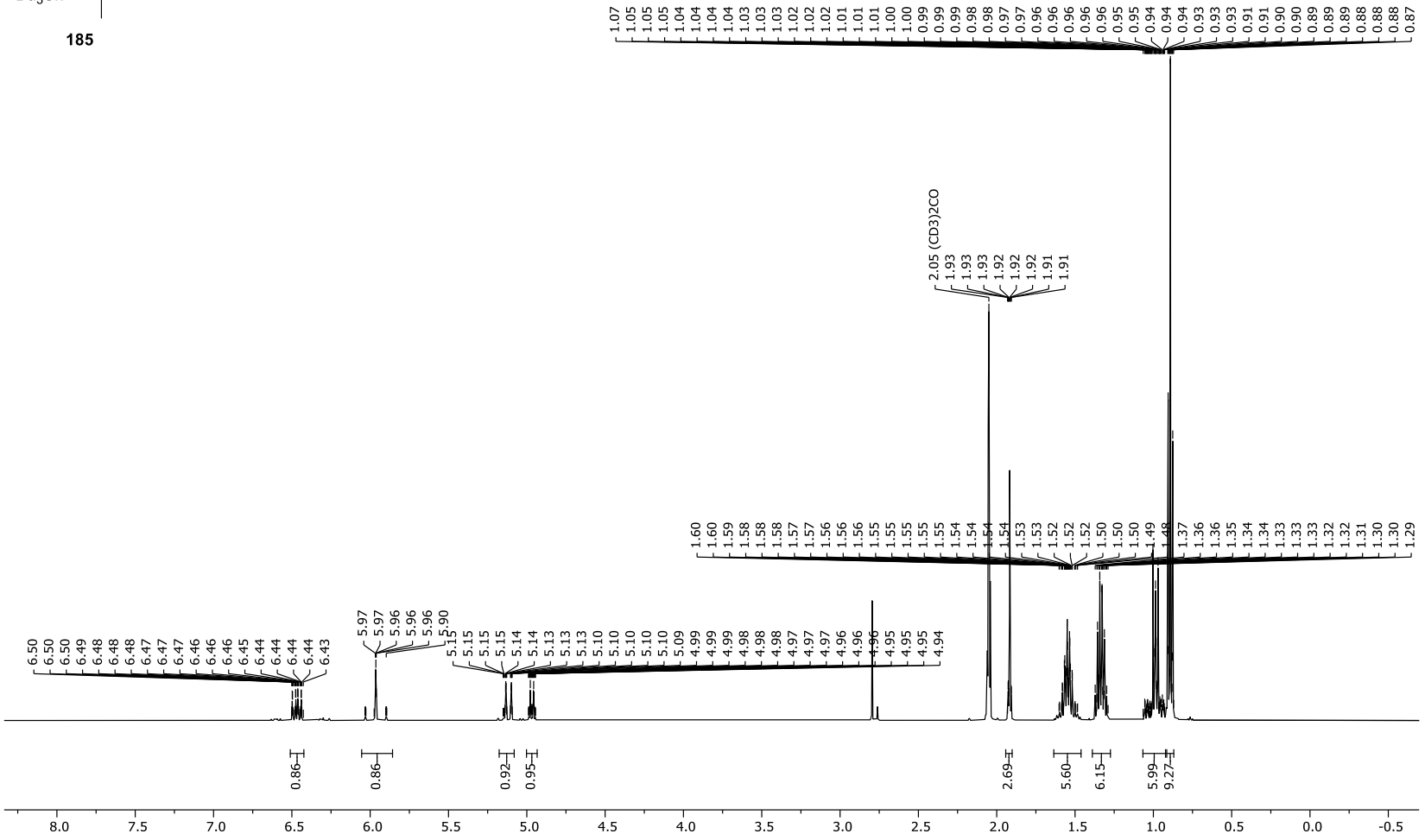

Appendix 74. ^{1}H-NMR spectrum of (*E*)-tributyl(2-methylbuta-1,3-dien-1-yl)stannane (**185**).

Nucleus: 13C
Frequency: 125.52 MHz
Solvent: Acetone
Temperature: 298.0 K

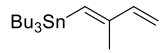

185

Appendix 75. ^{13}C-NMR spectrum of (*E*)-tributyl(2-methylbuta-1,3-dien-1-yl)stannane (**185**).

Nucleus: 1H
Frequency: 700.41 MHz
Solvent: Acetone
Temperature: 298.0 K

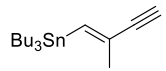

188

Appendix 76. ^{1}H-NMR spectrum of (*E*)-tributyl(2-methylbut-1-en-3-yn-1-yl)stannane (**188**).

Nucleus: 13C
Frequency: 176.14 MHz
Solvent: Acetone
Temperature: 298.0 K

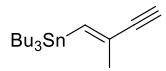

188

Appendix 77. ^{13}C-NMR spectrum of (*E*)-tributyl(2-methylbut-1-en-3-yn-1-yl)stannane (**188**).

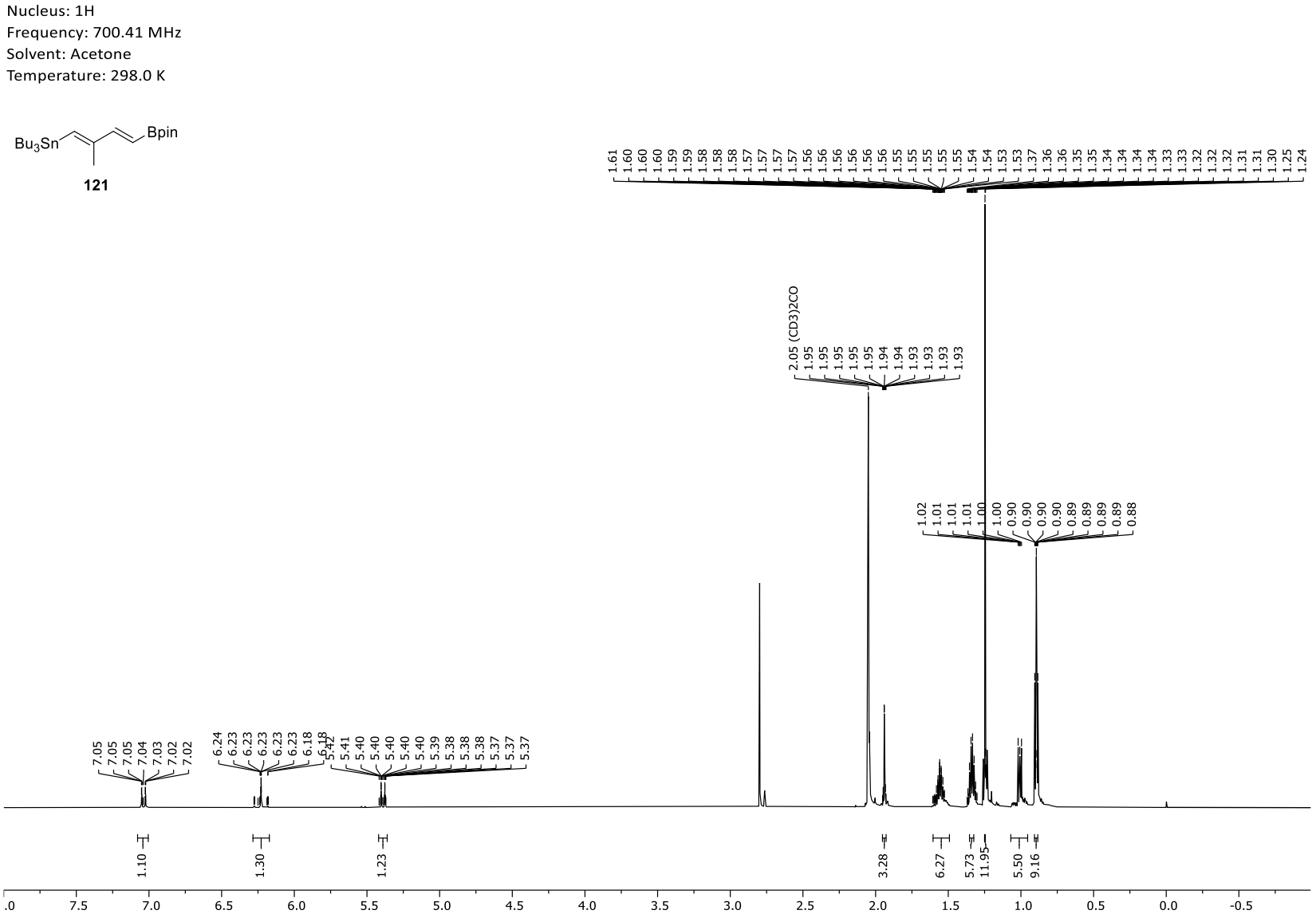

Appendix 78. ^{1}H-NMR spectrum of tributyl((1*E*,3*E*)-2-methyl-4-(4,4,5,5-tetramethyl-1,3,2-dioxaborolan-2-yl)buta-1,3-dien-1-yl) stannane (**121**).

Nucleus: 13C
Frequency: 176.14 MHz
Solvent: Acetone
Temperature: 298.0 K

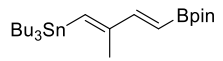

121

Appendix 79. ^{13}C-NMR spectrum of tributyl((1*E*,3*E*)-2-methyl-4-(4,4,5,5-tetramethyl-1,3,2-dioxaborolan-2-yl)buta-1,3-dien-1-yl) stannane (**121**).

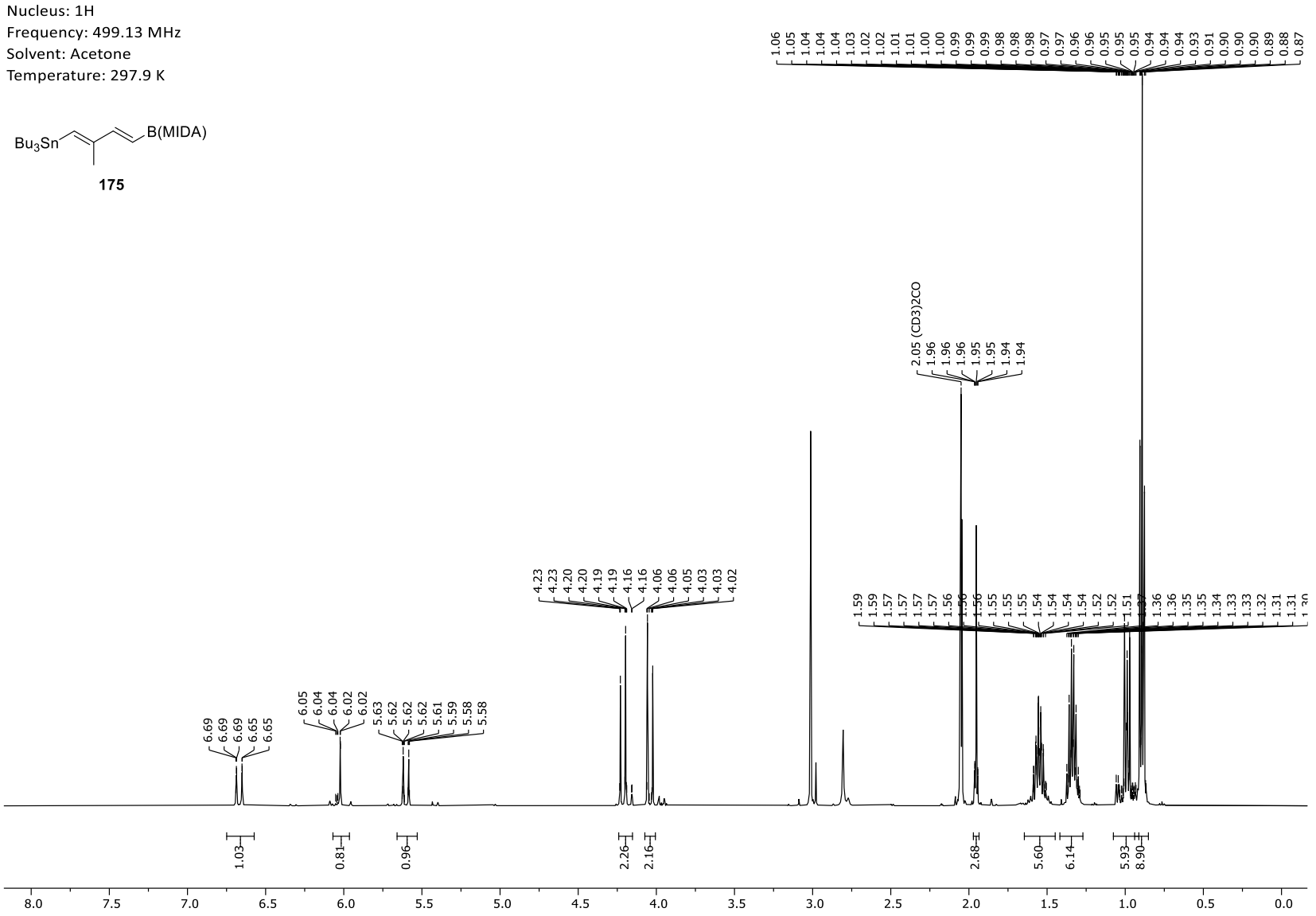

Appendix 80. ^{1}H-NMR spectrum of tributyl((1*E*,3*E*)-2-methyl-4-(1,3,6,2-dioxazaborocane-4,8-dione-2-yl)buta-1,3-dien-1-yl) stannane (**175**).

Nucleus: 13C
Frequency: 125.52 MHz
Solvent: Acetone
Temperature: 298.0 K

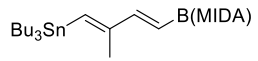

175

Appendix 81. ^{13}C-NMR spectrum of tributyl((1*E*,3*E*)-2-methyl-4-(1,3,6,2-dioxazaborocane-4,8-dione-2-yl)buta-1,3-dien-1-yl) stannane (**175**).

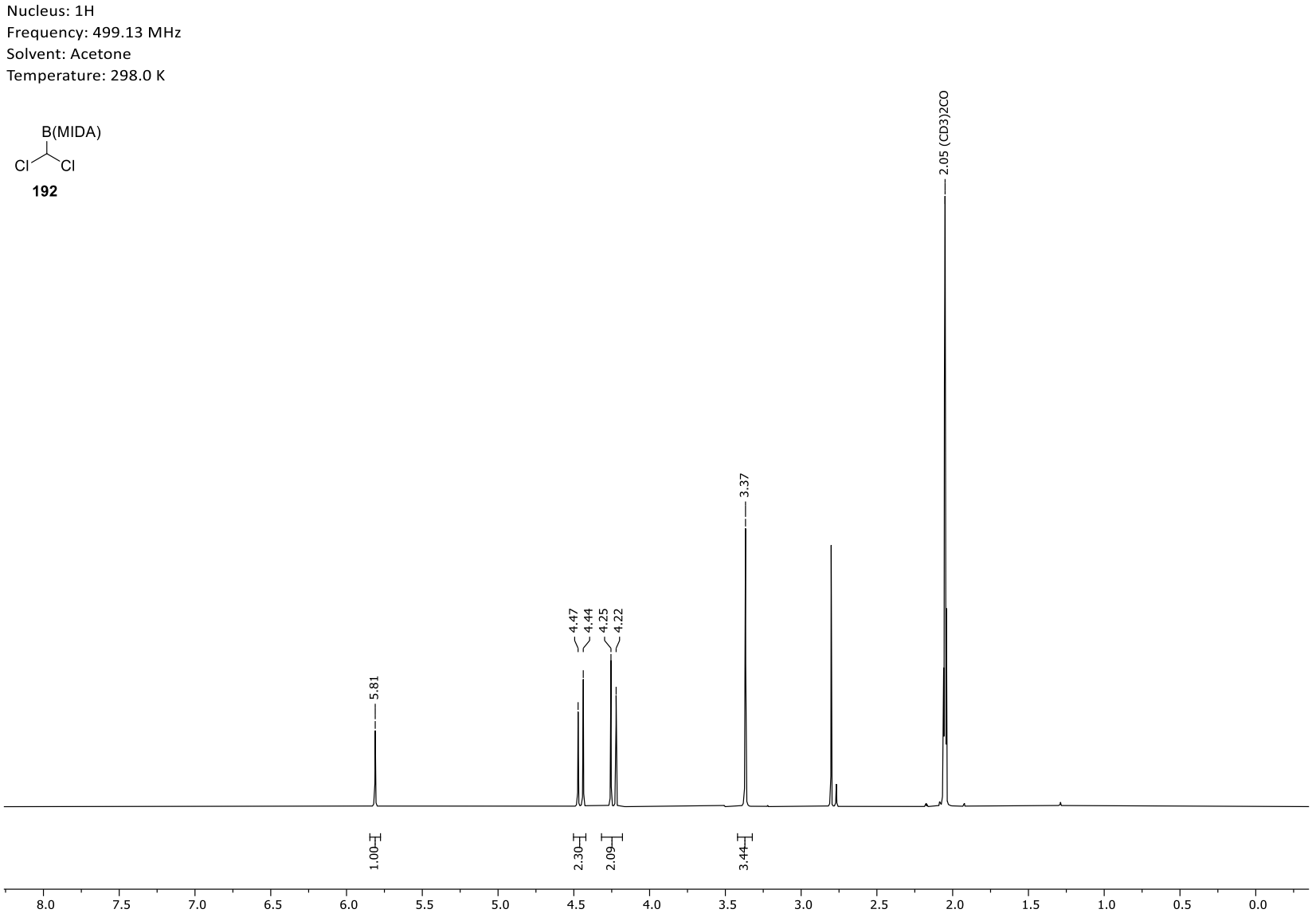

Appendix 82. ^{1}H-NMR spectrum of 2-(dichloromethyl)-1,3,6,2-dioxazaborocane-4,8-dione (**192**).

Nucleus: 13C
Frequency: 125.52 MHz
Solvent: Acetone
Temperature: 297.9 K

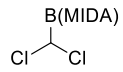

192

Appendix 83. ^{13}C-NMR spectrum of 2-(dichloromethyl)-1,3,6,2-dioxazaborocane-4,8-dione (**192**).

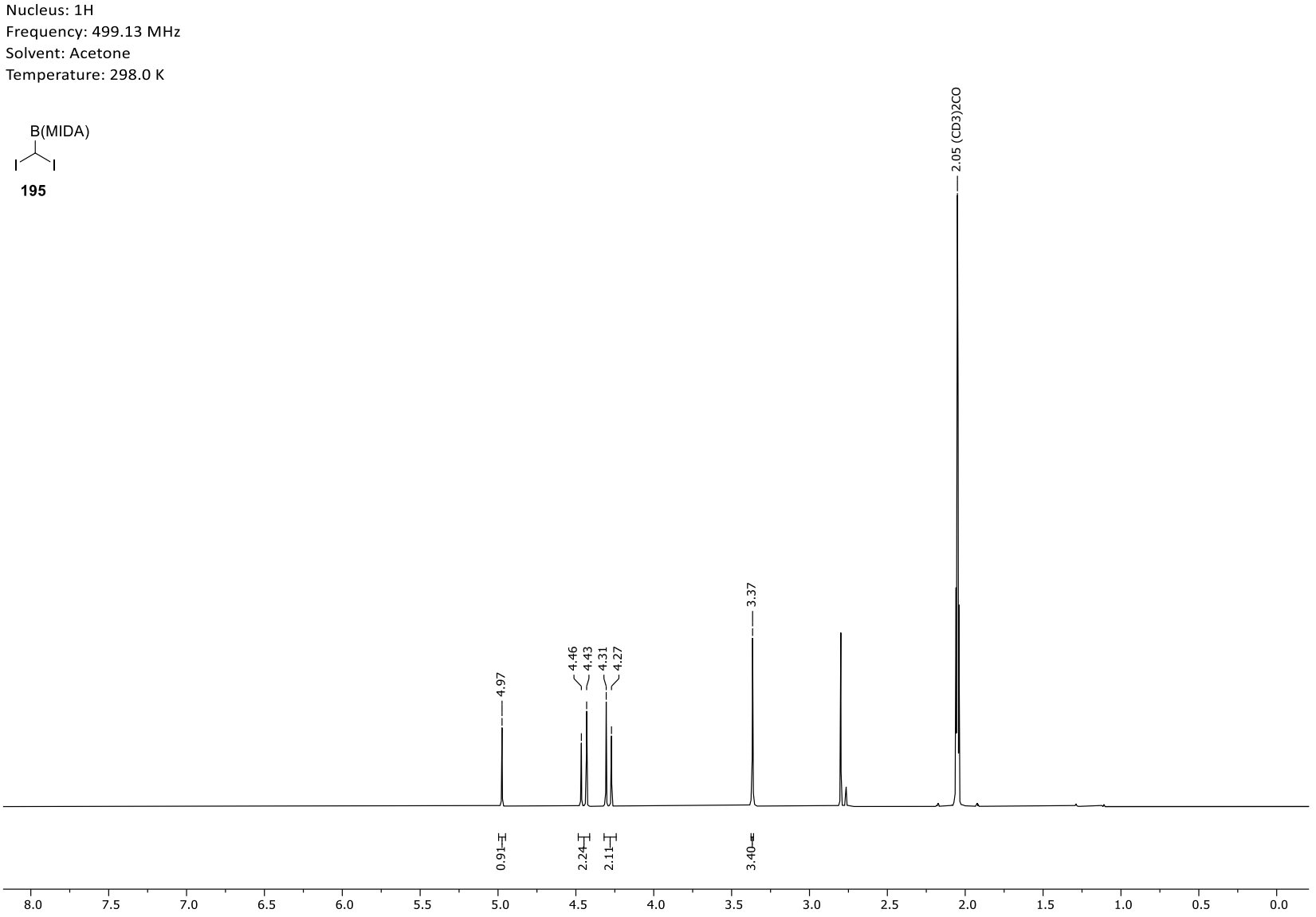

Appendix 84. ^{1}H-NMR spectrum of 2-(diiodomethyl)-1,3,6,2-dioxazaborocane-4,8-dione (**195**).

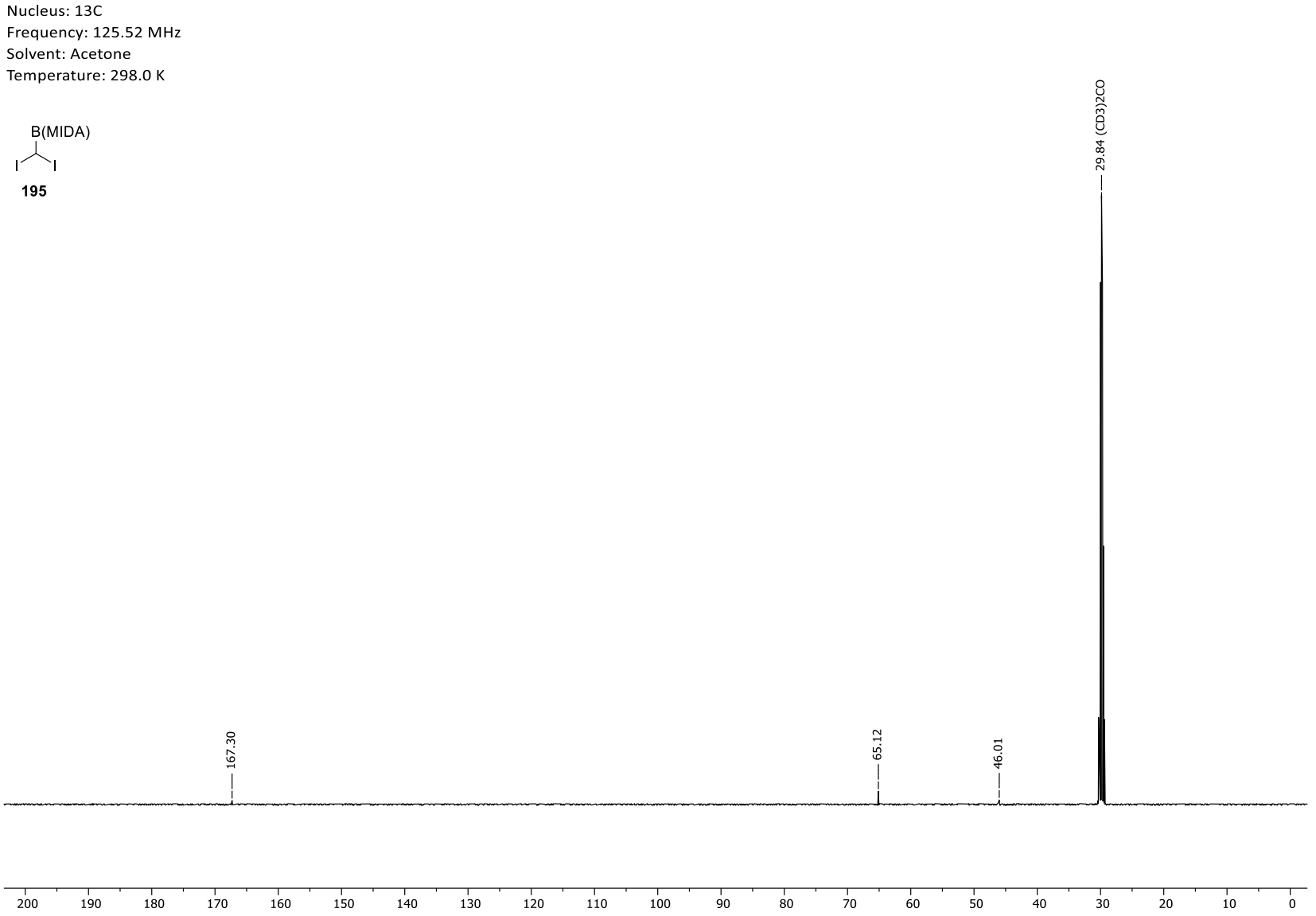

Appendix 85. ^{13}C-NMR spectrum of 2-(diiodomethyl)-1,3,6,2-dioxazaborocane-4,8-dione (**195**).

Nucleus: 1H
Frequency: 300.13 MHz
Solvent: Acetone
Temperature: 298.0 K

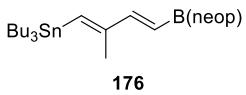

176

Appendix 86. ^{1}H-NMR spectrum of tributyl((1*E*,3*E*)-4-(5,5-dimethyl-1,3,2-dioxaborinan-2-yl)-2-methylbuta-1,3-dien-1-yl)stannane (**176**).

Nucleus: 1H
Frequency: 500.04 MHz
Solvent: Acetone
Temperature: 298.0 K

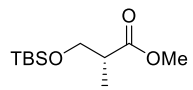

S-4

Appendix 87. ^{1}H-NMR spectrum of methyl (*R*)-3-((*tert*-butyldimethylsilyl)oxy)-2-methylpropanoate (**S-4**).

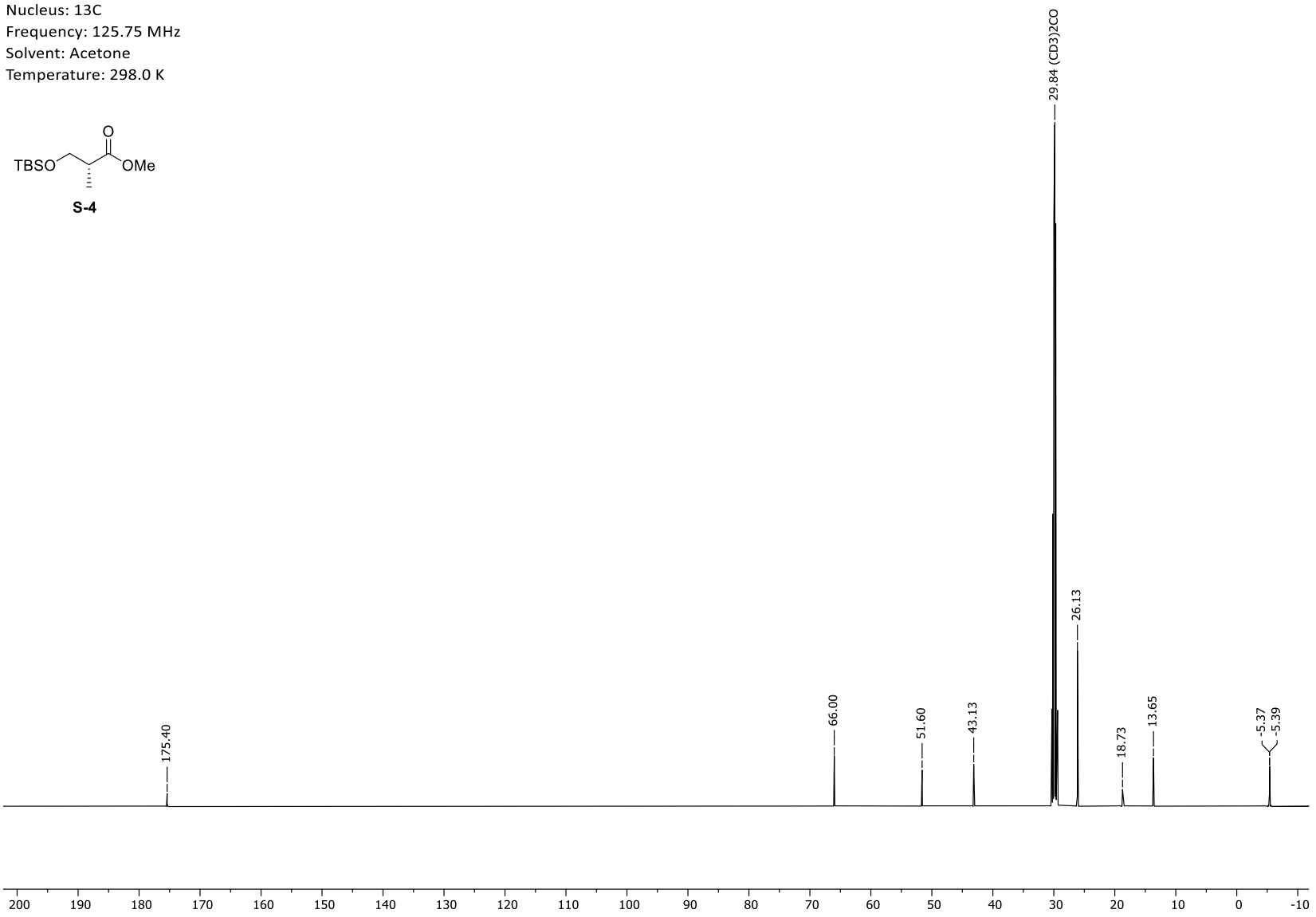

Appendix 88. ^{13}C-NMR spectrum of methyl (*R*)-3-((*tert*-butyldimethylsilyl)oxy)-2-methylpropanoate (**S-4**).

Nucleus: 1H
Frequency: 500.04 MHz
Solvent: Acetone
Temperature: 298.0 K

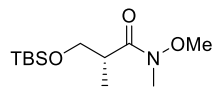

S-5

Appendix 89. ^{1}H-NMR spectrum of (*R*)-3-((*tert*-Butyldimethylsilyl)oxy)-*N*-methoxy-*N*,2-dimethylpropanamide (**S-5**).

Nucleus: 13C
Frequency: 125.75 MHz
Solvent: Acetone
Temperature: 298.0 K

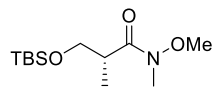

S-5

Appendix 90. ^{13}C-NMR spectrum of (*R*)-3-((*tert*-butyldimethylsilyl)oxy)-*N*-methoxy-*N*,2-dimethylpropanamide (**S-5**).

Nucleus: 1H
Frequency: 500.04 MHz
Solvent: Acetone
Temperature: 298.0 K

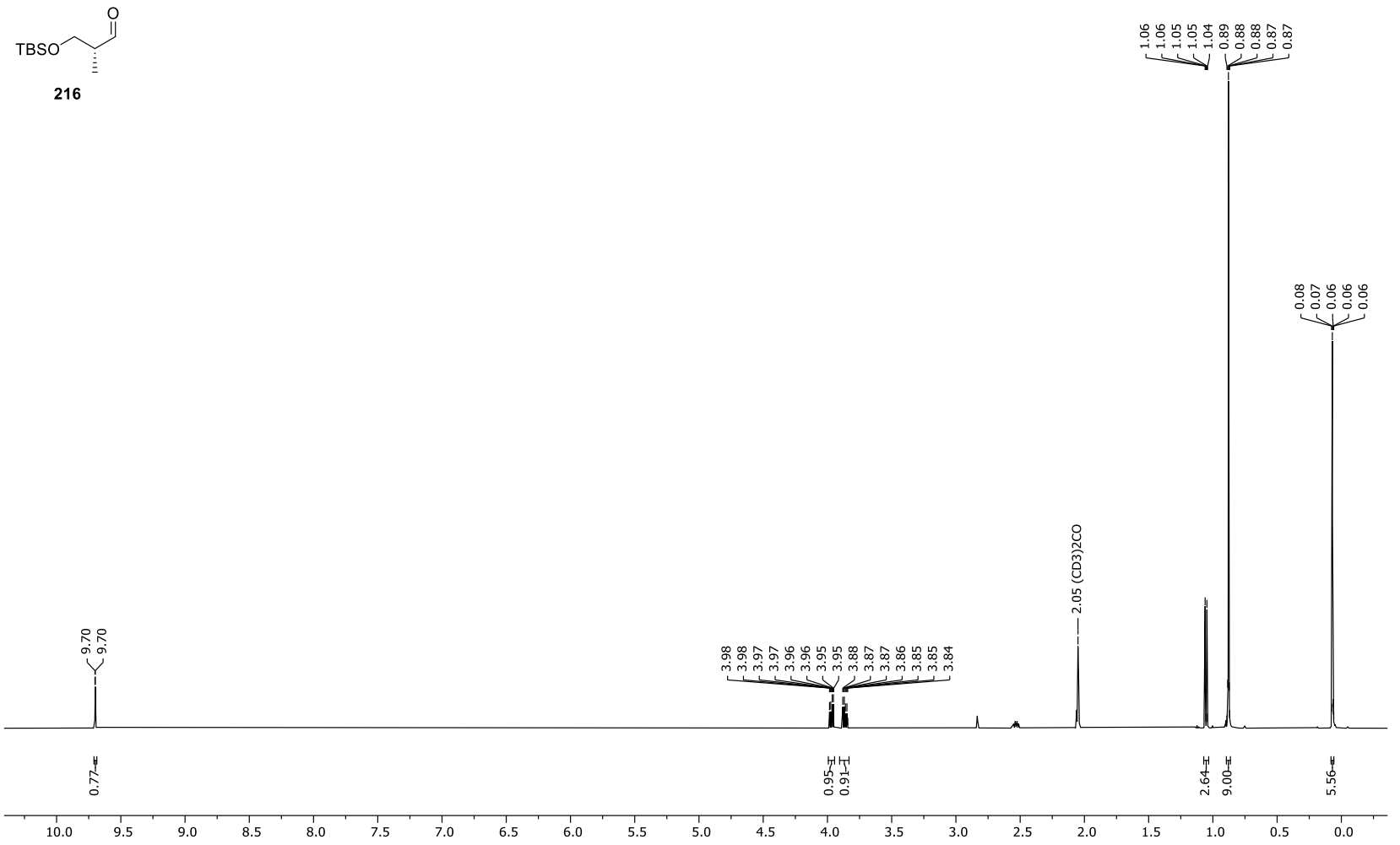

Appendix 91. ^{1}H-NMR spectrum of (2*R*)-3-(*tert*-butyldimethylsilyl)oxy-2-methylpropanal (**216**).

Nucleus: 13C
Frequency: 125.75 MHz
Solvent: Acetone
Temperature: 298.0 K

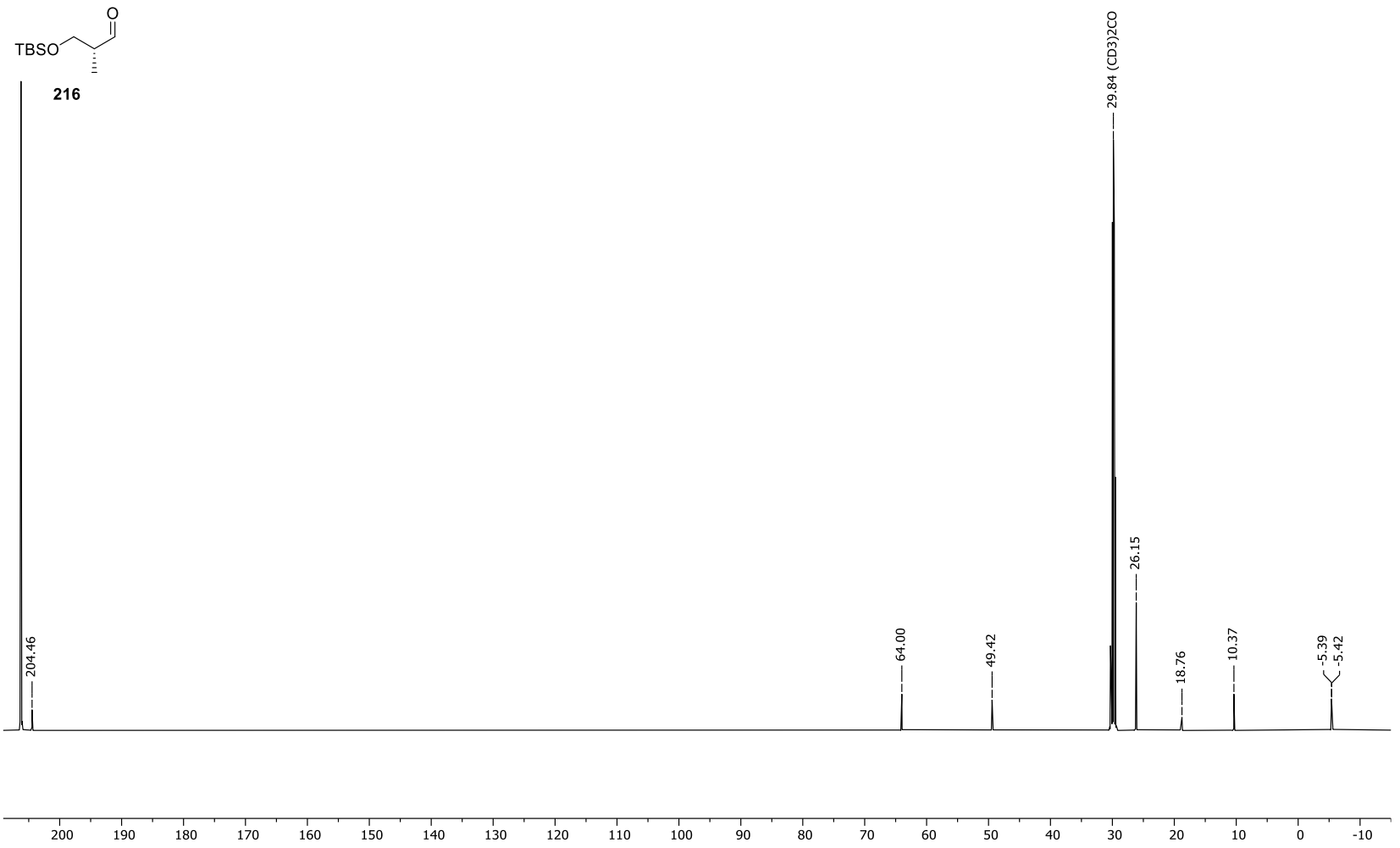

Appendix 92. ^{13}C-NMR spectrum of (2*R*)-3-(*tert*-Butyldimethylsilyl)oxy-2-methylpropanal (**216**).

Nucleus: 1H
Frequency: 500.04 MHz
Solvent: Acetone
Temperature: 298.0 K

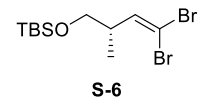

S-6

Appendix 93. ^{1}H-NMR spectrum of (2*S*)-1-(*tert*-Butyldimethylsilyloxy)-4,4-dibromo-2-methylbut-3-ene (**S-6**).

Nucleus: 13C
Frequency: 125.75 MHz
Solvent: Acetone
Temperature: 298.0 K

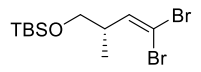

S-6

Appendix 94. ^{13}C-NMR spectrum of (2*S*)-1-(*tert*-Butyldimethylsilyloxy)-4,4-dibromo-2-methylbut-3-ene (**S-6**).

Nucleus: 1H
Frequency: 499.13 MHz
Solvent: CDCl3
Temperature: 298.1 K

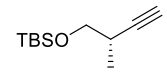

217

Appendix 95. ^{1}H-NMR spectrum of (2*S*)-1-(*tert*-butyldimethylsilyl)oxy-2-methylbut-3-yne (**217**).

Nucleus: 13C
Frequency: 125.52 MHz
Solvent: CDCl3
Temperature: 298.0 K

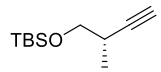

217

Appendix 96. ^{13}C-NMR spectrum of (2*S*)-1-(*tert*-Butyldimethylsilyl)oxy-2-methylbut-3-yne (**217**).

Nucleus: 1H
Frequency: 499.13 MHz
Solvent: Acetone
Temperature: 298.1 K

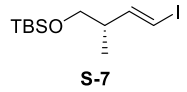

S-7

Appendix 97. ^{1}H-NMR spectrum of (2*S*, 3*E*)-1-(*tert*-butyldimethylsilyl)oxy-4-iodo-2-methylbut-3-ene (**S-7**).

Nucleus: 13C
Frequency: 125.52 MHz
Solvent: Acetone
Temperature: 298.2 K

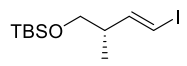

S-7

Appendix 98. ^{13}C-NMR spectrum of (2*S*, 3*E*)-1-(*tert*-Butyldimethylsilyl)oxy-4-iodo-2-methylbut-3-ene (**S-7**).

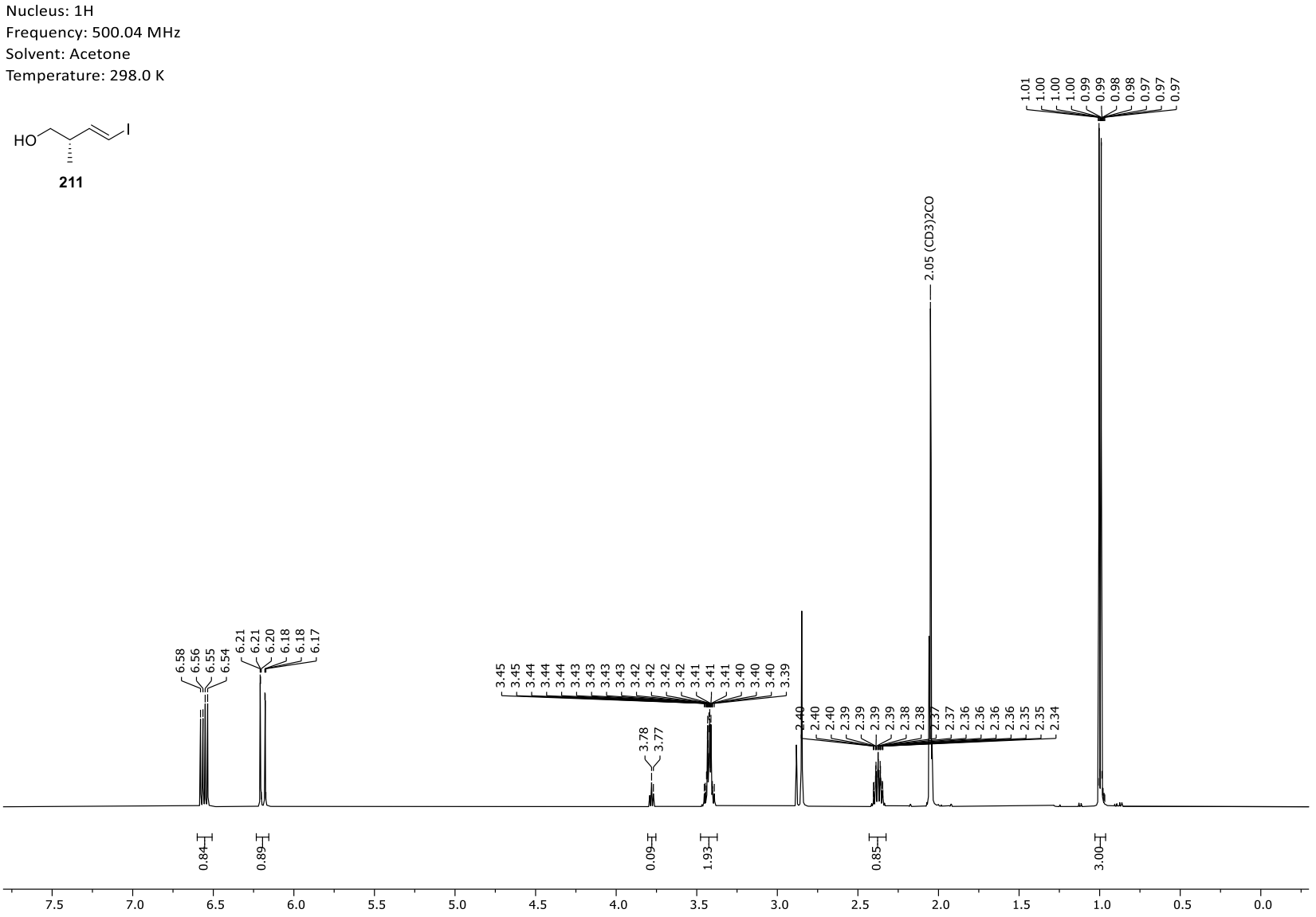

Appendix 99. ^{1}H-NMR spectrum of (2*S*,3*E*)-4-Iodo-2-methyl-3-buten-1-ol (**211**).

Nucleus: 13C
Frequency: 125.75 MHz
Solvent: Acetone
Temperature: 298.0 K

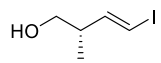

211

Appendix 100. ^{13}C-NMR spectrum of (2*S*,3*E*)-4-Iodo-2-methyl-3-buten-1-ol (**211**).

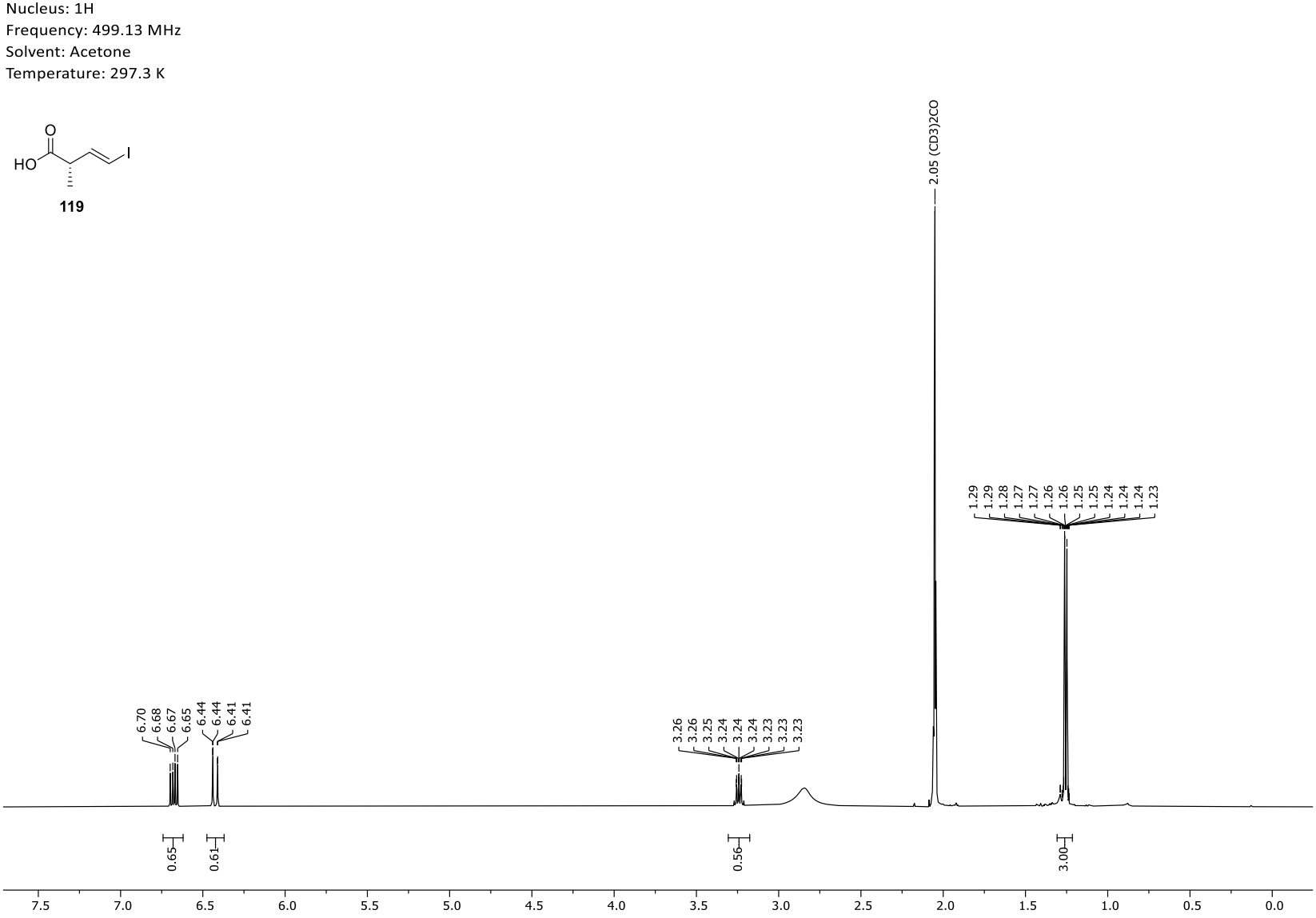

Appendix 101. ^{1}H-NMR spectrum of (2*S*, 3*E*)-4-Iodo-2-methyl-3-butenoic acid (**119**).

Nucleus: 13C
Frequency: 125.52 MHz
Solvent: Acetone
Temperature: 298.1 K

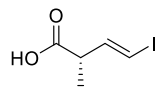

119

Appendix 102. ^{13}C-NMR spectrum of (2*S*, 3*E*)-4-Iodo-2-methyl-3-butenoic acid (**119**).

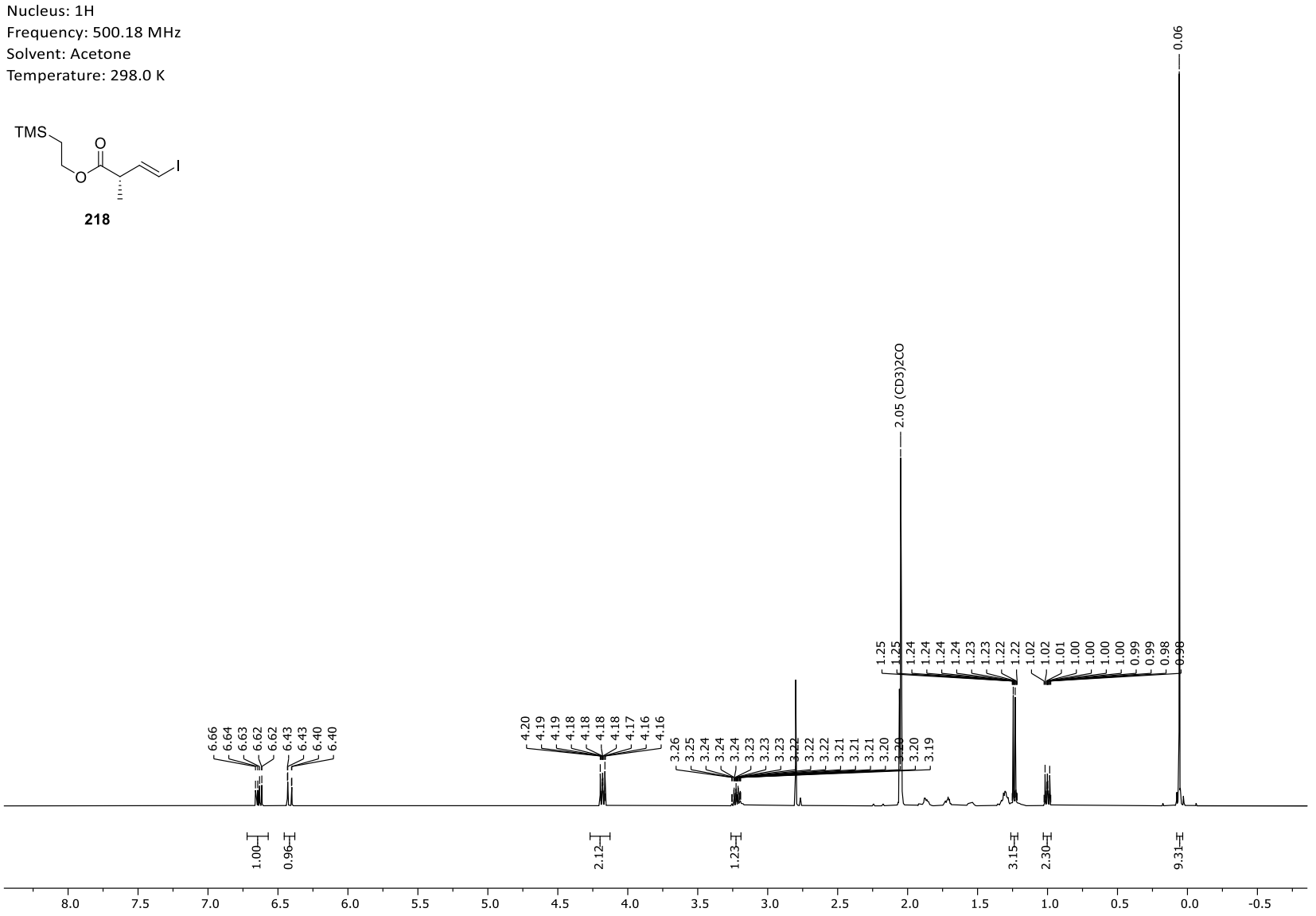

Appendix 103. ^{1}H-NMR spectrum of 2-(trimethylsilyl)ethyl (*S*,*E*)-4-iodo-2-methylbut-3-enoate (**218**).

Nucleus: 13C
Frequency: 125.78 MHz
Solvent: Acetone
Temperature: 298.0 K

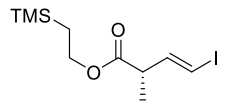

218

Appendix 104. ^{13}C-NMR spectrum of 2-(trimethylsilyl)ethyl (*S*,*E*)-4-iodo-2-methylbut-3-enoate (**218**).

Nucleus: 1H
Frequency: 499.13 MHz
Solvent: CDCl3
Temperature: 298.2 K

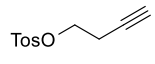

225

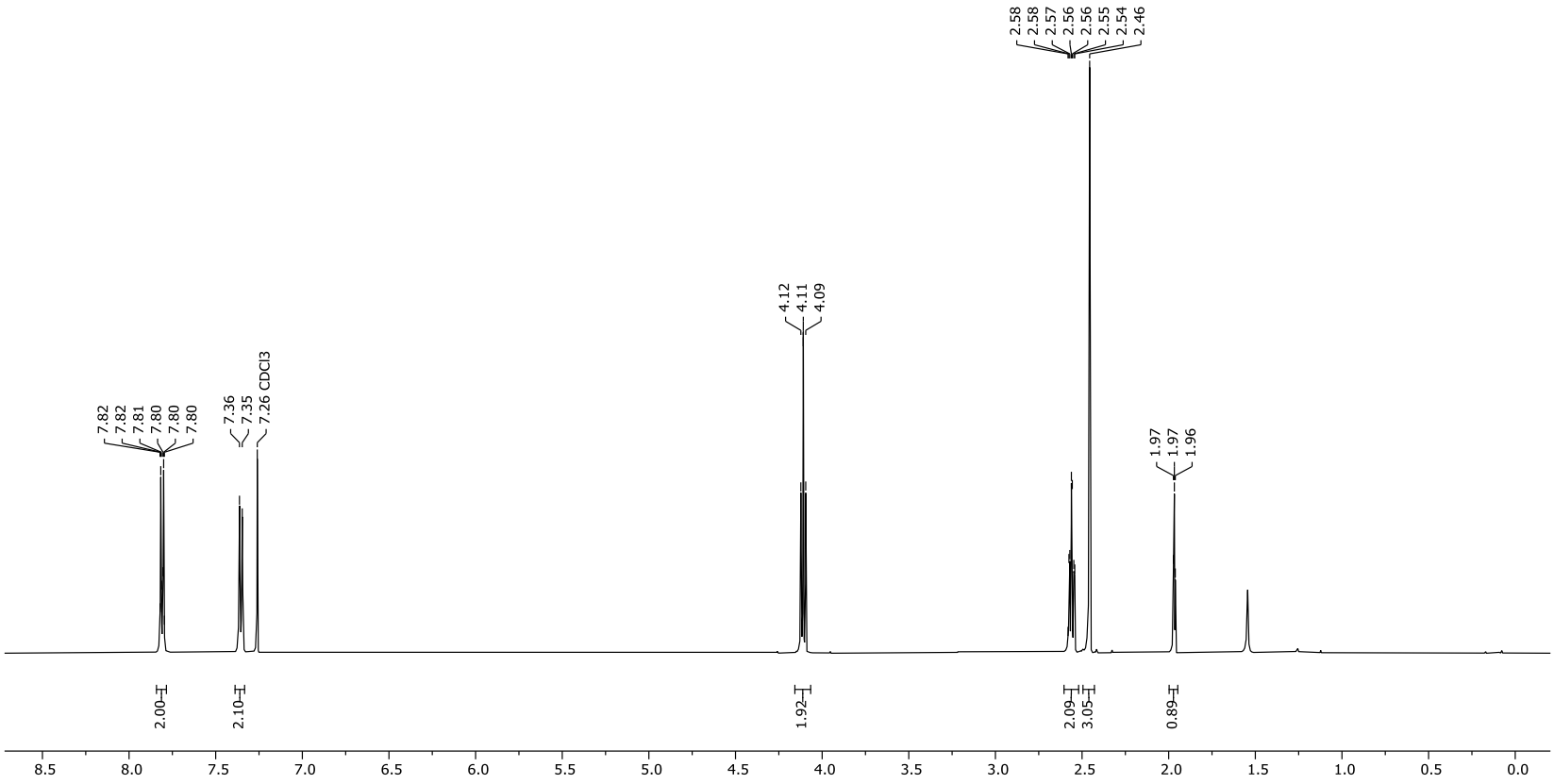

Appendix 105. ^{1}H-NMR spectrum of but-3-yn-1-yl 4-methylbenzenesulfonate (**225**).

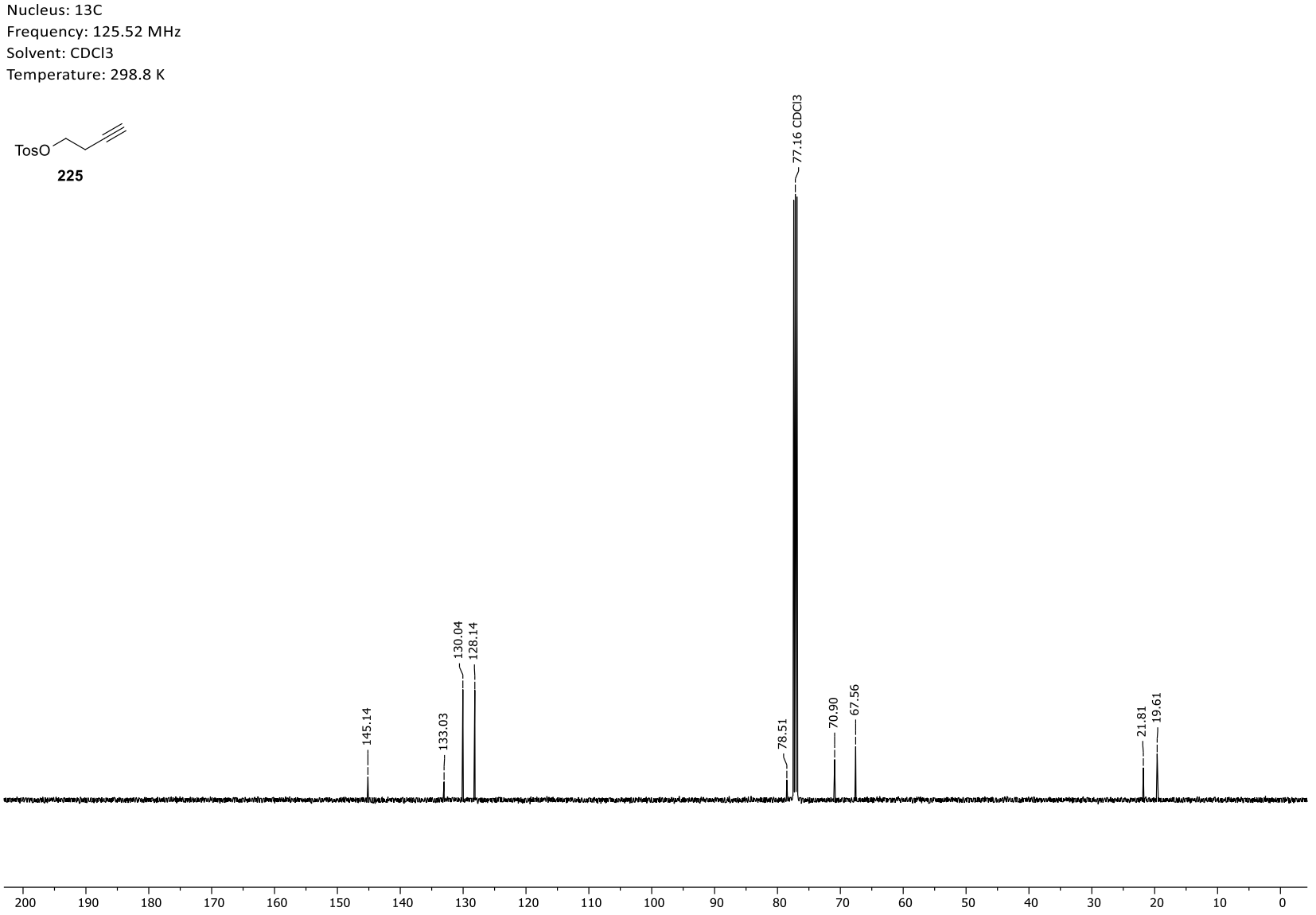

Appendix 106. ^{13}C-NMR spectrum of but-3-yn-1-yl 4-methylbenzenesulfonate (**225**).

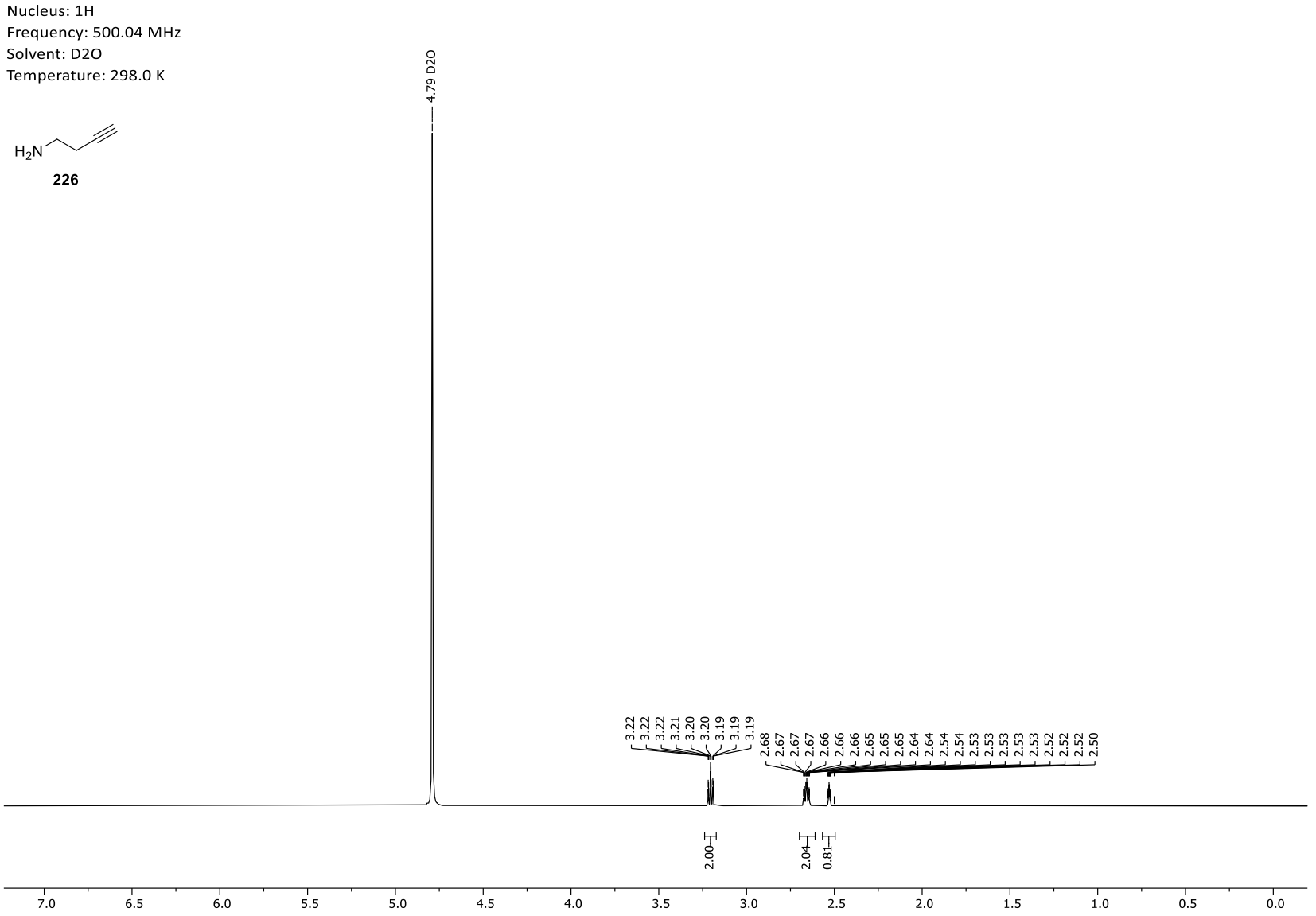

Appendix 107. ^{1}H-NMR spectrum of but-3-yn-1-amine hydrochloride (**226**).

Nucleus: 13C
Frequency: 125.75 MHz
Solvent: D2O
Temperature: 298.0 K

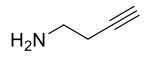

226

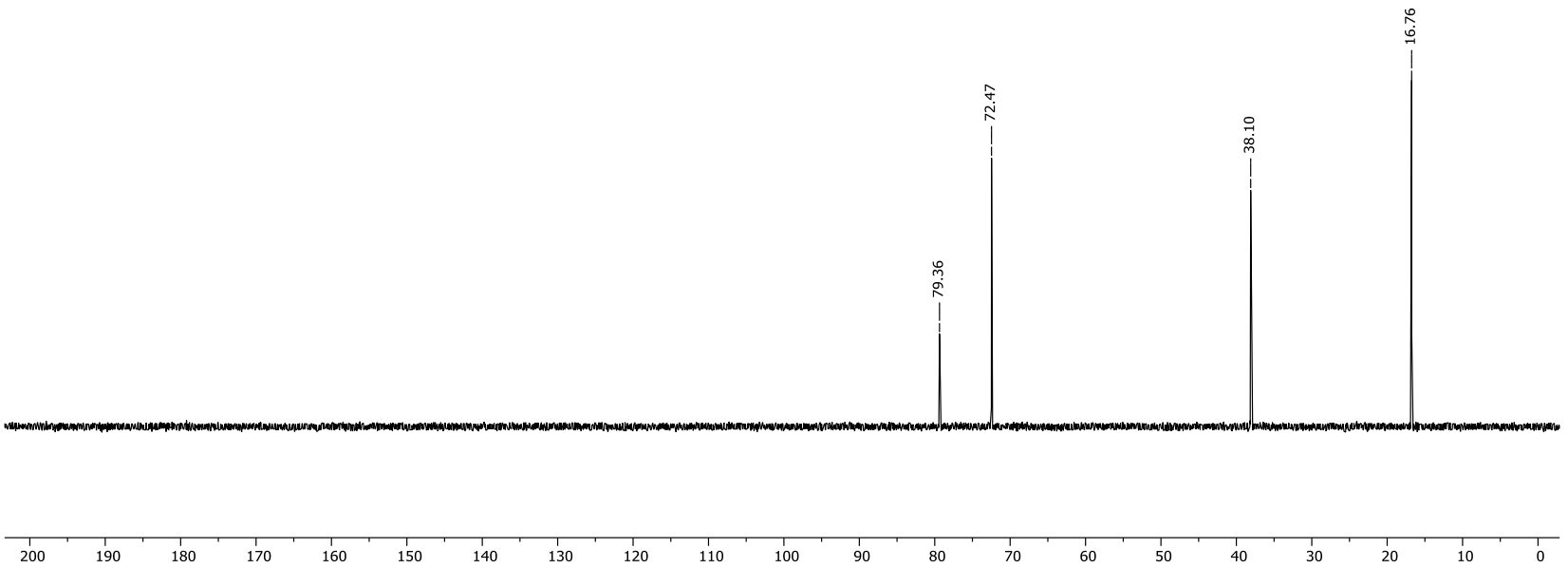

Appendix 108. ^{13}C-NMR spectrum of but-3-yn-1-amine hydrochloride (**226**).

Nucleus: 1H
Frequency: 499.13 MHz
Solvent: Acetone
Temperature: 298.0 K

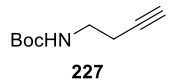

227

Appendix 109. ^{1}H-NMR spectrum of *tert*-butyl but-3-yn-1-ylcarbamate (**227**).

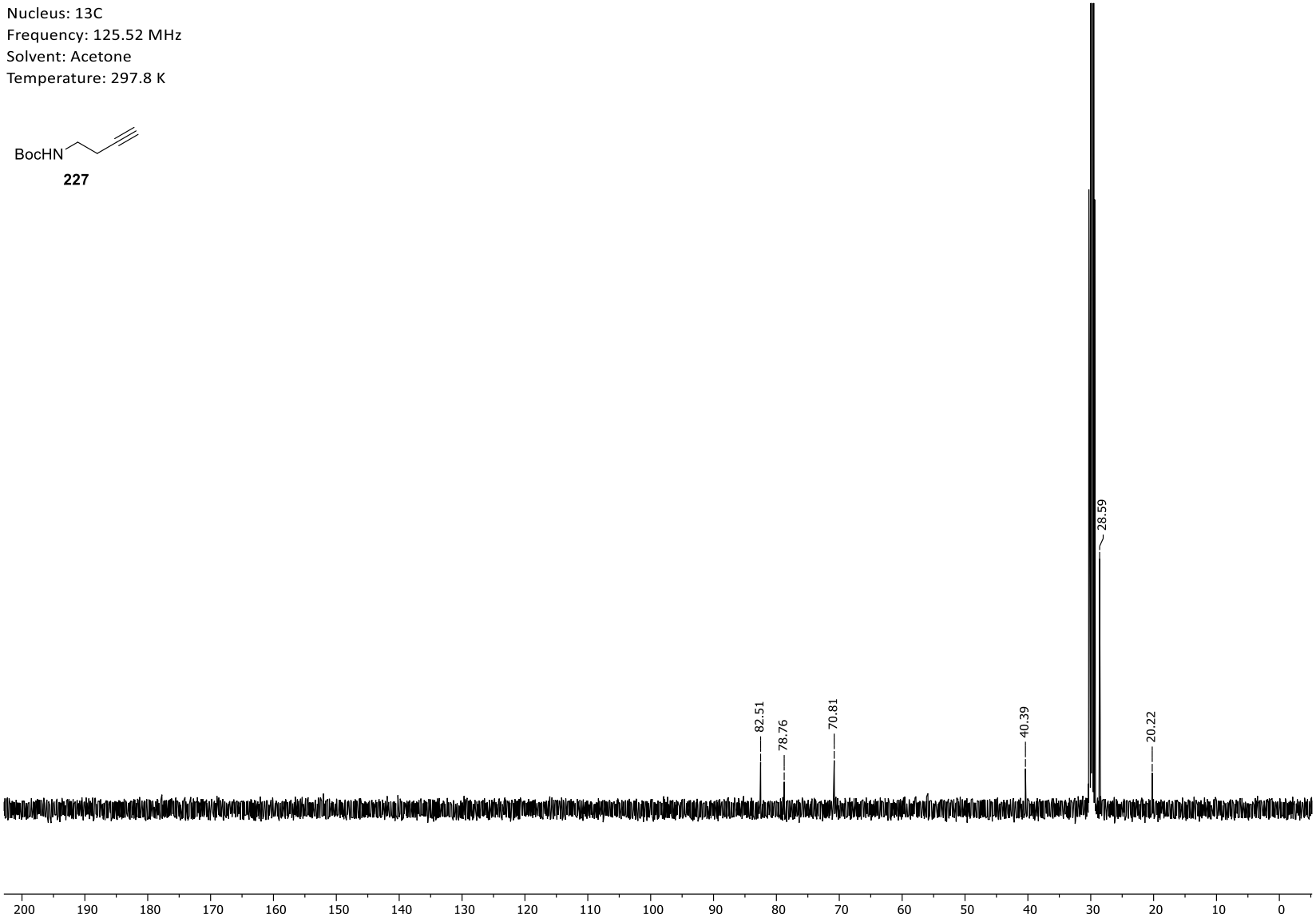

Appendix 110. ^{13}C-NMR spectrum of *tert*-butyl but-3-yn-1-ylcarbamate (**227**).

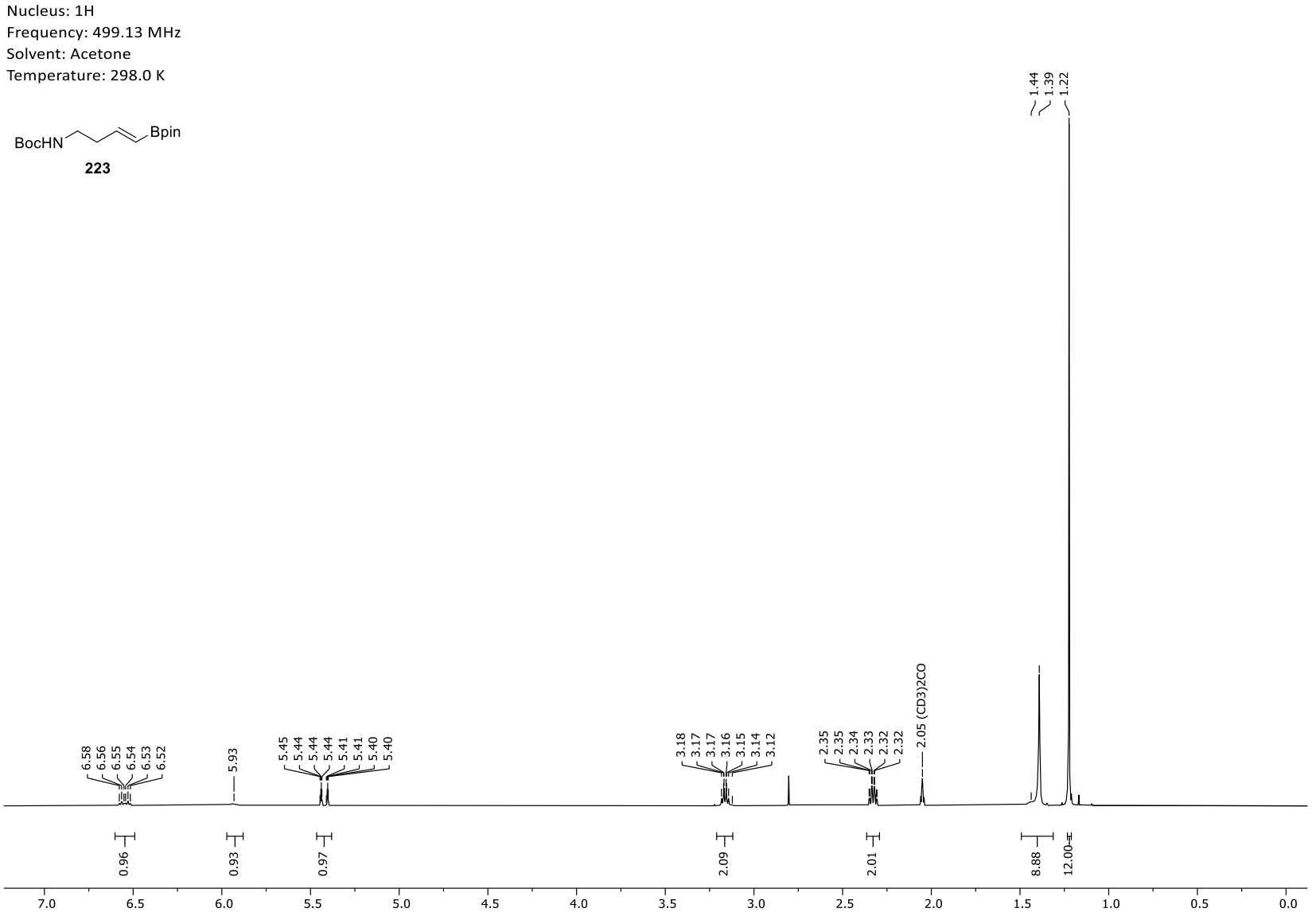

Appendix 111. ^{1}H-NMR spectrum of *tert*-butyl (*E*)-(4-(4,4,5,5-tetramethyl-1,3,2-dioxaborolan-2-yl)but-3-en-1-yl)carbamate (**223**).

Nucleus: 13C
Frequency: 125.52 MHz
Solvent: Acetone
Temperature: 297.8 K

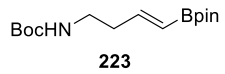

223

Appendix 112. ^{13}C-NMR spectrum of *tert*-butyl (*E*)-(4-(4,4,5,5-tetramethyl-1,3,2-dioxaborolan-2-yl)but-3-en-1-yl)carbamate (**223**).

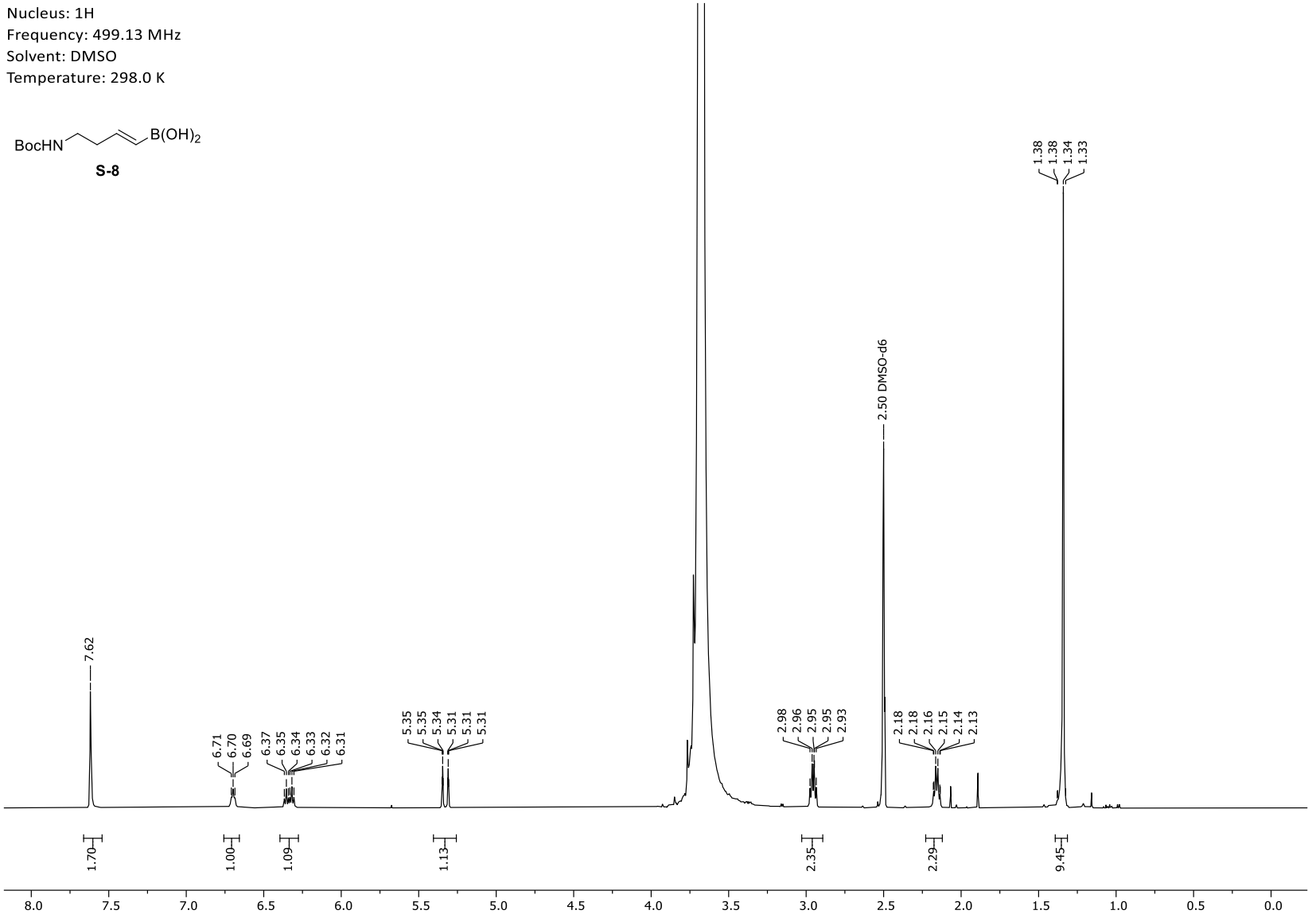

Appendix 113. ^{1}H-NMR spectrum of (*E*)-(4-((*tert*-butoxycarbonyl)amino)but-1-en-1-yl)boronic acid (**S-8**).

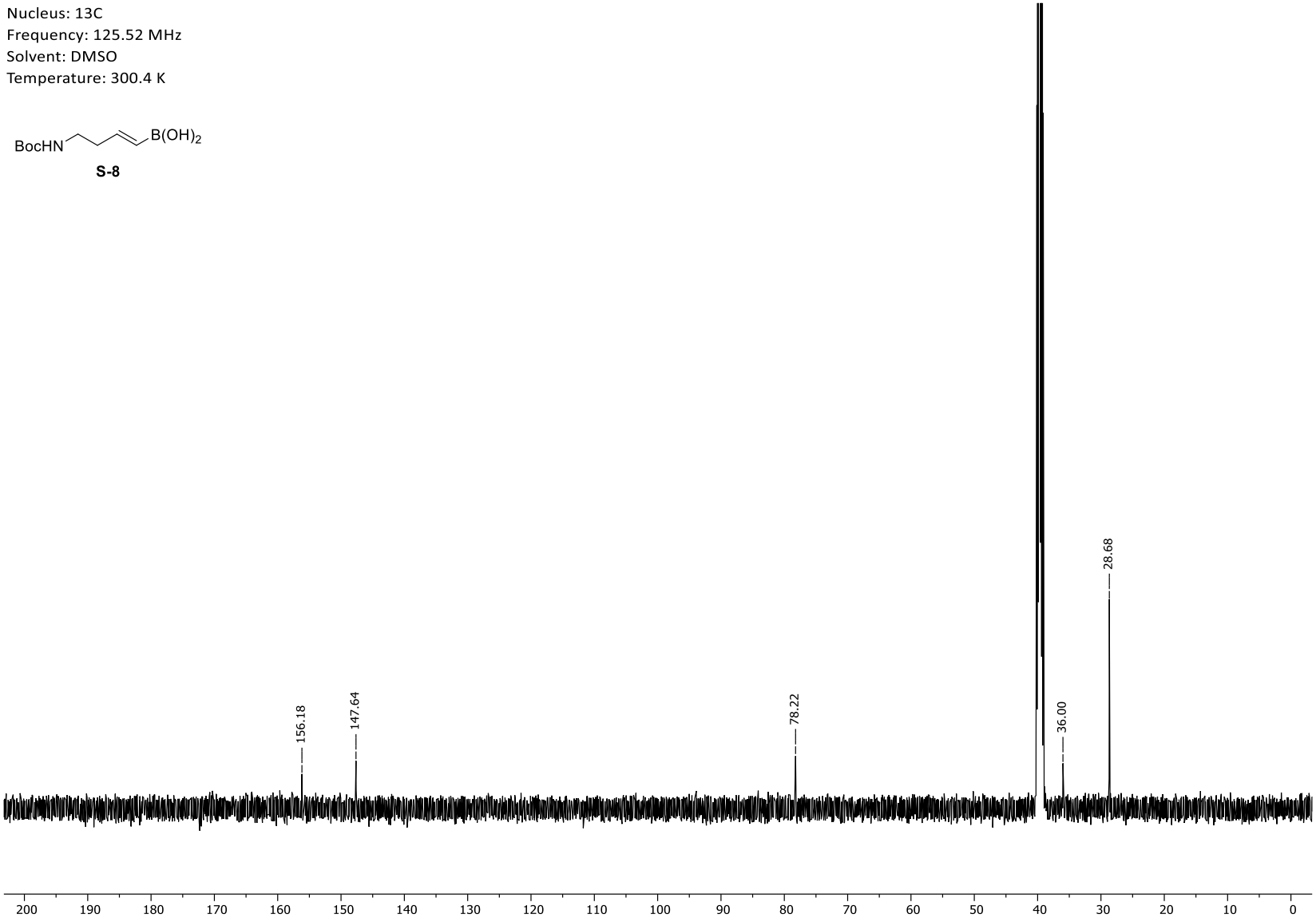

Appendix 114. ^{13}C-NMR spectrum of (*E*)-(4-((*tert*-butoxycarbonyl)amino)but-1-en-1-yl)boronic acid (**S-8**).

Nucleus: 1H
Frequency: 500.04 MHz
Solvent: Acetone
Temperature: 298.0 K

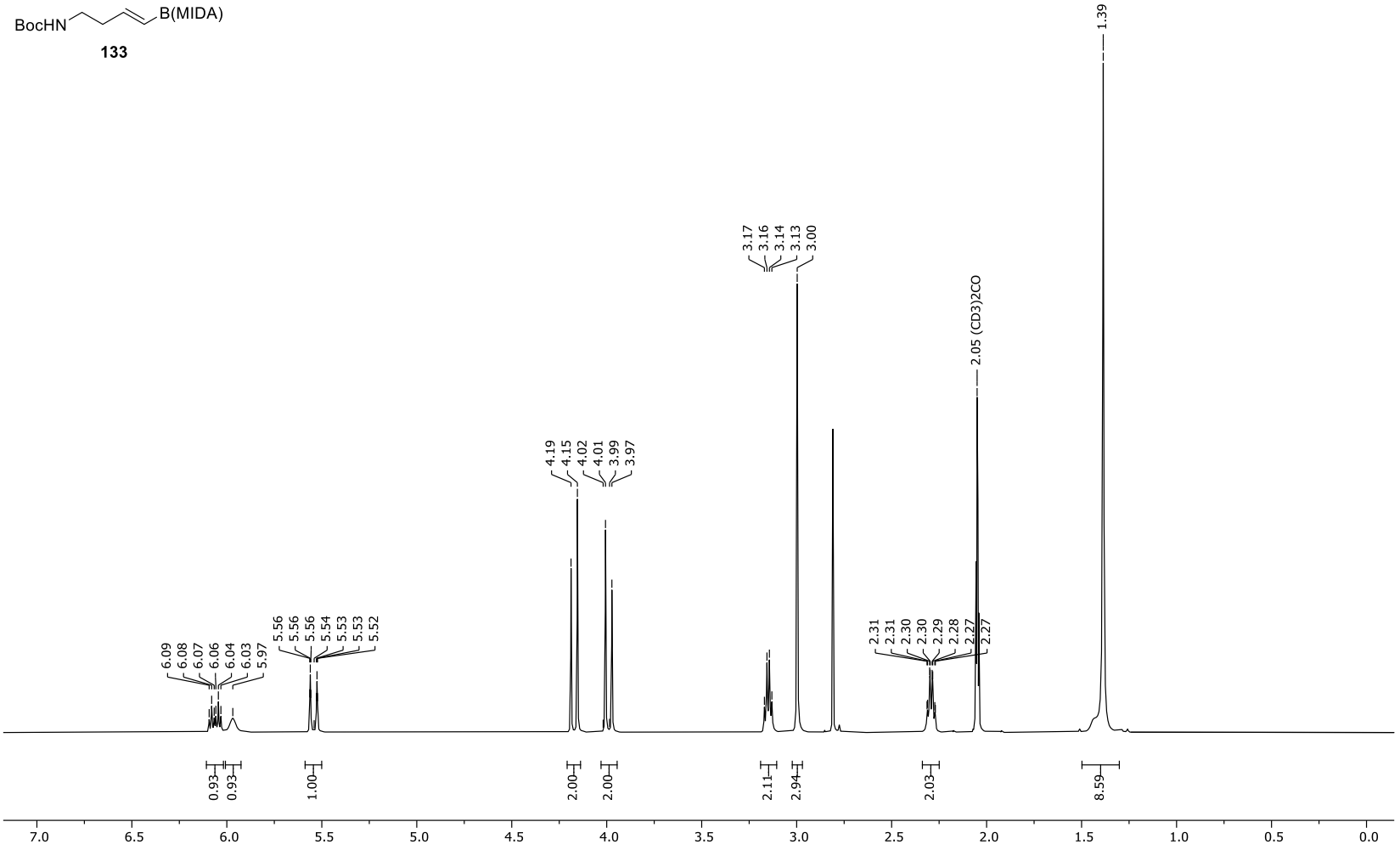

Appendix 115. ^{1}H-NMR spectrum of *tert*-butyl (*E*)-(4-(1,3,6,2-dioxazaborocane-4,8-dione-2-yl)but-3-en-1-yl)carbamate (**133**).

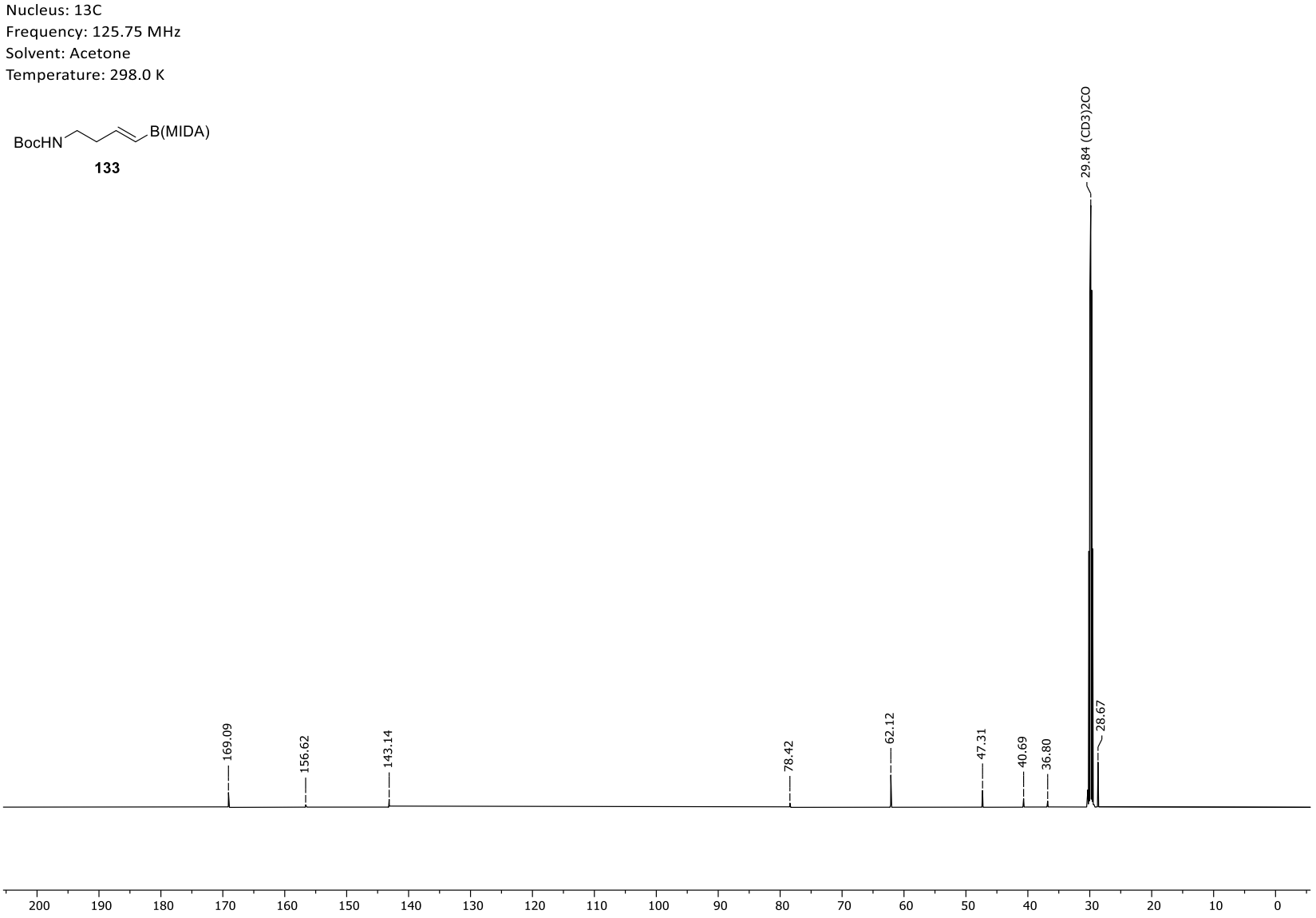

Appendix 116. ^{13}C-NMR spectrum of *tert*-butyl (*E*)-(4-(1,3,6,2-dioxazaborocane-4,8-dione-2-yl)but-3-en-1-yl)carbamate (**133**).

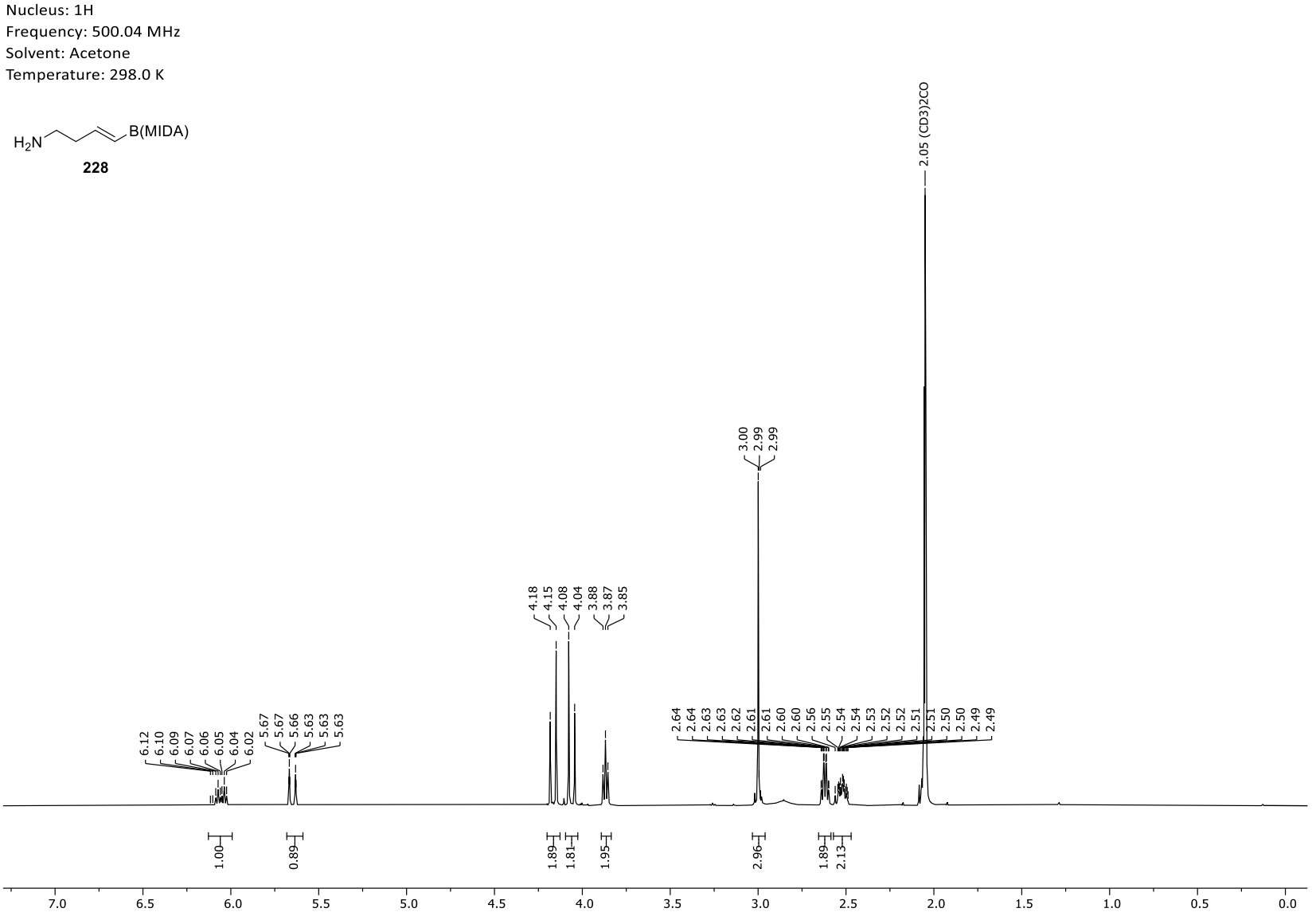

Appendix 117. ^{1}H-NMR spectrum of *tert*-butyl (*E*)-(4-(1,3,6,2-dioxazaborocane-4,8-dione-2-yl)but-3-en-1-yl)amine (**228**).

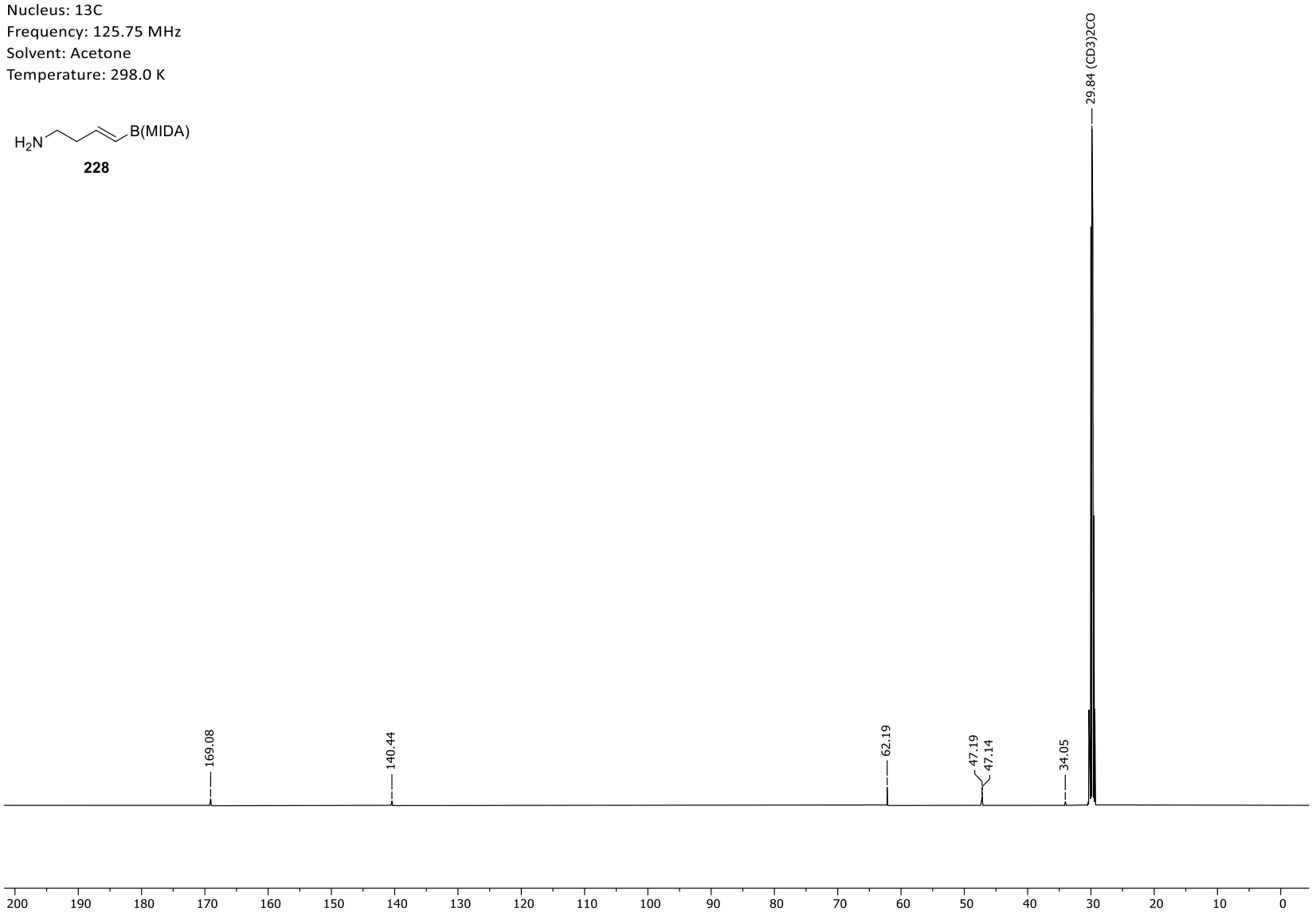

Appendix 118. ^{13}C-NMR spectrum of *tert*-butyl (*E*)-(4-(1,3,6,2-dioxazaborocane-4,8-dione-2-yl)but-3-en-1-yl)amine (**228**).

Nucleus: 1H
Frequency: 499.13 MHz
Solvent: CD2Cl2
Temperature: 298.7 K

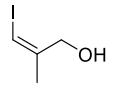

229

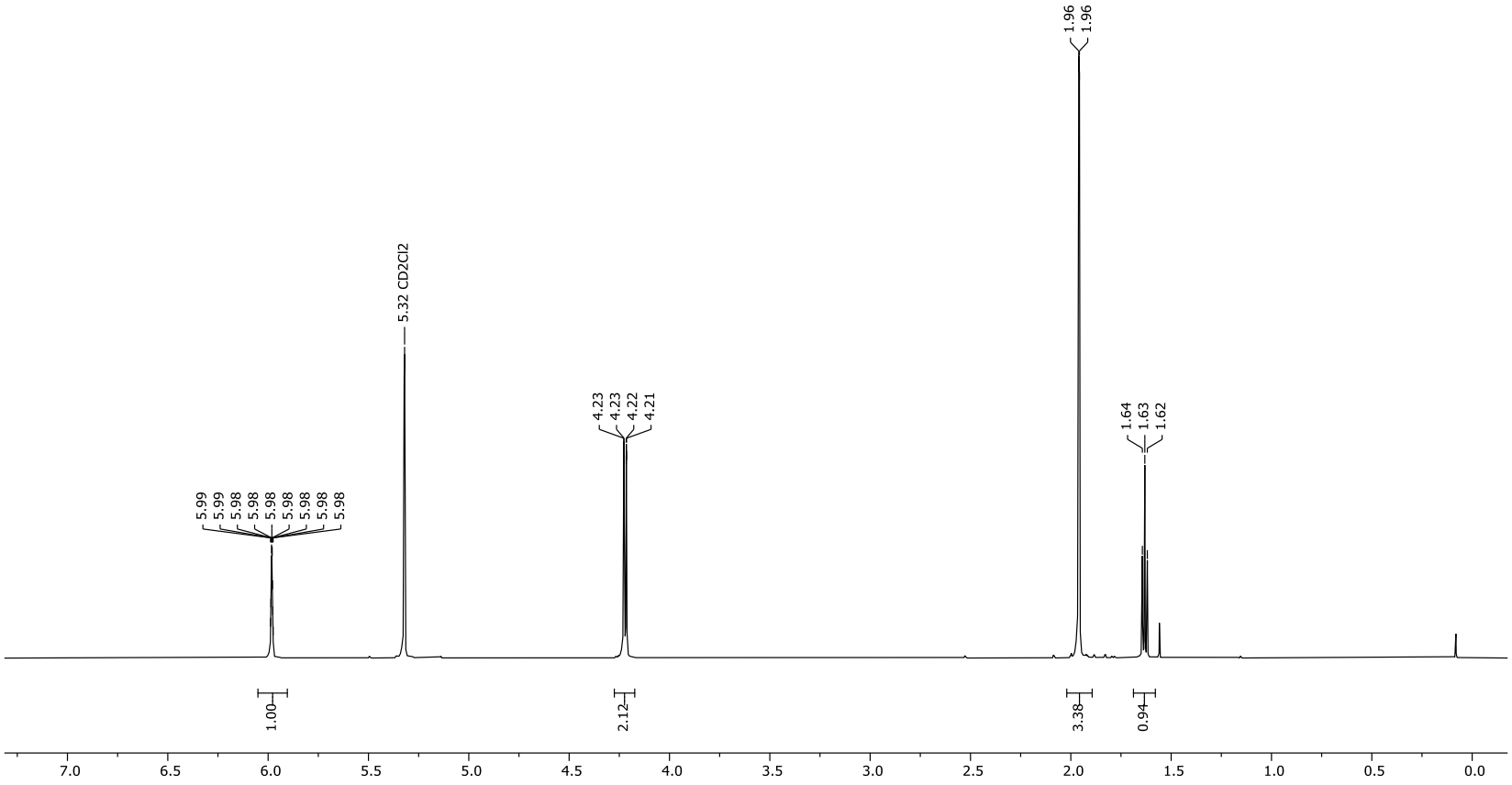

Appendix 119. ^{1}H-NMR spectrum of (*Z*)-3-Iodo-2-methylprop-2-en-ol (**229**).

Nucleus: 13C
Frequency: 125.52 MHz
Solvent: CD2Cl2
Temperature: 299.2 K

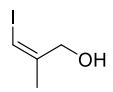

229

Appendix 120. ^{13}C-NMR spectrum of (*Z*)-3-Iodo-2-methylprop-2-en-ol (**229**).

Nucleus: 1H
Frequency: 499.13 MHz
Solvent: CDCl3
Temperature: 298.2 K

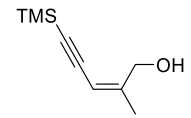

230

Appendix 121. ^{1}H-NMR spectrum of (*Z*)-2-methyl-5-(trimethylsilyl)pent-2-en-4-yn-1-ol (**230**).

Nucleus: 13C
Frequency: 125.52 MHz
Solvent: CDCl3
Temperature: 298.1 K

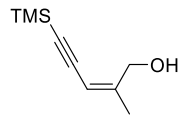

230

Appendix 122. ^{13}C-NMR spectrum of (*Z*)-2-methyl-5-(trimethylsilyl)pent-2-en-4-yn-1-ol (**230**).

Nucleus: 1H
Frequency: 499.13 MHz
Solvent: Acetone
Temperature: 297.9 K

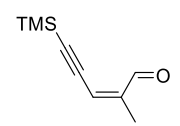

231

Appendix 123. ^{1}H-NMR spectrum of (2*Z*)-2-Methyl-5-(trimethylsilyl)pent-2-en-4-ynal (**231**).

Nucleus: 13C
Frequency: 125.52 MHz
Solvent: Acetone
Temperature: 298.0 K

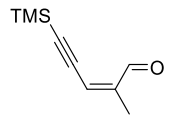

231

Appendix 124. ^{13}C-NMR spectrum of (2*Z*)-2-Methyl-5-(trimethylsilyl)pent-2-en-4-ynal (**231**).

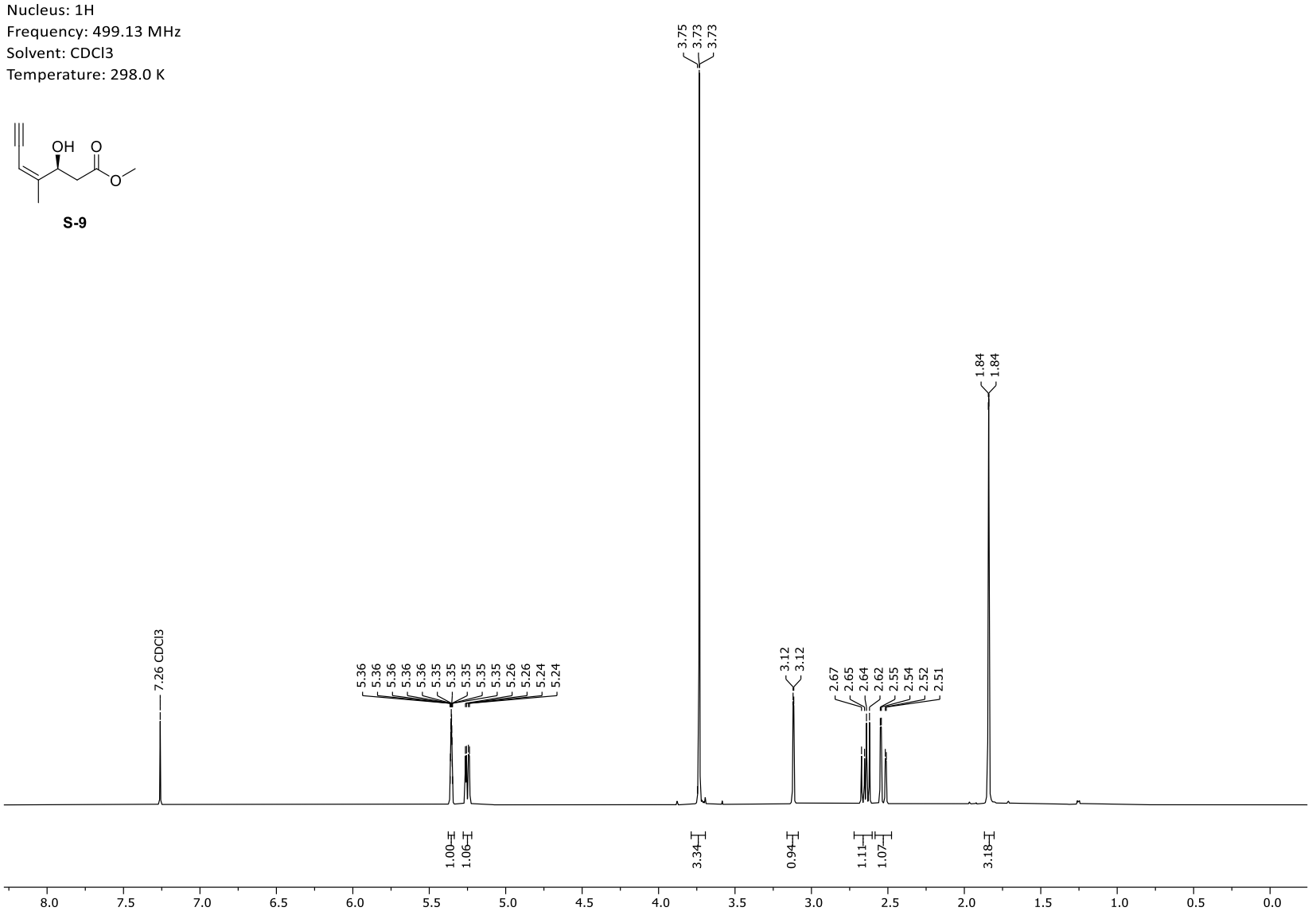

Appendix 125. ^{1}H-NMR spectrum of methyl (4*Z*,3*S*)-3-hydroxy-4-methyl-hept-4-en-6-ynoate (**S-9**).

Nucleus: 13C
Frequency: 125.52 MHz
Solvent: CDCl3
Temperature: 298.0 K

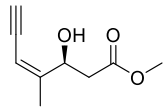

S-9

Appendix 126. ^{13}C-NMR spectrum of methyl (4*Z*,3*S*)-3-hydroxy-4-methyl-hept-4-en-6-ynoate (**S-9**).

Nucleus: 1H
Frequency: 499.13 MHz
Solvent: CDCl3
Temperature: 296.8 K

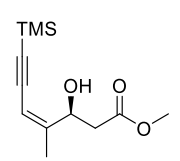

238

Appendix 127. ^{1}H-NMR spectrum of methyl (4*Z*,3*S*)-3-hydroxy-4-methyl-7-(trimethylsilyl)hept-4-en-6-ynoate (**238**).

Nucleus: 13C
Frequency: 125.52 MHz
Solvent: CDCl3
Temperature: 297.4 K

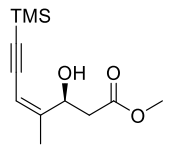

238

Appendix 128. ^{13}C-NMR spectrum of methyl (4*Z*,3*S*)-3-hydroxy-4-methyl-7-(trimethylsilyl)hept-4-en-6-ynoate (**238**).

Nucleus: 1H
Frequency: 700.41 MHz
Solvent: Acetone
Temperature: 298.0 K

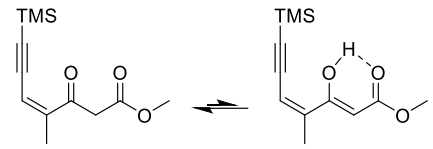

S-10

Appendix 129. ^{1}H-NMR spectrum of methyl (*Z*)-4-methyl-3-oxo-7-(trimethylsilyl)hept-4-en-6-ynoate (**S-10**) – major keto-tautomer picked.

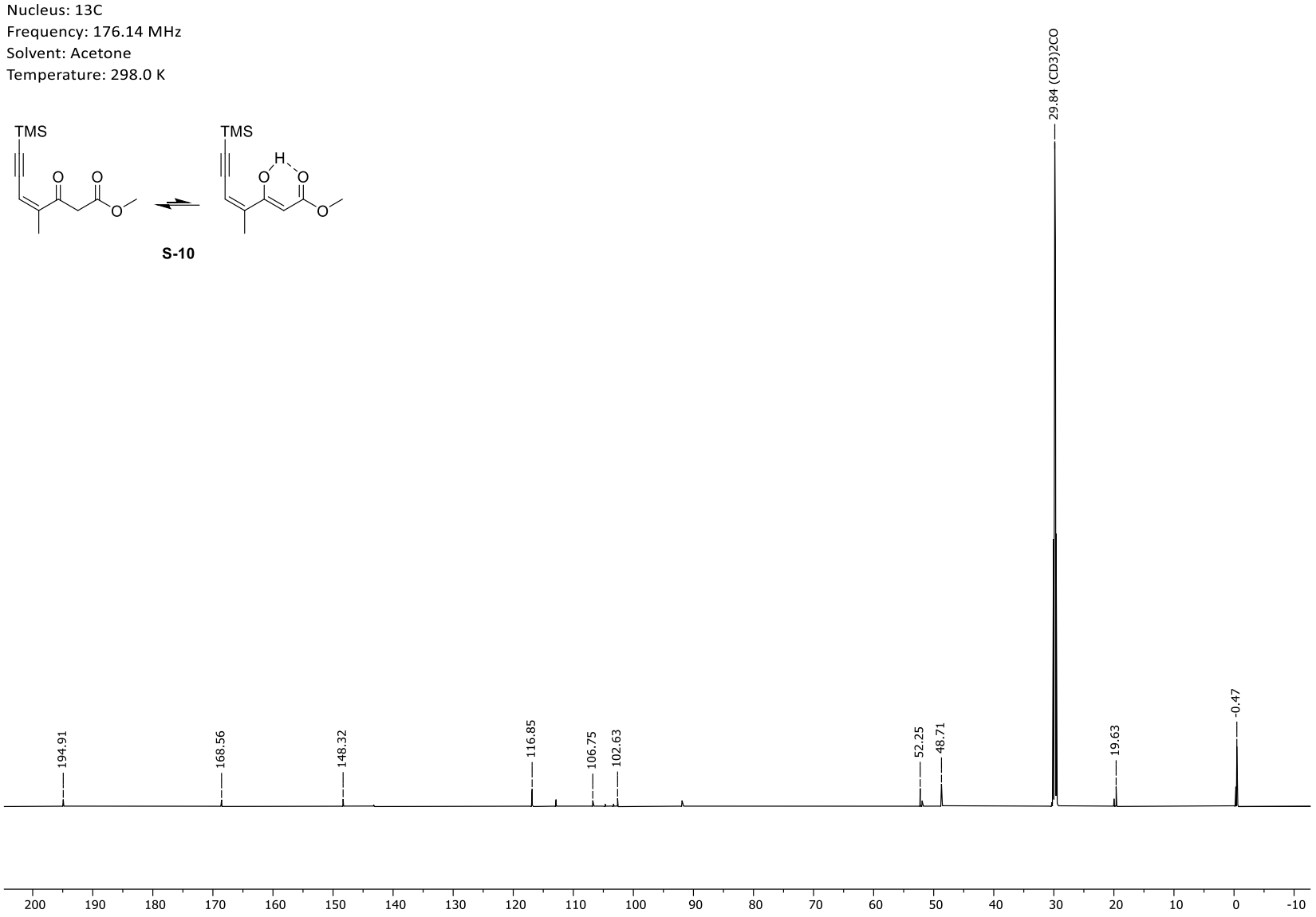

Appendix 130. ^{13}C-NMR spectrum of methyl (*Z*)-4-methyl-3-oxo-7-(trimethylsilyl)hept-4-en-6-ynoate (**S-10**) – major keto-tautomer picked.

Nucleus: 1H
Frequency: 700.41 MHz
Solvent: CDCl3
Temperature: 298.0 K

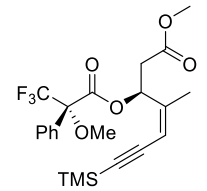

S-**238-M**

Appendix 131. ^{1}H-NMR: methyl (4*Z*,3*S*)-4-methyl-3-((2*S*)-3,3,3-trifluoro-2-methoxy-2-phenylpropanoyl)oxy-7-trimethylsilylhept-4-en-6-ynoate **(*S*)-238-M**

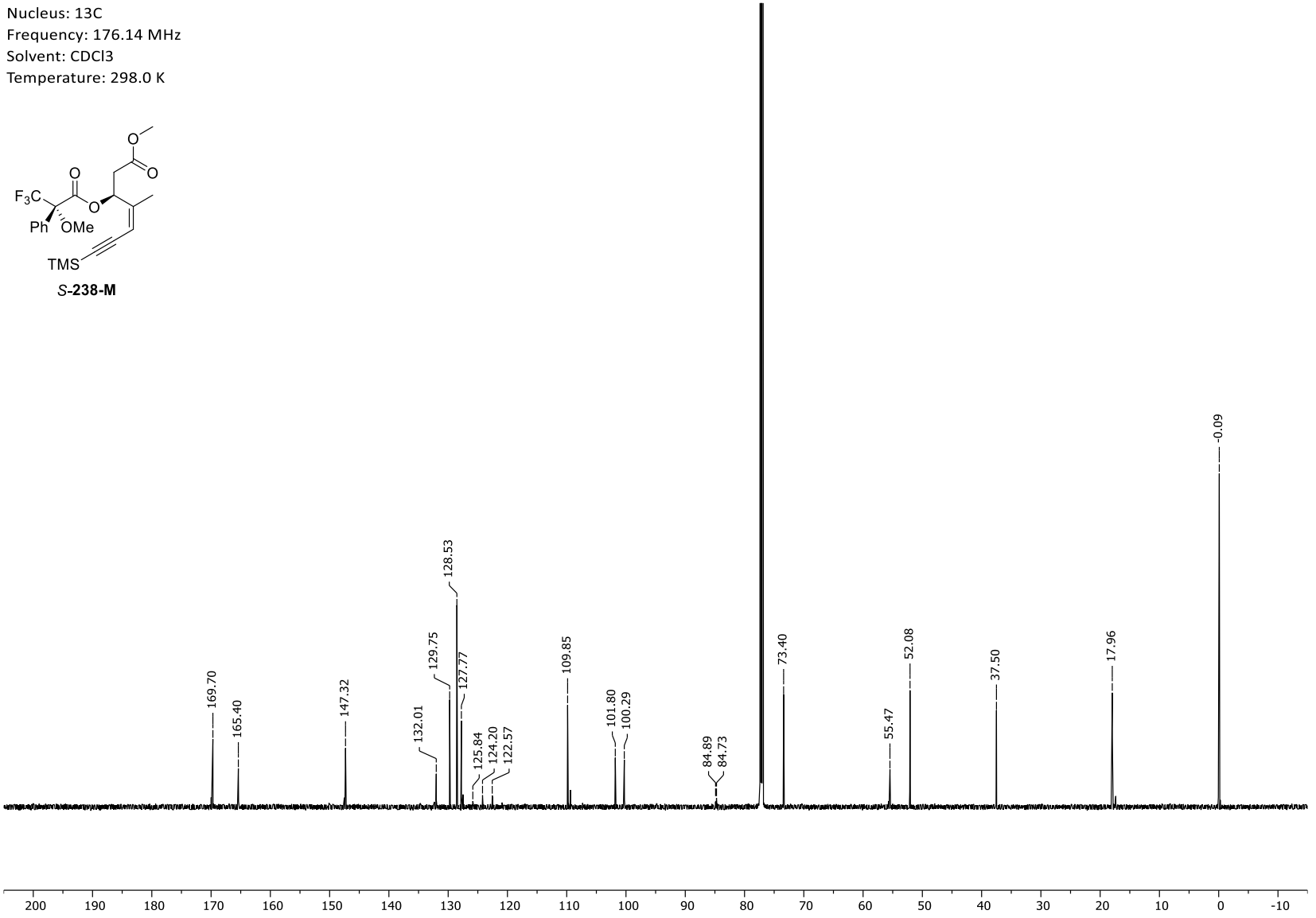

Appendix 132. ^{13}C-NMR: methyl (4*Z*,3*S*)-4-methyl-3-((2*S*)-3,3,3-trifluoro-2-methoxy-2-phenylpropanoyl)oxy-7-trimethylsilylhept-4-en-6-ynoate **(*S*)-238-M**

Nucleus: 1H
Frequency: 700.41 MHz
Solvent: CDCl3
Temperature: 298.0 K

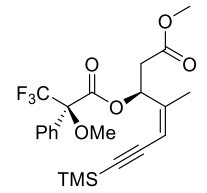

R-238-M

Appendix 133. ^{1}H-NMR: methyl (4*Z*,3*S*)-4-methyl-3-((2*R*)-3,3,3-trifluoro-2-methoxy-2-phenylpropanoyl)oxy-7-trimethylsilylhept-4-en-6-ynoate **(*R*)-238-M**

Nucleus: 13C
Frequency: 176.14 MHz
Solvent: CDCl3
Temperature: 298.0 K

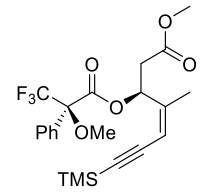

R-238-M

Appendix 134. ^{13}C-NMR: methyl (4*Z*,3*S*)-4-methyl-3-((2*R*)-3,3,3-trifluoro-2-methoxy-2-phenylpropanoyl)oxy-7-trimethylsilylhept-4-en-6-ynoate **(*R*)-238-M**

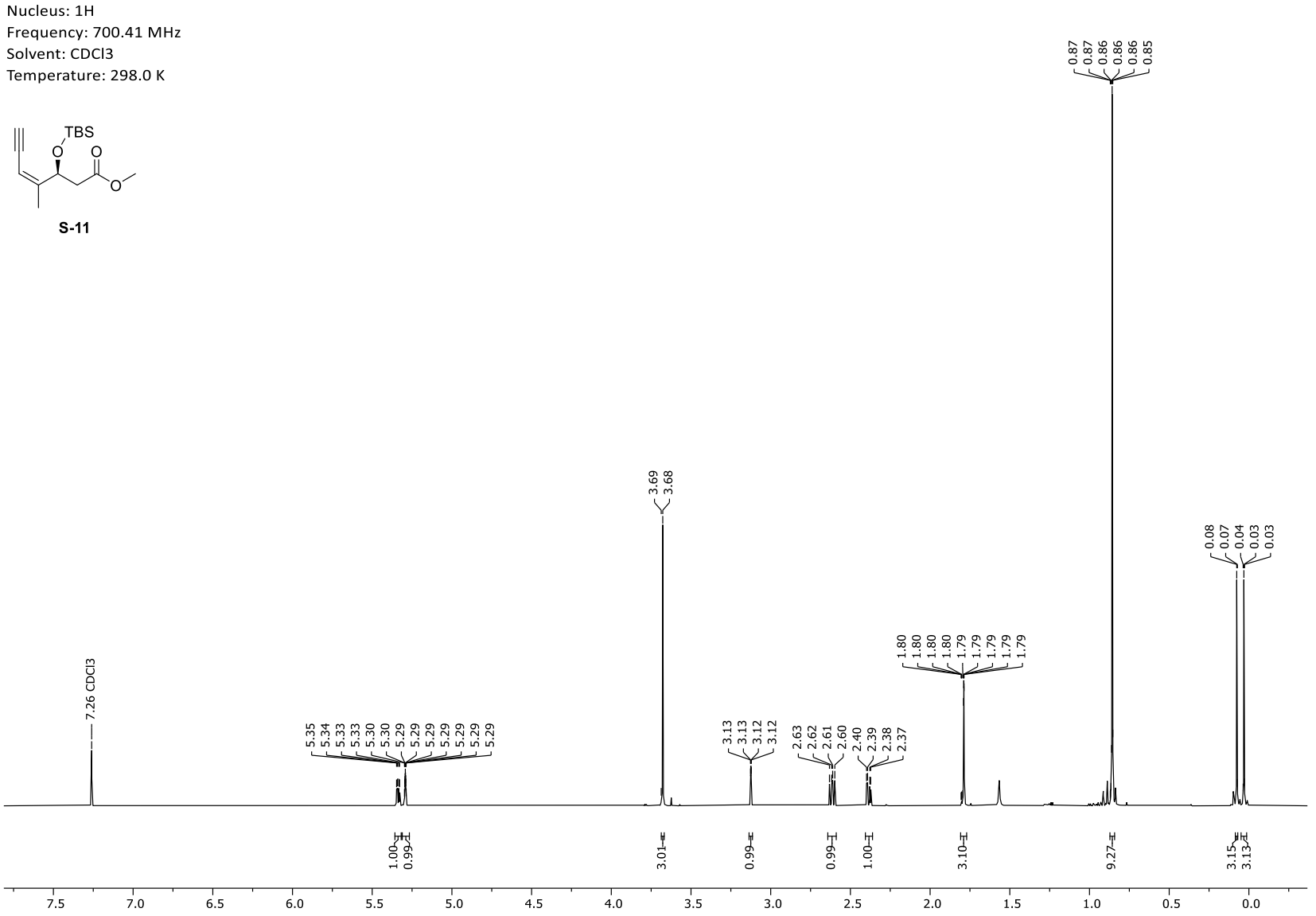

Appendix 135. ^{1}H-NMR spectrum of methyl (4*Z*,3*S*)-3-((*tert*-butyldimethylsilyl)oxy)-4-methyl-hept-4-en-6-ynoate (**S-11**).

Nucleus: 13C
Frequency: 176.14 MHz
Solvent: CDCl3
Temperature: 298.0 K

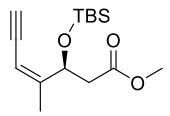

S-11

Appendix 136. ^{13}C-NMR spectrum of methyl (4*Z*,3*S*)-3-((*tert*-butyldimethylsilyl)oxy)-4-methyl-hept-4-en-6-ynoate (**S-11**).

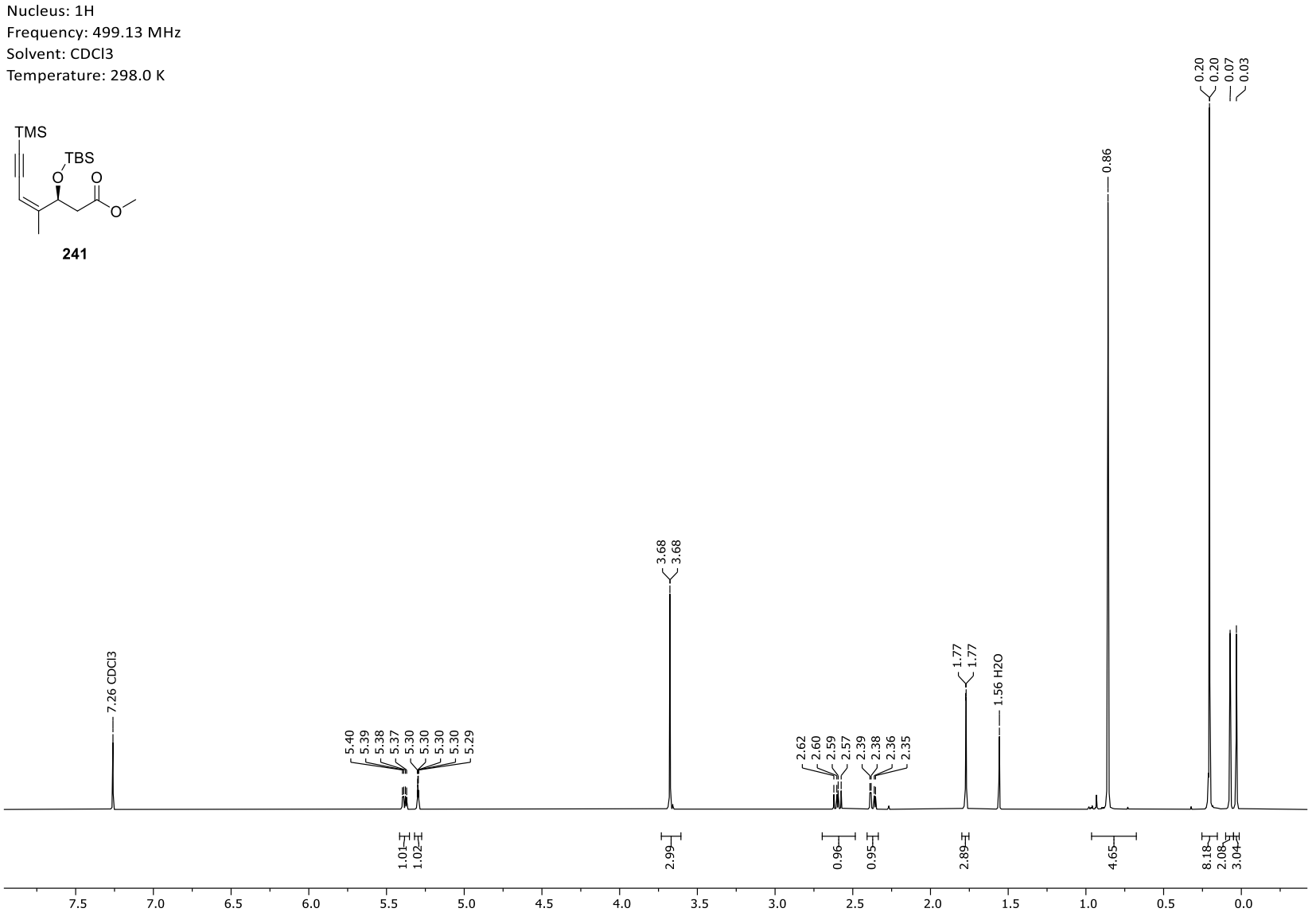

Appendix 137. ^{1}H-NMR spectrum of methyl (4*Z*,3*S*)-3-((*tert*-butyldimethylsilyl)oxy)-4-methyl-7-(trimethylsilyl)-hept-4-en-6-ynoate (**241**).

Nucleus: 13C
Frequency: 125.52 MHz
Solvent: CDCl3
Temperature: 298.2 K

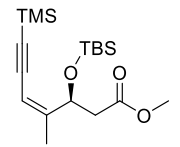

241

Appendix 138. ^{13}C-NMR spectrum of methyl (4*Z*,3*S*)-3-((*tert*-butyldimethylsilyl)oxy)-4-methyl-7-(trimethylsilyl)-hept-4-en-6-ynoate (**241**).

Nucleus: 1H
Frequency: 700.41 MHz
Solvent: CDCl3
Temperature: 298.0 K

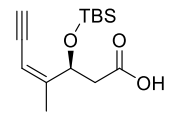

129

Appendix 139. ^{1}H-NMR spectrum of (*S*,*Z*)-3-((*tert*-butyldimethylsilyl)oxy)-4-methylhept-4-en-6-ynoic acid (**129**).

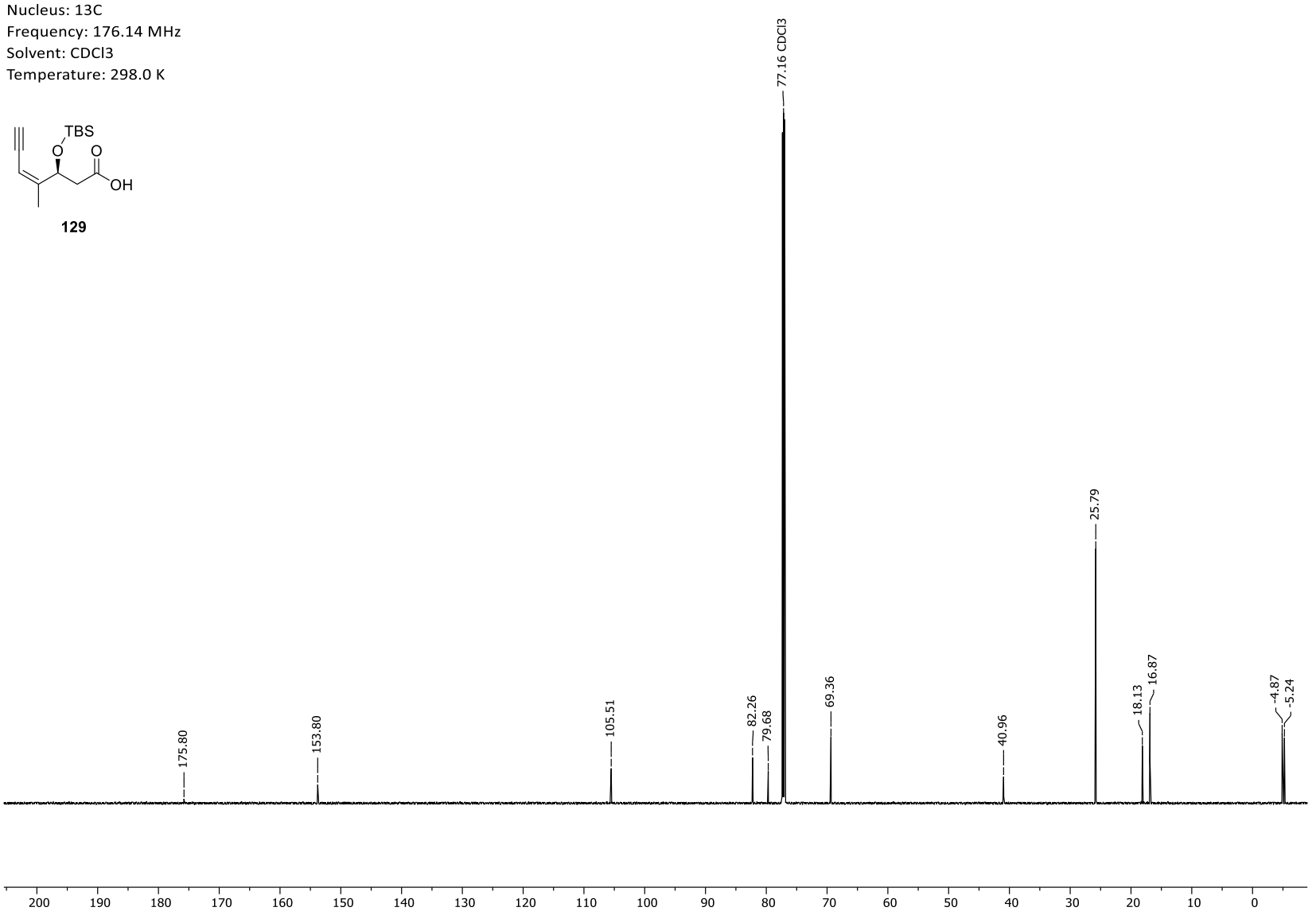

Appendix 140. ^{13}C-NMR spectrum of (*S*,*Z*)-3-((*tert*-Butyldimethylsilyl)oxy)-4-methylhept-4-en-6-ynoic acid (**129**).

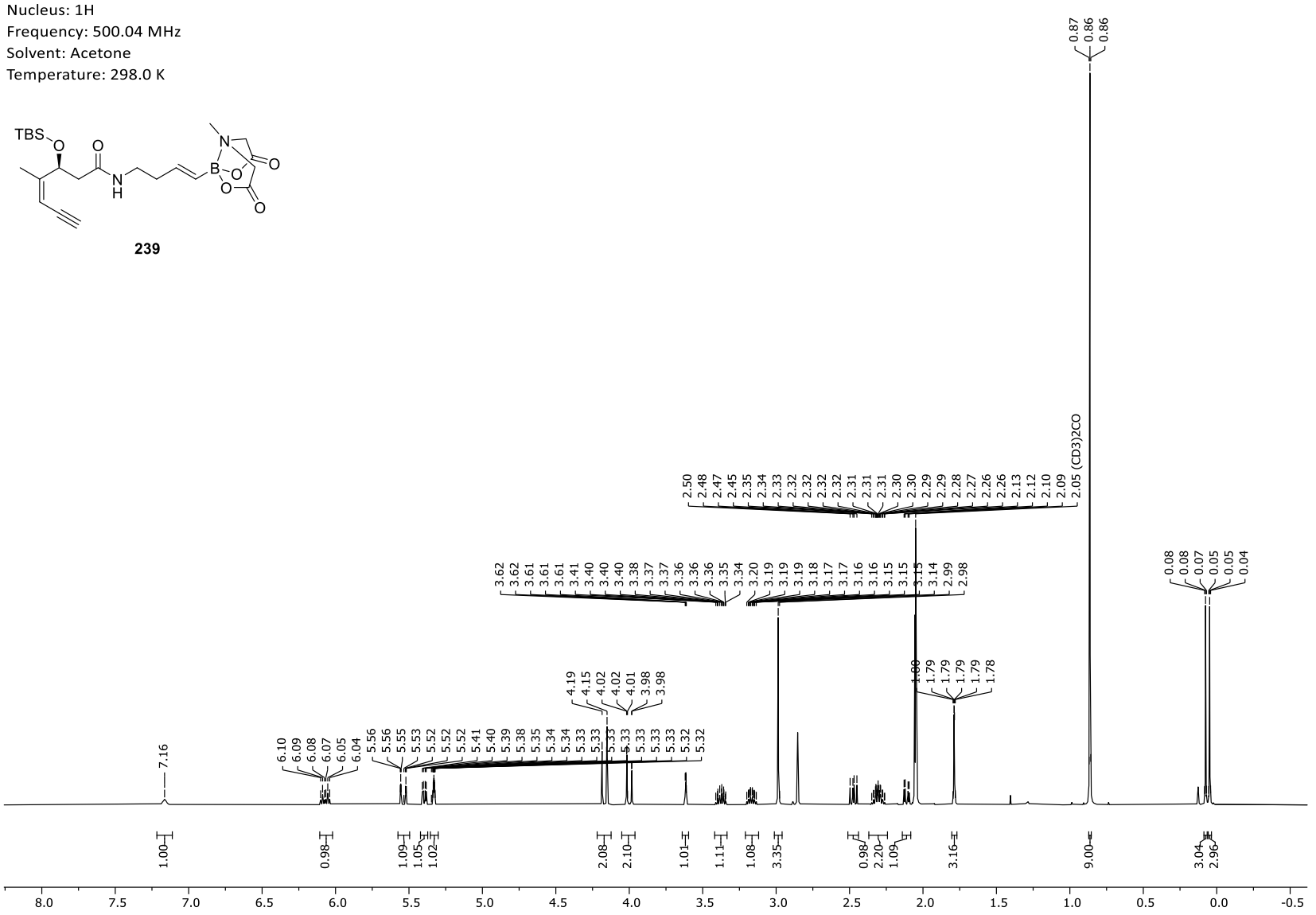

Appendix 141. ^{1}H-NMR: (*S*,4*Z*)-3-((*tert*-butyldimethylsilyl)oxy)-4-methyl-*N*-((*E*)-4-(1,3,6,2-dioxazaborocane-4,8-dione-2-yl)but-3-en-1-yl)hepta-4-en-6-ynamide (**239**).

Nucleus: 13C
Frequency: 125.75 MHz
Solvent: Acetone
Temperature: 298.0 K

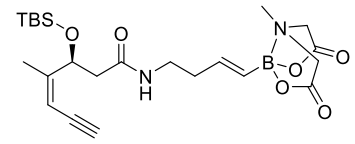

239

Appendix 142. ^{13}C-NMR: (*S*,4*Z*)-3-((*tert*-butyldimethylsilyl)oxy)-4-methyl-*N*-((*E*)-4-(1,3,6,2-dioxazaborocane-4,8-dione-2-yl)but-3-en-1-yl)hepta-4-en-6-ynamide (**239**).

Nucleus: 1H
Frequency: 500.04 MHz
Solvent: Acetone
Temperature: 298.0 K

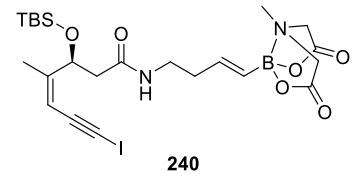

240

Appendix 143. ^{1}H-NMR: (*S*,4*Z*)-3-((*tert*-butyldimethylsilyl)oxy)-7-iodo-4-methyl-*N*-((*E*)-4-(1,3,6,2-dioxazaborocane-4,8-dione-2-yl)but-3-en-1-yl)hepta-4-en-6-ynamide (**240**).

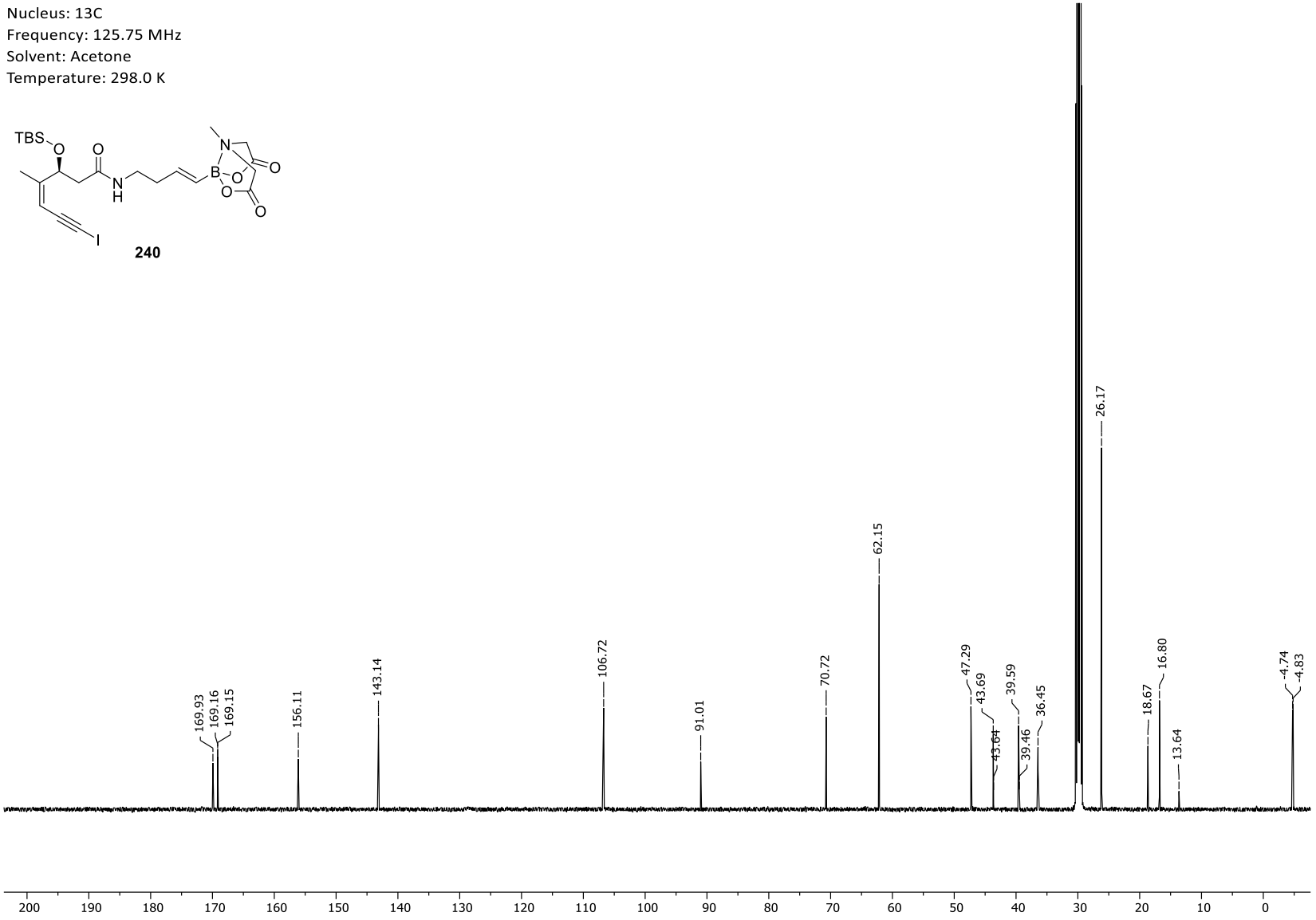

Appendix 144. ^{13}C-NMR: (*S*,4*Z*)-3-((*tert*-butyldimethylsilyl)oxy)-7-iodo-4-methyl-*N*-((*E*)-4-(1,3,6,2-dioxazaborocane-4,8-dione-2-yl)but-3-en-1-yl)hepta-4-en-6-ynamide (**240**).

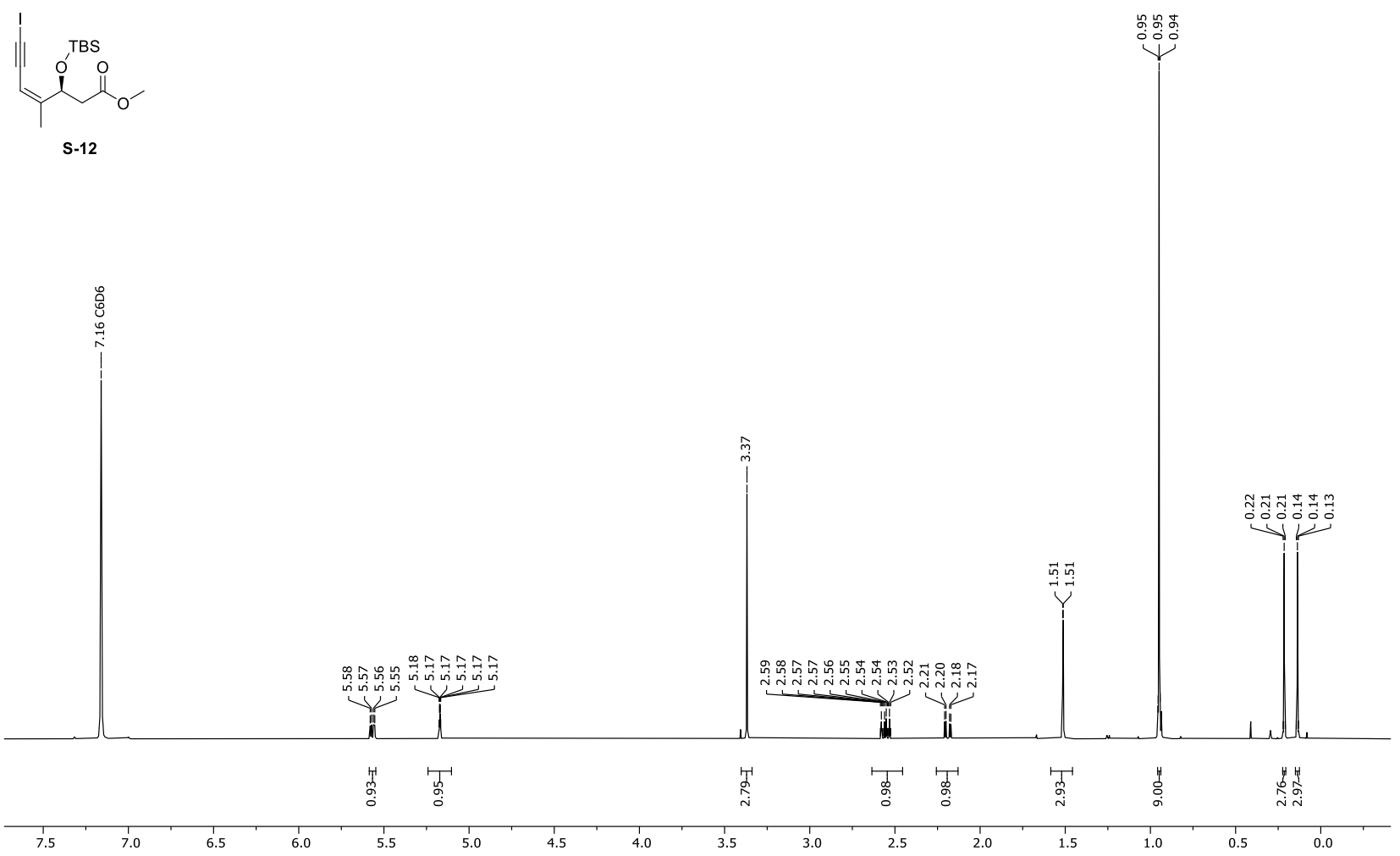

Appendix 145. ^{1}H-NMR spectrum of methyl (*S*,*Z*)-3-((*tert*-butyldimethylsilyl)oxy)-7-iodo-4-methylhept-4-en-6-ynoate (**S-12**).

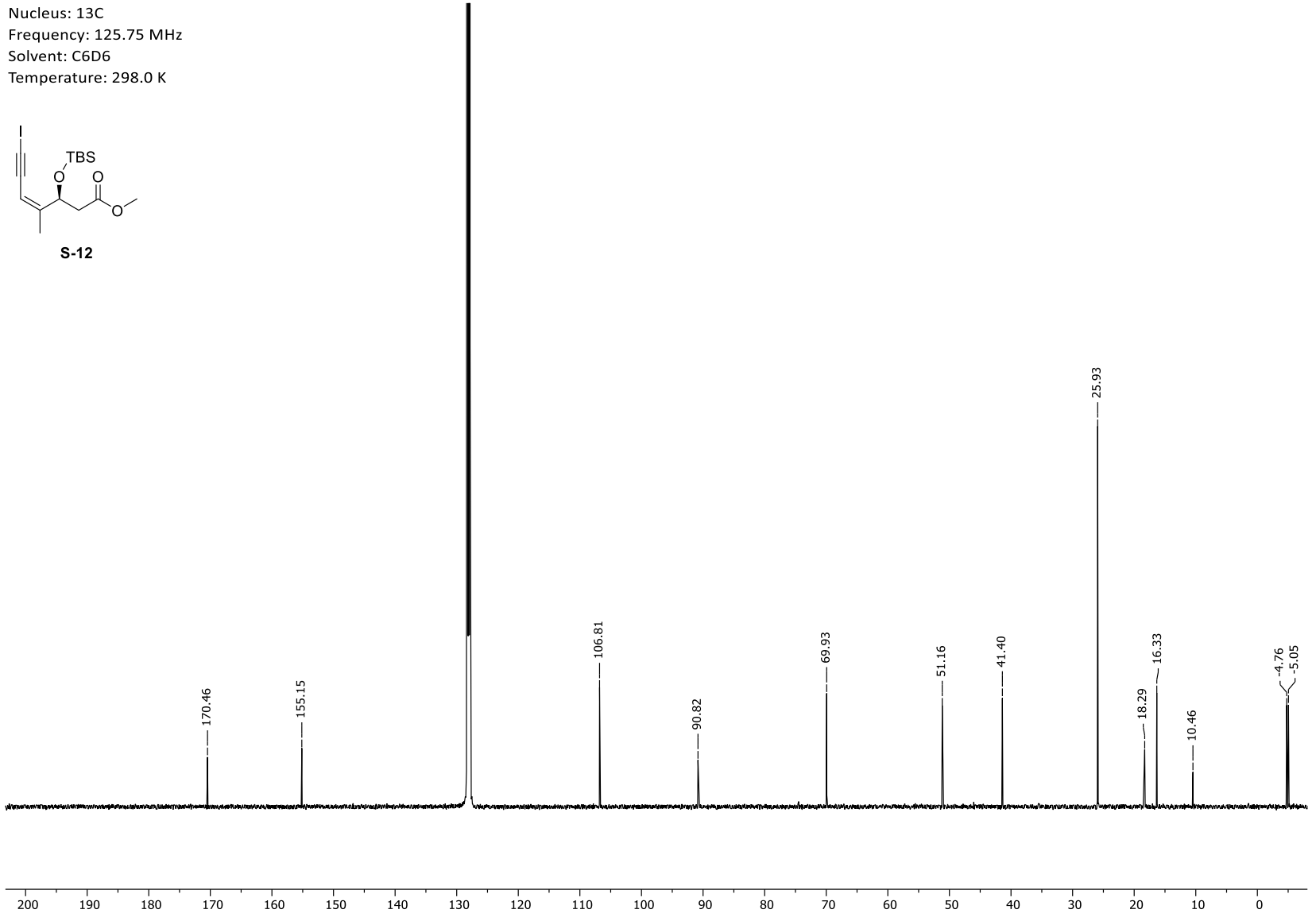

Appendix 146. ^{13}C-NMR spectrum of methyl (*S*,*Z*)-3-((*tert*-butyldimethylsilyl)oxy)-7-iodo-4-methylhept-4-en-6-ynoate (**S-12**).

Nucleus: 1H
Frequency: 700.41 MHz
Solvent: Acetone
Temperature: 298.0 K

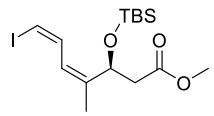

245

Appendix 147. ^{1}H-NMR spectrum of methyl (4*Z*,6*Z*,3*S*)-3-((*tert*-butyldimethylsilyl)oxy)-7-iodo-4-methyl-hept-4,6-dienoate (**245**).

Nucleus: 13C
Frequency: 176.14 MHz
Solvent: Acetone
Temperature: 298.0 K

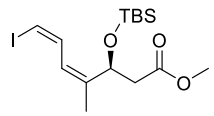

245

Appendix 148. ^{13}C-NMR spectrum of methyl (4*Z*,6*Z*,3*S*)-3-((*tert*-butyldimethylsilyl)oxy)-7-iodo-4-methyl-hept-4,6-dienoate (**245**).

Nucleus: 1H
Frequency: 500.04 MHz
Solvent: Acetone
Temperature: 298.0 K

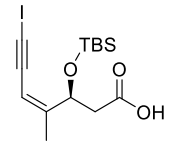

243

Appendix 149. ^{1}H-NMR spectrum of (*S*,*Z*)-3-((*tert*-butyldimethylsilyl)oxy)-7-iodo-4-methylhept-4-en-6-ynoic acid (**243**).

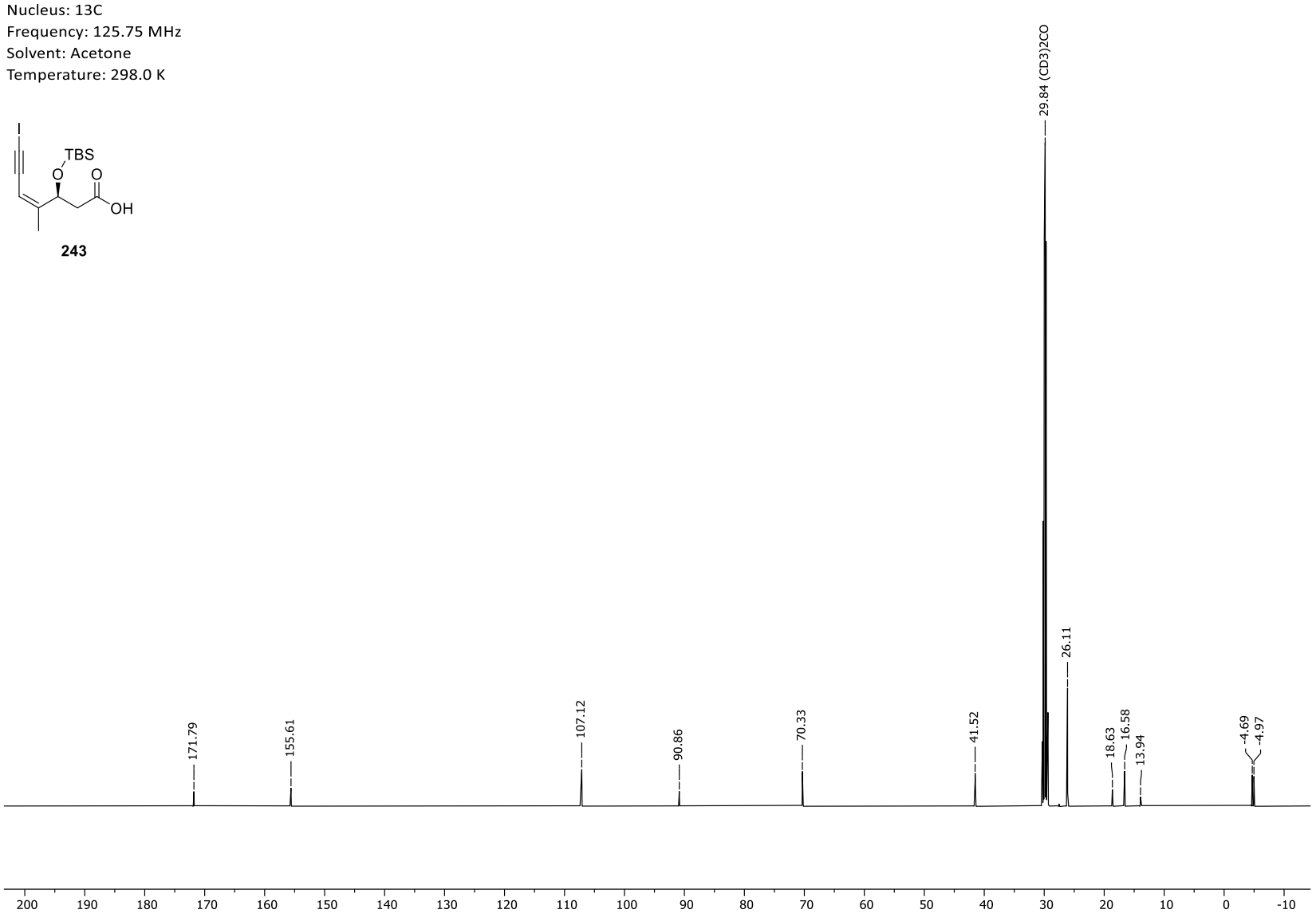

Appendix 150. ^{13}C-NMR spectrum of (*S*,*Z*)-3-((*tert*-butyldimethylsilyl)oxy)-7-iodo-4-methylhept-4-en-6-ynoic acid (**243**).

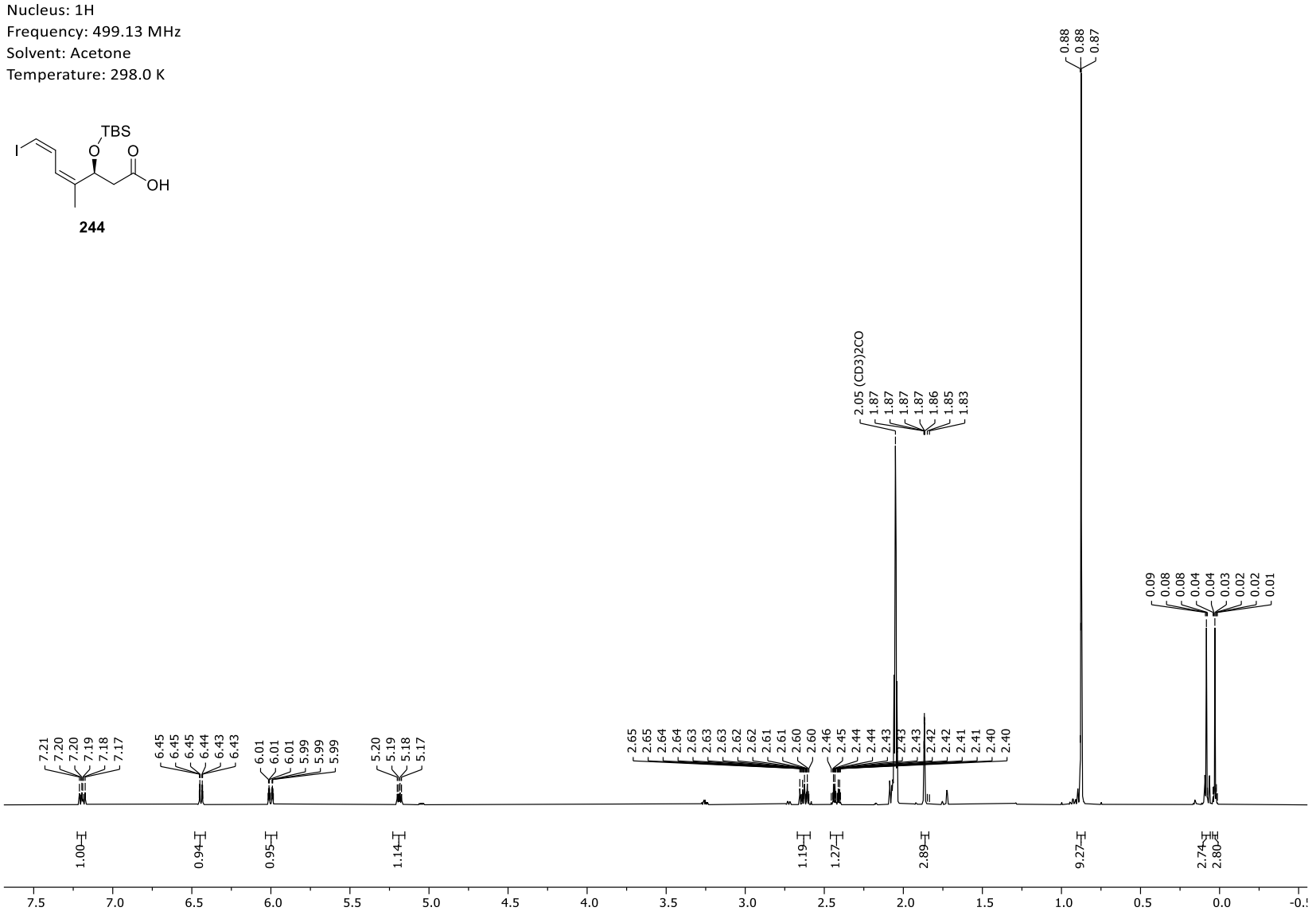

Appendix 151. ^{1}H-NMR spectrum of (4*Z*,6*Z*,3*S*)-3-((*tert*-butyldimethylsilyl)oxy)-7-iodo-4-methyl-hept-4,6-dienoic acid (**244**).

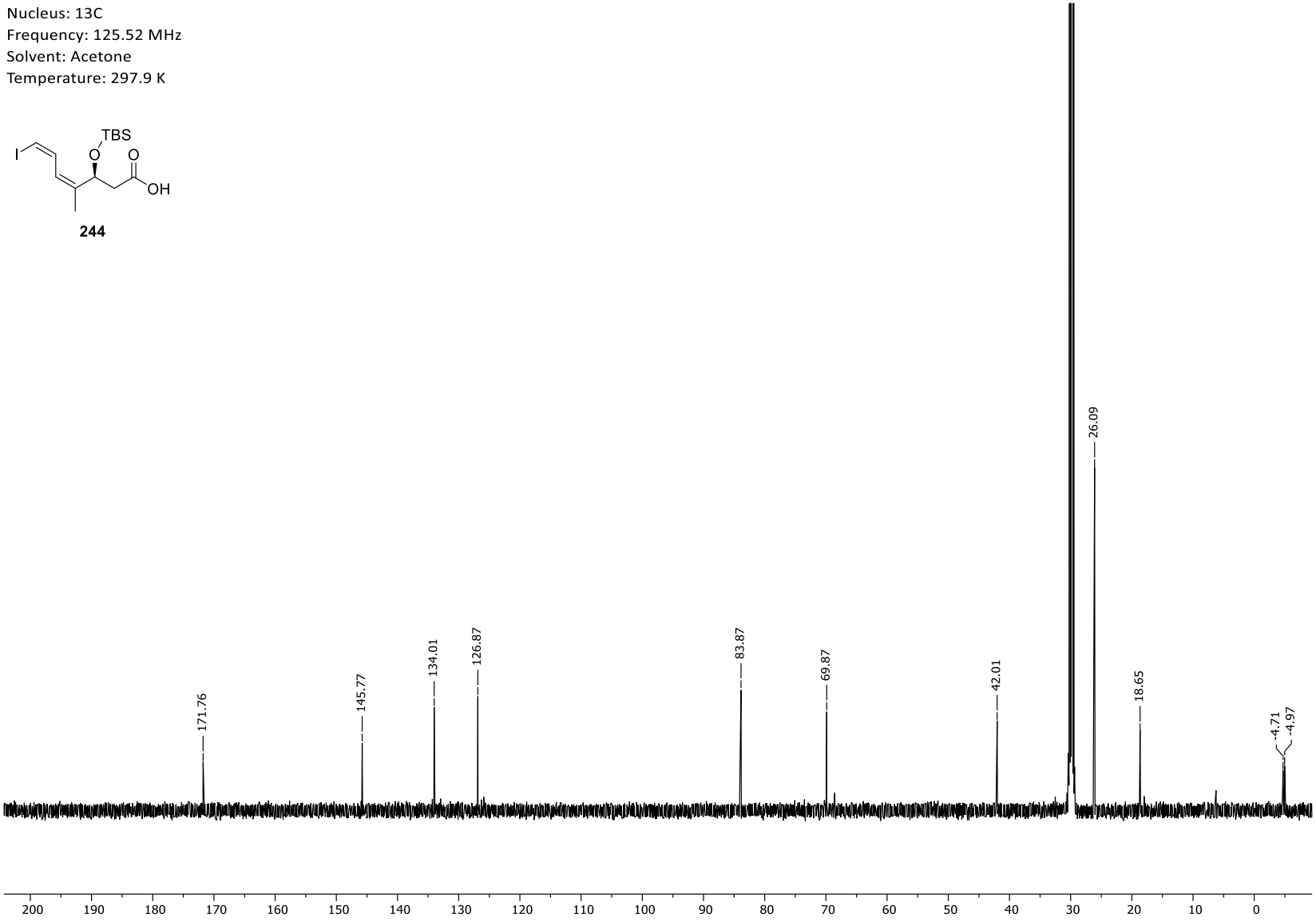

Appendix 152. ^{13}C-NMR spectrum of (4*Z*,6*Z*,3*S*)-3-((*tert*-butyldimethylsilyl)oxy)-7-iodo-4-methyl-hept-4,6-dienoic acid (**244**).

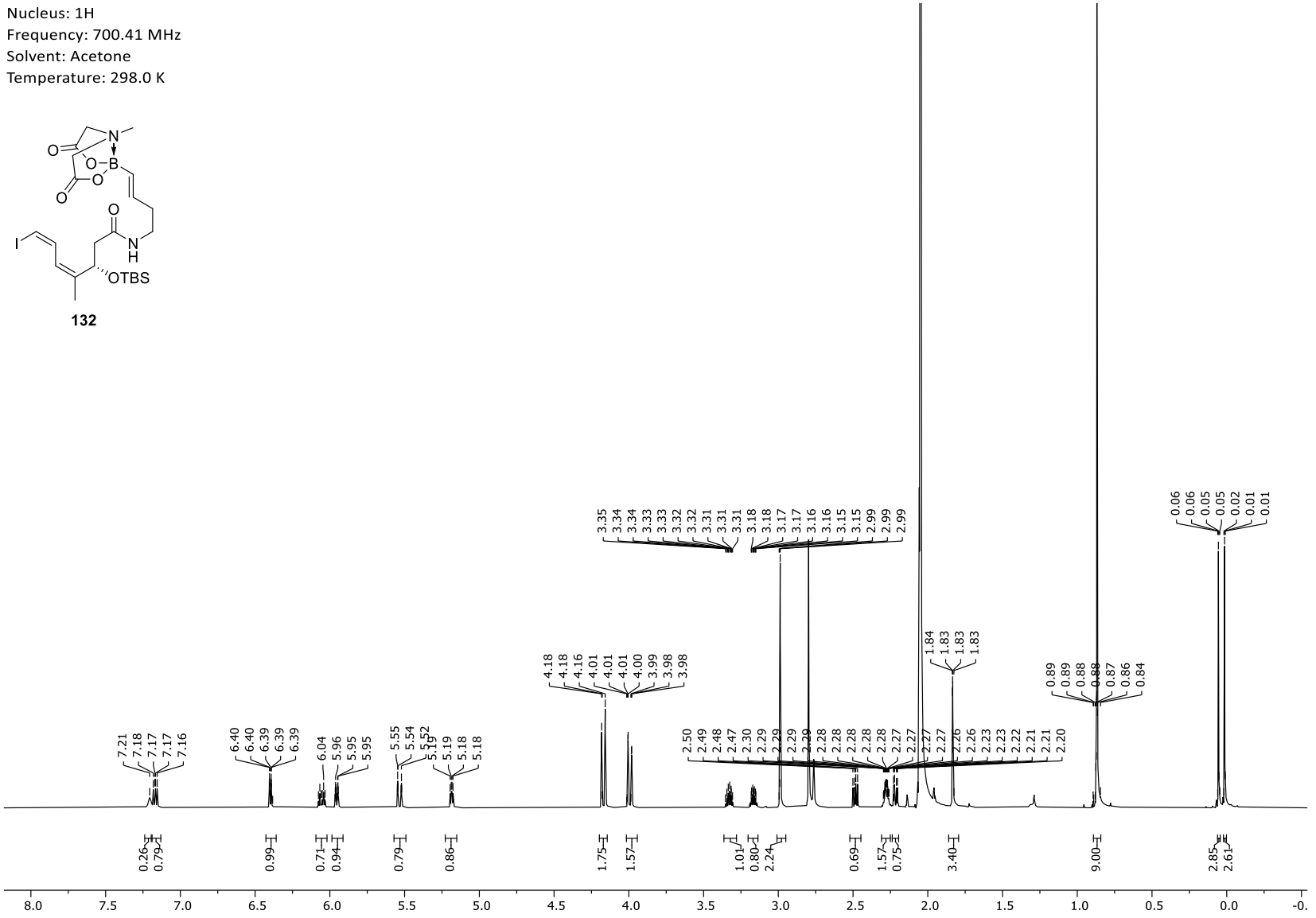

Appendix 153. ^{1}H-NMR: (*S*,4*Z*,6*Z*)-3-((*tert*-butyldimethylsilyl)oxy)-7-iodo-4-methyl-*N*-((*E*)-4-(1,3,6,2-dioxazaborocane-4,8-dione-2-yl)but-3-en-1-yl)hepta-4,6-dienamide (**132**).

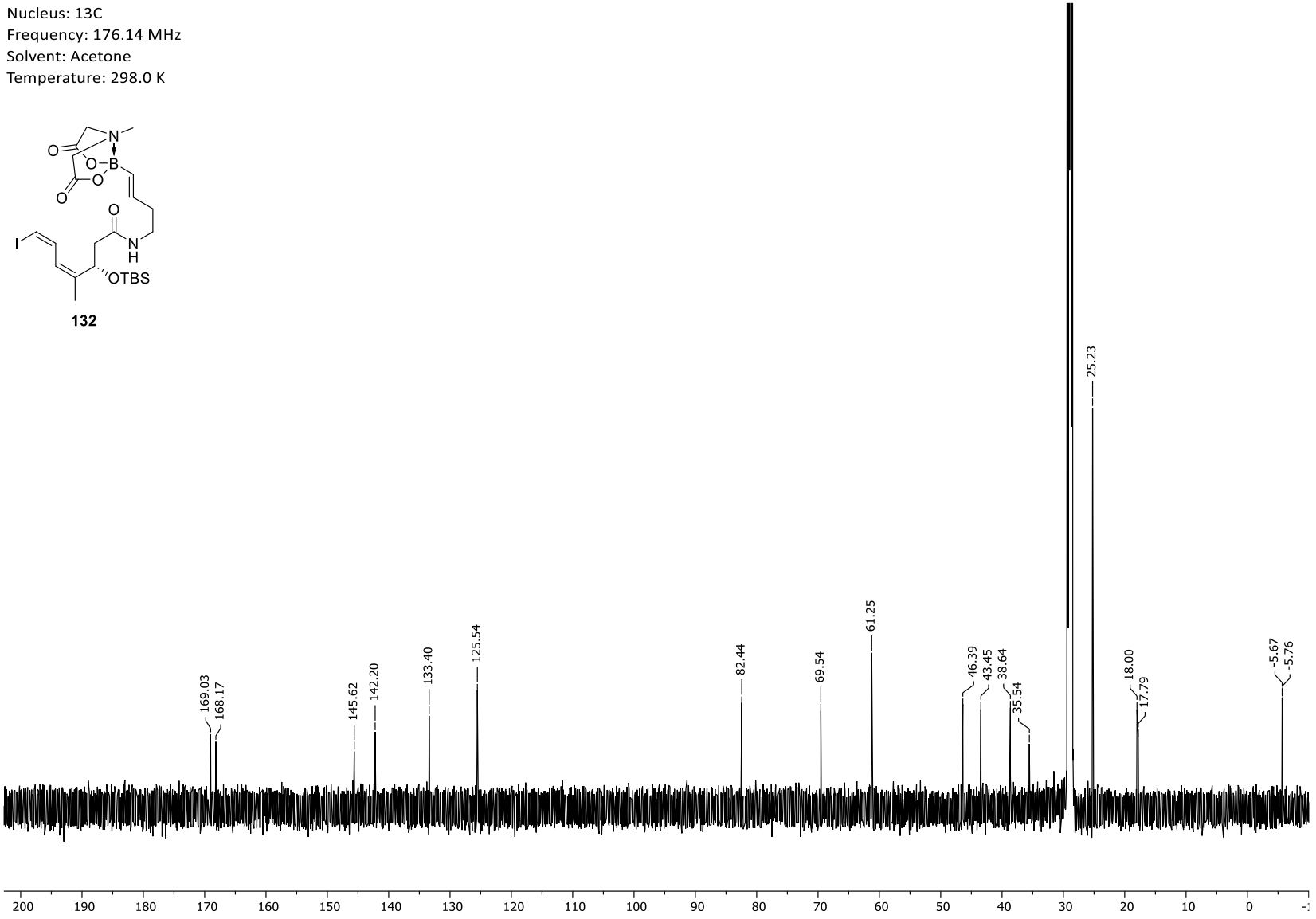

Appendix 154. ^{13}C-NMR: (*S*,4*Z*,6*Z*)-3-((*tert*-butyldimethylsilyl)oxy)-7-iodo-4-methyl-*N*-((*E*)-4-(1,3,6,2-dioxazaborocane-4,8-dione-2-yl)but-3-en-1-yl)hepta-4,6-dienamide (**132**).

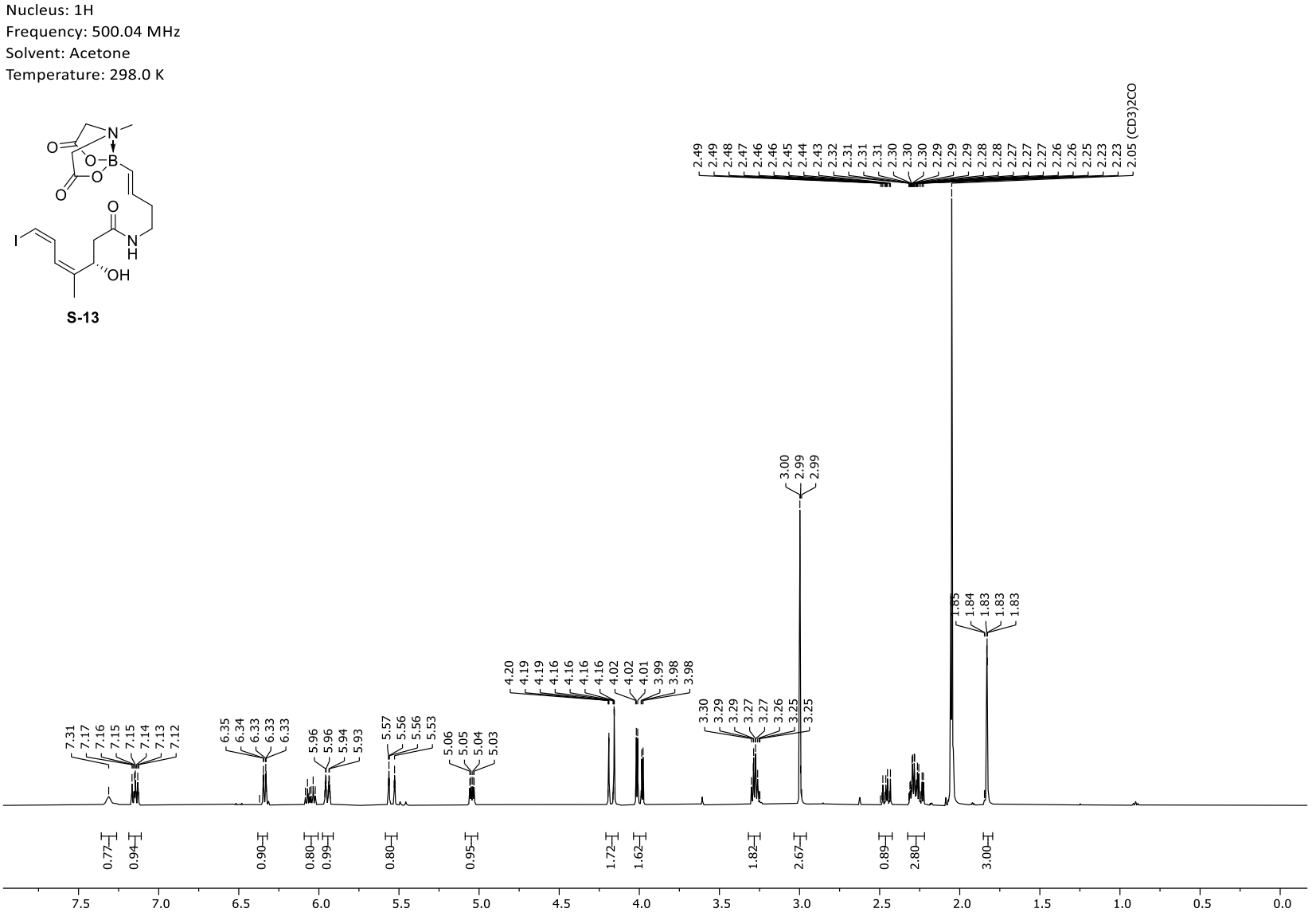

Appendix 155. ^{1}H-NMR: (*S*,4*Z*,6*Z*)-3-hydroxy-7-iodo-4-methyl-*N*-((*E*)-4-(1,3,6,2-dioxazaborocane-4,8-dione-2-yl)but-3-en-1-yl)hepta-4,6-dienamide (**S-13**).

Nucleus: 13C
Frequency: 125.75 MHz
Solvent: Acetone
Temperature: 298.0 K

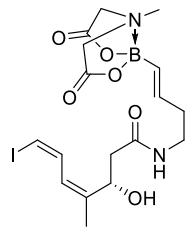

S-13

Appendix 156. ^{13}C-NMR: (*S*,4*Z*,6*Z*)-3-hydroxy-7-iodo-4-methyl-*N*-((*E*)-4-(1,3,6,2-dioxazaborocane-4,8-dione-2-yl)but-3-en-1-yl)hepta-4,6-dienamide (**S-13**).

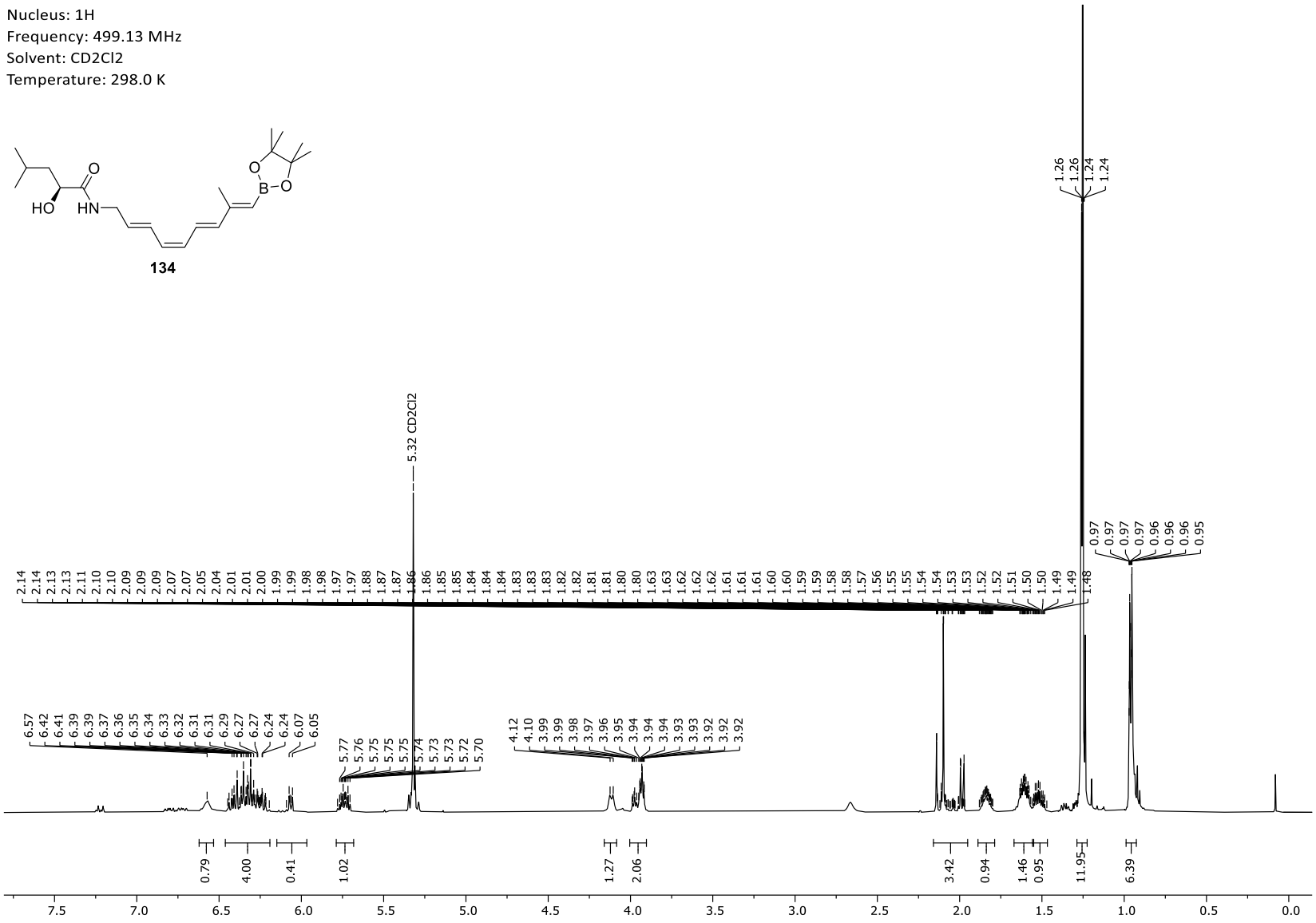

Appendix 157. ^{1}H-NMR spectrum of tetraene II (**134**).

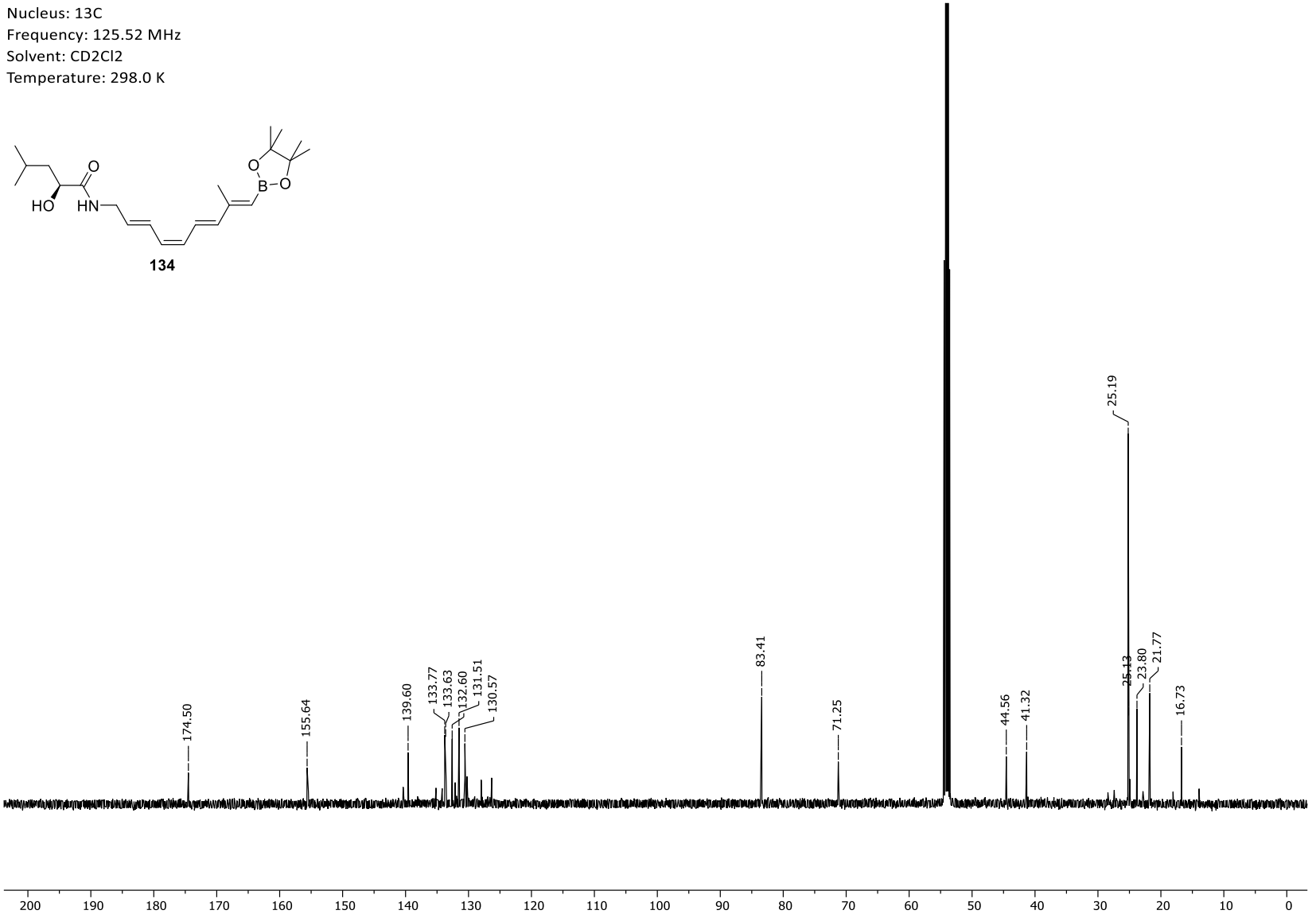

Appendix 158. ^{13}C-NMR spectrum of tetraene II (**134**).

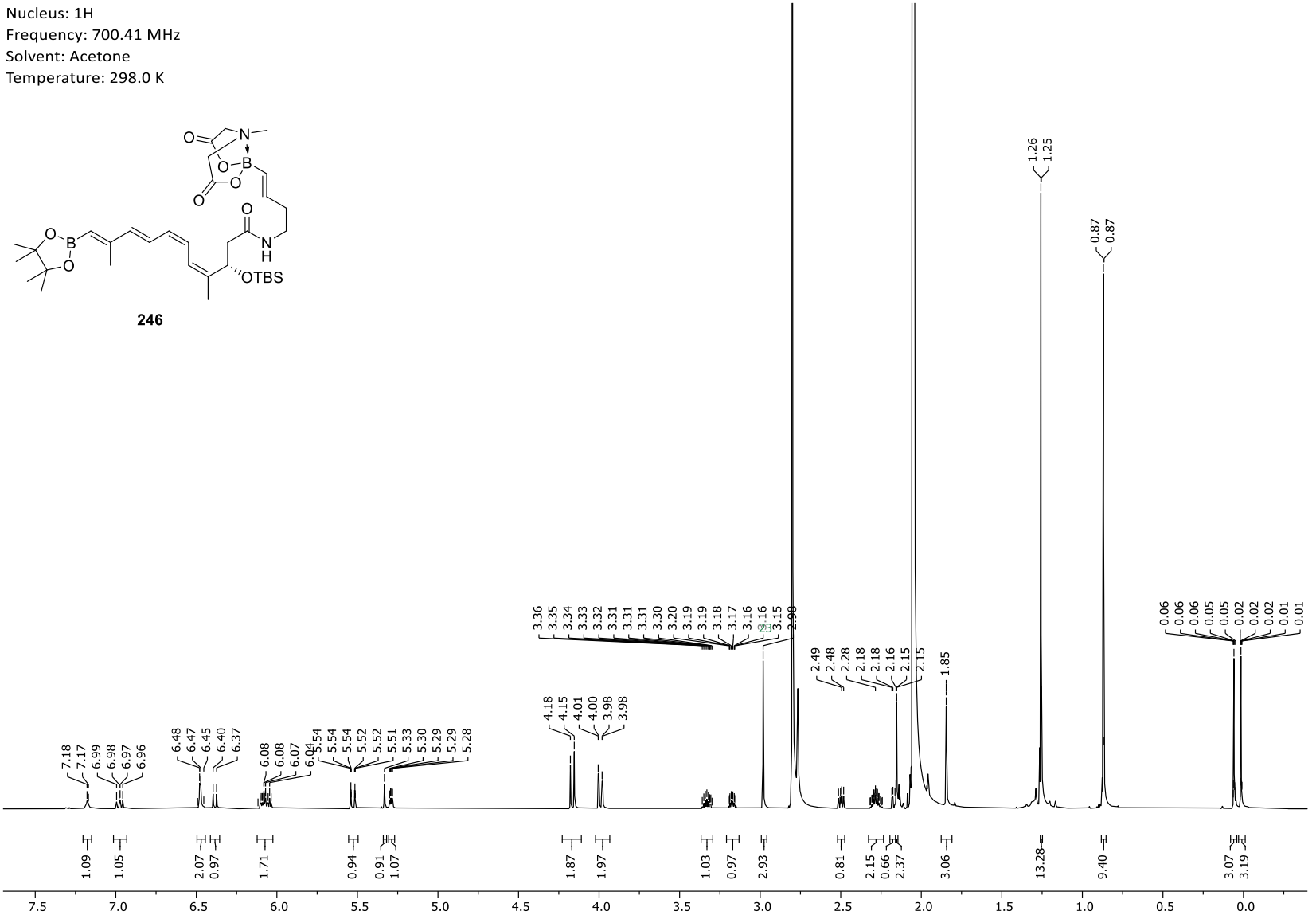

Appendix 159. ^{1}H-NMR spectrum of tetraene III (**246**).

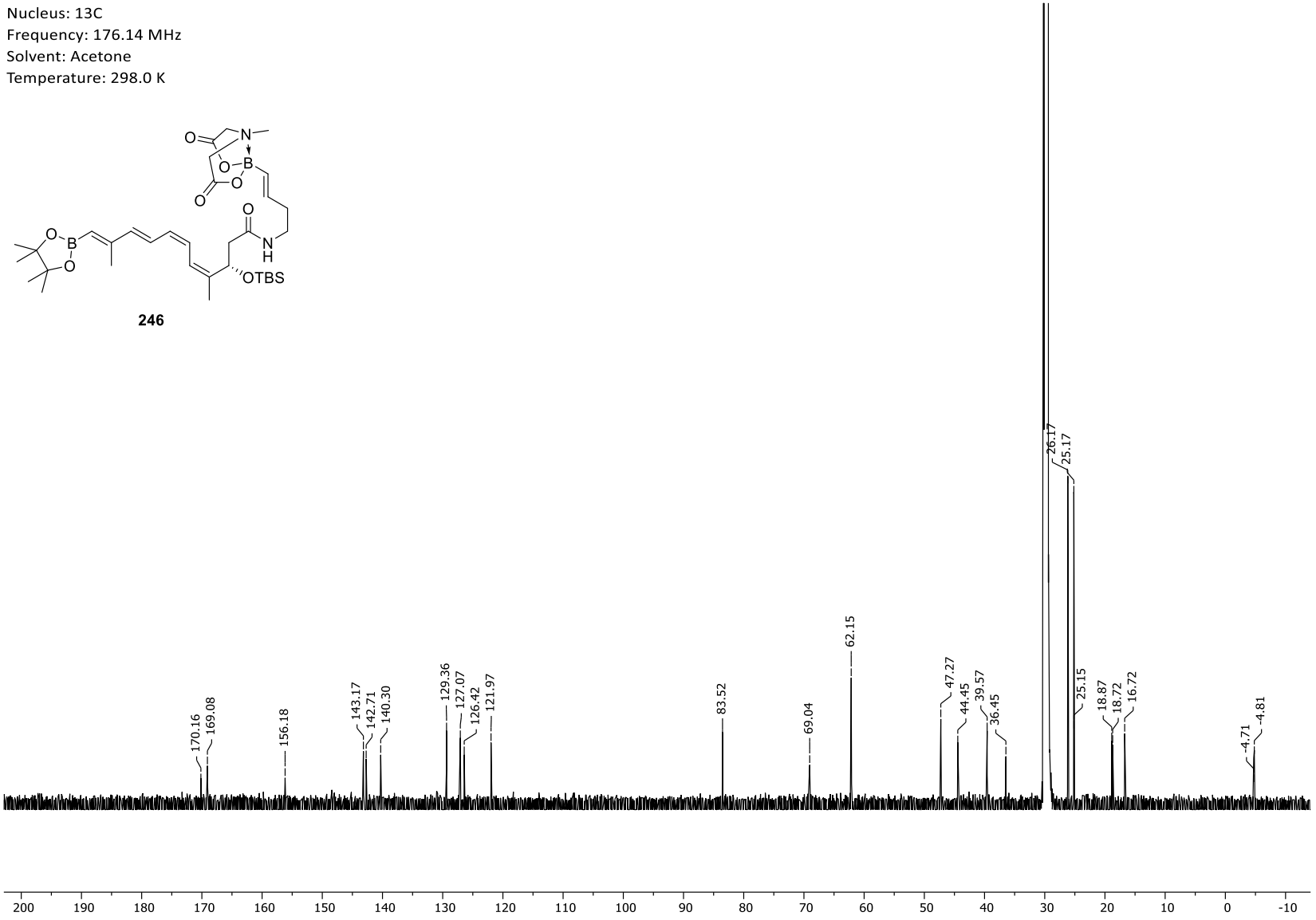

Appendix 160. ^{13}C-NMR spectrum of tetraene III (**246**).

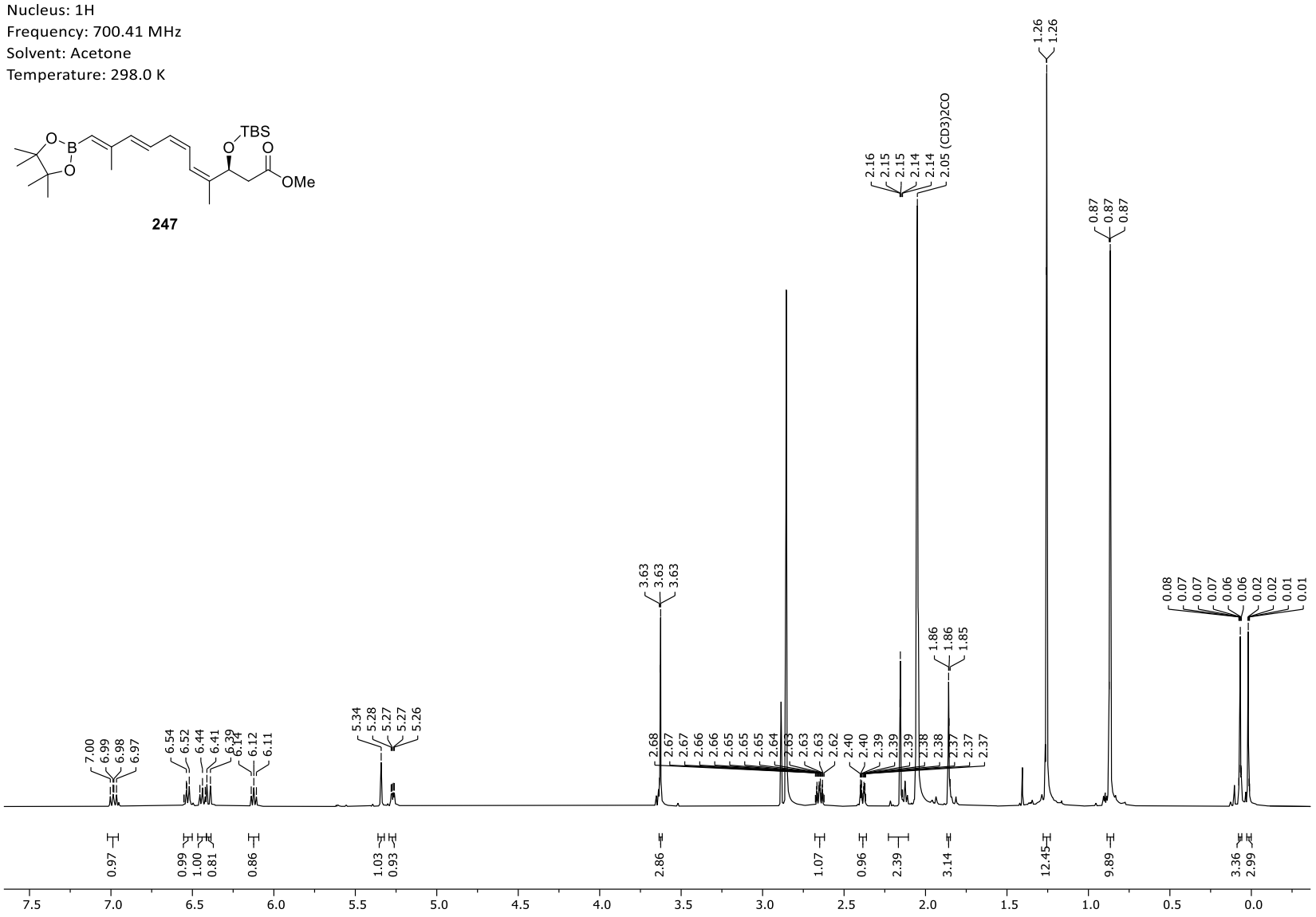

Appendix 161. ^{1}H-NMR spectrum of tetraene IV (**247**).

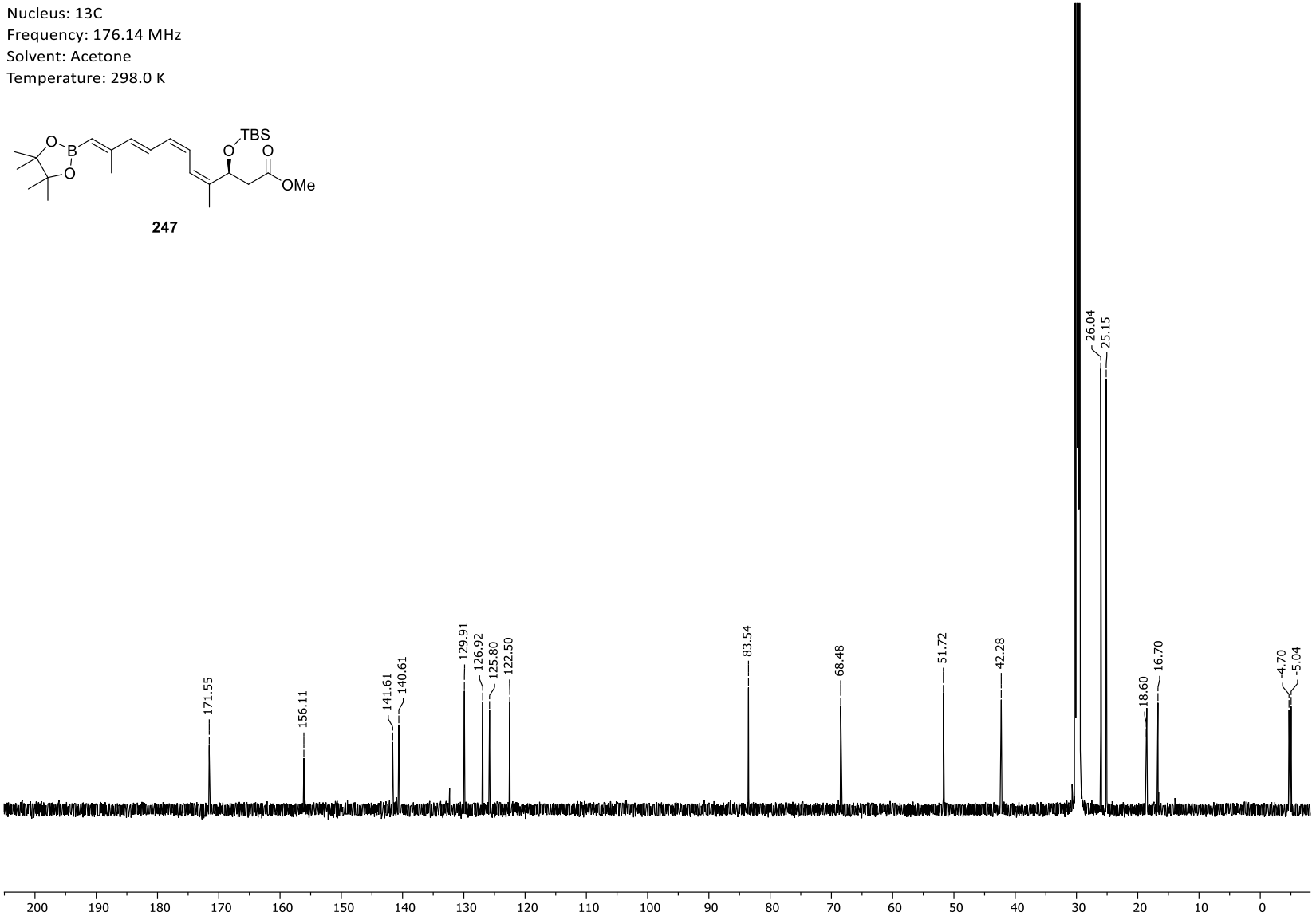

Appendix 162. ^{13}C-NMR spectrum of tetraene IV (**247**).

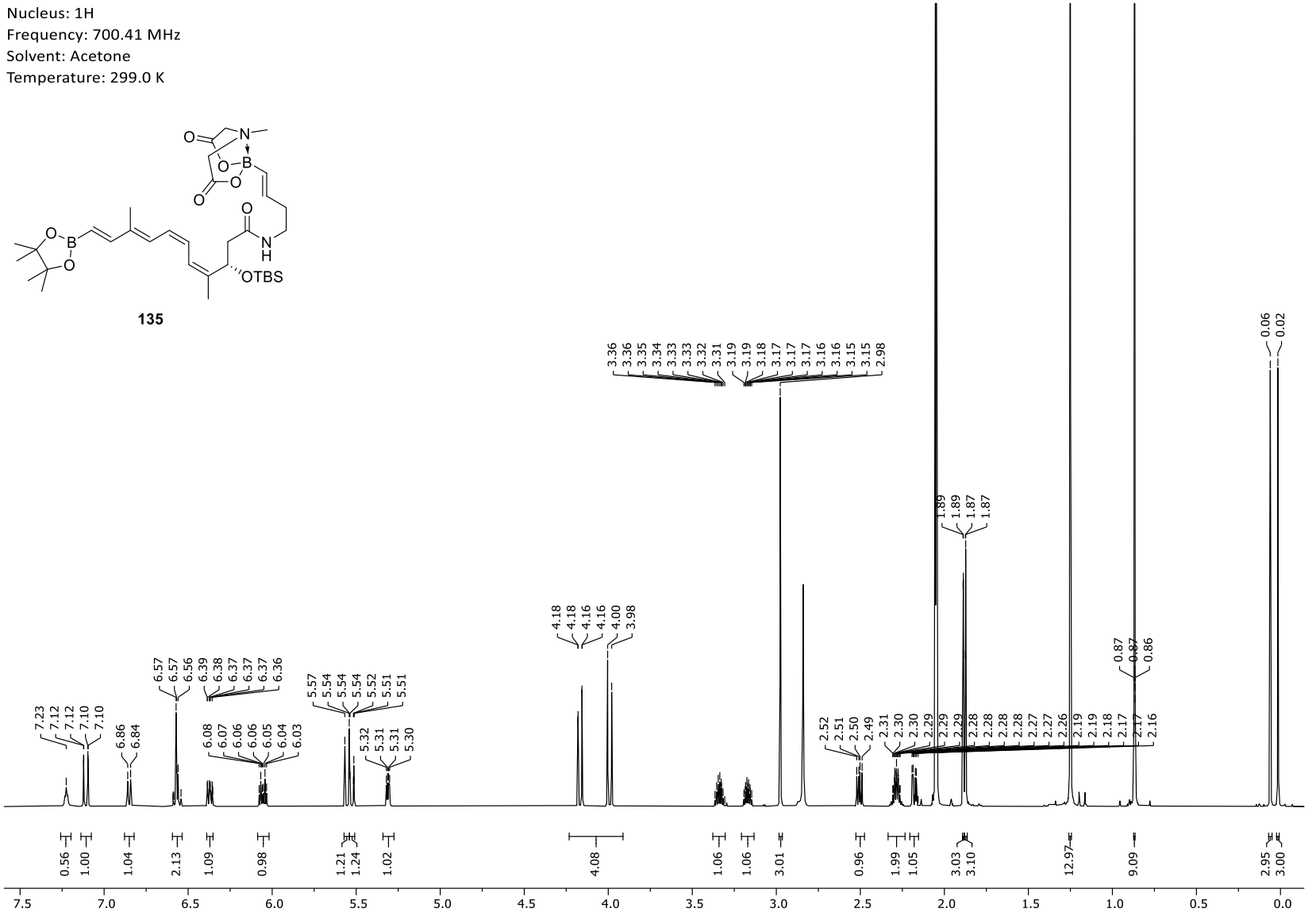

Appendix 163. ^{1}H-NMR spectrum of tetraene V (**135**).

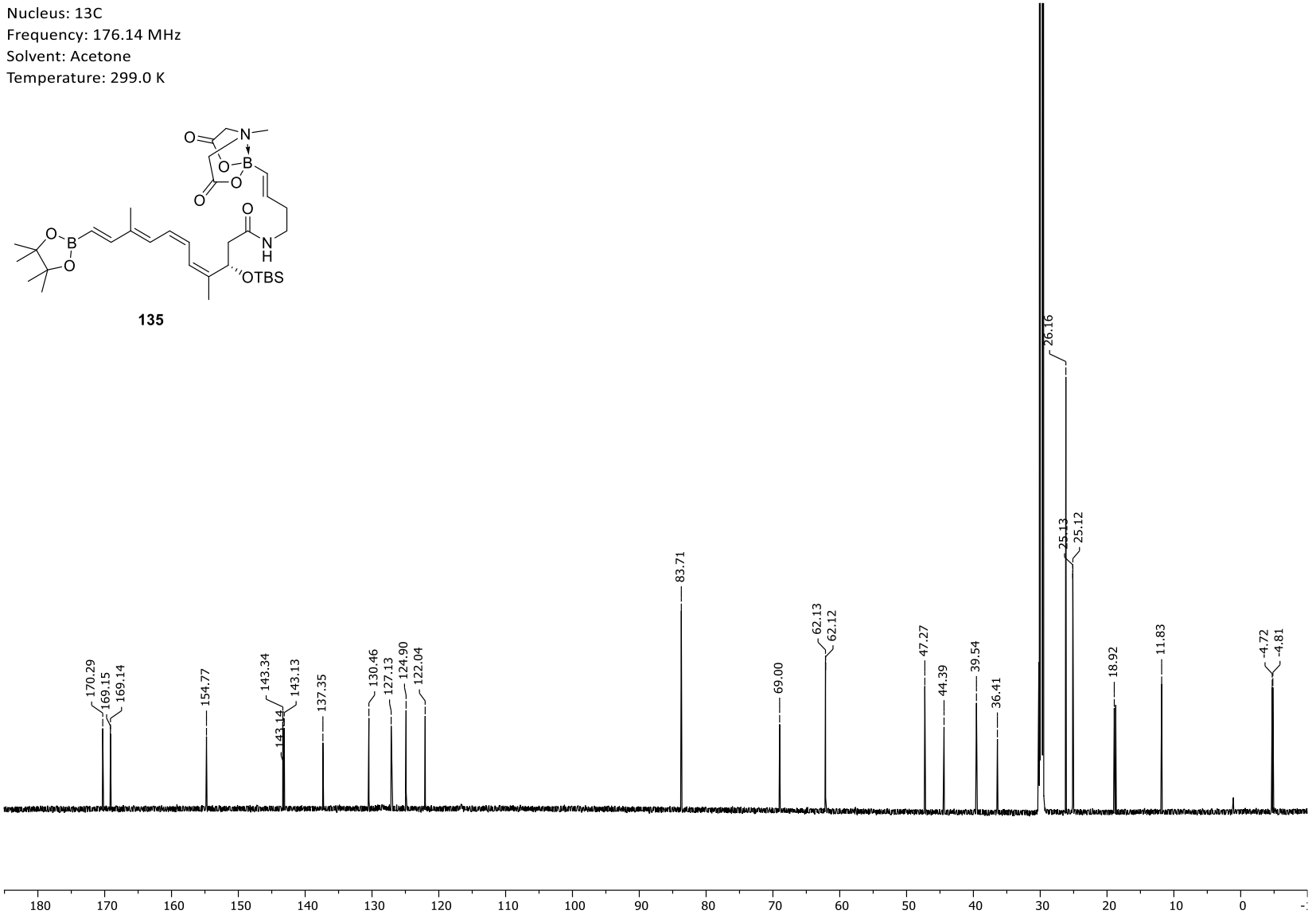

Appendix 164. ^{13}C-NMR spectrum of tetraene V (**135**).

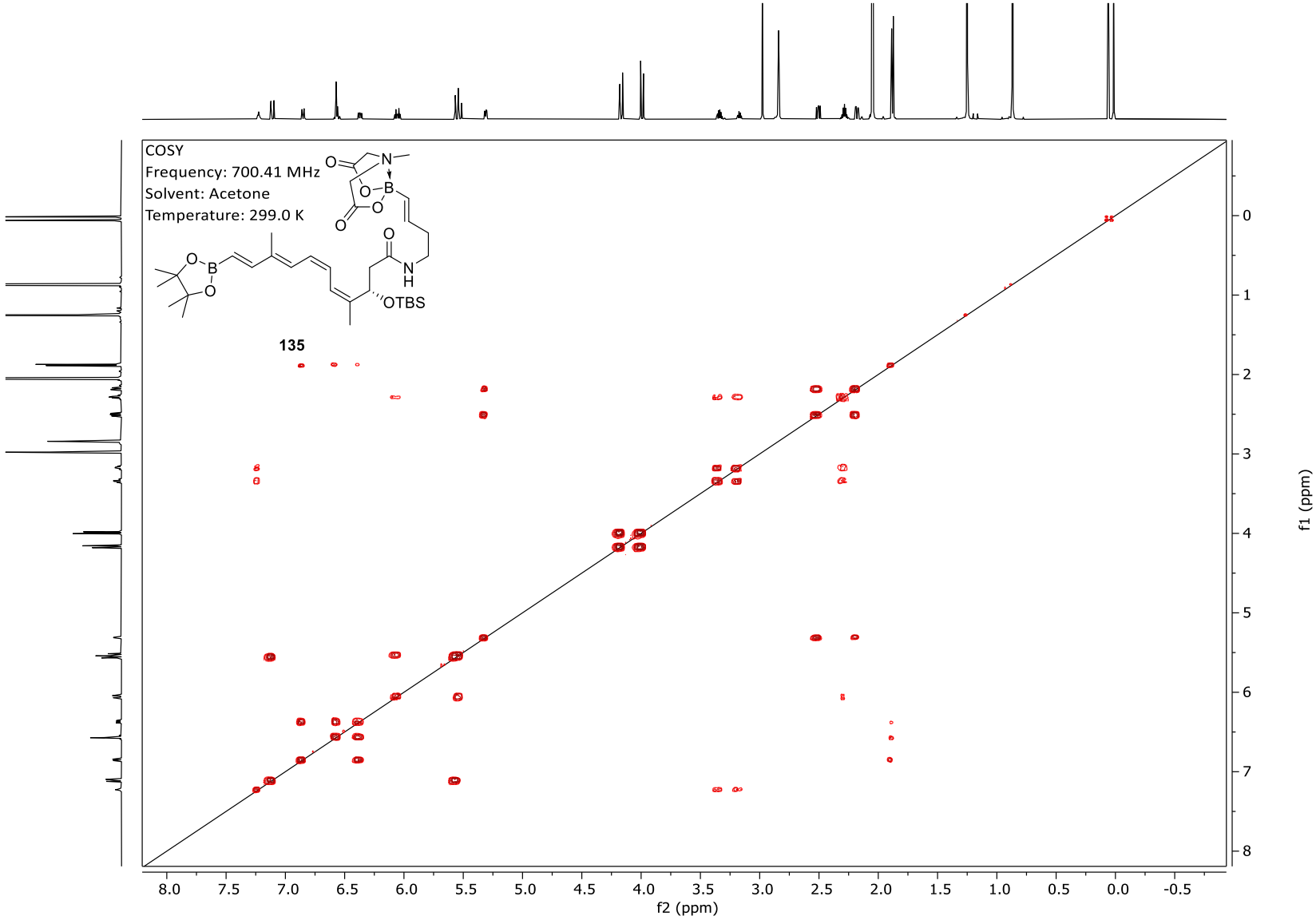

Appendix 165. COSY-spectrum of tetraene V (**135**).

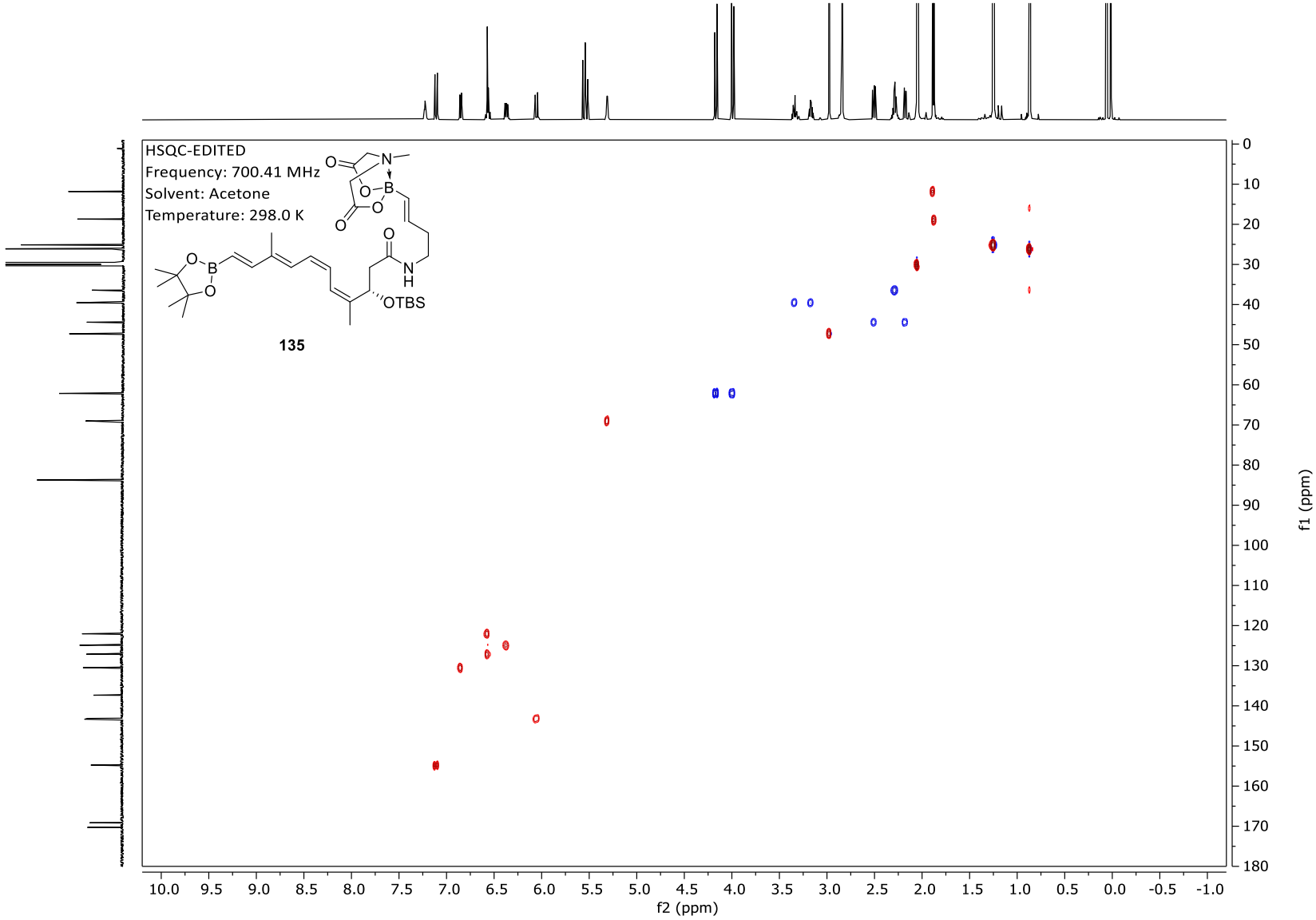

Appendix 166. HSQC-spectrum of tetraene V (**135**).

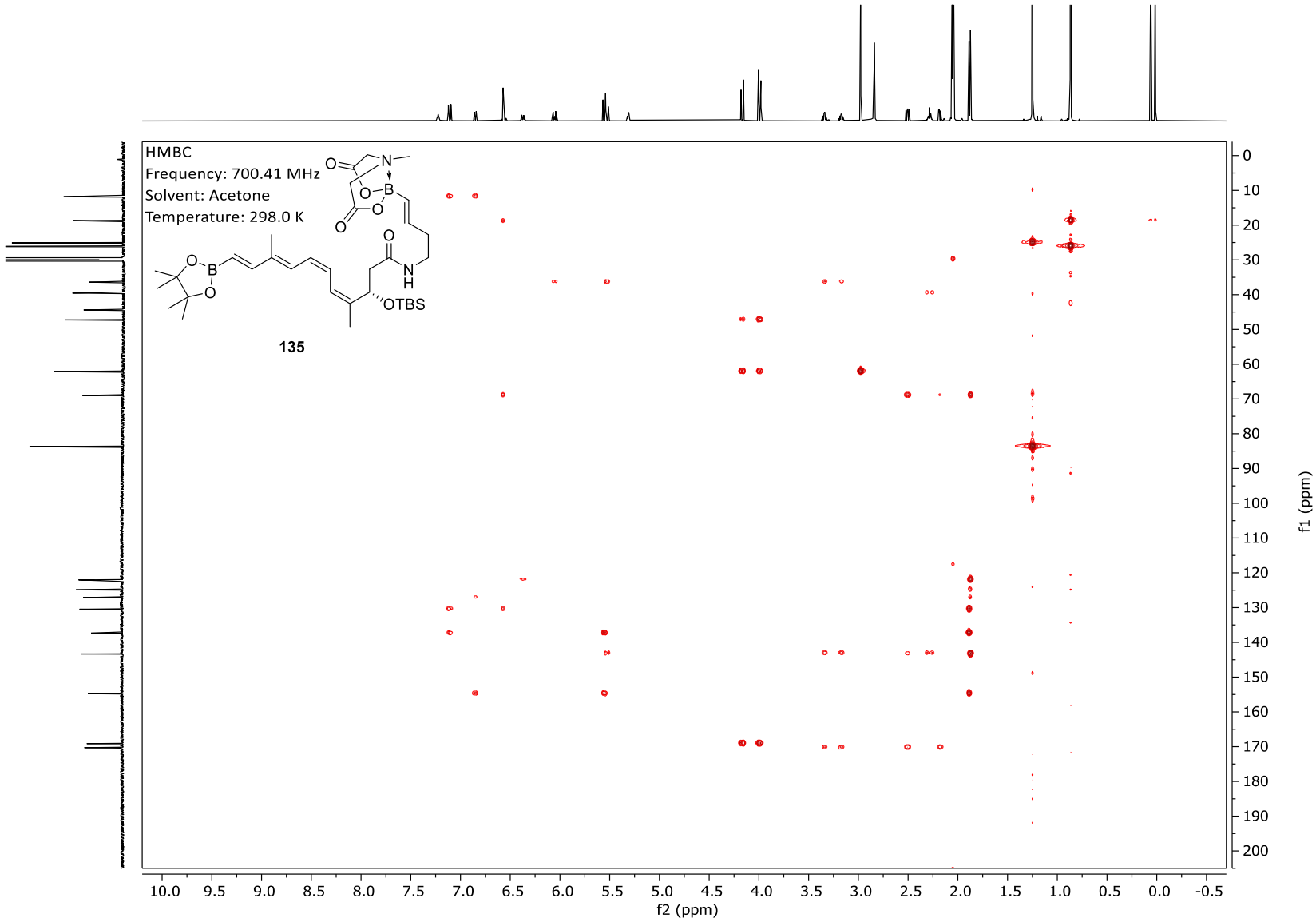

Appendix 167. HMBC-spectrum of tetraene V (**135**).

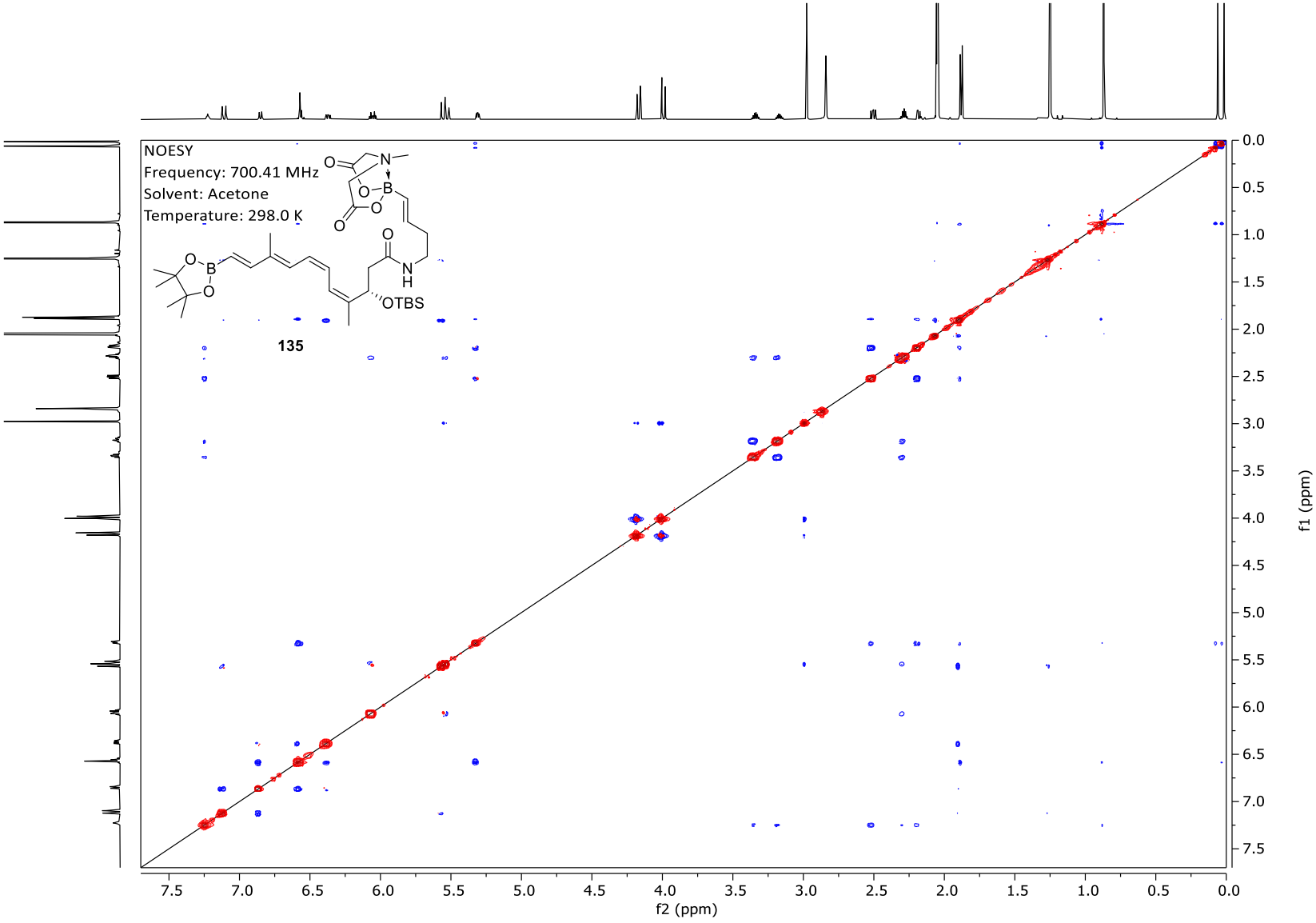

Appendix 168. NOESY-spectrum of tetraene V (**135**).

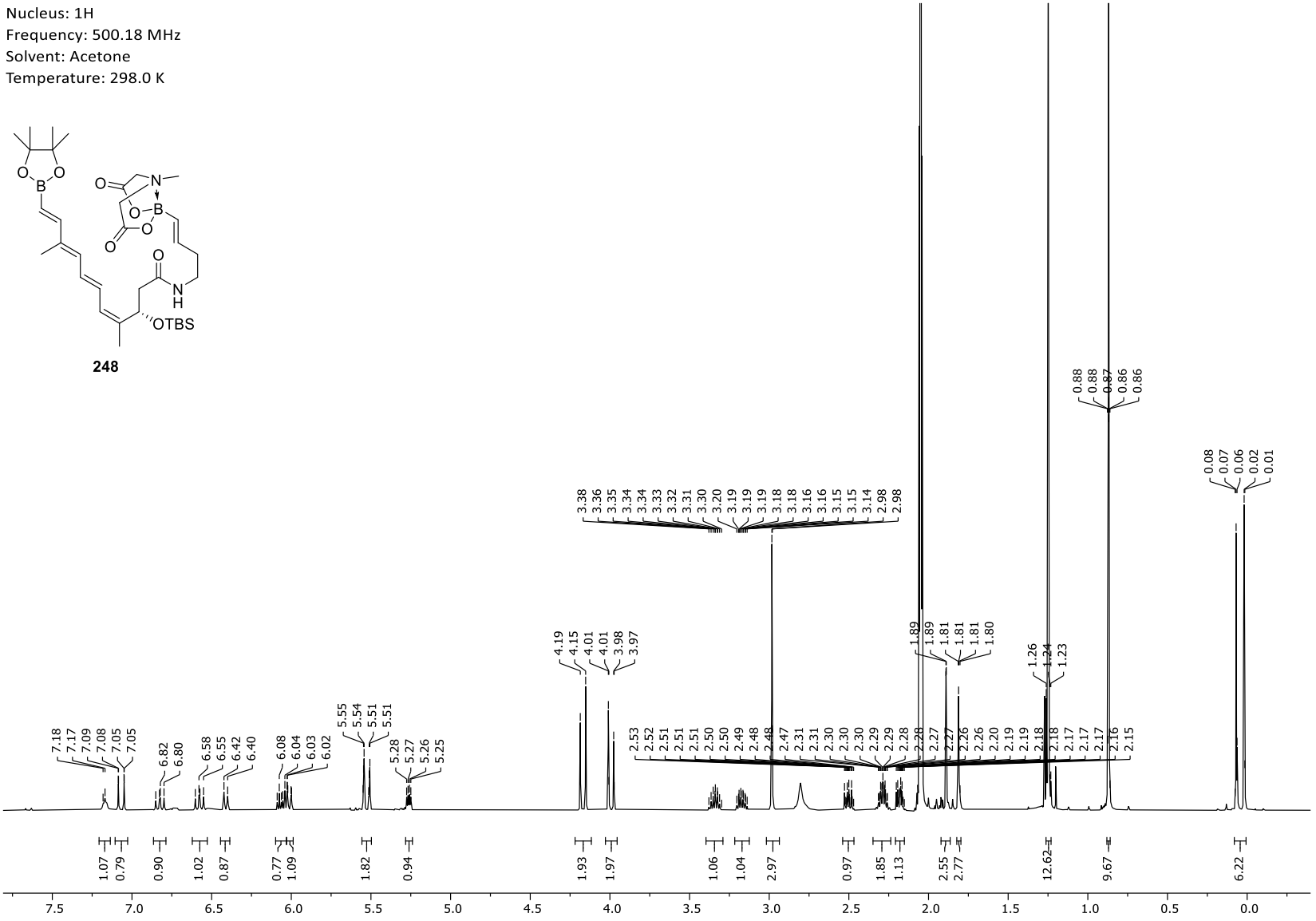

Appendix 169. ^{1}H-NMR spectrum of tetraene VI (**248**).

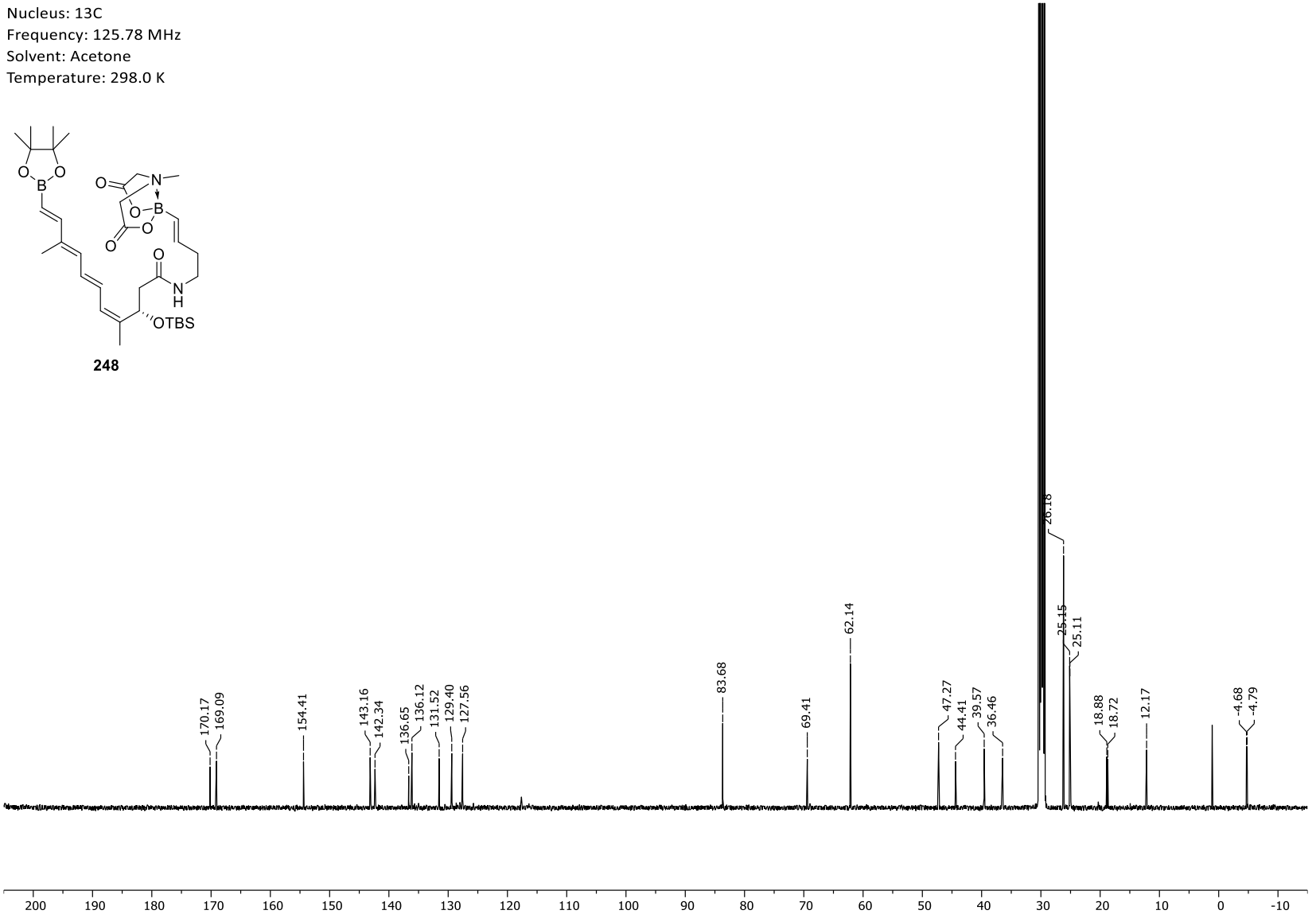

Appendix 170. ^{13}C-NMR spectrum of tetraene VI (**248**).

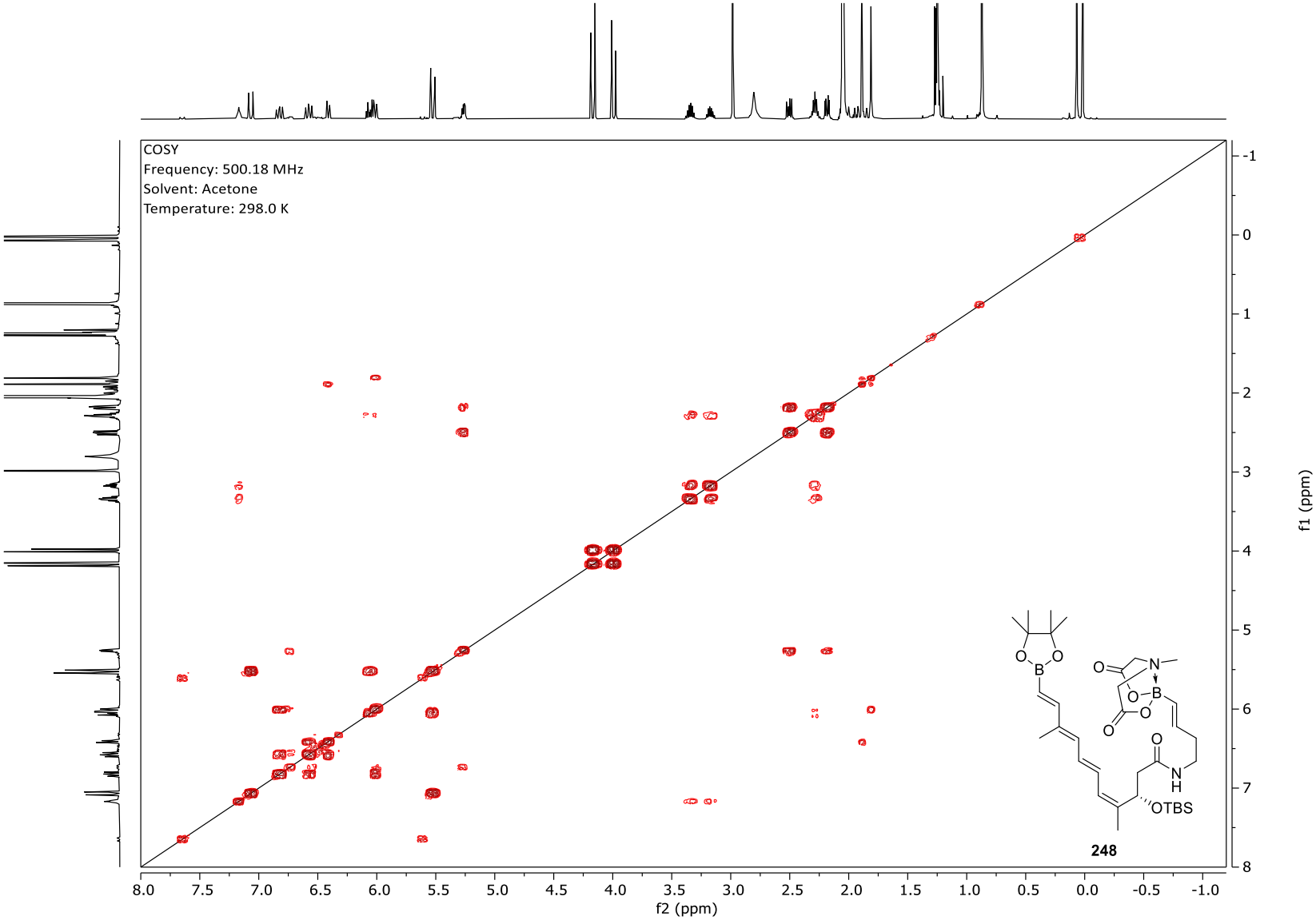

Appendix 171. COSY-NMR spectrum of tetraene VI (**248**).

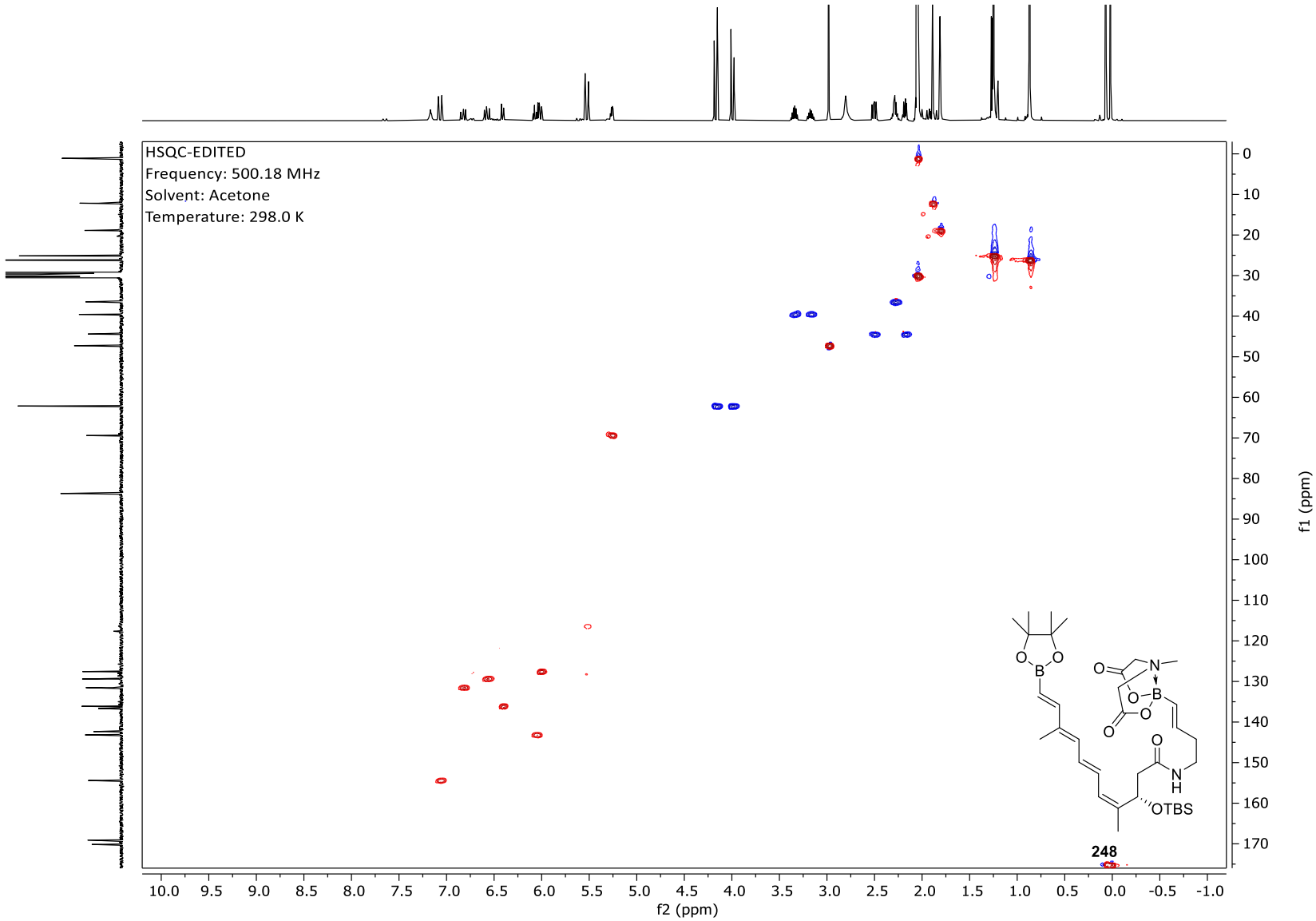

Appendix 172. HSQC-NMR spectrum of tetraene VI (**248**).

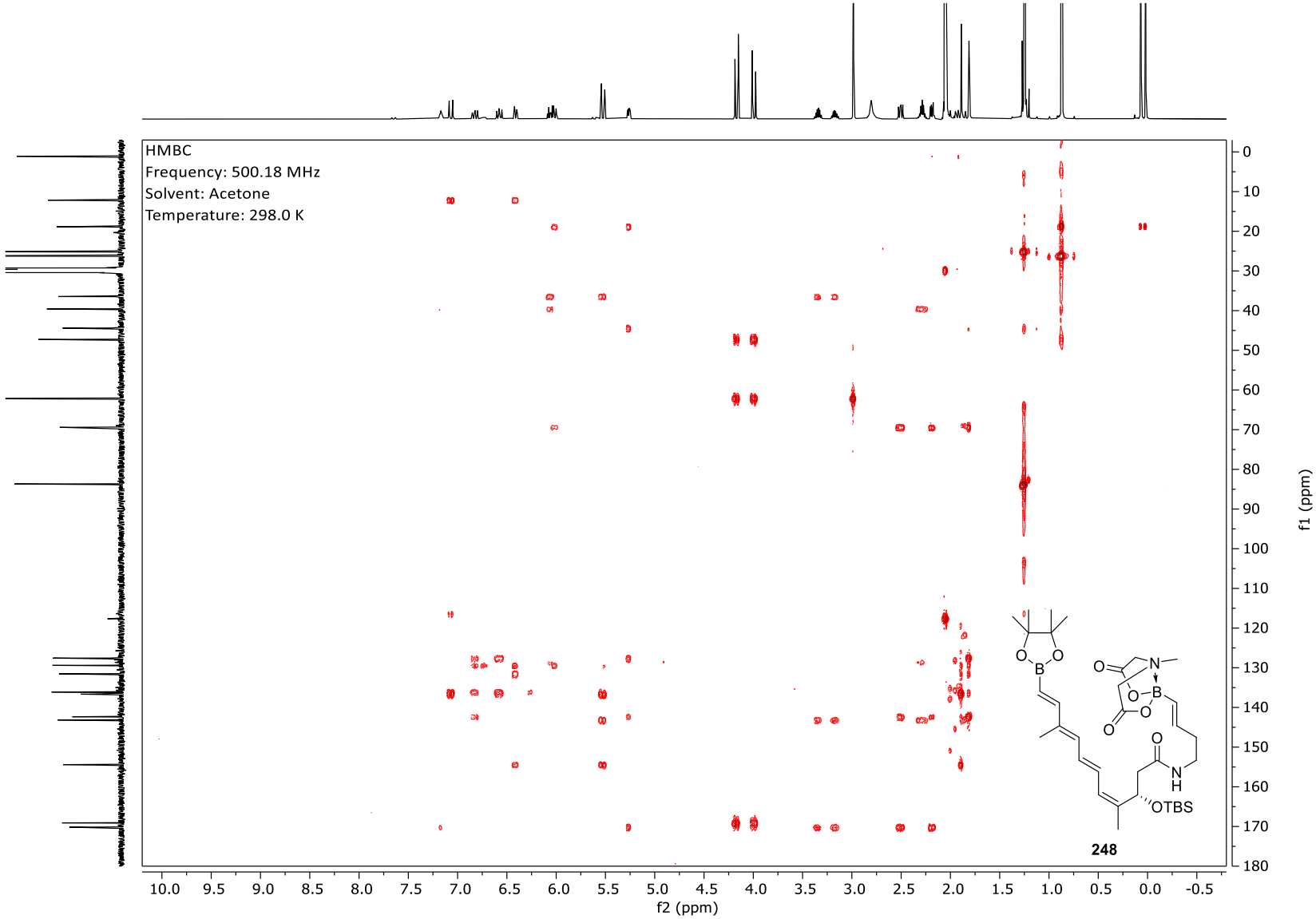

Appendix 173. HMBC-NMR spectrum of tetraene VI (**248**).

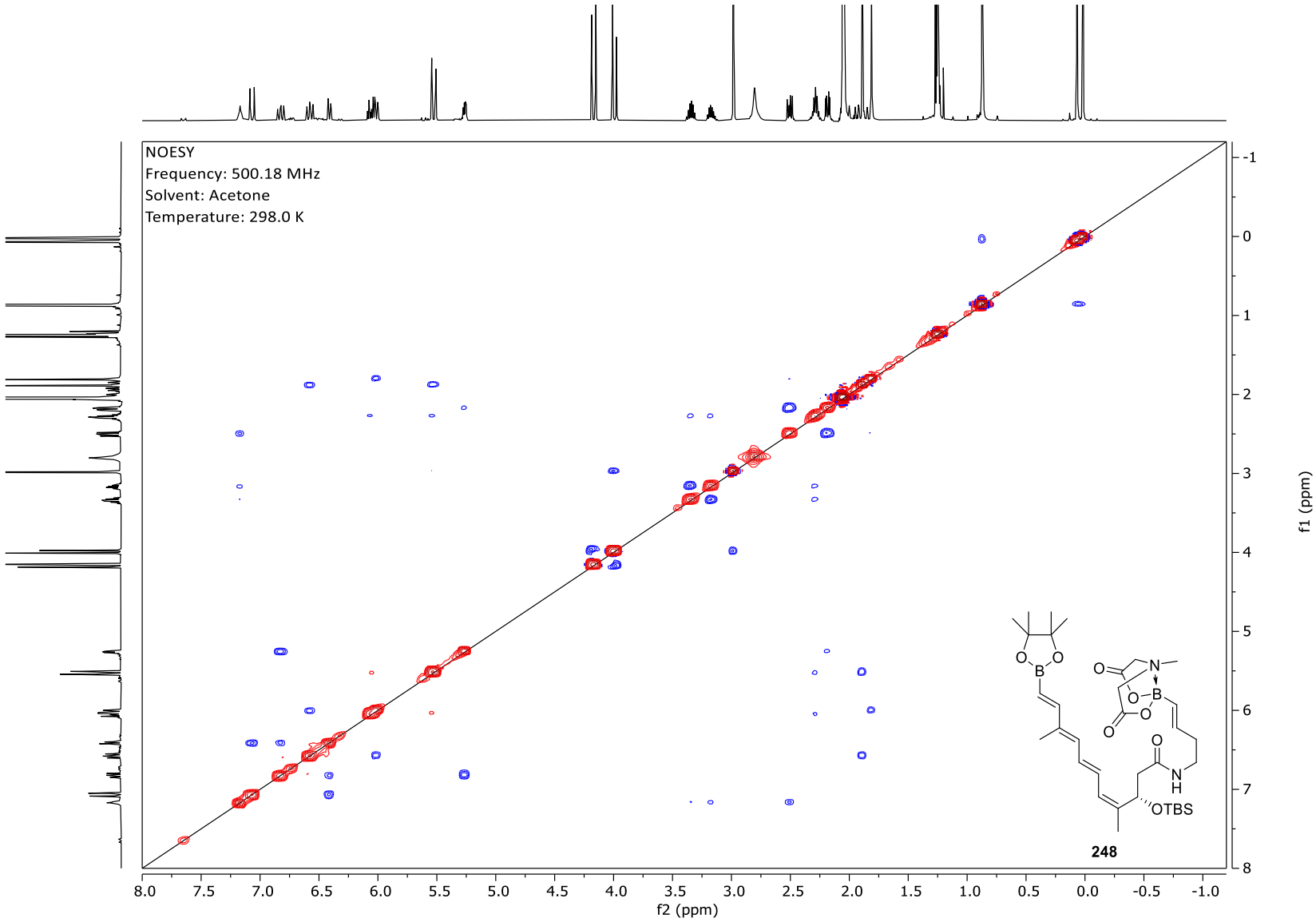

Appendix 174. NOESY-NMR spectrum of tetraene VI (**248**).

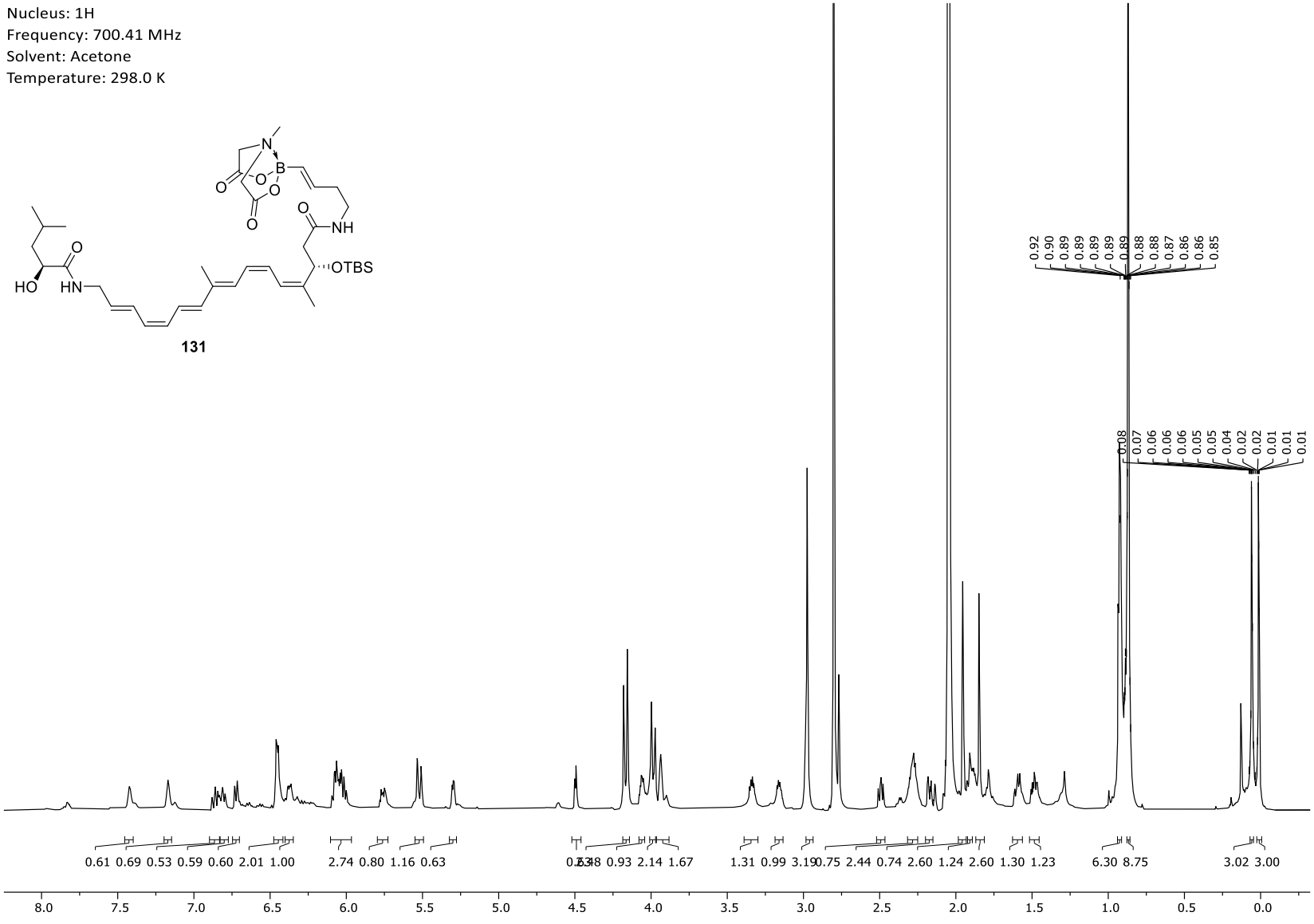

Appendix 175. ^{1}H-NMR spectrum of hexaene II (**131**) – after HPLC purification.

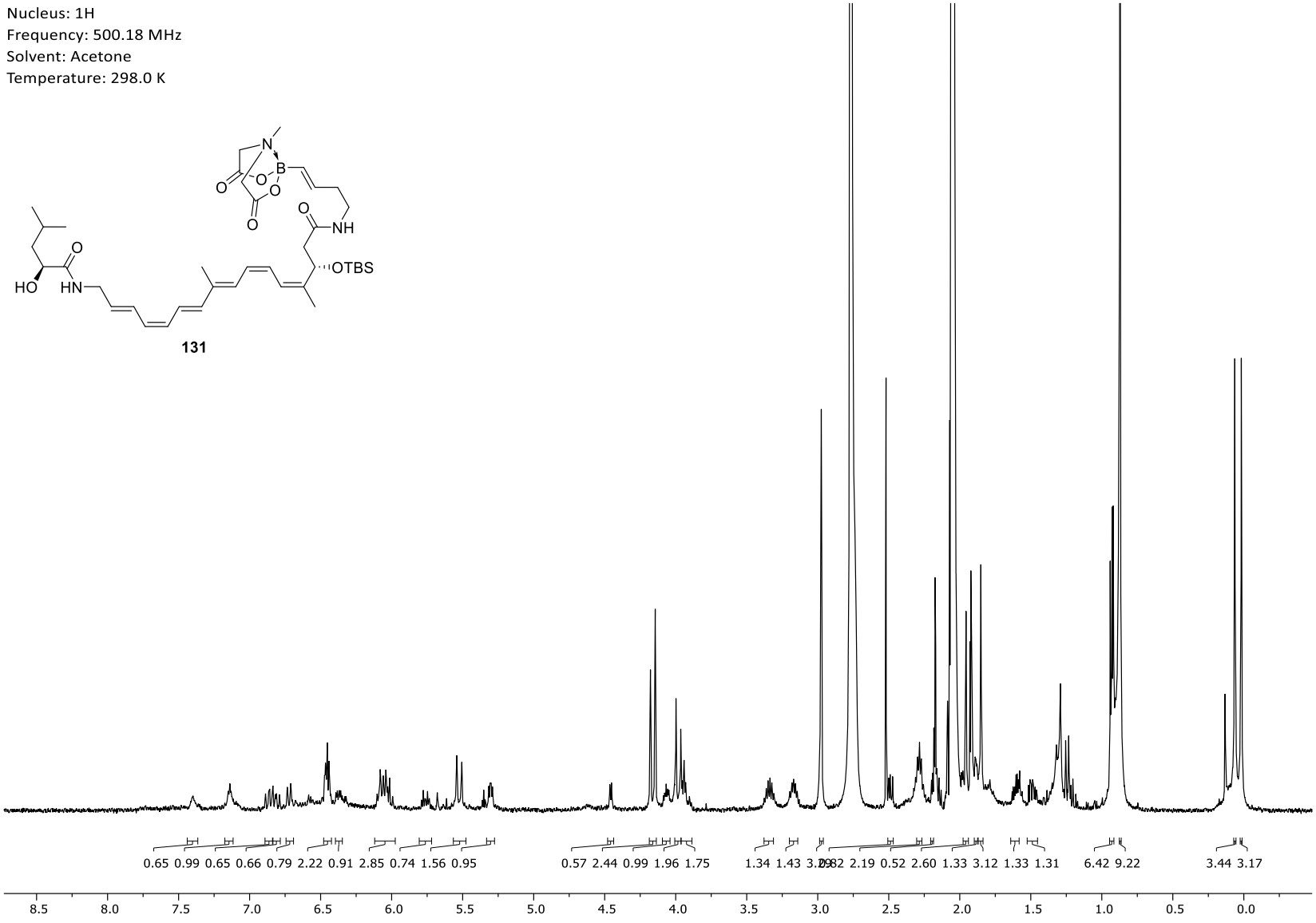

Appendix 176. ^{1}H-NMR spectrum of hexaene II (**131**) – after SPE purification.

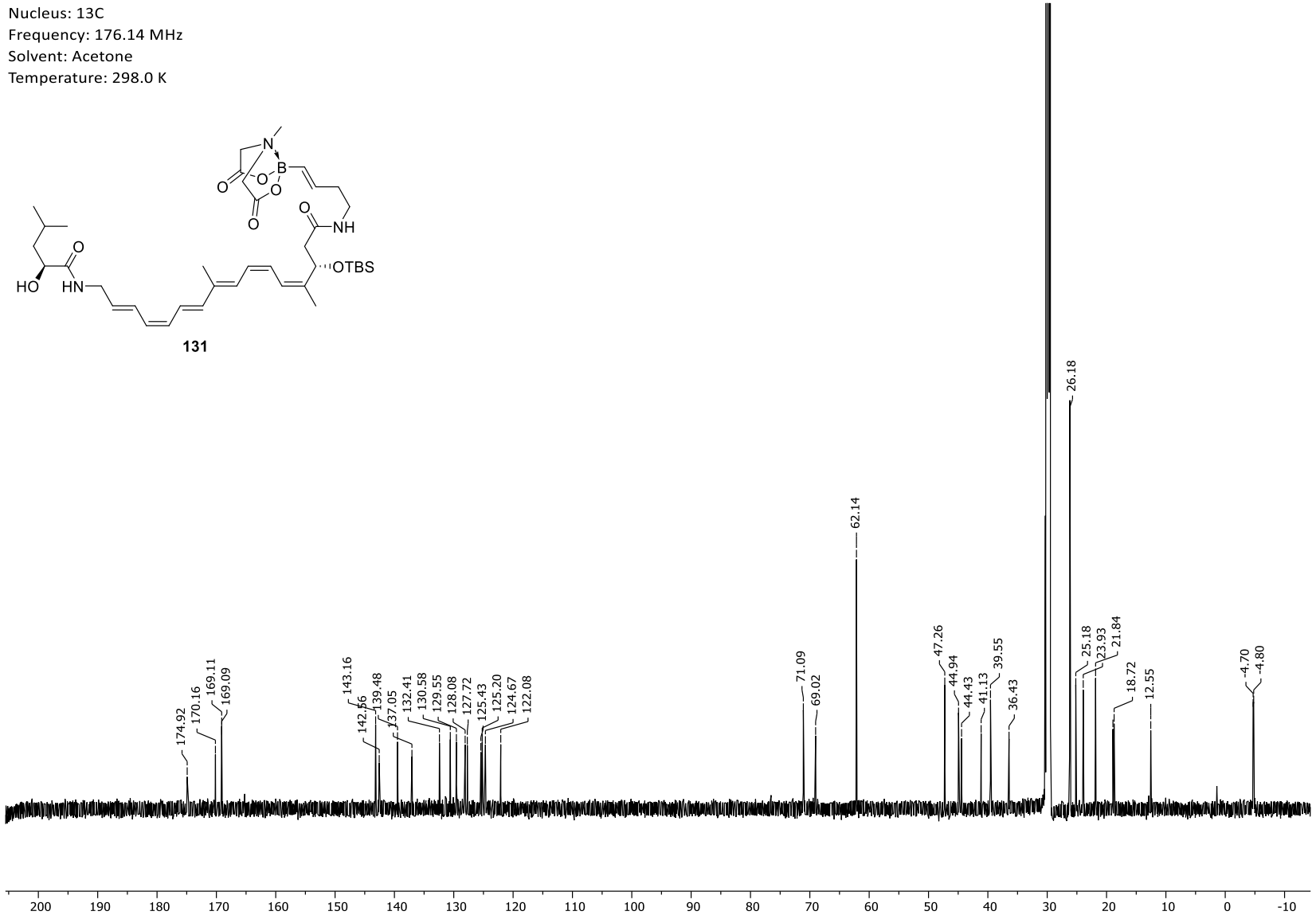

Appendix 177. ^{13}C-NMR spectrum of hexaene II (**131**).

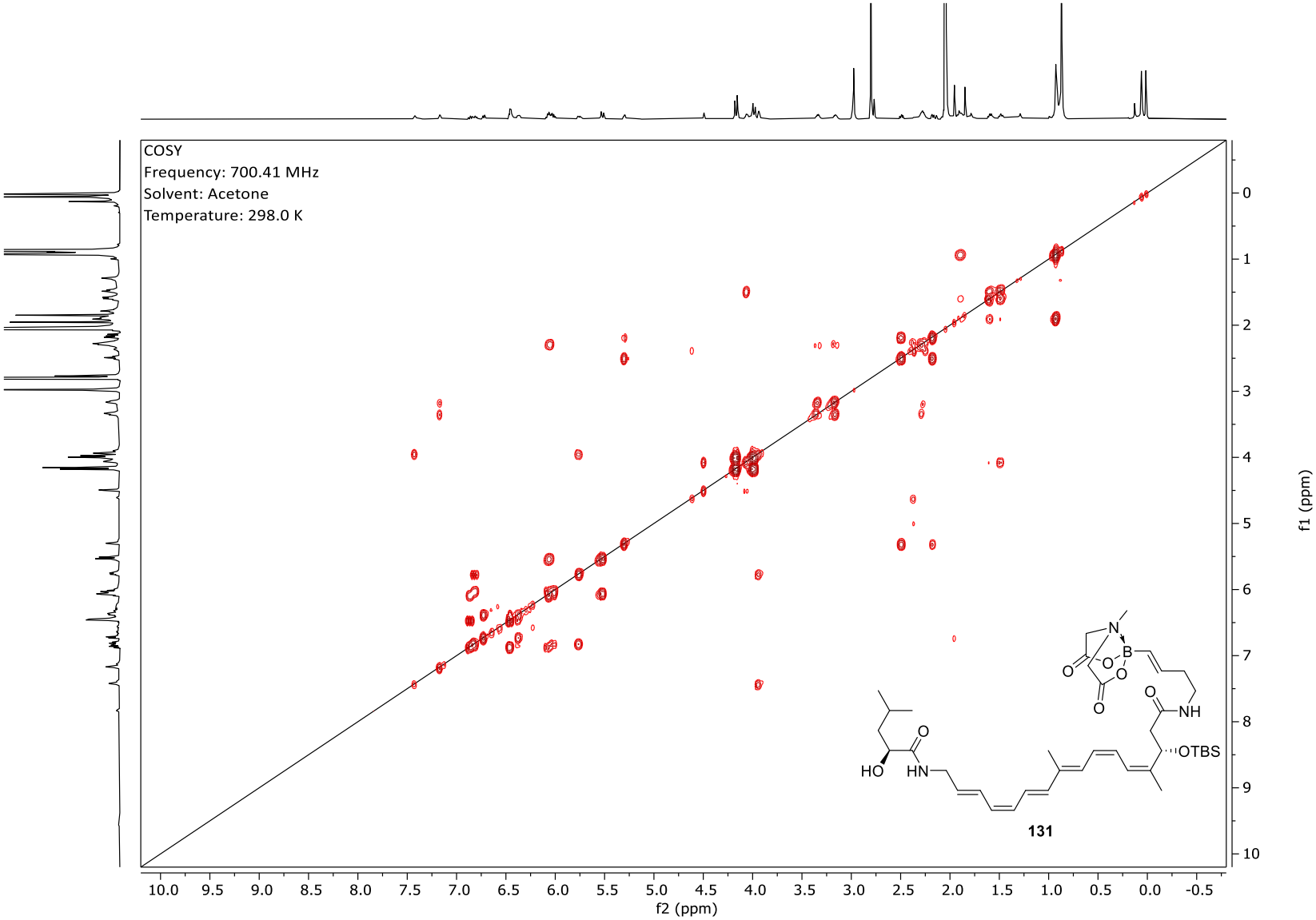

Appendix 178. COSY-NMR spectrum of hexaene II (**131**).

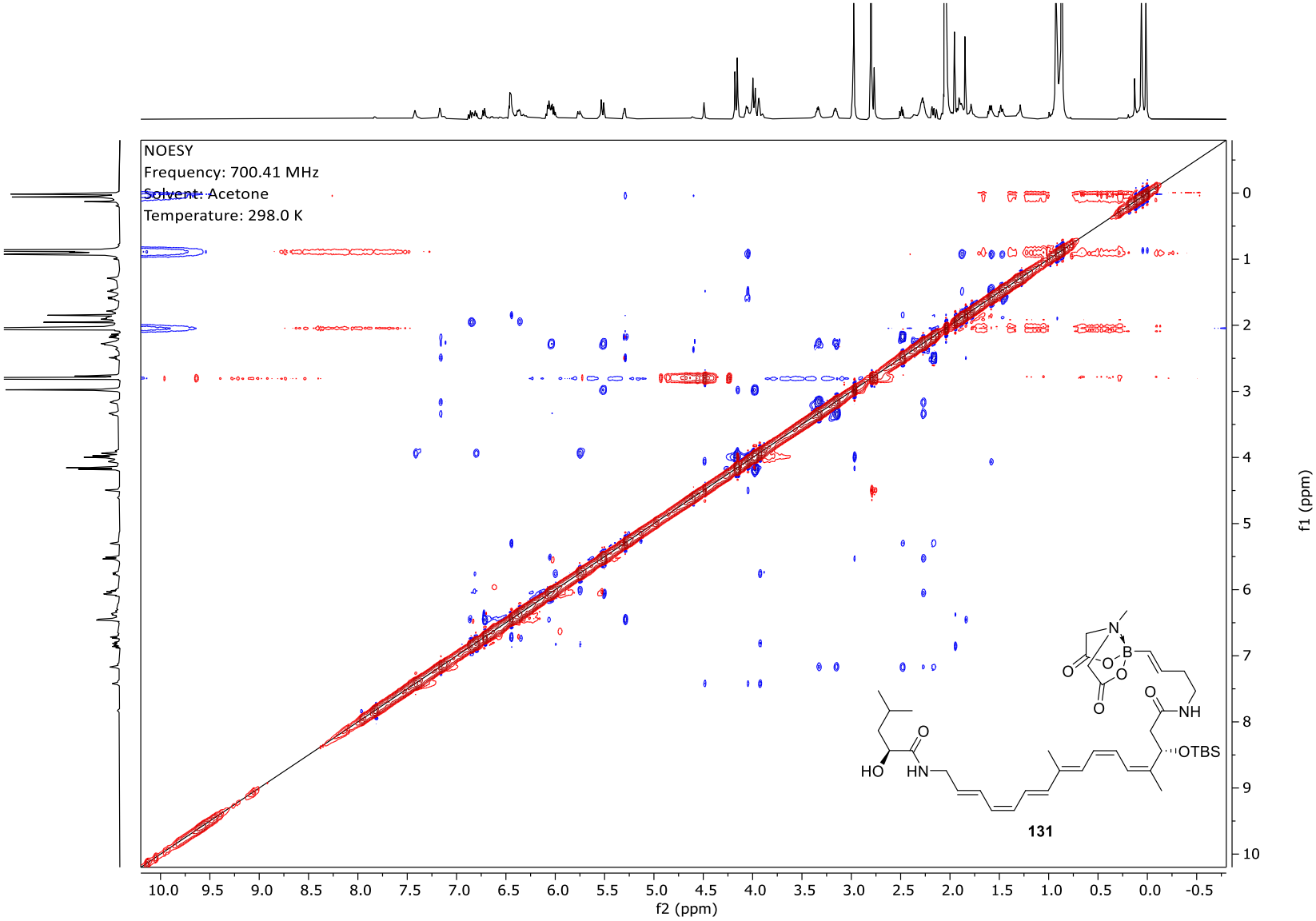

Appendix 179. NOESY-NMR spectrum of hexaene II (**131**).

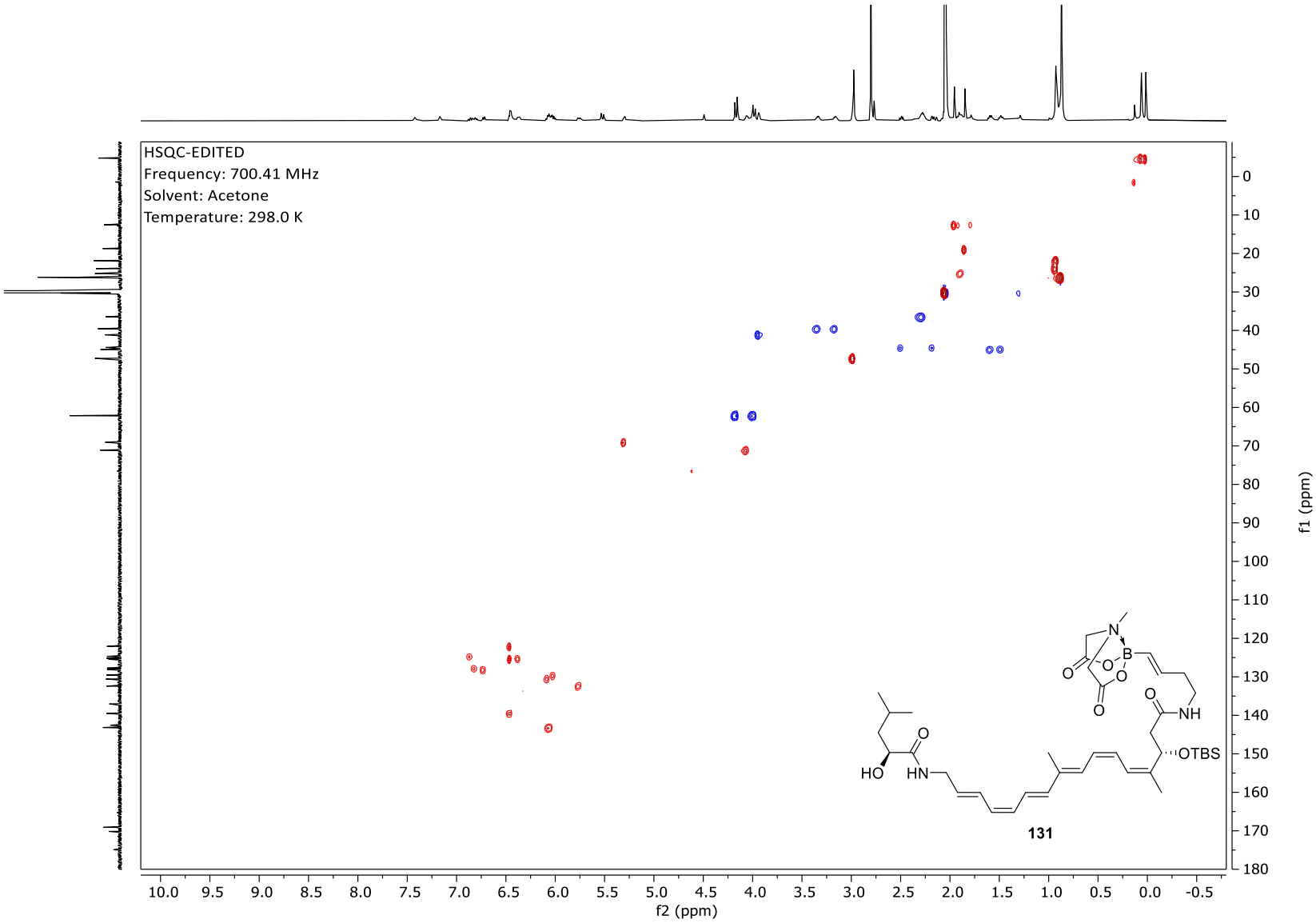

Appendix 180. HSQC-NMR spectrum of hexaene II (**131**).

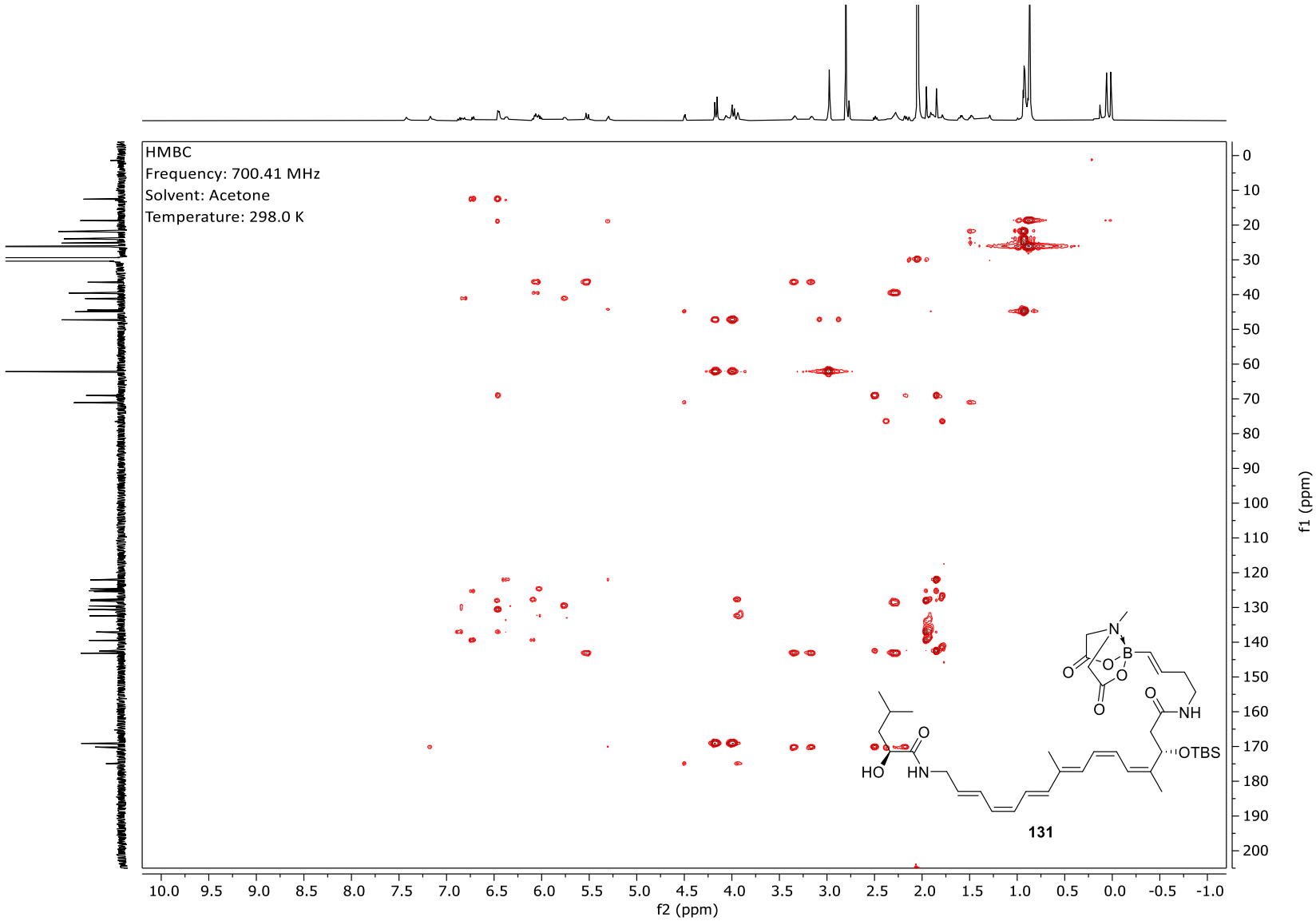

Appendix 181. HMBC-NMR spectrum of hexaene II (**131**).

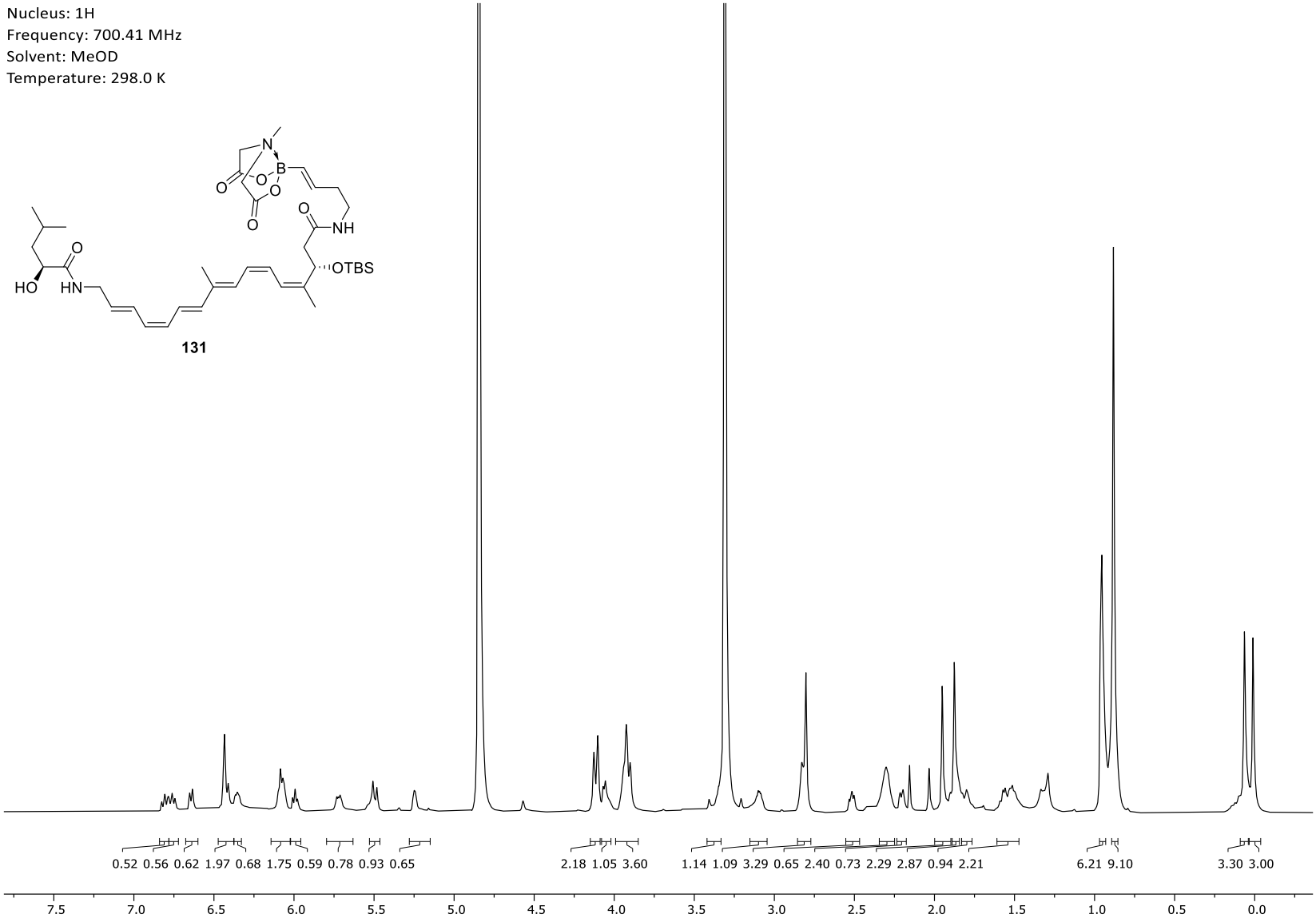

Appendix 182. ^{1}H-NMR spectrum of hexaene II (**131**) – in MeOD.

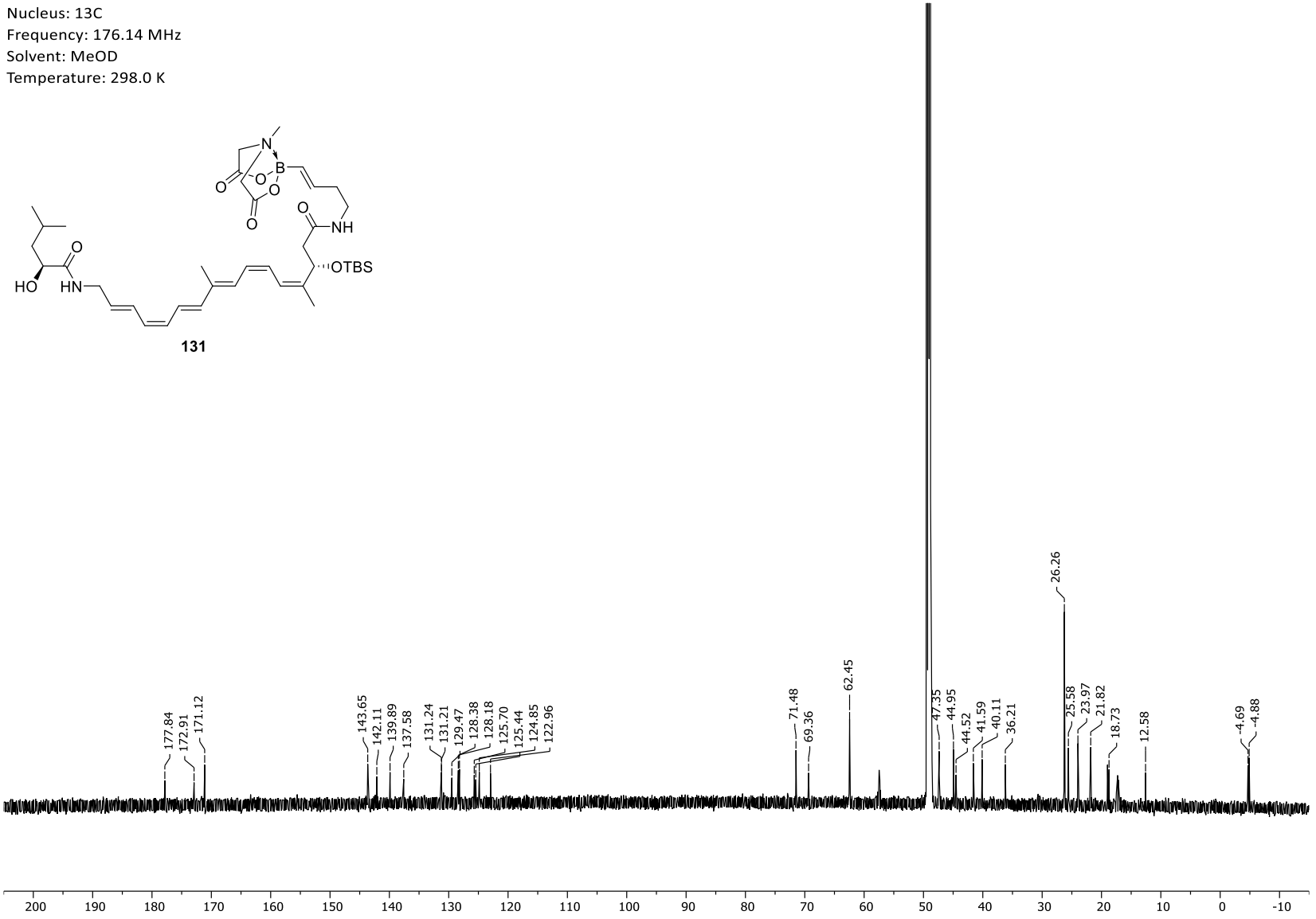

Appendix 183. ^{13}C-NMR spectrum of hexaene II (**131**) – in MeOD.

Nucleus: 1H
Frequency: 499.96 MHz
Solvent: Acetone
Temperature: 298.0 K

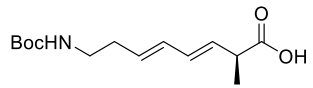

249

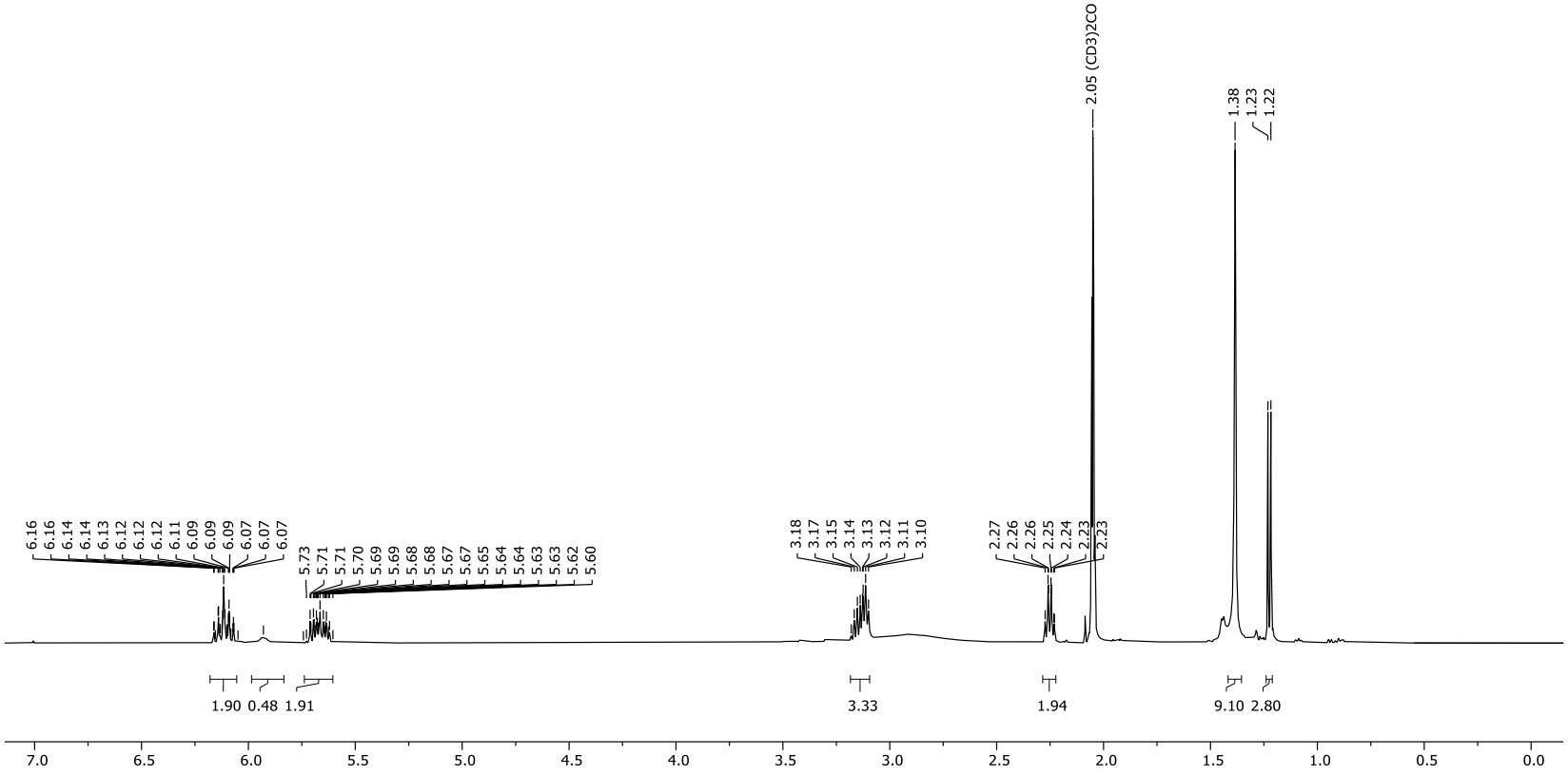

Appendix 184. ^{1}H-NMR spectrum of acid **249** - reproduced with permission from *Johannes Herbst*.[X]

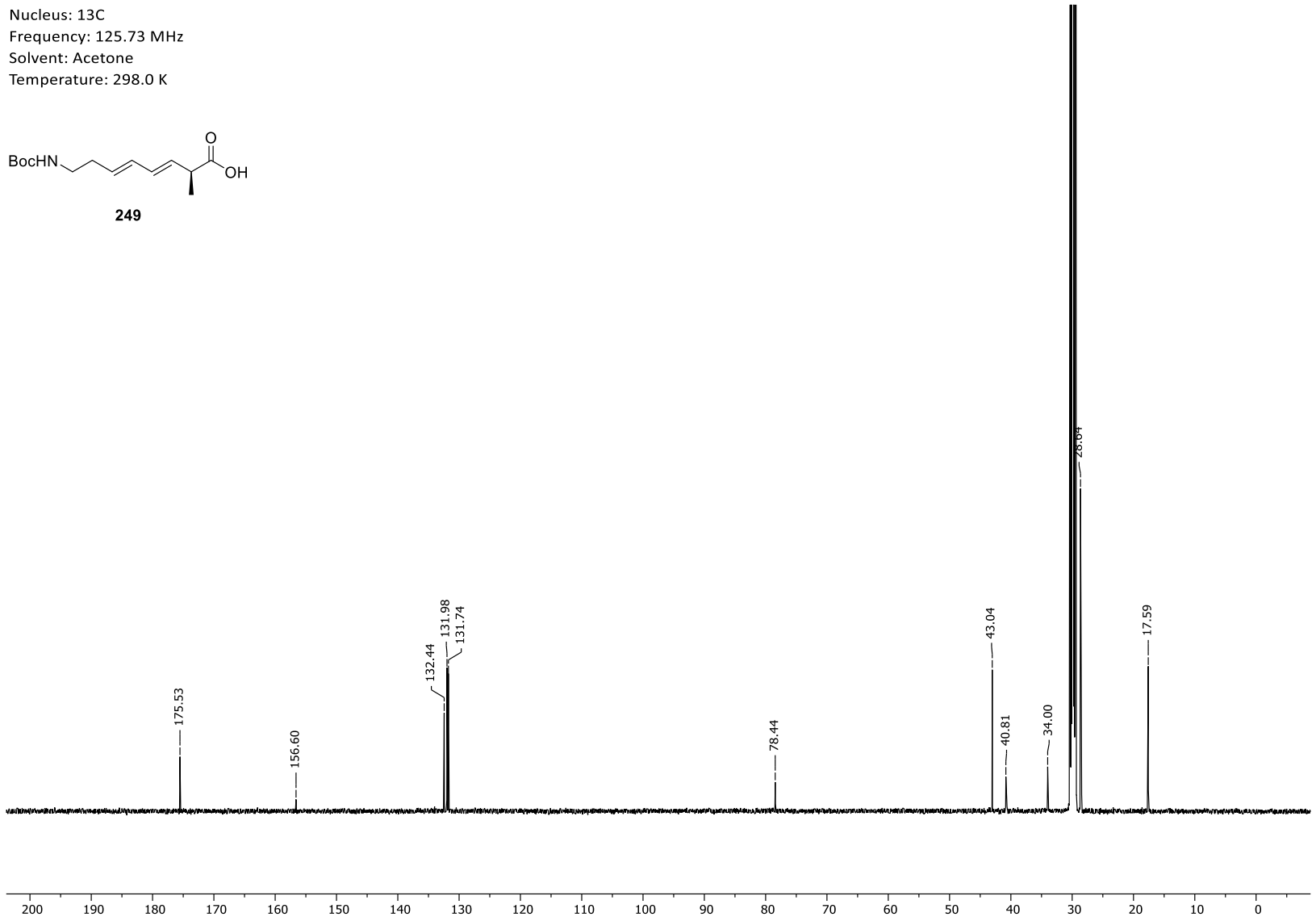

Appendix 185. ^{13}C-NMR spectrum of acid **249** - reproduced with permission from *Johannes Herbst*.[X]

Nucleus: 1H
Frequency: 499.13 MHz
Solvent: Acetone
Temperature: 298.0 K

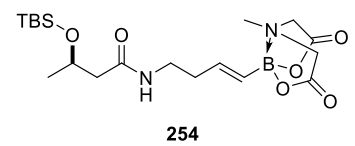

254

Appendix 186. ^{1}H-NMR spectrum of test system **254**.

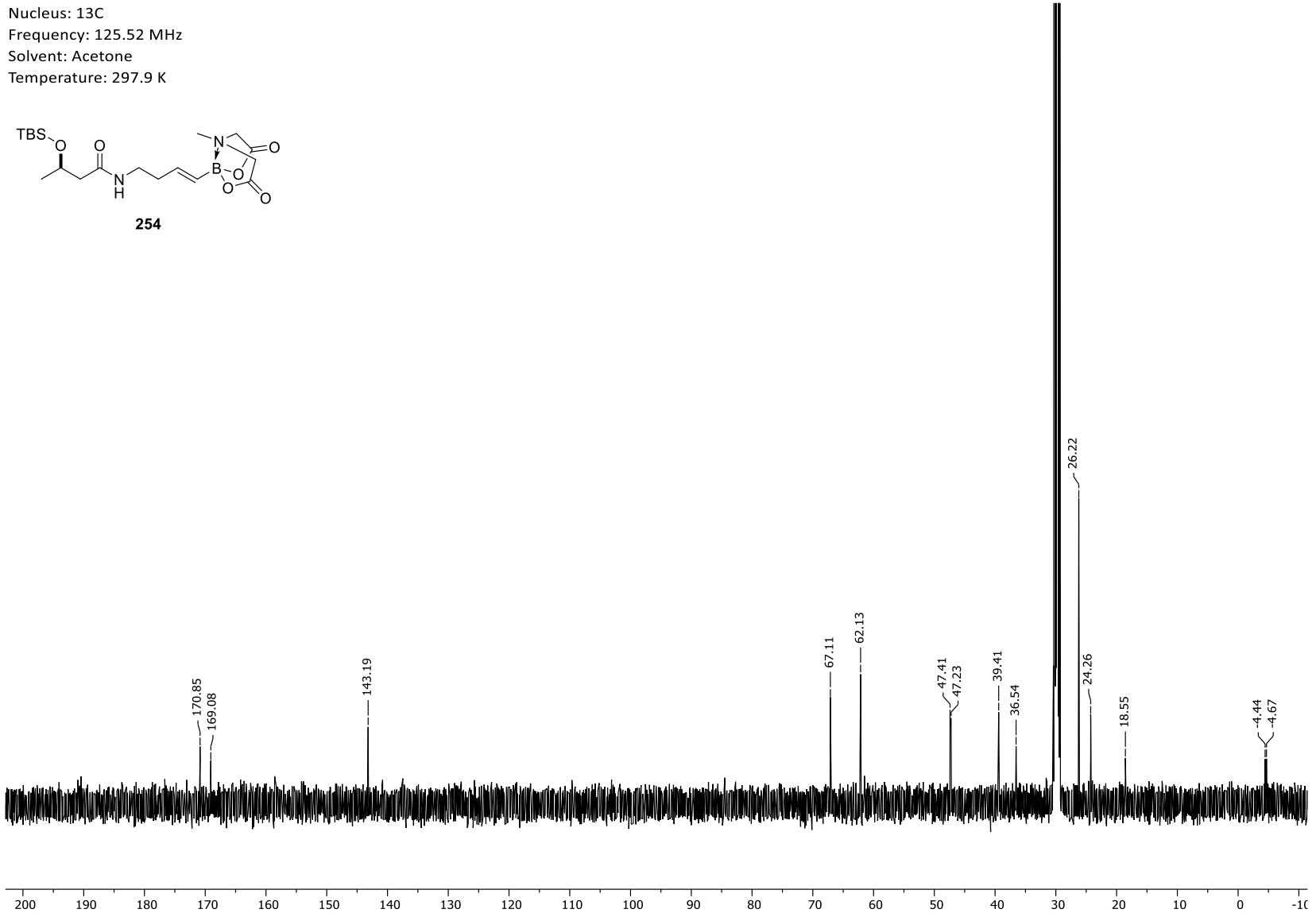

Appendix 187. ^{13}C-NMR spectrum of test system **254**.

Nucleus: 1H
Frequency: 500.04 MHz
Solvent: Acetone
Temperature: 298.0 K

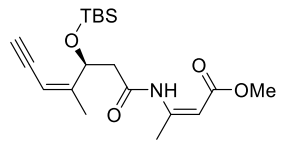

257

Appendix 188. ^{1}H-NMR spectrum of methyl (*Z*)-3-((*S*,*Z*)-3-((*tert*-butyldimethylsilyl)oxy)-4-methylhept-4-en-6-ynamido)but-2-enoate (**257**).

Nucleus: 13C
Frequency: 125.75 MHz
Solvent: Acetone
Temperature: 298.0 K

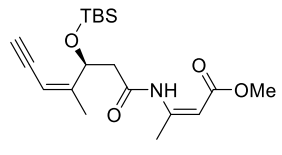

257

Appendix 189. ^{13}C-NMR spectrum of methyl (*Z*)-3-((*S*,*Z*)-3-((*tert*-butyldimethylsilyl)oxy)-4-methylhept-4-en-6-ynamido)but-2-enoate (**257**).

Nucleus: 1H
Frequency: 500.04 MHz
Solvent: Acetone
Temperature: 298.0 K

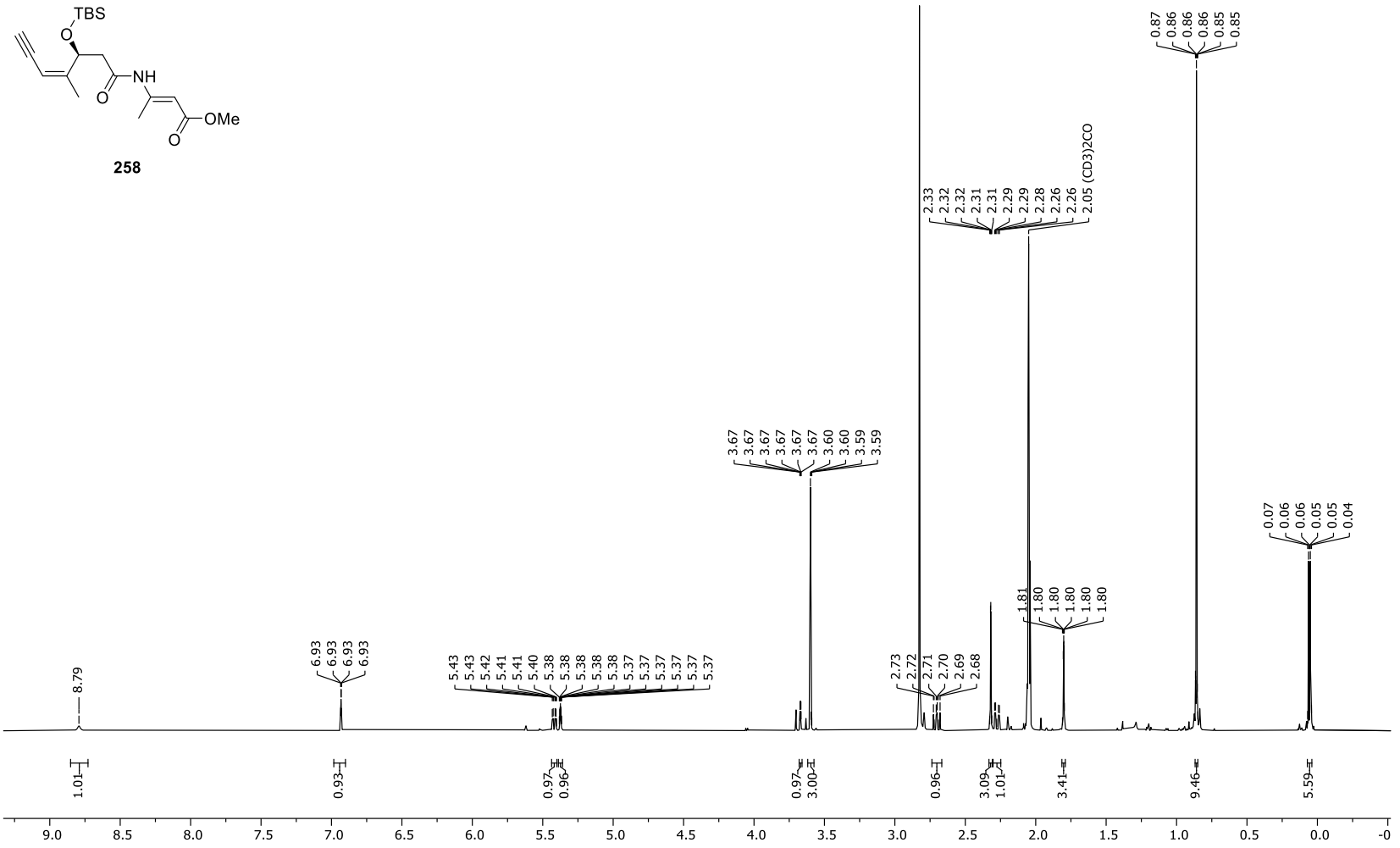

Appendix 190. ^{1}H-NMR spectrum of methyl (*E*)-3-((*S*,*Z*)-3-((*tert*-butyldimethylsilyl)oxy)-4-methylhept-4-en-6-ynamido)but-2-enoate (**258**).

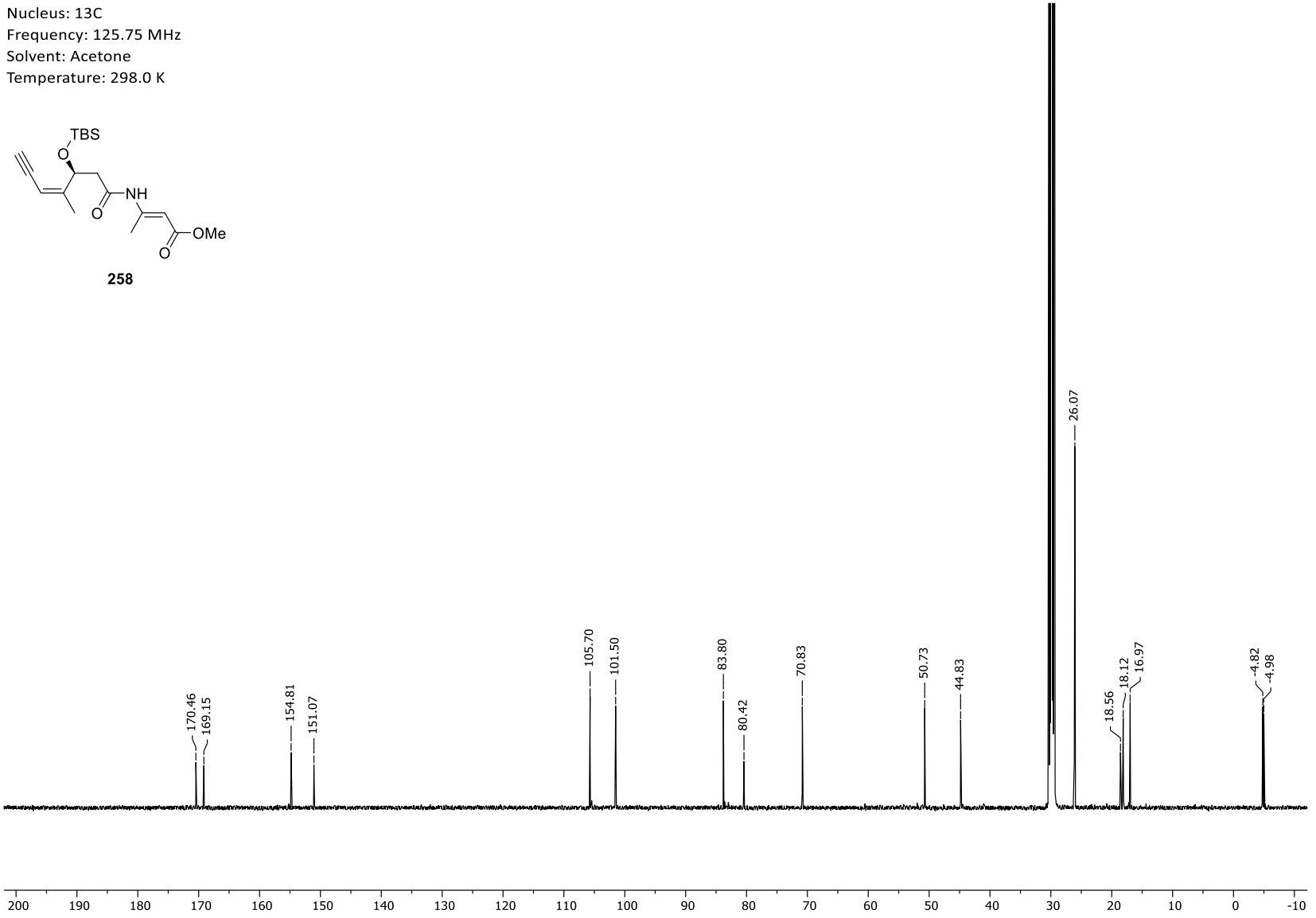

Appendix 191. ^{13}C-NMR spectrum of methyl (*E*)-3-((*S*,*Z*)-3-((*tert*-butyldimethylsilyl)oxy)-4-methylhept-4-en-6-ynamido)but-2-enoate (**258**).

Nucleus: 1H
Frequency: 499.13 MHz
Solvent: CDCl3
Temperature: 297.9 K

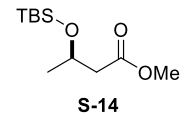

S-14

Appendix 192. ^{1}H-NMR spectrum of (*rac*)-methyl 3-((*tert*-butyldimethylsilyl)oxy)butanoate (**S-14**).

Nucleus: 13C
Frequency: 125.52 MHz
Solvent: CDCl3
Temperature: 298.0 K

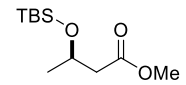

S-14

Appendix 193. ^{13}C-NMR spectrum of (*rac*)-methyl 3-((*tert*-butyldimethylsilyl)oxy)butanoate (**S-14**).

Nucleus: 1H
Frequency: 500.04 MHz
Solvent: Acetone
Temperature: 298.0 K

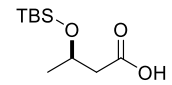

253

Appendix 194. ^{1}H-NMR spectrum of (*rac*)-3-((*tert*-butyldimethylsilyl)oxy)butanoic acid (**253**).

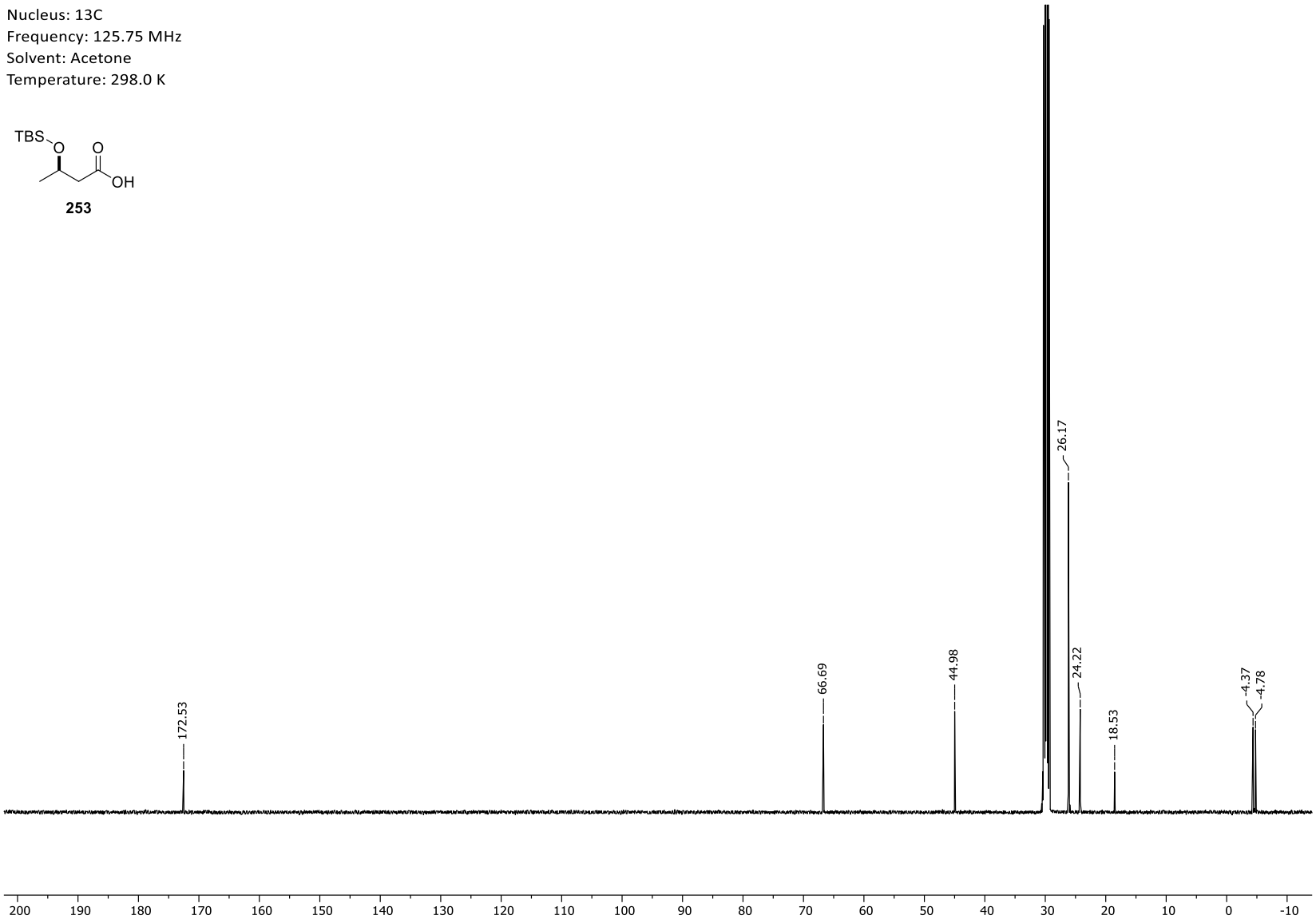

Appendix 195. ^{13}C-NMR spectrum of (*rac*)-3-((*tert*-butyldimethylsilyl)oxy)butanoic acid (**253**).

Nucleus: 1H
Frequency: 499.13 MHz
Solvent: Acetone
Temperature: 297.9 K

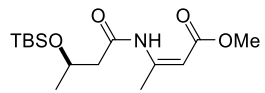

259

Appendix 196. ^{1}H-NMR spectrum of (*rac*)-methyl (*Z*)-3-(3-((*tert*-butyldimethylsilyl)oxy)butanamido)but-2-enoate (**259**).

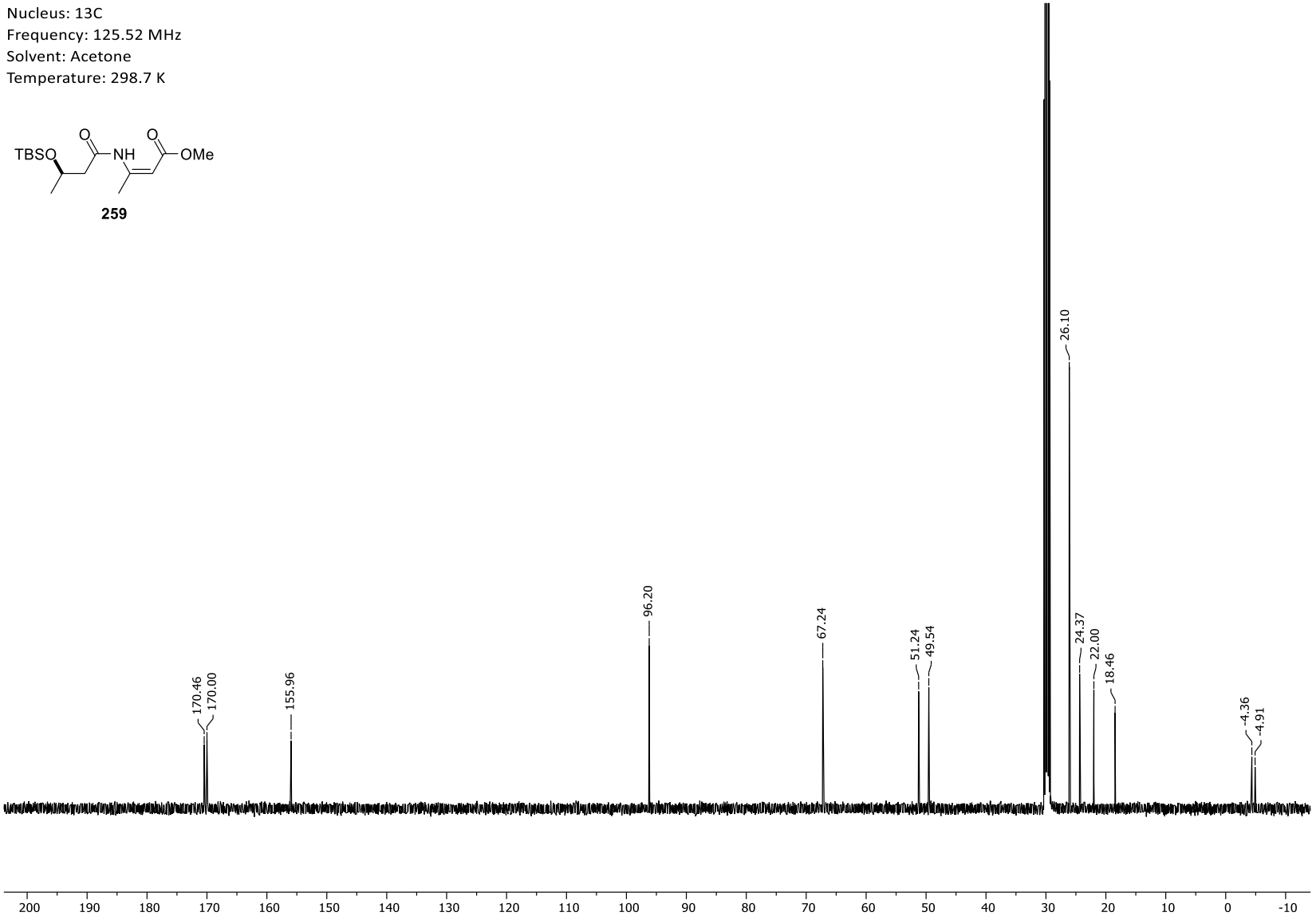

Appendix 197. ^{13}C-NMR spectrum of (*rac*)-methyl (*Z*)-3-(3-((*tert*-butyldimethylsilyl)oxy)butanamido)but-2-enoate (**259**).

Nucleus: 1H
Frequency: 499.13 MHz
Solvent: Acetone
Temperature: 298.0 K

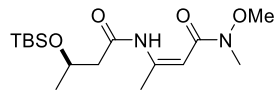

261

Appendix 198. ^{1}H-NMR spectrum of (*rac*)-(*Z*)-3-(3-((*tert*-butyldimethylsilyl)oxy)butanamido)-*N*-methoxy-*N*-methylbut-2-enamide (**261**).

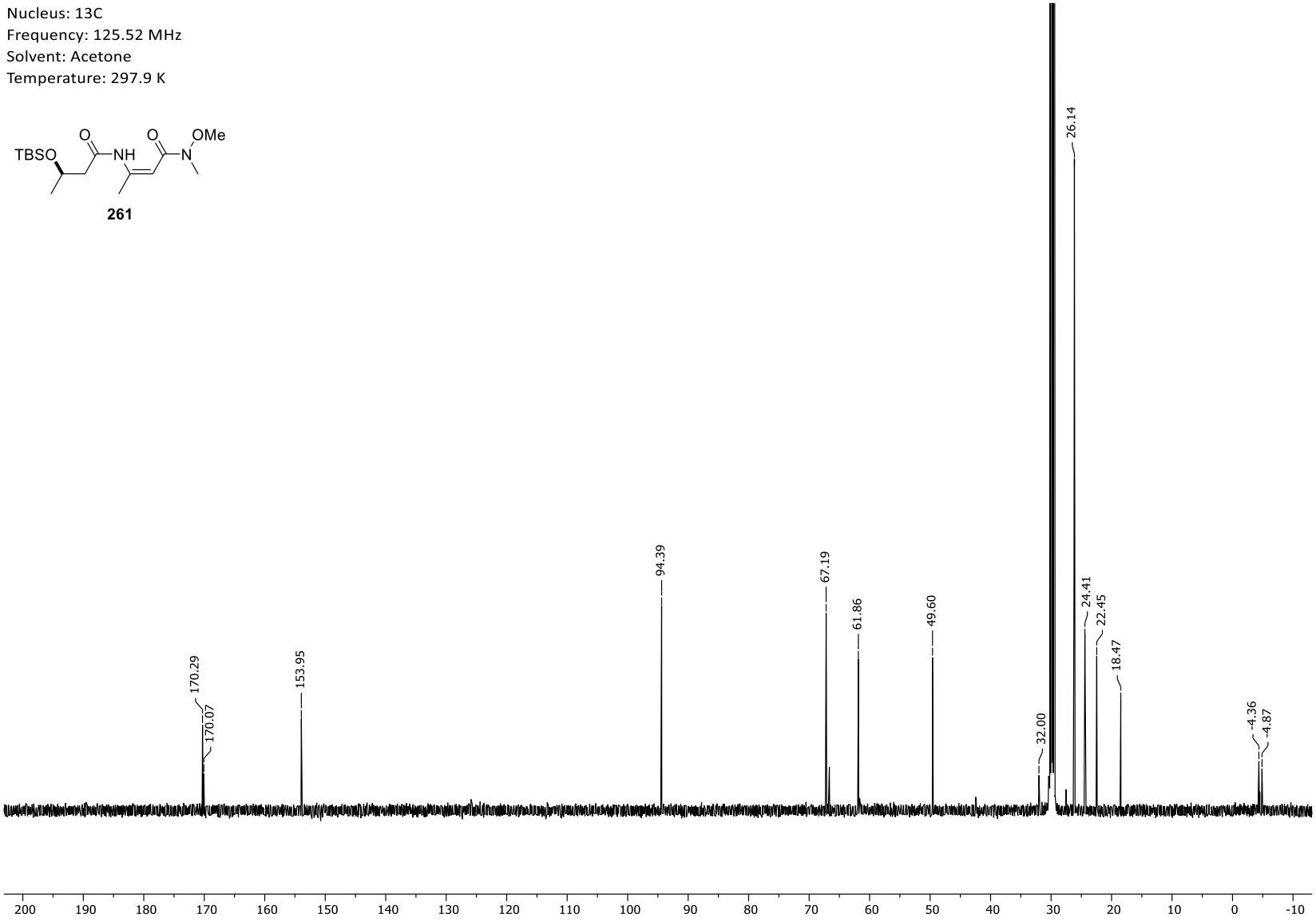

Appendix 199. ^{13}C-NMR spectrum of (*rac*)-(*Z*)-3-(3-((*tert*-butyldimethylsilyl)oxy)butanamido)-*N*-methoxy-*N*-methylbut-2-enamide (**261**).

Nucleus: 1H
Frequency: 499.13 MHz
Solvent: Acetone
Temperature: 298.0 K

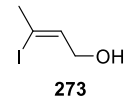

273

Appendix 200. ^{1}H-NMR spectrum of (*Z*)-3-iodobut-2-en-1-ol (**273**).

Nucleus: 13C
Frequency: 125.52 MHz
Solvent: Acetone
Temperature: 298.0 K

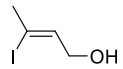

273

Appendix 201. ^{13}C-NMR spectrum of (*Z*)-3-iodobut-2-en-1-ol (**273**).

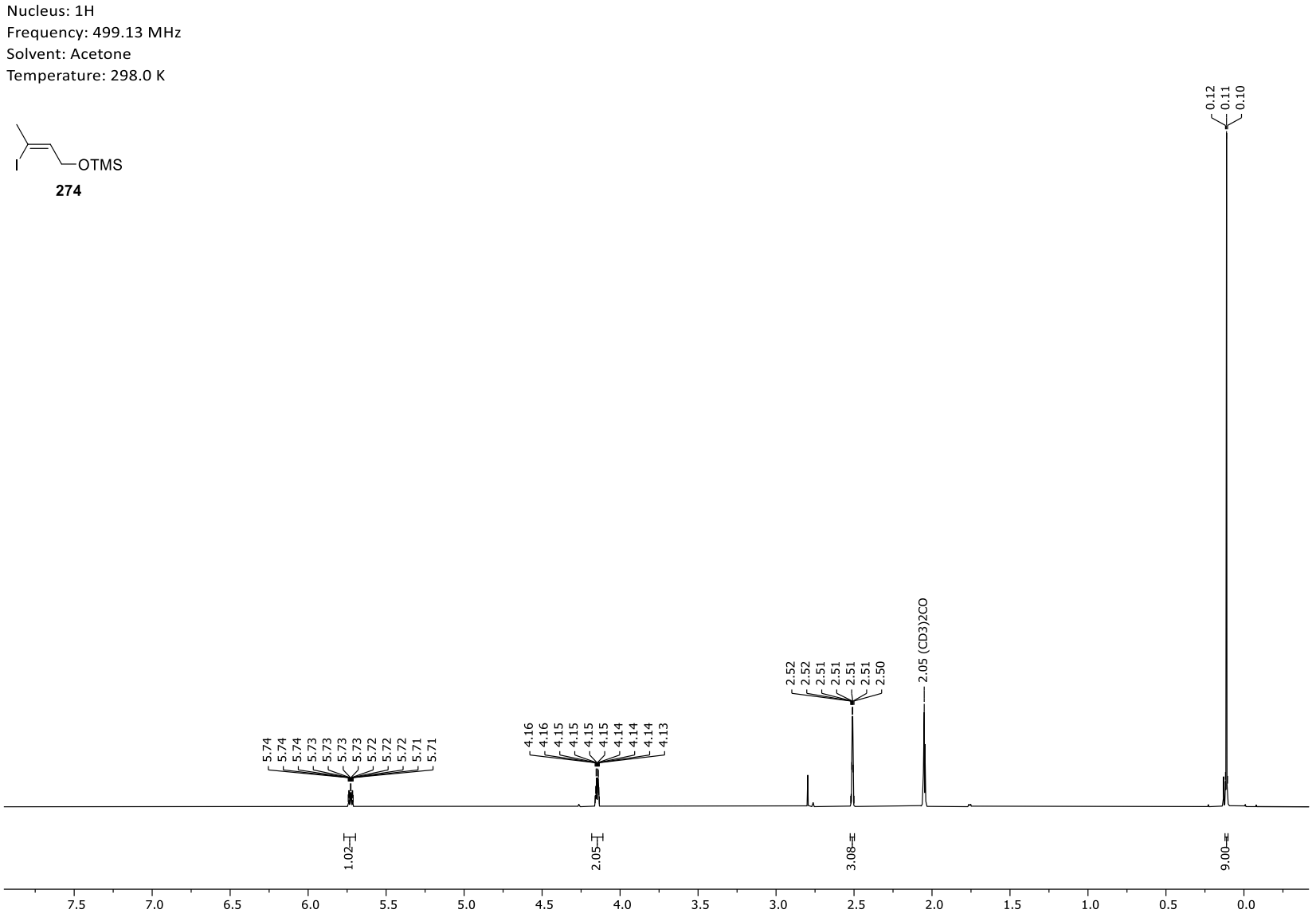

Appendix 202. ^{1}H-NMR spectrum of (*Z*)-((3-iodobut-2-en-1-yl)oxy)trimethylsilane (**274**).

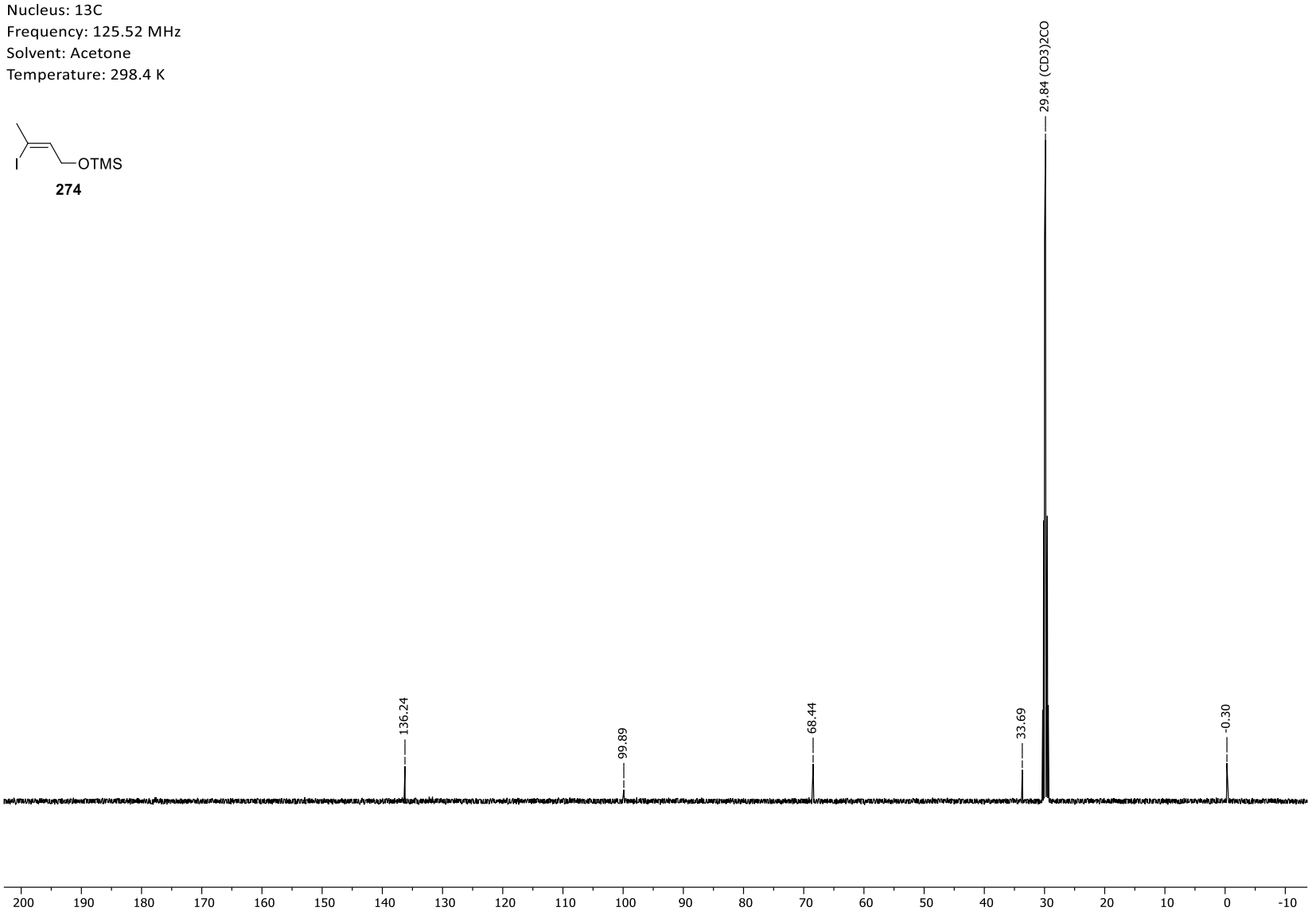

Appendix 203. ^{13}C-NMR spectrum of (*Z*)-((3-iodobut-2-en-1-yl)oxy)trimethylsilane (**274**).

Nucleus: 1H
Frequency: 499.13 MHz
Solvent: Acetone
Temperature: 298.0 K

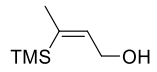

270

Appendix 204. ^{1}H-NMR spectrum of (*Z*)-3-(trimethylsilyl)but-2-en-1-ol (**270**).

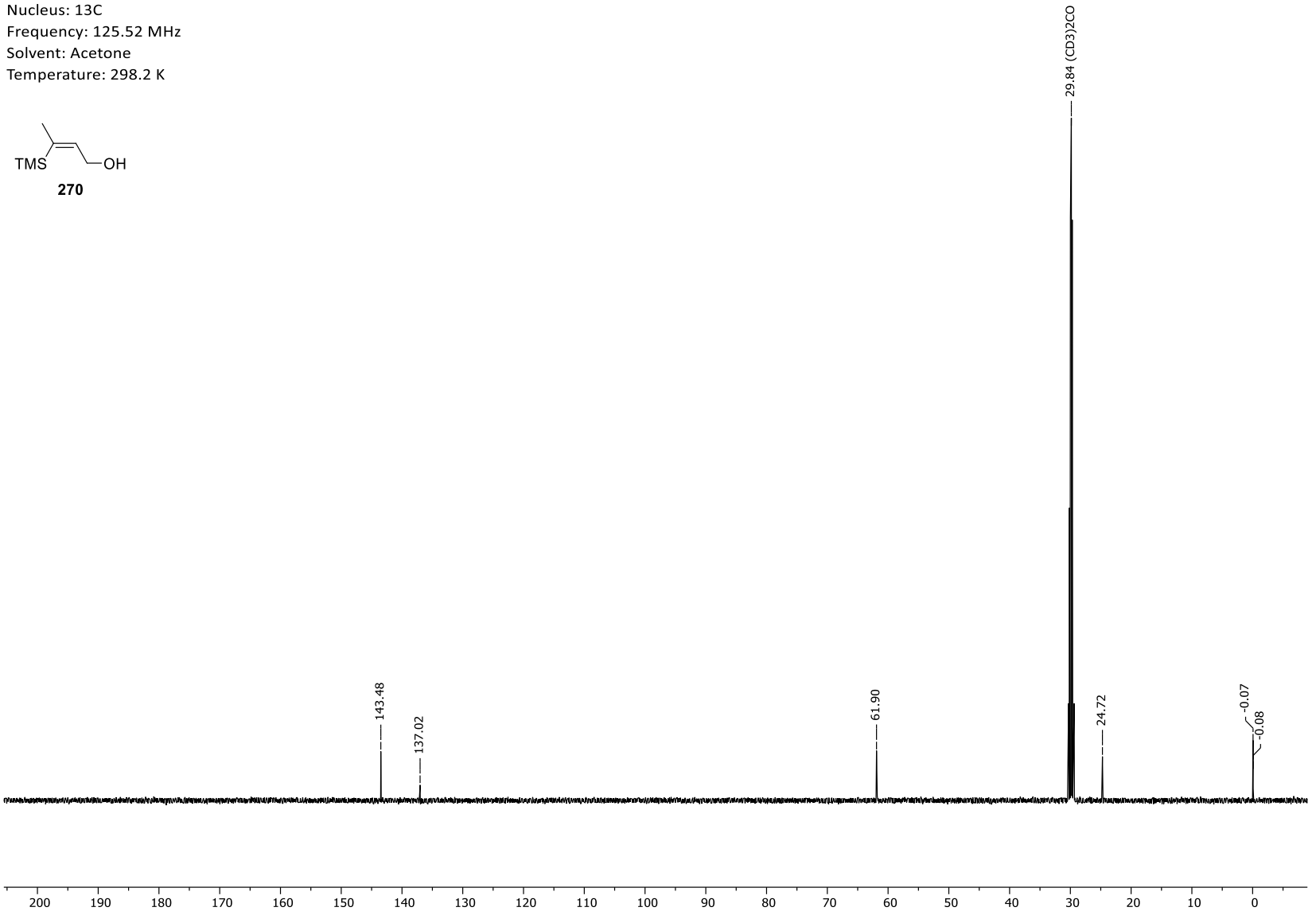

Appendix 205. ^{13}C-NMR spectrum of (*Z*)-3-(trimethylsilyl)but-2-en-1-ol (**270**).

Nucleus: 1H
Frequency: 499.96 MHz
Solvent: Acetone
Temperature: 298.0 K

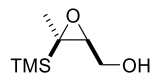

269

Appendix 206. ^{1}H-NMR spectrum of (2*S**,3*R**)-3-methyl-3-(trimethylsilyl)oxiran-2-yl)methanol (**269**).

Nucleus: 13C
Frequency: 125.73 MHz
Solvent: Acetone
Temperature: 298.0 K

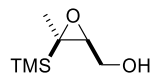

269

Appendix 207. ^{13}C-NMR spectrum of (2*S**,3*R**)-3-methyl-3-(trimethylsilyl)oxiran-2-yl)methanol (**269**).

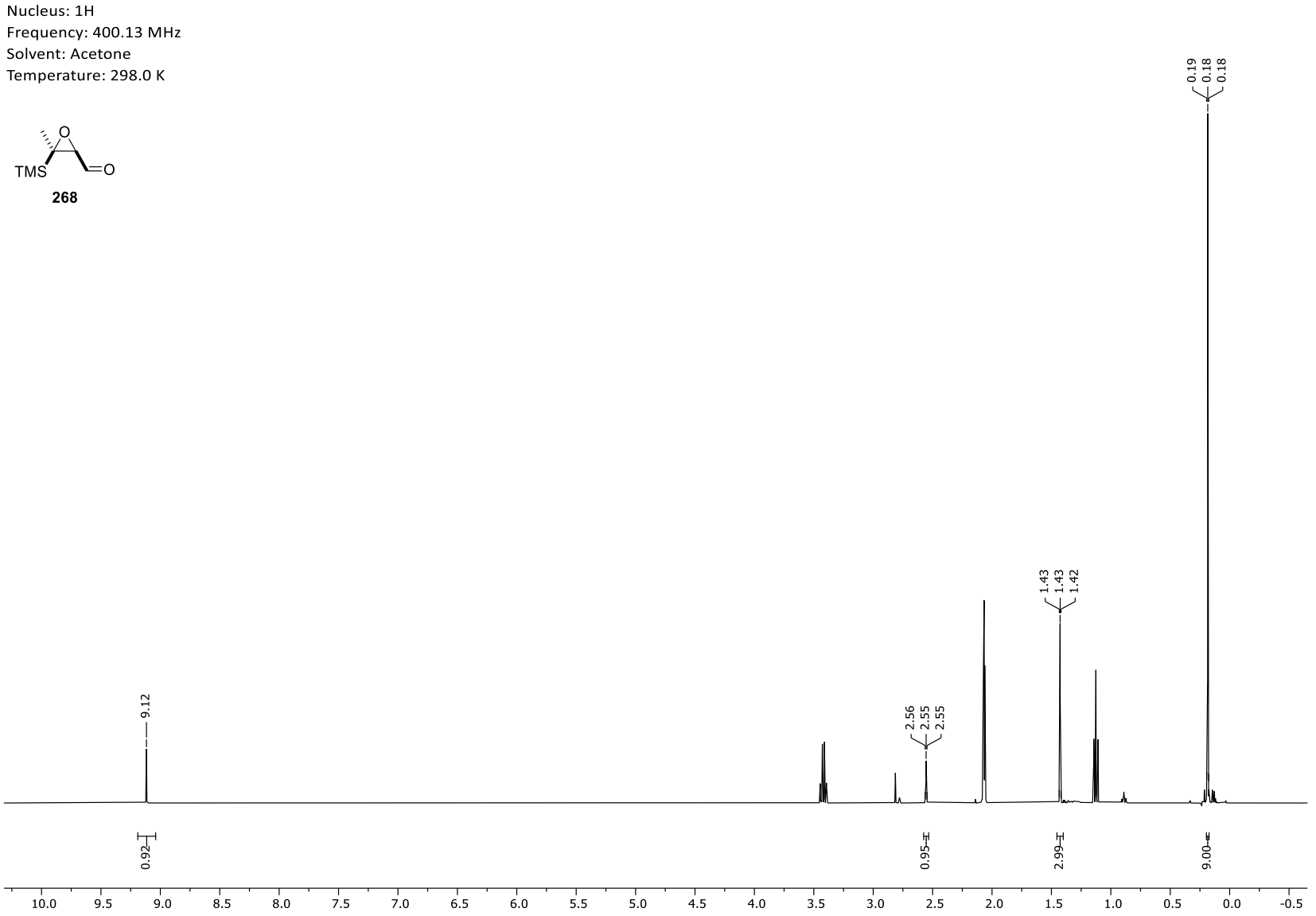

Appendix 208. ^{1}H-NMR spectrum of (2*S**,3*R**)-3-methyl-3-(trimethylsilyl)oxirane-2-carbaldehyde (**268**).

Nucleus: 1H
Frequency: 499.13 MHz
Solvent: Acetone
Temperature: 298.0 K

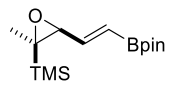

267

Appendix 209. ^{1}H-NMR spectrum of trimethyl((2*R**,3*S**)-2-methyl-3-((*E*)-2-(4,4,5,5-tetramethyl-1,3,2-dioxaborolan-2-yl)vinyl)oxiran-2-yl)silane (**267**).

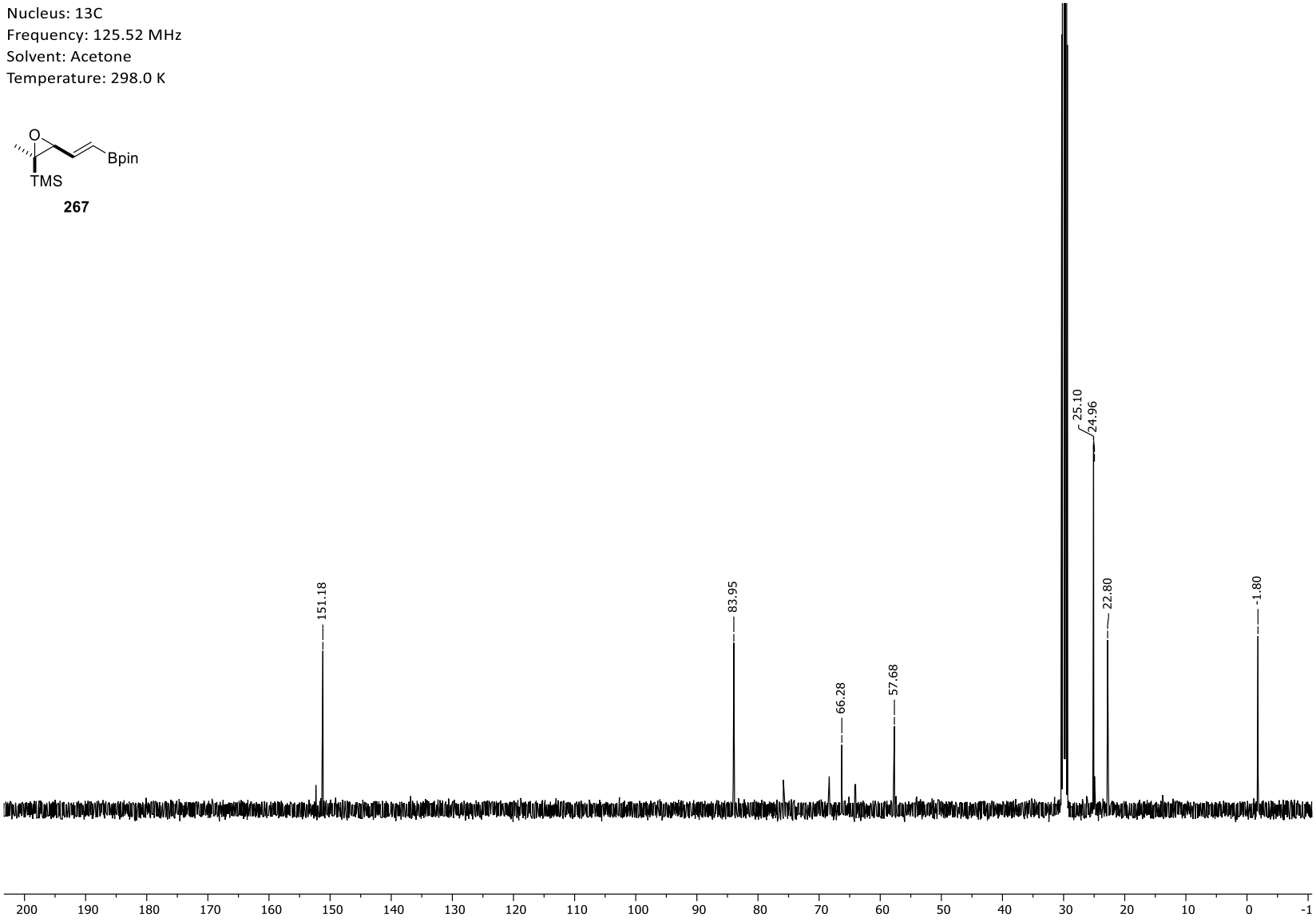

Appendix 210. ^{13}C-NMR spectrum of trimethyl((2*R**,3*S**)-2-methyl-3-((*E*)-2-(4,4,5,5-tetramethyl-1,3,2-dioxaborolan-2-yl)vinyl)oxiran-2-yl)silane (**267**).

Nucleus: 1H
Frequency: 499.13 MHz
Solvent: Acetone
Temperature: 297.9 K

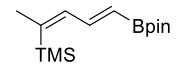

278

Appendix 211. ^{1}H-NMR spectrum of trimethyl((2*Z*,4*E*)-5-(4,4,5,5-tetramethyl-1,3,2-dioxaborolan-2-yl)penta-2,4-dien-2-yl)silane (**278**).

Nucleus: 13C
Frequency: 125.52 MHz
Solvent: Acetone
Temperature: 297.8 K

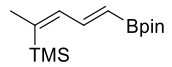

278

Appendix 212. ^{13}C-NMR spectrum of trimethyl((2*Z*,4*E*)-5-(4,4,5,5-tetramethyl-1,3,2-dioxaborolan-2-yl)penta-2,4-dien-2-yl)silane (**278**).

Nucleus: 1H
Frequency: 499.96 MHz
Solvent: Acetone
Temperature: 298.0 K

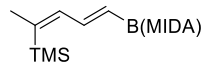

279

Appendix 213. ^{1}H-NMR spectrum of trimethyl((2*Z*,4*E*)-5-(1,3,6,2-dioxazaborocane-4,8-dione-2-yl)penta-2,4-dien-2-yl)silane (**279**).

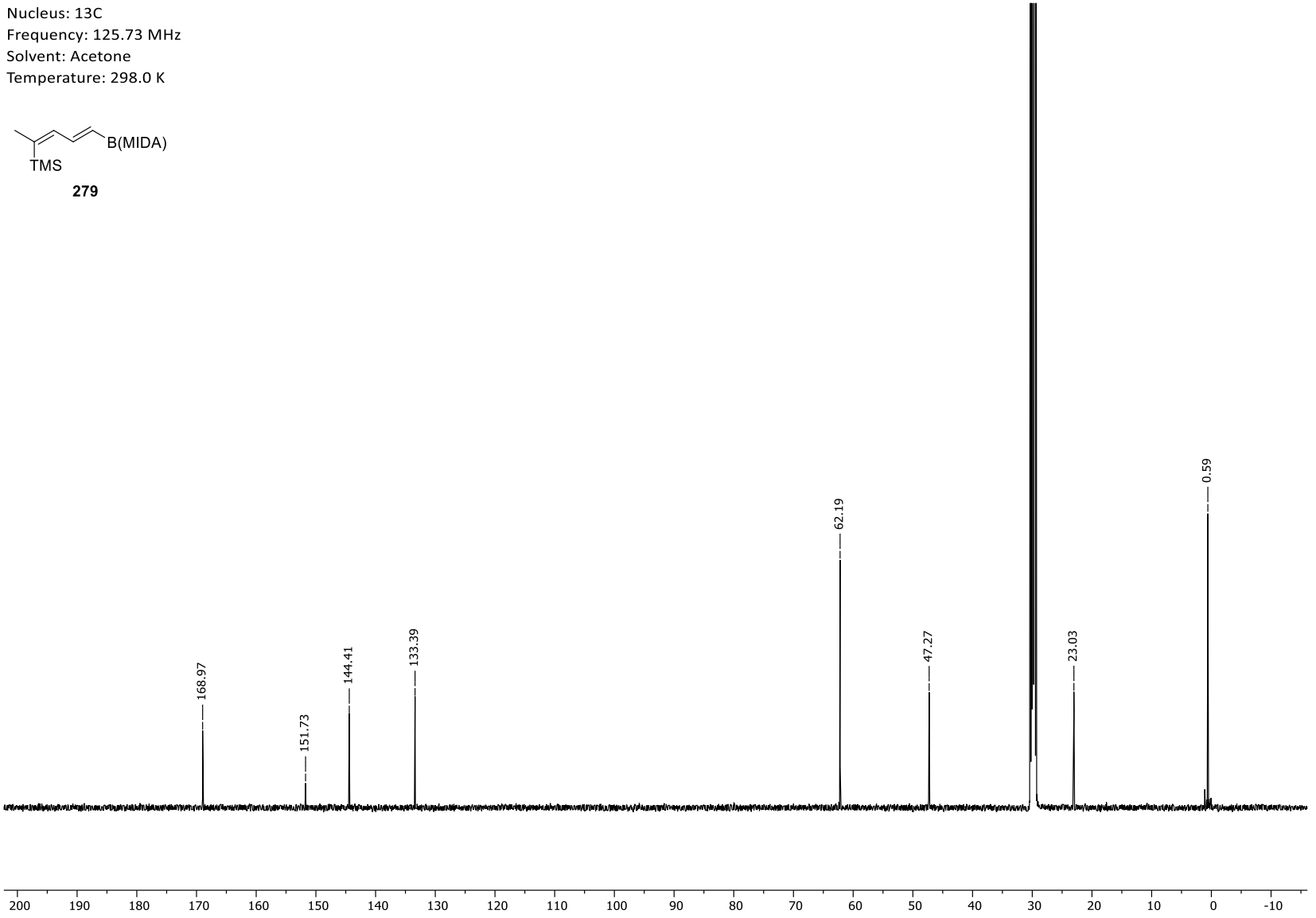

Appendix 214. ^{13}C-NMR spectrum of trimethyl((2*Z*,4*E*)-5-(1,3,6,2-dioxazaborocane-4,8-dione-2-yl)penta-2,4-dien-2-yl)silane (**279**).

Nucleus: 1H
Frequency: 499.96 MHz
Solvent: Acetone
Temperature: 298.0 K

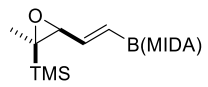

266

Appendix 215. ^{1}H-NMR spectrum of trimethyl((2*Z*,4*E*)-5-(1,3,6,2-dioxazaborocane-4,8-dione-2-yl)vinyl)oxiran-2-yl)silane (**266**).

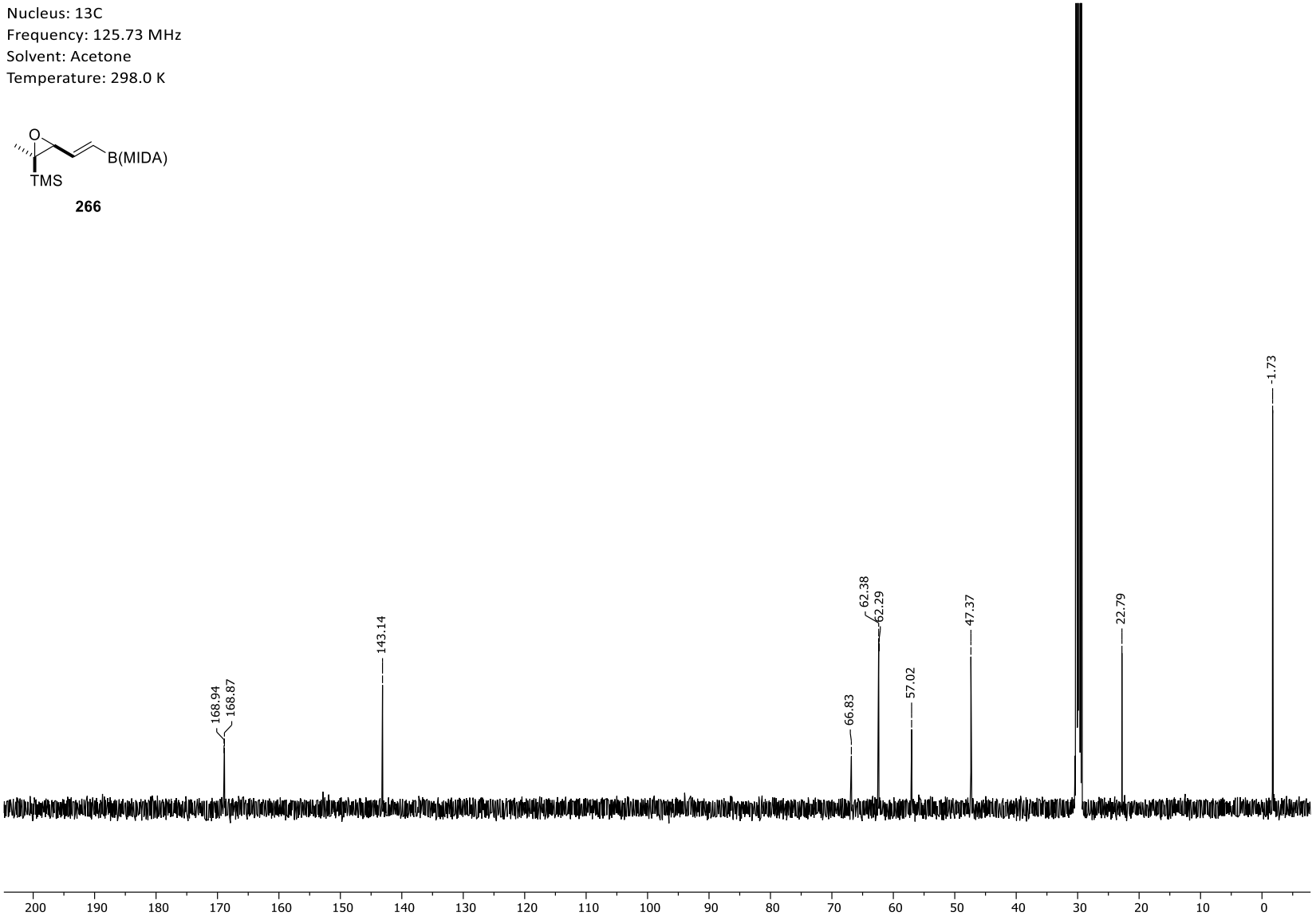

Appendix 216. ^{13}C-NMR spectrum of trimethyl((2*Z*,4*E*)-5-(1,3,6,2-dioxazaborocane-4,8-dione-2-yl)vinyl)oxiran-2-yl)silane (**266**).

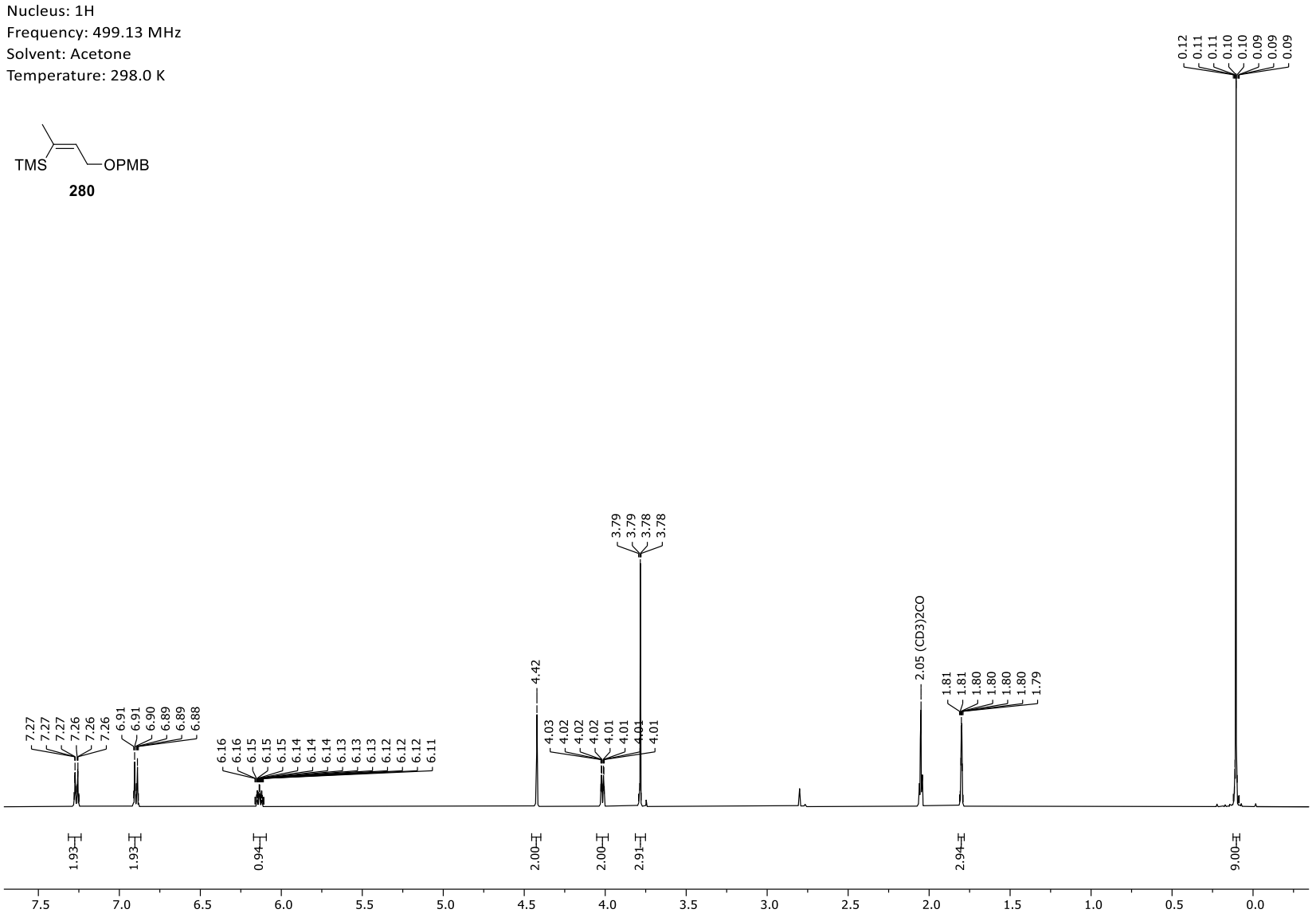

Appendix 217. ^{1}H-NMR spectrum of (*Z*)-(4-((4-methoxybenzyl)oxy)but-2-en-2-yl)trimethylsilane (**280**).

Nucleus: 13C
Frequency: 125.52 MHz
Solvent: Acetone
Temperature: 298.0 K

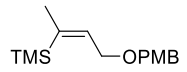

280

Appendix 218. ^{13}C-NMR spectrum of (*Z*)-(4-((4-methoxybenzyl)oxy)but-2-en-2-yl)trimethylsilane (**280**).

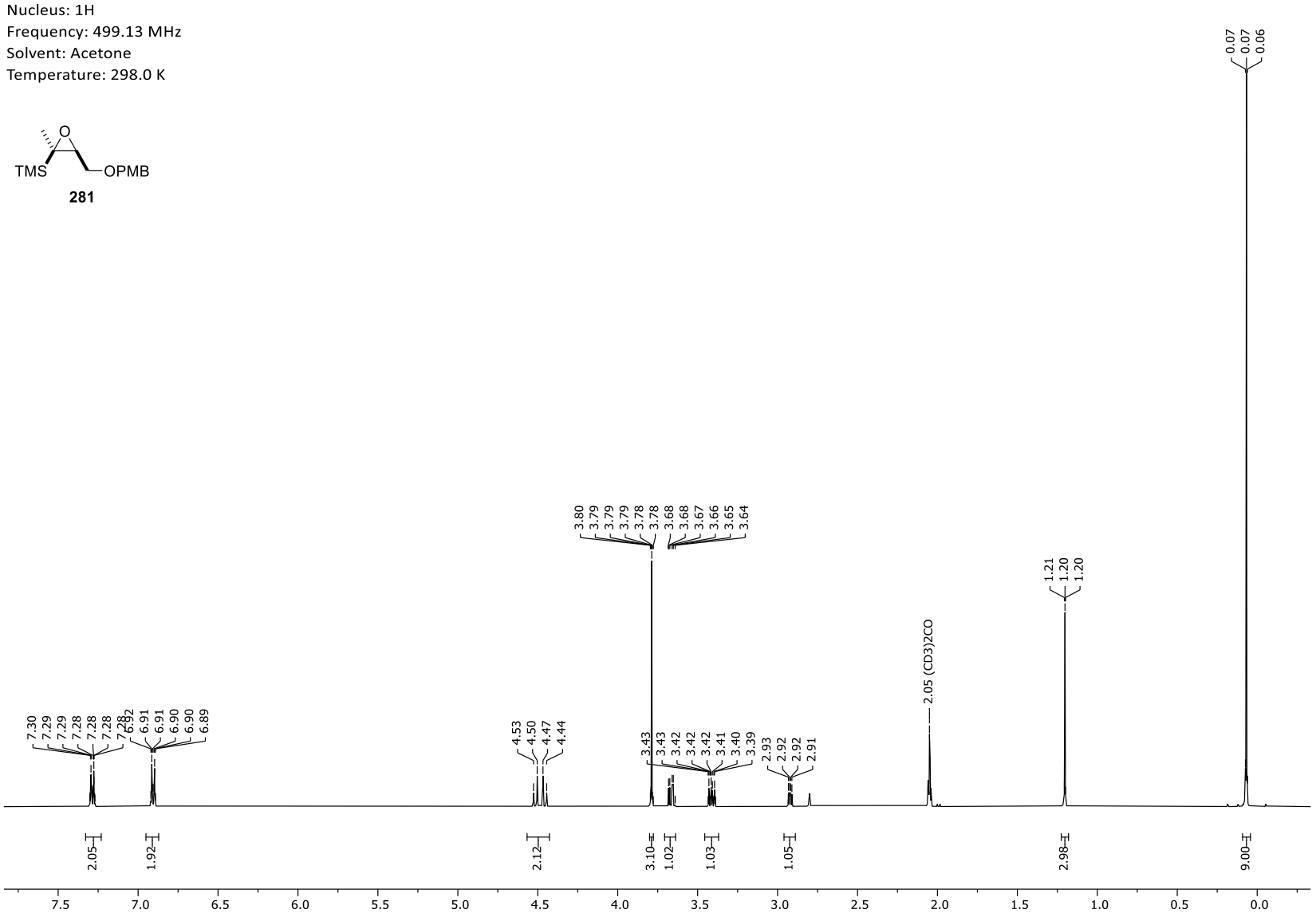

Appendix 219. ^{1}H-NMR spectrum of ((2*R**,3*S**)-3-(((4-methoxybenzyl)oxy)methyl)-2-methyloxiran-2-yl)trimethylsilane (**281**).

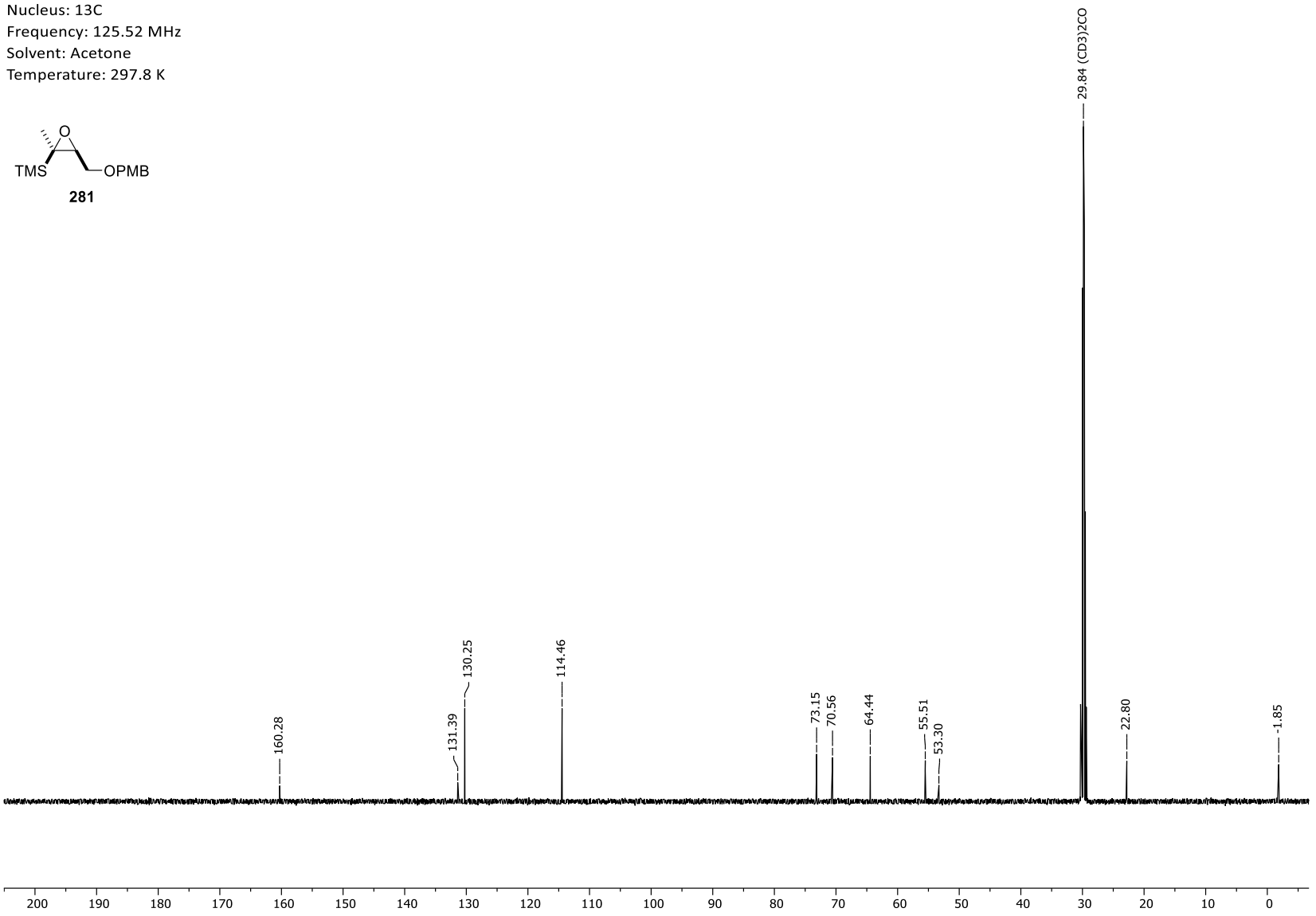

Appendix 220. ^{13}C-NMR spectrum of ((2*R**,3*S**)-3-(((4-methoxybenzyl)oxy)methyl)-2-methyloxiran-2-yl)trimethylsilane (**281**).

Nucleus: 1H
Frequency: 499.13 MHz
Solvent: Acetone
Temperature: 298.5 K

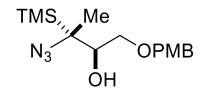

282

Appendix 221. ^{1}H-NMR spectrum of (2*R**,3*R**)-3-azido-1-((4-methoxybenzyl)oxy)-3-(trimethylsilyl)butan-2-ol (**282**).

Nucleus: 13C
Frequency: 125.52 MHz
Solvent: Acetone
Temperature: 298.9 K

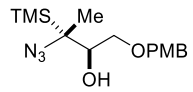

282

Appendix 222. ^{13}C-NMR spectrum of (2*R**,3*R**)-3-azido-1-((4-methoxybenzyl)oxy)-3-(trimethylsilyl)butan-2-ol (**282**).

Nucleus: 1H
Frequency: 499.13 MHz
Solvent: Acetone
Temperature: 298.0 K

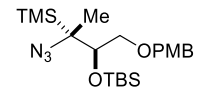

283

Appendix 223. ^{1}H-NMR spectrum of (((2*R**,3*R**)-3-azido-1-((4-methoxybenzyl)oxy)-3-(trimethylsilyl)butan-2-yl)oxy)(tert-butyl) dimethylsilane (**283**).

Nucleus: 13C
Frequency: 125.52 MHz
Solvent: Acetone
Temperature: 298.0 K

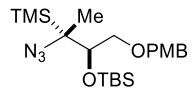

283

Appendix 224. ^{13}C-NMR spectrum of (((2*R**,3*R**)-3-azido-1-((4-methoxybenzyl)oxy)-3-(trimethylsilyl)butan-2-yl)oxy)(tert-butyl) dimethylsilane (**283**).

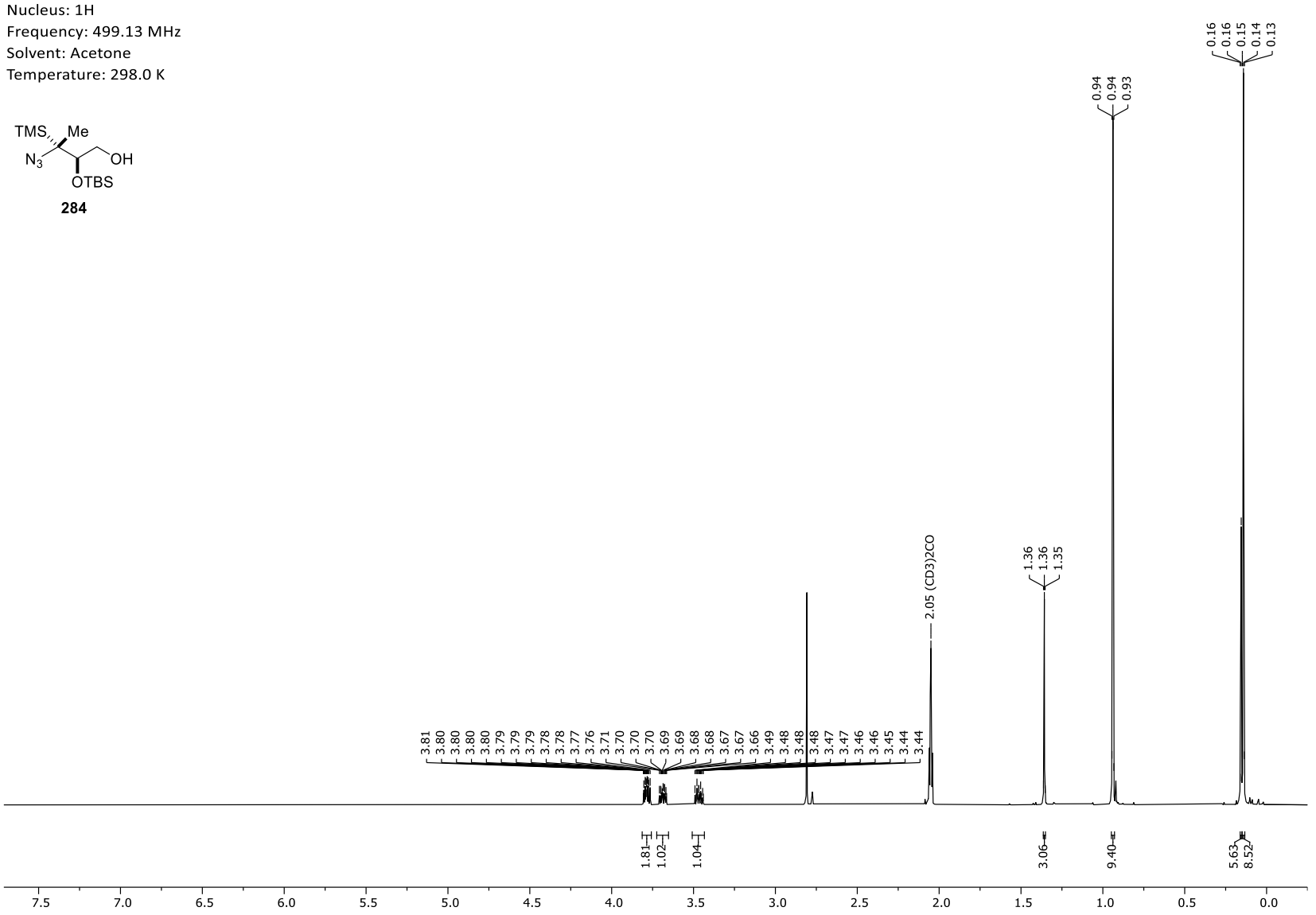

Appendix 225. ^{1}H-NMR spectrum of (2*R**,3*R**)-3-azido-2-((*tert*-butyldimethylsilyl)oxy)-3-(trimethylsilyl)butan-1-ol (**284**).

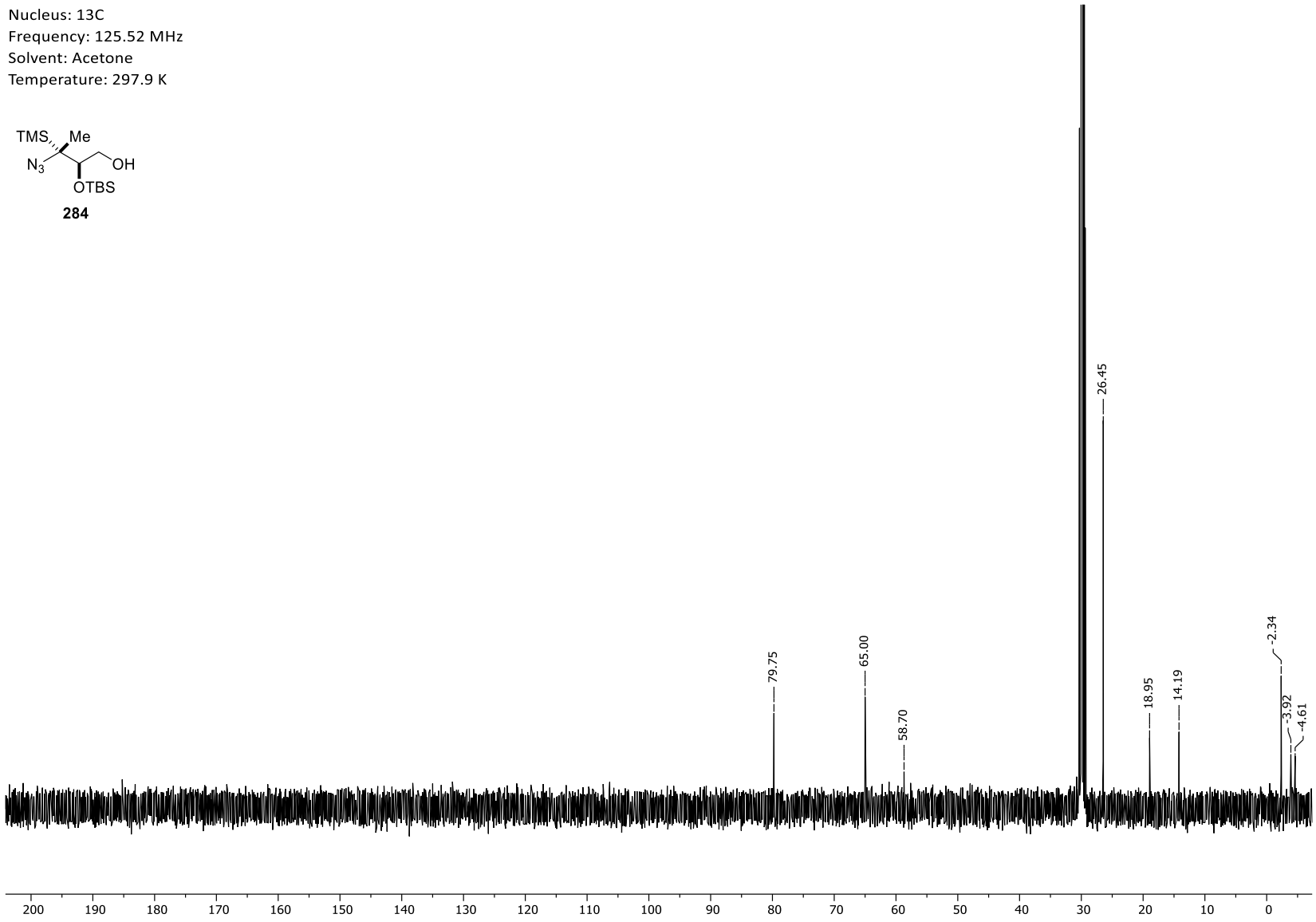

Appendix 226. ^{13}C-NMR spectrum of (2*R**,3*R**)-3-azido-2-((*tert*-butyldimethylsilyl)oxy)-3-(trimethylsilyl)butan-1-ol (**284**).

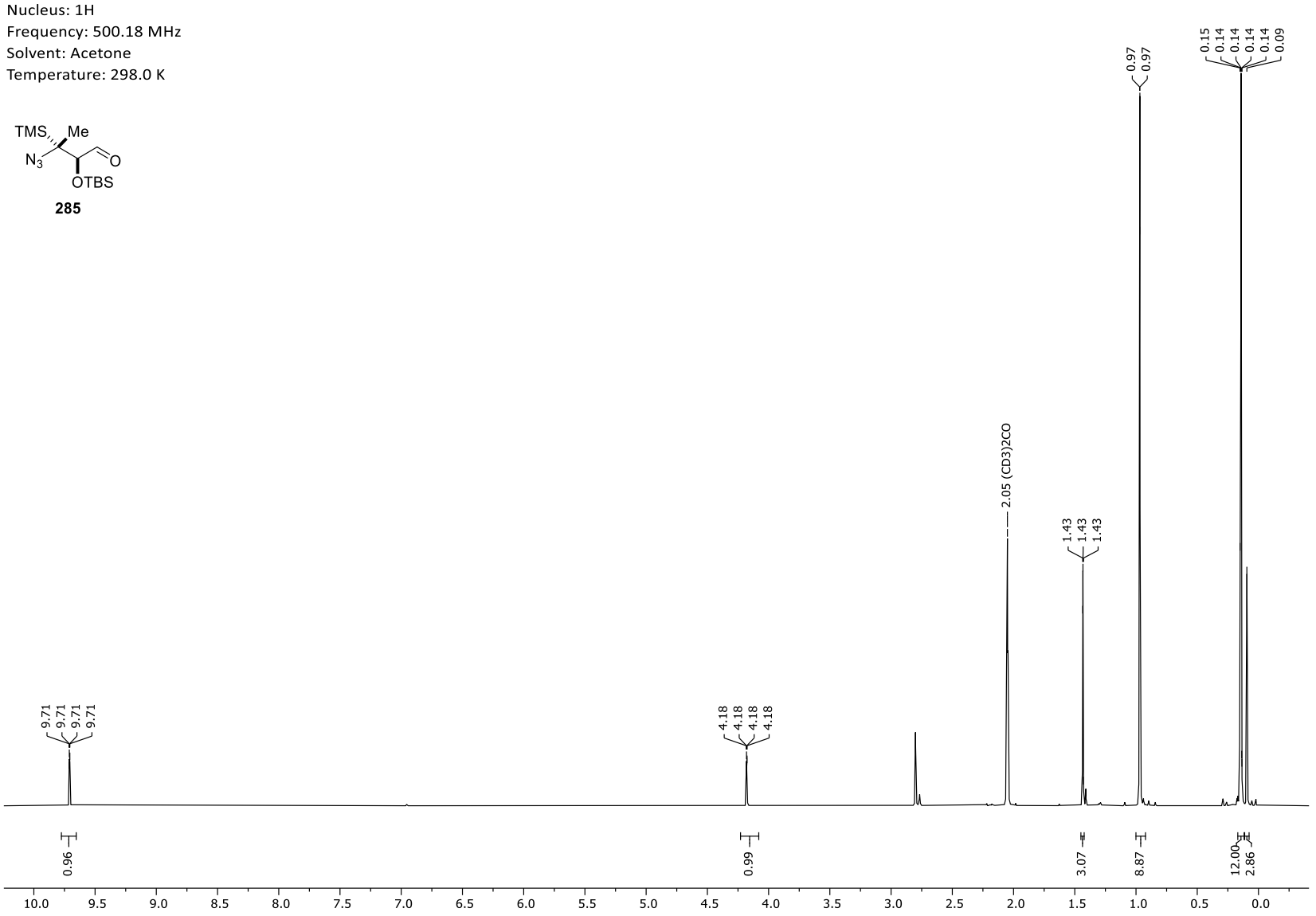

Appendix 227. ^{1}H-NMR spectrum of (2*R**,3*R**)-3-azido-2-((*tert*-butyldimethylsilyl)oxy)-3-(trimethylsilyl)butanal (**285**).

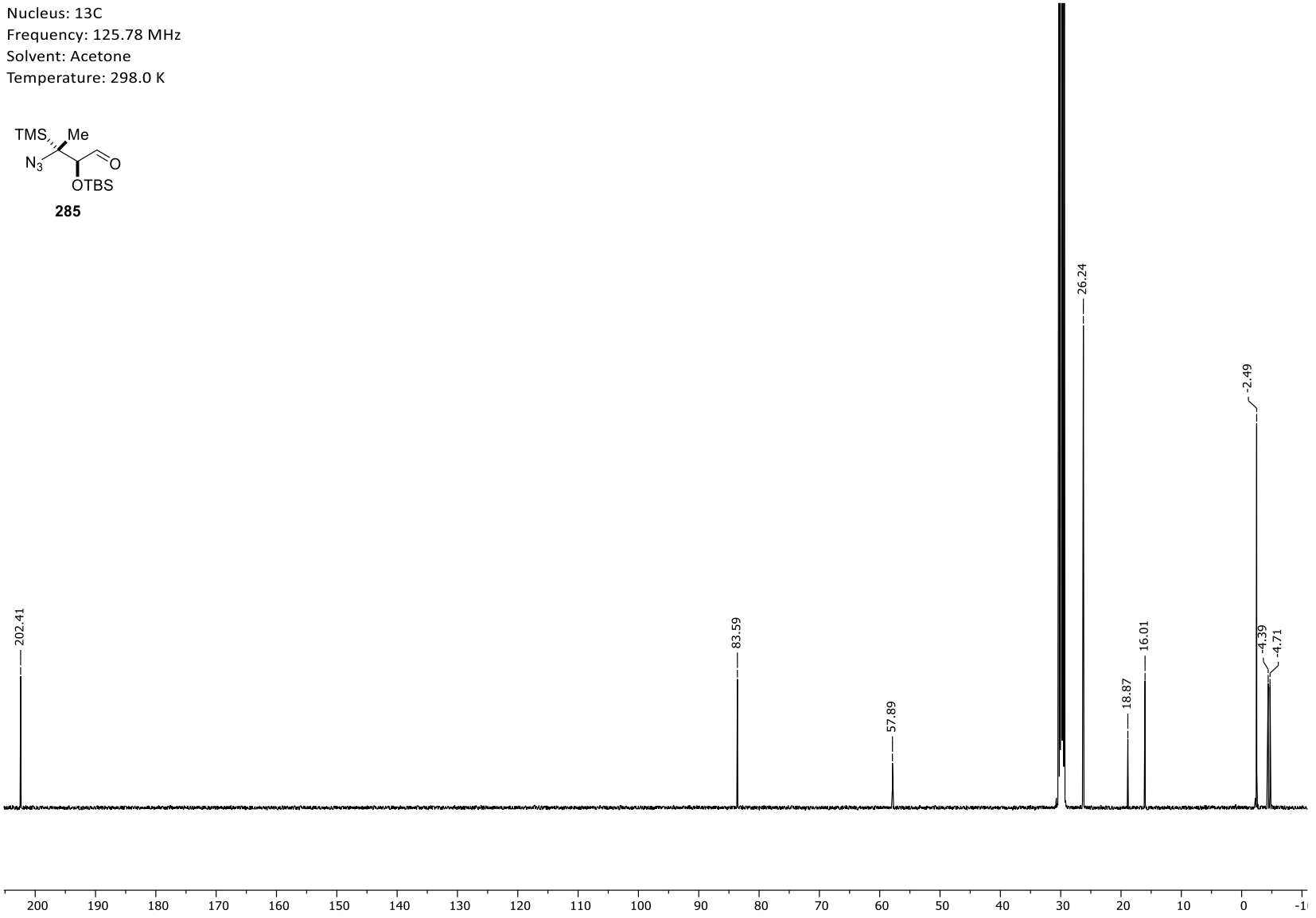

Appendix 228. ^{13}C-NMR spectrum of (2*R**,3*R**)-3-azido-2-((*tert*-butyldimethylsilyl)oxy)-3-(trimethylsilyl)butanal (**285**).

Nucleus: 1H
Frequency: 700.41 MHz
Solvent: Acetone
Temperature: 298.0 K

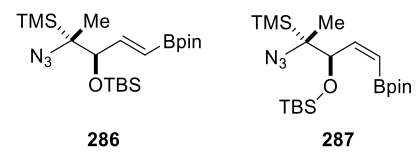

286

287

Appendix 229. ^{1}H-NMR spectrum of boronate **286** – major (*E*)-isomer picked.

Nucleus: 13C
Frequency: 176.14 MHz
Solvent: Acetone
Temperature: 298.0 K

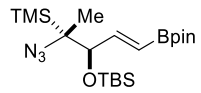

286

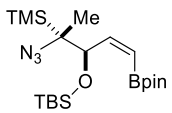

287

Appendix 230. ^{13}C-NMR spectrum of boronate **286** – major (*E*)-isomer picked.

Nucleus: 1H
Frequency: 500.18 MHz
Solvent: Acetone
Temperature: 298.0 K

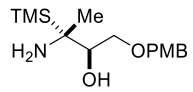

291

Appendix 231. ^{1}H-NMR spectrum of (2*R**,3*R**)-3-amino-1-((4-methoxybenzyl)oxy)-3-(trimethylsilyl)butan-2-ol (**291**).

Nucleus: 13C
Frequency: 125.78 MHz
Solvent: Acetone
Temperature: 298.0 K

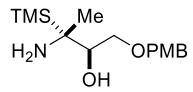

291

Appendix 232. ^{13}C-NMR spectrum of (2*R**,3*R**)-3-amino-1-((4-methoxybenzyl)oxy)-3-(trimethylsilyl)butan-2-ol (**291**).

Nucleus: 1H
Frequency: 700.41 MHz
Solvent: Acetone
Temperature: 298.0 K

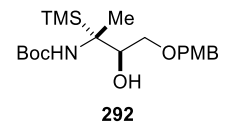

292

Appendix 233. ^{1}H-NMR spectrum of *tert*-butyl ((2*R**,3*R**)-3-hydroxy-4-((4-methoxybenzyl)oxy)-2-(trimethylsilyl)butan-2-yl)carbamate (**292**).

Nucleus: 13C
Frequency: 176.14 MHz
Solvent: Acetone
Temperature: 298.0 K

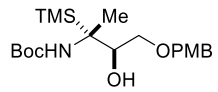

292

Appendix 234. ^{13}C-NMR spectrum of *tert*-butyl ((2*R**,3*R**)-3-hydroxy-4-((4-methoxybenzyl)oxy)-2-(trimethylsilyl)butan-2-yl)carbamate (**292**).

Nucleus: 1H
Frequency: 500.18 MHz
Solvent: Acetone
Temperature: 298.0 K

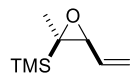

300

Appendix 235. ^{1}H-NMR spectrum of trimethyl((2*R**,3*S**)-2-methyl-3-vinyloxiran-2-yl)silane (**300**).

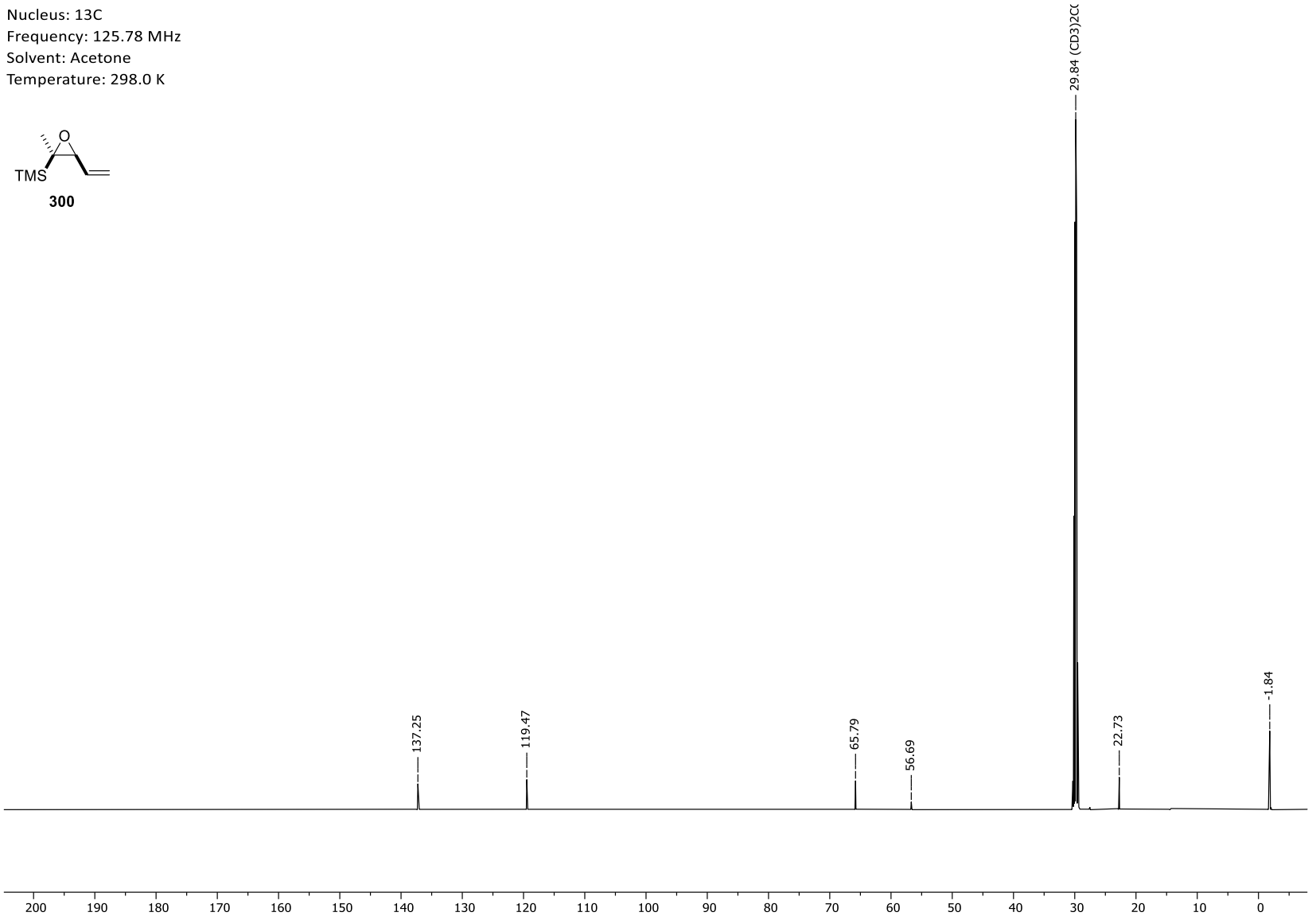

Appendix 236. ^{13}C-NMR spectrum of trimethyl((2*R**,3*S**)-2-methyl-3-vinyloxiran-2-yl)silane (**300**).

Nucleus: 1H
Frequency: 500.18 MHz
Solvent: Acetone
Temperature: 298.0 K

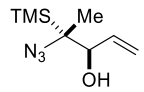

301

Appendix 237. ^{1}H-NMR spectrum of (3*R**,4*R**)-4-azido-4-(trimethylsilyl)pent-1-en-3-ol (**301**).

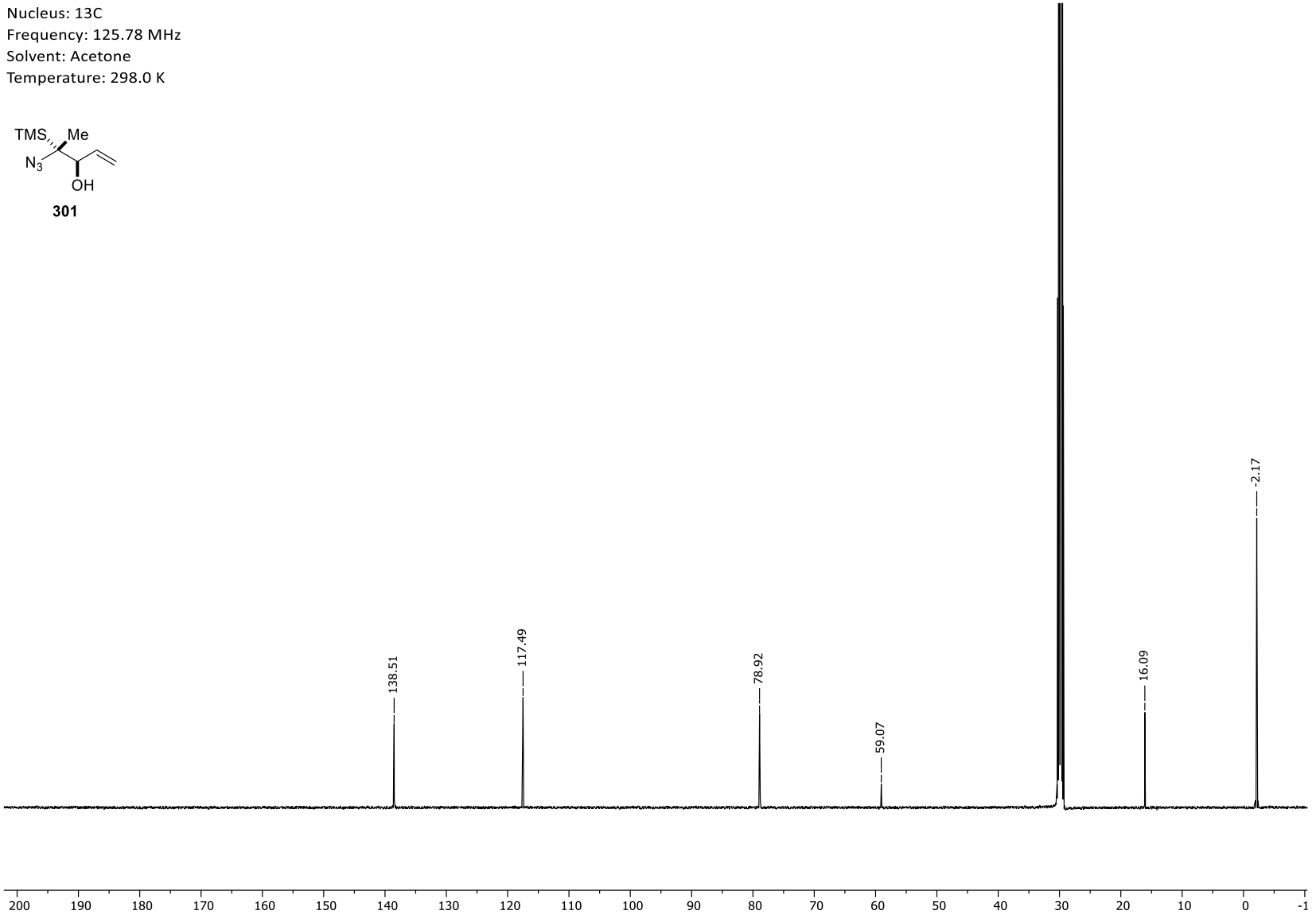

Appendix 238. ^{13}C-NMR spectrum of (3*R**,4*R**)-4-azido-4-(trimethylsilyl)pent-1-en-3-ol (**301**).

Nucleus: 1H
Frequency: 500.18 MHz
Solvent: Acetone
Temperature: 298.0 K

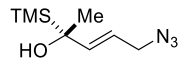

302

Appendix 239. ^{1}H-NMR spectrum of (*R**,*E*)-5-azido-2-(trimethylsilyl)pent-3-en-2-ol (**302**).

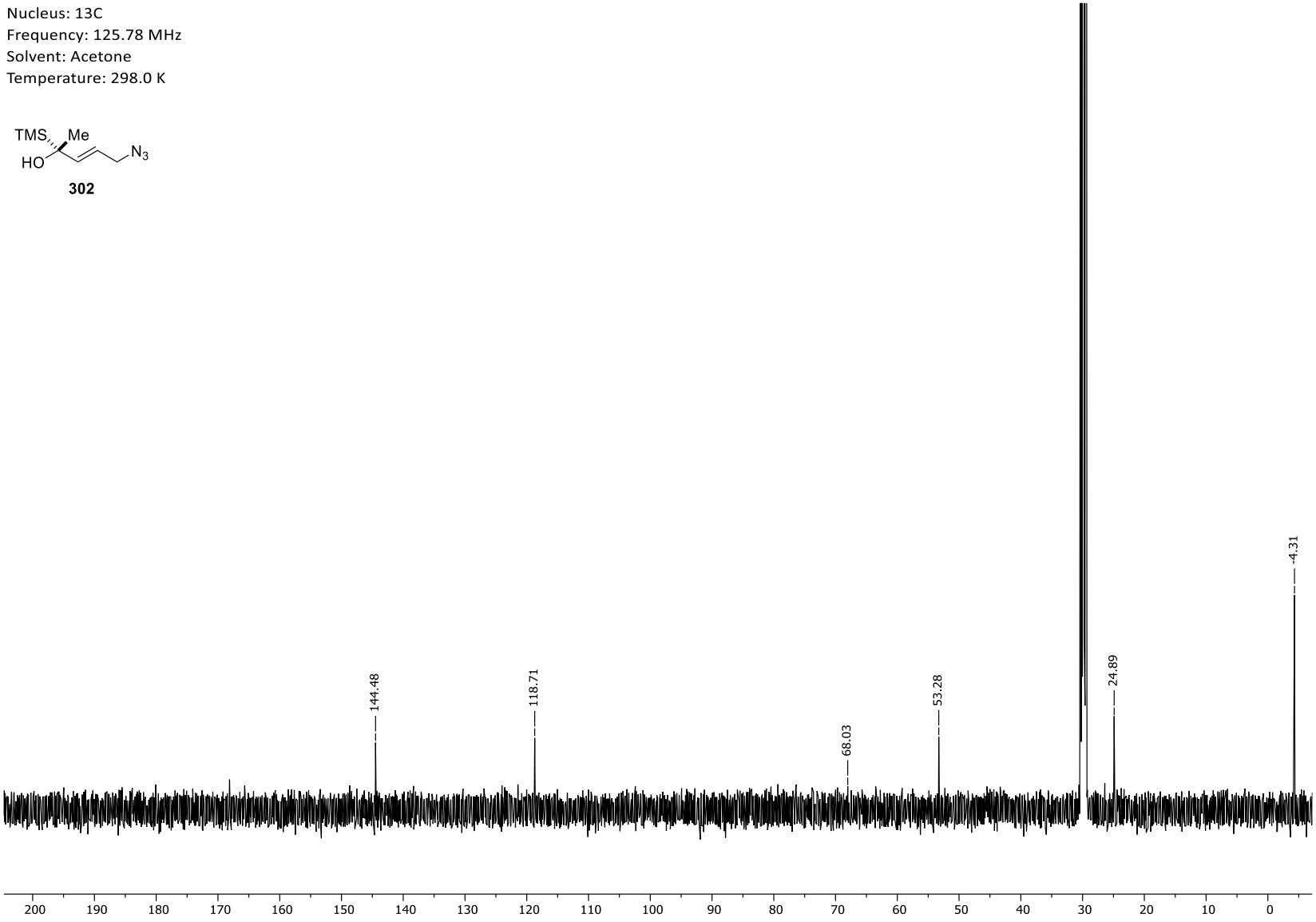

Appendix 240. ^{13}C-NMR spectrum of (*R**,*E*)-5-azido-2-(trimethylsilyl)pent-3-en-2-ol (**302**).

Nucleus: 1H
Frequency: 499.13 MHz
Solvent: Acetone
Temperature: 298.9 K

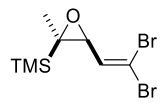

303

Appendix 241. ^{1}H-NMR spectrum of ((2*R**,3*S**)-3-(2,2-dibromovinyl)-2-methyloxiran-2-yl)trimethylsilane (**303**).

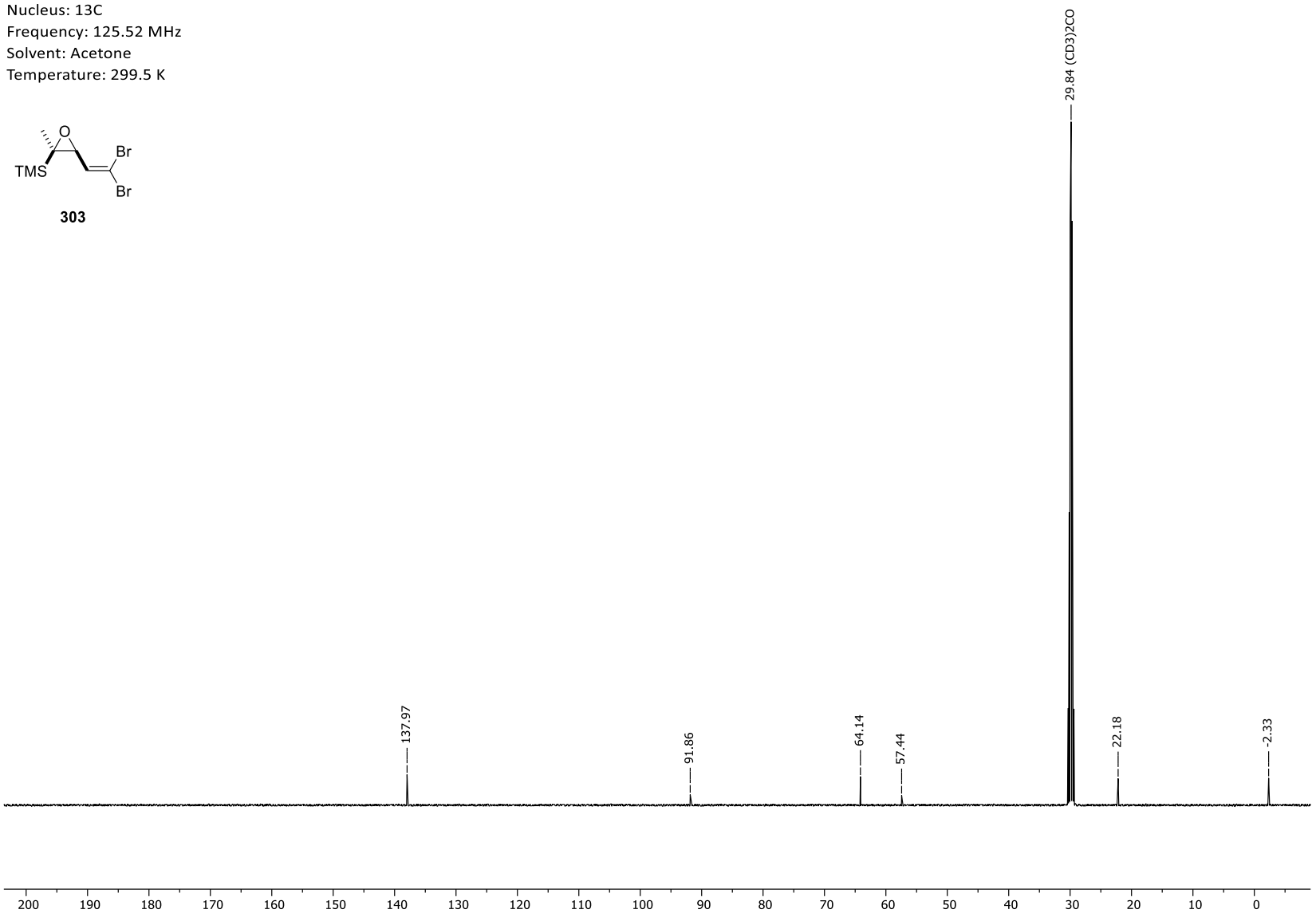

Appendix 242. ^{13}C-NMR spectrum of ((2*R**,3*S**)-3-(2,2-dibromovinyl)-2-methyloxiran-2-yl)trimethylsilane (**303**).

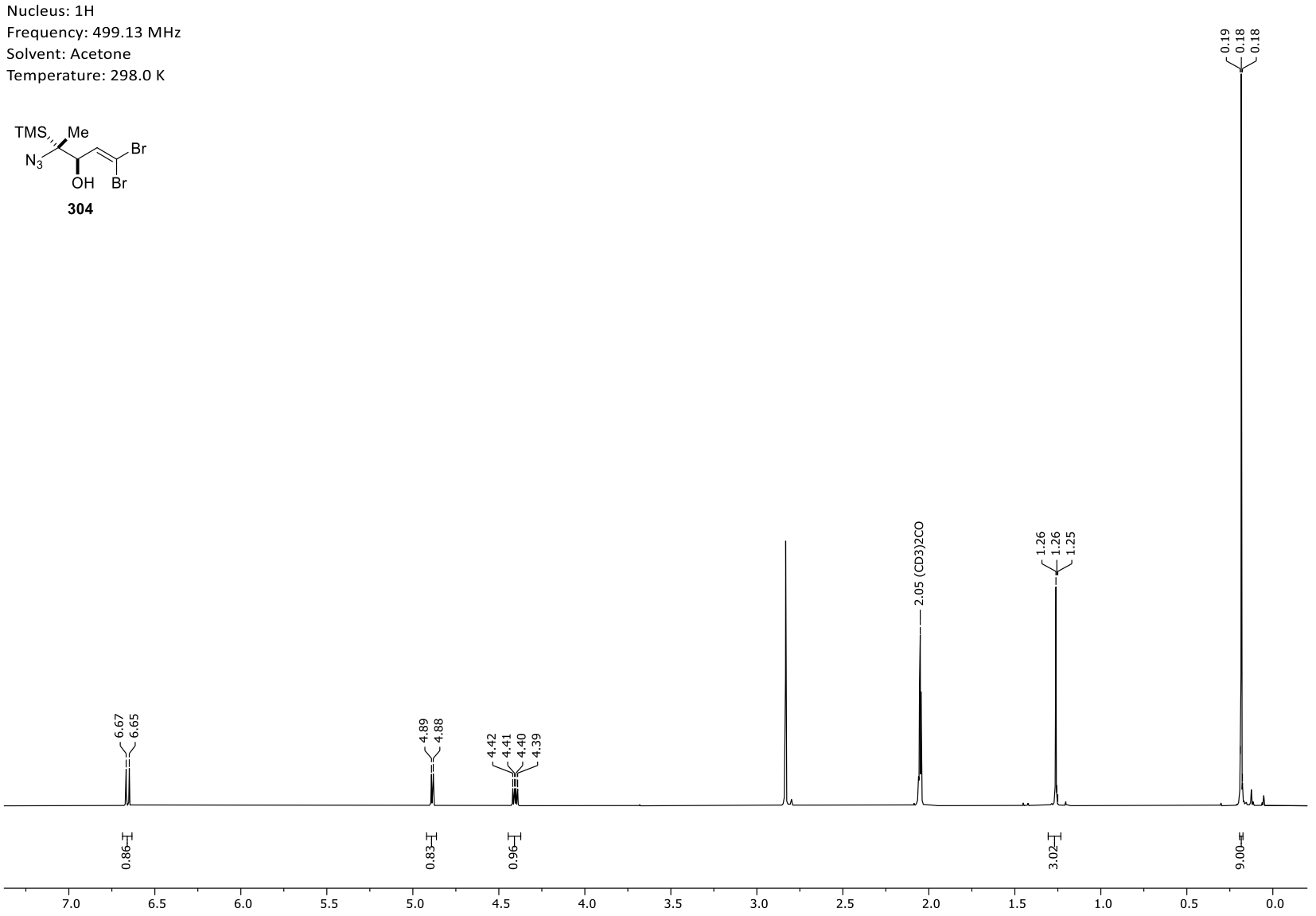

Appendix 243. ^{1}H-NMR spectrum of (3*R**,4*R**)-4-azido-1,1-dibromo-4-(trimethylsilyl)pent-1-en-3-ol (**304**).

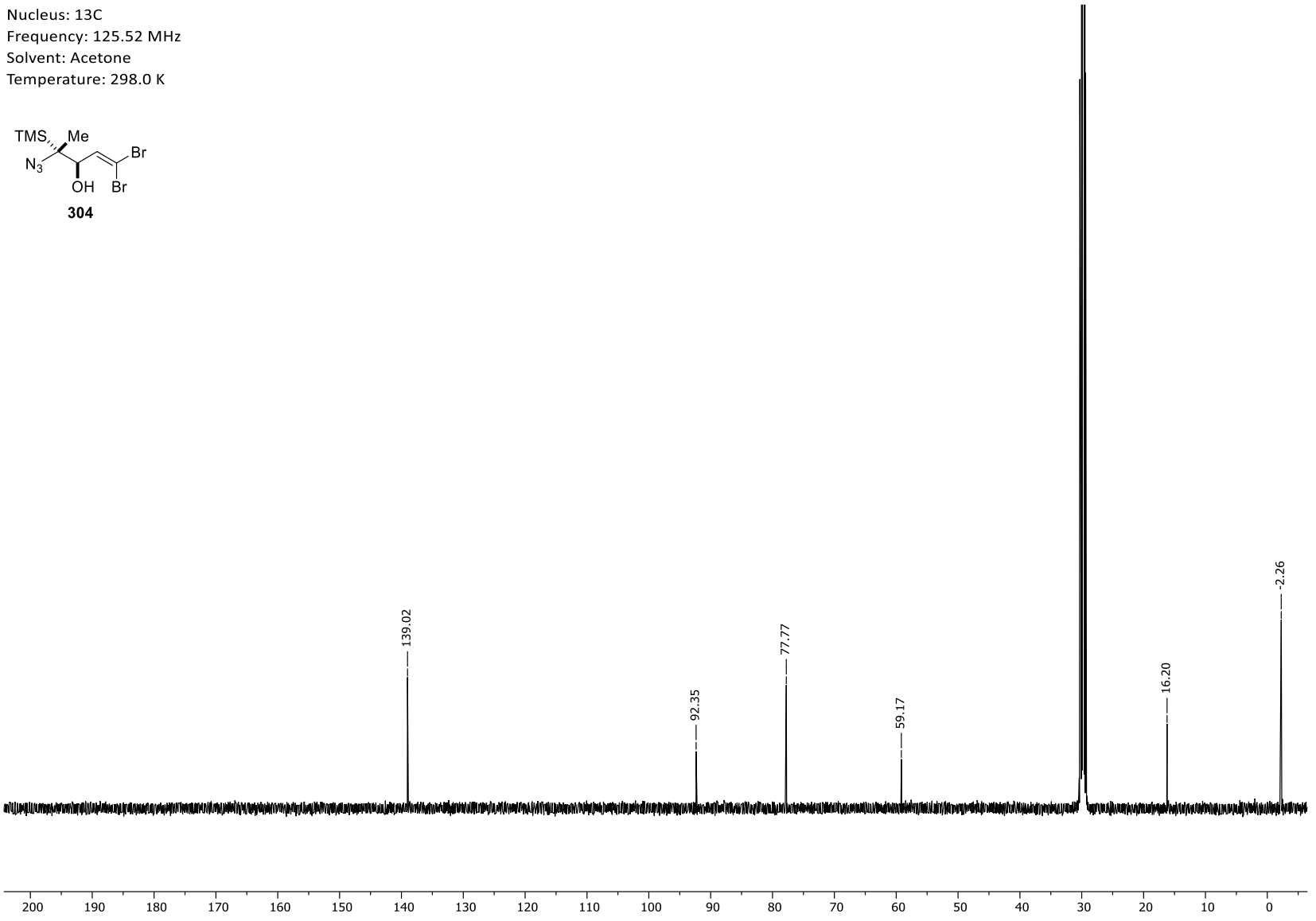

Appendix 244. ^{13}C-NMR spectrum of (3*R**,4*R**)-4-azido-1,1-dibromo-4-(trimethylsilyl)pent-1-en-3-ol (**304**).

Nucleus: 1H
Frequency: 500.18 MHz
Solvent: Acetone
Temperature: 298.0 K

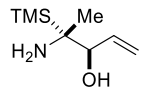

306

Appendix 245. ^{1}H-NMR spectrum of (3*R**,4*R**)-4-amino-4-(trimethylsilyl)pent-1-en-3-ol (**306**).

Nucleus: 13C
Frequency: 125.78 MHz
Solvent: Acetone
Temperature: 298.0 K

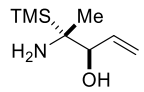

306

Appendix 246. ^{13}C-NMR spectrum of (3*R**,4*R**)-4-amino-4-(trimethylsilyl)pent-1-en-3-ol (**306**).

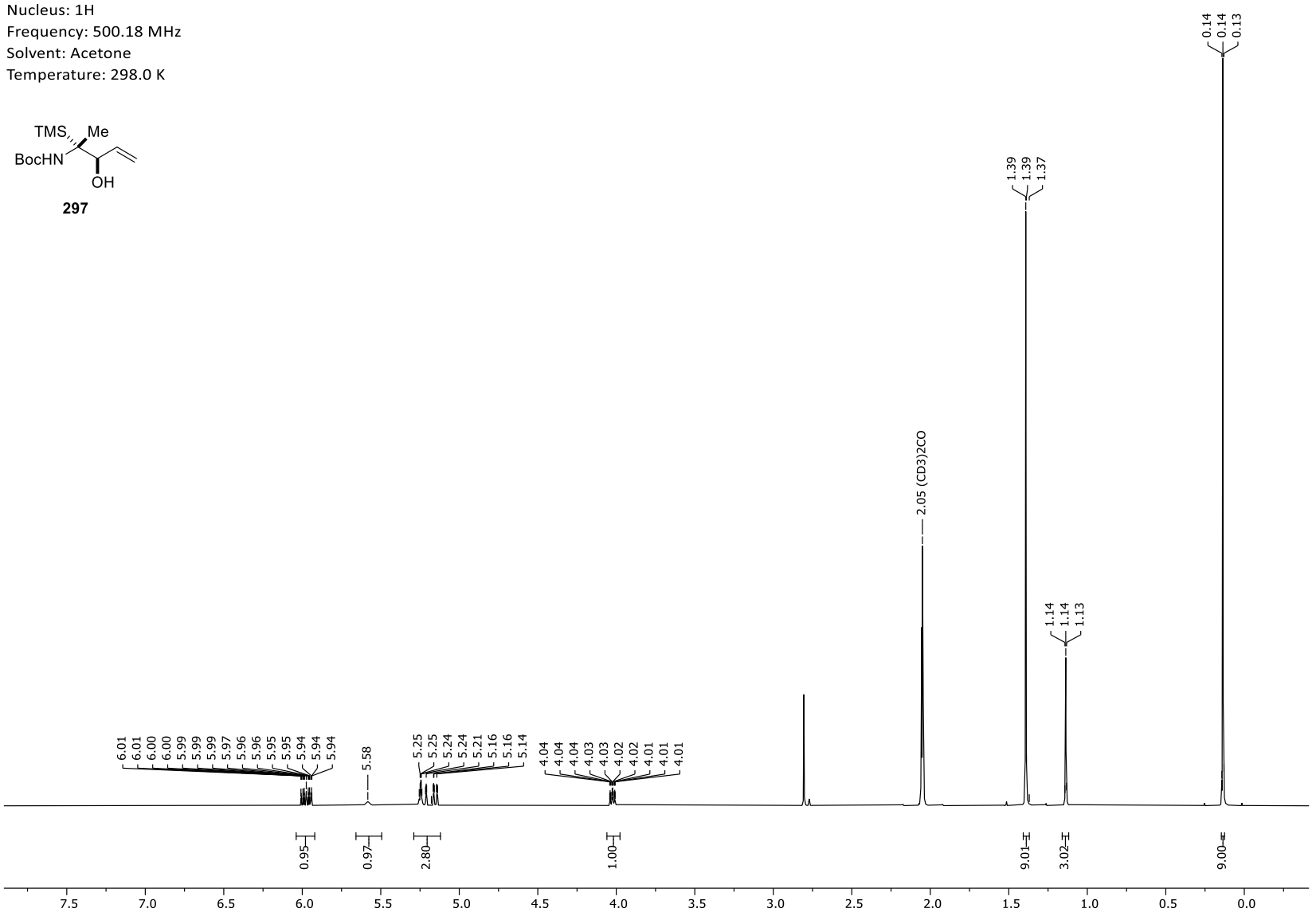

Appendix 247. ^{1}H-NMR spectrum of *tert*-butyl ((2*R**,3*R**)-3-hydroxy-2-(trimethylsilyl)pent-4-en-2-yl)carbamate (**297**).

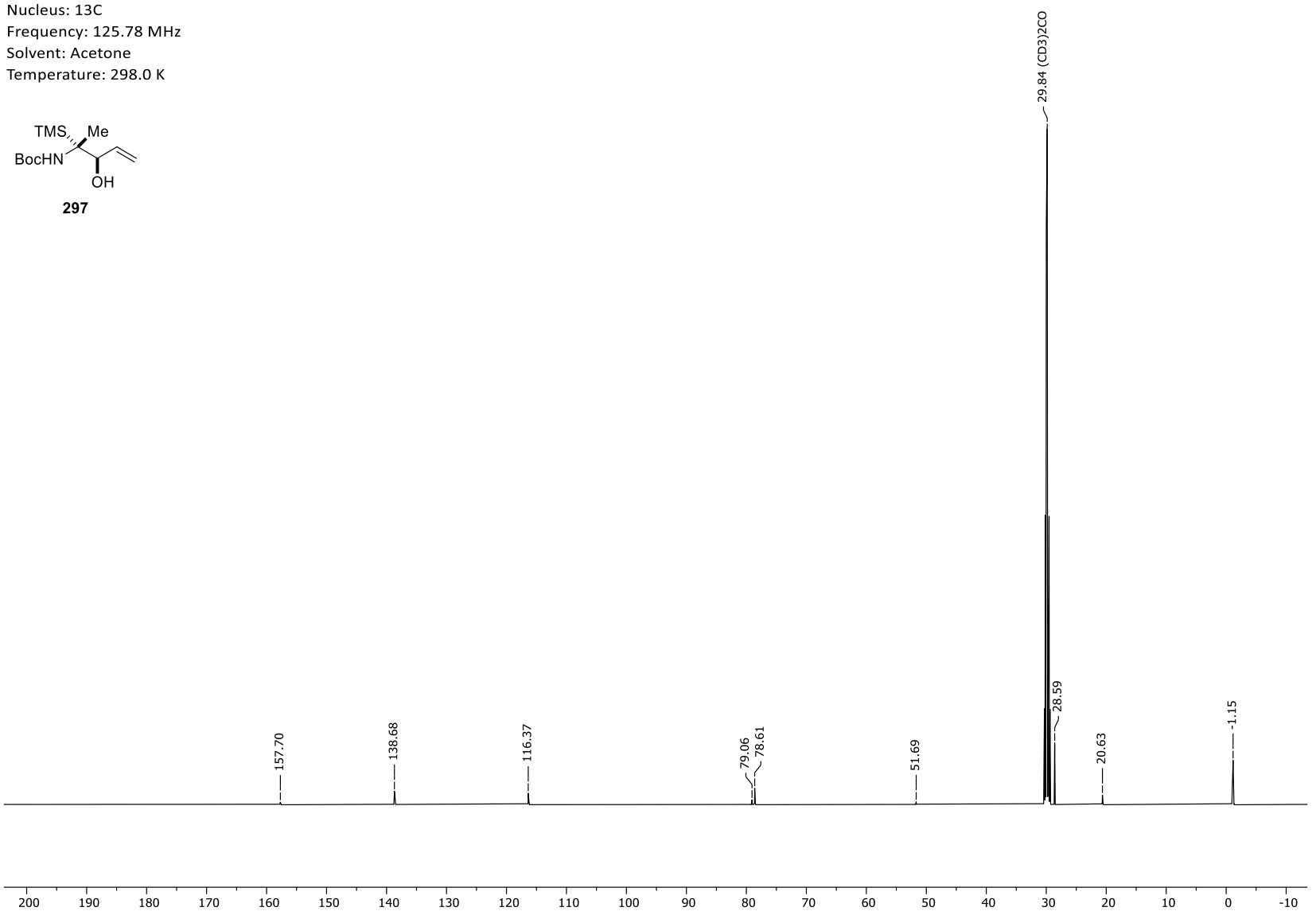

Appendix 248. ^{13}C-NMR spectrum of *tert*-butyl ((2*R**,3*R**)-3-hydroxy-2-(trimethylsilyl)pent-4-en-2-yl)carbamate (**297**).

Nucleus: 1H
Frequency: 499.13 MHz
Solvent: Acetone
Temperature: 298.0 K

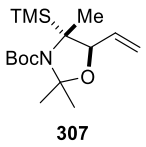

307

Appendix 249. ^{1}H-NMR spectrum of *tert*-butyl (4*R**,5*R**)-2,2,4-trimethyl-4-(trimethylsilyl)-5-vinyloxazolidine-3-carboxylate (**307**).

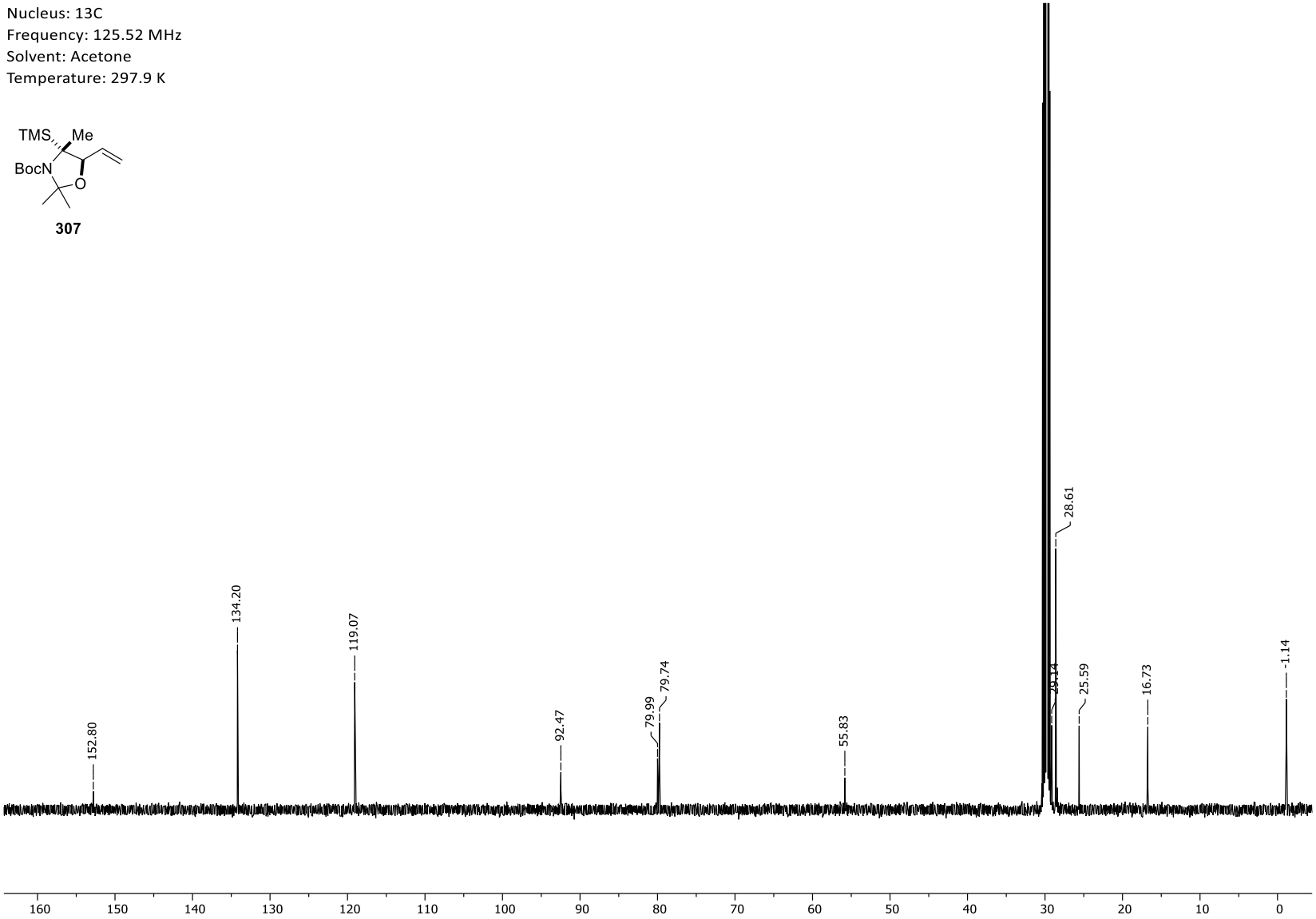

Appendix 250. ^{13}C-NMR spectrum of *tert*-butyl (4*R**,5*R**)-2,2,4-trimethyl-4-(trimethylsilyl)-5-vinyloxazolidine-3-carboxylate (**307**).

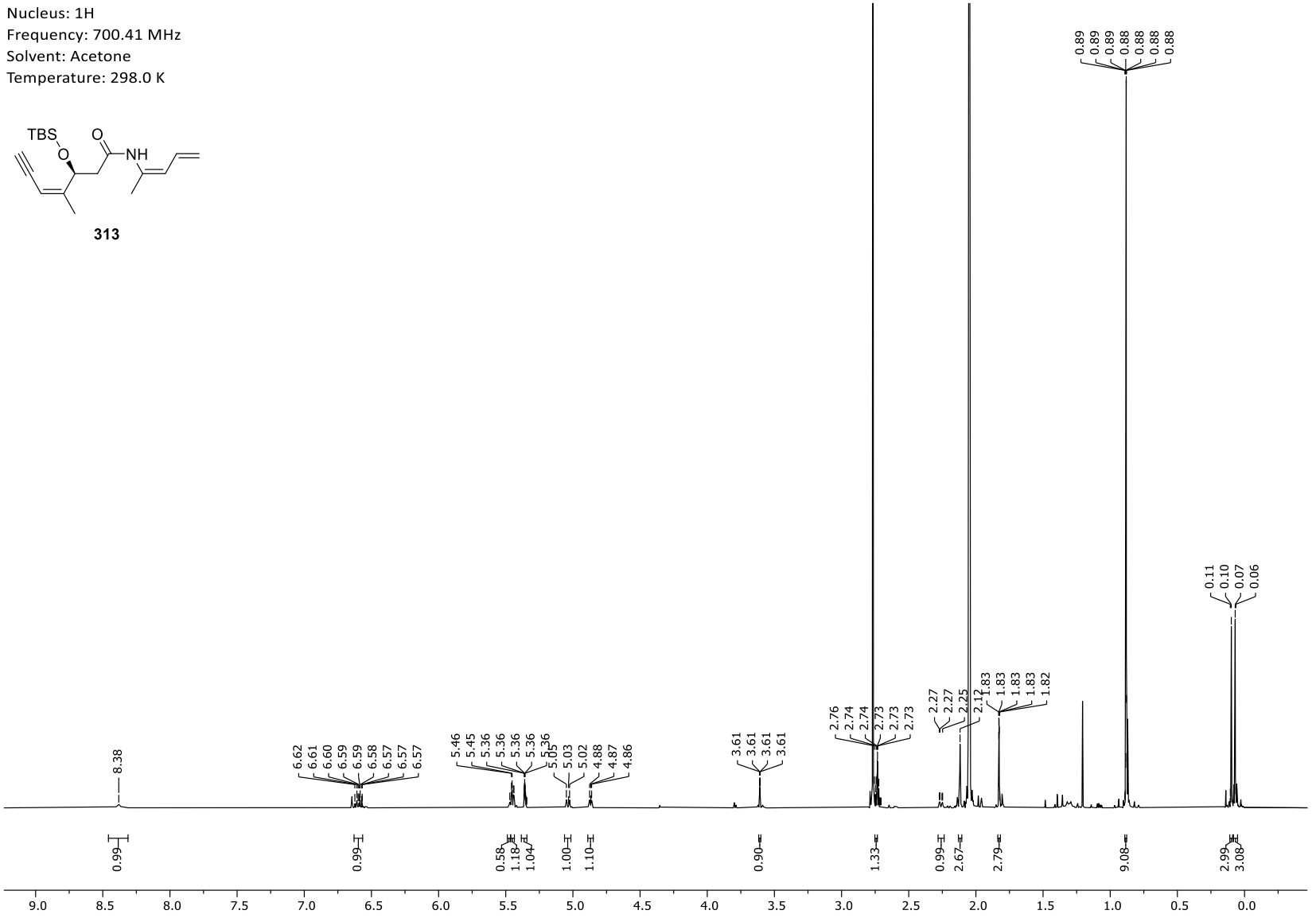

Appendix 251. ^{1}H-NMR spectrum of dienamide **313**.

Nucleus: 13C
Frequency: 176.14 MHz
Solvent: Acetone
Temperature: 298.0 K

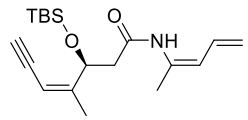

313

Appendix 252. ^{13}C-NMR spectrum of dienamide **313**.

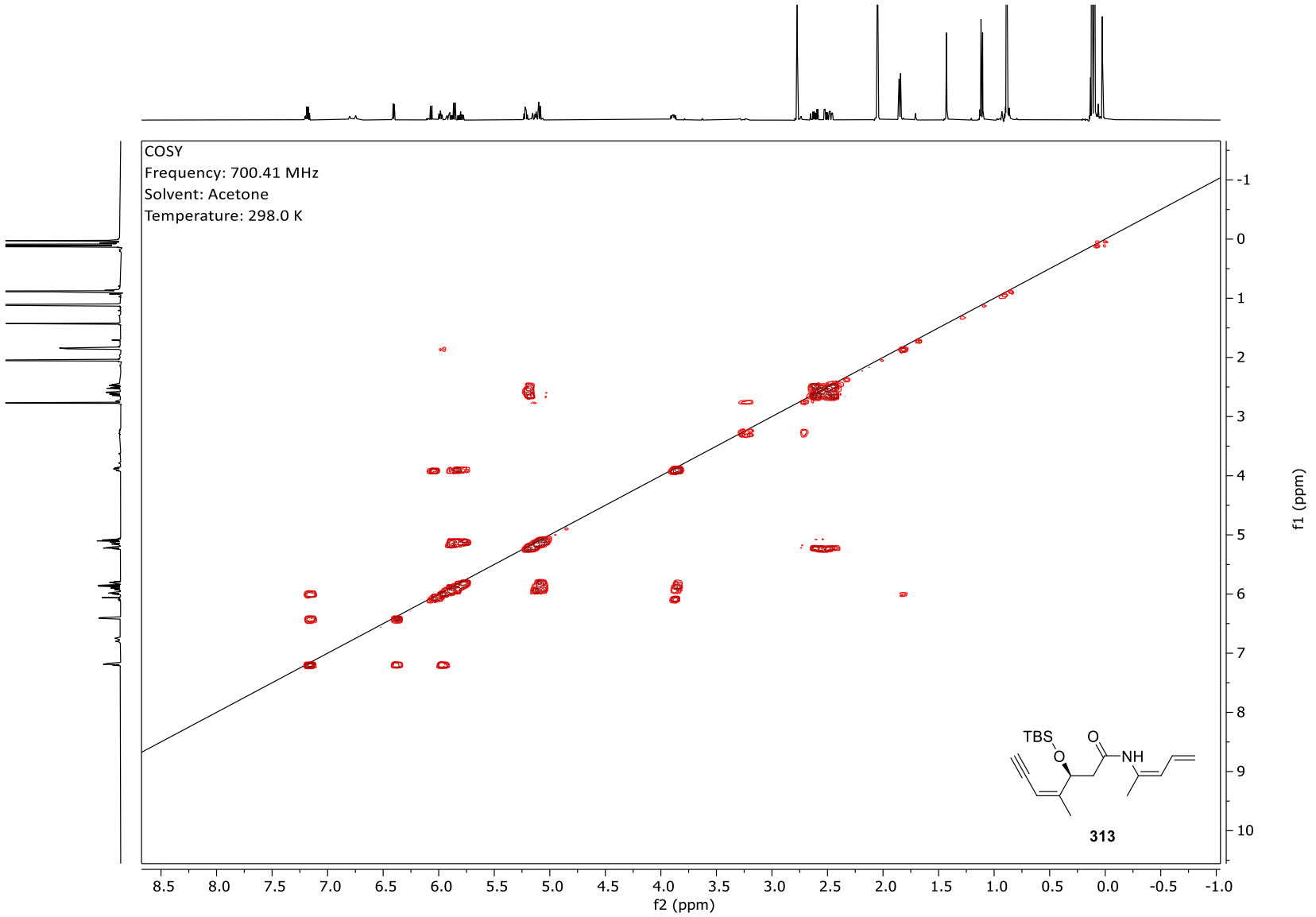

Appendix 253. COSY-NMR spectrum of dienamide **313**.

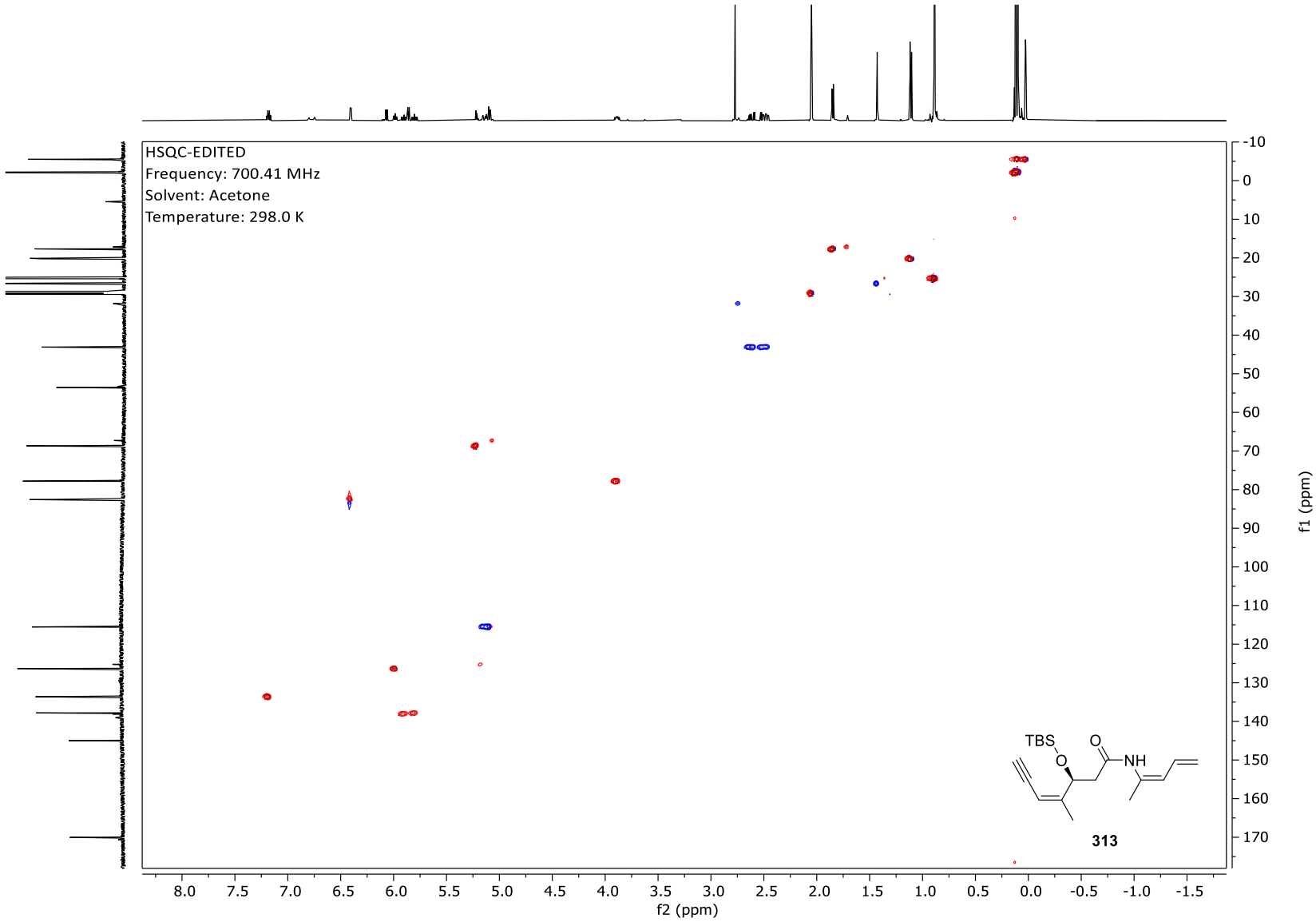

Appendix 254. HSQC-NMR spectrum of dienamide **313**.

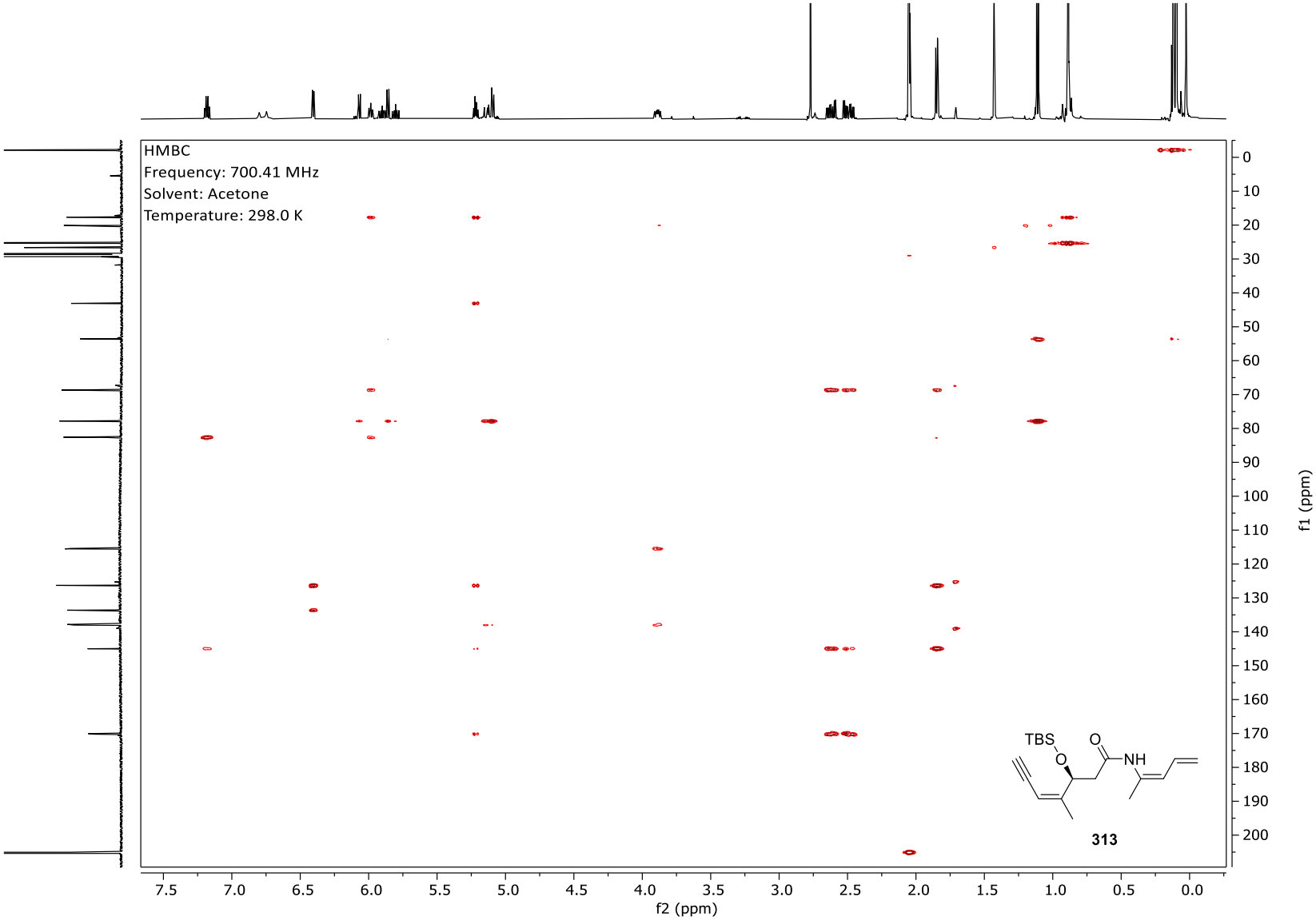

Appendix 255. HMBC-NMR spectrum of dienamide **313**.

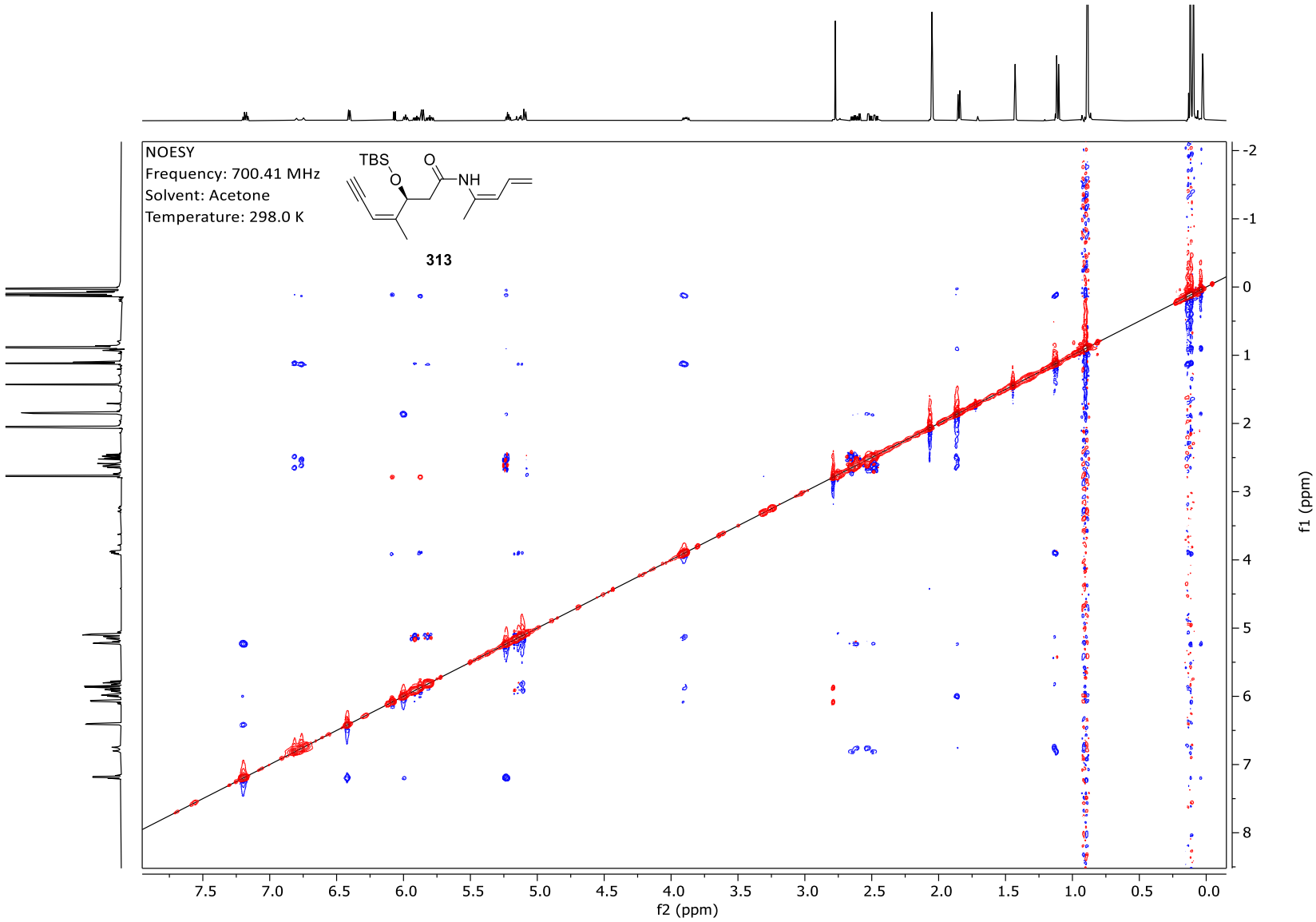

Appendix 256. NOESY-NMR spectrum of dienamide **313**.

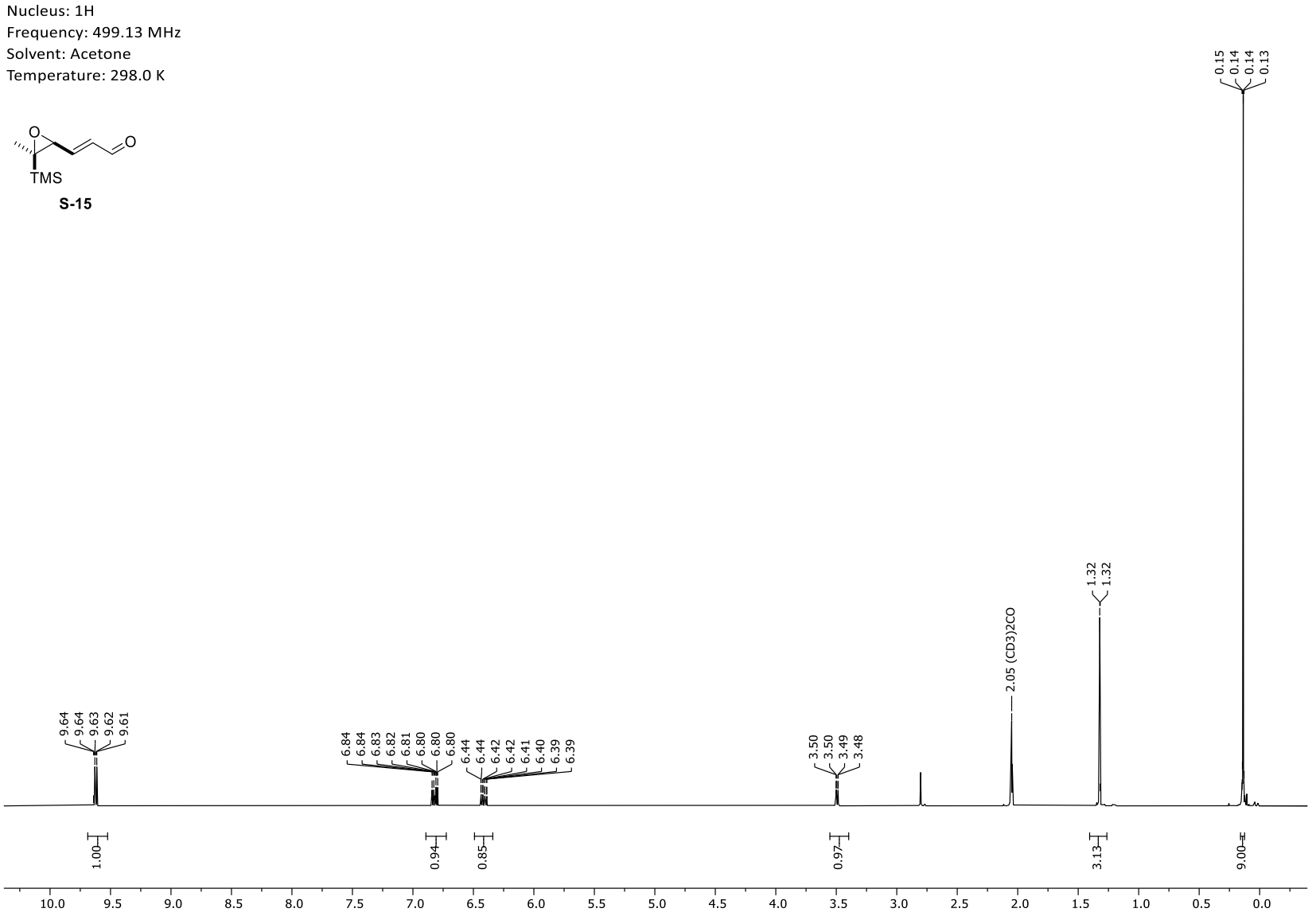

Appendix 257. ^{1}H-NMR spectrum of (*E*)-3-((2*S**,3*R**)-3-methyl-3-(trimethylsilyl)oxiran-2-yl)acrylaldehyde (**S-15**).

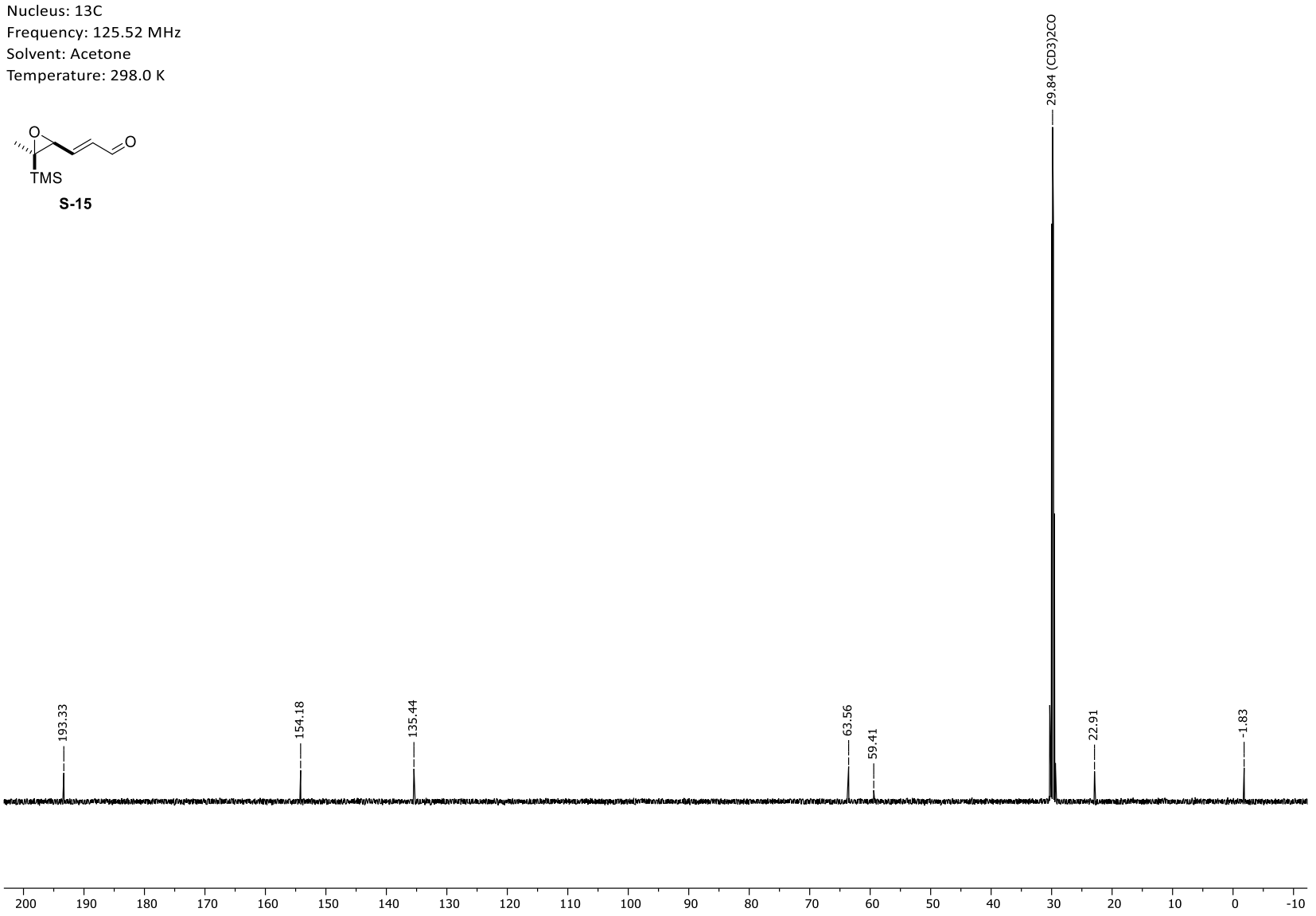

Appendix 258. ^{13}C-NMR spectrum of (*E*)-3-((2*S**,3*R**)-3-methyl-3-(trimethylsilyl)oxiran-2-yl)acrylaldehyde (**S-15**).

Nucleus: 1H
Frequency: 499.13 MHz
Solvent: Acetone
Temperature: 298.0 K

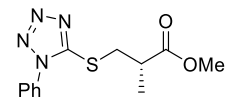

S-16

Appendix 259. ^{1}H-NMR spectrum of methyl (*S*)-2-methyl-3-((1-phenyl-1H-tetrazol-5-yl)thio)propanoate (**S-16**).

Nucleus: 13C
Frequency: 125.52 MHz
Solvent: Acetone
Temperature: 298.4 K

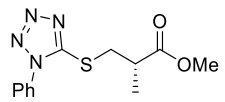

S-16

Appendix 260. ^{13}C-NMR spectrum of methyl (*S*)-2-methyl-3-((1-phenyl-1H-tetrazol-5-yl)thio)propanoate (**S-16**).

Nucleus: 1H
Frequency: 499.13 MHz
Solvent: Acetone
Temperature: 298.0 K

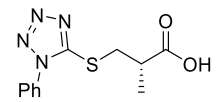

S-17

Appendix 261. ^{1}H-NMR spectrum of (*S*)-2-methyl-3-((1-phenyl-1H-tetrazol-5-yl)thio)propanoIc acid (**S-17**).

Nucleus: 13C
Frequency: 125.52 MHz
Solvent: Acetone
Temperature: 298.3 K

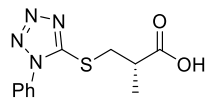

S-17

Appendix 262. ^{13}C-NMR spectrum of (*S*)-2-methyl-3-((1-phenyl-1H-tetrazol-5-yl)thio)propanoIc acid (**S-17**).

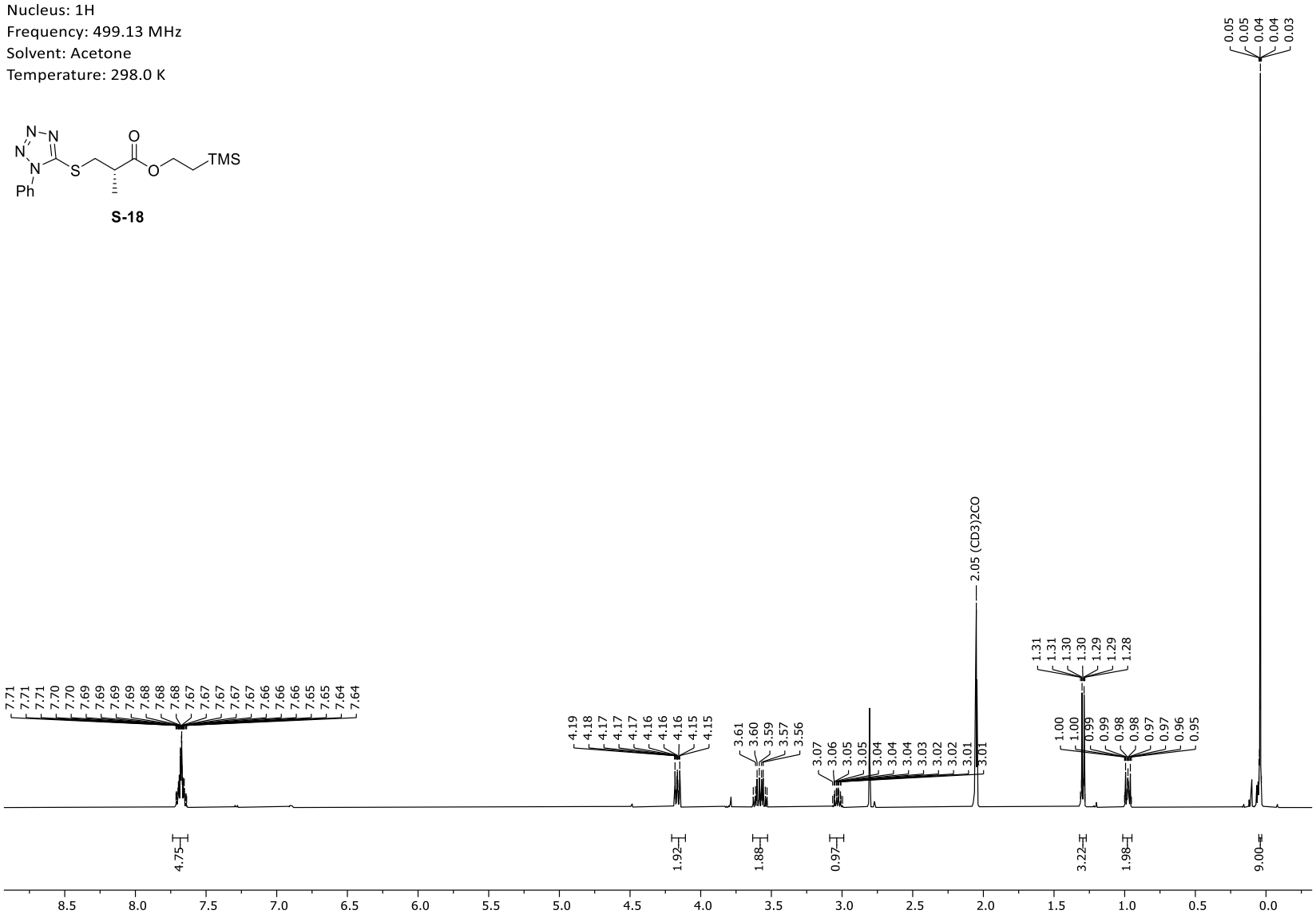

Appendix 263. ^{1}H-NMR spectrum of 2-(trimethylsilyl)ethyl (S)-2-methyl-3-((1-phenyl-1H-tetrazol-5-yl)thio)propanoate (**S-18**).

Nucleus: 13C
Frequency: 125.52 MHz
Solvent: Acetone
Temperature: 298.2 K

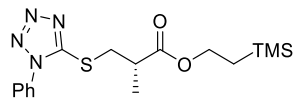

S-18

Appendix 264. ^{13}C-NMR spectrum of 2-(trimethylsilyl)ethyl (S)-2-methyl-3-((1-phenyl-1H-tetrazol-5-yl)thio)propanoate (**S-18**).

Nucleus: 1H
Frequency: 499.13 MHz
Solvent: Acetone
Temperature: 298.0 K

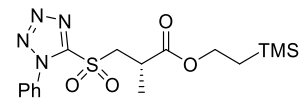

S-19

Appendix 265. ^{1}H-NMR spectrum of 2-(trimethylsilyl)ethyl (*S*)-2-methyl-3-((1-phenyl-1H-tetrazol-5-yl)sulfonyl)propanoate (**S-19**).

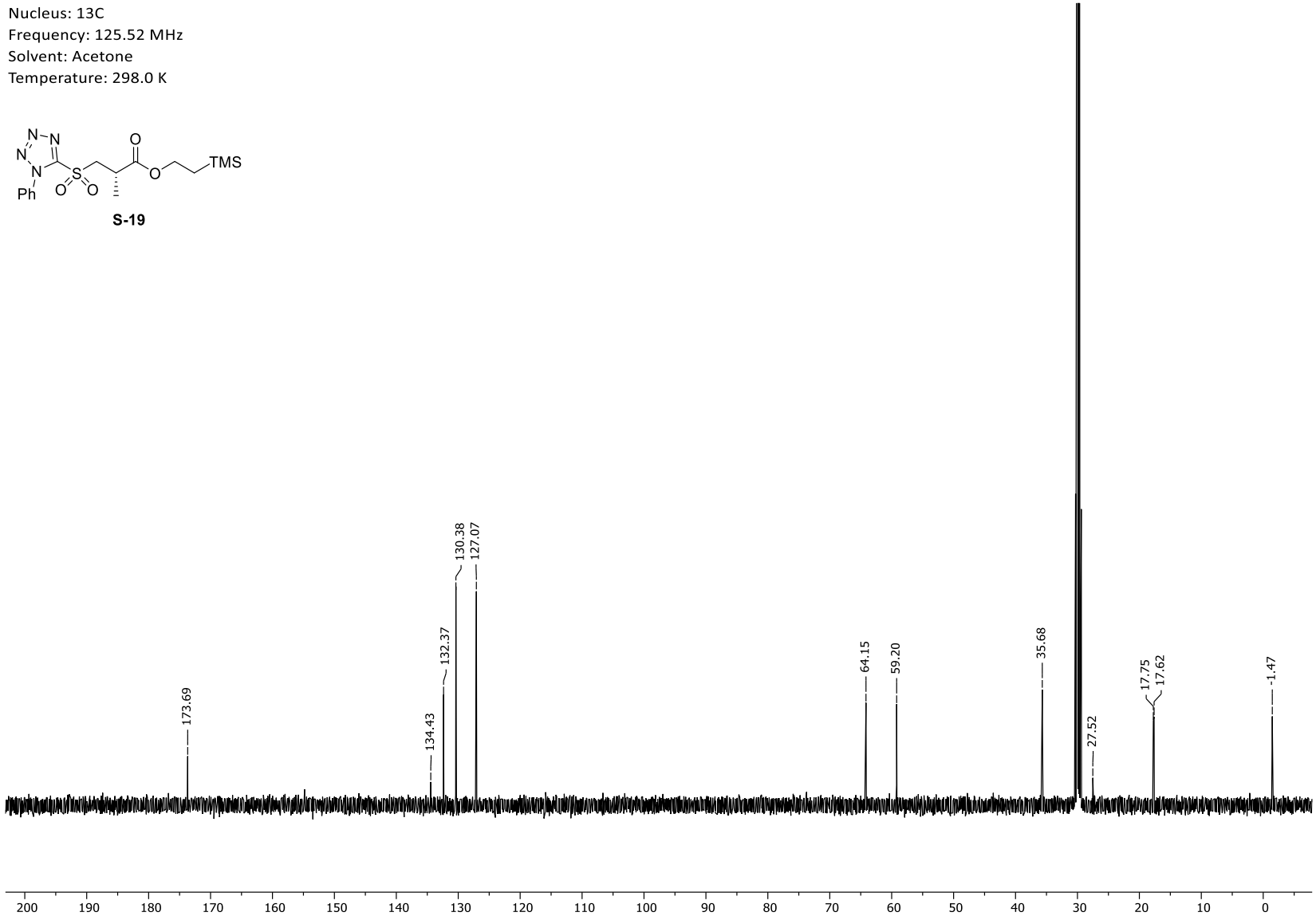

Appendix 266. ^{13}C-NMR spectrum of 2-(trimethylsilyl)ethyl (*S*)-2-methyl-3-((1-phenyl-1H-tetrazol-5-yl)sulfonyl)propanoate (**S-19**).

Nucleus: 1H
Frequency: 500.18 MHz
Solvent: Acetone
Temperature: 298.0 K

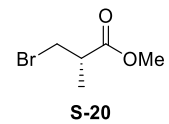

S-20

Appendix 267. ^{1}H-NMR spectrum of methyl (*S*)-3-bromo-2-methylpropanoate (**S-20**).

Nucleus: 13C
Frequency: 125.78 MHz
Solvent: Acetone
Temperature: 298.0 K

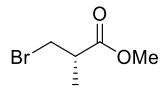

S-20

Appendix 268. ^{13}C-NMR spectrum of methyl (*S*)-3-bromo-2-methylpropanoate (**S-20**).

Nucleus: 1H
Frequency: 499.13 MHz
Solvent: Acetone
Temperature: 298.0 K

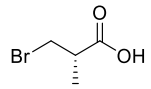

S-21

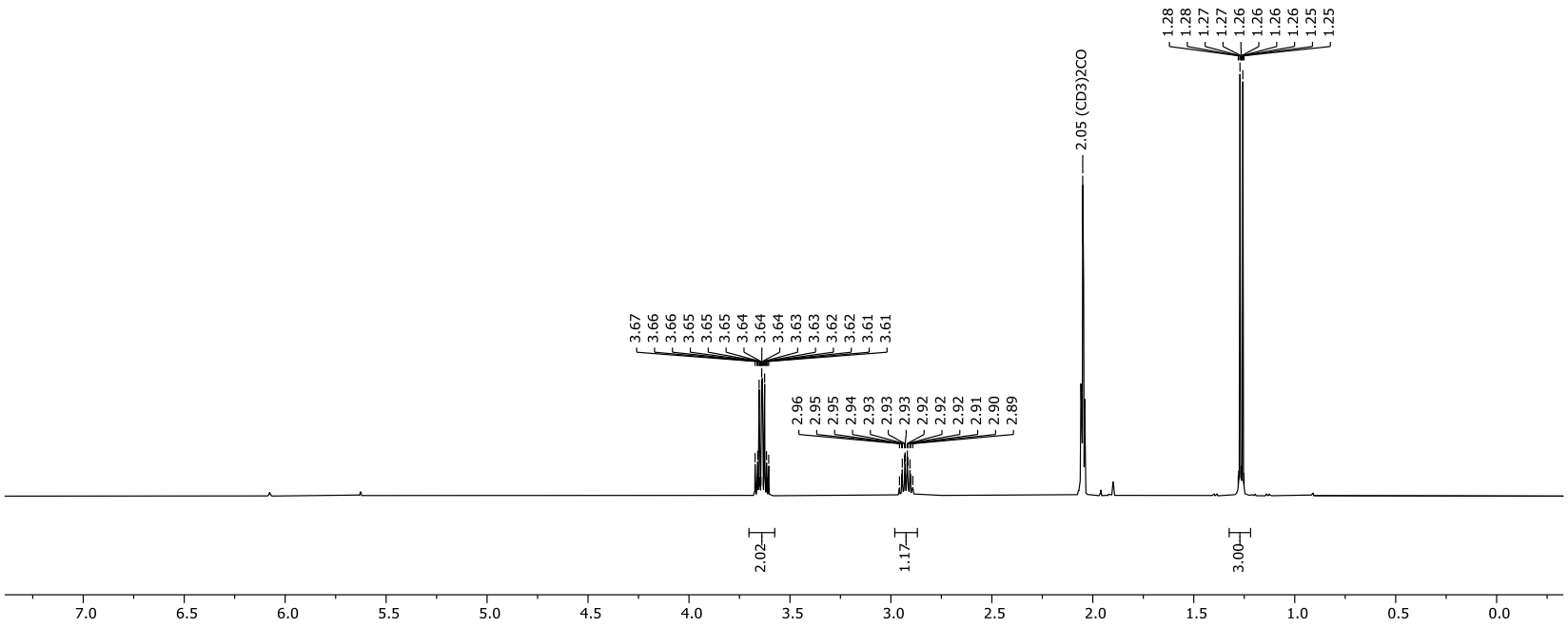

Appendix 269. ^{1}H-NMR spectrum of methyl (*S*)-3-bromo-2-methylpropanoic acid (**S-21**).

Nucleus: 13C
Frequency: 125.52 MHz
Solvent: Acetone
Temperature: 298.2 K

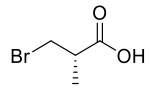

S-21

Appendix 270. ^{13}C-NMR spectrum of methyl (*S*)-3-bromo-2-methylpropanoic acid (**S-21**).

Nucleus: 1H
Frequency: 500.04 MHz
Solvent: Acetone
Temperature: 298.0 K

S-22

Appendix 271. ^{1}H-NMR spectrum of 2-(dichloromethyl)-4,4,5,5-tetramethyl-1,3,2-dioxaborolane (**S-22**).

Nucleus: 13C
Frequency: 125.75 MHz
Solvent: Acetone
Temperature: 298.0 K

S-22

Appendix 272. ^{13}C-NMR spectrum of 2-(dichloromethyl)-4,4,5,5-tetramethyl-1,3,2-dioxaborolane (**S-22**).

Nucleus: 1H
Frequency: 500.04 MHz
Solvent: CDCl3
Temperature: 298.0 K

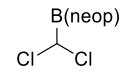

S-23

Appendix 273. ^{1}H-NMR spectrum of 2-(dichloromethyl)-5,5-dimethyl-1,3,2-dioxaborinane (**S-23**).

Nucleus: 13C
Frequency: 125.75 MHz
Solvent: CDCl3
Temperature: 298.0 K

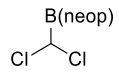

S-23

Appendix 274. ^{13}C-NMR spectrum of 2-(dichloromethyl)-5,5-dimethyl-1,3,2-dioxaborinane (**S-23**).

10. Mass spectra

10.1 mass spectrum of 250

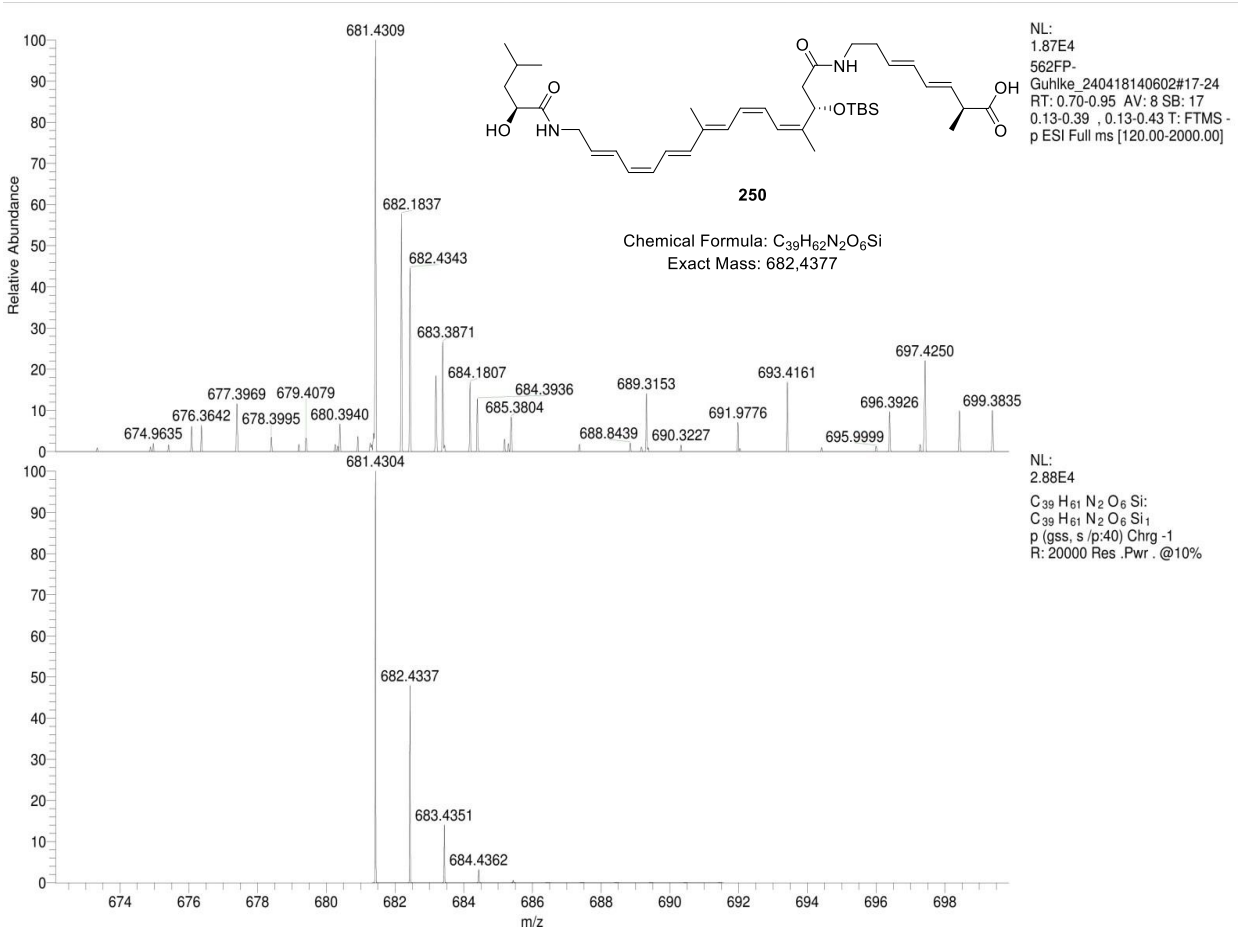

10.2 mass spectrum of bacillaene analogue (7)

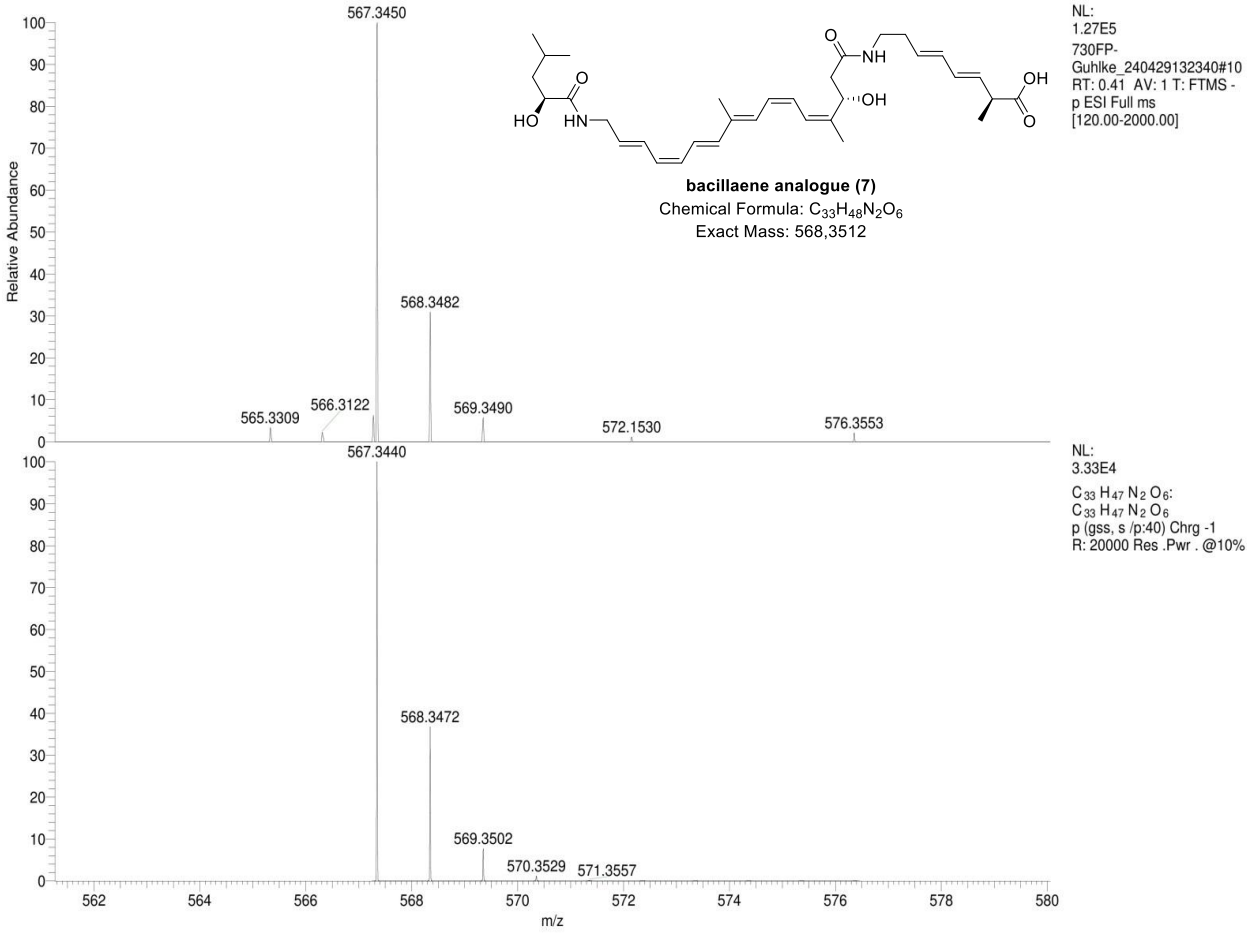

11. Chromatograms

11.1 Irradiation experiments of tetraene V (135)

Data File: F:\Enterprise\Europa\Result\2024\2024 - AK Menche\ME-069-Max Guhlke\ME-069-37D1-01H-050224-01.dat
Method: F:\Enterprise\Europa\Method\U - 0.5ml - 75-25 - C4 - 190-600nm - 05,0min - 230-260-330nm - 25-23°C - 50 Hz.met

Max Guhlke - MG-F005-RP - ME-069-36 Light 310nm 1,2,4,24h auf MN Nucleodur 100-3 Gravity C18 3µm; 2,0 x 100mm - 330nm

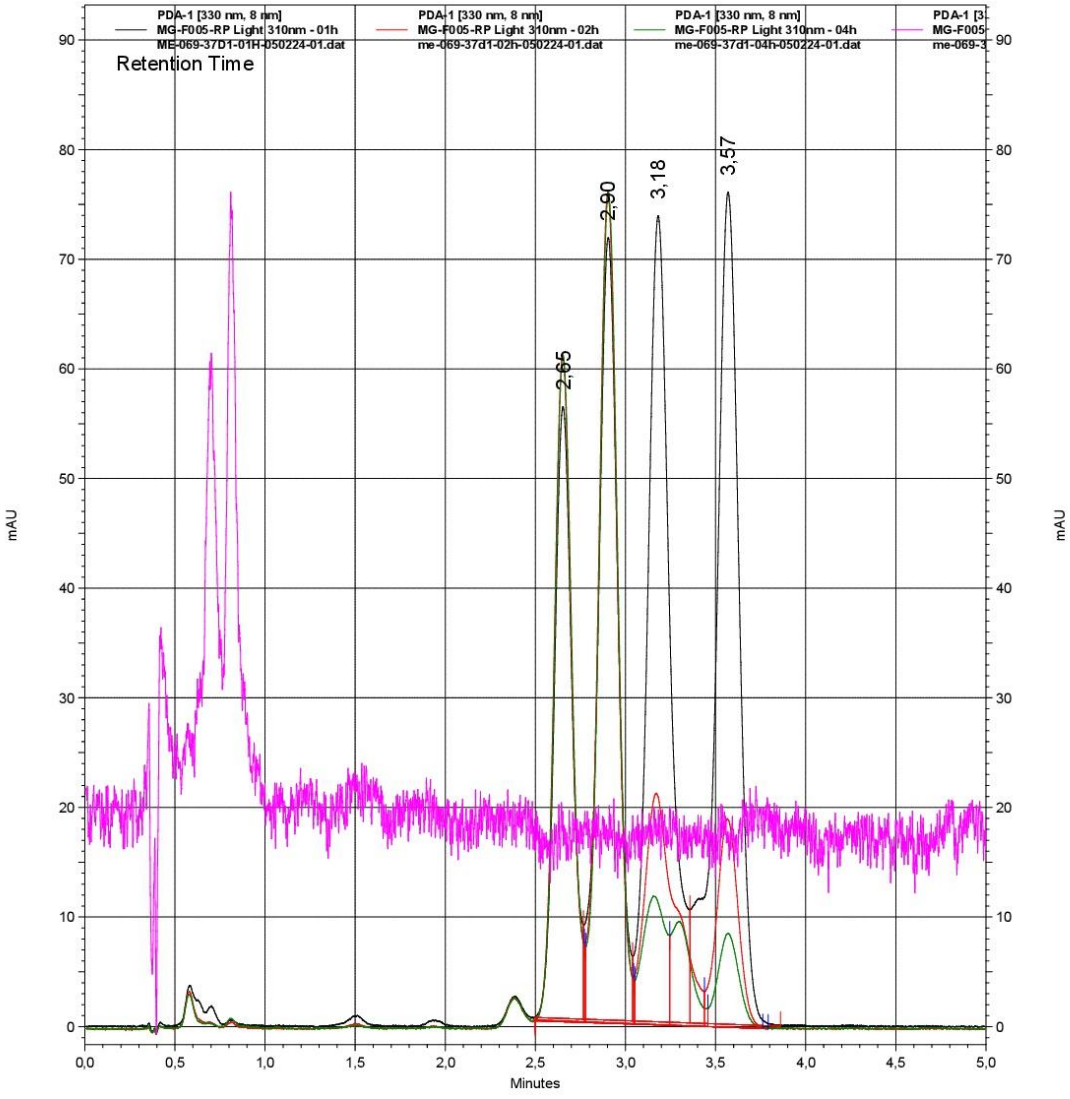

PDA-1 [330 nm, 8 nm] Results

Retention Time	Area	Area %	Height	Height %
2,654	375906	16,88	55799	20,17
2,904	541886	24,33	71360	25,80
3,182	631150	28,34	73524	26,58
3,569	678113	30,45	75911	27,44
Totals	2227055	100,00	276594	100,00

PDA-1 [330 nm, 8 nm] Results

Retention Time	Area	Area %	Height	Height %
2,650	591532	29,78	86905	34,36
2,902	798108	40,18	108510	42,91
3,172	369403	18,60	30232	11,95
3,565	227389	11,45	27253	10,78
Totals	1986432	100,00	252900	100,00

PDA-1 [330 nm, 8 nm] Results

Retention Time	Area	Area %	Height	Height %
2,654	585816	34,19	85169	36,55
2,906	780148	45,53	106149	45,55
3,154	145833	8,51	16440	7,05
3,298	103913	6,06	13298	5,71
3,573	97752	5,70	11971	5,14
Totals	1713462	100,00	233027	100,00

PDA-1 [330 nm, 8 nm] Results

Retention Time	Area	Area %	Height	Height %

Data File: F:\Enterprise\Europa\Result\2024\2024 - AK Menche\ME-069-Max Guhlke\ME-069-37D2-01H-050224-01.dat
Method: F:\Enterprise\Europa\Method\U - 0.5ml - 75-25 - C4 - 190-600nm - 05,0min - 230-260-330nm - 25-23°C - 50 Hz.met

Max Guhlke - MG-F005-RP - ME-069-36 Light 325nm 1,2,4,24h auf MN Nucleodur 100-3 Gravity C18 3µm; 2,0 x 100mm - 330nm

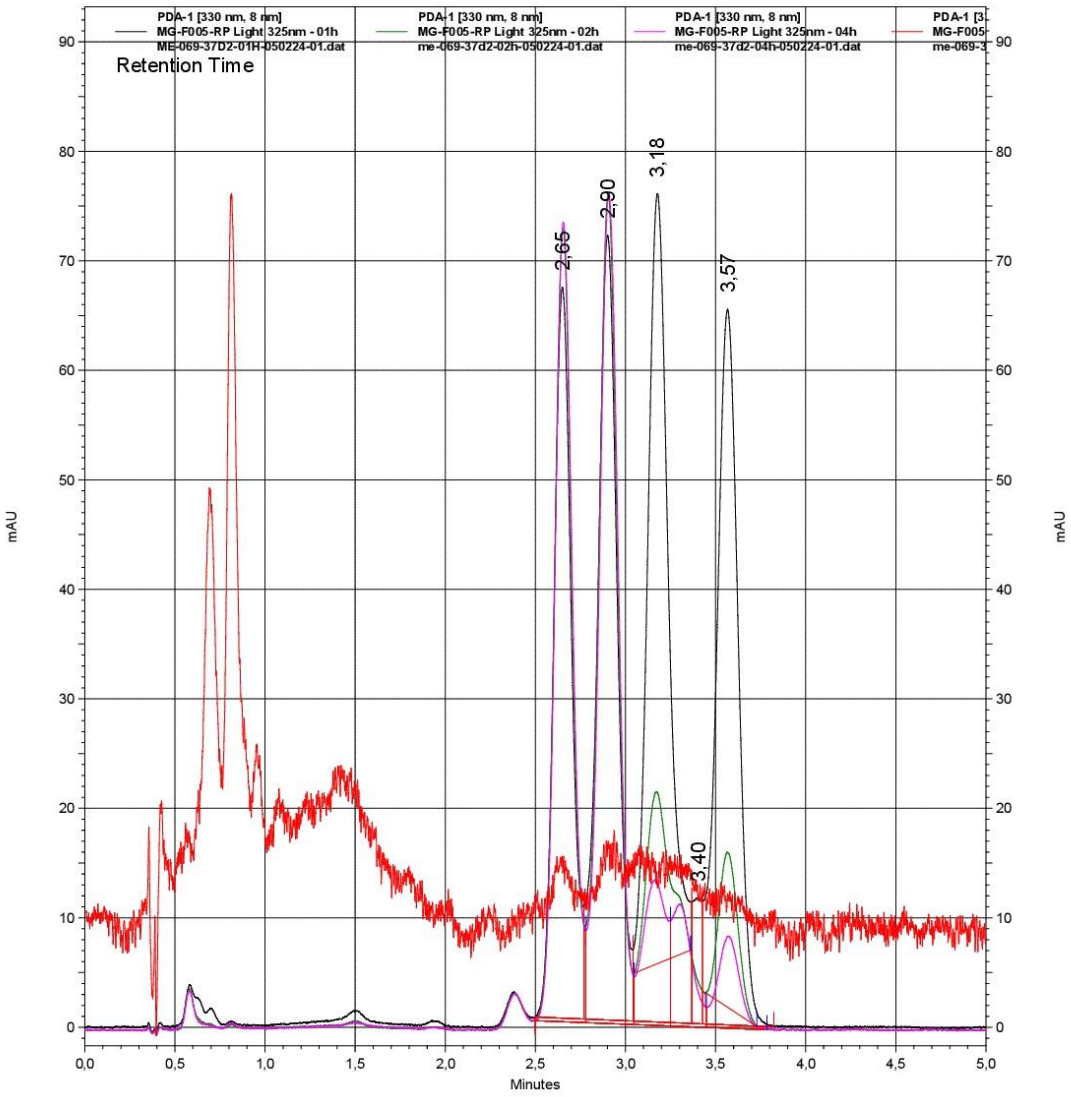

PDA-1 [330 nm, 8 nm] Results

Retention Time	Area	Area %	Height	Height %
2,650	451857	20,05	66727	22,94
2,900	550552	24,43	71684	24,64
3,177	664070	29,47	75639	26,00
3,402	40281	1,79	11471	3,94
3,567	546378	24,25	65354	22,47
Totals	2253138	100,00	290875	100,00

PDA-1 [330 nm, 8 nm] Results

Retention Time	Area	Area %	Height	Height %
2,654	371941	46,94	54242	50,34
2,904	267869	33,80	35062	32,54
3,166	75106	9,48	8186	7,60
3,295	47263	5,96	6515	6,05
3,572	30250	3,82	3736	3,47
Totals	792429	100,00	107741	100,00

PDA-1 [330 nm, 8 nm] Results

Retention Time	Area	Area %	Height	Height %
2,655	713821	37,14	104733	40,19
2,909	811738	42,24	108695	41,71
3,165	172637	8,98	19079	7,32
3,300	121965	6,35	16054	6,16
3,567	101698	5,29	12056	4,63
Totals	1921859	100,00	260617	100,00

PDA-1 [330 nm, 8 nm] Results

Retention Time	Area	Area %	Height	Height %

Data File: F:\Enterprise\Europa\Result\2024\2024 - AK Menche\ME-069-Max Guhlke\ME-069-37D3-01H-050224-01.dat
Method: F:\Enterprise\Europa\Method\U - 0.5ml - 75-25 - C4 - 190-600nm - 05,0min - 230-260-330nm - 25-23°C - 50 Hz.met

Max Guhlke - MG-F005-RP - ME-069-37 Light 365nm 1,2,4,24h auf MN Nucleodur 100-3 Gravity C18 3µm; 2,0 x 100mm - 330nm

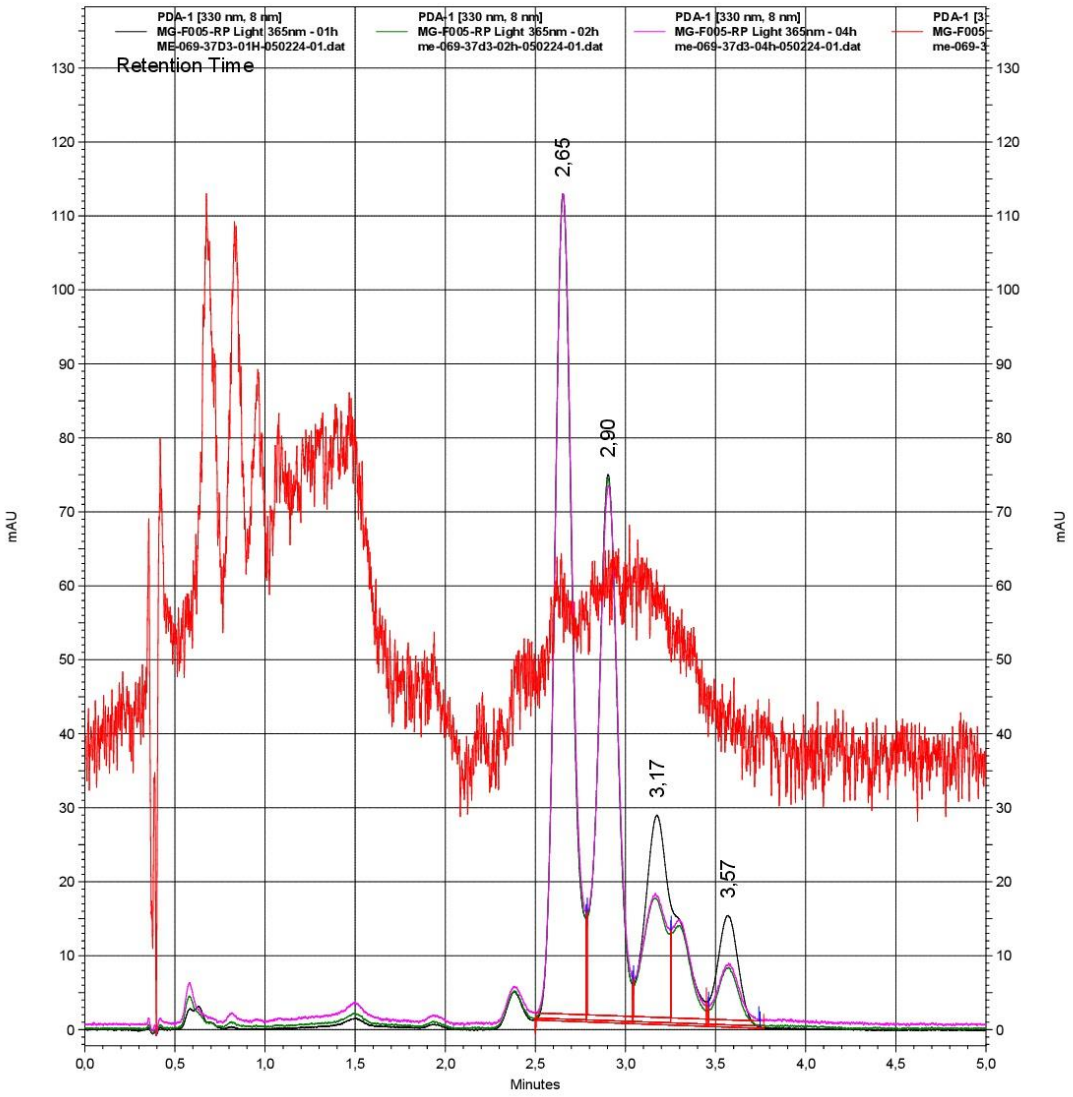

PDA-1 [330 nm, 8 nm] Results

Retention Time	Area	Area %	Height	Height %
2,653	754766	42,24	111837	48,76
2,903	561466	31,42	74089	32,30
3,175	346384	19,38	28323	12,35
3,571	124371	6,96	15117	6,59
Totals	1786987	100,00	229366	100,00

PDA-1 [330 nm, 8 nm] Results

Retention Time	Area	Area %	Height	Height %
2,654	565557	46,66	82980	50,15
2,903	412355	34,02	54429	32,90
3,162	114817	9,47	12508	7,56
3,288	72722	6,00	9775	5,91
3,572	46533	3,84	5767	3,49
Totals	1211984	100,00	165459	100,00

PDA-1 [330 nm, 8 nm] Results

Retention Time	Area	Area %	Height	Height %
2,654	371941	46,94	54242	50,34
2,904	267869	33,80	35062	32,54
3,166	75106	9,48	8186	7,60
3,295	47263	5,96	6515	6,05
3,572	30250	3,82	3736	3,47
Totals	792429	100,00	107741	100,00

PDA-1 [330 nm, 8 nm] Results

Retention Time	Area	Area %	Height	Height %

Data File: F:\Enterprise\Europa\Result\2024\2024 - AK Menche\ME-069-Max Guhlke\ME-069-37D4-01H-050224-01.dat
Method: F:\Enterprise\Europa\Method\U - 0.5ml - 75-25 - C4 - 190-600nm - 05,0min - 230-260-330nm - 25-23°C - 50 Hz.met

Max Guhlke - MG-F005-RP Light White 1,2,4,24 h - ME-069-37 auf MN Nucleodur 100-3 Gravity C18 3µm; 2,0 x 100mm - 330nm

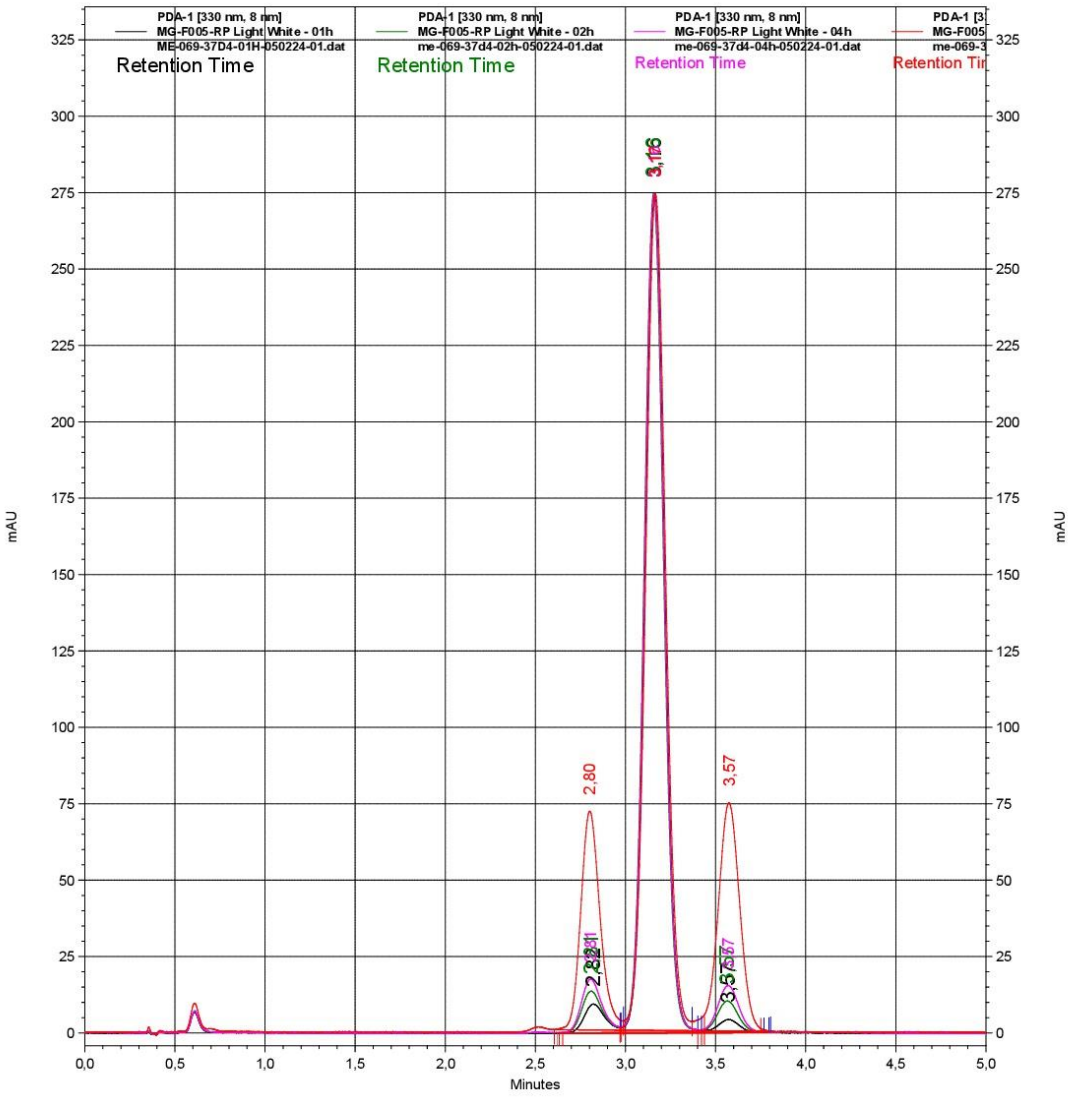

PDA-1 [330 nm, 8 nm] Results

Retention Time	Area	Area %	Height	Height %
2,822	80222	3,62	9617	3,33
3,161	2096788	94,72	274680	95,15
3,571	36604	1,65	4392	1,52
Totals	2213614	100,00	288689	100,00

PDA-1 [330 nm, 8 nm] Results

Retention Time	Area	Area %	Height	Height %
2,811	109437	4,94	13291	4,60
3,155	2023554	91,31	265736	91,93
3,566	83177	3,75	10043	3,47
Totals	2216168	100,00	289070	100,00

PDA-1 [330 nm, 8 nm] Results

Retention Time	Area	Area %	Height	Height %
2,807	133067	5,98	16434	5,71
3,158	1972579	88,69	257138	89,30
3,571	118589	5,33	14370	4,99
Totals	2224235	100,00	287942	100,00

11.2 Catalyst-screening for hexaene II (131)

Data File: F:\Enterprise\Europa\Result\2024\2024 - AK Menche\ME-069-Max Guhlke\ME-069-39a-220324.dat
Method: F:\Enterprise\Europa\Method\Europa+ HPG\0.5ml - A1-B1 - 50-50 0min - 100-00 4,0min - C3 - 6,0min - 190-600nm - 230-330-365nm - 25-23°C - 50 Hz.met

Max Guhlke - XPhos MeCN (1) - ME-069-39a auf KNAUER Eurospher II 100-3 C18P 3µm; 2,0 x 100mm - 330nm

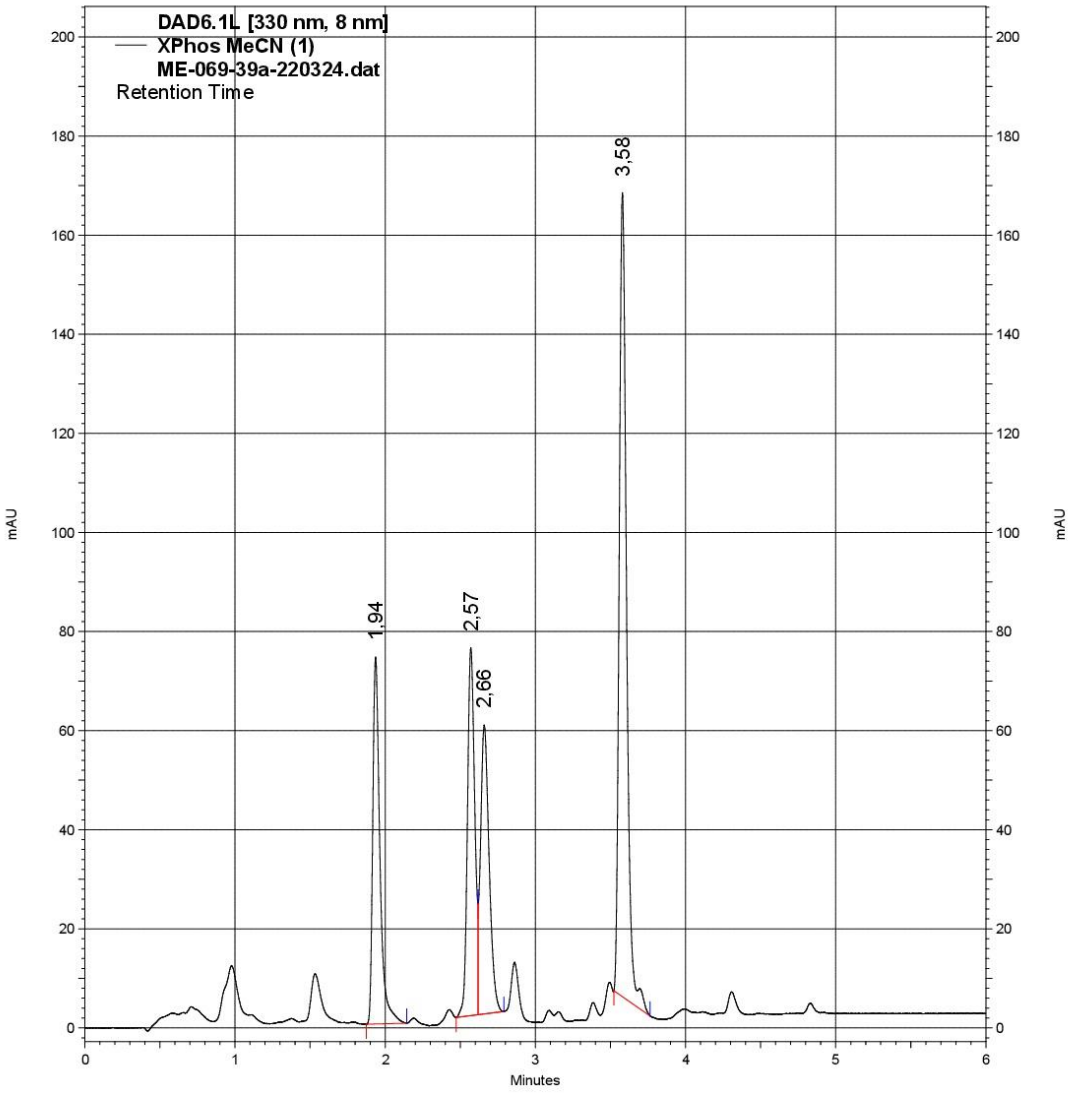

UV-Spektren

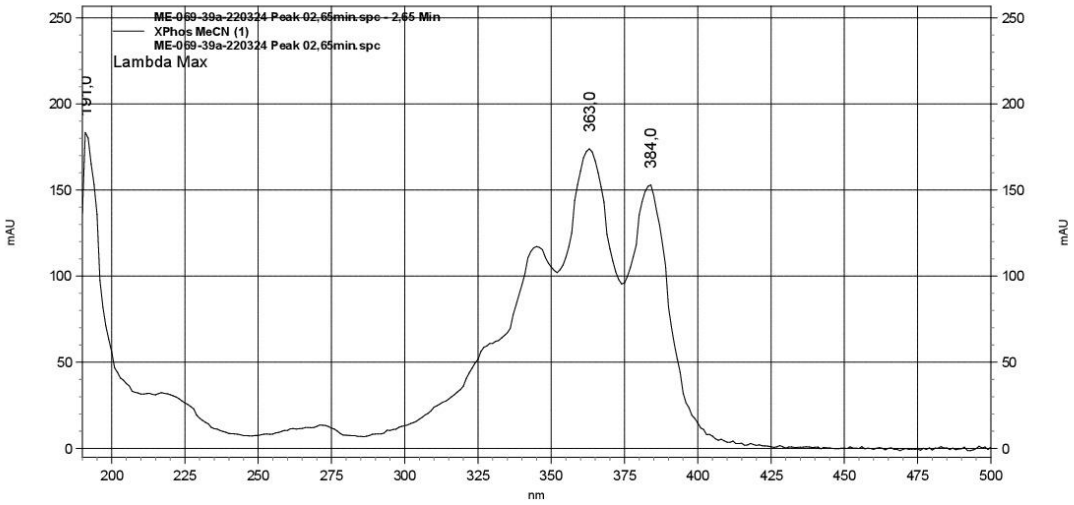

DAD6.1L [230 nm, 8 nm] Results

Retention Time	Area	Area %	Height	Height %
1,936	323897784	100,00	98862380	100,00
Totals	323897784	100,00	98862380	100,00

DAD6.1L [330 nm, 8 nm] Results

Retention Time	Area	Area %	Height	Height %
1,936	24490017	19,15	7405905	20,08
2,570	25111294	19,63	7424016	20,13
2,659	23444945	18,33	5831236	15,81
3,580	54865758	42,89	16225492	43,99
Totals	127912014	100,00	36886649	100,00

DAD6.1L [365 nm, 8 nm] Results

Retention Time	Area	Area %	Height	Height %
2,570	73860816	51,91	21817365	55,97
2,660	62054030	43,61	15338880	39,35
3,580	6384807	4,49	1822195	4,67
Totals	142299653	100,00	38978440	100,00

Data File: F:\Enterprise\Europa\Result\2024\2024 - AK Menche\ME-069-Max Guhlke\ME-069-39c-220324.dat
Method: F:\Enterprise\Europa\Method\Europa+ HPG\0.5ml - A1-B1 - 50-50 0min - 100-00 4,0min - C3 - 6,0min - 190-600nm - 230-330-365nm - 25-23°C - 50 Hz.met

Max Guhlke - SPhos MeCN (1) - ME-069-39c auf KNAUER Eurospher II 100-3 C18P 3µm; 2,0 x 100mm - 330nm

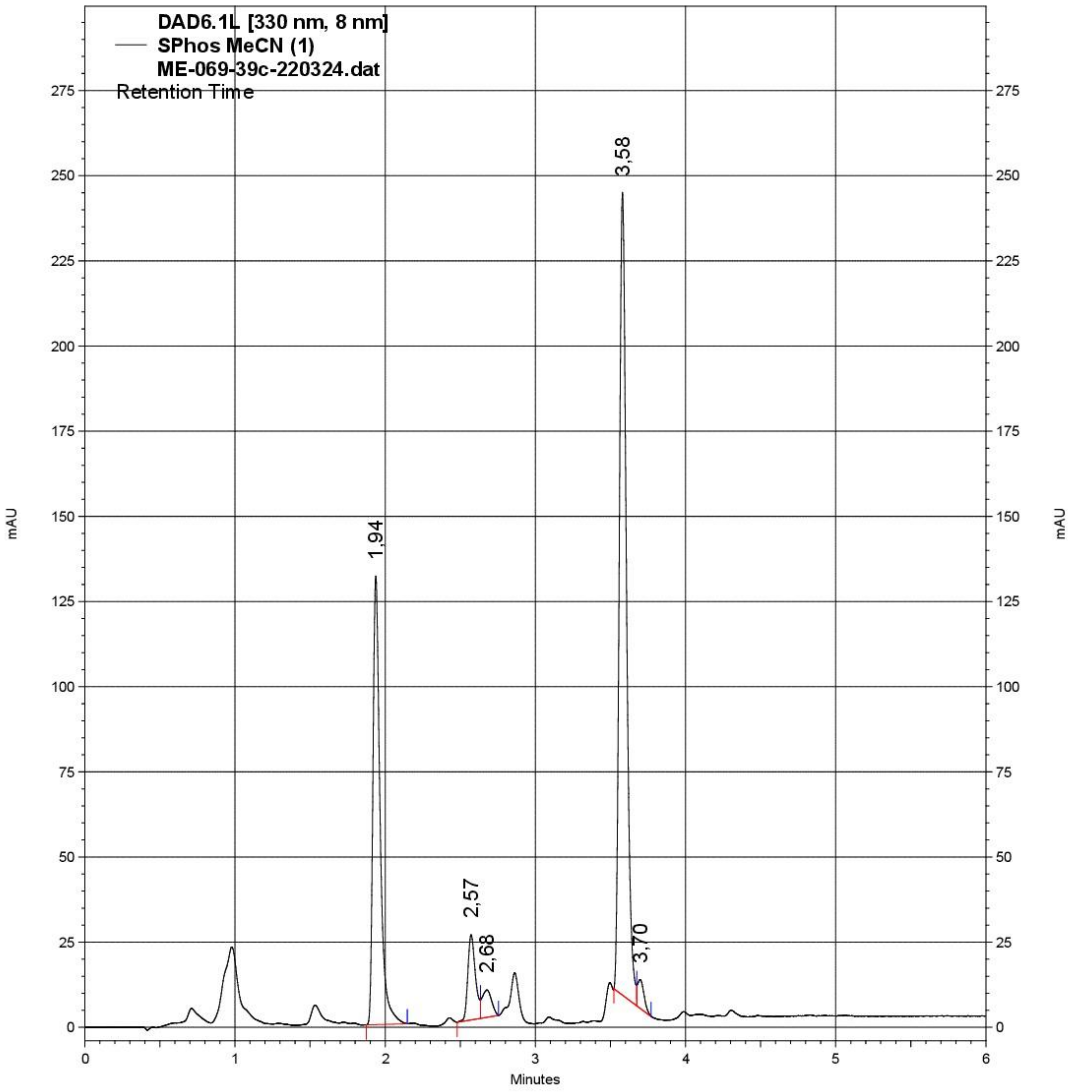

UV-Spektren

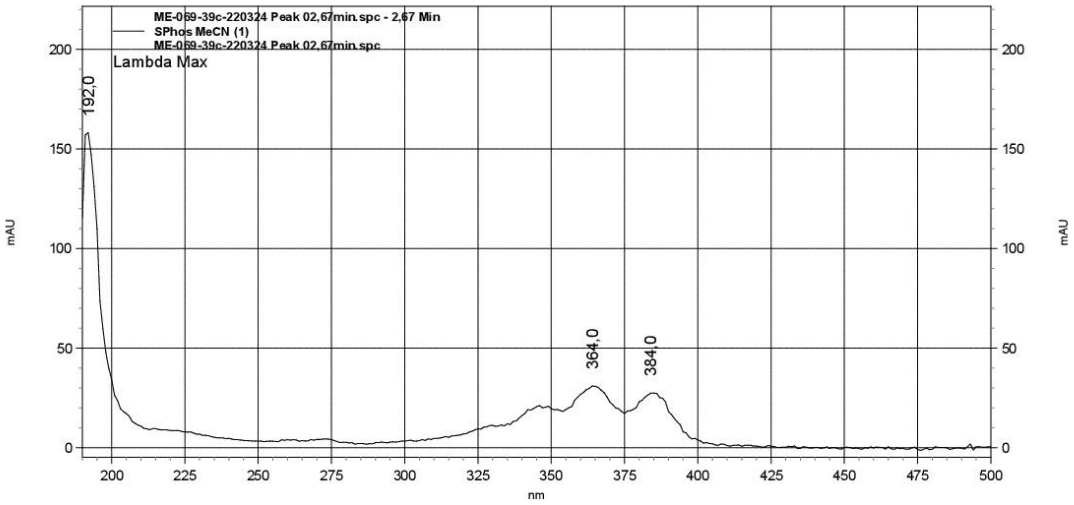

DAD6.1L [230 nm, 8 nm] Results

Retention Time	Area	Area %	Height	Height %
1,938	572264436	100,00	172076240	100,00

Totals				
	572264436	100,00	172076240	100,00

DAD6.1L [330 nm, 8 nm] Results

Retention Time	Area	Area %	Height	Height %
1,937	43535930	31,90	13169948	32,21
2,572	8792531	6,44	2500064	6,12
2,677	3503070	2,57	803579	1,97
3,580	78090296	57,22	23562909	57,64
3,698	2541620	1,86	845779	2,07

Totals				
	136463447	100,00	40882279	100,00

DAD6.1L [365 nm, 8 nm] Results

Retention Time	Area	Area %	Height	Height %
2,572	25910235	58,07	7380592	60,51
2,679	9651300	21,63	2221242	18,21
3,579	9060011	20,30	2596384	21,28

Totals				
	44621546	100,00	12198218	100,00

Data File: F:\Enterprise\Europa\Result\2024\2024 - AK Menche\ME-069-Max Guhlke\ME-069-39e-220324.dat
Method: F:\Enterprise\Europa\Method\Europa+ HPG\0.5ml - A1-B1 - 50-50 0min - 100-00 4,0min - C3 - 6,0min - 190-600nm - 230-330-365nm - 25-23°C - 50 Hz.met

Max Guhlke - JackiePhos MeCN (1) - ME-069-39e auf KNAUER Eurospher II 100-3 C18P 3µm; 2,0 x 100mm - 330nm

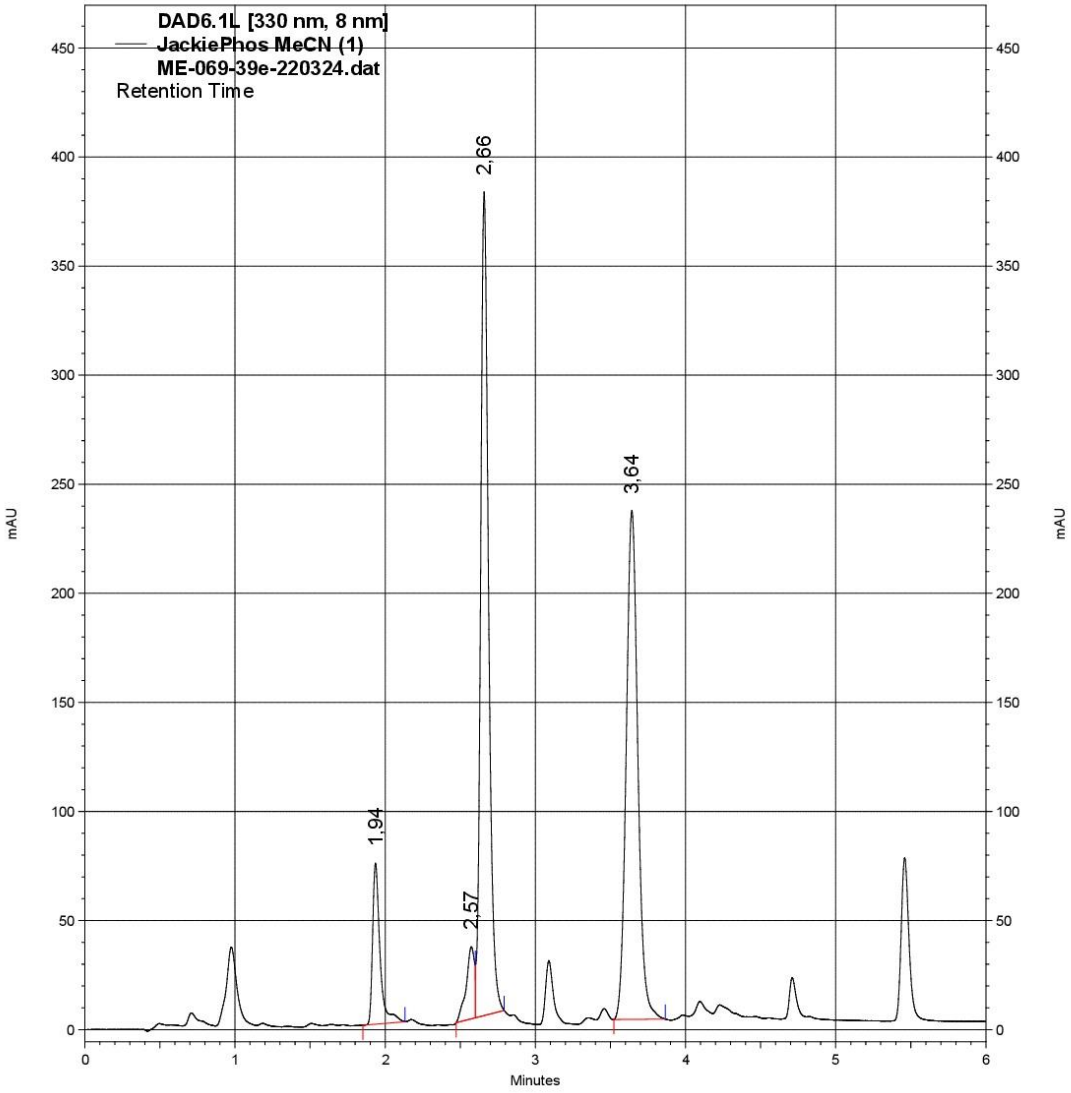

UV-Spektren

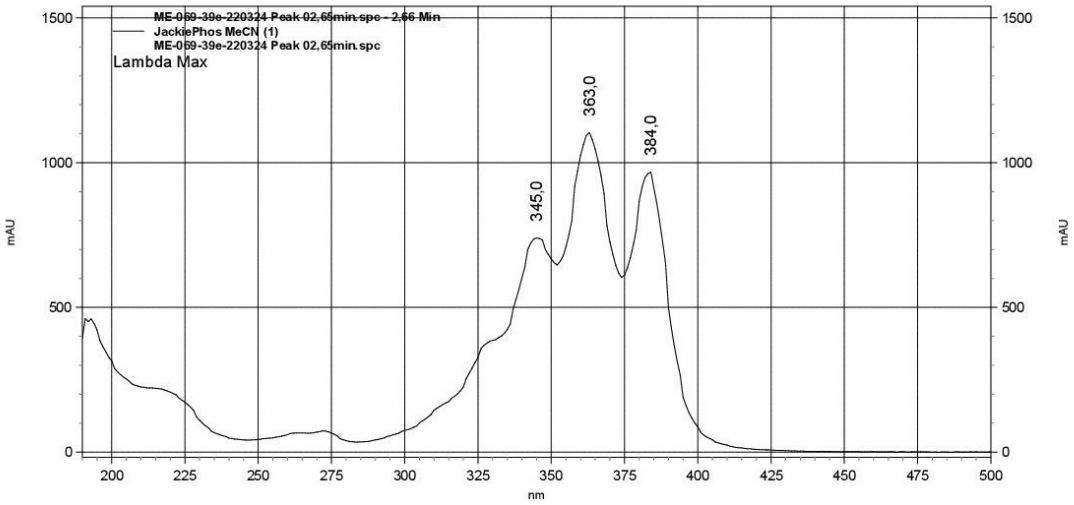

DAD6.1L [230 nm, 8 nm] Results

Retention Time	Area	Area %	Height	Height %
1,935	320782192	100,00	97388697	100,00

Totals				
	320782192	100,00	97388697	100,00

DAD6.1L [330 nm, 8 nm] Results

Retention Time	Area	Area %	Height	Height %
1,935	25337631	8,39	7380590	10,28
2,574	12534865	4,15	3300460	4,60
2,659	138566757	45,90	37758273	52,61
3,643	125445543	41,55	23325858	32,50

Totals				
	301884796	100,00	71765181	100,00

DAD6.1L [365 nm, 8 nm] Results

Retention Time	Area	Area %	Height	Height %
2,574	36533350	6,47	9702375	6,97
2,659	363211584	64,31	97947164	70,37
3,642	165072375	29,23	31539741	22,66

Totals				
	564817309	100,00	139189280	100,00

Data File: F:\Enterprise\Europa\Result\2024\2024 - AK Menche\ME-069-Max Guhlke\ME-069-39g-220324.dat
Method: F:\Enterprise\Europa\Method\Europa+ HPG\0.5ml - A1-B1 - 50-50 0min - 100-00 4,0min - C3 - 6,0min - 190-600nm - 230-330-365nm - 25-23°C - 50 Hz.met

Max Guhlke - Dppf MeCN (1) - ME-069-39g auf KNAUER Eurospher II 100-3 C18P 3µm; 2,0 x 100mm - 330nm

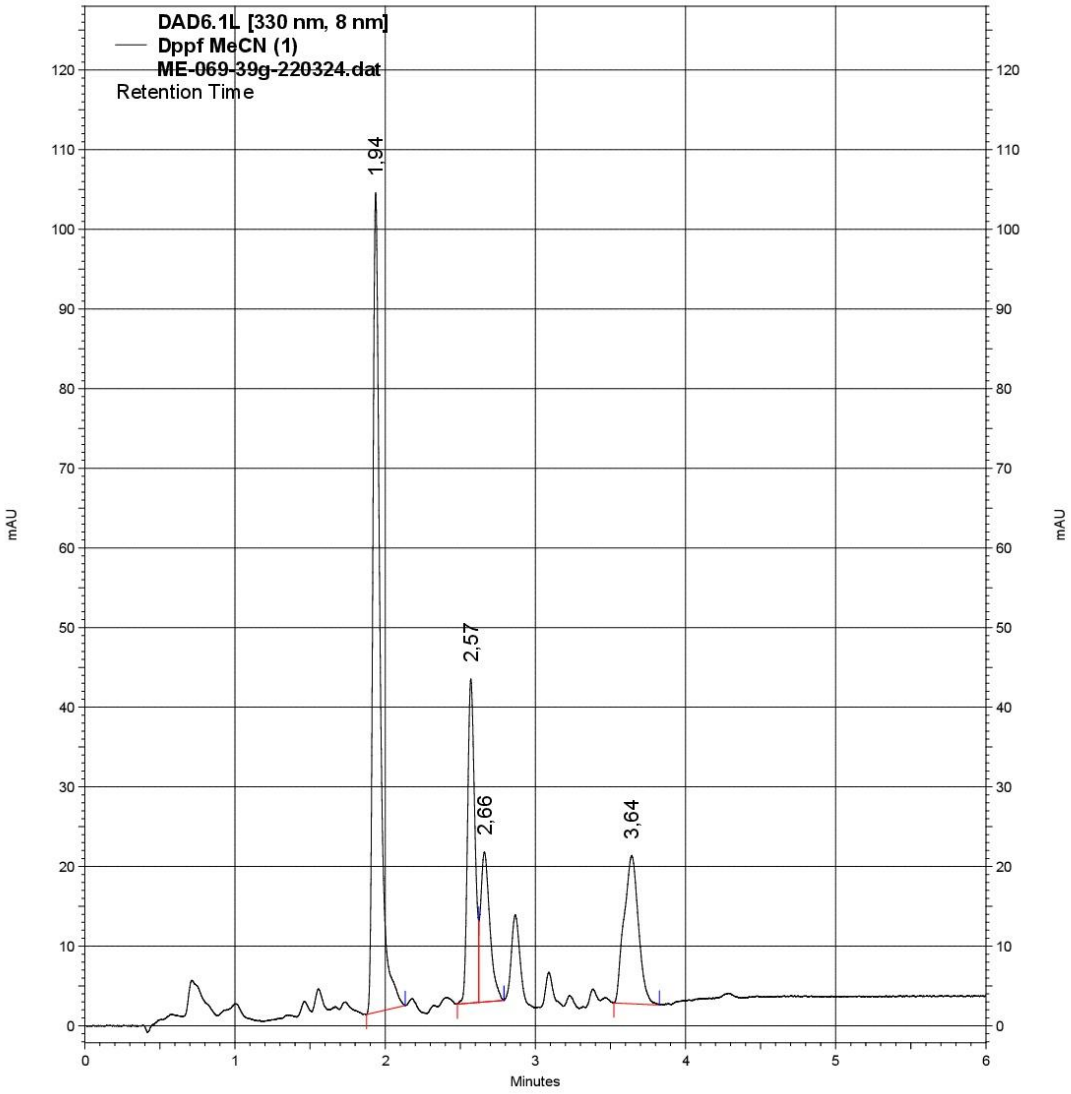

UV-Spektren

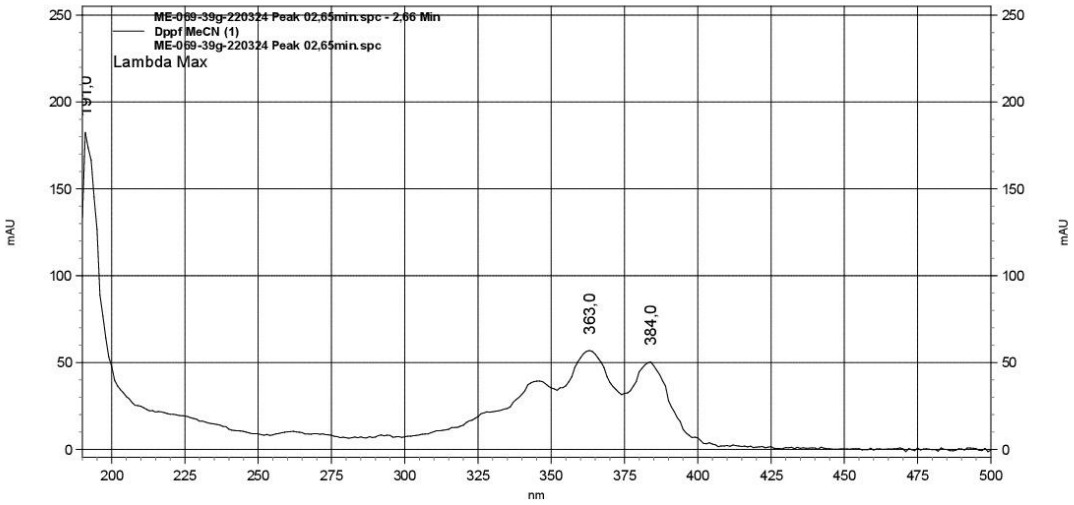

DAD6.1L [230 nm, 8 nm] Results

Retention Time	Area	Area %	Height	Height %
1,937	447493489	100,00	135138497	100,00
Totals	447493489	100,00	135138497	100,00

DAD6.1L [330 nm, 8 nm] Results

Retention Time	Area	Area %	Height	Height %
1,937	34392147	50,06	10289110	56,84
2,570	13806426	20,10	4067416	22,47
2,661	8071357	11,75	1882227	10,40
3,642	12432336	18,10	1861979	10,29
Totals	68702266	100,00	18100732	100,00

DAD6.1L [365 nm, 8 nm] Results

Retention Time	Area	Area %	Height	Height %
2,570	41434884	54,83	12064903	62,22
2,661	20477286	27,10	4860401	25,07
3,643	13653831	18,07	2463908	12,71
Totals	75566001	100,00	19389212	100,00

Data File: F:\Enterprise\Europa\Result\2024\2024 - AK Menche\ME-069-Max Guhlke\ME-069-39i-220324.dat
Method: F:\Enterprise\Europa\Method\Europa+ HPG\0.5ml - A1-B1 - 50-50 0min - 100-00 4,0min - C3 - 6,0min - 190-600nm - 230-330-365nm - 25-23°C - 50 Hz.met

Max Guhlke - Pd(PPh3)4 MeCN (1) - ME-069-39i auf KNAUER Eurospher II 100-3 C18P 3µm; 2,0 x 100mm - 330nm

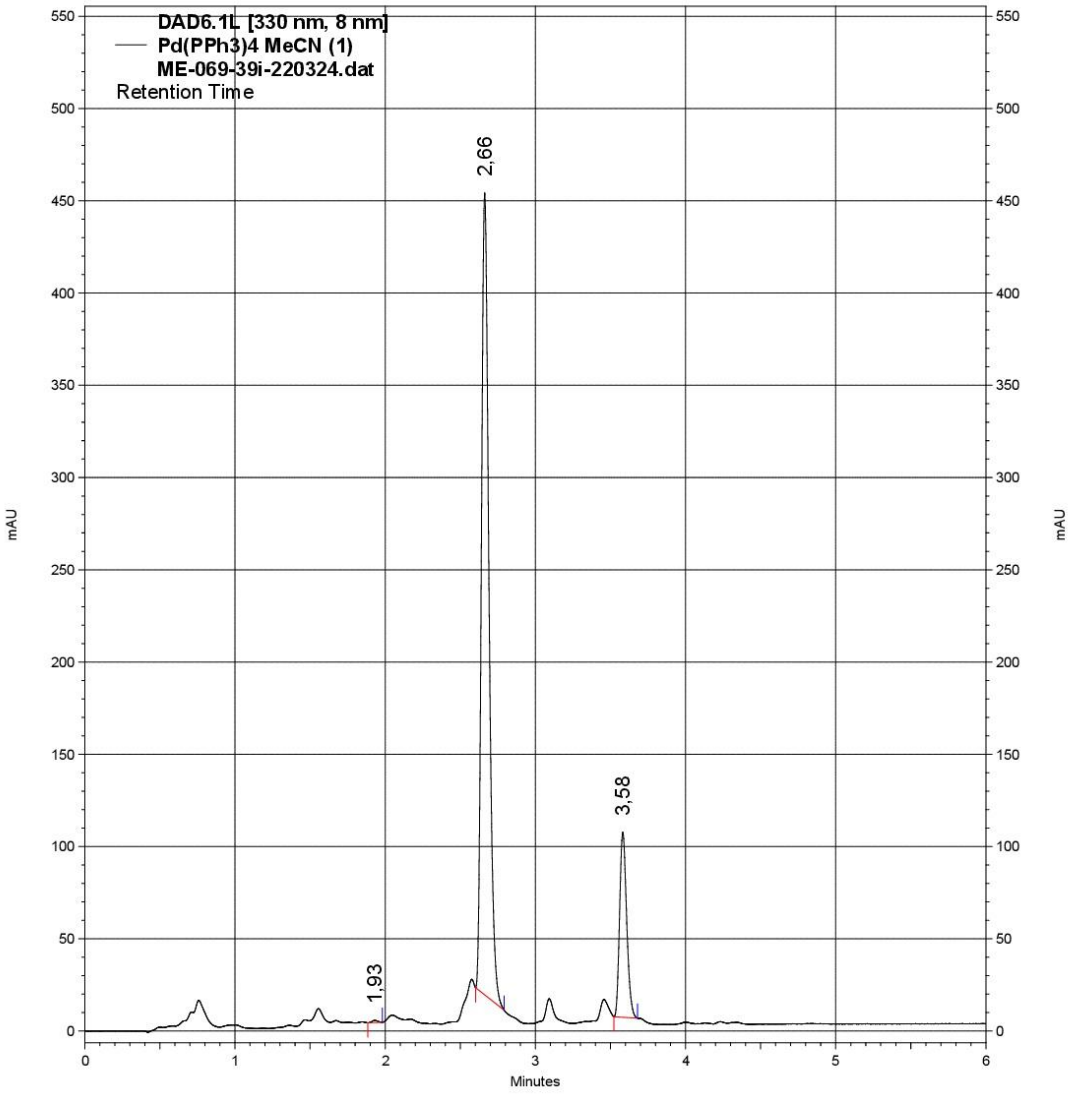

UV-Spektren

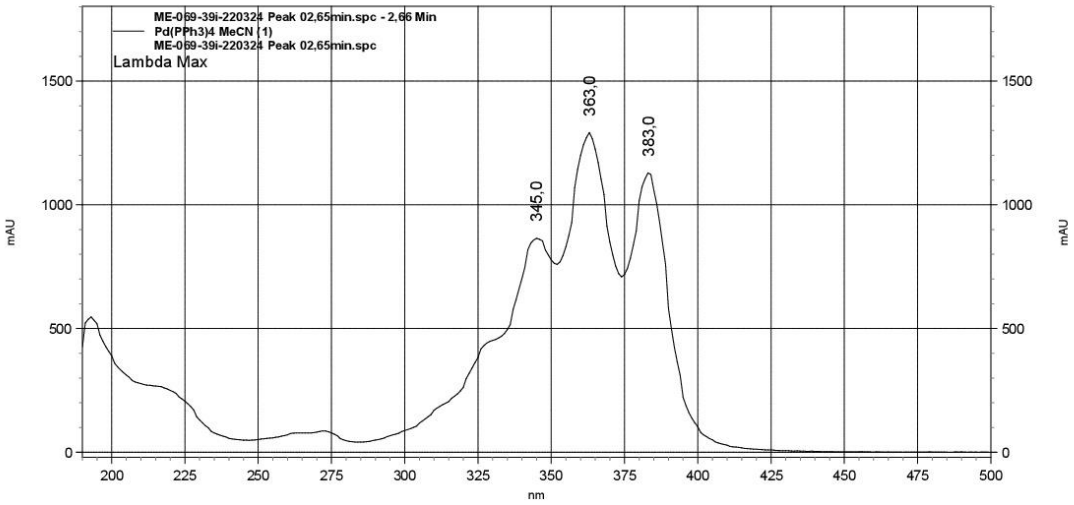

DAD6.1L [230 nm, 8 nm] Results

Retention Time	Area	Area %	Height	Height %
1,825	238	100,00	614	100,00
Totals	238	100,00	614	100,00

DAD6.1L [330 nm, 8 nm] Results

Retention Time	Area	Area %	Height	Height %
1,931	296806	0,16	116369	0,22
2,663	150124472	82,00	43471527	81,07
3,582	32667056	17,84	10032504	18,71
Totals	183088334	100,00	53620400	100,00

DAD6.1L [365 nm, 8 nm] Results

Retention Time	Area	Area %	Height	Height %
2,663	388258945	99,15	111781749	99,08
3,582	3336212	0,85	1037563	0,92
Totals	391595157	100,00	112819312	100,00

Data File: F:\Enterprise\Europa\Result\2024\2024 - AK Menche\ME-069-Max Guhlke\ME-069-39k-220324.dat
Method: F:\Enterprise\Europa\Method\Europa+ HPG\0.5ml - A1-B1 - 50-50 0min - 100-00 4,0min - C3 - 6,0min - 190-600nm - 230-330-365nm - 25-23°C - 50 Hz.met

Max Guhlke - Pd(P-oTol)2 MeCN (1) - ME-069-39k auf KNAUER Eurospher II 100-3 C18P 3µm; 2,0 x 100mm - 330nm

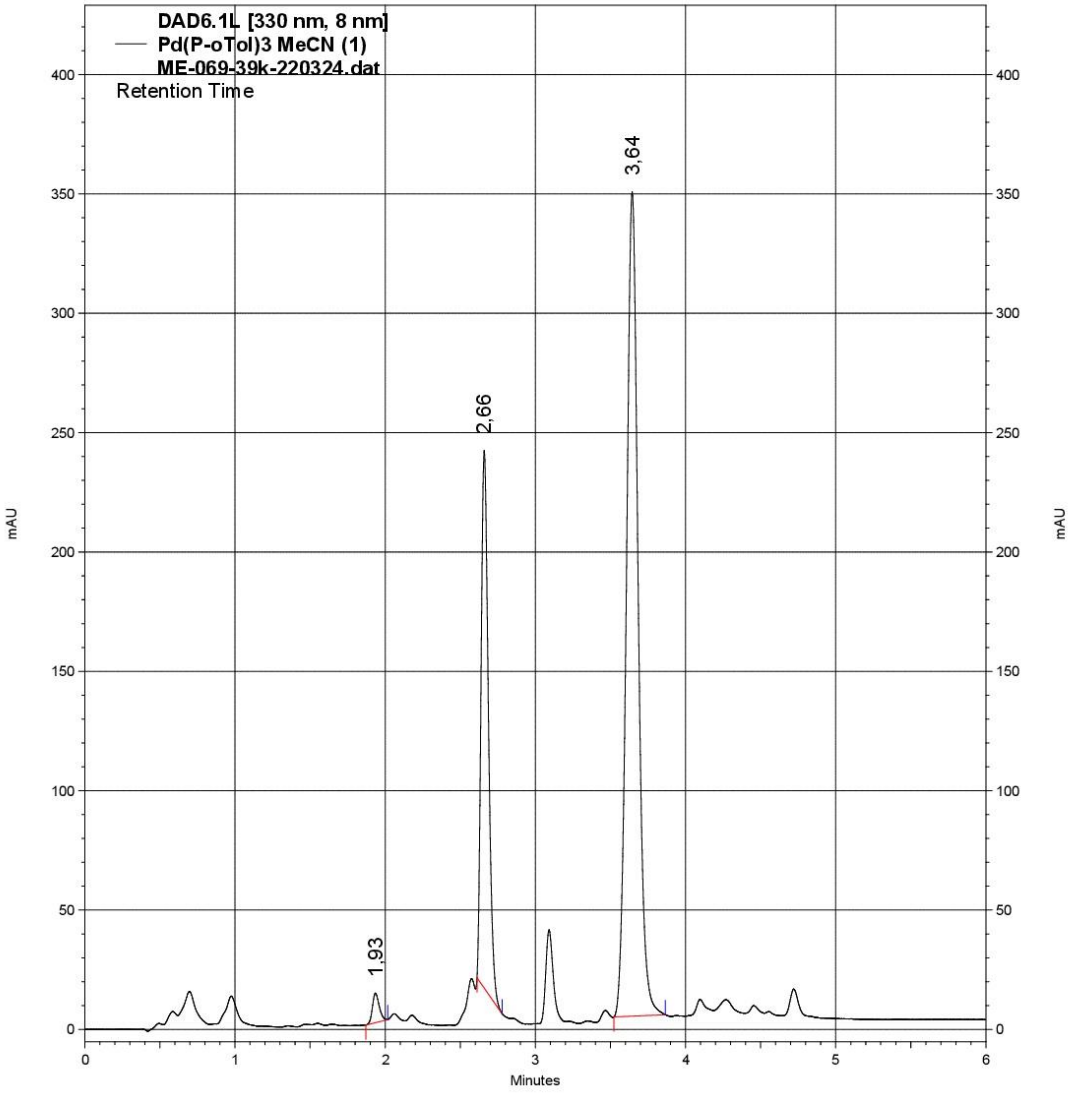

UV-Spektren

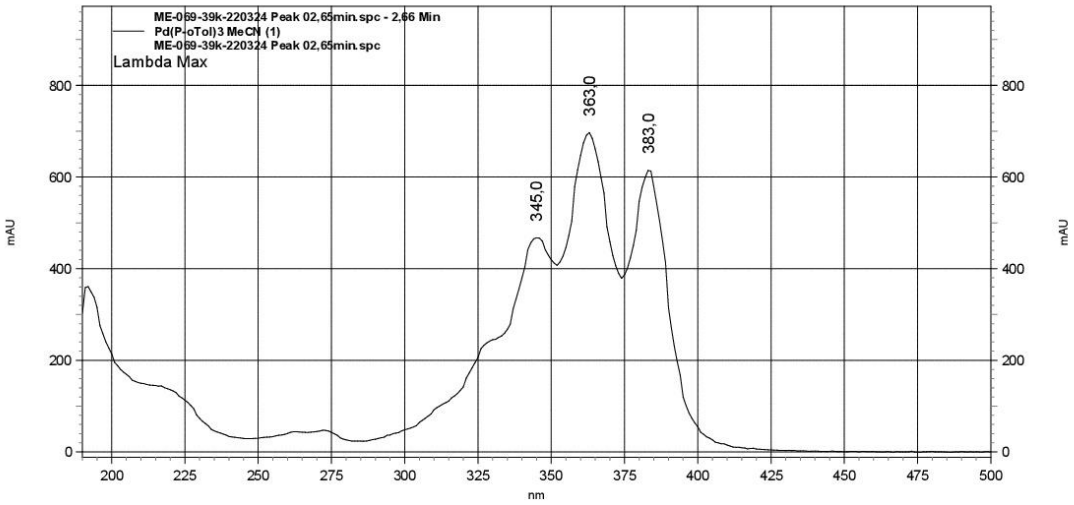

DAD6.1L [230 nm, 8 nm] Results

Retention Time	Area	Area %	Height	Height %
1,936	49831112	100,00	13793061	100,00

Totals				
	49831112	100,00	13793061	100,00

DAD6.1L [330 nm, 8 nm] Results

Retention Time	Area	Area %	Height	Height %
1,935	3886352	1,46	1239988	2,13
2,660	75827465	28,52	22526283	38,64
3,645	186186341	70,02	34529553	59,23

Totals				
	265900158	100,00	58295824	100,00

DAD6.1L [365 nm, 8 nm] Results

Retention Time	Area	Area %	Height	Height %
2,660	203428754	45,57	59374888	56,02
3,644	242955612	54,43	46617513	43,98

Totals				
	446384366	100,00	105992401	100,00

KNAUER

Raum 5.067 / 5.068
Telefon: 73-5817
Mail: hplcpool@uni-bonn.de

Rheinische Friedrich-Wilhelms-Universität Bonn
Kekulé-Institut für Organische Chemie und Biochemie
HPLC-Pool – **hplcpool.uni-bonn.de**

Messprotokoll ANALYTISCHE HPLC-Trennung

Datum: 22. 03. 2024	Name: Max Guhlke	AK-Nr.: ME-069
Chiffre Substanz: siehe unten	Chiffre HPLC : ME-069-39X (siehe unten)	

PROBENVORBEREITUNG

Menge: -- mg	gelöst in Acetonitril	Ultraschallbad? JA ☐ NEIN X
Filtriert? JA X NEIN ☐	Filterbezeichnung: SARTORIUS MiniSart RC4 (reg. Cellulose) 0,2 µm	
Anmerkungen: klare, farblose oder gelbliche Lösungen (**nach SPE-C18ec-Vorreinigung**)		

SYSTEMANGABEN

System KALLISTO+ ☐	System GANYMED+² ☐	System EUROPA+ X	230, 330, 365 nm
UV/Vis-DAD X	Meßbereich: X 190 – 600 nm ☐ 190 – 900 nm – 50 Hz / 0,02 sec		
Ri-Detektor ☐	Range : ☐ 125 ☐ 256 ☐ 512		
Eluenten	A: Acetonitril *HPLCgrade*	B: Wasser *PureLab*	

LAUF 01	Flussrate: 0,5 ml/min	Druck: 231 - 97 bar	Injektion: 2 µl	Temperatur: 25°C
Pumpe	%A: 50	%B: 50	Vial: 1	Laufzeit: 06,0 Minuten
Isokratisch ☐	Gradient X – Details:	Start: 50% A + 50% B 04:00 min: 100% A 06:00 min: 100% A		
Säule: KNAUER Eurospher II 100-3 C18P; 3 µm; 2,0 x 100 mm (19120315187)				
Dateiname: ME-069-39a-220324	Anmerkungen: **XPhos MeCN (1)**			**Plot? JA X NEIN ☐**

LAUF 03	Flussrate: 0,5 ml/min	Druck: 231 - 97 bar	Injektion: 2 µl	Temperatur: 25°C
Pumpe	%A: 50	%B: 50	Vial: 3	Laufzeit: 06,0 Minuten
Isokratisch ☐	Gradient X – Details:	Start: 50% A + 50% B 04:00 min: 100% A 06:00 min: 100% A		
Säule: KNAUER Eurospher II 100-3 C18P; 3 µm; 2,0 x 100 mm (19120315187)				
Dateiname: ME-069-39c-220324	Anmerkungen: **SPhos MeCN (1)**			**Plot? JA X NEIN ☐**

LAUF 05	Flussrate: 0,5 ml/min	Druck: 231 - 97 bar	Injektion: 2 µl	Temperatur: 25°C
Pumpe	%A: 50	%B: 50	Vial: 5	Laufzeit: 06,0 Minuten
Isokratisch ☐	Gradient X – Details:	Start: 50% A + 50% B 04:00 min: 100% A 06:00 min: 100% A		
Säule: KNAUER Eurospher II 100-3 C18P; 3 µm; 2,0 x 100 mm (19120315187)				
Dateiname: ME-069-39e-220324	Anmerkungen: **JackiePhos MeCN (1)**			**Plot? JA X NEIN ☐**

KNAUER

Raum 5.067 / 5.068
Telefon: 73-5817
Mail: hplcpool@uni-bonn.de

Rheinische Friedrich-Wilhelms-Universität Bonn
Kekulé-Institut für Organische Chemie und Biochemie
HPLC-Pool – **hplcpool.uni-bonn.de**

Messprotokoll ANALYTISCHE HPLC-Trennung

LAUF 07	Flussrate: 0,5 ml/min	Druck: 231 - 97 bar	Injektion: 2 µl	Temperatur: 25°C
Pumpe	%A: 50	%B: 50	Vial: 7	Laufzeit: 06,0 Minuten
Isokratisch ☐	Gradient X – Details:	Start: 50% A + 50% B 04:00 min: 100% A 06:00 min: 100% A		
Säule: KNAUER Eurospher II 100-3 C18P; 3 µm; 2,0 x 100 mm (19120315187)				
Dateiname: ME-069-39g-220324	Anmerkungen: **Dppf MeCN (1)**			**Plot? JA X NEIN ☐**
LAUF 09	Flussrate: 0,5 ml/min	Druck: 231 - 97 bar	Injektion: 2 µl	Temperatur: 25°C
Pumpe	%A: 50	%B: 50	Vial: 9	Laufzeit: 06,0 Minuten
Isokratisch ☐	Gradient X – Details:	Start: 50% A + 50% B 04:00 min: 100% A 06:00 min: 100% A		
Säule: KNAUER Eurospher II 100-3 C18P; 3 µm; 2,0 x 100 mm (19120315187)				
Dateiname: ME-069-39i-220324	Anmerkungen: **$Pd(PPh_3)_4$ MeCN (1)**			**Plot? JA X NEIN ☐**
LAUF 11	Flussrate: 0,5 ml/min	Druck: 231 - 97 bar	Injektion: 2 µl	Temperatur: 25°C
Pumpe	%A: 50	%B: 50	Vial: 11	Laufzeit: 06,0 Minuten
Isokratisch ☐	Gradient X – Details:	Start: 50% A + 50% B 04:00 min: 100% A 06:00 min: 100% A		
Säule: KNAUER Eurospher II 100-3 C18P; 3 µm; 2,0 x 100 mm (19120315187)				
Dateiname: ME-069-39k-220324	Anmerkungen: **$Pd(P\text{-}oTol)_3$ MeCN (1)**			**Plot? JA X NEIN ☐**

11.3 Purity control of hexaene II (135)

Data File: F:\Enterprise\Europa\Result\2024\2024 - AK Menche\ME-069-Max Guhlke\ME-069-40a-180424-01.dat
Method: F:\Enterprise\Europa\Method\Europa+ HPG\0.5ml - A1-B1 - 50-50 0min - 100-00 4,0min - C3 - 6,0min - 190-600nm - 230-330-365nm - 25-23°C - 50 Hzb.met

Max Guhlke - MG-F007 Fr. - ME-069-40a auf MN Nucleodur 100-3 Isis C18 3µm; 2,0 x 100mm - 365nm

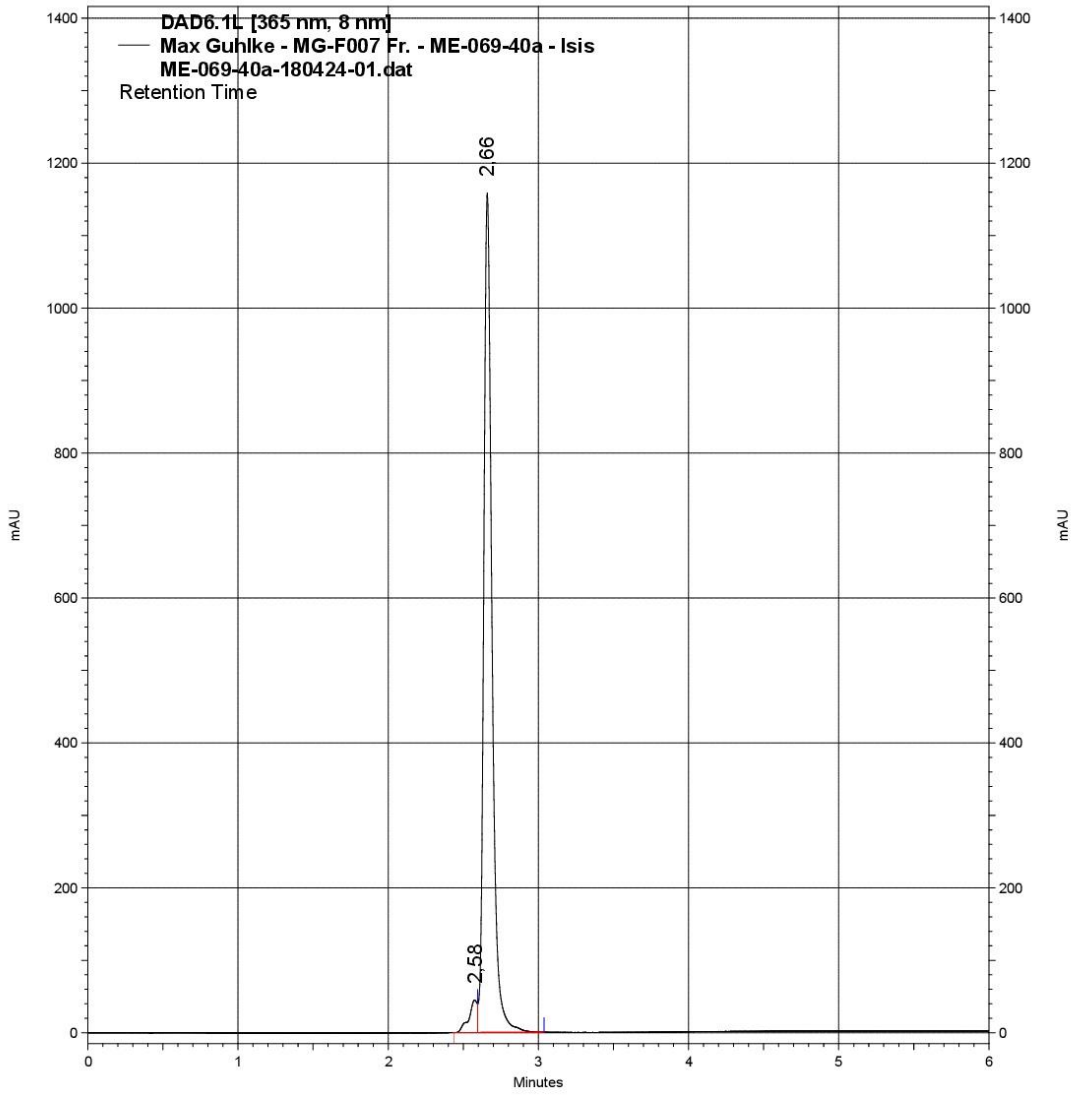

UV-Spektren

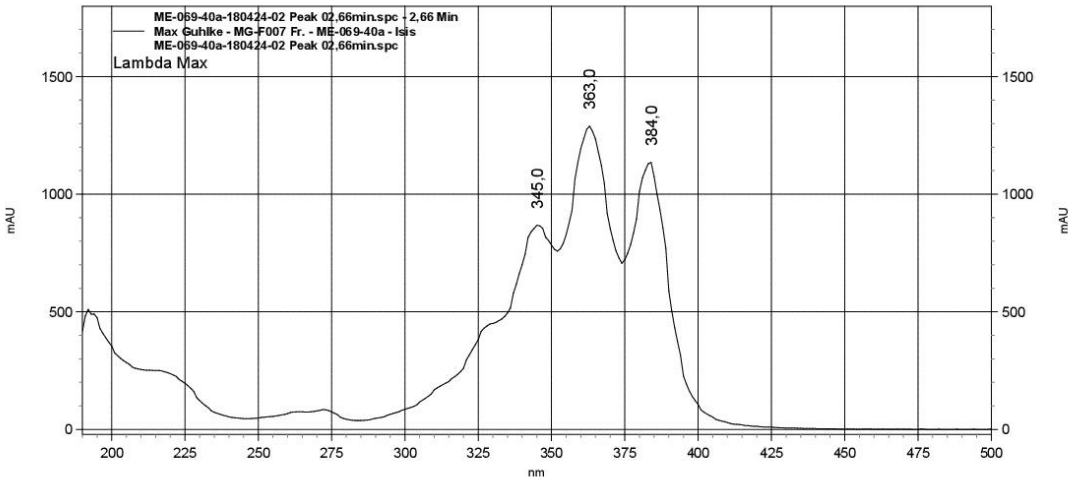

DAD6.1L [230 nm, 8 nm] Results

Retention Time	Area	Area %	Height	Height %	Name
2,577	1201377	2,29	304517	2,29	
2,660	51358804	97,71	12975499	97,71	
Totals	52560181	100,00	13280016	100,00	

DAD6.1L [330 nm, 8 nm] Results

Retention Time	Area	Area %	Height	Height %	Name
2,574	6122124	3,46	1558561	3,36	
2,660	171002840	96,54	44846414	96,64	
Totals	177124964	100,00	46404975	100,00	

DAD6.1L [365 nm, 8 nm] Results

Retention Time	Area	Area %	Height	Height %	Name
2,575	17101115	3,74	4471050	3,72	
2,660	439544320	96,26	115799863	96,28	
Totals	456645435	100,00	120270913	100,00	

KNAUER

Raum 5.067 / 5.068
Telefon: 73-5817
Mail: hplcpool@uni-bonn.de

Rheinische Friedrich-Wilhelms-Universität Bonn
Kekulé-Institut für Organische Chemie und Biochemie
HPLC-Pool – **hplcpool.uni-bonn.de**

Messprotokoll ANALYTISCHE HPLC-Trennung

Datum: 18. 04. 2024	Name: Max Guhlke	AK-Nr.: ME-069
Chiffre Substanz: MG-F007 Fr.	Chiffre HPLC : ME-069-40a	

PROBENVORBEREITUNG

Menge: -- mg	gelöst in Acetonitril / Wwasser	Ultraschallbad? JA ☐ NEIN X
Filtriert? JA ☐ NEIN X	Filterbezeichnung:	
Anmerkungen: Direktentnahme Fr. aus präp. Trennung ME-069-40 (TITAN+)		

SYSTEMANGABEN

System KALLISTO+ ☐	System GANYMED+^{2} ☐	System EUROPA+ X	230, 330, 365 nm
UV/Vis-DAD X	Meßbereich: X 190 – 600 nm	☐ 190 – 900 nm – 50 Hz / 0,02 sec	
Ri-Detektor ☐	Range : ☐ 125 ☐ 256 ☐ 512		
Eluenten	A: Acetonitril *HPLCgrade*	B: Wasser *PureLab*	

LAUF 01	Flussrate: 0,5 ml/min	Druck: 232 – 96 bar	Injektion: 1 µl	Temperatur: 25°C
Pumpe	%A: 50	%B: 50	Vial: 2	Laufzeit: 06,0 Minuten
Isokratisch ☐	Gradient X – Details:	Start: 50% A + 50% B 04:00 min: 100% A 06:00 min: 100% A		
Säule: MACHERERY-NAGEL Nucleodur 100-3 Isis C18; 3 µm; 2,0 x 100 mm (N2300006)				
Dateiname: ME-069-40a-180424-01	Anmerkungen: ca. 3 – 4% Dreck			Plot? JA ☐ NEIN X
LAUF 02	Flussrate: 0,5 ml/min	Druck: 232 – 96 bar	Injektion: 1 µl	Temperatur: 25°C
Pumpe	%A: 50	%B: 50	Vial: 2	Laufzeit: 06,0 Minuten
Isokratisch ☐	Gradient X – Details:	Start: 50% A + 50% B 04:00 min: 100% A 06:00 min: 100% A		
Säule: MACHERERY-NAGEL Nucleodur 100-3 Isis C18; 3 µm; 2,0 x 100 mm (N2300006)				
Dateiname: ME-069-40a-180424-02	Anmerkungen: reprod. Lauf 01			**Plot? JA X NEIN ☐**

References

[1] H. S. Elshafie, I. Camele , Amira A. Mohamed, *Int. J. Mol. Sci.* **2023**, *24*, 3266.

[2] A. Banoa,T. A. Qadrib, Mahnoora, N. Khan, *S. Afr. J. Bot.* **2023**, *159*, 98–109.

[3] G. Muteeb, M. T. Rehman, M. Shahwan, M. Aatif, *Pharmaceuticals* **2023**, *16*, 1615.

[4] K. C. Nicolaou, S. Rigol, *J. Antibiot.* **2018**, *71*, 153–184.

[5] A. G. Atanasov, S. B. Zotchev2, V. M. Dirsch, C. T. Supuran, *Nat. Rev. Drug Discov.* **2021**, *20*, 200–216.

[6] N. Y. S. Lam, I. Paterson, *Eur. J. Org. Chem.* **2020**, *16*, 2310–2320.

[7] P. S. Baran, *J. Am. Chem. Soc.* **2018**, *140*, 4751−4755.

[8] C. M. Rath, J. B. Scaglione, J. D. Kittendorf, D. H. Sherman, *Comprehensive Natural Products II Chemistry and Biology* **2010**, *1*, 453–492.

[9] D. Aprilia, A. Miftakhurohmat, Sutarman, *Earth Environ. Sci.* **2021**, 819 012009.

[10] S. Miao, J. Liang, Y. Xu, G. Yu, M. Shao, *J. Cell Physiol.* **2024**, 239:e30974.

[11] P. S. Patel, S. Huang, S. Fisher, D. Pirnik, C. Aklonis, L. Dean, E. Meyers, P. Fernandes, F. Mayerl, *J. Antibiot.* **1995**, *48*, 997–1003.

[12] R. A. Butcher, F. C. Schroeder, M. A. Fischbach, P. D. Straight, R. Kolter, C. T. Walsh, J. Clardy, *Proc. Natl. Acad. Sci. USA* **2007**, *105*, 1506–1509.

[13] J. Moldenhauer, X. Chen, R. Borriss, J. Piel, *Angew. Chem.* **2007**, *119*, 8343 –8345.

[14] H. Li, X. Han, J. Zhang, Y. Dong, S. Xu, Y. Bao, C. Chen, Y. Feng, Q. Cui, W. Li, *J. Nat. Prod.* **2019**, *82*, 3340–3346.

[15] C. T. Calderone, S. B. Bumpus, N. L. Kelleher, C. T. Walsh, N. A. Magarvey, *Proc. Natl. Acad. Sci. USA*, **2008**, *105*, 12809–12814.

[16] M. Guhlke, J. Herbst, T. G. Nguyen, A. Schneider, J. S. Dickschat, D. Menche, *Org. Lett.* **2025**, *27*, 2317–2322.

[17] R. Reid, M. Piagentini, E. Rodriguez, G. Ashley, N. Viswanathan, J. Carney, D. V. Santi, C. R. Hutchinson, R. McDaniel, *Biochemistry* **2003**, *42*, 72-79.

[18] P. Caffrey, *ChemBioChem.* **2003**, *4*, 649–662.

[19] P. Nonejuie, R. M. Trial, G. L Newton, A. Lamsa, V. R. Perera, J. Aguilar, W. Liu, P. C. Dorrestein, J. Pogliano, K. Pogliano*, J. Antibiot.* **2016**, *69*, 353–361.

[20] H. Li, X. Han, Y. Dong, S. Xu, C. Chen, Y. Feng, Q. Cui, W. Li, *ACS Omega* **2021**, *6*, 1093–1098.

[21] X. Chen, J. Vater, J. Piel, P. Franke, R. Scholz, K. Schneider, A. Koumoutsi, G. Hitzeroth, N. Grammel, A. W. Strittmatter, G. Gottschalk, R. D. Süssmuth, R. Borriss, *J. Bacteriol.* **2006**, *188*, 4024–4036.

[22] J. Moldenhauer, D. C. G. Götz, C. R. Albert, S. K. Bischof, K. Schneider, R. D. Süssmuth, M. Engeser, H. Gross, G. Bringmann, J. Piel, *Angew. Chem.* **2010**, *122*, 1507–1509.

[23] A. Hashem, B. Tabassum, E. F. Abd Allah, *Saudi J. Biol. Sci.* **2019**, *26*, 1291–1297.

[24] K. Chen, Z. Tian, Y. Luo, Y. Cheng, C. Long, *Phytopathol.* **2018**, *108*, 1252–1262.

[25] L. Chen, J. Heng, S. Qin, K. Bian, *PloS ONE* **2018**, *13*, e0198560.

[26] C. Molina-Santiago, D. Vela-Corcia, D. Petras, P. C. Dorrestein, A. de Vicente, D. Romero, *Cell Reports* **2021**, *36*, 109449.

[27] S. Shoji, S. E. Walker, K. Fredrick, *ACS Chem. Biol.* **2009**, *4*, 93–107.

[28] A. Erega, P. Stefanic, I. Dogsa, T. Danevcic, K. Simunovic, A. Klancnik, S. Smole Možina, I. M. Mulec, *Appl. Environ. Microbiol.* **2021**, *87*, e02955-20.

[29] S. F. Altekruse, N. J. Stern, P. I. Fields, D. L. Swerdlow, *Emerg. Infect. Dis*. **1999**, *5*, 28–35.

[30] P. D. Straight, M. A. Fischbach, C. T. Walsh, D. Z. Rudner, R. Kolter, *Proc. Natl. Acad. Sci. USA* **2007**, *104*, 305–310.

[31] E. J. N. Helfrich, J. Piel, *Nat. Prod. Rep.* **2016**, *33*, 231–316.

[32] Z. Yin, J. S. Dickschat, *Beilstein J. Org. Chem.* **2024**, *20*, 734–740.

[33] Y. Liu, W. Qin, Q. Liu, J. Zhang, H. Li, S. Xu, P. Ren, L. Tian, W. Li, *Environ. Microbiol.* **2016**, *18*, 4770–4781.

[34] Y. Liu, W. Qin, Q. Liu, J. Zhang, H. Li, S. Xu, P. Ren, L. Tian, W. Li, *ChemBioChem* **2014**, *15*, 2747–2753.

[35] A. Bayer, M. E. Maier, *Tetrahedron* **2004**, *60*, 6665–6677.

[36] Y. Wu, X. Liao, R. Wang, X. Xie, J. K. De Brabander, *J. Am. Chem. Soc.* **2002**, *124*, 3245–3253.

[37] K. S. Madden, F. A. Mosa, A. Whiting, *Org. Biomol. Chem.* **2014**, *12*, 7877–7899.

[38] B. Hudson, B. Kohler, *Annu. Rev. Phys. Chem.* **1974**, *25*, 437–460.

[39] T. Maoka, *J. Nat. Med.* **2020**, *74*, 1–16.

[40] E. H. Harrison, *Nutrients* **2022**, *14*, 1411–1420.

[41] L. F. Maia, V. E. De Oliveira, H. G. M. Edwards, L. C. De Oliveira, *ChemPhysChem* **2021**, *22*, 231–249.

[42] T. Haro-Reyes, L. Diaz-Peralta, A. Galván-Hernández, A. Rodríguez-López, L. Rodríguez-Fragoso, I. Ortega-Blake, *Membranes* **2022**, *12*, 681.

[43] K. B. Vu, V. V. Vu, H. P. T. Thu, H. N. Giang, N. M. Tam, S. T. Ngo, *Synth. Met.* **2018**, *246*, 128–136.

[44] J. Cornil, A. Guérinot, J. Cossy, *Org. Biomol. Chem.* **2015**, *13*, 4129–4142.

[45] R. S. Coleman, M. C. Walczak, *J. Org. Chem.* **2006**, *71*, 9841–9844.

[46] E. P. Gillis, M. D. Burke, *J. Am. Chem. Soc.* **2007**, *129*, 6716–6717.

[47] E. P. Gillis, dissertation, University of Illinois at Urbana-Champaign, **2010**.

[48] D. Aich, P. Kumar, D. Ghorai, K. K. Das, S. Panda, *Chem. Commun.* **2022**, *58*, 13298-13316.

[49] K. C. Gray, D. S. Palacios, I. Dailey, M. M. Endo, B. E. Uno, B. C. Wilcock, M. D. Burke, *Proc. Natl. Acad. Sci. USA* **2012**, *109*, 2234–2239.

[50] V. P. Ananikov, A. S. Kashina, O. V. Hazipova, I. P. Beletskaya, Z. A. Starikova, *Synlett.* **2011**, *14*, 2021–2024.

[51] F. Babudri, G. M. Farinola, F. Naso, R. Ragni, G. Spina, *Synthesis* **2007**, *19*, 3088–3092.

[52] P. M. Pihko, A. M. P. Koskinen, *Synlett* **1999**, *12*, 1966–1968.

[53] A. Babczyk, D. Menche, *J. Am. Chem. Soc.* **2023**, *145*, 10974−10979.

[54] A. Sorg, R. Brückner, *Angew. Chem. Int. Ed.* **2004**, *43*, 4523 –4526.

[55] L. A. Paquette, *Acc. Chem. Res.* **1968**, *1*, 209–216.

[56] B. H. Lipshutz, C. Lindsley, *J. Am. Chem. Soc.* **1997**, *119*, 4555–4556.

[57] K. Takai, N. Shinomiya, H. Kaihara, N. Yoshida, T. Moriwake, K. Utimoto, *Synlett* **1995**, *9*, 963–964.

[58] M. Altendorfer,D. Menche, *Chem. Commun.* **2012**, *48*, 8267–8269.

[59] A. Darwish, A. Lang, T. Kim, J. M. Chong, *Org. Lett.* **2008**, *10*, 861–864.

[60] A. Barbero, F. J. Pulido, *Chem. Soc. Rev.* **2005**, *34*, 913–920.

[61] S. Ahn, C. Lee, C. Cheon, *Adv. Synth. Catal.* **2014**, *356*, 1767–1772.

[62] J. W. Lehmann, D, J. Blair, M. D. Burke, *Nat. Rev. Chem.* **2018**, *2*, 0115.

[63] T. Kuranaga, Y. Sesoko, M. Inoue, *Nat. Prod. Rep.* **2014**, *31*, 514–532.

[64] T. Courant, G. Dagousset, G. Masson, *Synthesis* **2015**, *47*, 1799–1826.

[65] T. K. Chakraborty, P. Laxman, *Tetrahedron Lett.* **2003**, *44*, 4989–4992.

[66] J. T. Feutrill, M. J. Lilly, M. A. Rizzacasa, *Org. Lett.* **2002**, *4*, 525–527.

[67] A. B. Smith, M. O. Duffey, K. Basu, S. P. Walsh, H. W. Suennemann, M. Frohn, *J. Am. Chem. Soc.* **2008**, *130*, 422–423.

[68] A. Fürstner, T. Dierkes, O. R. Thiel, G. Blanda, *Chem. Eur. J.* **2001**, *7*, 5286–5298.

[69] D. R. Carbery, *Org. Biomol. Chem.* **2008**, *6*, 3455–3460.

[70] C. Cativiela, J. I. Garcia, J. A. Mayoral, L. Salvatella, *J. Mol. Struct. THEOCHEM* **1996**, *368*, 57–66.

[71] A. J. Clark, D. P. Curran, D. J. Fox, F. Ghelfi, C. S. Guy, B. Hay, N. James, J. M. Phillips, F. Roncaglia, P. B. Sellars, P. Wilson, H. Zhan, *J. Org. Chem.* **2016**, *81*, 5547–5565.

[72] R. Shen, J. A. Porco, *Org. Lett.* **2000**, *2*, 1333–1336.

[73] I. Goldberg, *Chem. Ber.* **1906**, *39*, 1691–1692.

[74] A. Klapars, J. C. Antilla, X. Huang, S. L. Buchwald, *J. Am. Chem. Soc.* **2001**, *123*, 7727–7729.

[75] L.C. Dias, L. G. de Oliveira, J. D. Vilcachagua, F. Nigsch, J. *Org. Chem.* **2005**, *70*, 2225–2234.

[76] L. Jiang, G. E. Job, A. Klapars, S. L. Buchwald, *Org. Lett.* **2003**, *5*, 3667–3669.

[77] J. C. Cuevas, P. Patil, V. Snieckus, *Tetrahedron Lett.* **1989**, *30*, 5841–5844.

[78] C. Palomo, J. M. Aizpurua, M. Legido, *Tetrahedron Lett.* **1992**, *33*, 3903–3906.

[79] A. Fürstner, C. Brehm, Y. Cancho-Grande, *Org. Lett.* **2001**, *3*, 3955–3957.

[80] T. K. Chakraborty, G. V. Reddy, *Tetrahedron Lett.* **1990**, *31*, 1335–1338.

[81] P. F. Hudrlik, D. Peterson, *J. Am. Chem. Soc.* **1975**, *97*, 1464–1468.

[82] V. M. Csizmadia, K. M. Koshy, K. C. M. Lau, R. A. McClelland, V. J. Nowlan, T. T. Tidwell, *J. Am. Chem. Soc.* **1979**, *101*, 974–979.

[83] I. Stefanuti, S. A. Smith, R. J. K. Taylor, *Tetrahedron Lett.* **2000**, *41*, 3735–3738.

[84] R. Brettle, A. J. Mosedale, *J. Chem. Soc., Perkin Trans. 1,* **1988**, 2185–2195.

[85] K. Kuramochi, H. Watanabe, T. Kitahara, *Synlett* **2000**, *3*, 397–399.

[86] A. Mukherjee, K. K. Mahalanabis, *Indian J. Chem.* **2021**, *60B*, 291–302.

[87] H. Hebbache, Z. Hank, C. Bruneau, J.-L. Renaud, *Synthesis* **2009**, *15*, 2627-2633.

[88] S. Kang, J. Lv1 , T. Wang, B. Wu, M. Wang, Z. Shi, *Nat. Commun.* **2024**, *15*, 7380.

[89] G. Lemière, S. Sedehizadeh, J. Toueg, N. Fleary-Roberts, J. Clayden, *Chem. Commun.* **2011**, *47*, 3745–3747.

[90] S. J. Lee, K. C. Gray, J. S. Paek, M. D. Burke, *J. Am. Chem. Soc.* **2008**, *130*, 466–468.

[91] M. Guhlke, master thesis, University of Bonn, **2019**.

[92] D. Menche, J. Hassfeld, J. Li, K. Mayer, S. Rudolph, *J. Org. Chem.* **2009**, *74*, 7220–7229.

[93] I. Shin, M. Lee, J. Lee, M. Jung, W. Lee, J. Yoon, *J. Org. Chem.* **2000**, *65*, 7667–7675.

[94] S. Deechongkit, S.You, J. W. Kelly, *Org. Lett.* **2004**, *6*, 497–500.

[95] J. Coste, D. Le-Nguyen, B. Castro, *Tetrahedron Lett.* **1990**, *31*, 205–208.

[96] R. Pappo, D. S. Allen Jr., R. U. Lemieux, W. S. Johnson, *J. Org. Chem.* **1956**, *21*, 478–479.

[97] W. S. Wadsworth, W. D. Emmons, *J. Am. Chem. Soc.* **1961**, *83*, 1733.

[98] P. Li, J. Li, F. Arikan, W. Ahlbrecht, M. Dieckmann, D. Menche, *J. Org. Chem.* **2010**, *75*, 2429–2444.

[99] G. Stork, K. Zhao, *Tetrahedron Lett.* **1989**, *30*, 2173–2174.

[100] H. C. Brown, C. D. Blue, D. J. Nelson, N. G. Bhat, *J. Org. Chem.* **1989**, *54*, 6064–6067.

[101] C. Lüthy, P. Konstantin, K. G. Untch, *J. Am. Chem. Soc.* **1978**, *100*, 6211–6217.

[102] F. Rami, B. Klinnert, J. Nowak, F. Ullwer, M. Zheng, W. Frey, B. Plietker, *Org. Lett.* **2024**, *26*, 6370–6374.

[103] R. J. Nachman, G. M. Coast, C. Douat, J. Fehrentz, K. Kaczmarek, J. Zabrocki, N. W. Pryor, J. Martinez, *Peptides* **2003**, *24*, 1615–1621.

[104] Wi. E. Luttrell, C. B. Giles, *J. Chem. Health Saf.* **2007**, *14*, 40–41.

[105] C. Breuer, C. Lemke, J. Schmitz, U. Bartz, M. Gütschow, *Bioorg. Med. Chem. Lett.* **2018**, *28*, 2008–2012.

[106] B. Kim, R. Ratnayake, H. Lee, G. Shi, S. L. Zeller, C. Li, H. Luesch, J. Hong, *Bioorg. Med. Chem.* **2017**, *25*, 3077–3086.

[107] K. Eto, M. Yoshino, K. Takahashi, J. Ishihara, S. Hatakeyama, *Org. Lett.* **2011**, *13*, 5398–5401.

[108] L. A. Carpino, *Acc. Chem. Res.* **1987**, *20*, 401–407.

[109] M. Charpenay, A. Boudhar, G. Blond, J. Suffert, *Angew. Chem. Int. Ed.* **2012**, *51*, 4379–4382.

[110] R. C. Elgersma , L. M.J. Kroon-Batenburg , G. Posthuma, J. D. Meeldijk, D.T.S. Rijkers, R. M.J. Liskamp, *Eur. J. Med. Chem.* **2014**, *88*, 55–65.

[111] B. H. Lipshutz, E. L. Ellsworth, S. H. Dimock, D. C. Reuter, *Tetrahedron Lett.* **1989**, *30*, 2065–2068.

[112] S. Caddick, V.M. Delisser, V.E. Doyle, S. Khan, A. G. Avent, S. Vile, *Tetrahedron Lett.* **1999**, *55*, 2737–2754.

[113] M. Biagetti, F. Bellina, A. Carpita, S. Viel, L. Mannina, R. Rossi, *Eur. J. Org. Chem.* **2002**, 1063–1076.

[114] D. C. Harrowven, D. P. Curran, S. L. Kostiuk, I. L. Wallis-Guy, S. Whiting, K. J. Stenning, B. Tang, E. Packard, L. Nanson, *Chem. Commun.* **2010**, *46*, 6335–6337.

[115] M. J. Dabdoub, V. B. Dabdoub, A. C. M. Baroni, *J. Am. Chem. Soc.* **2001**, *123*, 9694–9695.

[116] A. E. Pasqua, F. D. Ferrari, J. J. Crawford, W. G. Whittingham, R. Marquez, *Bioorg. Med. Chem.* **2015**, *23*, 1062–1068.

[117] G. Wang, S. Mohan, E. Negishi, *Proc. Natl. Acad. Sci. USA* **2011**, *108*, 11344–11349.

[118] I. Marek, C. Meyer, J. F. Normant, *Org. Synth.* **1998**, *9*, 510.

[119] N. Tseng, M. Lautens, *J. Org. Chem.* **2009**, *74*, 2521–2526.

[120] B. M. Trost, M. U. Frederiksen, J. P. N. Papillon, P. E. Harrington, S. Shin, B. T. Shireman, *J. Am. Chem. Soc.* **2005**, *127*, 3666–3667.

[121] S. Caddick, D. B. Judd, A. K. de K. Lewis, M. T. Reich, M. R. V. Williams, *Tetrahedron* **2003**, *59*, 5417–5423.

[122] R. Appel, *Angew. Chem. Int. Ed.* **1975**, *14*, 801 –811.

[123] H. Staudinger, J. Meyer, *Helv. Chim. Acta.***1919**, *2*, 635–646.

[124] H. Zhou, S. Yan, J. Ma, L. Lian, W. Song, *Environ. Sci. Technol.* **2017**, *51*, 11066−11074.

[125] University of California Santa Barbara. "Laboratory Safety Fact Sheet #26: Synthesizing, Purifying, and Handling Organic Azides. https://www.ehs.ucsb.edu/sites/default/files/docs/ls/factsheets/Azides_FS26.pdf (07.04.2025)

[126] S. Bräse, C. Gil, K. Knepper, V. Zimmermann, *Angew. Chem. Int. Ed.* **2005**, *44*, 5188–5240.

[127] E. Colvin, B. J. Hamill, *J. Chem. Soc., Chem. Commun.* **1973**, 151–152.

[128] M. Tortosa, N. A. Yakelis, W. R. Roush, *J. Am. Chem. Soc.* **2008**, *130*, 2722–2723.

[129] O. Zhurakovskyi, R. M. P. Dias, A. Noble, V. K. Aggarwal, *Org. Lett.* **2018**, *20*, 3136−3139.

[130] I. Marek, A. Alexakis, J. F. Normant, *Tetrahedron Lett.* **1991**, *32*, 6337–6340.

[131] Y. Nishioka, Y. Yano, N. Kinashi, N. Oku, Y. Toriyama, S. Katsumura, T. Shinada, K. Sakaguchi, Synlett **2016**, *28*, 327-332.

[132] K. Sakaguchi, Y. Nishioka, N. Kinashi, N. Yukihira, T. Shinada, T. Nishimura, H. Hashimoto, S. Katsumura, *Synthesis* **2020**, *52*, 3007–3017.

[133] S. Xu, E. Negishi, *Acc. Chem. Res.* **2016**, *49*, 2158−2168.

[134] D. R. Brandt, K. M. Pannone, J. J. Romano, E. G. Casillas, *Tetrahedron* **2013**, *69*, 9994−10002.

[135] N. Kotoku, N. Tamada, A. Hayashi, M. Kobayashi, *Bioorg. Med. Chem. Lett.* **2008**, *18*, 3532–3535.

[136] M. Asano, M. Inoue, K. Watanabe, H. Abe, T. Katoh, *J. Org. Chem.* **2006**, *71*, 6942–6951.

[137] A. B. Cuenca, E. Fernandez, *Chem. Soc. Rev.* **2021**, *50*, 72–86.

[138] Y. Liu, C. Li, C. Liu, J. He, X. Zhao, S.g Cao, *Tetrahedron Lett.* **2020**, *61*, 151940.

[139] C. C. Roberts, D. M. Matías, M. J. Goldfogel, S. J. Meek, *J. Am. Chem. Soc.* **2015**, *137*, 6488−6491.

[140] I. T. Raheem, S. N. Goodman, E. N. Jacobsen, *J. Am. Chem. Soc.* **2004**, *126*, 706–707.

[141] G. Benoit, A. B. Charette, *J. Am. Chem. Soc.* **2017**, *139*, 1364–1367.

[142] T. Boultwood, J. A. Bull, *ACS Omega* **2019**, *4*, 870−879.

[143] D. Werner, R. Anwander, *J. Am. Chem. Soc.* **2018**, *140*, 14334−14341.

[144] C. P. Delaney, V. M. Kassel, S. E. Denmark, *ACS Catal.* **2020**, *10*, 73−80.

[145] A. V. Kalinin, S. Scherer, V. Snieckus, *Angew. Chem.* **2003**, *115*, 3521–3526.

[146] H. E. Zimmerman, M. D. Traxler, *J. Am. Chem. Soc.* **1957**, 79, 1920–1923.

[147] Z. Bao, M. Huang, Y. Xu, X. Zhang,Y. Wu, J. Wang, *Angew. Chem. Int. Ed.* **2023**, *62*, e202216356.

[148] D. J. Blair, S. Zhong, M. J. Hesse, N. Zabaleta, E. L. Myers, V. K. Aggarwal, *Chem. Commun.* **2016**, *52*, 5289–5292.

[149] E. J. Corey, P. L. Fuchs, *Tetrahedron Lett.* **1972**, *36*, 3769–3772.

[150] K. Bowden, I. M. Heilbron, E. R. H. Jones, B. C. L. Weedon, *J. Chem. Soc.* **1946**, 39–45.

[151] S. Hanessian, P. Lavallee, *Can. J. Chem.* **1975**, *53*, 2975–2977.

[152] B. Göricke, M. F. Bieber, K. E. Mohr, D. Menche, *Angew. Chem. Int. Ed.* **2019**, *58*, 13019 –13023.

[153] I. Paterson, G. J. Florence, K. Gerlach, J. P. Scott, N. Sereinig, *J. Am. Chem. Soc.* **2001**, 123, 9535–9544.

[154] C. Rink, V. Navickas, M. E. Maier, *Org. Lett.* **2011**, *13*, 2334–2337.

[155] J. Herbst, master thesis, University of Bonn, **2023**.

[156] R. M. Lanes, D. G. Lee, *J. Chem. Educ.* **1968**, *45*, 269.

[157] L. Schmieder-van de Vondervoort, S. Bouttemy, J.M. Padrón, J. Le Bras, J. Muzart, Paul L. Alsters, *Synlett* **2002**, *2*, 243–246.

[158] G. W. Kabalka, D. E. Bierer, *Synth. Commun.* **1989**, *19*, 2783-2787.

[159] L. M. Wingen, M. Rausch, T. Schneider, D. Menche, *J. Org. Chem.* **2020**, *85*, 10206−10215.

[160] Y. Chen, G. Coussanes, C. Souris, P. Aillard, D. Kaldre, K. Runggatscher, S. Kubicek, G. Di Mauro, B. Maryasin, N. Maulide, *J. Am. Chem. Soc.* **2019**, *141*, 13772−13777.

[161] E. Otieno Onyango, J. Tsurumoto, N. Imai, K. Takahashi, J. Ishihara, S. Hatakeyama, *Angew. Chem. Int. Ed.* **2007**, *46*, 6703–6705.

[162] M. Roche, S. Specklin, M. Richard, F. Hinnen, K. Génermont, B. Kuhnast, *J. Label Compd. Radiopharm.* **2019**, *62*, 95–108.

[163] L. Adriaenssens, J. L. A. Sánchez, X. Barril, C. K. O´Sullivan, P. Ballester, *Chem. Sci.* **2014**, *5*, 4210–4215.

[164] M. J. Wen, M. T. Jackson, C. M. Garner, *Dalton Trans.* **2019**, *48*, 11575–11582.

[165] A. J. Zhang, D. H. Russell, J. Zhu, K. Burgess, *Tetrahedron Lett.* **1998**, *39*, 7439–7442.

[166] C. Zhu, X. Shen, S. G. Nelson, *J. Am. Chem. Soc.* **2004**, *126*, 5352–5353.

[167] A. G. Myers, B. Zheng, M. Movassaghi, *J. Org. Chem.* **1997**, *62*, 7507.

[168] J.G. Duboudin, B. Jousseaume, *J. Organomet. Chem.* **1979**, *168*, 1–11.

[169] J. D. More, N. S. Finney, *Org. Lett.* **2002**, *4*, 3001–3003.

[170] P. Nösel, T. Lauterbach, M. Rudolph, F. Rominger, A. Stephen, K. Hashmi, *Chem. Eur. J.* **2013**, *19*, 8634–8641.

[171] K. R. Buszek, N. Brown, *J. Org. Chem.* **2007**, *72*, 3125–3128.

[172] J. K. Stille, B. L. Groht, *J. Am. Chem. Soc.* **1987**, *109*, 813–817.

[173] K. Maruyama, Y. Kuramoto, M. Yagi and Y. Tanizaki, *Polymer* **1988**, *29*, 24–29.

[174] S. A. Frank, H. Chen, R. K. Kunz, M. J. Schnaderbeck, W. R. Roush, *Org. Lett.* **2000**, *2*, 2691–2694.

[175] F. Lehmann, *Synlett* **2004**, 13, 2447–2448.

[176] R. A. Raubach, A. V. Guzzo, *J. Phys. Chem.* **1973**, *77*, 889–892.

[177] A. L. Dobryakov, D. Schriever, M. Quick, J. L. Perez-Lustres, I. N. Ioffe, S. A. Kovalenko, *J. Am. Chem. Soc.* **2024**, *146*, 32463−32478.

[178] T. G. Nguyen, master thesis, University of Bonn, **2024**.

[179] J. D. Hicks, A. M. Hyde, A. M. Cuezva, S. L. Buchwald, *J. Am. Chem. Soc.* **2009**, *131*, 16720–16734.

[180] G. Lu, K. R. Voigtritter, C. Cai, B. H. Lipshutz, *J. Org. Chem.* **2012**, *77*, 3700−3703.

[181] H. Suzuki, *Bull. Chem. Soc. Jpn.* **1959**, *32*, 1340–1350.

[182] F. R. Hartley, *J. Organomet. Chem.* **1970**, *21*, 227–236.

[183] C.P. Delaney, D. P. Marron, A. S. Shved, R. N. Zare, R. M. Waymouth, S. E. Denmark, *J. Am. Chem. Soc.* **2022**, *144*, 4345–4364.

[184] H. Koyama1, H. Doi, M. Suzuki, *Int. J. Org. Chem.* **2013**, *3*, 220–223.

[185] J. Uenishi, J. M. Beau, R. W. Armstrong, Y. Kishi, *J. Am. Chem. Soc.* **1987**, *109*, 4756–4758.

[186] I. E. Marko, F. Murphy, S. Dolan, *Tetrahedron Lett.* **1996**, *37*, 2507–2510.

[187] J. J. Fuentes-Rivera, M. E. Zick, M. A. Düfert, P. J. Milner, *Org. Process Res. Dev.* **2019**, *23*, 1631−1637.

[188] L. Wagner, M. Zargar, C. Kalli, E. O. Fridjonsson, N. N. A. Ling, E. F. May, J. Zhen, M. L. Johns, *Ind. Eng. Chem. Res.* **2020**, *59*, 20836−20844.

[189] P. A. Cox, A. G. Leach, A. D. Campbell, G. C. Lloyd-Jones, *J. Am. Chem. Soc.* **2016**, *138*, 9145−9157.

[190] J. A. Gonzalez, O. M. Ogba, G. F. Morehouse, N. Rosson, K. N. Houk, A. G. Leach, P. H. Y. Cheong, M. D. Burke, G. C. Lloyd-Jones, *Nat. Chem.* **2016**, *8*, 1067–1075.

[191] N. Oka, T. Yamada, H. Sajiki, S. Akai, T. Ikawa, *Org. Lett.* **2022**, *24*, 3510−3514.

[192] B. P. Carrow, J. F. Hartwig, *J. Am. Chem. Soc.* **2011**, *133*, 2116–2119.

[193] M. Filipan-Litvić, M. Litvić, I. Cepanec, V. Vinković, *Molecules* **2007**, *12*, 2546–2558.

[194] S. E. Lyubimov, E. A. Rastorguev, V. A. Davankov, *Chirality* **2011**, *8*, 624-627.

[195] X. Jie, Y. Shang, Z.-N. Chen, X. Zhang, W. Zhuang, W. Su, *Nat. Commun.* **2018**, *9*, 5002.

[196] X. Zhang, K. Huang, G. Hou, B. Cao, X. Zhang, *Angew. Chem. Int. Ed.* **2010**, *49*, 6421–6424.

[197] A. P. Davis, J. J. Walsh, *Tetrahedron Lett.* **1994**, *35*, 4865–4868.

[198] M. J. Totleben, J. P. Freeman, J. Szmuszkovicz, *J. Org. Chem.* **1997**, *62*, 7319-7323.

[199] L. A. Carpino, *J. Am. Chem. Soc.* **1993**, *115*, 4397-4398.

[200] V. Dourtoglou, J.-C. Ziegler, B. Gross, *Tetrahedron Lett.* **1978**, *15*, 1269-1272.

[201] L. Hu, J. Zhao, *Synlett* **2017**, *28*, 1663–1670.

[202] M. S. Kim, Y. M. Choi, D. K. An, *Tetrahedron Lett.* **2007**, *48*, 5061–5064.

[203] K. Soai, A. Ookawa, *J. Org. Chem.* **1986**, *51*, 4000–4005.

[204] J. T. Spletstoser, J. M. White, A. R. Tunoori, G. I. Georg, *J. Am. Chem. Soc.* **2007**, *129*, 3408–3419.

[205] J. M. Williams, R. B. Jobson, N. Yasuda, G. Marchesini, U.-H. Dolling, E. J. J. Grabowski, *Tetrahedron Lett.* **1995**, *36*, 5461–5464.

[206] I. Cheng-Sánchez, C. García-Ruiz, G. A. Guerrero-Vásquez, F. Sarabia, *J. Org. Chem.* **2017**, *82*, 4744 −4757.

[207] Y. Ono, A. Nakazaki, K. Ueki, K. Higuchi, U. Sriphana, M. Adachi, T. Nishikawa, *J. Org. Chem.* **2019**, *84*, 9750−9757.

[208] H. Urabe, T. Matsuka, F. Sate, *Tetrahedron Lett.* **1992**, *33*, 4179−4182.

[209] Y. Ukaji, K. Sada, K. Inomata, *Chem. Lett.* **1993**, *22*, 1227−1230.

[210] O. V. Konstantinova, A. M. P. Koskinen, *Synthesis* **2019**, *51*, 285–295.

[211] K. D. Kim, P. A. Wagtiotis, *Tetrahedron Lett.* **1990**, 131, 6137–6140.

[212] N. Prilezhaev, *Ber. dtsch. Chem. Ges.* **1909**, *42*, 4811–4815.

[213] J. R. Parikh, W. V. E. Doering, *J. Am. Chem. Soc.* **1967**, *89*, 5505–5507.

[214] R. Johnsson, M. Ohlin, U. Ellervik, *J. Org. Chem.* **2010**, *75*, 8003–8011.

[215] M. Pastó, A. Moyano, M. A. Pericks, A. Riera, *Tetrahedron: Asymmetry* **1995**, *6*, 2329–2342.

[216] J. Wang, M. A. Horwitz, A. B. Dürr, F. Ibba, G. Pupo, Y. Gao, P. Ricci, K. E. Christensen, T. P. Pathak, T. D. W. Claridge, G. C. Lloyd-Jones, R. S. Paton, V. Gouverneur, *J. Am. Chem. Soc.* **2022**, *144*, 4572−4584.

[217] B. E. Uno, E. P. Gillis, M. D. Burke, *Tetrahedron* **2009**, *65*, 3130–3138.

[218] J. He, J. Ling, P. Chiu, *Chem. Rev.* **2014**, *114*, 8037−8128.

[219] A. Tenaglia, B. Waegell, *Tetrahedron Lett.* **1988**, 29,4851−4854.

[220] A. K. Chatterjee, T.-L. Choi, D. P. Sanders, R. H. Grubbs, *J. Am. Chem. Soc.* **2003**, *125*, 11360−11370.

[221] I. C. Stewart, T. Ung, A. A. Pletnev, J. M. Berlin, R. H. Grubbs, Y. Schrodi, *Org. Lett.* **2007**, *9*, 1589−1592.

[222] A. Michrowska, R. Bujok, S. Harutyunyan, V. Sashuk, G. Dolgonos, K. Grela, *J. Am. Chem. Soc.* **2004**, *126*, 9318−9325.

[223] T. R. Hoye, C. S. Jeffrey, F. Shao, *Nat. Protoc.* **2007**, *2*, 2451–2458.

[224] K. Sugimoto, Y. Kobayashi, A. Hori, T. Kondo, N. Toyooka, H. Nemoto, Y. Matsuya, *Tetrahedron* **2011**, *67*, 7681−7685.

[225] D. P. Curran, M. K. Sinha, K. Zhang, J. J. Sabatini, D.-H. Cho, *Nat. Chem.* **2012**, *4*, 124–129.

[226] C. Jasper, R. Wittenberg, M. Quitschalle, J. Jakupovic, A. Kirschning, *Org. Lett.* **2005**, *7*, 479–482.

[227] V. Atlan, S. Racouchot, M. Rubin, C. Bremer, J. Ollivier, A. de Meijere, J. Salaün, *Tetrahedron: Asymmetry* **1998**, *9*, 1131–1135.

[228] C. J. Salomon, E. G. Mata, O. A. Mascaretti, *J. Org. Chem.* **1994**, *59*, 7259–7266.

[229] M. Sayes, G. Benoit, A. B. Charette, *Angew. Chem. Int. Ed.* **2018**, *57*, 13514–13518.